Nuclear Science NEA/NSC/DOC(2010)7

Shielding Aspects of Accelerators, Targets and Irradiation Facilities – SATIF-9

Proceedings of the 9th Meeting

21-23 April 2008
Spallation Neutron Source
Oak Ridge National Laboratory
Oak Ridge, TN USA

© OECD 2010

NUCLEAR ENERGY AGENCY
Organisation for Economic Co-operation and Development

ORGANISATION FOR ECONOMIC CO-OPERATION AND DEVELOPMENT

The OECD is a unique forum where the governments of 30 democracies work together to address the economic, social and environmental challenges of globalisation. The OECD is also at the forefront of efforts to understand and to help governments respond to new developments and concerns, such as corporate governance, the information economy and the challenges of an ageing population. The Organisation provides a setting where governments can compare policy experiences, seek answers to common problems, identify good practice and work to co-ordinate domestic and international policies.

The OECD member countries are: Australia, Austria, Belgium, Canada, the Czech Republic, Denmark, Finland, France, Germany, Greece, Hungary, Iceland, Ireland, Italy, Japan, Korea, Luxembourg, Mexico, the Netherlands, New Zealand, Norway, Poland, Portugal, the Slovak Republic, Spain, Sweden, Switzerland, Turkey, the United Kingdom and the United States. The Commission of the European Communities takes part in the work of the OECD.

OECD Publishing disseminates widely the results of the Organisation's statistics gathering and research on economic, social and environmental issues, as well as the conventions, guidelines and standards agreed by its members.

This work is published on the responsibility of the Secretary-General of the OECD. The opinions expressed and arguments employed herein do not necessarily reflect the official views of the Organisation or of the governments of its member countries.

NUCLEAR ENERGY AGENCY

The OECD Nuclear Energy Agency (NEA) was established on 1st February 1958 under the name of the OEEC European Nuclear Energy Agency. It received its present designation on 20th April 1972, when Japan became its first non-European full member. NEA membership today consists of 28 OECD member countries: Australia, Austria, Belgium, Canada, the Czech Republic, Denmark, Finland, France, Germany, Greece, Hungary, Iceland, Ireland, Italy, Japan, Luxembourg, Mexico, the Netherlands, Norway, Portugal, Republic of Korea, the Slovak Republic, Spain, Sweden, Switzerland, Turkey, the United Kingdom and the United States. The Commission of the European Communities also takes part in the work of the Agency.

The mission of the NEA is:

- to assist its member countries in maintaining and further developing, through international co-operation, the scientific, technological and legal bases required for a safe, environmentally friendly and economical use of nuclear energy for peaceful purposes, as well as
- to provide authoritative assessments and to forge common understandings on key issues, as input to government decisions on nuclear energy policy and to broader OECD policy analyses in areas such as energy and sustainable development.

Specific areas of competence of the NEA include safety and regulation of nuclear activities, radioactive waste management, radiological protection, nuclear science, economic and technical analyses of the nuclear fuel cycle, nuclear law and liability, and public information.

The NEA Data Bank provides nuclear data and computer program services for participating countries. In these and related tasks, the NEA works in close collaboration with the International Atomic Energy Agency in Vienna, with which it has a Co-operation Agreement, as well as with other international organisations in the nuclear field.

Corrigenda to OECD publications may be found on line at: *www.oecd.org/publishing/corrigenda*.
© OECD 2010

You can copy, download or print OECD content for your own use, and you can include excerpts from OECD publications, databases and multimedia products in your own documents, presentations, blogs, websites and teaching materials, provided that suitable acknowledgment of OECD as source and copyright owner is given. All requests for public or commercial use and translation rights should be submitted to *rights@oecd.org*. Requests for permission to photocopy portions of this material for public or commercial use shall be addressed directly to the Copyright Clearance Center (CCC) at *info@copyright.com* or the Centre français d'exploitation du droit de copie (CFC) *contact@cfcopies.com*.

Foreword

Nuclear energy covers a field much wider than nuclear power. In fact, atomic and nuclear energy applications involve a large range of scientific and technological activities using a variety of machines and analysis techniques. Activities in this area have increased over the years and consequently the OECD/NEA Nuclear Science Committee is sponsoring more activities in this area.

One of these activities concerns "Shielding Aspects of Accelerators, Targets and Irradiation Facilities" (SATIF). A series of workshops has been held during the last decade: SATIF-1 was held on 28-29 April 1994 in Arlington, Texas; SATIF-2 on 12-13 October 1995 at CERN in Geneva, Switzerland; SATIF-3 on 12-13 May 1997 at Tohoku University in Sendai, Japan; SATIF-4 on 17-18 September 1998 in Knoxville, Tennessee; SATIF-5 on 17-21 July 2000 at the OECD in Paris, France; SATIF-6 on 10-12 April 2002 at the Stanford Linear Accelerator Center (SLAC), Menlo Park, California, United States; SATIF-7 on 17-18 May 2004 at ITN, Sacavém, Portugal; and SATIF-8 was held on 22-24 May 2006 at the Pohang Accelerator Laboratory (PAL) POSTECH, Republic of Korea. SATIF-9 was held on 21-23 April 2008 at the Spallation Neutron Source, Oak Ridge National Laboratory, United States. SATIF-10 is scheduled to be held on 2-4 June 2010 at CERN in Geneva, Switzerland.

Each workshop is hosted by organisations having accelerator facilities and experts that enhance the interaction between local expertise and experts from the international community. SATIF-9 was held at the Spallation Neutron Source, Oak Ridge National Laboratory (SNS), Oak Ridge, United States, and the chairman of the workshop, Phillip D. Ferguson (SNS), arranged a visit to their facility.

This event was jointly organised by the:

- OECD Nuclear Energy Agency;
- Spallation Neutron Source (SNS);
- Radiation Safety Information Computational Center (RSICC);
- Shielding Working Group of the Reactor Physics Committee of Japan.

The current proceedings provide a summary of the discussions, decisions and conclusions together with the text of the presentations made at the eighth SATIF meeting.

This text is published on the responsibility of the Secretary-General of the OECD. The views expressed do not necessarily correspond to those of the national authorities concerned.

Acknowledgements

Acknowledgements are due to the members of the SATIF-9 Technical Programme Committee and in particular to P.D. Ferguson, chair of the workshop, for their contribution in shaping the technical programme, and to all participants who contributed valuable work and ideas described in these proceedings.

Table of contents

Executive summary

The OECD/NEA Expert Group on Shielding Aspects of Accelerators, Targets and Irradiation Facilities (SATIF) meets every two years, and organises its workshops in places where world-class facilities are operated, alternating between North America, Europe and the Far East. During these workshops progress and results form an agreed programme of work are presented and common actions and research initiatives promoted and undertaken with the aim of achieving progress and enhancing international co-operation in this area of research.

The ninth SATIF workshop took place on 21-23 April 2008 and was hosted by the Spallation Neutron Source (SNS) (see Figures 1 and 2), Oak Ridge National Laboratory in the United States. The local organiser and Chair of the workshop was Dr. Phil Ferguson from the SNS. It was attended by 35 specialists in radiation protection, radiation shielding and radiation dosimetry from 10 countries representing 20 different organisations active in this field (see Annex 1: List of participants).

The objectives of SATIF-9 are as follows:

- To promote the exchange of information among experts in the field of accelerator shielding and related topics.
- To identify areas where international co-operation can be fruitful. Recommend actions with strong need for international work on theoretical models, experimental work and benchmarking.
- To carry on a programme of work in order to achieve progress in specific priority areas.
- To present and assess achievements on actions agreed upon previously.

Figure 1: SATIF-9 workshop venue and facility visited

Figure 2: Spallation Neutron Source (SNS)

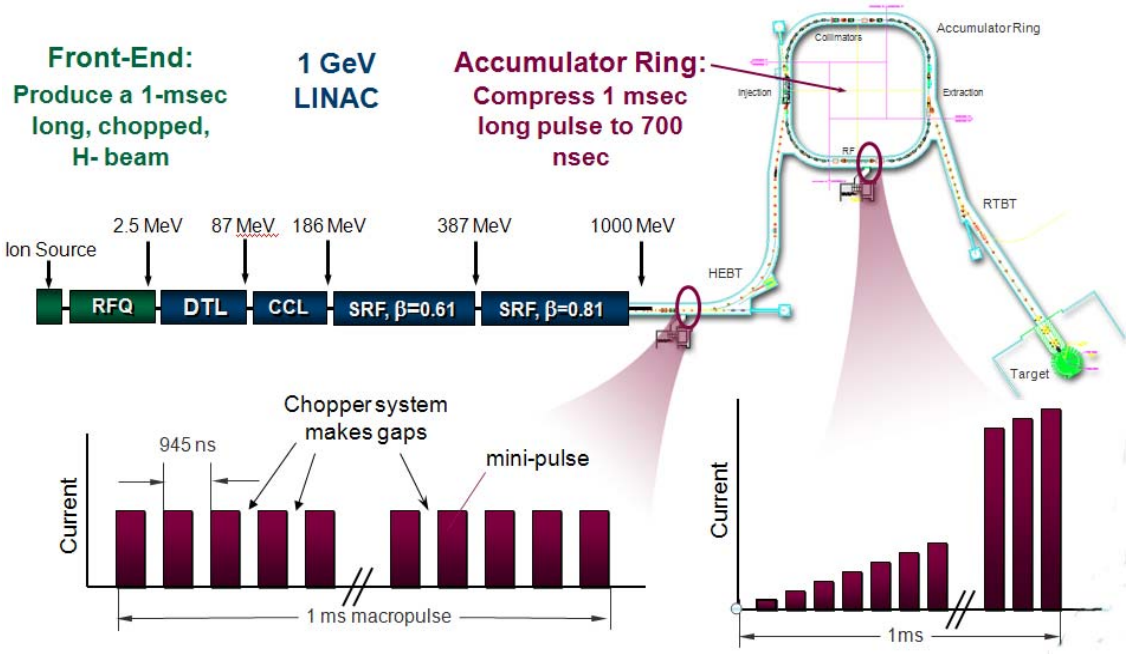

Thirty presentations followed by discussions were made, organised into six topical sessions:

1) source terms and related topics;
2) measurements and calculations of induced radioactivity and activation data;
3) shielding in medical and industrial accelerator applications;
4) benchmarking – calculations and results;
5) dose and related issues;
6) status of computer codes, cross-sections and shielding data libraries.

The detailed programme is provided in Annex 2.

Future directions for the expert group discussed and agreed upon include the following actions:

- Enhance visibility of work:
  - state-of-the-art handbook(s);
  - publications in archival journals.
- Target new applications:
  - medical radiation applications;
  - dosimetry-related calculations for different applications (industrial, material/tissue damage, irradiations of specimens, radiation fields in and around irradiation facilities);
  - shielding of transmutation and high-power accelerator facilities.
- Increase interaction with other groups (*e.g.*):
  - CONRAD activities (quality assurance and benchmarking, monitoring in workplace, review of HE facilities, carbon beams for therapy, etc.);
  - Computation Medical Physics Working Group (ANS);
  - close co-operation with joint PSI/ORNL ARIA activity.

- Training courses/tutorials (good codes and competent users).
- Enhance effectiveness:
  - form sub-groups on topics of common interest – project-oriented;
  - exchange via videoconferencing;
  - make use of SATIF forum via *satif@nea.fr* Q/A.

The important aspects of the work were identified as follows:

- Activation and dose rates estimation for facility maintenance planning is requested and it is particularly crucial if the targets are changed, to identify "hot spots" and how to prevent them
- Dismantling of facilities requires estimation of remnant dose for dose management, for the characterisation of waste to be able to declare it free from radiation. Lack of such a capability may lead to very expensive solutions. Relevant data on activation and their evaluation contributing to waste disposal and hazard classification of accelerators. The SINBAD database should be expanded to include such compilations, in particular, as EXFOR does not seem to be an adequate format for it. More basic data on mass distributions and spallation products are also needed and should be integrated in the databases.
- Shield designs of high-power accelerator facilities require best-estimate/state-of-the art methods to reduce the cost of facilities.
- The activities of SATIF can provide reliable evaluated data and guidance for model selection; strong support and stimulation for making data available should be provided, and such experimental data should be presented at the SATIF meetings.
- The group does not just meet and hold workshops, it co-ordinates analysis, proposes action items; examples are the collaboration on attenuation length up to 10 GeV. The consensus for certain parameters, reached though independent but co-ordinated work, is of high value.
- Code comparisons present a challenge for code developers and lead to valuable insight for users and code developers.
- For the energy region where it becomes difficult to distinguish phenomena such as fission and spallation, requirements exist for additional development of models as the discrepancies are still very high. SATIF should devote efforts to resolving such issues by proposing experiments that help choosing the right model.
- In accelerator shield design simple codes are still used quite often. This normally leads to overdesign. With today's state-of-the-art methods only few safety factors need to be applied
- Experimental databases and benchmarking are key elements for building confidence in data and codes used; this is an essential activity of SATIF that enforces objective comparison and facilitates access to the information needed. It is felt that official endorsement of benchmarks by NEA NSC WPRS is essential.
- The discussions and exchange of views at SATIF relative to mechanisms that are not well understood provide new ideas for design experiments that lead to problem-solving.
- It was noted that there is lack of photonuclear data available for light elements and those available are for a limited range and often of poor quality. Data for production of d, t and alphas with their spectra are required (work by Fassò and available facilities for such measurements).
- Concerning computer programs it is essential that all responsible developers of the relevant codes contribute to the discussion and share their models; they should also generate a table describing the quality (good or bad) of their features. This should be presented and discussed by authors at SATIF-10. A session should also be devoted to "event generators" to facilitate common ways of solving problems. Release of standard routines and of tools for geometry conversion from one code input to others, to minimise benchmarking efforts and cost should be strongly encouraged.

The know-how and experience amassed by the SATIF group over recent years will be synthesised into an "Accelerator Shielding Handbook", for the benefit of an increasingly large community of accelerator shielders. No current handbook exists on this subject and, a strong need for it being expressed, its production was agreed upon. The editors of the handbook were designated among those SATIF members having editing experience: P. Vaz and Nikolai Mokhov and a number of co-ordinators and authors (*e.g.* T. Nakamura, S. Mashnik, P. Ferguson, F. Gallmeier, A. Fassò, M. Silari, W. Dittrich, L. Waters, etc.) as well as others who confirmed their availability. The agreed upon structure of the handbook is provided in Annex 3.

The following chapters have been drafted thus far:

- W. Dittrich:
  - 2.3 Radiological standards and limits, legal dose
  - 2.5 Practical aspects
  - 3.6 Environmental impact

Comments: Explain that legal dose limits are in practice never approached: (F. Gallemeier will provide examples). As to environmental impacts, contamination should be included in particular as concerns facilities in support of fusion reactors (Ph. Joyer will contribute issues relevant to fusion).

- T. Nakamura:
  - 7.1 Thick target yields
  - 7.2 Shielding experiments
  - 11.4 Heavy ions

Comments: Provide feedback to T. Nakamura.

Actions specific to the shielding handbook were discussed, and include the following:

- Editors will contact co-ordinators to verify structure of handbook and confirm contributors.
- Verify co-ordinator/authors for Chapter 2 (R. Thomas, H. Menzel, A. Fassò). If not available, verify if M. Pelliccioni would be available.
- Verify whether Y. Titarenko would be willing to contribute parts of the text.
- Chapter co-ordinators will contact authors in the near future to provide instructions and monitor progress on a regular basis with the aim of having drafts of most chapters/sections by March/April 2009.
- Arrange meeting of editors and chapter co-ordinators in March/April 2009 to discuss draft chapters and ensure coherence of presentation, identification of gaps, etc. (E. Sartori).
- Add handbook to the NEA publication schedule for 2010/11.

The benchmark and related activities were discussed, proposals made and several choices made during SATIF-8 confirmed and complemented with new ones. The following is a summary of items discussed and deemed of importance. Preservation of evaluated experiments in the SINBAD database was recommended:

1) Production yields of the radionuclides induced from various targets in concrete shield at the 500-MeV neutron irradiation facility of KENS by H. Matsumura (KEK), N. Nakao (KEK), K. Masumoto (KEK), K. Oishi (Shimizu Co.), M. Kawai (KEK), T. Aze (U.Tokyo), A. Toyoda (KEK), M. Numajiri (KEK), K. Takahashi (KEK), M. Fujimura (Nihon U.), Q. Wang (IHEP), K. Bessho (KEK), T. Sanami (KEK).
2) Thick target yield (TTY) at 0 degree by 250 and 350 MeV protons at the Research Center of Nuclear Physics (RCNP) cyclotron by Y. Iwamoto (JAEA).
3) AGS Spallation Target Experiment by H. Nakashima and the ASTE collaboration team.
4) Benchmarks on photon-neutron spectrum, differential yields, and angular distribution from targets irradiated by 2 GeV electrons based on measurements carried out at PAL by H-S. Lee.

5) Heavy ion benchmark based on data from HIMAC by K. Niita.

6) Proposal for a ADS and high power accelerator facilities benchmark, by P. Vaz (ITN).

7) Benchmark experiments using 140-392 MeV p-Li quasi monoenergetic neutrons at RCNP (T. Nakamura).

8) Propose priority targets for ITEP-ISTC project with p up to 2.6 GeV (Cr, Ni and Zr-4 + others) (P. Ferguson).

9) Investigate possible release of material assay data for low activation concrete (K. Kimura).

10) Possible general release of BRIEFF, FLUKA and PHITS computer codes.

11) Upgrade models for TOF experiments and undertake a quality review of accelerator shielding benchmarks in SINBAD.

12) Revise/submit additional solutions for inter-comparison of the "Neutron Attenuation in Iron and Concrete (7)" report results from improved modelling/experimental data for resolving discrepancy, by Hideo Hirayama (KEK) (N.V. Mokhov will suggest a list of published lambda measurements; results on an experiment with 120 GeV p into a beam dump will be available by SATIF-10).

13) Contact should be made with G. Gualdrini and S. Agosteo for sharing results from the EURADOS benchmark activities (E. Sartori).

14) Make MCNP input for inter-comparison of the medium-energy neutron attenuation in iron and concrete available (F. Maekawa).

15) Computational Medical Physics Benchmark(s), report progress on database of Dosimetry Benchmarks for Radiation Transport at SATIF-10.

16) SHARE benchmark exercise (for modellers and code developers) by S. Leray (CEA) now organised within IAEA: proposed reporting at SATIF-10.

17) There is a need for releasing data for production of d, t, and alphas with their spectra. The collection by A. Fassò would be a good source for it and its general release would be useful.

It was agreed to hold the tenth workshop at CERN, Geneva on 2-4 June 2010. Executive Group members from Japan will investigate the possibility of hosting SATIF-11 in 2012 in Japan.

The new Executive/Scientific Committee for SATIF-10 was elected as follows: M. Brugger (CERN), Ph. Ferguson (ORNL, current Chair), A. Ferrari (CERN), H. Hirayama (KEK), B.L. Kirk (RSICC), H-S. Lee (PAL), N.V. Mokhov (FNAL), G. Muhrer (LANL), T. Nakamura (U. Tohoku), H. Nakashima (JAEA), S. Roesler (CERN), S. Rokni (SLAC), M. Silari (CERN, new Chair), P. Vaz (ITN), M. Wohlmuther (PSI).

To summarise, SATIF activities have contributed for over a decade to enhancing the role NEA plays in promoting international co-operation in scientific areas related to nuclear energy (at large), radiation physics and the application of ionising radiations in different fields of science and technology. They are in line with the NEA Programme of Work and the main areas of activity set out in the current NEA Strategic Plan.

Session I

Source terms and related topics

Chair: P. Vaz

Radiation shielding for the main injector collimation system

Igor Rakhno
Fermilab, Batavia, Illinois, USA

Fermilab

Motivation

- A Proton Plan was developed at Fermilab some time ago for the benefit of the existing neutrino programs as well as to increase anti-proton production for the Tevatron programs.
- As a part of the plan, the intensity of proton beams in the **Main Injector** should be increased by means of a slip-stacking injection.
- In order to localize beam loss associated with the injection, a collimation system was designed that satisfies all the radiation and engineering constraints. ***Recently commissioned.***

April 21, 2008 SATIF-9, Oak Ridge, TN 2

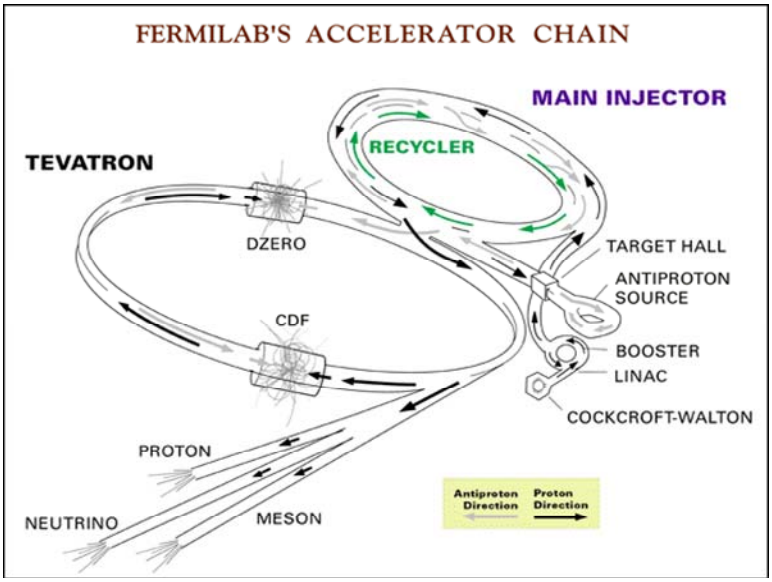

April 21, 2008 SATIF-9, Oak Ridge, TN 3

MI →

April 21, 2008 SATIF-9, Oak Ridge, TN 4

Fermilab

Outline

- **Collimation system.**
- **Model of the region.**
- **MAD-to-MARS beam line builder.**
- **Some results.**
- **Conclusions.**

April 21, 2008 SATIF-9, Oak Ridge, TN 5

Fermilab

Main Injector collimation system

- The collimation system itself comprises a ***primary*** collimator and ***four secondary*** collimators to which various masks are added.
- The entire length of the collimation region is ≈ 200 m.
- The corresponding part of the beam line consists of more than 30 magnets .
- An ***electron cooling system*** is installed in the region → the sensitive equipment should be protected against scattered radiation.

April 21, 2008 SATIF-9, Oak Ridge, TN 6

Fermilab

Model of the region

Plan view

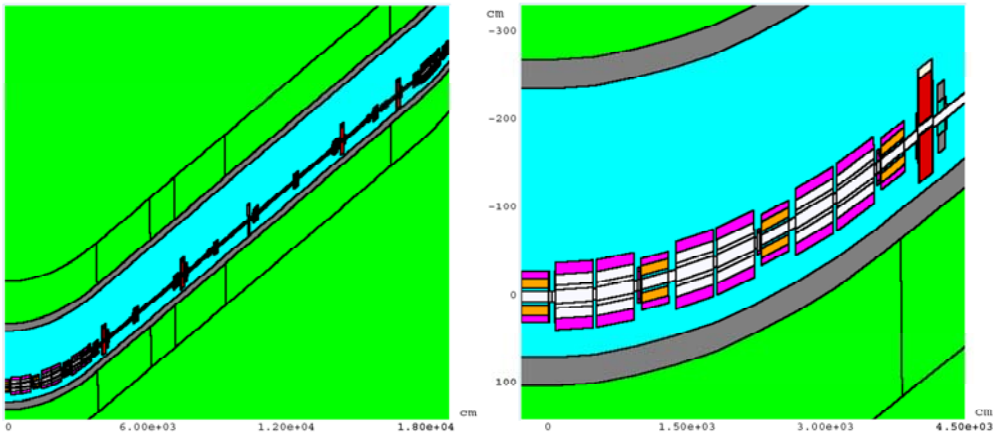

April 21, 2008 SATIF-9, Oak Ridge, TN 7

Fermilab

Model of a secondary collimator

(Steel core covered with marble layers)

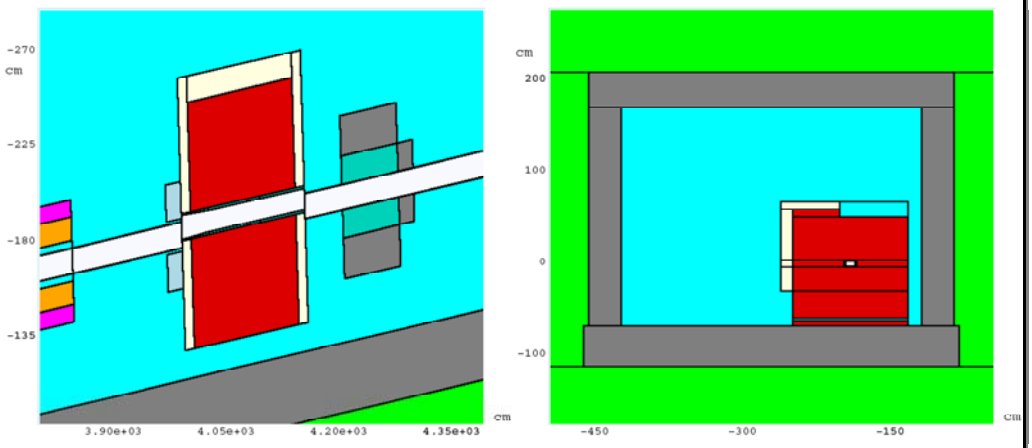

April 21, 2008 SATIF-9, Oak Ridge, TN 8

Fermilab

Real Primary Collimator
(Courtesy of Bruce Brown)

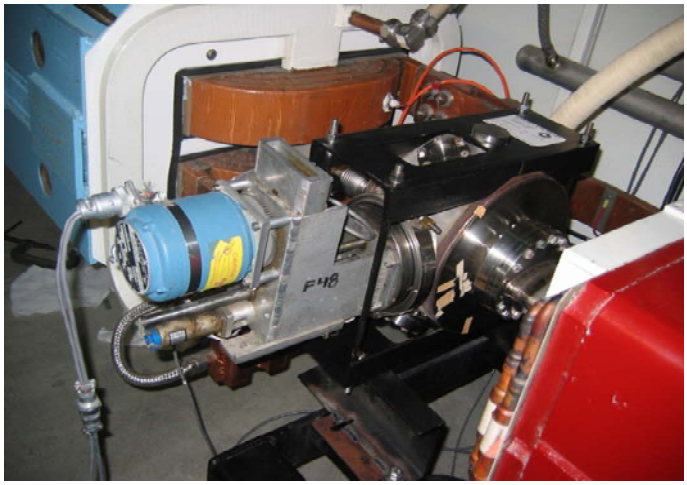

April 21, 2008 SATIF-9, Oak Ridge, TN 9

Fermilab

Real Secondary Collimator
Includes precise Radial & Vertical Motion
(Courtesy of Bruce Brown)

April 21, 2008 SATIF-9, Oak Ridge, TN 10

Fermilab

MAD-to-MARS beam line builder (MMBLB)

- The beam line itself was designed with the STRUCT code. Both **longitudinal** and **transverse alignment** of optical elements was calculated. Output in MAD format.
- For radiation studies with MARS code one has to 'attach' to this beam line all the **models of the magnets and collimators**.
- **MMBLB** is a built-in tool that reads in an optical output file in MAD format and builds a 3D model using also additional user-supplied info on transverse structure of our elements.
- ***Source term*** (beam loss spatial distribution) was transferred from STRUCT to MARS. High sensitivity on alignment.

April 21, 2008 SATIF-9, Oak Ridge, TN 11

Fermilab

Outcome

- According to a realistic operational schedule, **annual** number of 8-GeV protons is assumed to be 3.7×10^{20}.
- Given this number, one can determine thickness of the collimators and masks upstream and downstream of the collimators to meet ***safety requirements*** regarding ***surface and groundwater activation*** as well as ***residual activation*** of beam line components and tunnel.
- ***Absorbed dose*** in magnet coils → lifetime of a magnet. Varies with location. Average magnet lifetime is estimated to be 8 yrs.
- ***Marble*** layers are used as a cover for the collimators due to its unique feature of strong suppression of contact residual dose.

April 21, 2008 SATIF-9, Oak Ridge, TN 12

Fermilab

Calculated distribution of absorbed dose (Gy/yr)

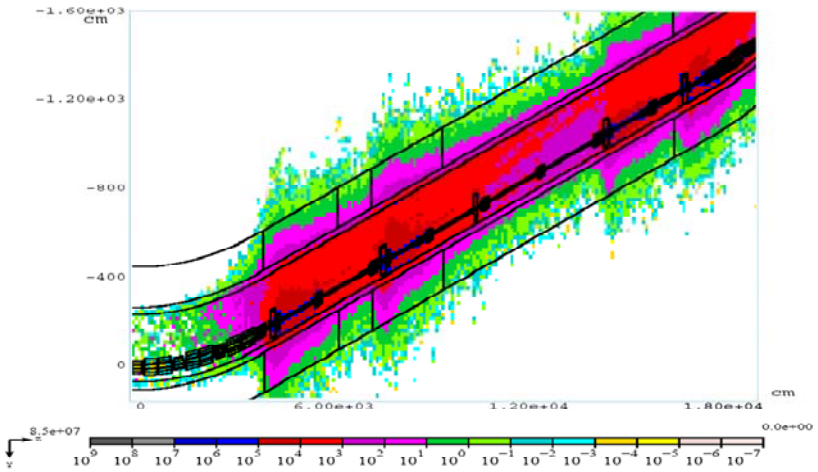

Fermilab

Calculated neutron spectrum ($cm^{-2}s^{-1}GeV^{-1}$) between Q301 and S1 with (red) and w/o (black) mask on upstream face of S1

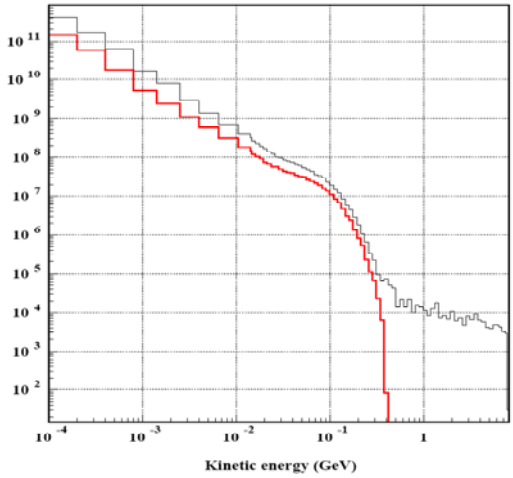

Fermilab

Calculated distribution of contact residual dose rate (mrem/hr) around the shower maximum in the secondary collimator S2

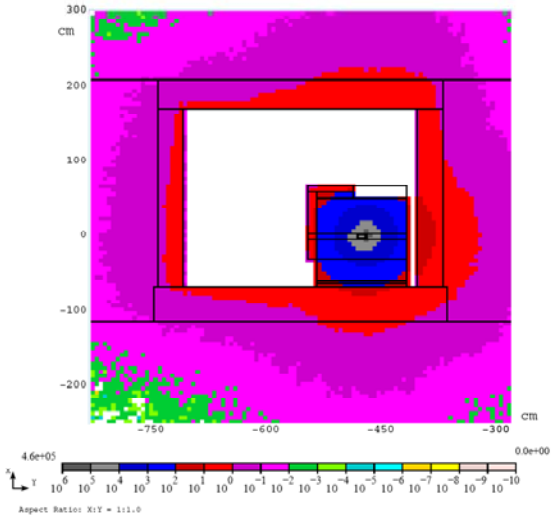

April 21, 2008 SATIF-9, Oak Ridge, TN 15

Fermilab

Conclusions

- The radiation shielding studies were performed for Main Injector Collimation System at Fermilab in order to satisfy safety constraints.
- Designed shielding provides an average magnet lifetime of about 8 years.
- Several predicted hot spots in the region (residual activity) require an extra local shielding, room permitting.
- Comparisons between predicted prompt dose and the 1st measurements performed after commissioning made the head of the MI department happy.

Ω

April 21, 2008 SATIF-9, Oak Ridge, TN 16

IFMIF/EVEDA accelerator nuclear safety issues and nuclear data needs

Philippe Joyer, Valentin Blideanu, Jean-Michel Dumas
CEA/IRFU/Saclay, Gif-sur-Yvette, France

Javier Sanz, Mauricio Garcia, Alicia Mayoral
Universidad National de Educacion a Distancia, Madrid, Spain

Abstract

In the frame of the nuclear fusion broader approach between Japan and Europe, EVEDA is the engineering validation and engineering design phase of the International Fusion Materials Irradiation Facility (IFMIF). In this phase, a prototype accelerator will be built to validate the concepts of the two accelerators of IFMIF.

Preliminary studies have been undertaken to assess safety issues (beam losses, neutron generation, activation, tritium production…). Preliminary calculations have been performed in order to pre-design the EVEDA accelerator vault. With regards to radioprotection issues, neutron source terms have been assessed at beam loss locations all along the accelerator and conservative assumptions have been defined. Depending on acceleration stage, neutron production can be related to both D(d,n)^{3}He reaction and deuteron interaction with various intercepting materials.

The present paper gives preliminary results on neutron transport and shielding calculations in order to verify the compliance with the targeted neutron dose rates outside the vault in accordance with Japanese regulation. In addition, several beam transport configurations have been studied with respect to their specific radiological constraints.

1 Introduction

International fusion materials irradiation facility (IFMIF) is one of the three projects of the fusion broader approach that is an agreement between Japan and the European Union. These three projects are planned to be performed in parallel of ITER project. The objective of IFMIF is to study the behaviour under irradiation of materials and components in conditions close to a nuclear fusion demonstration reactor (DEMO).

Engineering validation and engineering design activities (EVEDA) is the first phase of the IFMIF project and has begun on mid 2007. This phase that will last six years, up to mid 2013, includes in its scope the three main parts of the future IFMIF facility: the accelerator, the target and the test facilities.

A prototype of the accelerator will be built in Japan on Rokkasho-Mura site. The accelerator sub-systems and components will be provided by the European Team. Construction of the building for the prototype accelerator will start in 2008 and commissioning of the accelerator should start by mid-2010. Accelerator prototype will deliver a high power deuteron beam (125 mA @ 9 MeV) as required for IFMIF facility that will operate two deuteron beam lines delivering each 125 mA @40 MeV [1].

In the following sections, after a brief overview of the prototype accelerator, safety issues expected on EVEDA are described. Then methodology of calculations, nuclear reaction models and assumptions used in the calculations are detailed before presentation of the results followed by discussions and needs in nuclear data.

2 IFMIF EVEDA prototype accelerator overview

As shown on Figure 1, the prototype accelerator of IFMIF/EVEDA is composed of four main parts: the injector, the radiofrequency quadrupole (RFQ), the drift tube linac (DTL) and the beam dump.

The injector has to deliver a 140 mA deuteron beam at 100 keV with a high quality and a high reliability. The design of the EVEDA source is based on the SILHI H^+ source (High Intensity Light Ion Source) in Saclay [2].

The radiofrequency quadrupole (RFQ) will bunch and accelerate the deuteron beam from 100 keV to 5 MeV. Then the drift tube linac (DTL) will accelerate the deuterons up to 9 MeV while preserving the emittance and minimising beam halo and beam losses. On EVEDA, the DTL will use the superconducting technology that allows in particular linac length reduction and RF power saving.

Figure 1: Initial drawing of the accelerator prototype

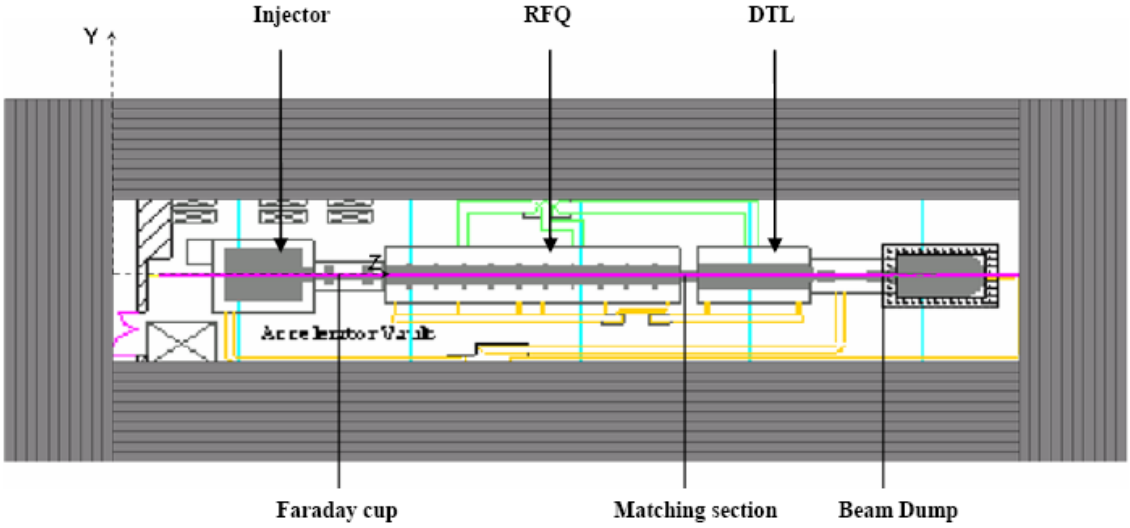

At the end of the beam line, the beam is stopped in the beam dump that will have to remove full power, *i.e.* 1.12 MW or 125 mA at 9 MeV in continuous operation.

3 Safety issues on IFMIF EVEDA prototype accelerator

Neutrons are produced by unfocused deuterons interacting with intercepting materials such as the beam line tube or with previous deuterons implanted in these materials through following typical reactions:

$$D(d,n)^{3}He \quad (1)$$

$$^{65}Cu(d,2n)^{65}Zn \quad (2)$$

The second kind of reactions are (d,Xn), (d,na) or (d,np) reactions with threshold of at least a few MeV, depending on the initial nucleus.

The Figure 2 shows the beam losses expected all along the EVEDA beam line. Main sources of neutron production are:

- The Faraday cup of the low energy beam transport (LEBT) line used for source commissioning or testing. In this Faraday cup, the entire beam coming from the injector will be intercepted.
- The matching section (MS) located between the radiofrequency quadrupole (RFQ) and the drift tube linac (DTL). The matching section is a collimator in normal conditions. Intercepting diagnostics may also be implemented in pulsed operation (low duty cycle). A maximum of 0.1% of the beam coming from the RFQ is expected to be lost and to interact with materials.
- The beam dump at the end of the line where the total power (1.12 MW) of the beam is stopped.

In the other parts of the beam line (RFQ, DTL and high energy beam transport) the beam losses have been assessed much lower. So only the three main sources mentioned above will be taken into account in the preliminary calculations for the design of the building.

Figure 2: Beam losses along the EVEDA beam line

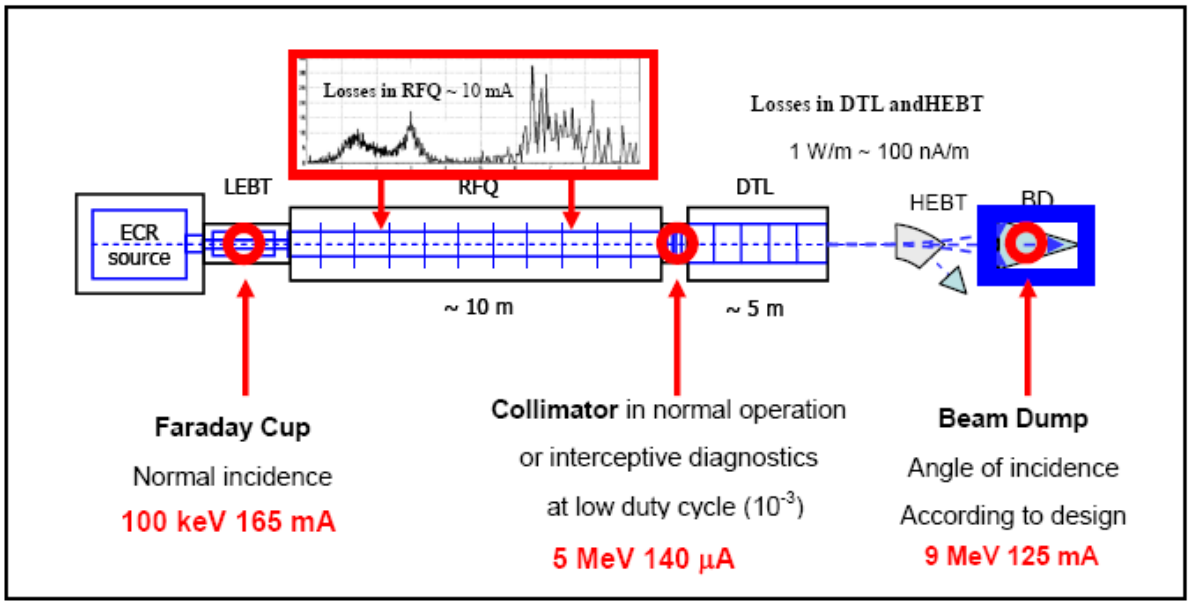

The generation of neutrons will induce:

- high neutron and gamma dose rates during accelerator operation;
- gamma dose rates when beam is off due to activation of all materials inside the accelerator vault;
- tritium production through $D(d,p)^{3}H$ reactions on deuterium implanted in materials;
- other nuclides such as ^{41}Ar in air or corrosion products in water cooling systems.

Figure 3: Comparison of calculated and experimental data for $^{58}Ni(d,n)^{59}Cu$ cross-section

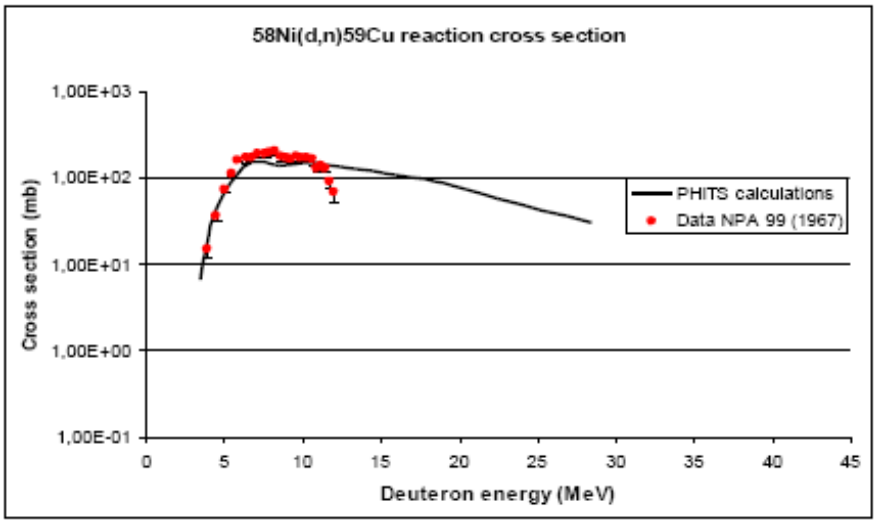

Figure 4: Comparison of calculated and experimental data for $^{65}Cu(d,2n)^{65}Zn$ cross-section

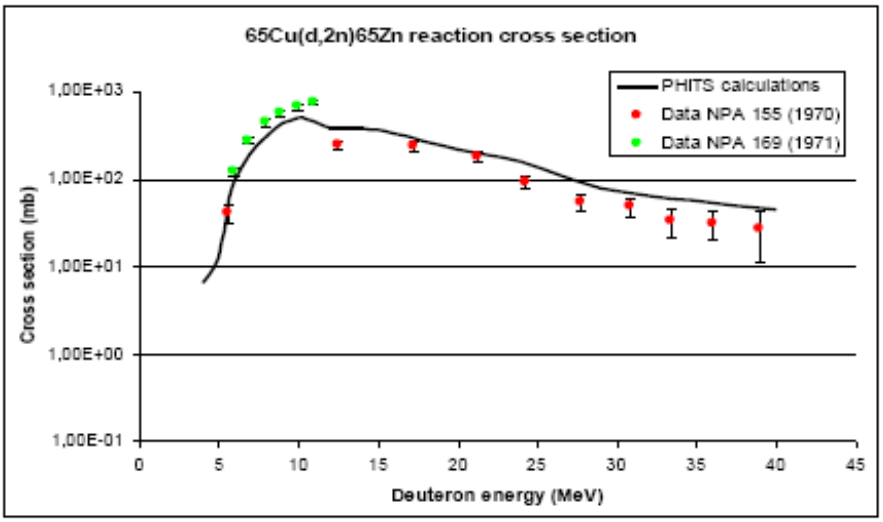

4 Calculations

4.1 Methodology

Calculations have been performed into two steps.

In the first one, PHITS [3] and MCNPX [4] codes have been used for 3-D transport of particles in order to assess neutron and gamma fluxes and prompt doses. An accurate 3-D geometry description and a basic material composition for flux attenuation are required. The main issue in this step is the validation of cross-section libraries and of nuclear reaction models.

In the second step, induced activity is calculated here with Cinder'90 and DChain-SP codes to assess specific activities and residual gamma dose rates from the different materials. This step requires an accurate composition of the different materials irradiated during operation and an operating history of the facility. The activation code ACAB [5] is also considered to be used in this kind of calculations.

4.2 Nuclear reaction models

In PHITS transport code, quantum molecular dynamic (QMD) model is used for fast stage of reaction and generalised evaporation model (GEM) is used for evaporation and fission stage.

Comparisons of calculated cross-sections with experimental data are shown for typical reactions, (d,n) reactions on Figure 3 and (d,2n) reactions on Figure 4.

A good agreement is observed with PHITS models for materials such as Cu, Ni, Zn or Fe for primary reactions such as (d,Xn) reactions as well as for secondary reactions such as (d,p) or (p,n) reactions. Contributions for all kind of materials from primary reactions is approximately 50% for (d,n) reactions and 20% for (d,2n) reactions.

4.3 Assumptions

In the preliminary design (Figure 1) taken for preliminary calculations, the beam line is supposed to be a straight line centred in the vault. The vault is 38 m long, 8 m wide and 7 m high.

The dose rate objective outside the vault is 12.5 μSv/h according to the Japanese law.

In the calculations, the neutron source in the Faraday cup is assumed to be a point source. Due to the 100 keV energy of deuterons at the end of the injector, neutrons are only produced through d-d reaction on copper which is the material of the Faraday cup.

The matching section is modellised as a cylindrical disk made of copper. Its size is 1 cm thick and 3 cm in diameter.

The beam dump is at present time assumed to be a conical cartridge made of nickel surrounded by a cylindrical stainless steel water tank. The length of the cartridge is 2.5 m long and the aperture of the cone is 20 cm in diameter. The tank is a 3 m long cylinder with a 1 m diameter.

Figure 5: Neutron source from deuteron induced reaction on Ni of the beam dump

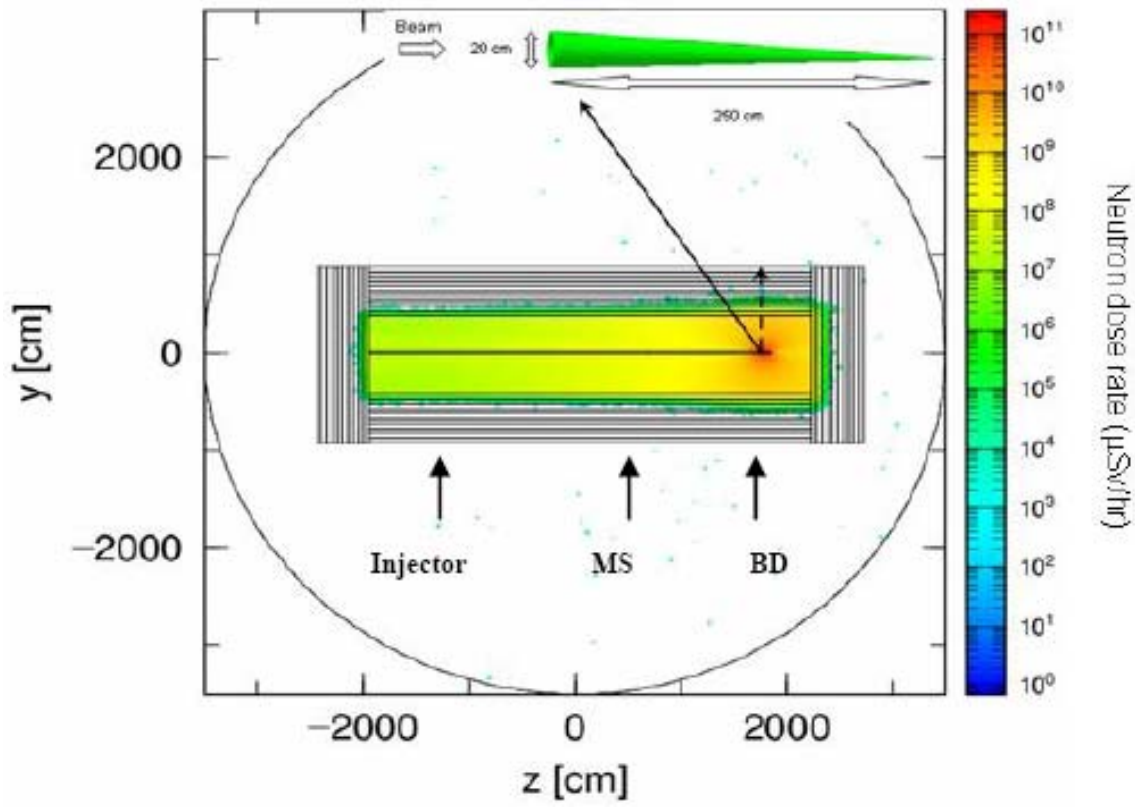

5 Results and discussions

5.1 Calculation results

Calculations have been performed for the three main sources identified in Section 3 (see Figure 2).

For the matching section and the beam dump, reaction cross-sections and angle and energy distributions have been calculated in PHITS code as mentioned in Section 3. In the injector case, the angle and energy distributions come from nuclear data tables [6]. At the entrance of the beam dump, the spatial distribution of the beam has a Gaussian shape with a FWHM around 15 cm.

Figure 5 shows the results obtained for the main neutron source produced in the beam dump. These results show that the three main neutron sources can be considered strictly independently from each other.

5.2 Benchmark

Neutron dose rate attenuation has been benchmarked between the two European home-teams involved in safety and radioprotection activities for EVEDA phase: CEA (France) and UNED (Spain).

The cross-check has been made through two independent calculations using PHITS for CEA and MCNPX (with neutron production cross-sections from nuclear interactions of deuterons with copper and nickel taken from EAF-2007 [7]) for UNED. In the injector case for d-d nuclear interactions, nuclear data tables [3] are used in CEA and cross-section data provided by the DROSG-2000/NEUYIE code [8] in UNED. The table 1 gives the number of calculated neutron per incident deuteron for each main source. A good agreement is obtained for these neutron yields (less than 30%).

Table 1: Calculated neutron yield per incident deuteron

Neutron source term	CIEMAT-UNED	CEA
Injector (d-d on Cu)	8.2E-09 n/d	6.0E-09 n/d
Matching section Cu(d,Xn) at 5 MeV	4.3E-05 n/d	3.1E-05 n/d
Beam dump Ni(d,Xn) at 9 MeV	2.5E-04 n/d	2.1E-04 n/d

Figure 6 shows the results of the crosscheck on dose rate attenuation and a good agreement is also observed for each main source term.

Figure 6: Cross-check UNED/CEA on neutron dose rate attenuation

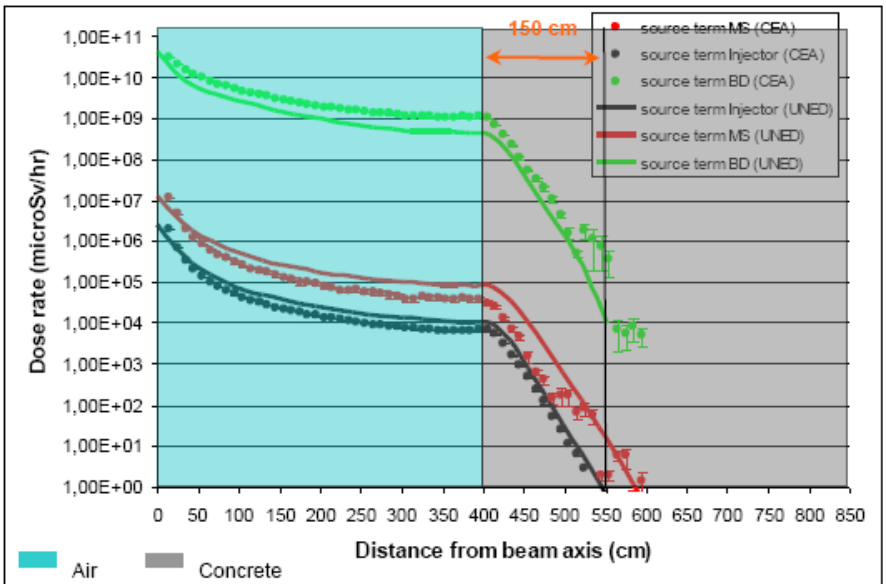

5.3 Present design of the building

Preliminary calculations have been used to improve the design of the building to take into account the commissioning phase and maintenance purposes. The beam line has then been shifted on the left side of the vault to keep space on the other side as shown on Figure 7.

Figure 7: Present design of the building

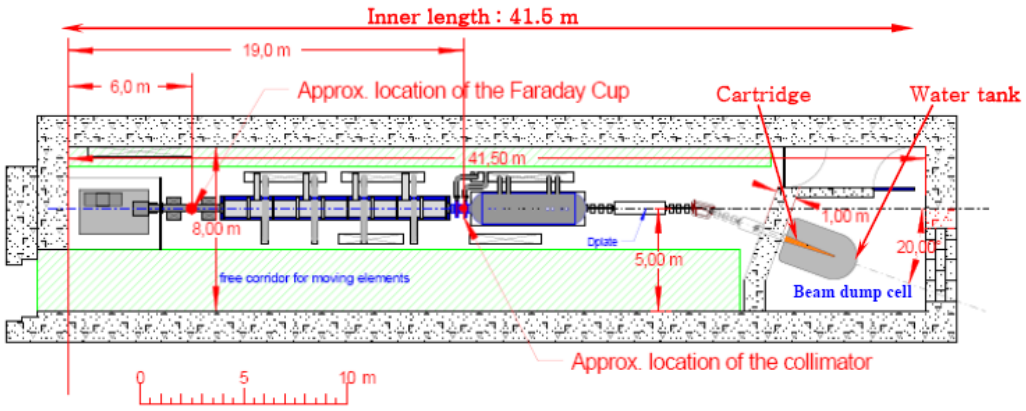

The beam line has also been tilted with an angle of 20 degrees before the high energy beam line transport for building size limitation knowing that the length has been increased from 38 m to 41.5 m and for space sparing near the beam dump.

The beam dump area is not yet frozen. Two options are still possible: a dedicated cell as drawn on Figure 7 or a concrete shielding close to the water tank.

The wall of the vault will be made of normal concrete (density = 2.1 g/cm^3). The thickness has been set to 1.50 metre to comply with the targeted dose rate outside the vault (12 µSv/h), assuming a minimum hydrogen content of 0.56% in ordinary concrete.

5.4 Beam dump and beam dump area

The main next safety issue on EVEDA prototype accelerator facility is the design of a high power beam dump (1.12 MW) able to remove power in any operational conditions, *i.e.* normal operations including continuous operation of the beam and non continuous operation with transient power increase coupled with abnormal conditions of operation.

The beam dump will be highly activated. At present time, the cartridge is planned to be made of nickel. Gamma dose rates higher than 500 µSv/h are expected near the cartridge alone after 1 day irradiation and 10 days cooling. The addition of a 1 m stainless steel water tank around the cartridge reduces the dose rates near the water tank to 80 µSv/h after 1 day irradiation and 1 day cooling.

High gamma dose rates are also expected in the high energy beam transport area when beam is off and have to be taken into account in the design of these components mainly for their maintenance.

The beam dump area has to be decided and is strongly dependent on the need to replace the cartridge of the beam dump.

5.5 Nuclear data needs

Experimental nuclear data are desirable in order to:

- improve our understanding on deuteron implantation in materials;
- accurately describe the neutron sources for radioprotection studies.

Such data will be useful to perform “less conservative” calculations and for extension calculations to higher energies up to 40 MeV in IFMIF.

An experimental campaign is planned at Saclay on the SILHI source during spring 2008 in order to perform systematic experiments as function of incident energy and different stopping material. SILHI source allows:

- a deuteron beam intensity of 25 mA;
- several deuteron energies: 40, 70, 100 keV;
- irradiation of different samples: C, Ni, Cu, Ta, W and stainless steel.

The objective of the experiments planned is to perform the following measurements:

- During beam operation:
  - energy and angular neutron distribution measurements;
  - prompt dose measurements.
- When beam is off:
  - measurements of profile and density of deuterons implanted in the different materials;
  - material activation measurements through gamma spectroscopy;
  - tritium behaviour (migration to cooling water).

For future calculations, a study on cross-sections is also planned at the end of the present year in order to:

- identify available experimental data;
- validate models used in the codes.

6 Conclusions

Safety issues have been identified for IFMIF/EVEDA prototype accelerator.

Preliminary calculations have shown that the three main neutron sources resulting from specific beam losses can be taken independently into account. Due to these main sources, the thickness of the wall of the building has been set to 1.5 metre of normal concrete with a minimum hydrogen content of 0.56%. This content comes from the experience feedback of nuclear facilities in Japan.

The beam dump is the next important issue regarding safety and radioprotection purposes. It will be the most activated and irradiated component in IFMIF/EVEDA and it has to remove a high power of 1.12 MW.

Finally, a better understanding of deuterium implantation in materials and of the associated neutron source is required. An experimental campaign is planned at Saclay on SILHI facility during spring 2008.

References

[1] *IFMIF Comprehensive Design Report*.

[2] R. Gobin, *et al.*, "A 140 mA CW Deuteron ECR Source for the IFMIF-EVEDA Project", *Review of Scientific Instruments*, 79, 02B303 (2008).

[3] H. Iwase, *et al.*, *Nucl. Instr. Meth. Phys. Res. B,* 183 (2001) 374.

[4] J.S. Hendricks, *et al.*, *MCNPX Extensions Version* 2.5.0, LA-UR-05-2675.

[5] J. San, *ACAB: Activation Code for Fusion Applications: User's Manual* V5.0, Lawrence Livermore National Laboratory, UCRL-MA-143238 (February 2000).

[6] H. Liskien, A. Paulsen, *Nuclear Data Tables* 11, 569-619 (1973).

[7] R.A. Forrest. J. Kopecky, J-Ch. Sublet, "The European Activation File: EAF-2007 Deuteron- and Proton-induced Cross Section Libraries", *UKAEA FUS* 536, March 2007.

[8] M. Drosg, *Neutron Source Reactions,* DROSG-2000/NEUYIE, Institute for Experimental Physics, University of Vienna, Austria.

Design of the shielding of the Materials Test Station

G. Muhrer, M. Wilson, Ch. Kelsey, E. Pitcher
Los Alamos National Laboratory, USA

Outlook

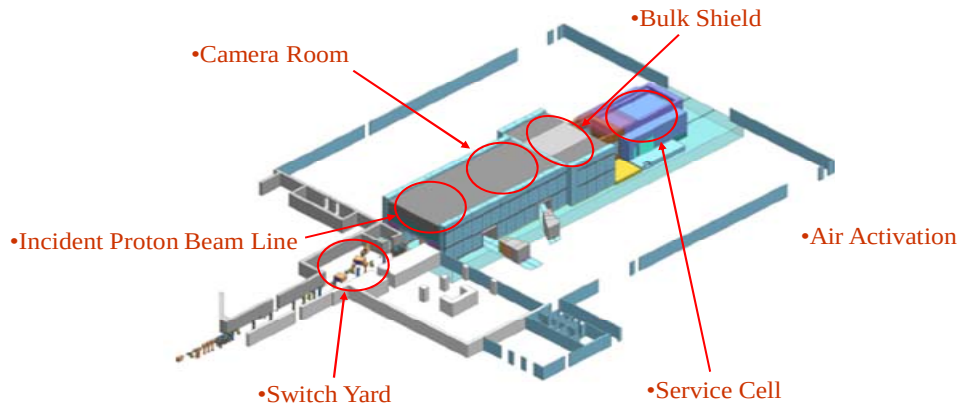

Los Alamos NATIONAL LABORATORY EST.1943

Operated by the Los Alamos National Security, LLC for the DOE/NNSA

LUJAN CENTER

NNSA

Shielding criteria

- Incident Proton Beamline:
  - normal: 1 nA/m, less than 0.25 mrem/h at the external shield surface.
  - off normal: full power (2MW), point spill on a thick target for one hour resulting in less than 5 rem exposure.
- Target:
  - normal: full power (2MW), less than 0.25 mrem/h at the external shield surface.
  - (off normal: full power (2MW), for one hour resulting in less than 5 rem.)
- Off-side
  - Total consequence for the public from air activation for the entire Los Alamos National Laboratory shall be less than 10 mrem/year

Los Alamos NATIONAL LABORATORY EST.1943
Operated by the Los Alamos National Security, LLC for the DOE/NNSA
LUJAN CENTER
NNSA

Methods: Moyer Model

Moyer Model:

$$H = I * H_0(E_p)/r^2 * e^{-\beta\theta} * e^{-d/\lambda}$$

- $H_0(E_p=800\ \text{MeV}) = 532.3\ \text{rem}\ h^{-1}\ m^2\ nA^{-1}$ = source term*
- r = distance from the spill point to the detector
- $\beta = 2.3/\text{radian}$*
- d = shielding thickness
- λ = dose attenuation length in the shielding material
- θ = angle between the proton beam and the direction from the spill to the detector

*Thomas and Thomas, Health Physics **46**, 954 (1984)

Los Alamos NATIONAL LABORATORY EST.1943
Operated by the Los Alamos National Security, LLC for the DOE/NNSA
LUJAN CENTER
NNSA

Incident Proton Beam Line Shield (1): criteria, results

- criteria:
  - –normal: 1 nA/m, less than 0.25 mrem/h at the external shield surface.
  - –off normal: full power (2MW), point spill on a thick target for one hour resulting in less than 5 rem exposure.

Table 1: Incident proton beamline shield thicknesses.

Steel (green blocks)	reg. concrete	concrete blocks
52"	122"	3x36"+1x18”=126"
78"	60"	2x36"=72"
104"	0"	1x18"=18"

Los Alamos NATIONAL LABORATORY EST.1943
Operated by the Los Alamos National Security, LLC for the DOE/NNSA
LUJAN CENTER
NNSA

Incident Proton Beam Line Shield (2): layout

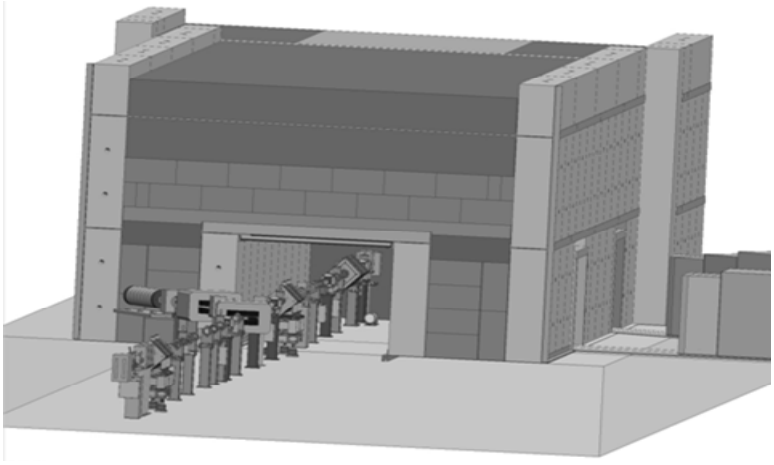

Los Alamos NATIONAL LABORATORY EST.1943
Operated by the Los Alamos National Security, LLC for the DOE/NNSA
LUJAN CENTER
NNSA

Materials test station geometry

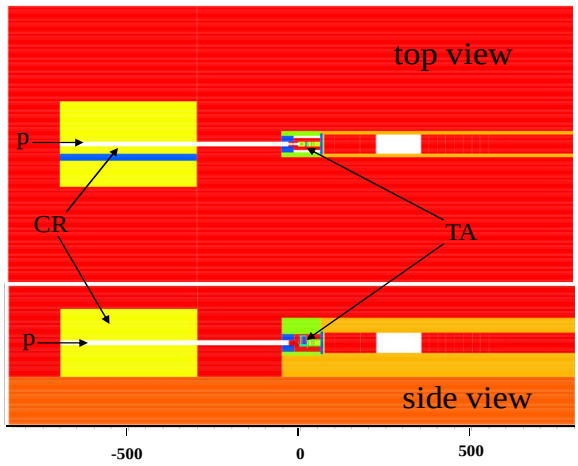

CR: camera room; TA: target assembly; p: incident proton beam

Los Alamos NATIONAL LABORATORY EST.1943
Operated by the Los Alamos National Security, LLC for the DOE/NNSA
LUJAN CENTER
NNSA

Beam pipe dose levels

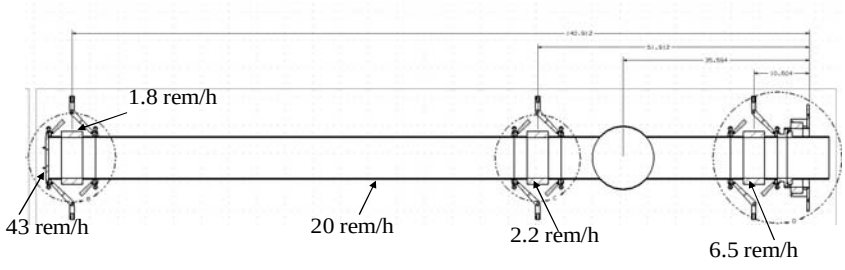

Los Alamos NATIONAL LABORATORY EST.1943
Operated by the Los Alamos National Security, LLC for the DOE/NNSA
LUJAN CENTER
NNSA

Camera room geometry

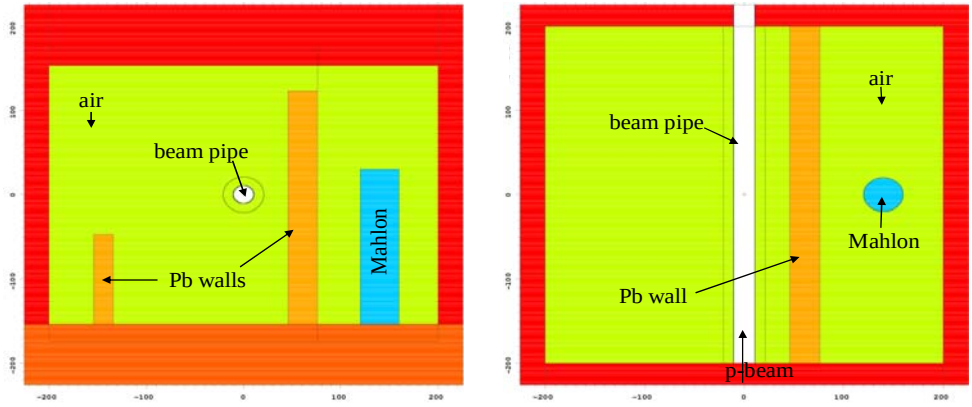

Los Alamos NATIONAL LABORATORY EST.1943

Operated by the Los Alamos National Security, LLC for the DOE/NNSA

LUJAN CENTER

NNSA

Beam pipe and shadow shield wall activation

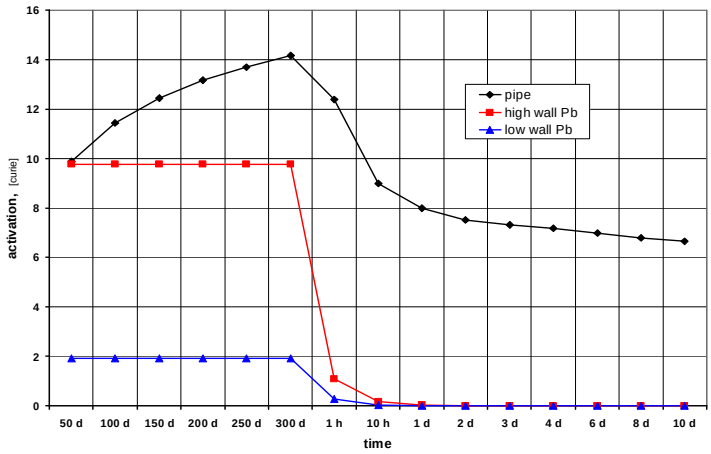

Los Alamos NATIONAL LABORATORY EST.1943

Operated by the Los Alamos National Security, LLC for the DOE/NNSA

LUJAN CENTER

NNSA

Effectiveness of the shadow shield

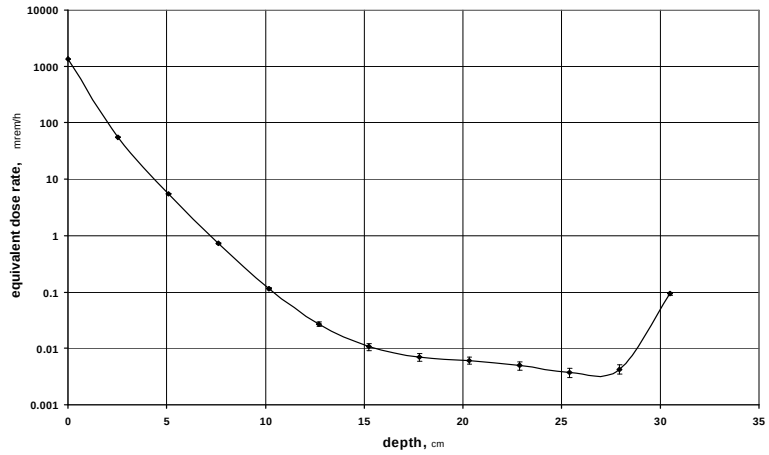

Los Alamos NATIONAL LABORATORY EST.1943

Operated by the Los Alamos National Security, LLC for the DOE/NNSA

LUJAN CENTER

NNSA

Neutron flux in the camera room

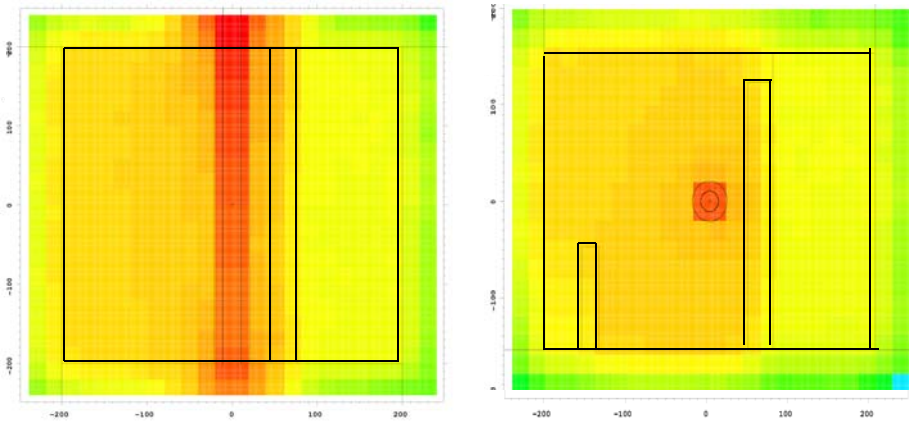

10^4 n/(cm^2,s) 10^5 n/(cm^2,s) 10^6 n/(cm^2,s) 10^7 n/(cm^2,s) 10^8 n/(cm^2,s)

Los Alamos NATIONAL LABORATORY EST.1943

Operated by the Los Alamos National Security, LLC for the DOE/NNSA

LUJAN CENTER

NNSA

Ceiling/wall/floor shine

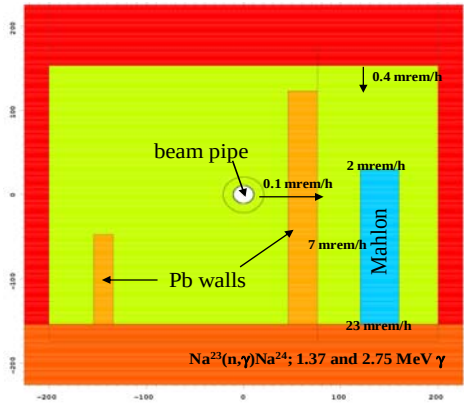

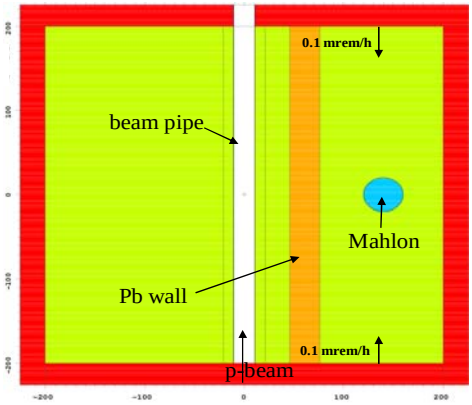

Los Alamos NATIONAL LABORATORY EST.1943

Operated by the Los Alamos National Security, LLC for the DOE/NNSA

LUJAN CENTER

NNSA

Bulk shield of the spallation target (1): criteria, method

- criteria:
  - –normal: full power (2MW), less than 0.25 mrem/h at the external shield surface.
  - –off normal: full power (2MW), for one hour resulting in less than 5 rem.

method:

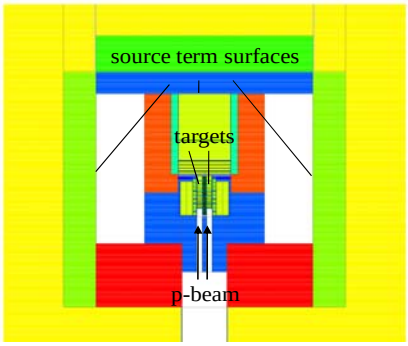

Los Alamos NATIONAL LABORATORY EST.1943

Operated by the Los Alamos National Security, LLC for the DOE/NNSA

LUJAN CENTER

NNSA

Bulk shield of the spallation target (2):results

Table 2: Material Test Station Bulk Shield Thickness

target area	He-tank (Fe)	total steel thickness	reg. concrete	concrete blocks
0.5m	3.15m	3.15m+26”=3.81m	1.14m	1x36”+1x18”=1.37m
0.5m	3.15m	3.15m+52”=4.47m	0.0m	1x18’=0.46m
0.5m	3.15m	13’ 3”=4.04m	0.91m	1x36”=0.91m
0.5m	3.15m	14’=4.27m	0.08m	1x18”=0.46m

Los Alamos NATIONAL LABORATORY EST.1943
Operated by the Los Alamos National Security, LLC for the DOE/NNSA
LUJAN CENTER
NNSA

Neutron flux in the camera room

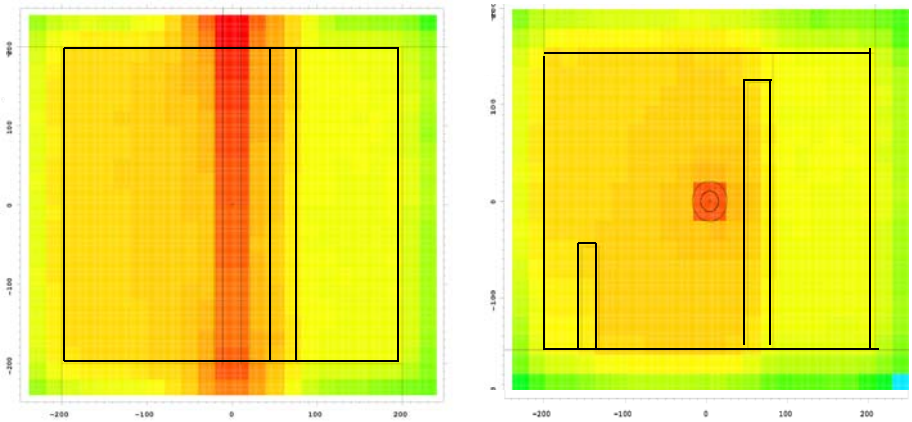

10^4 n/(cm^2,s) 10^5 n/(cm^2,s) 10^6 n/(cm^2,s) 10^7 n/(cm^2,s) 10^8 n/(cm^2,s)

Los Alamos NATIONAL LABORATORY EST.1943
Operated by the Los Alamos National Security, LLC for the DOE/NNSA
LUJAN CENTER
NNSA

Air activation(1): inside the camera room

Immediately after shutdown:

Isotope	CEDE*BR+CSDE [rem/Ci*m^3/s]	activity [Bq]	dose [mrem/h]
H^3	2.22E-02	1.75E+06	0.08
N^{13}	1.81E-01	7.28E+06	2.86
C^{14}	7.24E-01	1.19E+06	1.86
O^{15}	1.82E-01	9.71E+04	0.04
S^{35}	8.59E-01	3.25E+03	0.01
Ar^{37}	4.70E-07	2.46E+05	0.00
Cl^{38}	3.32E-01	7.68E+03	0.01
Cl^{39}	3.05E-01	7.28E+04	0.05
Ar^{39}	3.37E-05	1.27E+03	0.00
Ar^{41}	2.41E-01	1.01E+07	5.24
Kr^{83m}	5.55E-06	5.48E+03	0.00
total		2.07E+07	10.14

1 day after shutdown:

Isotope	CEDE*BR+CSDE [rem/Ci*m^3/s]	activity [Bq]	dose [mrem/h]
H^3	2.22E-02	1.75E+06	0.08
C^{14}	7.24E-01	1.19E+06	1.86
Ar^{37}	4.70E-07	2.41E+05	0.00
total		3.18E+06	1.95

Los Alamos NATIONAL LABORATORY EST.1943

Operated by the Los Alamos National Security, LLC for the DOE/NNSA

LUJAN CENTER

NNSA

Air activation(2): side boundary

Isotope	CEDE*BR+CSDE [rem/Ci*m^3/s]	production rate [Bq/s]	dose [mrem/year]
H^3	2.22E-02	3.11E-03	0.00
N^{13}	1.81E-01	8.45E+03	0.52
C^{14}	7.24E-01	4.58E-06	0.00
O^{15}	1.82E-01	5.52E+02	0.03
S^{35}	8.59E-01	2.98E-04	0.00
Ar^{37}	4.70E-07	5.64E-02	0.00
Cl^{38}	3.32E-01	2.39E+00	0.00
Cl^{39}	3.05E-01	1.51E+01	0.00
Ar^{39}	3.37E-05	1.03E-07	0.00
Ar^{41}	2.41E-01	1.06E+03	0.09
Kr^{83m}	5.55E-06	5.77E-01	0.00
total			0.64

Los Alamos NATIONAL LABORATORY EST.1943

Operated by the Los Alamos National Security, LLC for the DOE/NNSA

LUJAN CENTER

NNSA

Air activation (3): criterion, method

- Off-side criterion:
  - Total consequence for the public from air activation for the entire Los Alamos National Laboratory shall be less than 10 mrem/year

method:

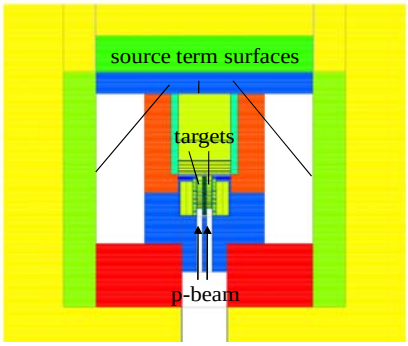

Los Alamos NATIONAL LABORATORY EST.1943
Operated by the Los Alamos National Security, LLC for the DOE/NNSA
LUJAN CENTER
NNSA

Air activation (4): attenuation length

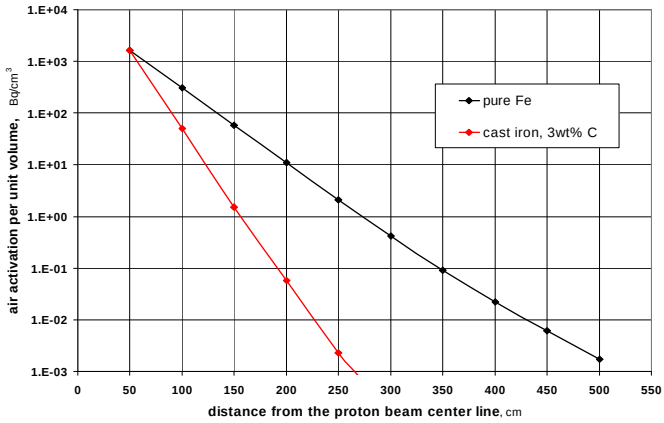

λ_{Cl} = 15cm λ_{Fe} = 30cm

Los Alamos NATIONAL LABORATORY EST.1943
Operated by the Los Alamos National Security, LLC for the DOE/NNSA
LUJAN CENTER
NNSA

Air activation (5): isotopes

Isotope	Contribution
H^{3}	0.4%
C^{14}	5.2%
N^{13}	1.8%
N^{16}	2.0%
O^{19}	0.7%
Ar^{37}	1.8%
Ar^{41}	86.8%
Kr^{83}	0.8%

Los Alamos NATIONAL LABORATORY EST.1943
Operated by the Los Alamos National Security, LLC for the DOE/NNSA
LUJAN CENTER
NNSA

Air activation (6): geometry

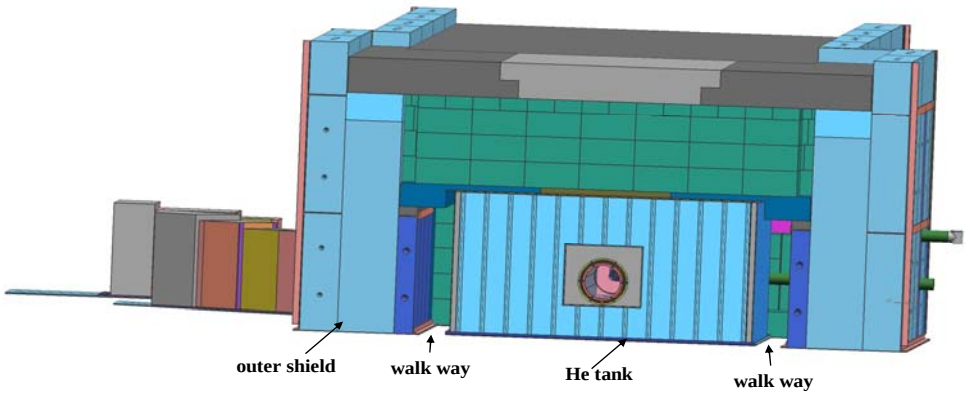

Los Alamos NATIONAL LABORATORY EST.1943
Operated by the Los Alamos National Security, LLC for the DOE/NNSA
LUJAN CENTER
NNSA

Air activation (7): inside the shielding

walk way: $A_{T1} = 4\pi r_1^2 A_o e^{-\lambda(r_1 - r_0)} d$ total activity: $4.8 \cdot 10^6$ Bq (Fe)

$1.25 \cdot 10^2$ Bq (CI)

outer shield:

$$A_{T2} = 4\pi c A_0 \frac{r_1^2}{r_2^2} e^{\lambda(r_0+d)} \left\{ e^{-\lambda r_2} \left[\frac{r_2^2}{\lambda} + \frac{2r_2}{\lambda^2} + \frac{2}{\lambda^3} \right] - e^{-\lambda r_3} \left[\frac{r_3^2}{\lambda} + \frac{2r_3}{\lambda^2} + \frac{2}{\lambda^3} \right] \right\}$$

total activity: $1.35 \cdot 10^5$ Bq (Fe)

1.67 Bq (CI)

$A_0 = 1640 \frac{\text{Bq}}{\text{cm}^3}$ $r_0 = 50$ cm $r_1 = 365$ cm $r_2 = 425$ cm $r_3 = 537$ cm

Dose to a person at the outer surface of the shielding: 6.3 mrem/year (Fe)

0.2 µrem/year (CI)

Air activation (8): in Area A/at the side boundary

In Area A: $A_{T3} = 4\pi r_3^2 A_o \frac{r_1^2}{r_2^2} e^{-\lambda(r_3 - r_0 - d)} d_{Area\ A}$

Total activity: $1.6 \cdot 10^7$ Bq (Fe)

9.4 Bq (CI)

Submerged cloud : $D_t = \sum_i \chi_i \cdot (CEDE_i \cdot BR + CSDE_i)$

Dose to the worker: 1.1 mrem/year (Fe)

0.6 nrem/year (CI)

Dose at the side boundary:

$$D = \int \chi/Q(\vec{r}) \cdot \sum_i Q_i(\vec{r}) \cdot (CEDE_i \cdot BR + CSDE_i) d\vec{r}$$

$\Rightarrow$**40 µrem/year (Fe)**

0.2 nrem/year (CI)

Service cell

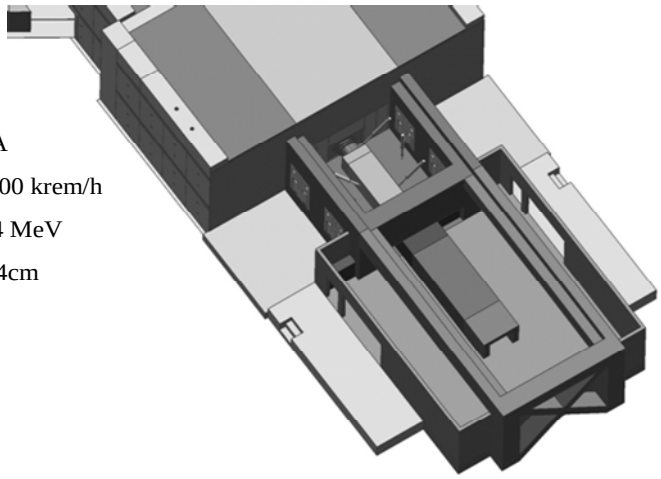

1.5 years @ 2.5 mA

activity: 10^{17} Bq; 100 krem/h

average energy: 0.4 MeV

regular concrete: 94cm

lead glass: 57cm

Los Alamos NATIONAL LABORATORY EST.1943

Operated by the Los Alamos National Security, LLC for the DOE/NNSA

LUJAN CENTER

NNSA

Switch yard (1): geometry

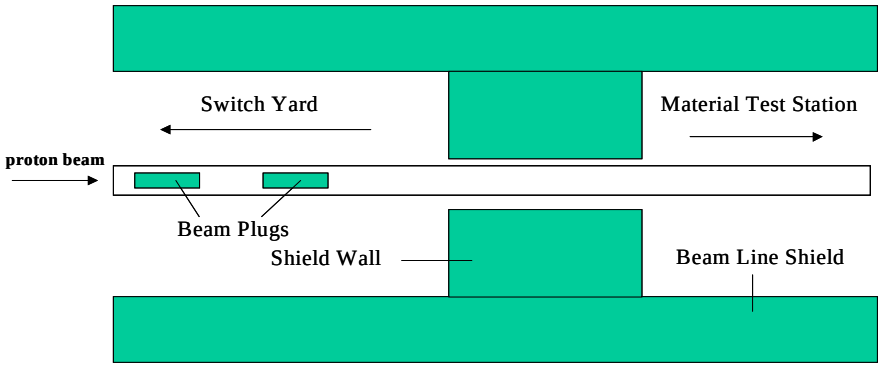

Los Alamos NATIONAL LABORATORY EST.1943

Operated by the Los Alamos National Security, LLC for the DOE/NNSA

LUJAN CENTER

NNSA

Switch yard (2): results

reg. Concrete			reg. Concrete/Fe		
H	4.2641	rem/h	H	4.71256	rem/h
I	2.50E+06	nA	I	2.50E+06	nA
H_0	532.3	rem/h m^2/nA	H_0	532.3	rem/h m^2/nA
r	15.86	meter	r	20.41	meter
R	22.86	meter	R	22.86	meter
β	2.3	$radian^{-1}$	β	2.3	$radian^{-1}$
θ	0	radian	θ	0	radian
d	7	meter	d	2.45	meter
λ	0.526316	meter	λ	0.2	meter

Los Alamos NATIONAL LABORATORY EST.1943
Operated by the Los Alamos National Security, LLC for the DOE/NNSA
LUJAN CENTER
NNSA

Conclusion

We have presented in the design criteria, shield thicknesses and material combinations to allow the engineers to utilize and reuse as much of the shielding material currently in stock at the Los Alamos Neutron Science Center. If implemented successfully this will lower the necessary budget for the construction of the Materials Test Station by a significant amount.

Los Alamos NATIONAL LABORATORY EST.1943
Operated by the Los Alamos National Security, LLC for the DOE/NNSA
LUJAN CENTER
NNSA

Benchmark neutron experiments using quasi-monoenergetic p-Li neutron sources of 140 to 392 MeV at RCNP, Osaka University

Takashi Nakamura, *et al.*
Tohoku University, Shimizu Corp.

Contents

- 1) Establishment of p-Li quasi-monoenergetic neutron field
- 2) Energy response measurements of NE213 scintillator
- 3) Neutron spectra from thick targets of C, Al, Fe and Pb at 0 and 90 degrees
- 4) Neutron shielding experiments through concrete and iron

Experimental facility

The experiments at the ring cyclotron facility at RCNP (Research Center of Nuclear Physics), Osaka University

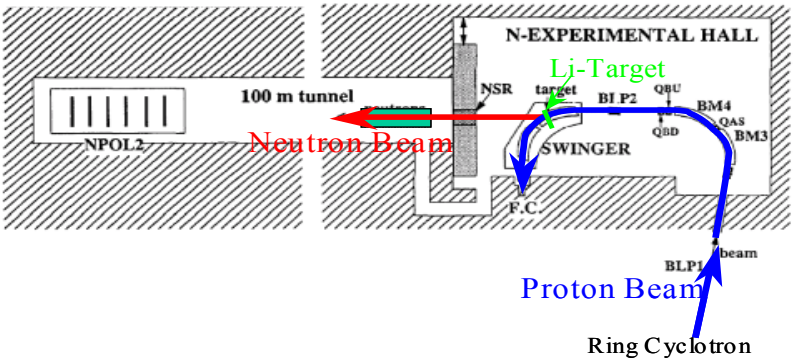

Neutron Experimental Hall and TOF room of RCNP, Osaka Univ., Japan

H. Sakai, H. Okamura, H. Otsu, T. Wakasa and S. Ishida, "Facility for the (p,n) polarization transfer measurement," *Nucl. Instrum. and Meth. in Phys. Res. Sec. A*, vol.369, pp.120-134, (1996).

TOF tunnel

95 m between detector and surface of the target

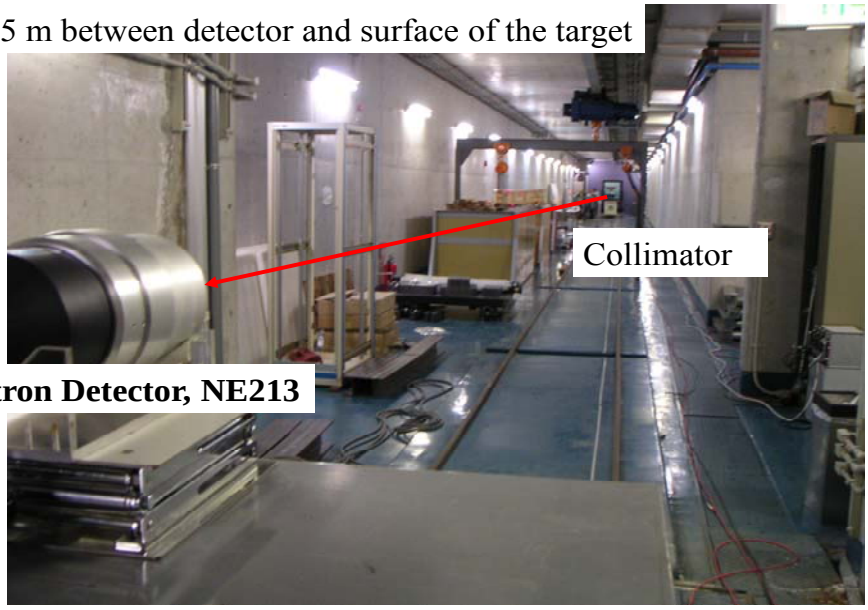

Experimental setup

The neutron TOF course of the RCNP

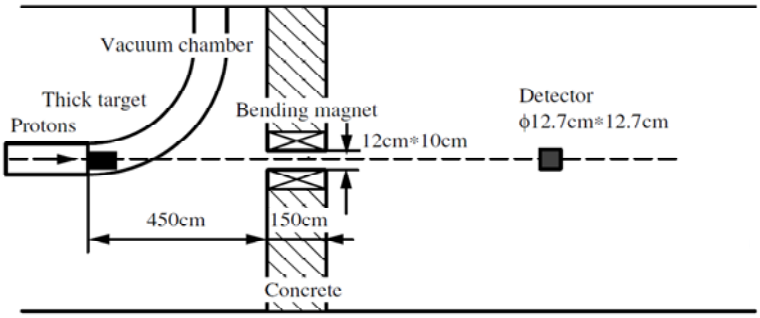

Protons:	140, 250 and 350 MeV
Angle:	0 degree
Beam current:	~20 nA
Flight path:	11.4 m and 60.0 m for 140 MeV proton
	11.4 m and 67.8 m for 250MeV proton
	11.4 m and 95.0 m for 350MeV proton

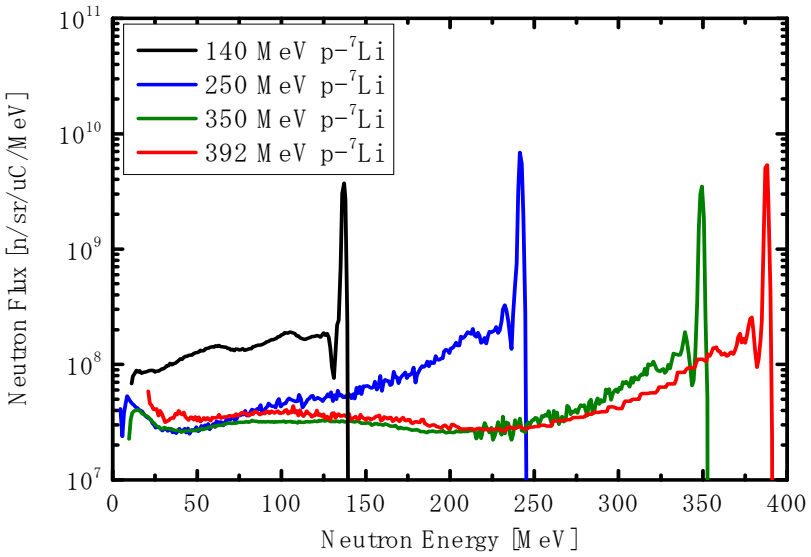

S. Taniguchi et al., Rad., Prot. Dosim., 126, 23 (2007) and M. Hagiwara et al., The ICRS-11 conference

Physical characteristics of p-Li neutron field at RCNP, Osaka Univ.

Proton energy [MeV]	140	250	350	392
Peak neutron energy [MeV]	137	248	348	390
Energy range of peak neutron [MeV]	135-140	236-250	344-350	383-392
Peak neutron intensity [n sr^{-1} μC^{-1}]	1.04×10^{10}	1.94×10^{10}	1.07×10^{10}	1.50×10^{10}
FWHM of peak neutron [MeV]	2.9	2.5	2.5	2.5
Energy range of tail neutron [MeV]	10-135	4-236	6-344	21-383
Tail neutron intensity [n sr^{-1} μC^{-1}]	1.70×10^{10}	1.70×10^{10}	1.35×10^{10}	1.76×10^{10}

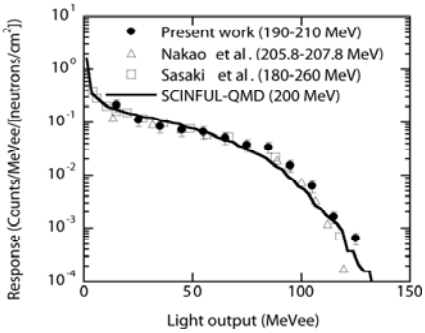

Measured response function of BC501A liquid organic scintillator for neutrons of 190-210 MeV. Other experimental data obtained by Nakao et al. and Sasaki et al. were for neutrons of 205.8-207.8 and 180-260 MeV, respectively. The calculation by SCINFUL-QMD was performed for incident neutrons of 200 MeV by D. Satoh et al., J. Nucl. Sci. Technol., 43, 714 (2006)

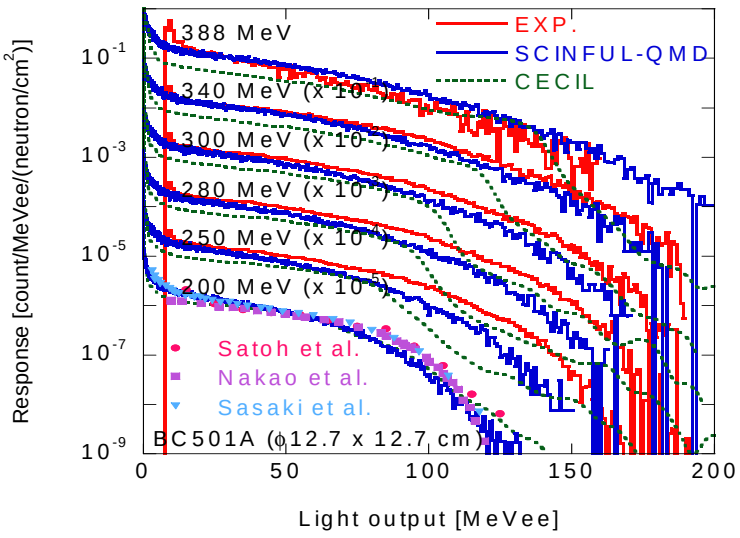

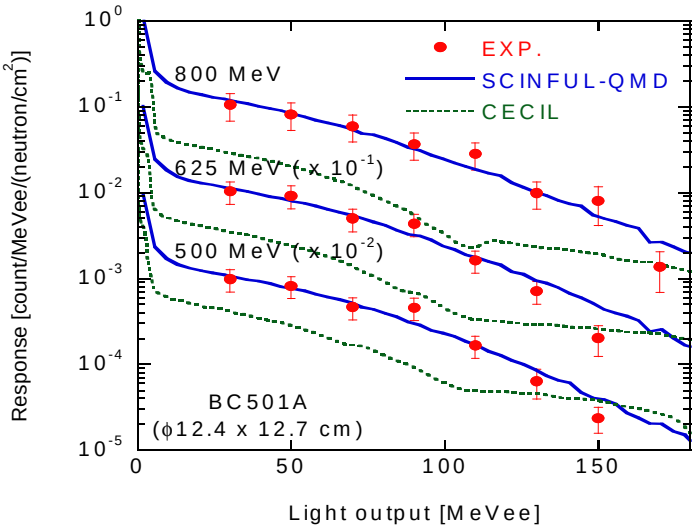

Response functions for neutrons of 500, 625, 800 MeV compared with the SCINFUL-QMD and CECIL calculations. The bin width of incident-neutron energies For the experimental data was ±10 MeV (except for 800-MeV neutrons, its width was 750-810 MeV). Monoenergetic neutrons were used in the calculations.

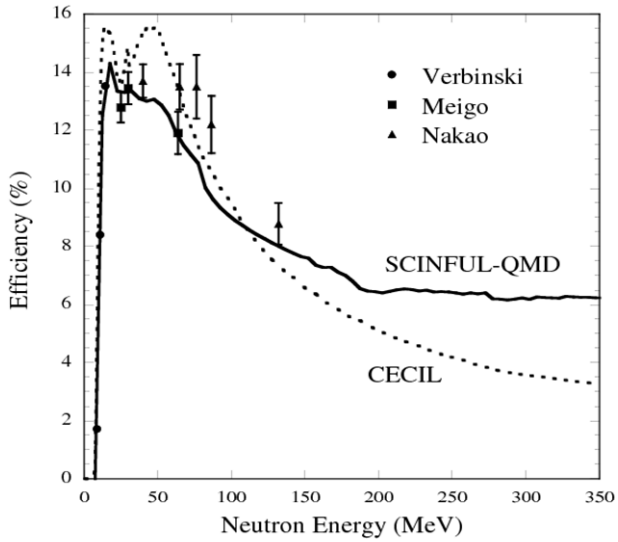

Comparison of CECIL and SCINFUL-QMD codes with experiments
D. Satoh et al., J. Nucl. Sci. Technol., 43, 714 (2006)

Thick target neutron yields at 0 degree for 140 MeV proton incidence.

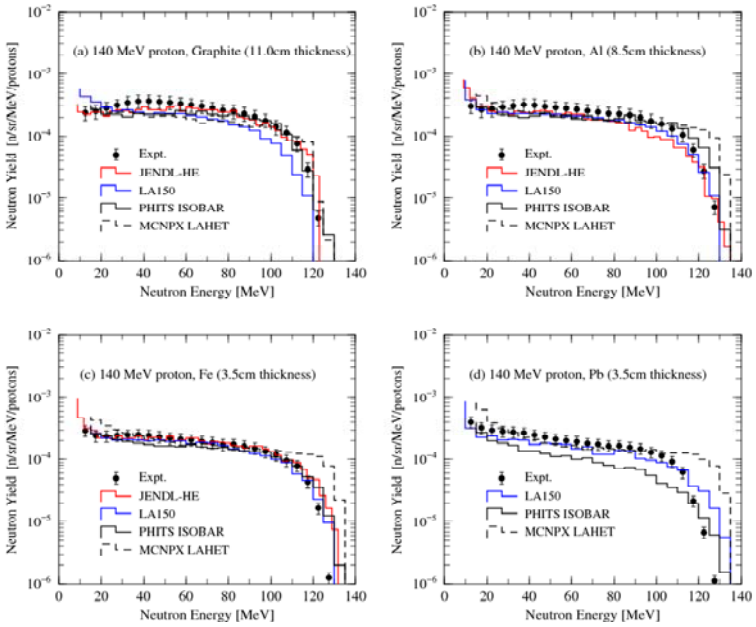

*Y. Iwamoto, et al., Nuclear Instrument and Methods A, to be submitted.

Thick target neutron yields at 0 degree for 250 MeV proton incidence.

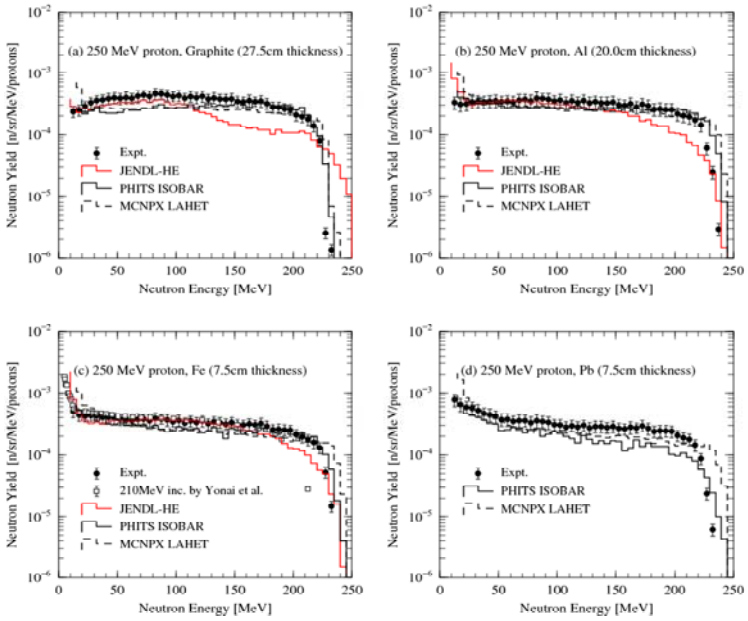

*Y. Iwamoto, et al., Nuclear Instrument and Methods A, to be submitted.

Thick target neutron yields at 0 degree for 350 MeV proton incidence.

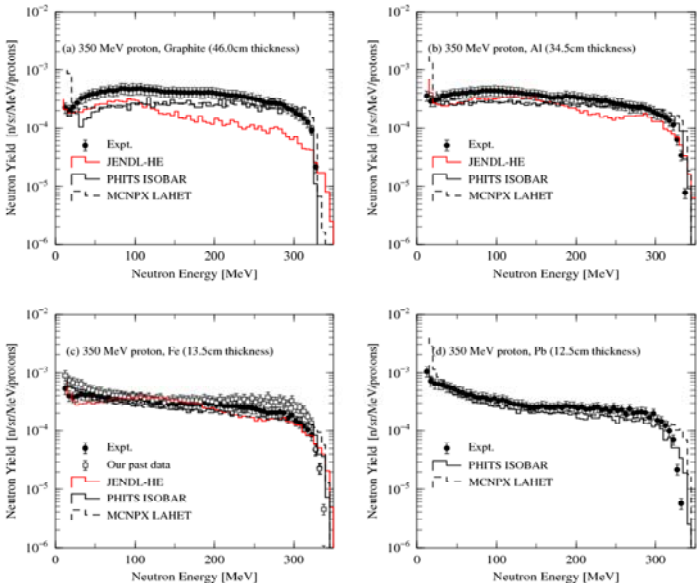

*Y. Iwamoto, et al., Nuclear Instrument and Methods A, 562, 789 (2006).

Thick target neutron yields at 0 and 90 degrees for 140 MeV proton incidence.

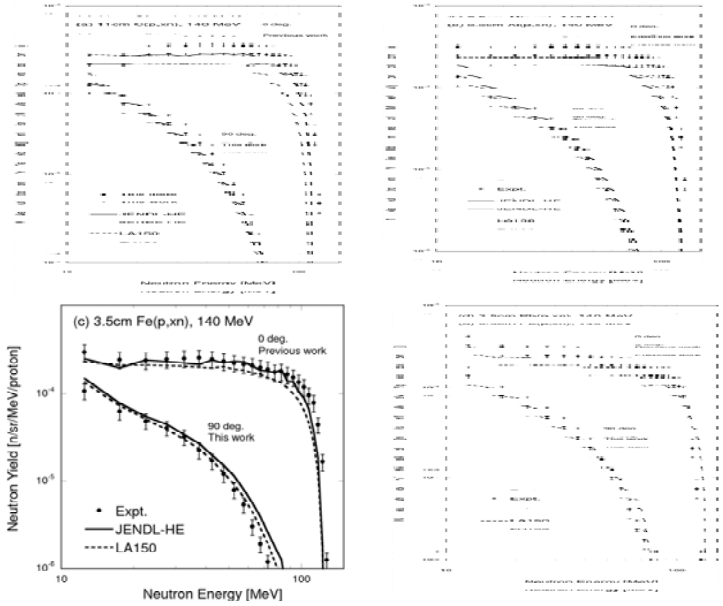

*Y. Iwamoto, et al., proceedings of ICRS11, to be submitted.

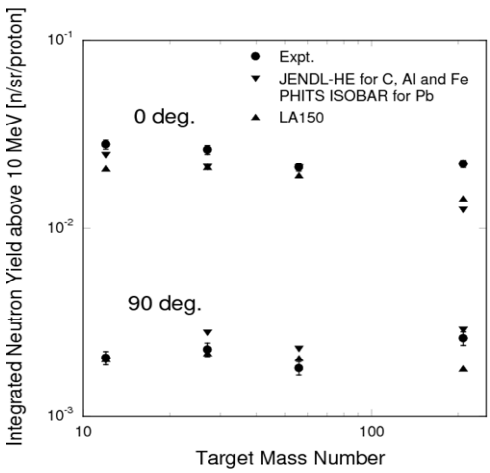

Thick target neutron yields above 10 MeV at 0 and 90 degrees as a function of target mass number compared with calculations

17

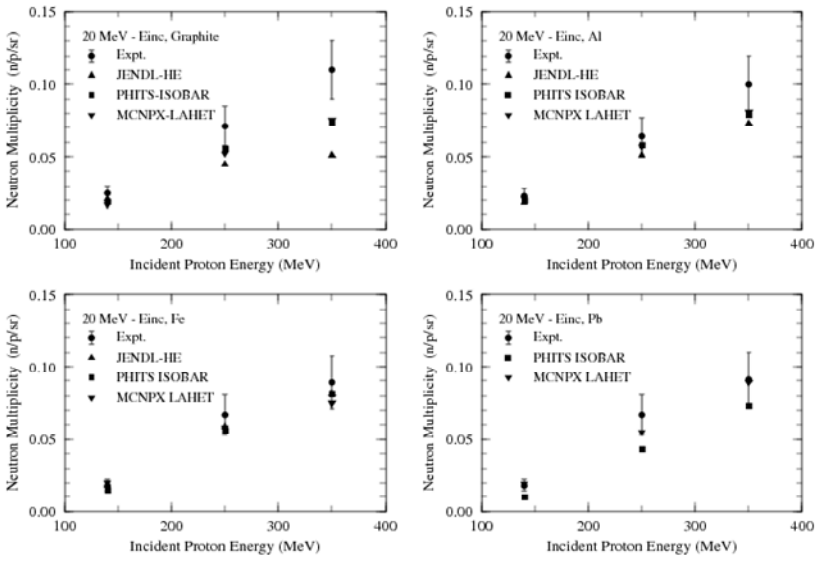

Thick target neutron yields above 20 MeV at 0 degree as a function of incident proton energy compared with calculations

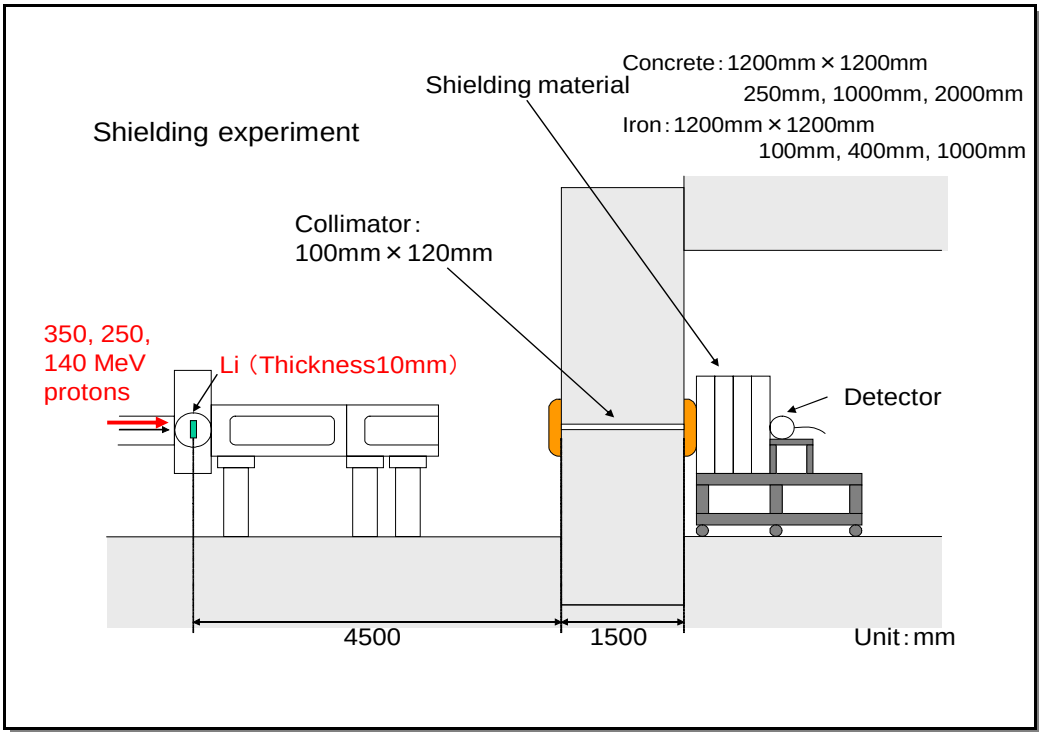

Neutron energy spectra for 140MeV p-Li neutron sources measured with NE213 detector

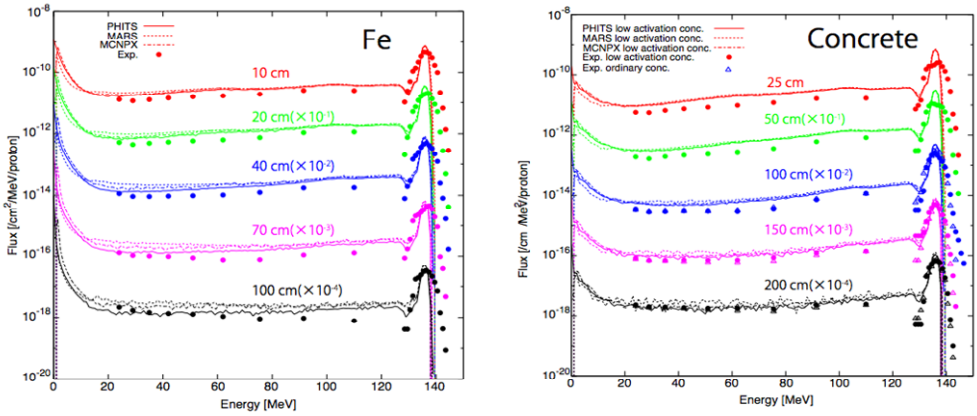

M. Hagiwara, Y. Kirihara et al., The ICRS-11 conference

Attenuation of peak neutron flux for 140 MeV p-Li neutron source

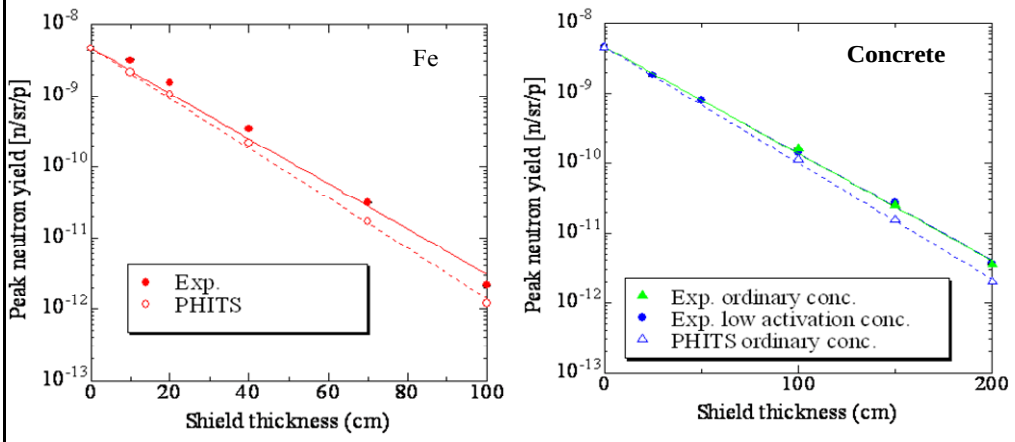

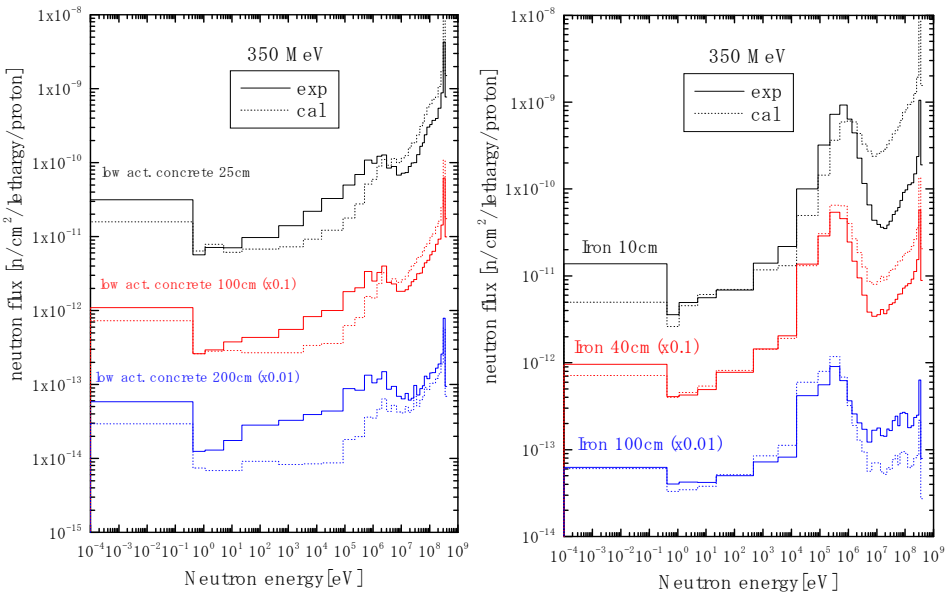

Neutron spectra measured with Bonner ball for 140 MeV p-Li neutron sources
H. Yashima et al., The ICRS-11 conference

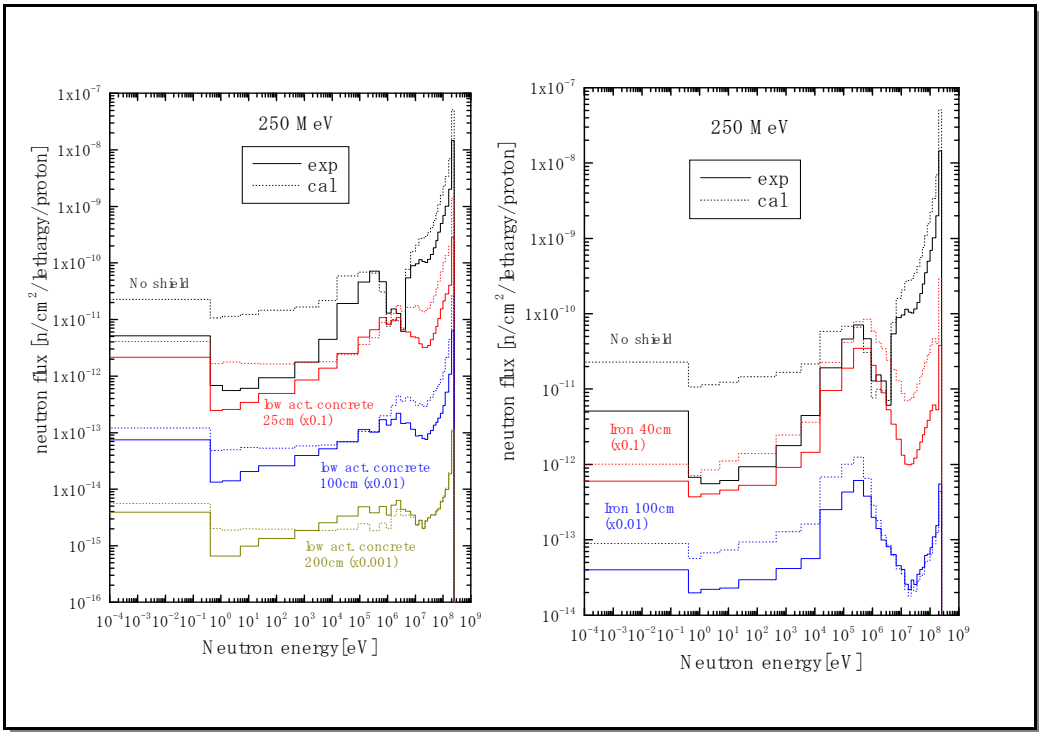
250 MeV
exp
cal
No shield
low act. concrete 25cm (x0.1)
low act. concrete 100cm (x0.01)
low act. concrete 200cm (x0.001)
neutron flux [n/cm²/lethargy/proton]
Neutron energy [eV]
250 MeV
exp
cal
No shield
Iron 40cm (x0.1)
Iron 100cm (x0.01)
neutron flux [n/cm²/lethargy/proton]
Neutron energy [eV]

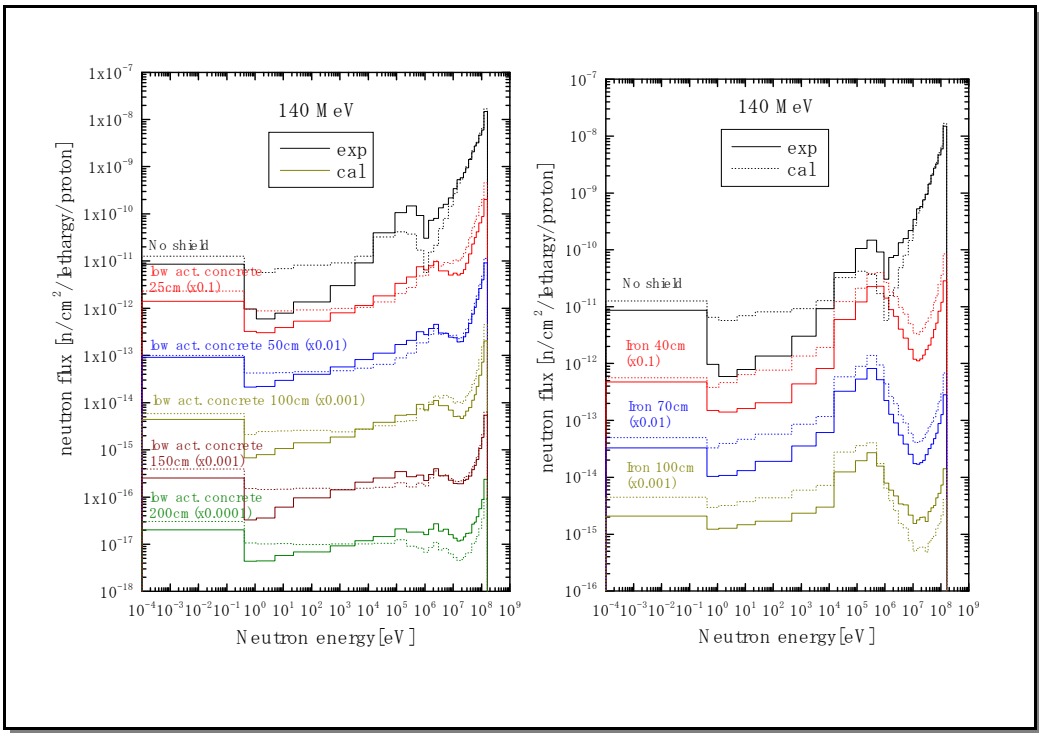
140 MeV
exp
cal
No shield
low act. concrete 25cm (x0.1)
low act. concrete 50cm (x0.01)
low act. concrete 100cm (x0.001)
low act. concrete 150cm (x0.001)
low act. concrete 200cm (x0.0001)
neutron flux [n/cm²/lethargy/proton]
Neutron energy [eV]
140 MeV
exp
cal
No shield
Iron 40cm (x0.1)
Iron 70cm (x0.01)
Iron 100cm (x0.001)
neutron flux [n/cm²/lethargy/proton]
Neutron energy [eV]

Attenuation of effective doses with iron and low activation concrete thicknesses

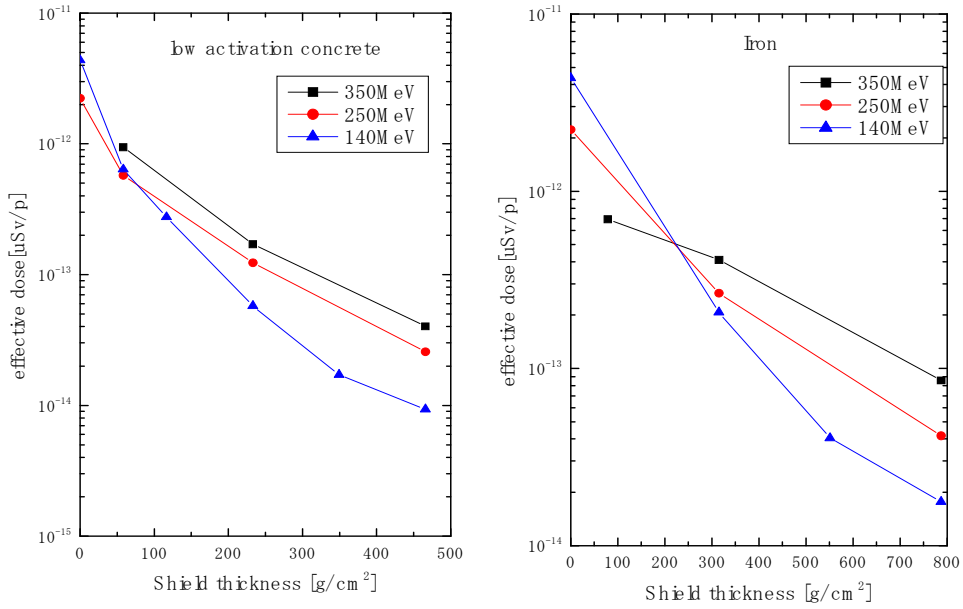

Conclusion

- **These experiments have been presented at ICRS-11 and some works have been published and are in preparation of submission.**

We are now planning to perform various DDX, TTY and shielding experiments at RCNP.

Electron linac based high energy radiation and neutron facility at PAL

Hee-Seock Lee
Pohang Accelerator Lab., POSTECH

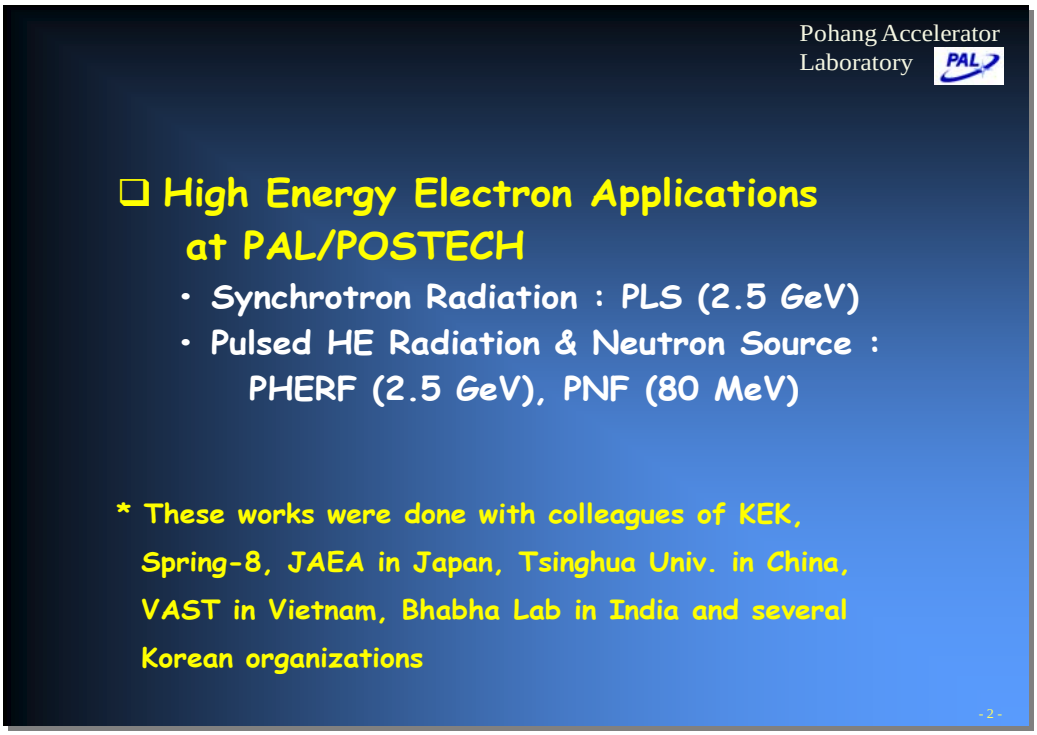

Pohang Accelerator Laboratory

Photo-Neutron Production and High Energy Radiation Applications at PHERF

- 3 -

Pohang Accelerator Laboratory

PAL-PHERF

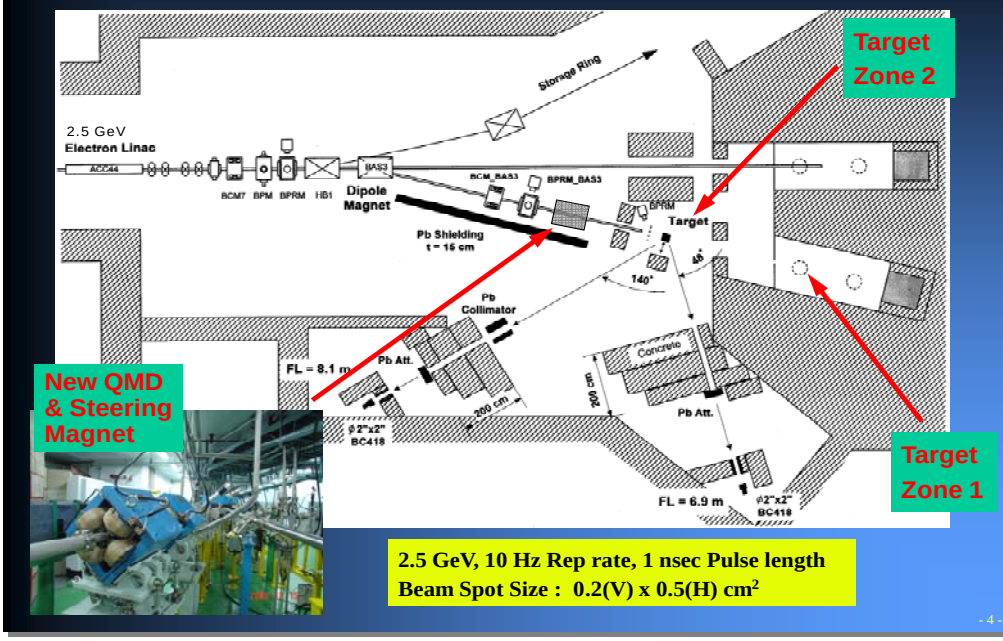

2.5 GeV, 10 Hz Rep rate, 1 nsec Pulse length
Beam Spot Size : 0.2(V) x 0.5(H) cm^2

- 4 -

Neutron TOF at 90º, 48º, 140º

Pohang Accelerator Laboratory

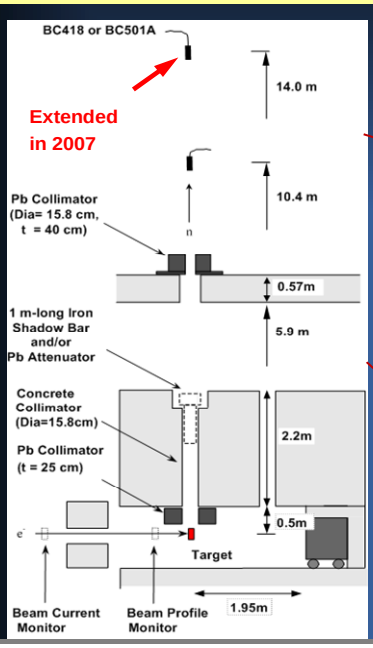

- Differential photo-neutron yields
  - Dependence on target conditions :
  - Atomic number, Target thickness

New TOF Tower

Experimental setup (90º case) .

Neutron TOF at 90º, 48º, 140º

Pohang Accelerator Laboratory

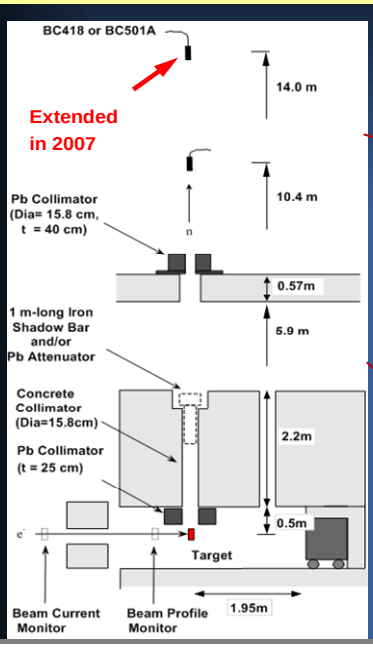

- Differential photo-neutron yields
  - Dependence on target conditions :
  - Atomic number, Target thickness

New TOF Tower

Experimental setup (90º case) .

- 5 -

Pohang Accelerator Laboratory

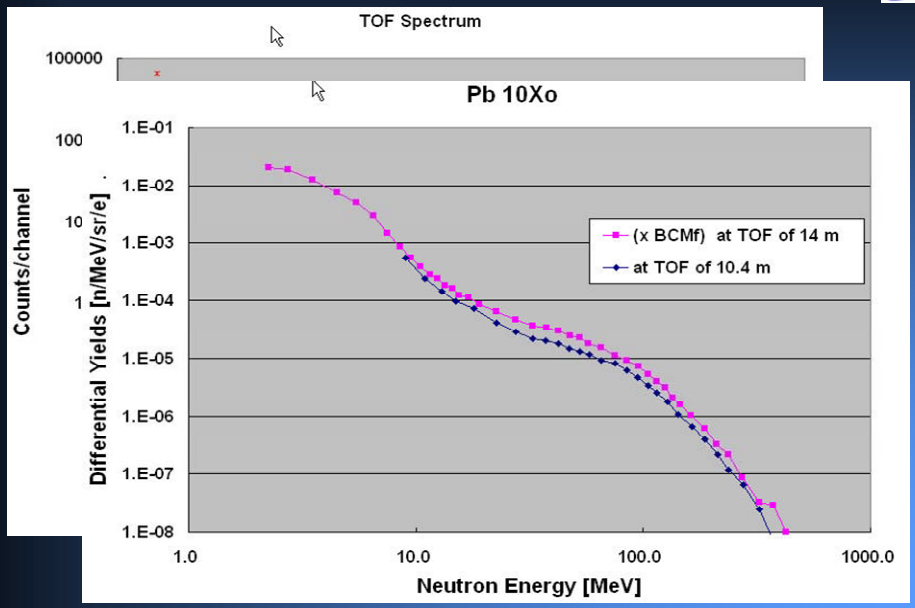

- 7 -

Low energy neutrons by BMS

Pohang Accelerator Laboratory

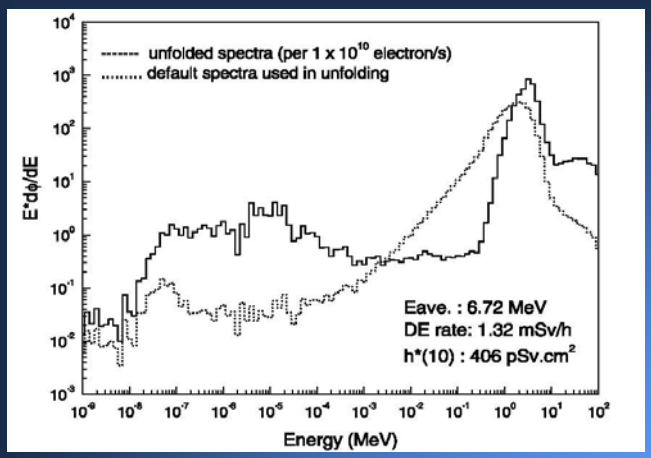

Published at Rad. Prot. Dosim. 110, 717 (2004)

Neutron Yields from 10 Xo-thick Pb target irradiated by 2.5 GeV electrons
- Using Au foil with enhanced Bonner Sphere (2" ~ 12" + lead shell 9" set)
- Measured at upper outlet of the neutron hole

- 8 -

Charged Particle Yields by TOF

Pohang Accelerator Laboratory

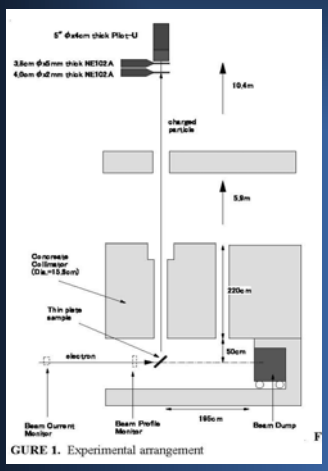

GURE 1. Experimental arrangement

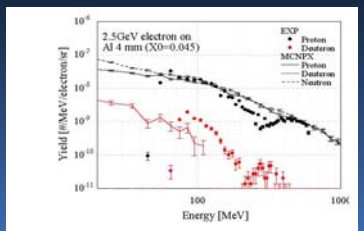

FIGURE 7. Secondary proton and deuteron energy spectrum at 90 degree for a 4 mm thick aluminum sample on 2.5 GeV electrons.

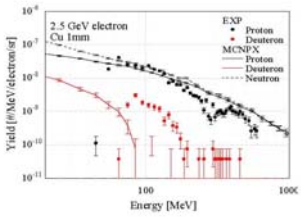

FIGURE 8. Secondary proton and deuteron energy spectrum at 90 degree for a 1 mm thick copper sample on 2.5 GeV electrons.

Presented by T. Sanami at ND2004

- 9 -

Interrogating Probe

Pohang Accelerator Laboratory

Using Transmission Method of Pulse Fast Neutron at TOF line
To confirm the feasibility, considered normal materials (Analysis Error = 35%)

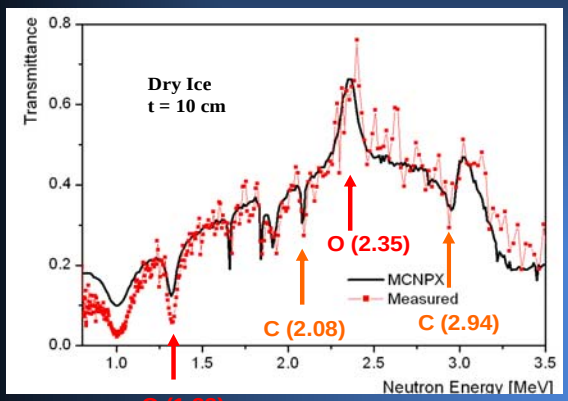

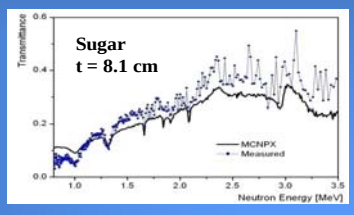

Published at NIM A562, 1076 (2006)

Small e-linac with high pulse rate is expected for the practical device using this method.

- 10 -

Demagnetization Study

Pohang Accelerator Laboratory

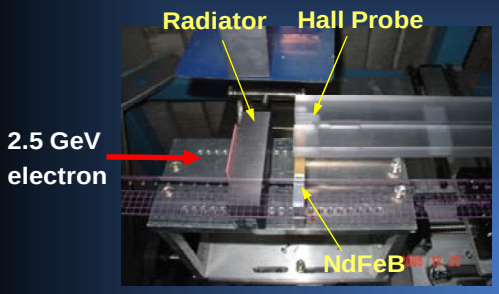

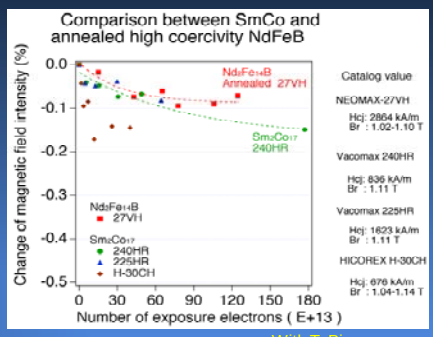

With T. Bizen
Published at Rad Meas V41 supplement (2007)

- In-situ type B-field Measuring System
  - 2D-Scanning over Nd-Fe-B magnet which used as main part of Undulator
  - Investigate radiation-dependent demagnetization property using Cu, Ta block

- 11 -

Thickness Dependence

2.5 GeV electron

Pohang Accelerator Laboratory

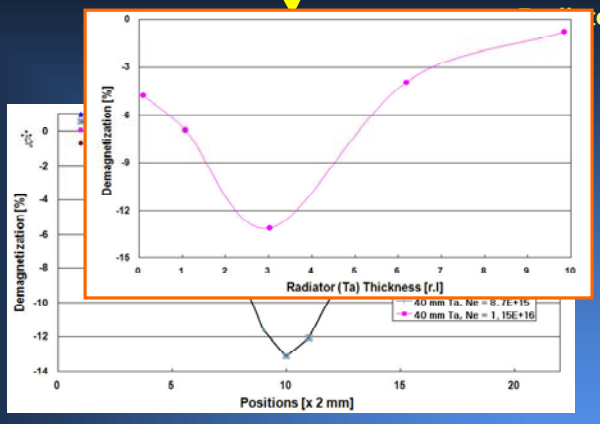

Normalized demagnetization at electron intensity of 5.44E+15

Presented at ICRS11 (2008)

- Demagnetization phenomena follow EM shower profile
  - Radiators (Thick Cu or Ta block) generate different EM shower profiles.
  - Photonuclear reactions and secondary particles are the source of demagnetization

- 12 -

Demagnetization Study

Pohang Accelerator Laboratory

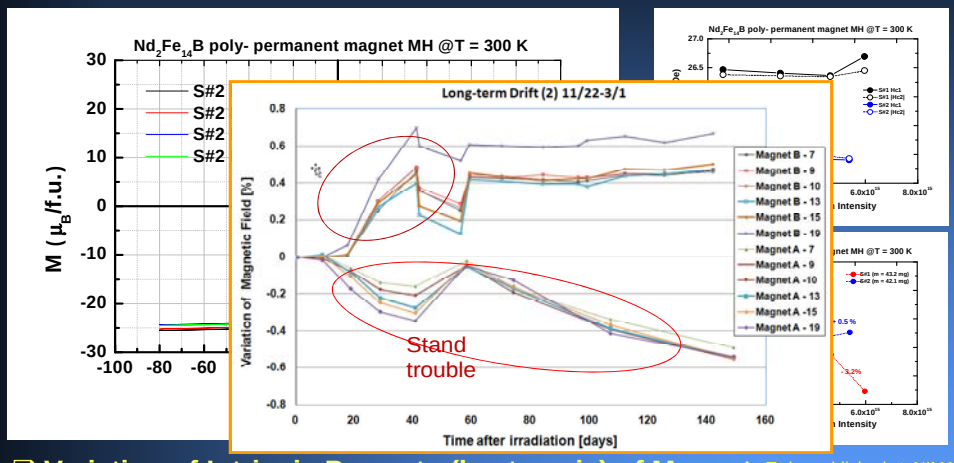

- Variation of Intrinsic Property (hysteresis) of Magnet — To be published at NIMA
  - No change of Coercive Field <--> Change of Saturated Magnetization
  - Irreversible Phenomena

- 13 -

Pohang Accelerator Laboratory

Nuclear Data Measurements and Applications at PNF

- 14 -

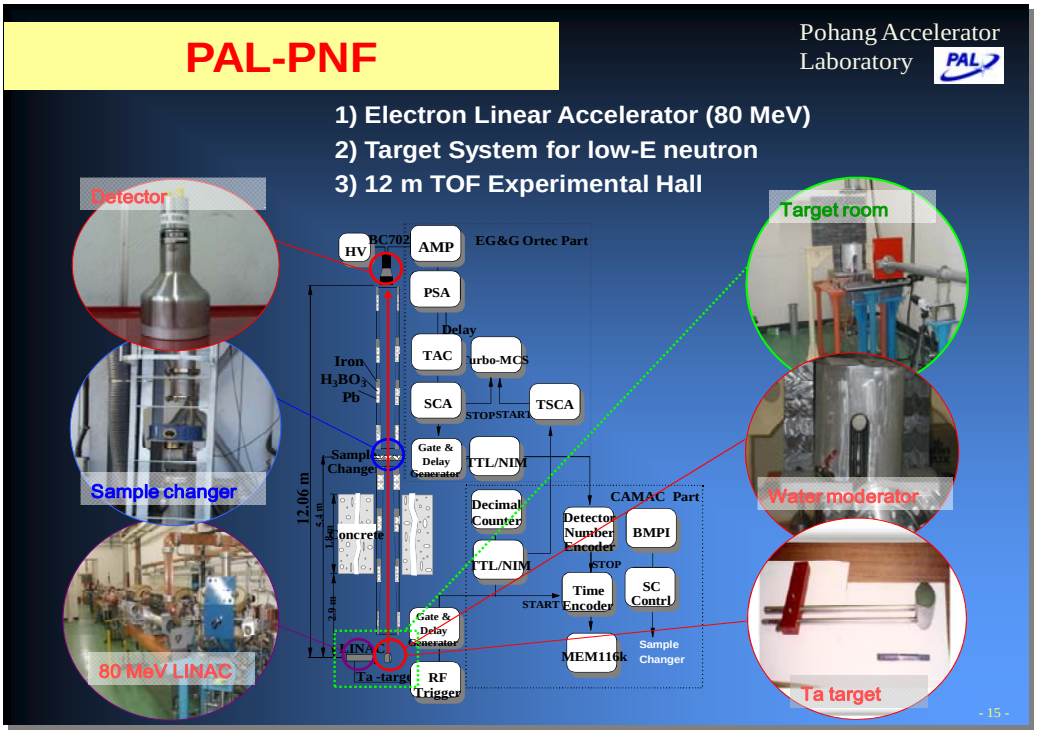
PAL-PNF
Pohang Accelerator Laboratory
PAL
1) Electron Linear Accelerator (80 MeV)
2) Target System for low-E neutron
3) 12 m TOF Experimental Hall
Detector
Sample changer
80 MeV LINAC
Target room
Water moderator
Ta target
HV
BC702
AMP
EG&G Ortec Part
PSA
Delay
TAC
Turbo-MCS
SCA
TSCA
STOP
START
Gate & Delay Generator
TTL/NIM
Sample Changer
Iron
H_3BO_3
Pb
Concrete
12.06 m
5.4 m
1.8 m
2.9 m
Decimal Counter
CAMAC Part
Detector Number Encoder
BMPI
TTL/NIM
STOP
Time Encoder
START
SC Control
Gate & Delay Generator
LINAC
Ta -target
RF Trigger
MEM116k
Sample Changer
- 15 -

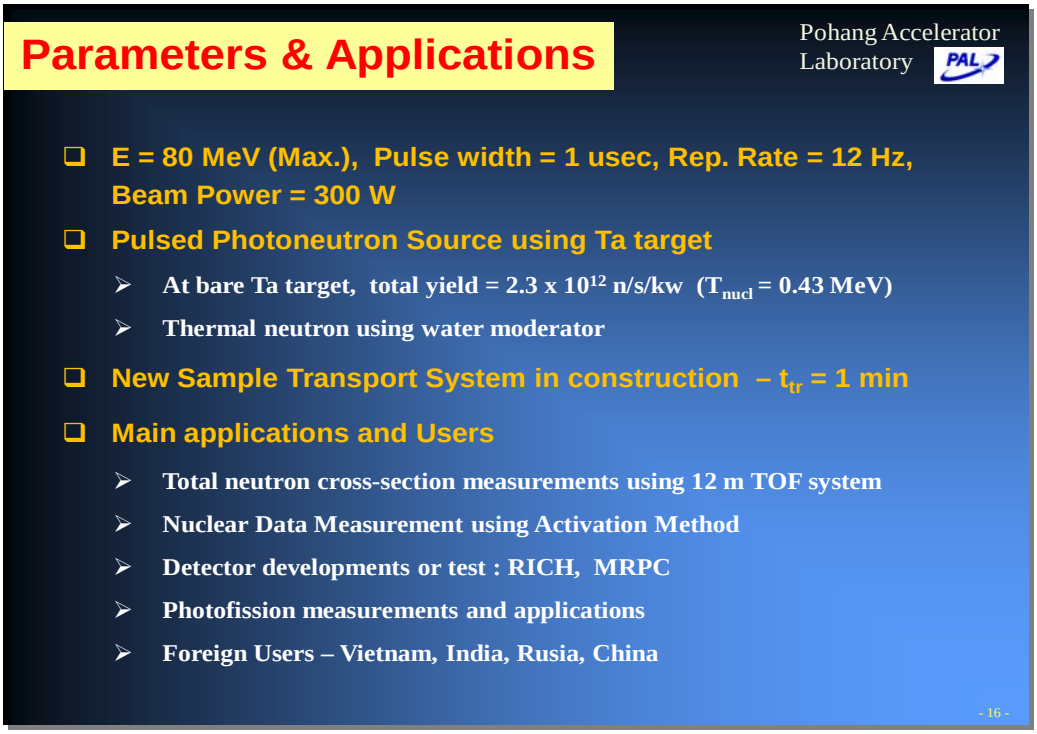
Parameters & Applications
Pohang Accelerator Laboratory
PAL
E = 80 MeV (Max.), Pulse width = 1 usec, Rep. Rate = 12 Hz, Beam Power = 300 W
Pulsed Photoneutron Source using Ta target
At bare Ta target, total yield = 2.3 x 10^{12} n/s/kw (T_{nucl} = 0.43 MeV)
Thermal neutron using water moderator
New Sample Transport System in construction – t_{tr} = 1 min
Main applications and Users
Total neutron cross-section measurements using 12 m TOF system
Nuclear Data Measurement using Activation Method
Detector developments or test : RICH, MRPC
Photofission measurements and applications
Foreign Users – Vietnam, India, Rusia, China
- 16 -

Neutron Spectrum & Distribution

Pohang Accelerator Laboratory

The spectrum agrees with evaporated neutron distribution
- using $^{115}In(n,\gamma)$, $^{65}Cu(n,p)$, $^{27}Al(n,p)$, $^{27}Al(n,\alpha)$

The flux distribution of thermal neutron generated from water-cooled Ta target along neutron guide tube

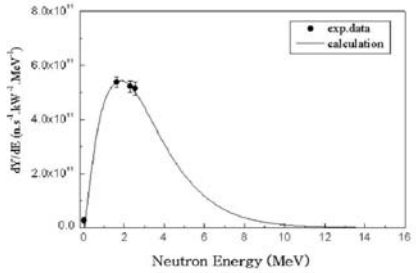

Fig. 5. Neutron energy spectrum from the thick Ta target bombarded by 65-MeV electrons.

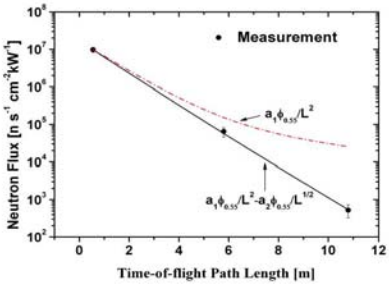

Fig. 9. Thermal neutron flux measured along the neutron guide tube and a fitting function.

Published at JKPS 48, 382(2006)

- 17 -

Total Cross-section by TOF

Pohang Accelerator Laboratory

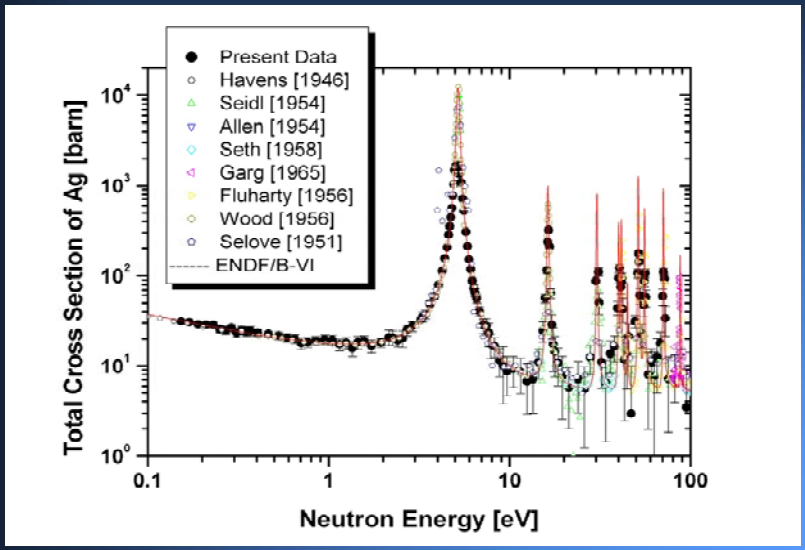

- 18 -

Nuclear Data Measurements

Pohang Accelerator Laboratory PAL

- Activation Method (monitored by using Au foil) : W, Hf
- Isomeric Cross-section, etc.

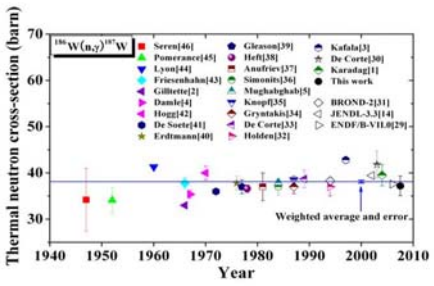

Fig. 4. Comparison of the evaluation and the experimental values for the thermal neutron cross-section of the $^{186}W(n,\gamma)^{187}W$ reaction. The line is the weighted average value for the experimental values included the present result.

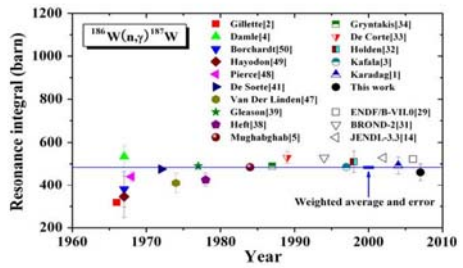

Fig. 5. Comparison of the evaluation and the experimental values for the resonance integral of the $^{186}W(n,\gamma)^{187}W$ reaction. The line is the weighted average value for the experimental values included the present result.

With Neuyen Van Do
Published at NIMB266 (2007)

- 19 -

Photofission Measurements

Pohang Accelerator Laboratory PAL

Electron Energy : 2.5 GeV, 45~75 MeV
Sample elements : Pb-208, Bi-209, Pb-nat
- planning : Th & U series
Detected isotopes : Fe-59, Zn-58m, As-74, Br-82,I-126, etc
(total 26 types) from Bi irradiated by Bremsstrahlung
from 2.5 GeV electron – now on analysis process
- Planning : Prompt & Delayed gamma & neutron measurements
using active detection system

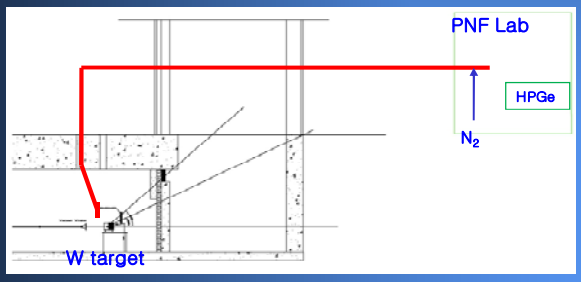

- 20 -

Summary

Pohang Accelerator Laboratory

- Electron-induced pulse neutron facilities developed at PAL service unique experimental infrastructure for nuclear and health physics
- Neutron and photon fields were defined well using TOF systems, BMS, passive detectors and damage monitors.
  - Bremsstrahlung from 2.5 GeV and 80 MeV electrons
  - High-E neutrons up to 500 MeV and low-E neutrons down to sub-eV
- Well-defined radiation facilities were used for several applications
  - Demagnetization of permanent magnet & Electronic devices for Space
  - Developing interrogating probe (explosive, nuclear material)
  - Total cross-section measurements
  - Detector development or test : RICH, MRPC
  - Photofission measurements and applications

- 21 -

Perspective Activities

Pohang Accelerator Laboratory

- PHERF and PNF will be upgraded more for Users and Applications
  - 12 m and 14.5 m TOF path length at 90° and others at 48° and 140°
  - Variable DAQ systems with N-γ discrimination
- Proton from 230 MeV Cyclotron at KNCC is available since 2008
- Construct I Linac of PAL-XFEL

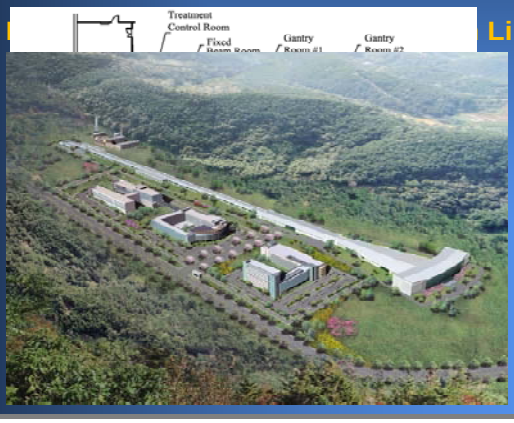

- 22 -

The MMW target station of EURISOL facility and its performance

M. Lindroos, Y. Kadi, C. Kharoua, R. Rocca, A. Herrera, K. Samec (CERN), **F. Groeschel, *et. al.*** (PSI), **J. Freibergs, *et al.*** (IPUL), **L. Tecchio, *et al.*** (INFN), **F. Negoita, *et al.*** (NIPNE)
European Organisation for Nuclear Research
Geneva, Switzerland

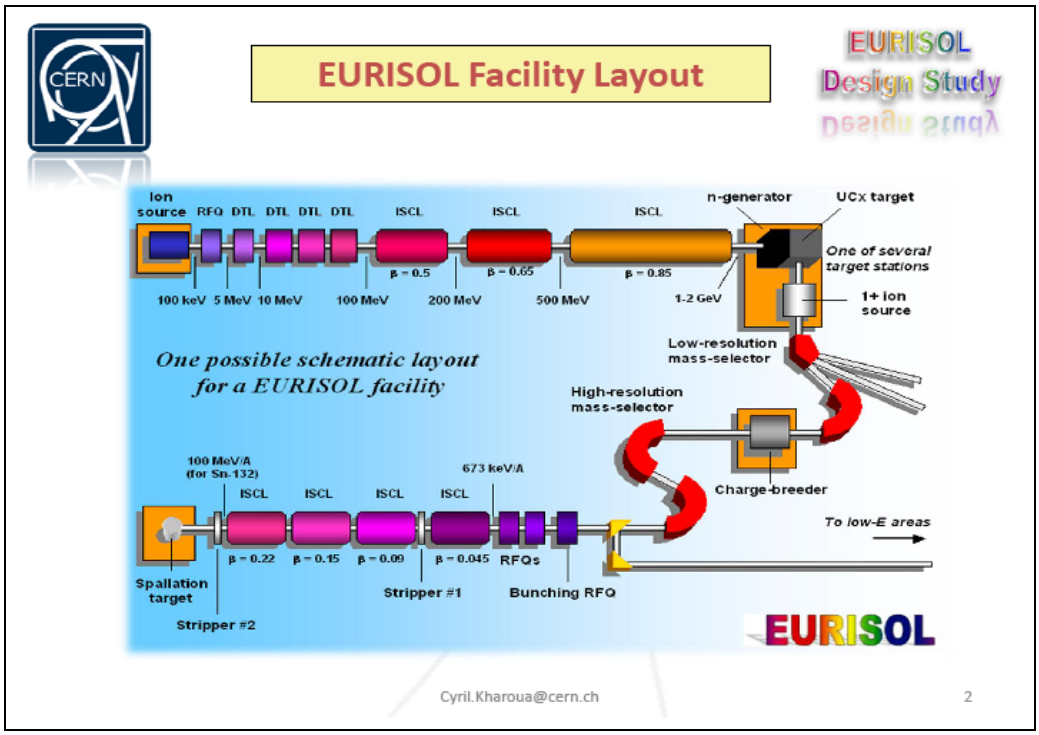

EURISOL Target Stations

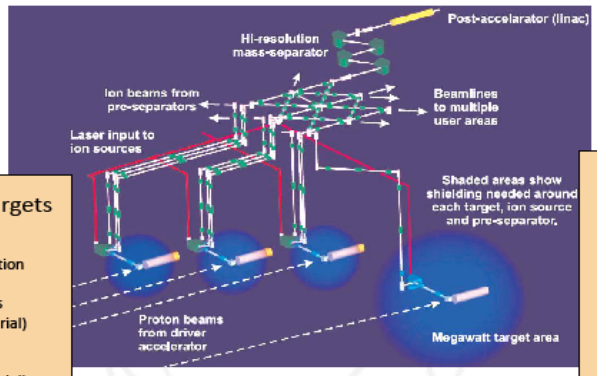

100 kW direct targets

RIB production:
- Spallation-evaporation
- Main: P-rich (10 to 15 elements below target material)
- Residues: N-rich (A few elements below target material)

Target materials:
- Oxides
- Carbides
- Metal foils
- Liquid metals

MMW target

RIB production:
- Fission (10^{15} fission/sec)
- N-rich (10^{13} Sn^{132}/s)
- Wide range Z = 10 to Z = 60

Target material:
- U (baseline)
- Th

Converter:
- Hg

Fast neutron fluxes: 10^{14} n/cm²/s/MW of beam

Cyril.Kharoua@cern.ch 3

EURISOL-DS Targetry Challenges

EURISOL shall deliver beams 3 orders of magnitude higher intensity than in presently operating facilities.

- Design of target containers dissipating a direct GeV p-beam dc-power of > 100 kW to produce spallation generated RIBs.
- Improve ion-source and release efficiencies
- Design high power density spallation n-source (10 MW/l)
- Design actinide targets intercepting efficiently the neutrons generated by high power density n- source.

Cyril.Kharoua@cern.ch 4

Multi-MW Liquid Hg Target

EURISOL Design Study

- Compact Hg-loop with beam widow
- Confined transverse film windowless

Deliverables:

1. Engineering study of the thermal hydraulics, fluid dynamics and construction materials of a window or window-free liquid-metal converter.
2. Study of an innovative waste management in the liquid Hg-loop e.g. by means of Hg distillation.
3. Engineering design and construction of a functional Hg-loop.
4. Off-line testing and validation of the thermal hydraulics and fluid dynamics.
5. Engineering design of the entire target station and its handling method

Coaxial Guided Stream (CGS) Design

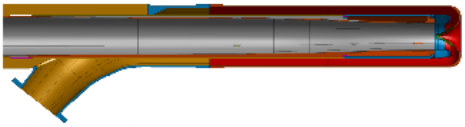

Windowless Transverse Film (WTF) design

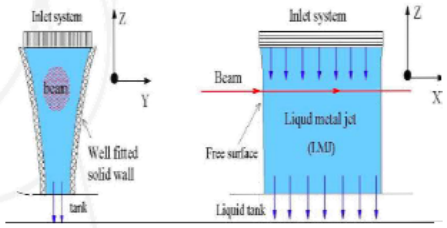

Cyril.Kharoua@cern.ch 5

Mercury loop parameter

EURISOL Design Study

	Value	Units
Beam power	4	MW (continuous)
Total Volume of Hg	0.9	m^3
Total Mass of Hg	12150	kg
Target length	100	cm
Target diameter	14	cm
Volume of liquid in the target	11.7	L
Mass of the target	178	Kg
Window and target material	T91	
Pump flow rates	15	L/s
Pump Pressure	7.5	bar
Pump power	160	KW
Total loss of pressure in the Loop	~4	bar

Cyril.Kharoua@cern.ch 6

Mercury target parameter

EURISOL Design Study

	Beam diameter		Units
Gaussian beam geometry	15 mm	25 mm	
Beam power	4		MW (continuous)
Beam particle energy	1		GeV
Beam current	4		mA
Beam escapes	$2x10^8$		primary/cm^2/s/MW of beam
Estimated peak temperature in the liquid	261	180	°C
Estimated peak temperature in the window	260	258	°C
Maximum velocity	6		m/s
Maximum loss of pressure	5		bar
Peak power density in the Mercury	1.8	0.8	kW/cm^3/MW of beam
Peak power density in the window	0.9	0.3	kW/cm^3/MW of beam
Beam power deposition in the Mercury	2.3	2.3	MW/cm^3/MW of beam
Estimated Stress level in the window	<140	<110	MPa

Cyril.Kharoua@cern.ch 7

Window Configuration
Coaxial Guided Stream design (CGS)

EURISOL Design Study

PAUL SCHERRER INSTITUT

Basic performances of the target

TM-34-07-05 K.Samec /Design of the EURISOL converter target. – PSI 2007

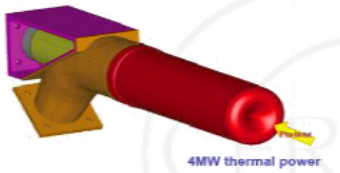

Parameter	symbol	value	unit
Liquid component	Hg	13.5	kg/l
Flow rate	ϕ	172	kg/s
Entrance temperature	T_{in}	< 60	C
Exit temperature	T_{out}	< 180	C
		> 150	
Pressure drop	ΔP	< 5	Bar
Static pressure	P_s	< 5	Bar

Ab.13 l/s

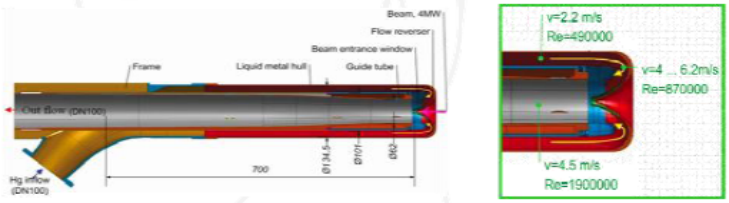

Paul Scherrer Institut - 5232 Villigen PSI PSI EURISOL converter target Hg test preparation Technical meeting PSI February 7 2008 DS34

Cyril.Kharoua@cern.ch 8

Window Configuration
Coaxial Guided Stream design (CGS)

EURISOL Design Study

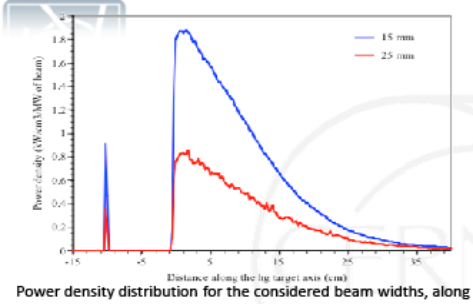

Power density distribution for the considered beam widths, along the beam axis and around the window

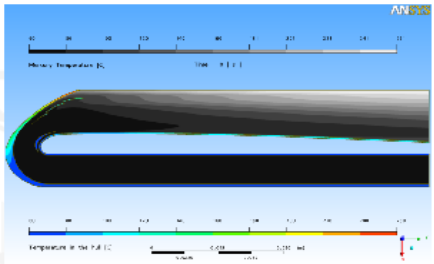

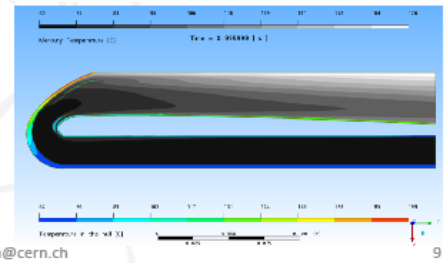

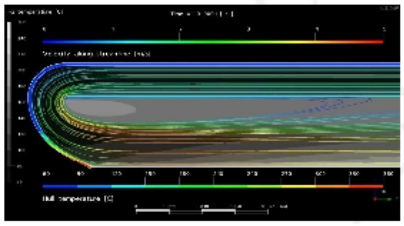

Cyril.Kharoua@cern.ch 9

3D CFD & Structural Analysis

EURISOL Design Study

- Maximum flow along beam axis
- Blade on the window to encourage flow on it and push liquid towards the centre axis
- Blade on leading edge use to attach the backflow and prevent cavitation (acts like a "fowler" on a wing)

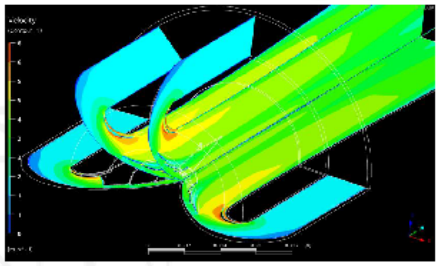

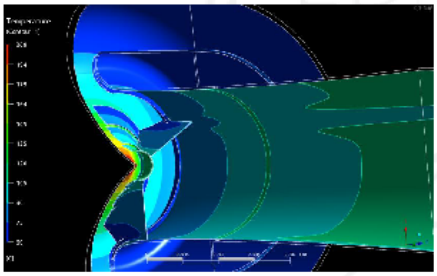

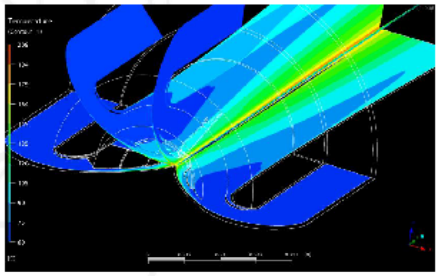

Cyril.Kharoua@cern.ch 10

Testing loop for the CGS design

EURISOL Design Study

PAUL SCHERRER INSTITUT

Measuring system

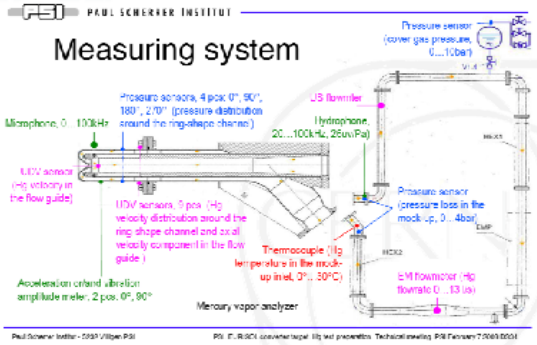

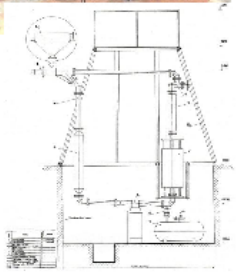

Existing Hg – loop in Institute of Physics (parameters of EMP p=4 bars; Q~12l/s)
Test planned for May 2008 and December 2008

Windowless Configuration Windowless Transverse Film design (WTF)

EURISOL Design Study

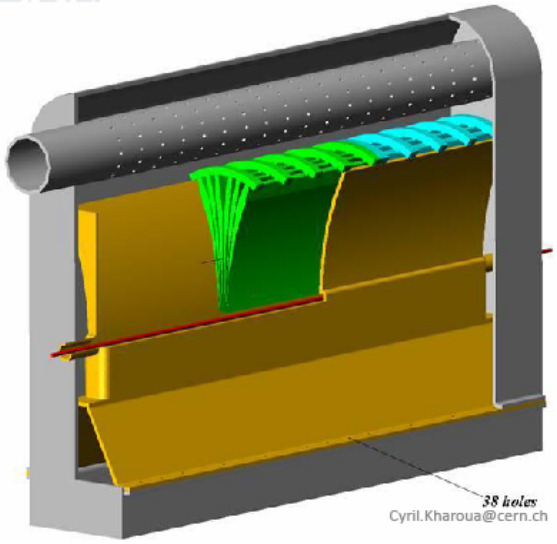

- The honeycomb is made to avoid the cavities in the falling mercury film.
- Such construction additionally gives possibility to distribute velocity in the film cross section according the local heat generation in the beam tract.
- The velocity becomes reduced along the tract by choosing sections with narrower gaps and reduced to sides by choosing narrower gaps in each section.

Windowless Configuration Windowless Transverse Film design (WTF)

EURISOL Design Study

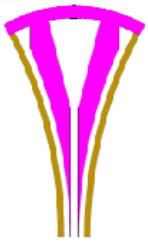

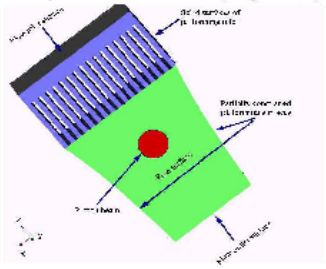

- Total Mercury flow-rate of ~ 12 l/s. Local velocity below the 3 mm gap will be 4.4m/s.
- The temperature increase of mercury is ~ 117.5 K when the heat deposition density on beam center line is 25 kW/cm3 (2mm σ).
- This design is under study at CERN and IPUL

Cyril.Kharoua@cern.ch 13

Testing loop for the WTF design (InGaSn loop)

EURISOL Design Study

Transverse Hg – film

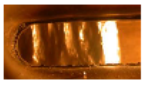
a


b


c

Modules of transverse film injectors


a


b


c

Test chambers

InGaSn test loop of transverse film target module

P=3 bar; Q~1.5 l/s

a – with rectangular cell inner structure
b – with round cell inner structure
c – with parallel separator inner structure

Cyril.Kharoua@cern.ch 14

Testing loop for the WTF design (Hg loop)

EURISOL Design Study

Engineering design and construction of a functional Hg loop for testing the integrity of the film

➔Inlet design proved
➔Complete CFD and Neutronics calculation on the way

Cyril.Kharoua@cern.ch 15

Integration of the fission target around the converter

EURISOL Design Study

Old Hg converter and secondary fission targets configuration

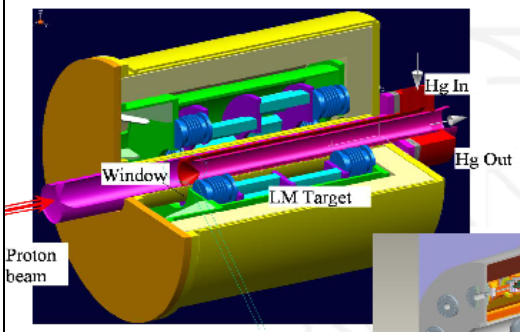

Problems:
- Sensitive instrument located in the harsh radioactive area
- Lack of flexibility
- Vaccum vessel
- Fission target vessel at 60KV and Hg target at ground

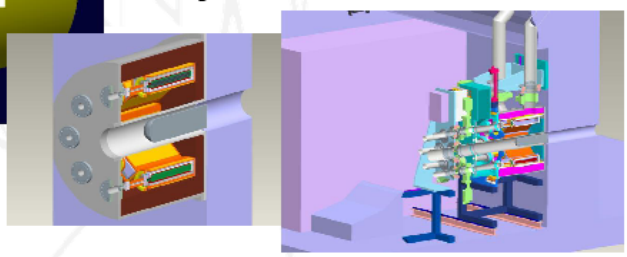

Cyril.Kharoua@cern.ch 16

Integration of the fission target around the converter

EURISOL Design Study

Integration inspired by the MAFF project

Fission target are located at the end of a long tube inserted in the concrete shielding

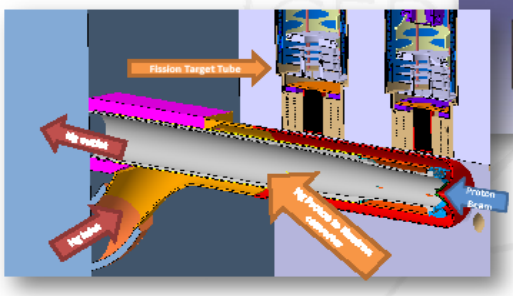

Fission target tube can be extracted separately from a remote system based in the hot cell above the concrete shielding of the neutron source

18/04/2008 Cyril.Kharoua@cern.ch Cyril Kharoua 17

Fission target design – MAFF/PIAFE

EURISOL Design Study

Florin Negoita (NIPNE)

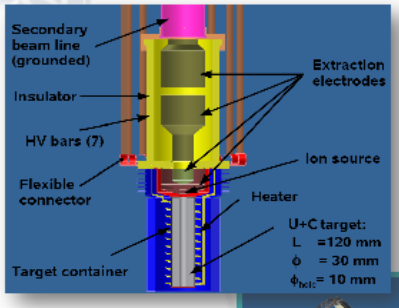

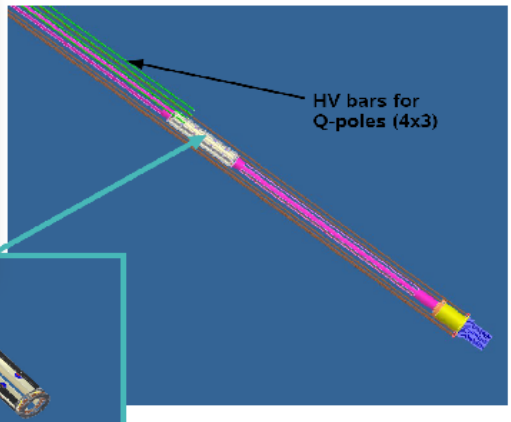

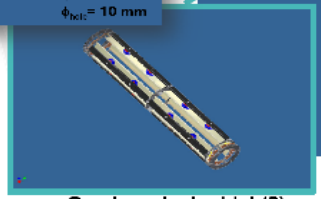

Quadrupole doublet (3)

Cyril.Kharoua@cern.ch 18

Fission Density

EURISOL Design Study

- Flexibility of the fission target arrangement (operation decoupled)
- Each target is independent from the others
- Moderator could be change in order to obtain different Neutron Spectra and so to produce different isotopes
- All the sensitive device could be placed away from the source of radiation
- The Shielding is now placed much closer to the source and

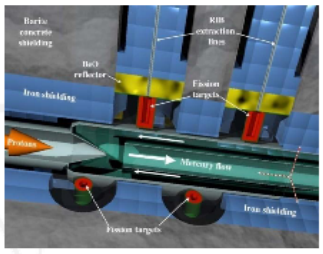

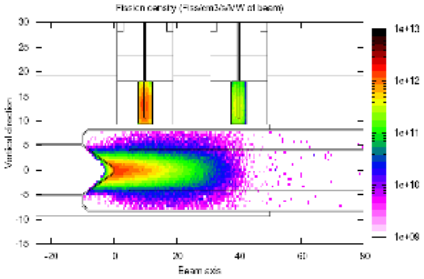

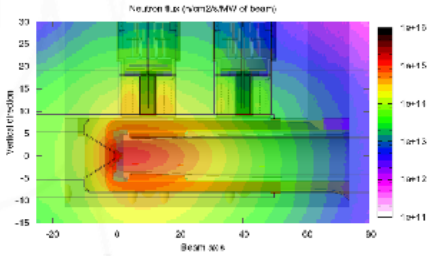

Cyril.Kharoua@cern.ch 19

Summary and Outlook

EURISOL Design Study

- The reference design of the 4 MW Hg spallation target and its ancillary equipment has advanced very significantly over the last year. The cases studied show the feasibility of the integration of the MAFF/PIAFE target into EURISOL Multi Megawatt target station.
- We are currently undertaking a detailed study of the Hg "windowless transverse film" which would allow a much more compact arrangement of the fission targets.
- The design of the fission target has been improved with the requirement to efficiently extract and ionize the fission fragments and to minimize the amount of fissionable material in the target assembly for a given beam intensity

Cyril.Kharoua@cern.ch 20

Fission target design – MAFF/PIAFE

EURISOL Design Study

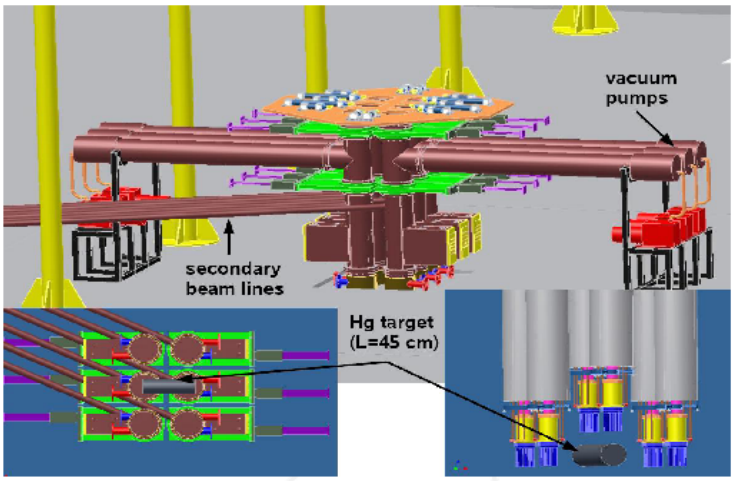

Cyril.Kharoua@cern.ch 22

Fission target design – MAFF/PIAFE

EURISOL Design Study

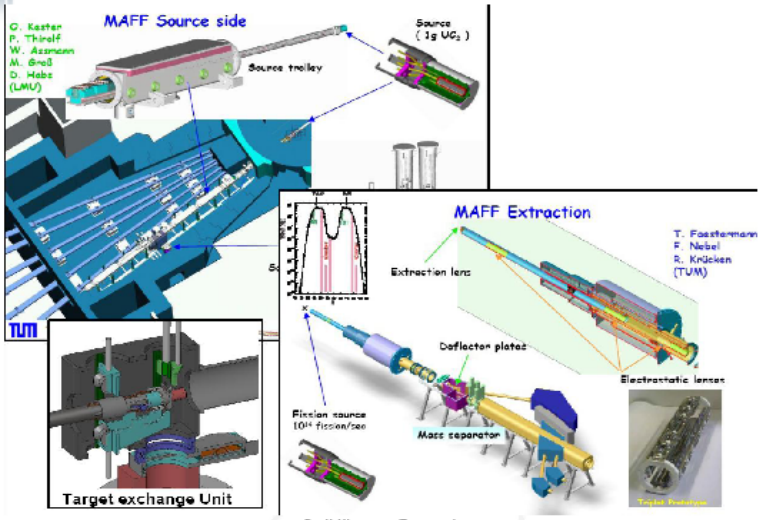

Cyril.Kharoua@cern.ch 23

Thermal Analysis of the fission target

EURISOL Design Study

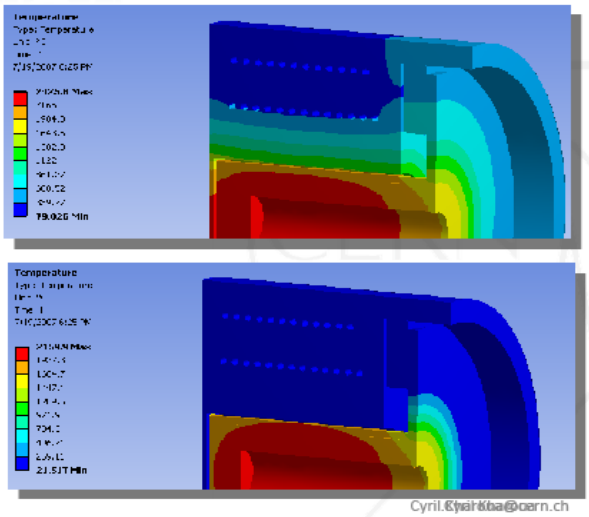

5.10^{14} fission per second (160W/cm3)
Graphite with Low conductivity (45W/m/K)

In order to perform a full thermal analysis of the proposed design, the graphite material imbibed with the desired quantity of Uranium need to be fully analyzed. The following properties need to be measured over the temperature range of the target usage condition (25°C up to 2500°C):

- specific heat
- thermal conductivity
- density

Cyril.Kharoua@cern.ch 24

Thermal Study

EURISOL Design Study

- Design parameter:
  - Pellets dimension (0.5mm thick, 30mm internal and 55mm external diameter)
  - 162 pellets spaced by 0.5mm=> 135 cm^3 of fissile material
  - Support of 0.5mm with same diameters
  - Support and container made of graphite
  - UCx of ISOLDE (1W/m/K) and High density (20W/m/K)
  - Container dimension : ~24cm high, ~6cm diameter
- Axisymmetric analysis
- Boundary condition:

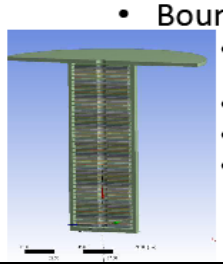

- 32KW deposited in the target = 10^{15} fission per second => 240W/cm^3
- Emissivity for the material UCx =0.6
- Emissivity for the container = 0.9
- Thermal conductivity of 50W/m/K for the container

Cyril.Kharoua@cern.ch 25

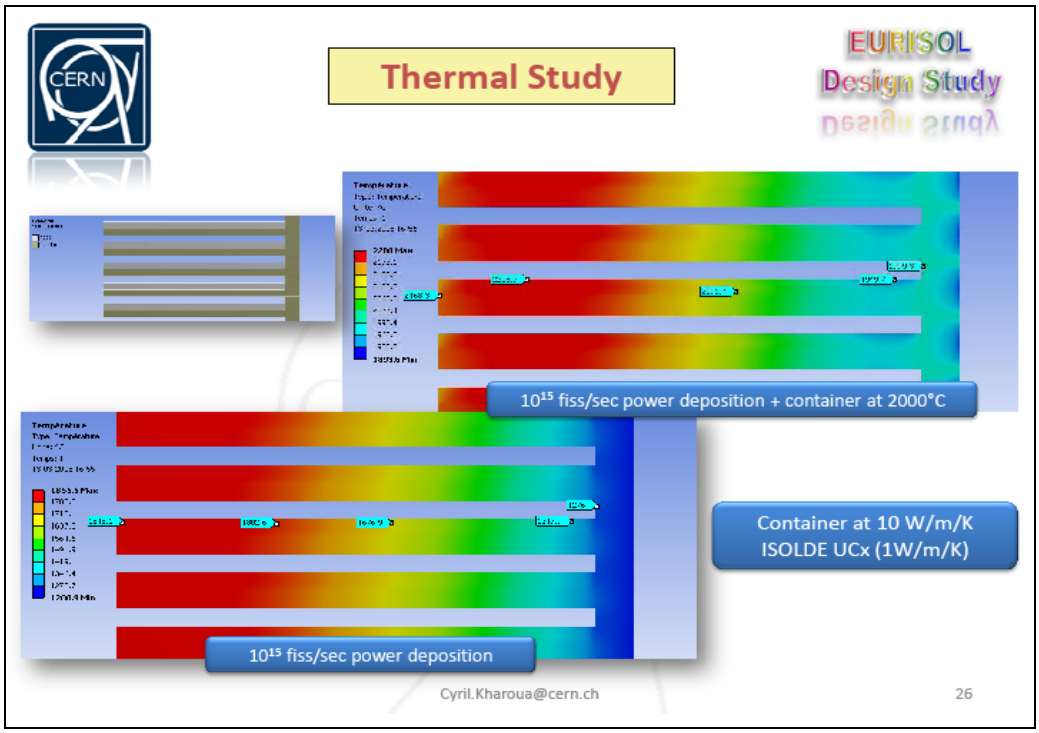
Thermal Study
EURISOL
Design Study
10¹⁵ fiss/sec power deposition + container at 2000°C
Container at 10 W/m/K
ISOLDE UCx (1W/m/K)
10¹⁵ fiss/sec power deposition
Cyril.Kharoua@cern.ch
26

Complementary shielding calculations for EURISOL postaccelerator

D. Ene, D. Ridikas, B. Rapp, J-C. David, D. Doré
CEA-Saclay, Gif-sur-Yvette, France

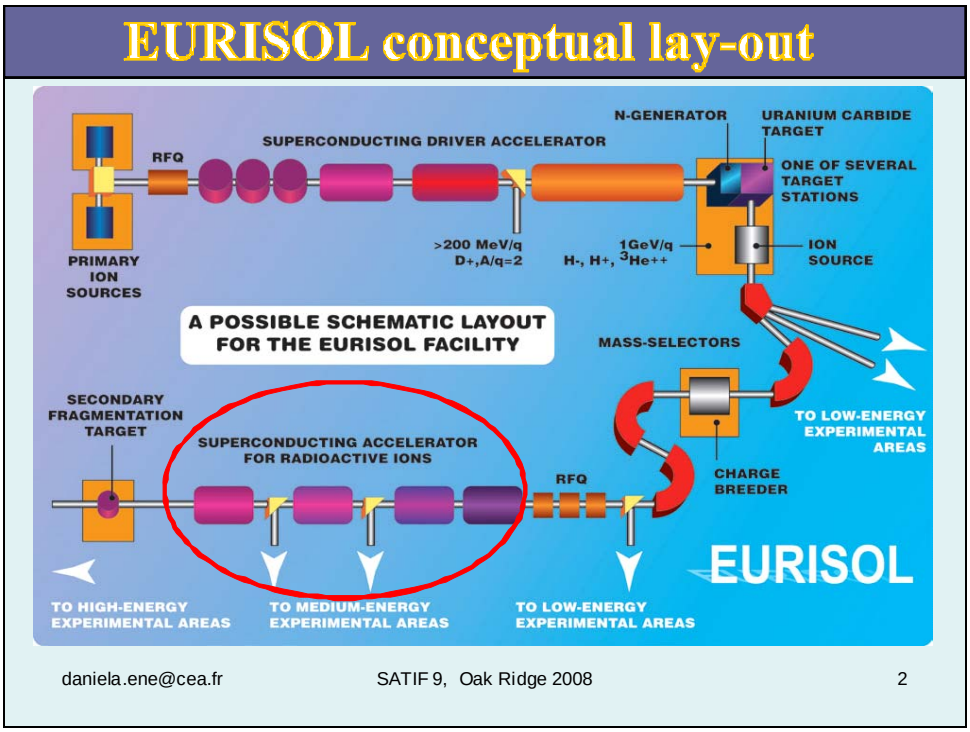

Schematic view of the EURISOL Linac

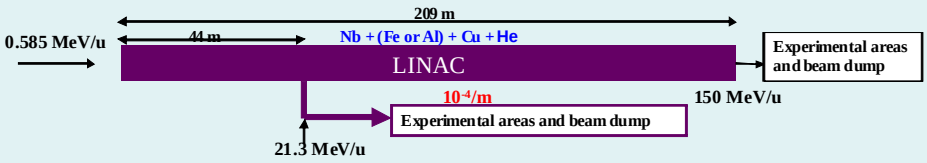

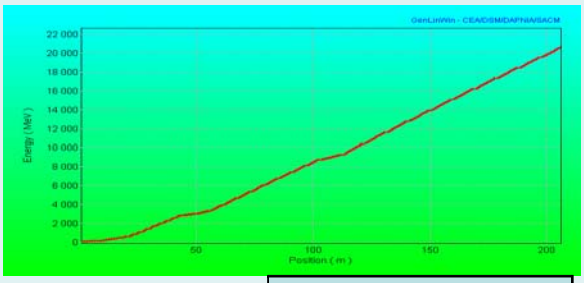

Energy gradient for $^{132}Sn^{25+}$

daniela.ene@cea.fr SATIF 9, Oak Ridge 2008 3

Goals:

- **Build confidence in PHITS1.94 estimates;**
- **Analysis of the possibility to reduce the thickness of the concrete shielding blocks;**
- **Preliminary analysis of a beam dump model, induced radioactivity and required shielding.**

daniela.ene@cea.fr SATIF 9, Oak Ridge 2008 4

Physics models: Benchmarck PHITS1.94 / MCNPX2.6.e

RIKEN

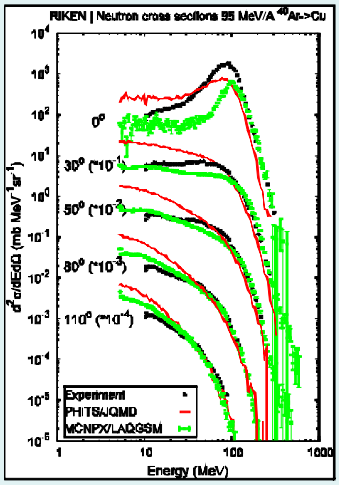

HIMAC

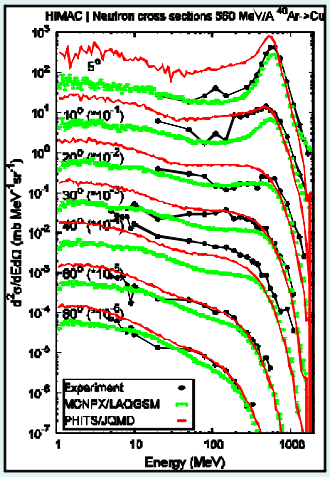

Shielding design requirements

	H*(10) [Sv h^{-1}]	Total_H*(10) [mSv y^{-1}]
Public areas	0.1	1
Controlled areas	10	20 / 2000 h
Accident beam loss: Total_H*(10) = 50 Sv		

Assumptions & Approach*

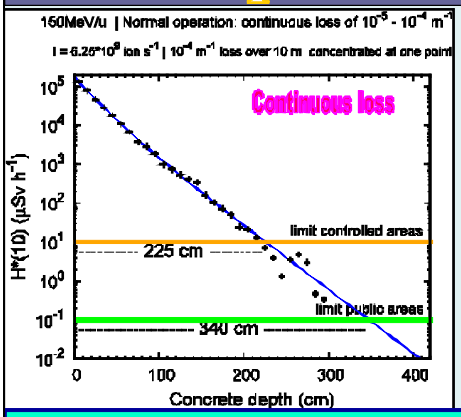

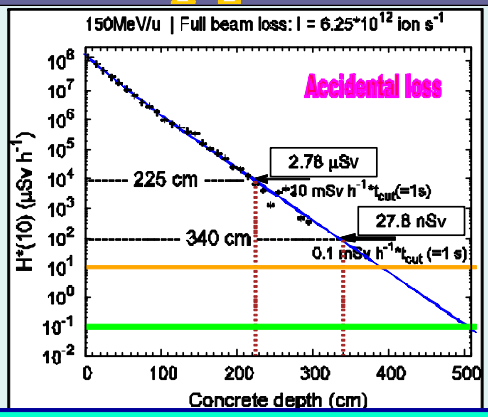

A shield designed for a continous beam loss of 10^{-4} m^{-1} (point loss of $6.25*10^9$ ion s^{-1}) during the routine operation is also adequate for an accident loss of the full beam at a localised point, providing that the linac cutoff time is less than 1s.

**A. Fasso, K. Göebel et all, Shielding against high energy radiation, Nuclear and Particle Physics, Vol 11, (1990)*

***S. Agosteo, M. Silari, CERN Note 088/ TIS-RP/TM/2001-028*

A full beam loss at a localised point must not give rise to a H*(10) > 100 mSv/h outside the shielding and the beam has to be swithed off within a time short enough that the H*(10) from this accident condition remains negligible.

Calculation model

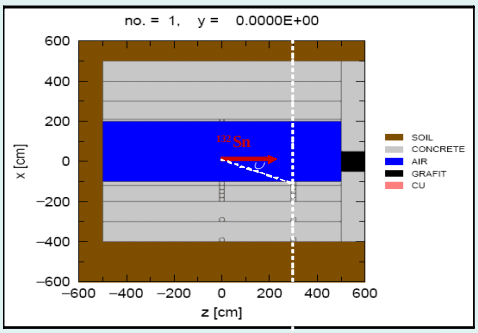

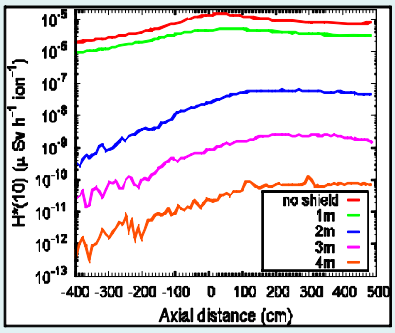

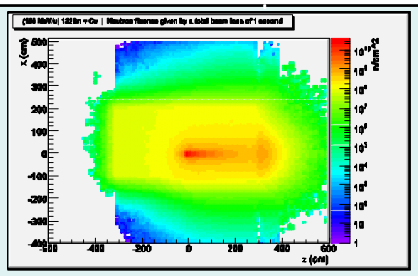

Results obtained for z=3m,

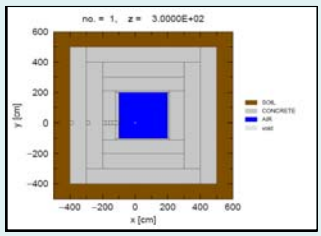

PHITS1.94 / MCNPX2.6.e comparison

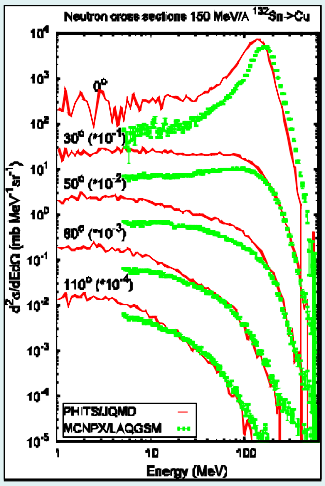

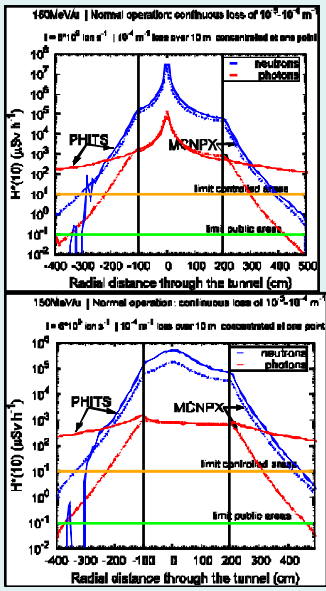

At z=0 neutrons factor 1.4

At z=3m neutrons: factor 2

Neutron attenuation curves in concrete

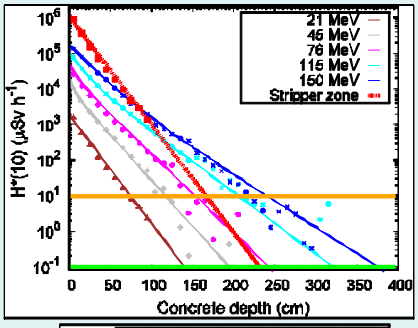

$$H^*(E_p, d/\lambda) = \frac{H_{1(E_p)}}{r^2}\exp\left[-\frac{d}{\lambda_1}\right] + \frac{H_{2(E_p)}}{r^2}\exp\left[-\frac{d}{\lambda_2}\right]$$

* Agosteo S, Nakamura T , at al. NIM/B 217, 2004

E [MeV/u]	∪ [Sv m² ion⁻¹]	∪ [g cm⁻²]	H∪ [Sv m² ion⁻¹]	∪ [g cm⁻²]
150	2.00E-10	38.78	7.98E-11	62.00
115	1.13E-10	23.50	6.14E-11	57.32
76	6.18E-11	21.36	1.27E-11	53.20
45.5	1.69E-11	12.19	1.55E-11	40.52
21.3	-	-	2.00E-12	33.57

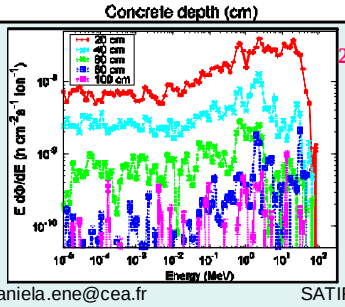

21MeV/u 150MeV/u

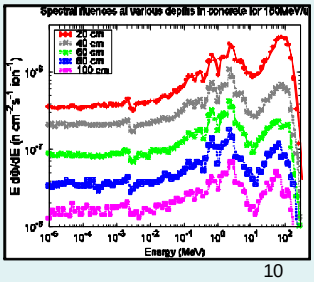

Schematic diagram of concrete shielding

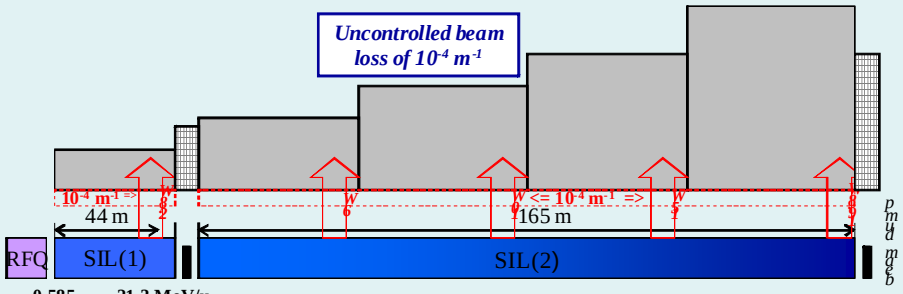

	staff	public
Dump / 2.8kW	165	230
Dump / 19.8kW	385	500

	Energy [MeV]	21.3	45.5	76	115	150
Staff	Length [m]	44	40	40	40	45
	Thickness (cm)	70	130	175	210	225
	V_{staff} (m^3)	338.05* → 7196.2 for a tunnel surface of 3 m x 4 m				
Public	Thickness (cm)	140	195	245	320	380
	V_{public} (m^3)	536.6* → 13663.7 for a tunnel surface of 3 m x 4 m				

*V_1, Unitary Volume (corresponding to a width = 1m)

Alternative shielding design: | 150MeV/u

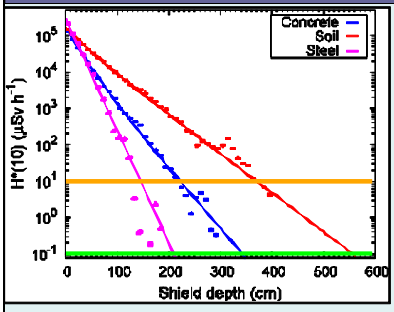

$$H^*(E_p, d/\lambda) = \frac{H_{1(E_p)}}{r^2}\exp\left[-\frac{d}{\lambda_1}\right] + \frac{H_{2(E_p)}}{r^2}\exp\left[-\frac{d}{\lambda_2}\right]$$

material	ω [Sv m²]	ω [g cm⁻²]	H_ω [Sv m²]	ω [g cm⁻²]	SHIELD [cm]	
					Staff	Public
concrete	1.248E+00	38.78	4.982E-01	62.00	*225*	*340*
soil	7.172E-01	34.04	9.959E+02	65.04	*375*	*570*
steel	-	-	2.996E+00	116.76	*145*	*215*

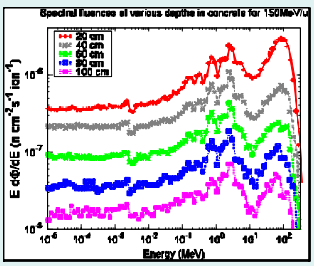

Concrete

Steel

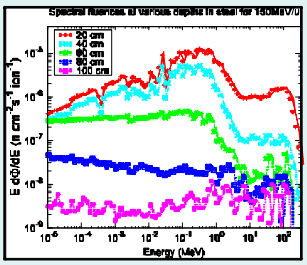

Alternative shielding design: "dirty" variant

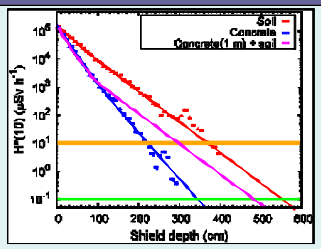

Composite concrete/soil structure

material	SHIELD [cm]	
	Public	Staff
concrete	Staff	Public
soil	375	570
concrete + soil	concrete (100cm) + soil (200cm)	concrete (100cm) + soil (380cm)

Specific activity [Bq cm^{-3}] in first 100 cm of soil surrounding the concrete wall after 40 y of continous irradiation

Isotope	$T_{1/2}$	Soil
^{3}H	12.33y	3.1550E-02
^{7}Be	53.12d	2.6720E-03
^{22}Na	2.6y	3.4640E-09
^{24}Na	14.96h	1.8190E-04
^{32}P	14.26d	6.1480E-05
^{35}S	87.32d	8.2220E-17
^{45}Ca	162.61d	4.9460E-04
^{46}Sc	83.79d	1.0750E-03
^{54}Mn	312.3d	4.5480E-04
^{55}Fe	2.73y	1.2610E-02
^{65}Zn	244.26d	1.5550E-04

A_tot [Bq] per year in a Volume of 1.672E+9 cm3

5.2752E+07 < 1E+12 (release LIMIT) *

5.7918E+00 < 1E+5 (release LIMIT) *

A_tot_soil = 0.38 Bq/g ; CI** = 4.53E-02 ⇨ Exempt wastes

V_{1}_dirty=0.56*V_{1}_concrete

V_{tot}_dirty=47/ 45 % V_{tot}_concrete

Cost problems:

- ~4 m thickness soil roof -> public constraint
- 2651 m^3 of digging soil to be removed

*IAEA TECDOC-1000, 1998

** IAEA TECDOC -855, 1996

Design of the BEAM DUMP*

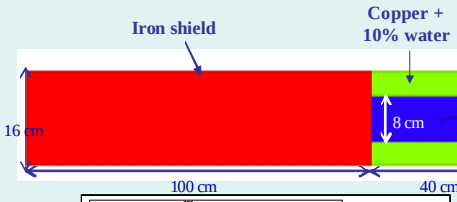

$^{132}Sn^{50+}$

Beam power = 19.8 kW (150 MeV/u)

Beam size s = 2 mm

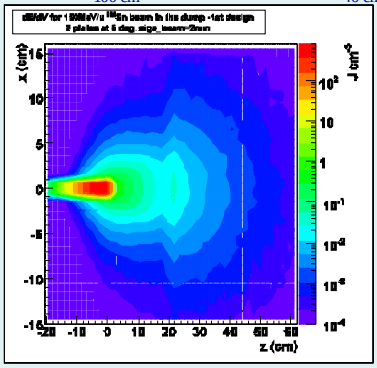

Beam size s = 2mm	
Ti [K]	?T_{max} [K]
293.15	535.7

⇨ Dump core under vacuum or inertial gas

!!! At the limit of the safety operational conditions

* Beam catcher FAIR Super-FRS | courtesy of H. WEICK (GSI)

Design of the BEAM DUMP: model comparison

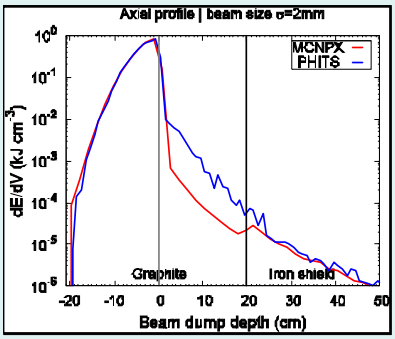

Axial profile of dE/dV : comparison

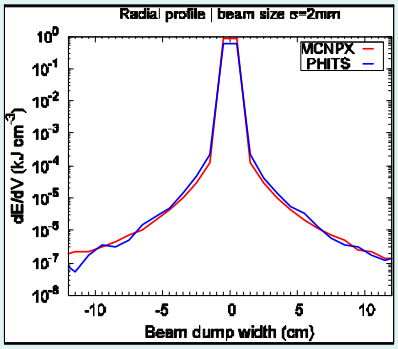

Radial profile of dE/dV : comparison

Design of the BEAM DUMP: beam size selection

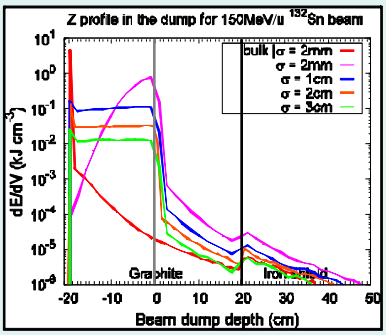

Axial profile of dE/dV variation with beam size

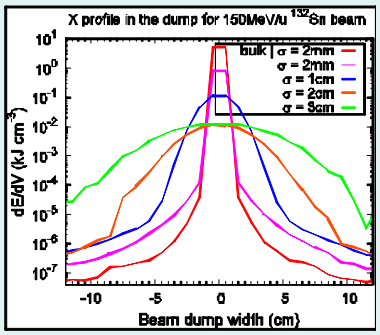

Radial profile of dE/dV variation with beam size

s = 1 cm -> kicker magnet length= 5m

Ti [K]	? T_{max} [K]
293.15	*374.43*

RESIDUAL RADIATION: Method

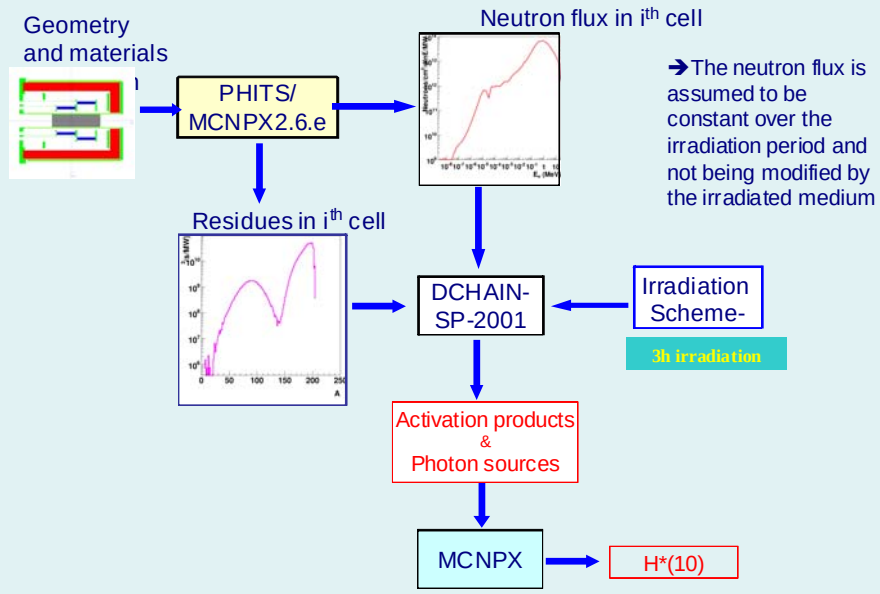

Design of the BEAM DUMP: Activation

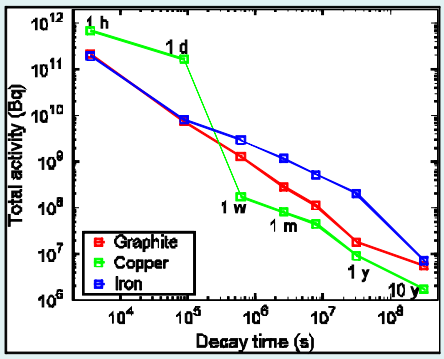

Total activity

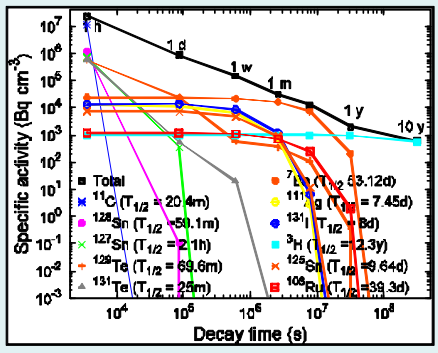

Graphite | dominant radionuclides

Design of the BEAM DUMP: Activation

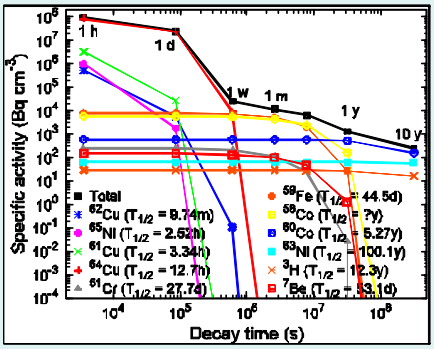

Copper | dominant radionuclides

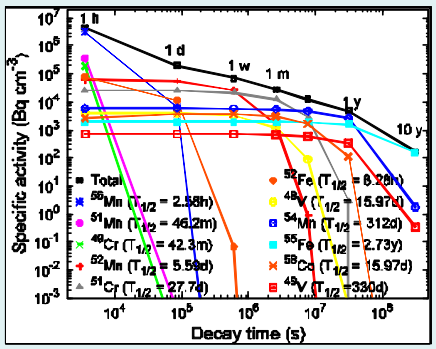

Steel | dominant radionuclides

Design of the BEAM DUMP: H*(10) | handling

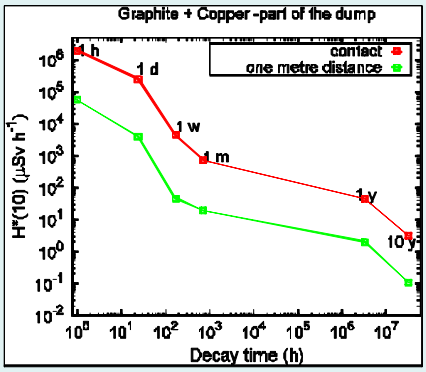

Core part | H*(10)

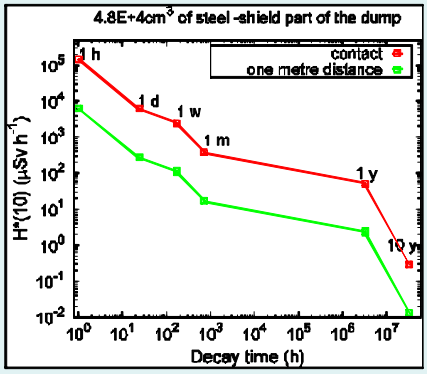

Shield part | H*(10)

Design of the BEAM DUMP: Shielding design

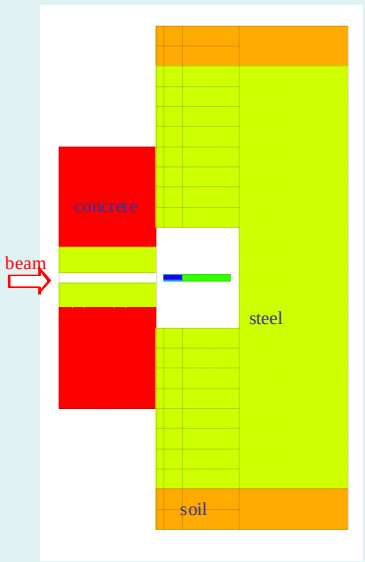

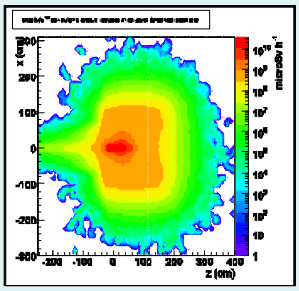

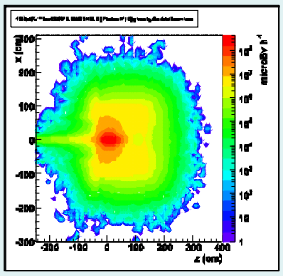

daniela.ene@cea.fr SATIF 9, Oak Ridge 2008 21

Design of the BEAM DUMP: Shielding design

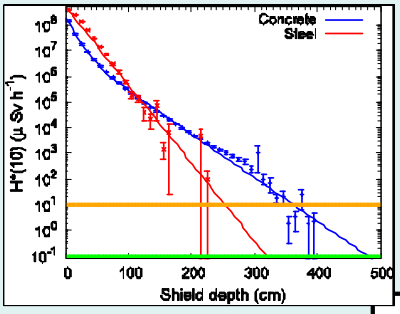

$$H^*(E_p, d/\lambda) = \frac{H_{1(E_p)}}{r^2}\exp\left[-\frac{d}{\lambda_1}\right] + \frac{H_{2(E_p)}}{r^2}\exp\left[-\frac{d}{\lambda_2}\right]$$

material	λ_1 [Sv m²]	λ_1 [g cm⁻²]	H_{λ_1} [Sv m²]	λ_2 [g cm⁻²]	SHIELD [cm]	
					Staff	Public
concrete	1.747E+03	23.7	1.338E+02	**60.36**	*364*	*480*
steel	-	-	5.000E+04	**112.14**	*254*	*320*

daniela.ene@cea.fr SATIF 9, Oak Ridge 2008 22

Conclusions

- *Both PHITS/JQMD and MCNPX/LAQGSM models are able to give a proper evaluation of the secondary neutron spectrum produced in heavy ions interactions around 100MeV/u;*
- *Placing the LINAC underground might reduce the shielding volume by ~45%;*
- *A preliminary analysis shows that the beam dump wedge shape with 40 cm graphite core and 100 cm iron shield might be a solution for the specific case;*
- *A kicker magnet 5 m long will be necessary to dilute the beam spot on the beam dump in order to assure safe operating conditions;*
- *Direct human access for the beam dump maintenance is not allowable;*
- *Two possible solutions for the beam dump lateral shielding were preliminary evaluated.*

daniela.ene@cea.fr SATIF 9, Oak Ridge 2008 23

Backup

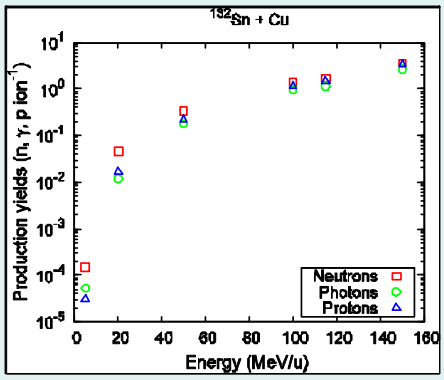

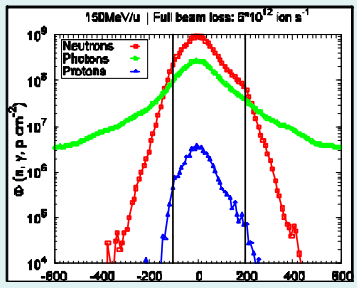

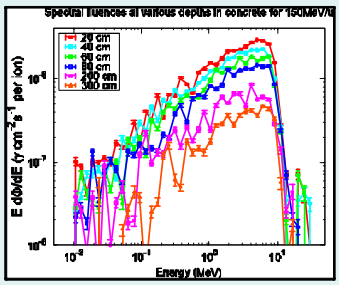

daniela.ene@cea.fr SATIF 9, Oak Ridge 2008 24

Session II

Measurements and calculations of induced radioactivity and activation data

Chair: F. Gallmeier

Radiological characterisation in support of intense pulsed neutron source D&D

B.J. Micklich
Argonne National Laboratory

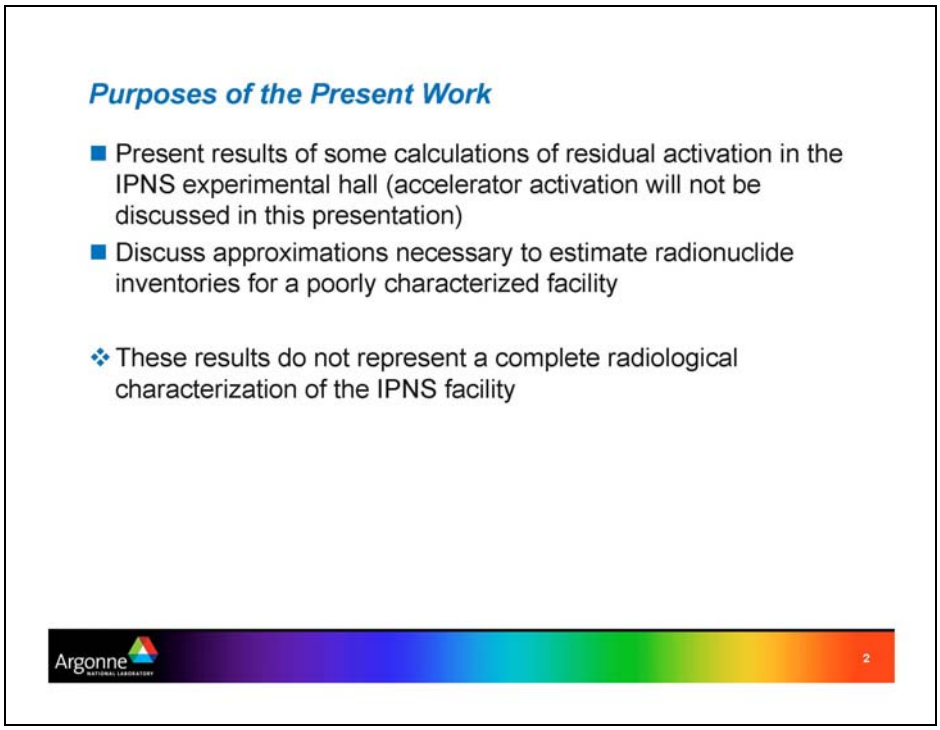

Attitudes About Safety

- When IPNS was first constructed, we had different ways of thinking about safety
  - Safety was someone else's business (our job was research)
  - Safety was incorporated into the job, but not necessarily planned for
  - IPNS personnel took pride in constructing and operating the facility on a very tight budget – but that is now coming back to haunt us
  - Modern facilities (e.g., SNS) are doing things the right way
- One big question is "At what point is IPNS no longer considered an accelerator facility?"
- And "If it's not an accelerator facility, would IPNS be considered a nuclear facility?"

Argonne NATIONAL LABORATORY 3

IPNS Facility

- IPNS was the first user-dedicated accelerator-driven neutron source in the world, commissioned in 1981
- Neutrons were produced by spallation/fission by 450-MeV protons striking depleted uranium target
- Proton beam pulsed at 30 Hz
- Average current 15 μA
- Target lifetime about four years operating 20-25 weeks per year
- Accelerated $2.63 \cdot 10^{22}$ protons (1.17252 A-hrs) in 9,368,550,687 pulses
- Liberated 0.53 g neutrons
- 95.4% reliability since 10/89

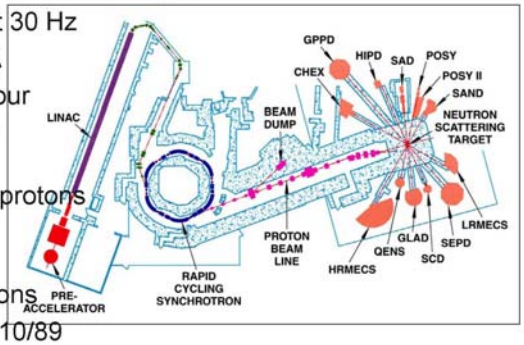

Argonne NATIONAL LABORATORY 4

IPNS Target / Moderators / Reflector

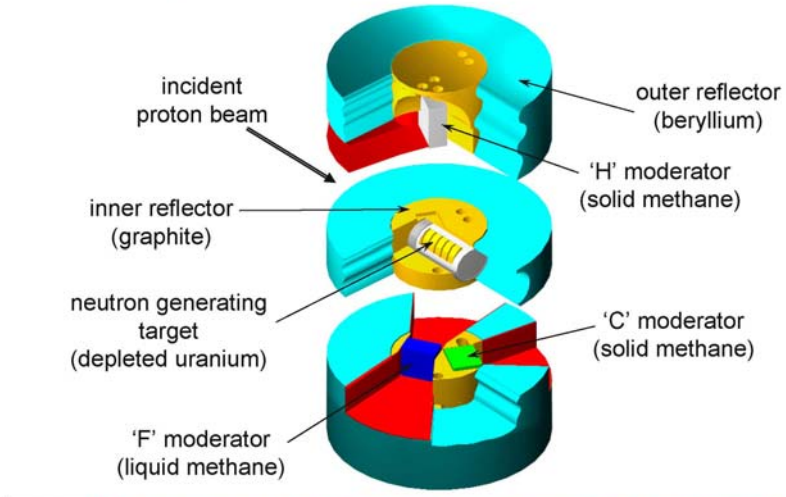

Argonne NATIONAL LABORATORY 5

Calculational Models

- The original MCNPX model of the IPNS target – moderator – reflector assembly was developed to study moderator neutronics, not to support calculations of component activation
- Many components were (are) not represented in the model
  - beamlines, choppers, windows, collimators, cooling lines for moderators, shielding
- No funds to pay to develop detailed target block model, and little interest in doing so
- D&D will rely on radioactive decay of activated materials, and in-situ characterization

Argonne NATIONAL LABORATORY 6

Calculational Method

- A Perl script is used to simplify the process of preparing input for and executing CINDER'90
- Irradiation histories from accelerator operations records
- A special version of MCNPX that directly tallies high-energy spallation products is used instead of writing the HISTP file
- The script is not currently able to run ALLCODE (used to order nuclides by activity, etc.)
- Stand-alone CINDER'90 must still be used for some applications

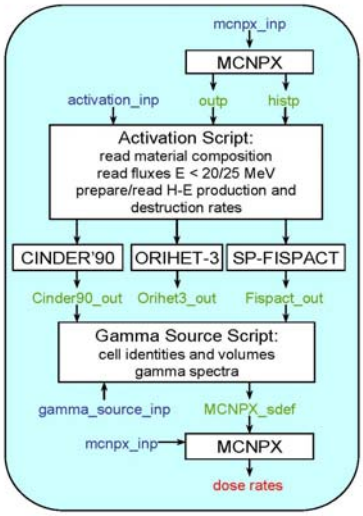

Argonne NATIONAL LABORATORY 7

IPNS Neutron Generating Target

- Eight depleted uranium disks in a stainless steel 304 housing
- Each disk 2.54 cm thick, 10.16 cm diameter
- Discs are clad with Zircaloy II, 0.5 mm on faces and 1.25 mm on edges

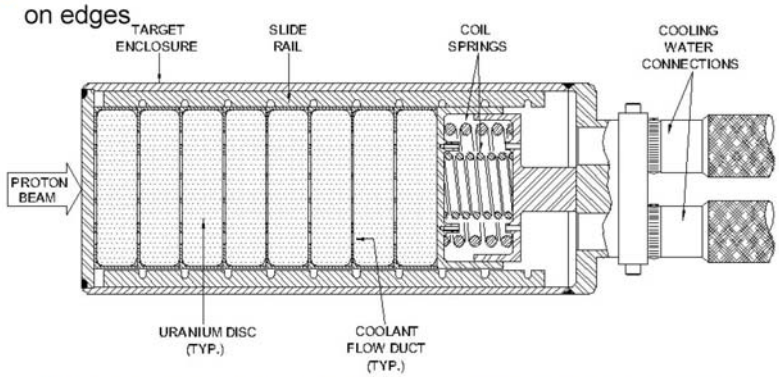

Argonne NATIONAL LABORATORY 8

IPNS Neutron Generating Target

- Three targets in facility, some disks from old targets in hot cells
- The last disk was SS304 in two targets, tantalum in one target
- The last target was composed of disks from two old targets

Argonne NATIONAL LABORATORY 9

Target Model

- Model as received (left), as modified (right)
- Largest difference is too much water in the old model
- Stainless steel target shell was completely missing

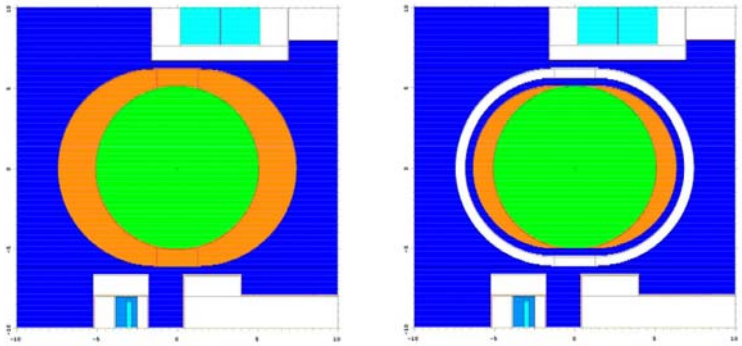

Argonne NATIONAL LABORATORY 10

Target Model

- Model as received (left), as modified (right)
- Beam incident from top
- Zircaloy cladding not modeled

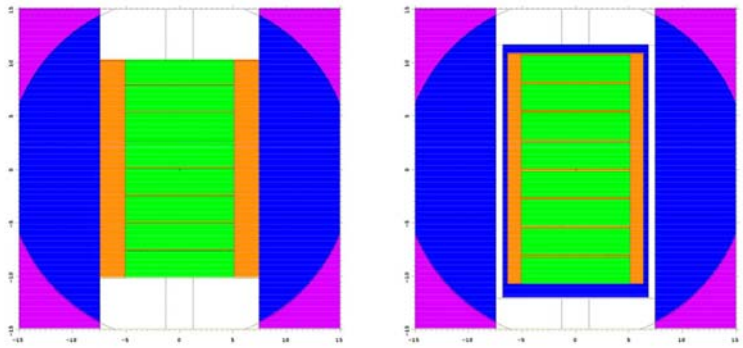

Argonne NATIONAL LABORATORY 11

Target Radionuclide Inventories

- The in-service target at the time of shutdown was fabricated using previously irradiated disks from the rear section of two previously irradiated targets
- Radionuclide inventory for disks from this target (NSU-4) was calculated in two steps
  - Initial activation script run to generate inventories after irradiation in first target
  - These inventories used as initial conditions for irradiation in second target
  - The second stage case had to be run with stand-alone CINDER'90 since the activation script cannot take results from one CINDER'90 run as initial conditions for another
- It is important to treat both irradiation periods, especially for the actinides

Argonne NATIONAL LABORATORY 12

Target Radionuclide Inventories

- Target inventories by activity on 31 March 08

Target nuclide	NSU-2 activity (GBq)	Target nuclide	NSU-3 activity (GBq)	Target nuclide	NSU-4 activity (GBq)
Fe 55	323	Fe 55	86	Ta182	18544
Cs137	269	Sb125	73	Nb 95	1874
Sb125	257	Pm147	71	Pr144	1508
Ba137*	254	Cs137	58	Ce144	1508
Pm147	246	Ba137*	55	Rh106	1464
Y 90	215	Y 90	48	Ru106	1464
Sr 90	215	Sr 90	48	Zr 95	1109
Co 60	164	Co 60	38	Y 91	824
H 3	136	Rh106	34	Fe 55	757
Rh106	78	Ru106	34	Pm147	750

Argonne NATIONAL LABORATORY 13

Target Radionuclide Inventories

- Target inventories by Category-3 fraction on 31 March 08

Target nuclide	NSU-2 Cat-3 frac.	Target nuclide	NSU-3 Cat-3 frac.	Target nuclide	NSU-4 Cat-3 frac.
Pu239	3.331E+0	Pu239	7.749E-1	Pu239	4.691E+00
Ac227	1.430E+0	Ac227	3.288E-1	Th228	1.935E+00
Th228	7.171E-1	Th228	1.993E-1	I 125	1.845E+00
U 232	4.449E-1	Pb210	1.039E-1	Ac227	1.468E+00
Rn220	3.736E-1	Rn220	9.731E-2	Rn220	1.010E+00
Sr 90	3.546E-1	U 232	7.872E-2	Ta182	8.083E-01
Pu238	1.299E-1	Sr 90	3.804E-2	Po210	5.993E-01
Cs137	1.212E-1	Cs137	2.623E-2	Pb210	5.410E-01
Pu240	6.107E-2	Po210	2.087E-2	U 232	4.553E-01
Pb210	5.701E-2	Pu238	1.209E-2	Sr 90	4.253E-01

Argonne NATIONAL LABORATORY 14

Target Radionuclide Inventories – NSU-4

- Activity (in GBq) for selected actinides on 31 March 08

nuclide	Second period only	Both periods	Ratio
Np237	1.02E-02	1.37E-02	1.34
Pu238	2.21E+00	3.33E+00	1.51
Pu239	4.93E+01	9.03E+01	1.83
Pu240	6.97E-01	2.45E+00	3.51
Pu241	3.13E+00	1.98E+01	6.32
Pu242	1.89E-07	2.47E-06	13.09
Am241	6.84E-03	1.17E-01	17.08
Am242*	4.34E-06	2.46E-04	56.62
Am242	4.32E-06	2.45E-04	56.62
Am243	9.72E-09	2.95E-07	30.40
Cm242	3.77E-03	9.69E-02	25.73
Cm243	1.20E-08	1.04E-06	86.27
Cm244	4.51E-09	2.86E-07	63.39

Argonne NATIONAL LABORATORY 15

Moderators Models

- Original model did not have moderator cans or vacuum jackets for “H” or “F” moderators, or vacuum jacket for “C” moderator

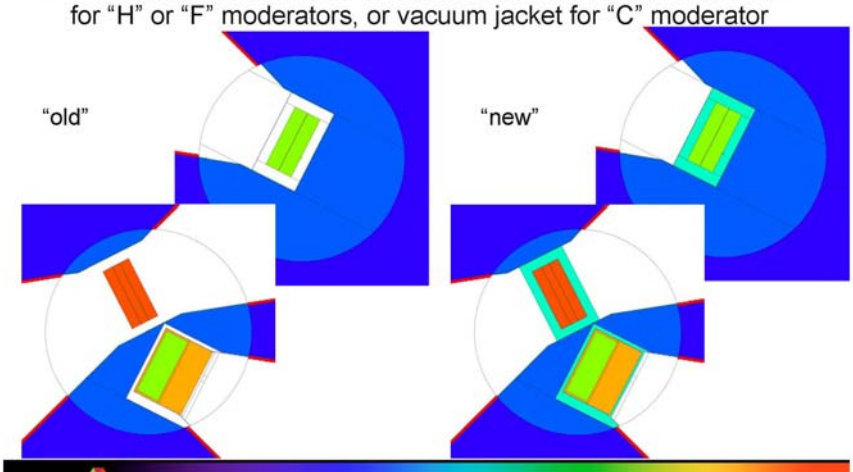

Argonne NATIONAL LABORATORY 16

IPNS Moderators – "C" Moderator

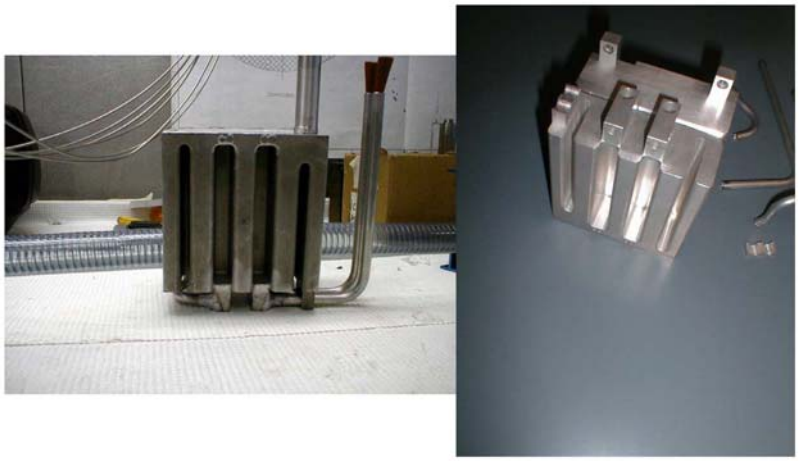

Argonne NATIONAL LABORATORY 17

Moderator Model – "F" Moderator

- Calculate mass of "F" moderator can from drawings – fill surrounding void space with appropriate density Al 6061 of representative composition (1.06% Mg, 0.69% Si, 0.55% Fe, 0.31% Cu, 0.21% Cr, 0.06% Mn, Zn, 0.02% Ti,V)
- Nuclides present in quantities > 37 MBq on 31 Mar 08
  - ^{22}Na (8.211e+7 s) 1490 MBq 48 mR/hr @ 1m
  - ^{55}Fe (8.615e+7 s) 266
  - ^{3}H (3.888e+8 s) 258
  - ^{54}Mn (2.697e+7 s) 146 1.86 mR/hr @ 1m
  - ^{65}Zn (2.107e+7 s) 100 0.73 mR/hr @ 1m
  - ^{51}Cr (2.393e+6 s) 40 0.02 mR/hr @ 1m

Argonne NATIONAL LABORATORY 18

Moderator Model – "H" Moderator

- Calculate mass of "H" moderator can from drawings – fill surrounding void space with appropriate density Al 6061 of representative composition (1.06% Mg, 0.69% Si, 0.55% Fe, 0.31% Cu, 0.21% Cr, 0.06% Mn, Zn, 0.02% Ti,V)
- Nuclides present in quantities > 37 MBq on 31 Mar 08
  - ^{22}Na (8.211e+7 s) 1366 MBq 44 mR/hr @ 1m
  - ^{55}Fe (8.615e+7 s) 244
  - ^{3}H (3.888e+8 s) 226
  - ^{54}Mn (2.697e+7 s) 112 1.43 mR/hr @ 1m
  - ^{65}Zn (2.107e+7 s) 75 0.55 mR/hr @ 1m
  - ^{51}Cr (2.393e+6 s) 39 0.02 mR/hr @ 1m

Argonne NATIONAL LABORATORY 19

Moderator Model – "C" Moderator

- Original model did not have vacuum jacket for "C" moderator
- Calculate mass of "C" moderator can from drawings – fill surrounding void space with appropriate density Al 6061 of representative composition (1.06% Mg, 0.69% Si, 0.55% Fe, 0.31% Cu, 0.21% Cr, 0.06% Mn, Zn, 0.02% Ti,V)
- Nuclides present in quantities > 37 MBq on 31 Mar 08
  - ^{22}Na (8.211e+7 s) 1414 MBq 46 mR/hr @ 1m
  - ^{55}Fe (8.615e+7 s) 474
  - ^{3}H (3.888e+8 s) 208
  - ^{65}Zn (2.107e+7 s) 148 1.08 mR/hr @ 1m
  - ^{51}Cr (2.393e+6 s) 114 0.05 mR/hr @ 1m
  - ^{54}Mn (2.697e+7 s) 85 1.08 mR/hr @ 1m

Argonne NATIONAL LABORATORY 20

Reflector Model – Inner Graphite Reflector

- Reflector made in several sections
- Aluminum plates top and bottom, support rings around center section, threaded rods to hold it all together
- Top and bottom plates added to model (Al 6061)
- Graphite is 'reactor-grade' (less than 0.5 ppm boron)

Argonne NATIONAL LABORATORY 21

Inner Graphite Reflector

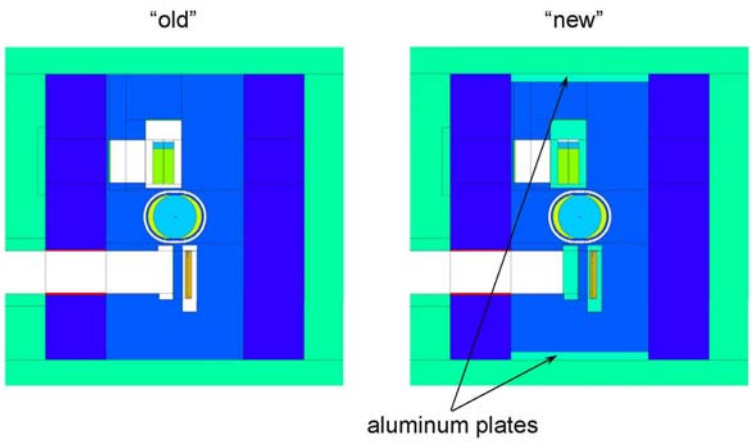

Argonne NATIONAL LABORATORY 22

Inner Graphite Reflector

- Radionuclide inventory of graphite on 31 Mar 08
  - ^{3}H 107 GBq
  - ^{7}Be 24.6 GBq
- Radionuclide inventory of aluminum top & bottom plate
  - ^{22}Na (8.211e+7 s) 1114 MBq 36 mR/hr @ 1m
  - ^{55}Fe (8.615e+7 s) 1043
  - ^{65}Zn (2.107e+7 s) 372 2.72 mR/hr @ 1m
  - ^{51}Cr (2.393e+6 s) 272 0.12 mR/hr @ 1m
  - ^{3}H (3.888e+8 s) 169
  - ^{54}Mn (2.697e+7 s) 91 1.16 mR/hr @ 1m

Argonne NATIONAL LABORATORY 23

Inner Graphite Reflector – Cadmium Decouplers

- In the final reflector stack, only 'F' and 'H' were decoupled
- Cadmium decouplers were included in model
- Radionuclide inventory of 'H' moderator cadmium decoupler
  - ^{113m}Cd (4.450e+8 s) 21.2 GBq
  - ^{115m}Cd (3.853e+6 s) 9.55 5.2 mR/hr @ 1m
  - ^{109m}Ag (3.960e+1 s) 6.29
  - ^{109}Cd (3.997e+7 s) 6.29
  - ^{110m}Ag (2.158e+7 s) 225 MBq 8.7 mR/hr @ 1m
  - ^{105}Ag (3.567e+6 s) 161
  - ^{101}Rh (1.040e+8 s) 59

Argonne NATIONAL LABORATORY 24

Inner Graphite Reflector – Cadmium Decouplers

- In the final reflector stack, only 'F' and 'H' were decoupled
- Cadmium decouplers were included in model
- Radionuclide inventory of 'F' moderator cadmium decoupler
  - ^{113m}Cd (4.450e+8 s) 22 GBq
  - ^{115m}Cd (3.853e+6 s) 9.6 5.2 mR/hr @ 1m
  - ^{109m}Ag (3.960e+1 s) 6.9
  - ^{109}Cd (3.997e+7 s) 6.9
  - ^{110m}Ag (2.158e+7 s) 235 MBq 9.1 mR/hr @ 1m
  - ^{105}Ag (3.567e+6 s) 176
  - ^{101}Rh (1.040e+8 s) 57

Argonne NATIONAL LABORATORY 25

Outer Beryllium Reflector

- Outer reflector has been in place for life of facility
- Aluminum cladding not modeled

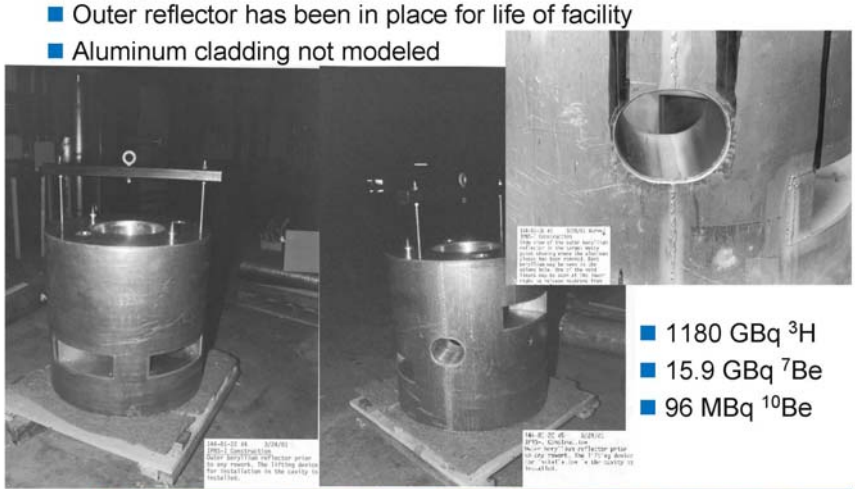

- 1180 GBq ^{3}H
- 15.9 GBq ^{7}Be
- 96 MBq ^{10}Be

Argonne NATIONAL LABORATORY 26

Monolith Shielding

- The IPNS shielding monolith contains ~2.5 meters of 'battleship steel' as the first layer of shielding (inside the atmosphere controlled volume)
- Dimensions known, material composition unknown (left over from Zero Gradient Synchrotron)
- Atmosphere not all that well controlled – was supposed to contain inert atmosphere of He, some reports that exhaust gas was only ½ helium – probably contains dispersible contamination
- Would the radionuclide inventory of the monolith steel shielding alone be sufficient to make IPNS a nuclear facility?
- Only the total amount of radioactivity matters (not specific activity Bq/g)

Argonne NATIONAL LABORATORY 27

Monolith Shielding

Argonne NATIONAL LABORATORY 28

Monolith Shielding

- Iron shielding extended out to approximate dimensions of atmospheric control barrier

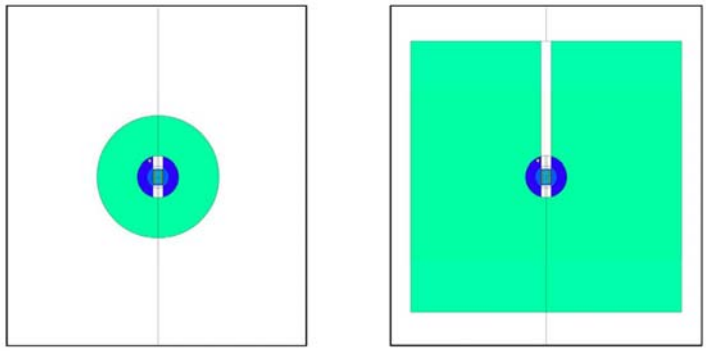

"old" "new"

Argonne NATIONAL LABORATORY 29

Activity in Monolith Shielding

- First calculation – assume shielding is 100% iron (on 31 Mar 08)
  - ^{55}Fe (8.615e+7 s) 18800 GBq Cat-3 fraction = 0.0943
  - ^{54}Mn (2.697e+7 s) 2930 GBq Cat-3 fraction = 0.0901
  - ^{59}Fe (3.844e+6 s) 242 GBq Cat-3 fraction = 0.0109
- Fe only would not cause an inventory above a Cat-3 level
- Estimate upper bound contribution from ^{60}Co – assume steel has 1000 ppm Co
  - ^{60}Co (1.664e+8 s) 13650 GBq Cat-3 fraction = 1.318
- Since it is unlikely that stainless steel would have been used as battleship steel, the radionuclide content of the iron shielding is probably under one Cat-3 equivalent

Argonne NATIONAL LABORATORY 30

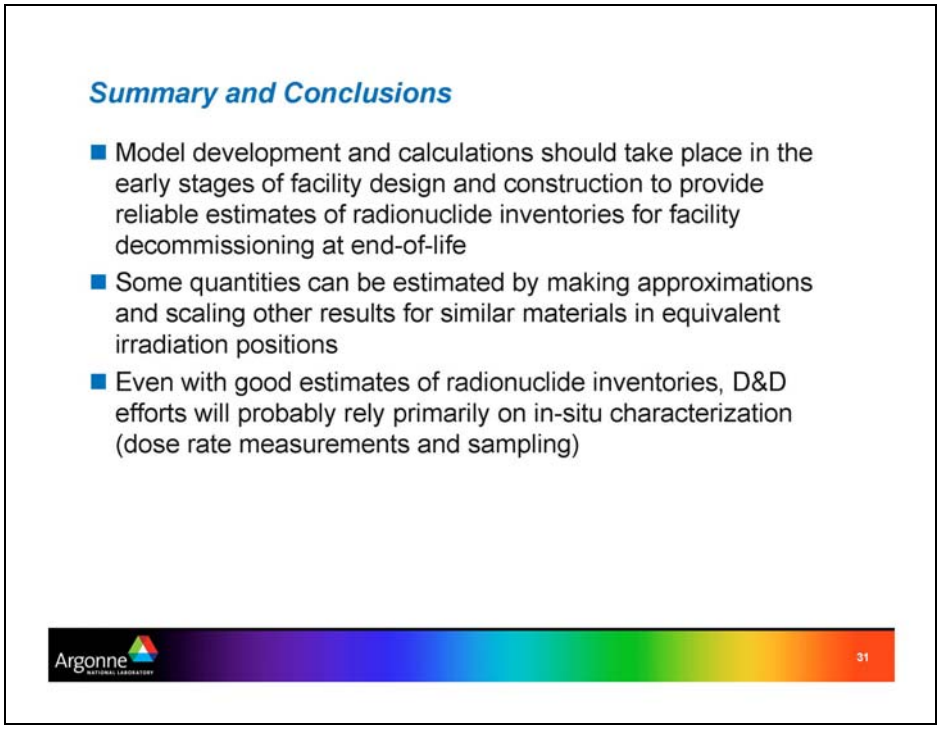
Summary and Conclusions
Model development and calculations should take place in the early stages of facility design and construction to provide reliable estimates of radionuclide inventories for facility decommissioning at end-of-life
Some quantities can be estimated by making approximations and scaling other results for similar materials in equivalent irradiation positions
Even with good estimates of radionuclide inventories, D&D efforts will probably rely primarily on in-situ characterization (dose rate measurements and sampling)
Argonne
31

Calculation of prompt and residual dose rates of the UCN guide system

M. Wohlmuther
Paul Scherrer Institut
Dep. Large Research Facilities

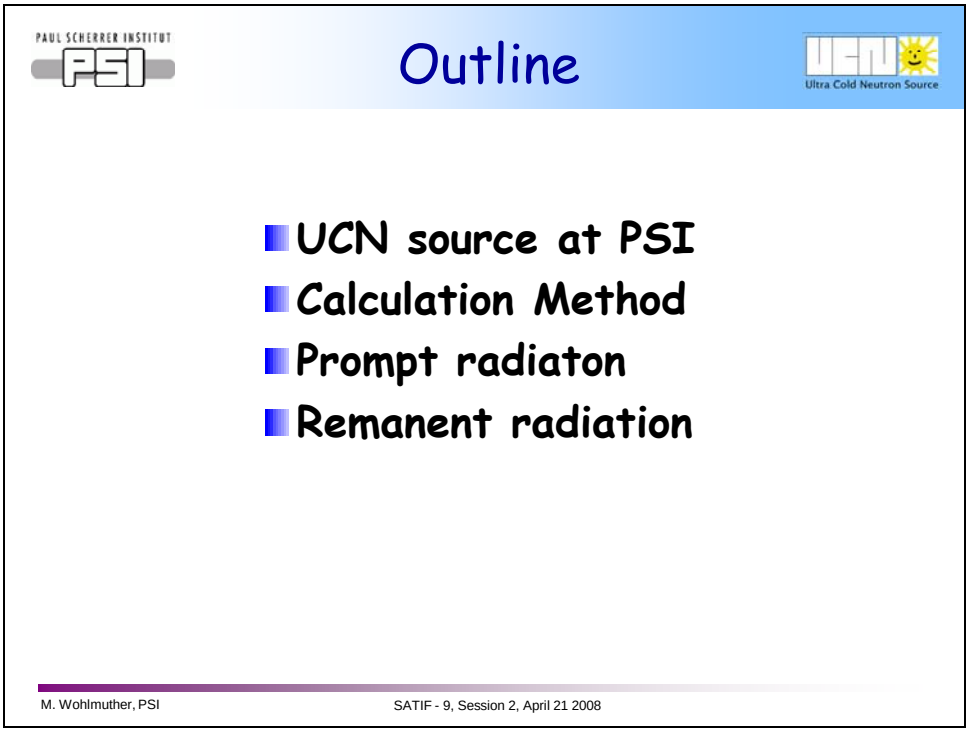

PSI p-Accelerators

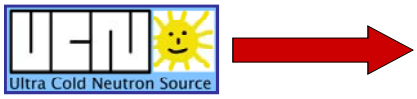

M. Wohlmuther, PSI SATIF - 9, Session 2, April 21 2008

The UCN source at PSI

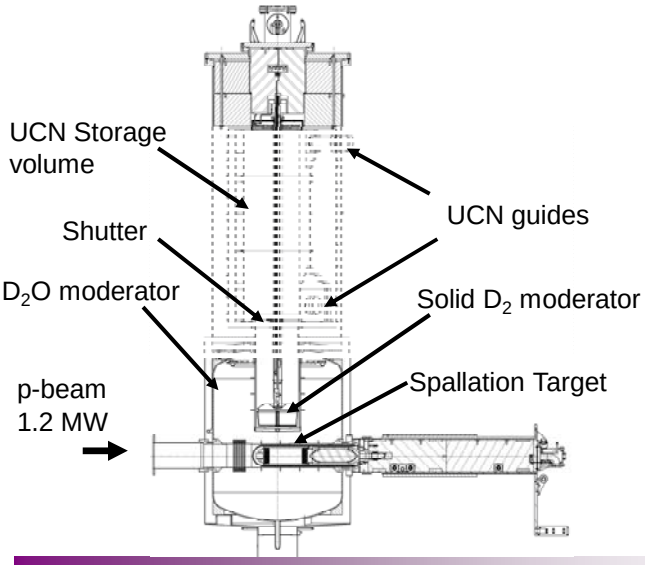

- Pulsed operation
- Full beam kicked from SINQ to UCN
- Duty cycle 1 %
- Proton pulse duration 4 – 8 s
- τ_n ~ 5 ms
- sD_2 @ 5K
- ρ_{UCN} ~ 1000 cm^{-3} in storage volume
- 3 UCN guides

M. Wohlmuther, PSI SATIF - 9, Session 2, April 21 2008

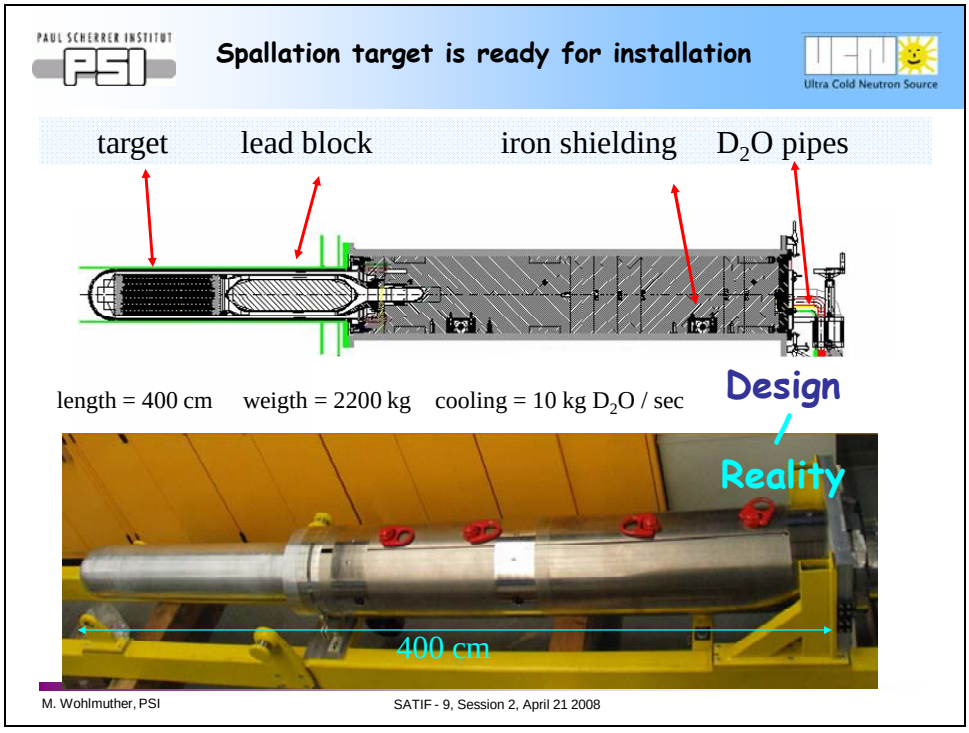
PAUL SCHERRER INSTITUT
PSI
Spallation target is ready for installation
Ultra Cold Neutron Source
target
lead block
iron shielding
D2O pipes
length = 400 cm
weigth = 2200 kg
cooling = 10 kg D2O / sec
Design
Reality
400 cm
M. Wohlmuther, PSI
SATIF - 9, Session 2, April 21 2008

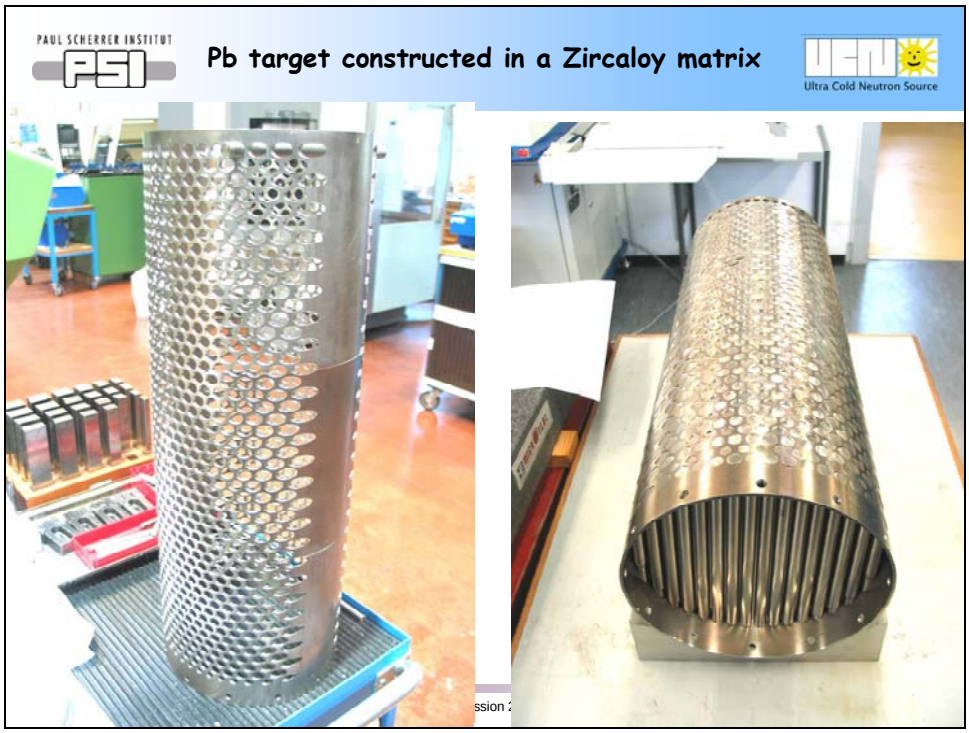
PAUL SCHERRER INSTITUT
PSI
Pb target constructed in a Zircaloy matrix
Ultra Cold Neutron Source

PAUL SCHERRER INSTITUT PSI

UCN Tank

Ultra Cold Neutron Source

To be installed soon …

M. Wohlmuther, PSI SATIF - 9, Session 2, April 21 2008

PAUL SCHERRER INSTITUT PSI

sD2 moderator – UCN window several shapes tested

Ultra Cold Neutron Source

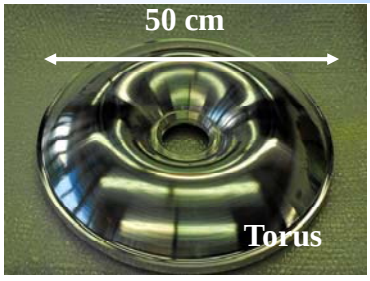

- Dome: AlMg3
- Pressure requirements
  i. p_i = 3 bar, p_a = 0 bar
  ii. p_i = 0 bar, p_a = 1 bar
- Thickness 0.5 mm
- measured UCN transmission 65%

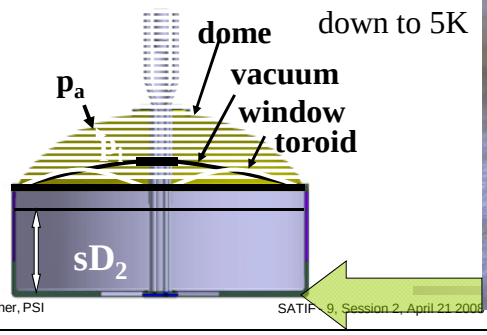

down to 5K

M. Wohlmuther, PSI SATIF - 9, Session 2, April 21 2008

sD2 moderator – UCN window several shapes tested

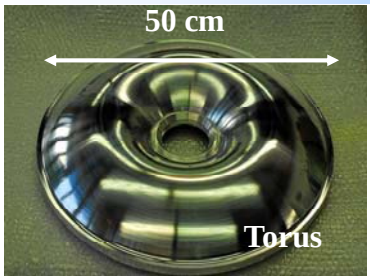

- Dome: AlMg3
- Thickness 0.5 mm
- measured UCN transmission 65%

down to 5K

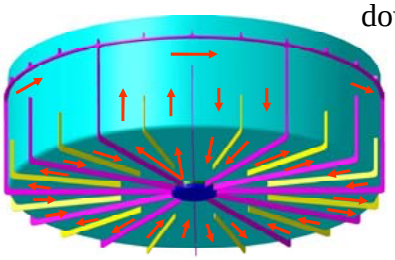

He flow direction

M. Wohlmuther, PSI SATIF - 9, Session 2, April 21 2008

UCN storage volume

Models of DLC coated storage volume tested for UCN performance
Phys. Rev. C 74, 055501 (2006)
and tightness: < 1.5 cm^2 total slit area in large storage volume expected
[losses ~ 10^{-4} per wall collision]

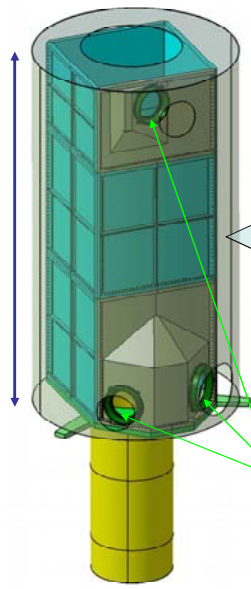

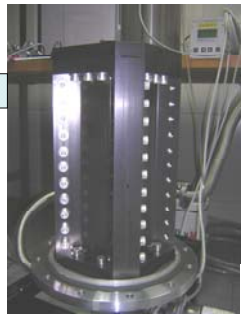

Design is finalized

3 openings for neutron guides which will serve 2 experiment areas and one test beam

M. Wol Session 2, April 21 2008

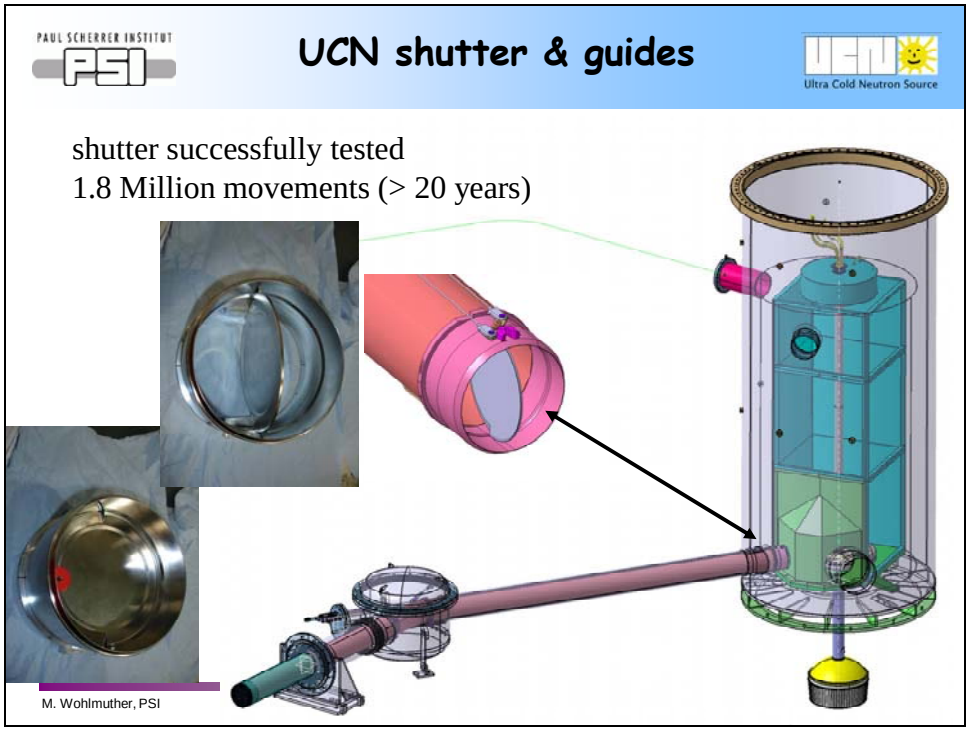
PAUL SCHERRER INSTITUT
PSI
UCN shutter & guides
Ultra Cold Neutron Source
shutter successfully tested
1.8 Million movements (> 20 years)
M. Wohlmuther, PSI

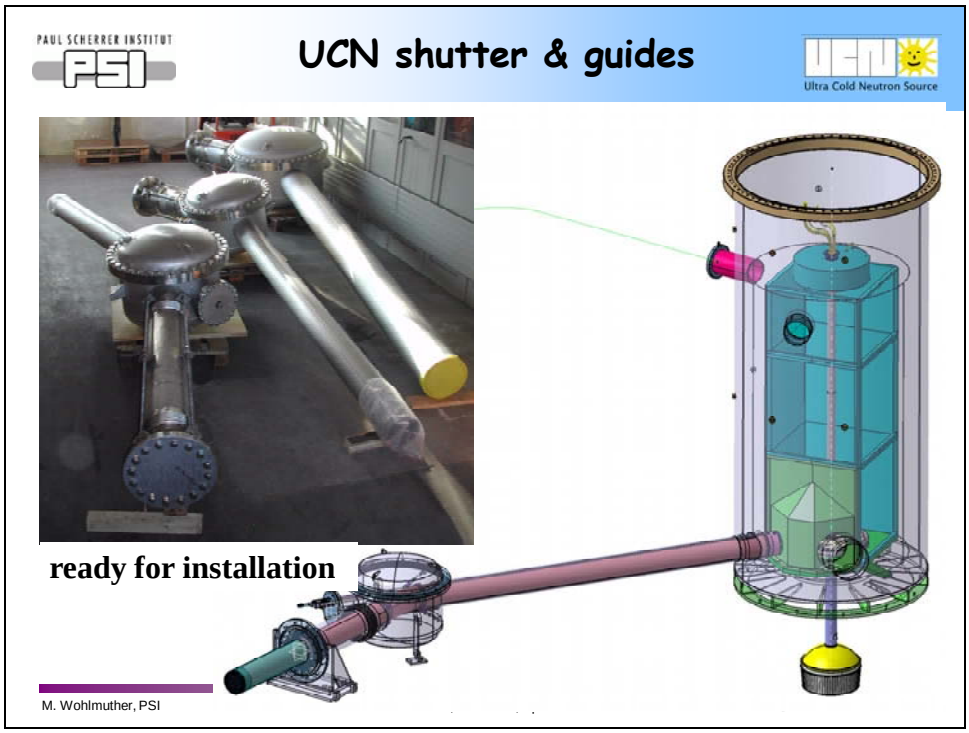
PAUL SCHERRER INSTITUT
PSI
UCN shutter & guides
Ultra Cold Neutron Source
ready for installation
M. Wohlmuther, PSI

Ultra Cold Neutron Guides

glass and stainless steel parts

UCN guides in production (Duran Glas)

Tests with UCN have started in Mainz and Grenoble

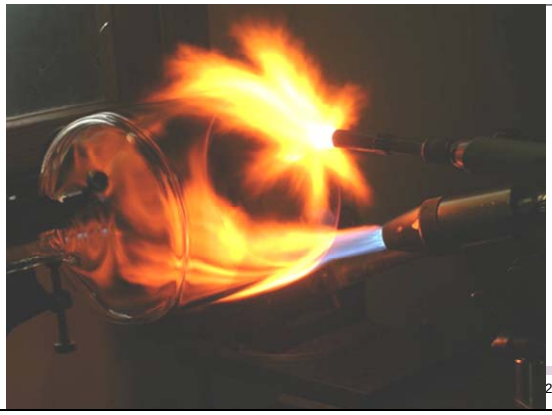

borosilicate glass
ID = 180 mm

coating: 300 nm NiMo non-magnetic (to be tested)

V_F ~ 230 neV measured

2008

Ultra Cold Neutron Guides

glass and stainless steel parts

UCN guides in production (Duran Glas)

Tests with UCN have started in Mainz and Grenoble

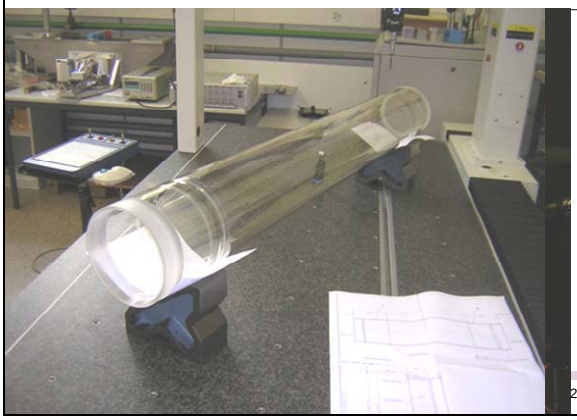

borosilicate glass
ID = 180 mm

coating: 300 nm NiMo non-magnetic (to be tested)

V_F ~ 230 neV measured

2008

Ultra Cold Neutron Guides

glass and stainless steel parts

UCN guides in production (Duran Glas)

Tests with UCN have started in Mainz and Grenoble

borosilicate glass
ID = 180 mm

coating: 300 nm NiMo
non-magnetic (to be tested)

V_F ~ 230 neV
measured

Experimental areas

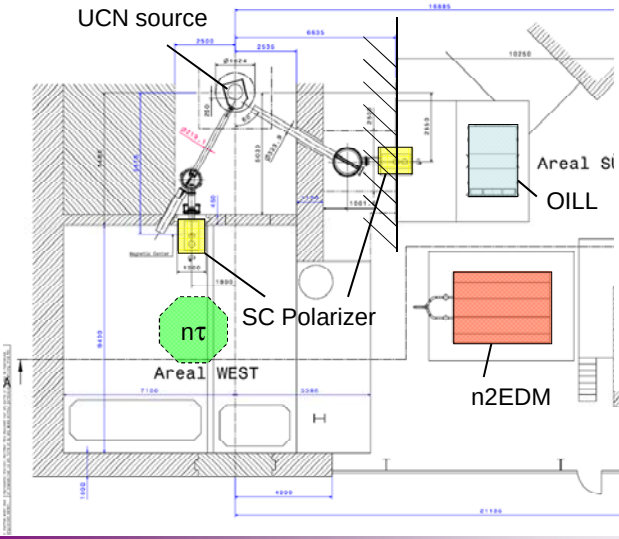

- Vacuum separation of source and experiment in maximum B-field
  ➔ gain factor of about 2 in intensity
- Deliver 100% UCN polarization to experiment
- 1 SC polarizer needed for EDM (prefer south area)

M. Wohlmuther, PSI SATIF - 9, Session 2, April 21 2008

The MCNPX model

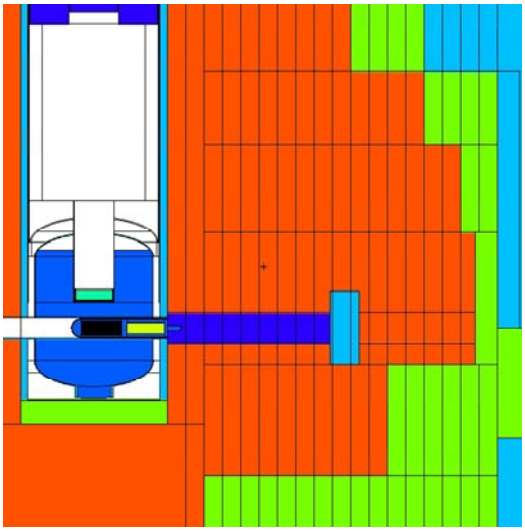

- Calculations performed with MCNPX 2.5.0
- Energy dependent weight windows were optimized iteratively
- Mesh size 10 x 12.5 x 15.5 cm^3
- ρ_{steel}=7.85 g/cm^3, ρ_{cast}=7.00 g/cm^3, $\rho_{concrete}$=2.4 g/cm^3

M. Wohlmuther, PSI SATIF - 9, Session 2, April 21 2008

The MCNPX model

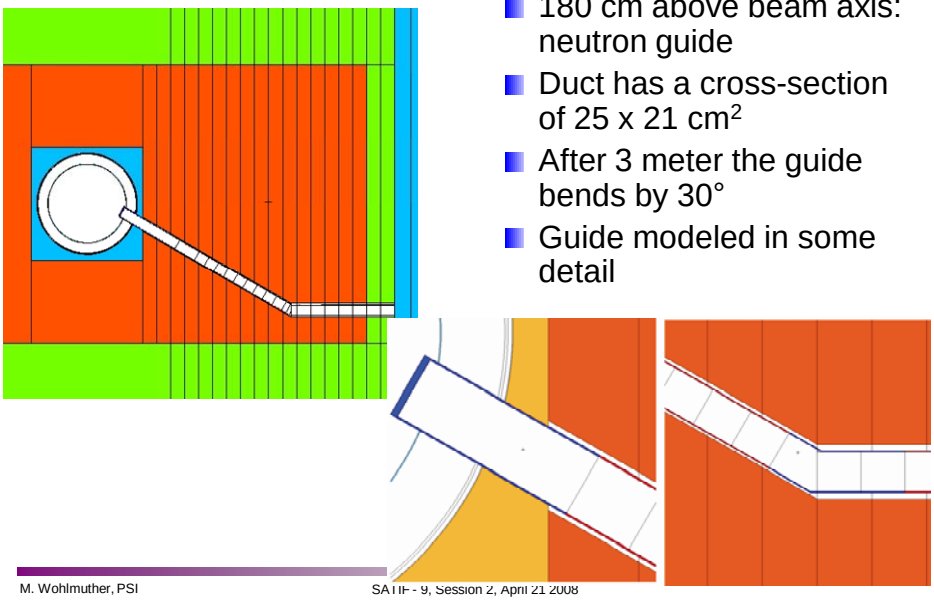

- 180 cm above beam axis: neutron guide
- Duct has a cross-section of 25 x 21 cm^2
- After 3 meter the guide bends by 30°
- Guide modeled in some detail

M. Wohlmuther, PSI SATIF - 9, Session 2, April 21 2008

Flux-to-Dose conversion

- An estimate of the prompt radiation is necessary, as the Duran glas parts of the UCN guide is glued to the steel parts.
- The UCN guide in forward direction with respect to the beam was used for the estimates of the prompt and remanent dose rates

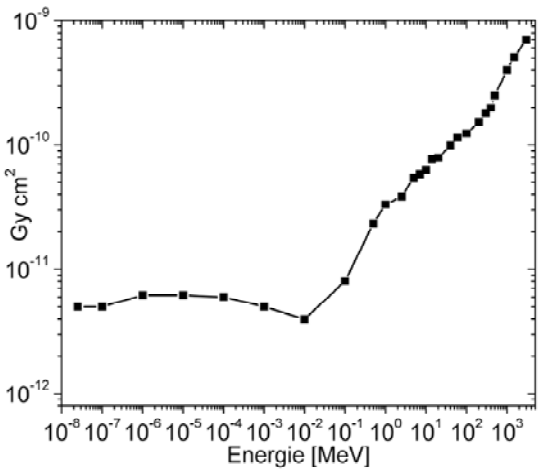

M. Wohlmuther, PSI SATIF - 9, Session 2, April 21 2008

Results

Description	Neutronflux	Neutronfluence	Prompt neutron Dose rate
	n/cm²/s/μA	n/cm²	Gy/h
Shutter (Steel) (2cm)	$2.637\ 10^{8}$	$1.823\ 10^{18}$	$2.001\ 10^{2}$
Steel Pipe (Steel) (50 cm)	$2.082\ 10^{8}$	$1.439\ 10^{18}$	$1.639\ 10^{2}$
1.Glas pipe (20 cm)	$6.610\ 10^{7}$	$4.569\ 10^{17}$	$6.934\ 10^{1}$
2.Glas pipe (20 cm)	$4.617\ 10^{7}$	$3.192\ 10^{17}$	$4.102\ 10^{1}$
3.Glas pipe (20 cm)	$3.266\ 10^{7}$	$2.257\ 10^{17}$	$2.530\ 10^{1}$
4.Glas pipe (20 cm)	$2.193\ 10^{7}$	$1.516\ 10^{17}$	$1.525\ 10^{1}$
5.Glas pipe (20 cm)	$1.420\ 10^{7}$	$9.815\ 10^{16}$	$9.055\ 10^{0}$
6.Glas pipe (20 cm)	$8.713\ 10^{6}$	$6.022\ 10^{16}$	$5.208\ 10^{0}$
7.Glas pipe (20 cm)	$5.263\ 10^{6}$	$3.638\ 10^{16}$	$3.010\ 10^{0}$
8.Glas pipe (20 cm)	$3.122\ 10^{6}$	$2.158\ 10^{16}$	$1.708\ 10^{0}$
9.Glas pipe (20 cm)	$1.793\ 10^{6}$	$1.239\ 10^{16}$	$9.550\ 10^{-1}$
10.Glas pipe (20 cm) before 30° bend	$1.040\ 10^{6}$	$7.192\ 10^{15}$	$5.406\ 10^{-1}$

M. Wohlmuther, PSI SATIF - 9, Session 2, April 21 2008

Results

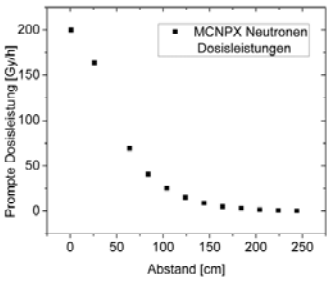

- Dose rates in the front part (steel) are dominated by thermal neutrons (25 %)
- As soon as bulk shielding neutrons in the keV range dominate
- All estimates have statistical errors lower than 3%.
- **The front steel part of the guide was constructed longer (~ 75 cm)**

Remanent dose rate

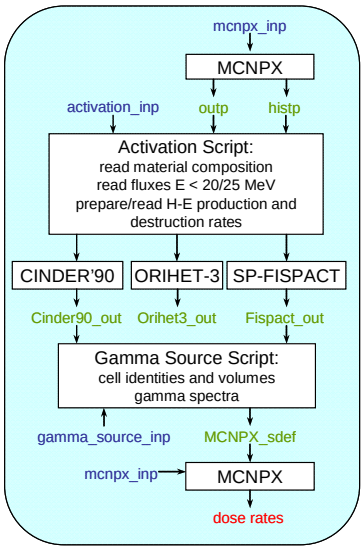

- The remanent dose rates of the guide were estimated to allow for the construction of an exchange mechanism for the UCN guide.
- Patched version of MCNPX 2.5.0 was used with the activation script and SP-FISPACT as the buildup and decay code.
- Subsequently an sdef was created with the Gamma script and a photon only transport was done with MCNPX 2.5.0

Remanent dose

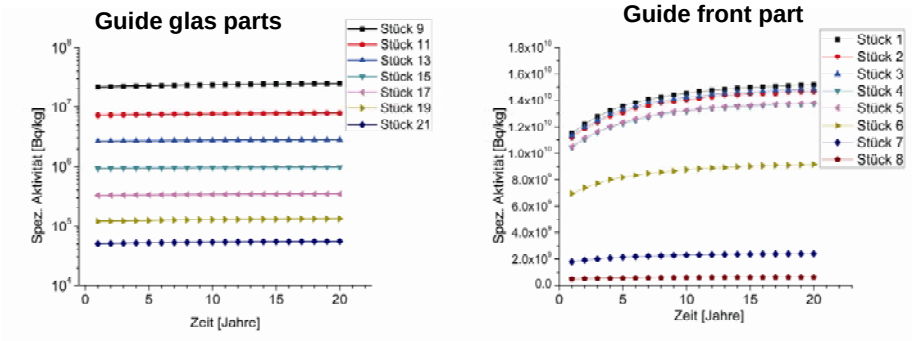

- Pieces 1 – 5 are made from steel, follow by the glas guide
- Equilibrium activity for glas activity reached very fast

M. Wohlmuther, PSI SATIF - 9, Session 2, April 21 2008

Remanent dose

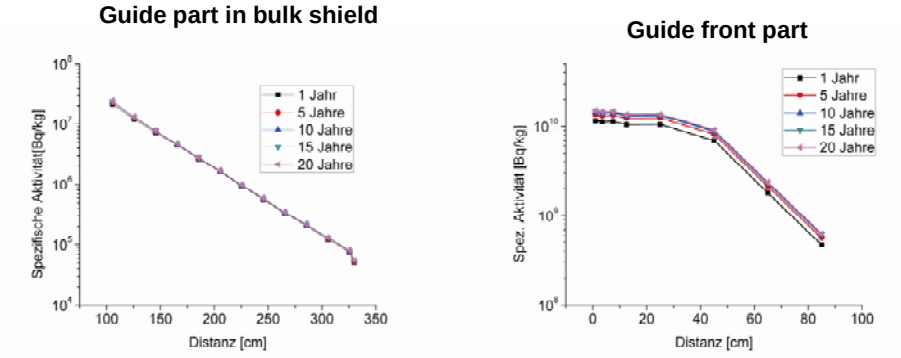

- After 15 years an equilibrium activity id reached for all parts of the UCN guide

M. Wohlmuther, PSI SATIF - 9, Session 2, April 21 2008

Remanent dose

Ultra Cold Neutron Source

Guide part in bulk shield

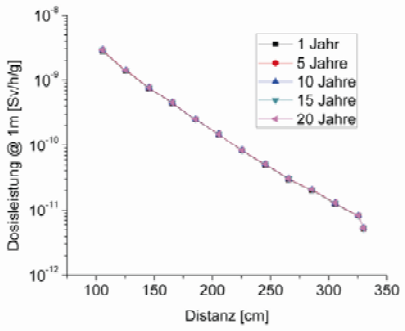

Guide front part

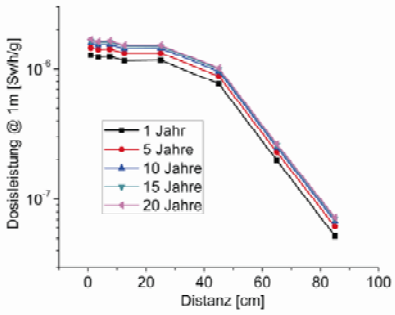

- Dose rates show the same behavior as activities

Remanent dose - cooling

Ultra Cold Neutron Source

Guide part in bulk shield

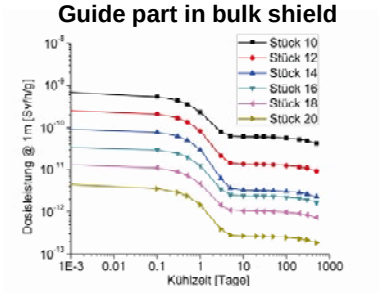

Guide front part

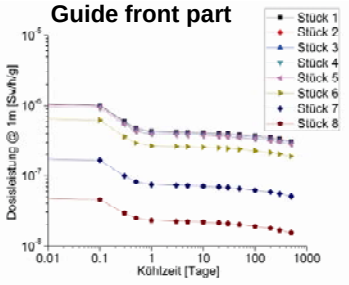

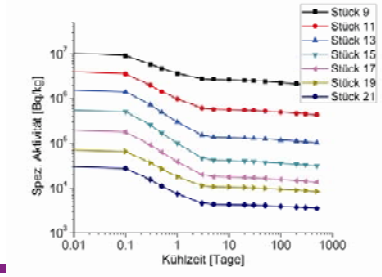

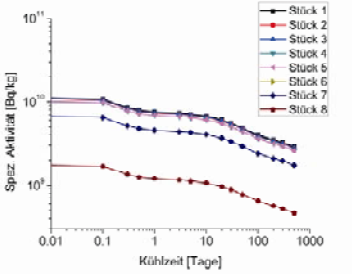

Remanent dose

Cooling time (days)	Gain factor dose rate Steel	Gain factor dose rate Glas	Gain factor spec. activity Steel	Gain factor spec. activity Glas
1	3.54	5.12	1.92	8.17
3	3.61	19.45	1.99	14.45
5	**3.65**	**28.73**	**2.04**	**15.68**
10	**3.70**	**30.69**	**2.17**	**16.00**
20	**3.79**	**30.95**	**2.39**	**16.37**
30	3.86	31.18	2.61	16.69
50	3.96	31.71	2.99	17.22
100	4.15	32.94	3.63	18.14
200	4.41	35.44	4.16	19.11

M. Wohlmuther, PSI SATIF - 9, Session 2, April 21 2008

Remanent dose

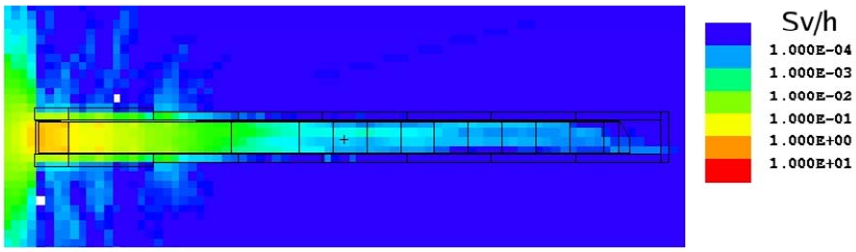

- Exchange mechanism, dose rates allowed (for transport):
  - 2 mSv/h at surface, 0.1 mSv/h @ 1m
- Over the first 70 cm 7.5 cm of Pb, followed by 5 cm steel
- Maximum dose rate 0.7 mSv/h @ surface

M. Wohlmuther, PSI SATIF - 9, Session 2, April 21 2008

An environment using nuclear inventory codes in combination with MCNPX for accelerator activation problems

F. Gallmeier,[1] **W.L. Wilson,**[2] **M. Wohlmuther,**[3] **B. Micklich,**[4] **E.B. Iverson,**[1]
E. Pitcher,[2] **W. Lu,**[1] **S. Cowell,**[2] **Ch. Kelsey,**[2] **G. Muhrer,**[2] **I.I. Popova,**[1] **P.D. Ferguson**[1]
[1]Oak Ridge National Laboratory, Oak Ridge, Tennessee, USA
[2]Los Alamos National Laboratory, Los Alamos, New Mexico, USA
[3]Paul Scherrer Institute, Villigen, Switzerland
[4]Argonne National Laboratory, Argonne, Illinois USA

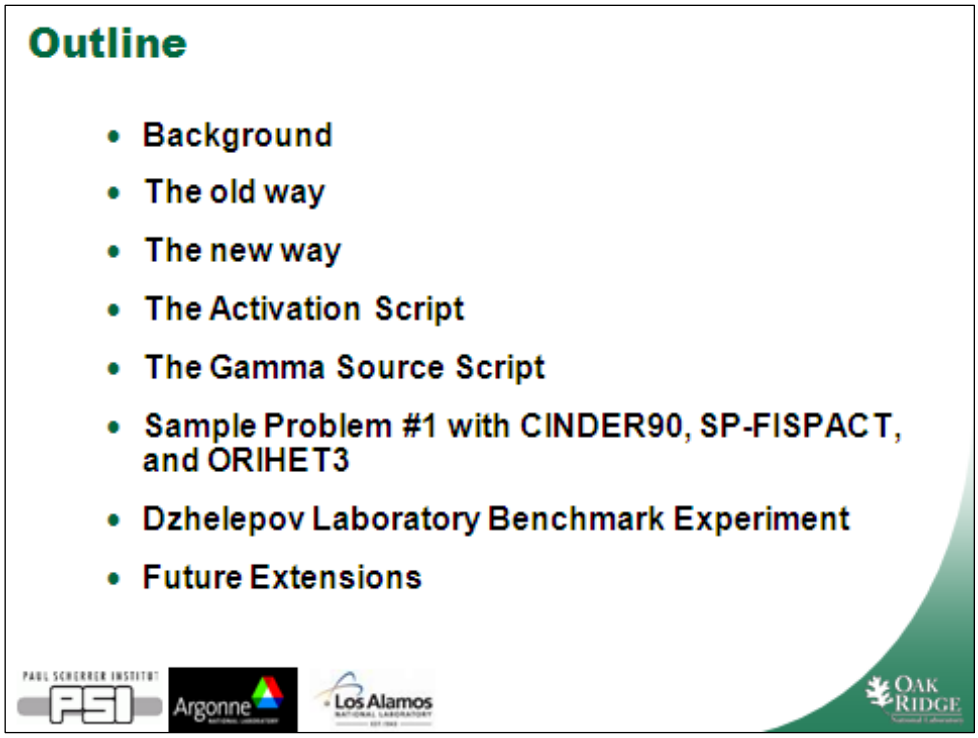

Background (1)

- An activation calculation involving high-energy applications involves typically two source terms:
  - HE cascade isotope production terms from event generators (spallation)
  - Low-E neutron activation from transport with evaluated data
- A analyst needs to provide and manipulate: material composition, volume, neutron fluxes, neutron activation cross sections, spallation product production rates for each cell/region of interest
- A tedious process

The Old Way

- Codes and shell scripts were available interfacing LAHET MCNP and CINDER'90
- Scripts were modified/extended to serve with MCNPX
- Complex system with multiple input files and user interaction

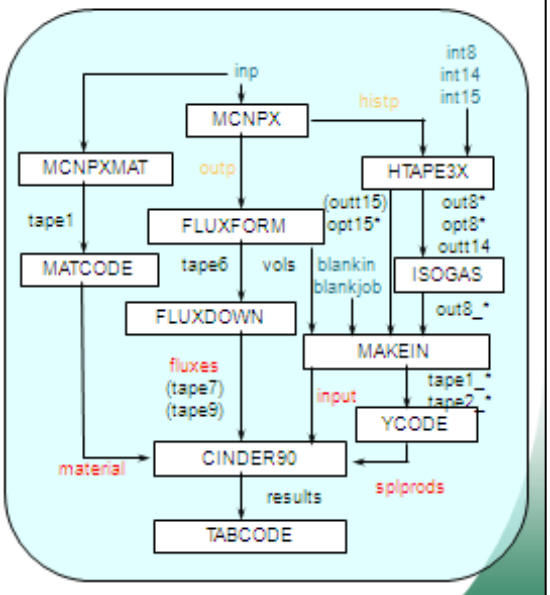

Background (2)

- Scripts dealt with the task of manipulating the flood of information for ADS
  - LANL scripts working with CINDER90
  - ORNL AAS framework working with ORIHET95 and FENDL2
  - PSI scripts working with SP-FISPACT and EAF
  - ...
- Meeting of users and CINDER90 developers at ICANS-XVI: it would be nice to have an easy to use tool to interface CINDER90 to MCNPX ⇒ launch a collaboration
- Meanwhile MCNPX started an effort to integrate CINDER90 to serve reactor burnup calculations

The New Way

- One script does a complete activation calculation with one user supplied input file minimizing the information needed
- Gamma Source Script prepares MCNPX source deck from decay gamma sources

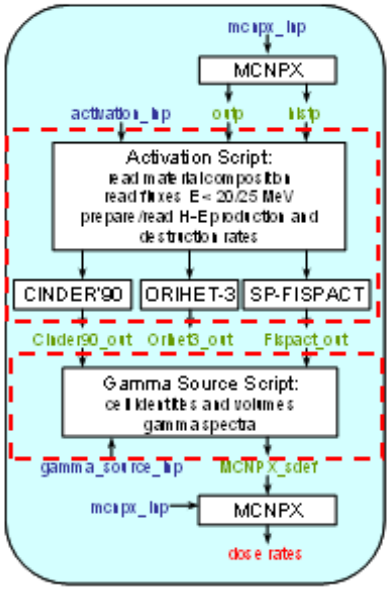

Instrumenting MCNPX_2.5.0

- Material and Cell information is obtained from regular MCNPX output
- Neutron fluxes for cells of interest are scored in any energy structure by tally f4:n; volume information is also read from tally output (mcnpx calculated, vol card, sd4 card) ⇒ f4:n card
- HE-isotope production/destruction information is written to HE event file histp on user request ⇒ post-process histp file ⇒ histp card
- Alternative: ORNL developed HE isotope production/destruction tally scores information within MCNPX and provides direct output ⇒ activ card
- Problem with Mix and Match:
  - Set transition from tabular to model regime to 20/25 MeV ⇒ phys:n 4j 20/25
  - Do not use tabular proton transport ⇒ phys:h 2j 1.0

PAUL SCHERRER INSTITUT PSI Argonne Los Alamos OAK RIDGE

Activation Script Input

- Ten blocks of input, each block separated by a blank line:
  - *codes:*
    specifies the executable code names of CINDER'90, ORIHET3, SP-FISPACT, HTAPE3X and the auxiliary codes TABCODE (from the CINDER'90 package), and GROUPIE (for generating multigroup activation cross sections from pointwise data) for the use with ORIHET3;
  - *title_lines:*
    allows the user to define descriptive text to be placed into the result files;
  - *files:*
    provides the file names of the MCNPX output and histp files, and a file of isotopic abundances by element;
  - *run_options:*
    provides directory names for storing the activation calculation input and output files, and switches to turn on/off spallation product and neutron activation based production terms in the activation analysis;
  - *cinder_options, fispact_options, orihet_options:*
    set parameters like choices of activation cross section data libraries, group structures, choice of weighting spectra for flux regrouping, output options and cutoff settings specific to the transmutation code to be used;
  - *normalization:*
    provides a normalization factor for scaling the activation calculation to the desired beam power;
  - *history:*
    provide irradiation and decay history in sub-blocks of time steps and relative power levels;
  - *cell_list:*
    provide a single MCNPX cell number or a list of MCNPX cell number for which an activation calculations is requested. Multiple cell numbers trigger a calculation for a merged cell conglomerate.

PAUL SCHERRER INSTITUT PSI Argonne Los Alamos OAK RIDGE

Typical Input

```
# modified sample problem 1
title_lines
  WNR Target 4  $RCSfile: inpactl
  test targets

codes
  cinder  cinder
  tabcode tabcode

files
  mcnpx_outp  act01o
  mcnpx_histp act01h
  biza_file   /look/here/bigza

# problem inputs and results end up
# in directory run_11
run_options
  dname    run
  dcounter 11

# CINDER90 is used
# for the activation analyses
cinder_options
```

```
…
# all n-fluxes and isotope prod./dest.
# rates are scaled by 2.8e13
normalization
  snorm     2.8e13

# two activation steps at full power
# are followed by three decay steps
history
2 1.0E+00
    1.0E+0 s -1.0 d
3 0.0E+00
    4.33 y  -4.5 y  -4.67 y

# a cell_list triggers a calculation
cell_list
  Hr target
  10

# now do case w/o low-E neutrons
run_options
  tabular  0

# for the cell we analysed before
cell_list
  Hr target
  10
```

CINDER'90 branch

- Database contains decay and activation cross sections, decay gamma spectra for 3400 isotopes
- Neutron activation cross sections in 65 energy groups
- Decay gamma structure fixed to 22 groups
- Considers material destruction in balance equations
- Activation script performs neutron flux rebinning with user defined spectra:
  flat, fission, fusion, spallation
- Tabulating of CINDER90 results with TABCODE

ORIHET3 branch

- Two decay libraries:
  - Nubasex: 3738 nuclides in decay library in 40 decay modes
  - Original ORIHET: 2456 nuclides in 7 decay modes
- Allows only isotope production rates as source terms
- Low-E neutron induced isotope production rates calculated in activation script using activation cross sections and neutron fluxes:
  - FENDL2 or EAF2003 continuous + GROUPIE (Cullen/LLNL) collapse
  - EAF2003/2001 multigroup (69,100,172,175,315 groups)
- Flexible decay gamma group structure

SP-FISPACT branch

- Original FISPACT modified by capability reading spallation induced isotope production rates to SP-FISPACT by M. Wohlmuther (originally by C. Petrovich/ENEA)
- Utilizes EAF neutron activation cross sections (EAF2003/2001) in multi-group structure (69,100,172,175,315 groups)
- Activation script performs neutron flux rebinning with user defined flux spectra:
  flat, fission, fusion

Execution

```
Prompt> activation.pl input output
```

Platforms

Activation script executes wherever Perl5 is installed and code executables are present

Cinder'90 is written in ANSI standard Fortran77

Activation Script+CINDER90 tested on Linux, Windows with various compilers

Activation Script+ORIHET3 or SP-FISPACT tested on LINUX

Outputs

- Script execution output reports flow of calculations
- File: cell_vol_dir_list

```
directory-name  total-volume  density region(cell-numbers)
testrun11  14.4792  6.49  10
testrun12  21.7187  16.6  20
```

- Input and Output files of all calculational steps in "directory-name" for respctive calculation

Example

- Sample problem #1: WNR experiment

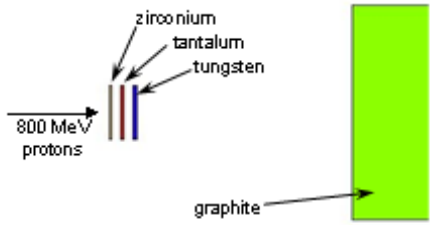

- Activity Buildup at 1second irradiation time for merged cells 10+20 (Zr+Ta)
- Comparing CINDER90/ORIHET3/SP-FISPACT performance

Example-Results

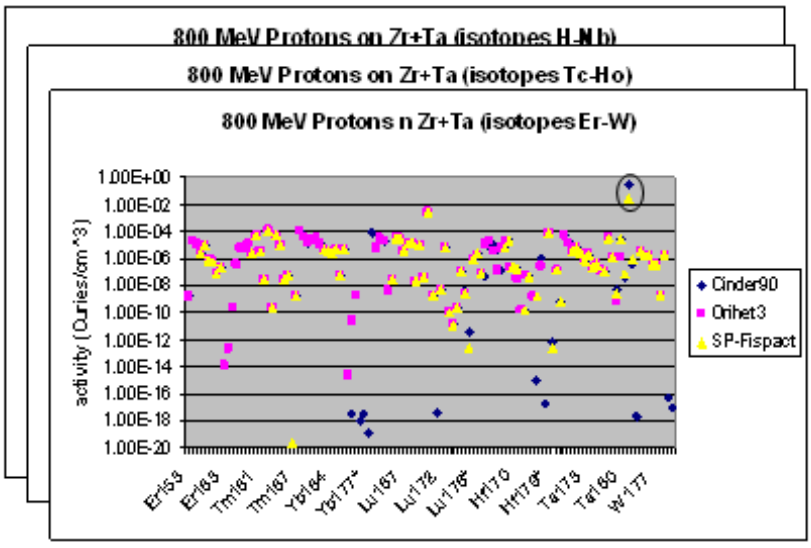

Benchmark Experiment

- Experiment conducted at the Dzhelepov Laboratory of Nuclear Problems in JINR Dubna (Russia)
- Experiment to determine axial distributions of radionuclide activity in a lead target
- Target was 80 mm diameter, composed of 32 1-mm samples separated by additional sections from 0.5 to 5 cm long
- Total target length 308 mm

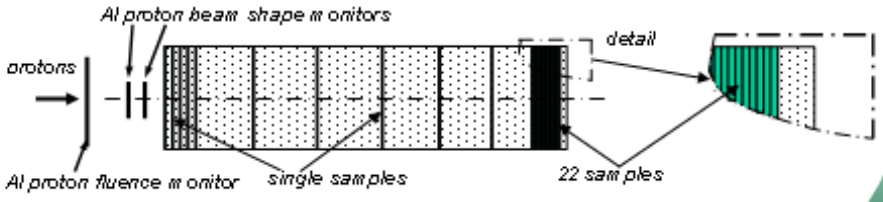

Code Comparison – 1 week

- Graph shows the twenty nuclides with greatest activity averaged over target disks (CINDER'90 ranking)
- Activity dominated by spallation products
- The three codes generally agree with a few differences > 2x

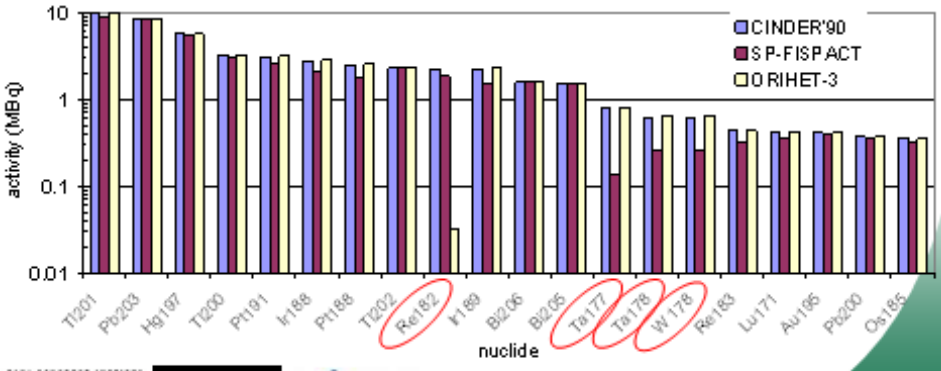

Comparison against experiment – fifth sample

- Activation within the 1-mm samples was provided for 28 nuclides
- Location: 2.4-2.5 cm from target front
- Underprediction compared to experiment for low & medium Z
- Overprediction compared to experiment for high Z

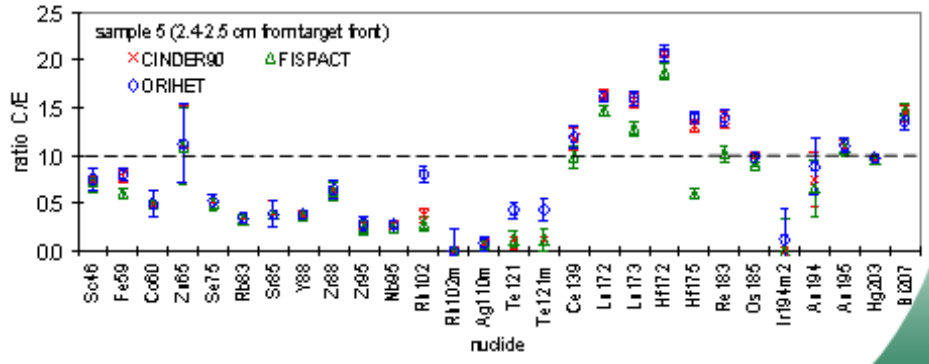

Activity vs. Depth

- The three codes agree with each other, but are about half of the measured values
- Shape of curve generally agrees with experiment

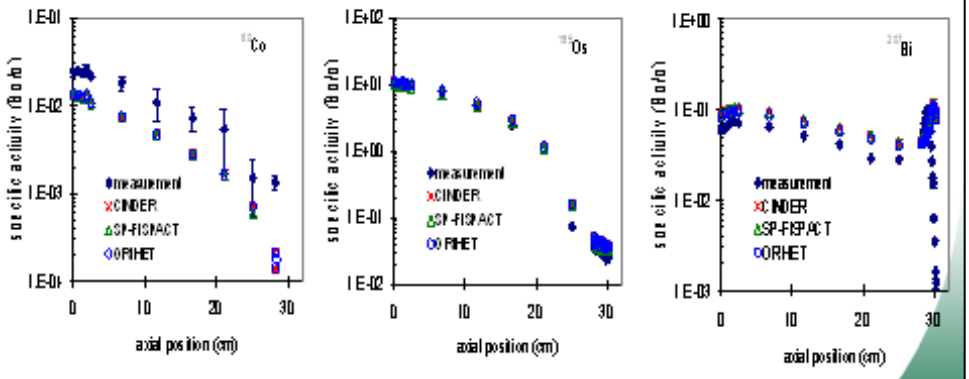

Concluding Remarks

- Activation script works reliably, and simplifies tremendously inventory calculation in combination with MCNPX
- Plans of a CINDER90 release including the activation and gamma source scripts
- Improvements underway:
  - Activation calculations produce a wealth of data
    ⇒ post-processing script is being developed to extact particular isotopic data or leading isotopes for a quantity of interest and a time step; graphical presentation desired
  - Spallation products of material impurities are insufficiently sampled in MCNPX
    ⇒ improvements by not sampling the collision partner at HE interactions, but perform a HE-interaction for each material component at each interaction point
- Improvements desired
  - Dealing with Mix&Match of MCNPX
  - Uncertainty analysis

Simulation of the radionuclide inventories in an ISAC TRIUMF UC_x target

I. Remec
Oak Ridge National Laboratory, USA

R.M. Ronningen
National Superconducting Cyclotron Laboratory, Michigan State University, USA

Introduction

- **ISAC (Isotope Separator and Accelerator) facility at TRIUMF**
  - **500-MeV proton beam**
  - **thick targets, typically 10-100 g cm^{-2}**
  - **target materials selected for the optimal yield of desired isotopes**
- **Currently actinide targets are under development**
  - **Isotopic inventories need to be predicted for planning targets operation and post-operation handling**
- **Motivation**
  - **Opportunity to compare code systems**
  - **Anne Trudell (TRIUMF) provided target geometry and suggested to compare against FLUKA simulations**

2 Managed by UT-Battelle
for the Department of Energy

Presentation_name

OAK RIDGE National Laboratory

Target Foil Materials

Typical target materials:
refractory metal foils W, Nb, Ta, ~0.025 mm thick

Composite foils of thin layers of refractory carbides (SiC, TiC, ZrC, ~ 0.2 mm thick, ~ 50-60% theoretical density) deposited on flexible exfoliated graphite sheet

Under development: composite foils with layers of UC, UC2, ThC on flexible graphite

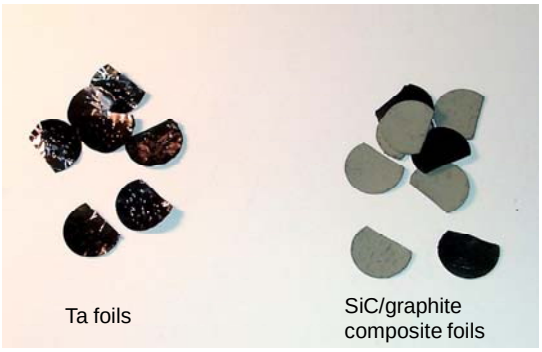

- Source: Marik Dombsky (ISAC, Triumf) Fabrication of ISAC High Thermal Conductivity Composite Target Materials, presented at WATD-2006

3 Managed by UT-Battelle for the Department of Energy

Presentation_name

Foil Details

- **UC_x target (from Anne Trudell):**
  - **foils of composite material**
  - **0.3 mm layers of UC2 at 6.2 gcm^{-3}**
  - **0.13 mm thin exfoliated C foil at 1.5 gcm^{-3}**
  - **0.1 mm thick gap between the foils**
  - **diameter 18 mm, truncated at one side at 5 mm from the center**
  - **foils stacked together to the total length of ~157 mm**
  - **total thickness is ~ 55 gcm^{-2} of UC2 and 4.5g/cm^{-2} of C**
  - **for simulations homogenized (3.88 g cm^{-3})**

4 Managed by UT-Battelle for the Department of Energy

Presentation_name

Driver Beam

- **500 MeV protons**
  - **(range ~ 526 mm in homogenized target material)**
- **Gaussian beam profile with FWHM = 6 mm**
- **200 µA current**
  - **100 kW**
  - **1.25 10^{15} protons/s**
- **Assumed 7 days irradiation**

Simulation Tools

- **MCNPX (particle transport) and**
- **CINDER90 (activation)**

- **PHITS (particle transport) and**
- **DCHAINSP 2001 (activation)**

Model of the Target for Simulations

Container tube (oven):
- 18 mm inner diameter
- 157 mm length (inside)
- 0.5 mm thick Ta

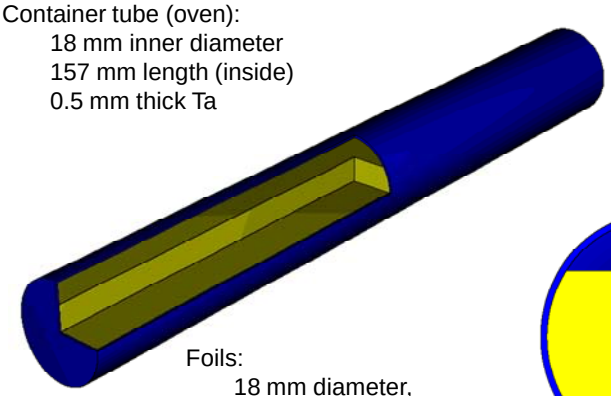

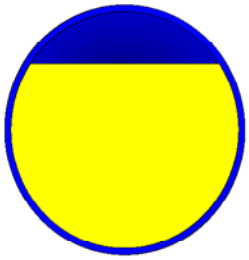

Foils:
- 18 mm diameter, truncated at 5 mm above the center (to provide effusion path)

7 Managed by UT-Battelle for the Department of Energy

Presentation_name

Comparison of Total Activity

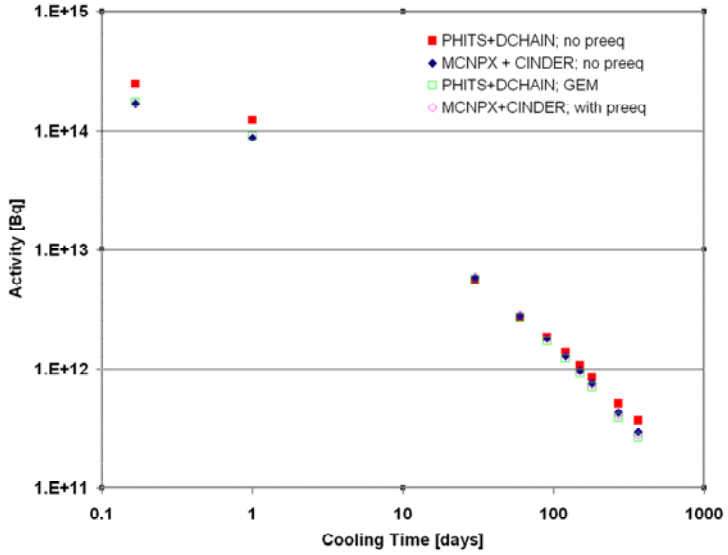

8 Managed by UT-Battelle for the Department of Energy

Presentation_name

Comparison of "Top Ten" at End Of Bombardment

	PHITS+ DCHAINSP 2001		MCNPX+ CINDER90		Ratio
Nuclide	Rank	[Bq]	Rank	[Bq]	
C 11	1	3.27E+13	1	1.67E+13	0.51
U 237	2	1.02E+13	2	8.39E+12	0.82
Rh105	3	8.23E+12	3	5.59E+12	0.68
Ag109m	4	7.59E+12	5	5.46E+12	0.72
Pd109	5	7.58E+12	8	5.02E+12	0.66
Rh107	6	7.52E+12	9	5.00E+12	0.67
Tc101	7	7.15E+12	4	5.51E+12	0.77
Ag112	8	7.06E+12	7	5.10E+12	0.72
Tc102	9	6.82E+12	6	5.21E+12	0.76
C 10	10	6.67E+12	294	6.82E+11	0.10
Pa237	13	6.25E+12	11	4.90E+12	0.78
Nb97	14	6.11E+12	10	4.94E+12	0.81
	Sum	1.14E+14		7.26E+13	0.64
	Total	6.62E+14		7.78E+14	1.18

9 Managed by UT-Battelle for the Department of Energy

Presentation_name

Sum of Threshold Quantity Ratios (TQR) For DOE Category 3 Nuclear Facility

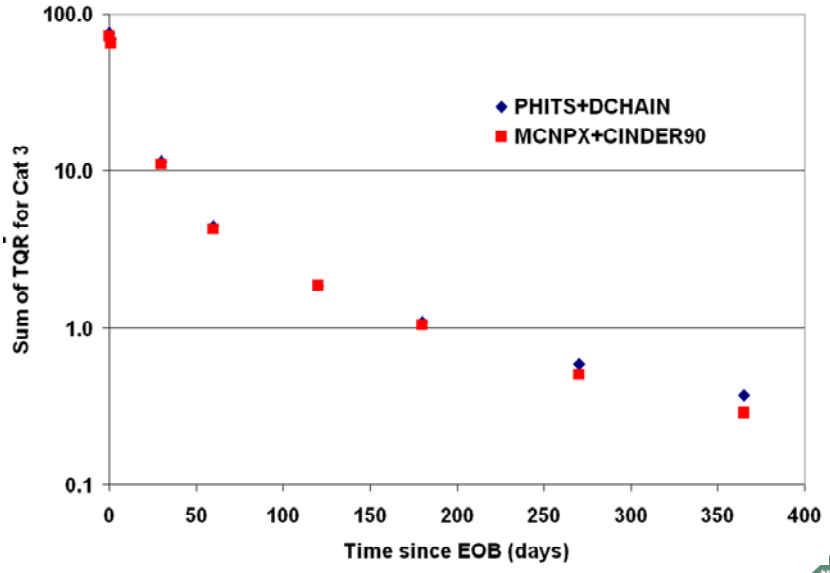

10 Managed by UT-Battelle for the Department of Energy

Presentation_name

RMR1

"Top Ten" Contributors to CAT-3 at EOB

Nuclide	PHITS + DCHAINSP		MCNPX + CINDER
I 131	37.06		37.87
I 126	20.51		16.38
I 124	5.69		5.86
I 125	4.89		5.44
I 133	2.91		3.58
Rn220	2.28		1.20
Po210	0.45		0.27
I 130	0.24		0.15
Kr 88	0.13		0.15
Nb 96	0.11	I 135	0.12
Sum	74.27		71.03
Total	76.40		73.16

11 Managed by UT-Battelle for the Department of Energy

Presentation_name

Decay Heat Comparison

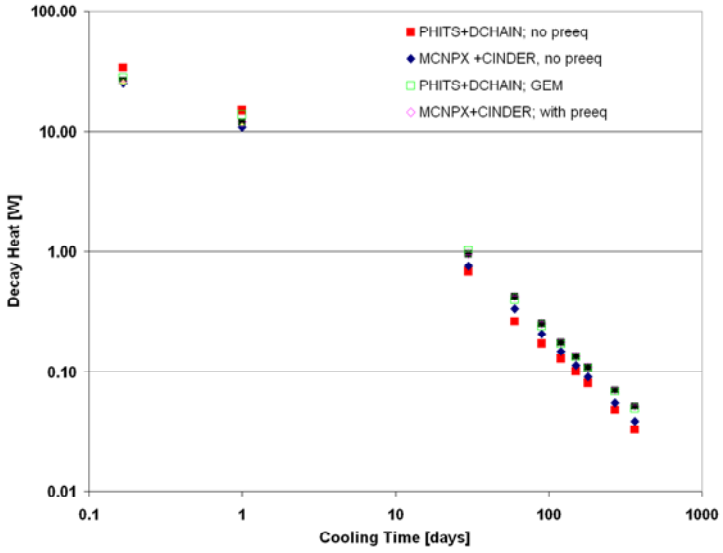

12 Managed by UT-Battelle for the Department of Energy

Presentation_name

Gamma Source Intensity Comparison

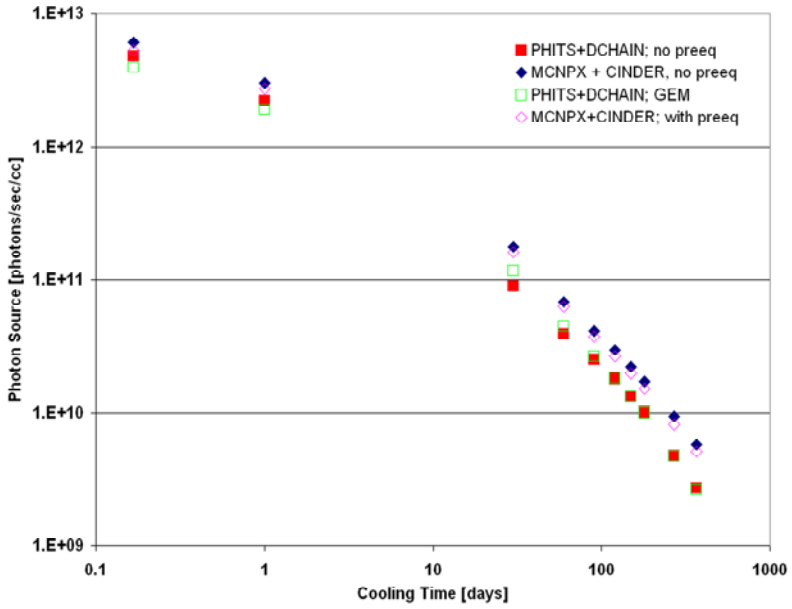

13 Managed by UT-Battelle
for the Department of Energy

Presentation_name

Energy Distribution of Gamma Source 7 Days Irradiation, 4 h Cooldown (UC_x Only)

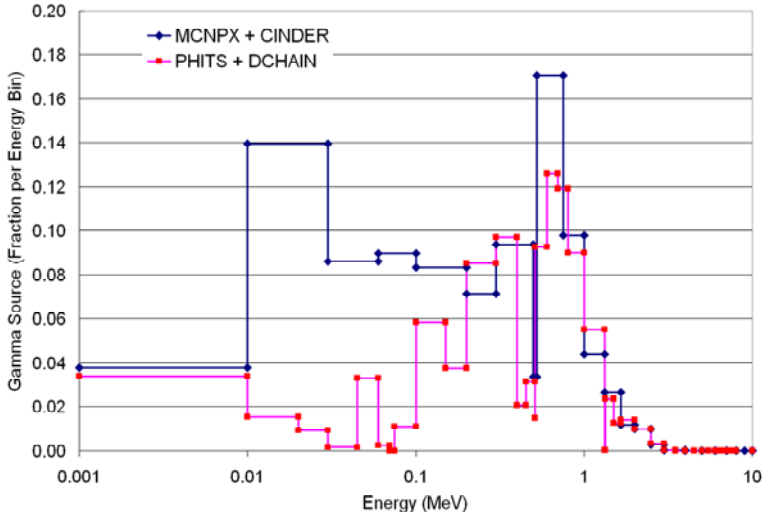

14 Managed by UT-Battelle
for the Department of Energy

Presentation_name

RMR1

Dose rate comparison @ 30 cm

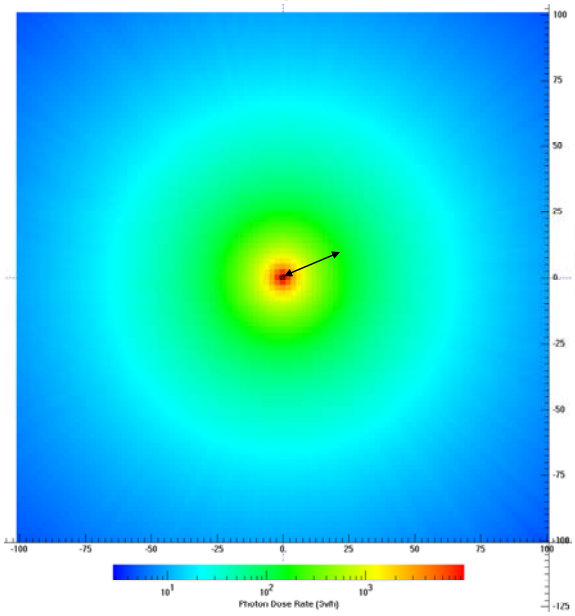

For 1 week irradiation,
at 4 h after EOB, at 30 cm:

PHITS +DCHAIN: 88 Sv/h
MCNPX+CINDER: 98 Sv/h
ISAC SAR Report: 68 Sv/h

15 Managed by UT-Battelle
for the Department of Energy

Dose rate distribution (horizontal plane)

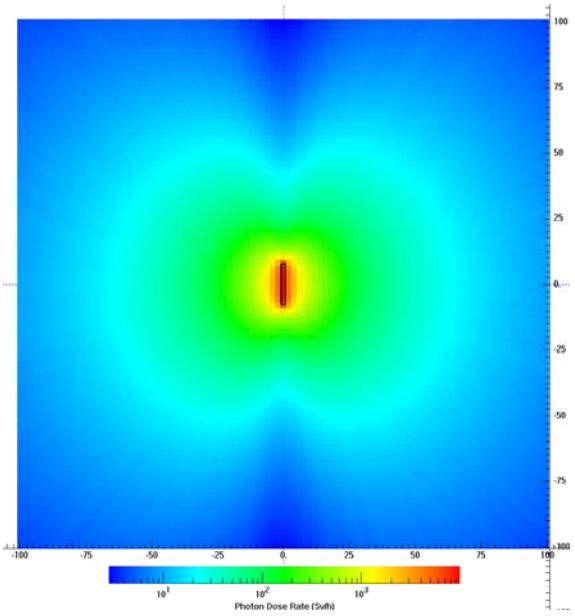

16 Managed by UT-Battelle
for the Department of Energy

Gamma Source and Dose Rate Contributions by Energy Bin

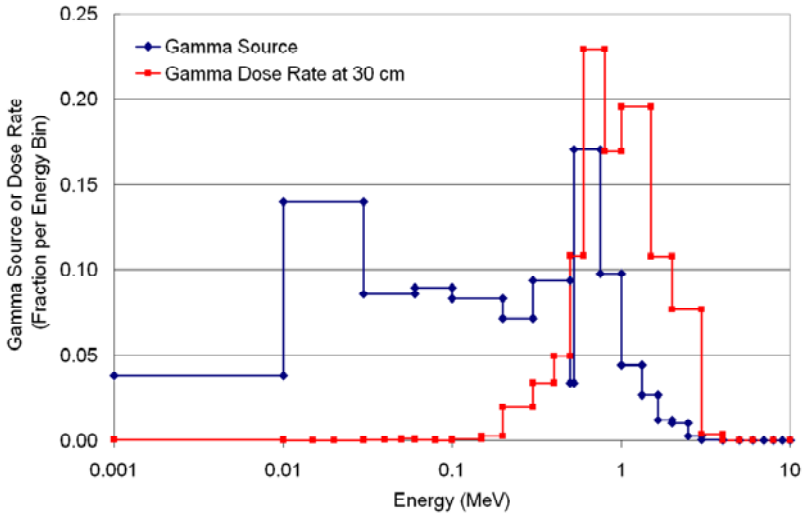

17 Managed by UT-Battelle for the Department of Energy

Presentation_name

Conclusions

The two code systems used:

- **PHITS + DCHAINSP 2000 and**
- **MCNPX +CINDER90**

Agreed reasonably well in predicting

- **Total activity**
- **Categorization (CAT-3 TQR)**
- **Decay heat**
- **Induced dose rates around the target (despite considerable differences in predicted gamma source spectrum)**

18 Managed by UT-Battelle for the Department of Energy

Presentation_name

Future Work

- **Would like to benchmark simulations against measurements (need suitable data)**
- **Investigate observed differences and improve consistency**
- **Compare to FLUKA results after developing geometry with foils**

19 Managed by UT-Battelle
for the Department of Energy

Presentation_name

Back-up slides

Koji Niita: PHITS *Particle and Heavy Ion Transport code System*

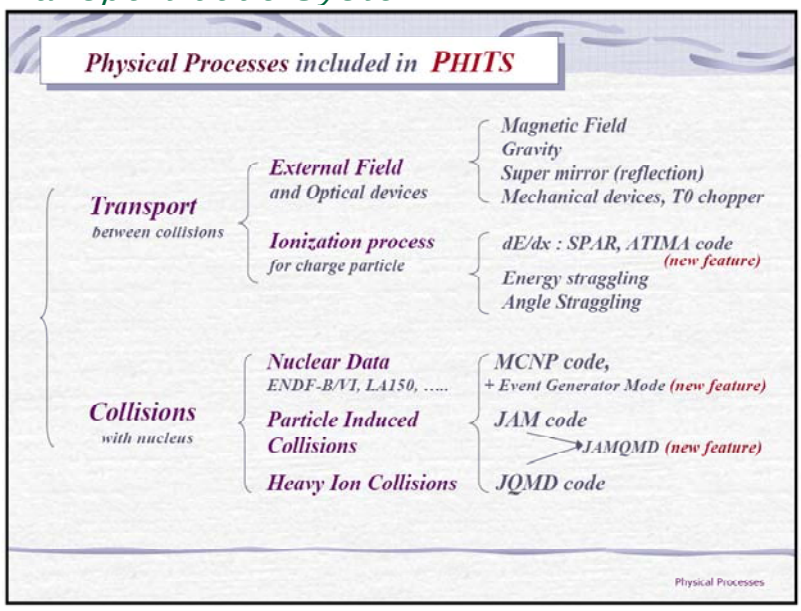

21 Managed by UT-Battelle
for the Department of Energy

Presentation_name

Koji Niita: PHITS *Particle and Heavy Ion Transport code System*

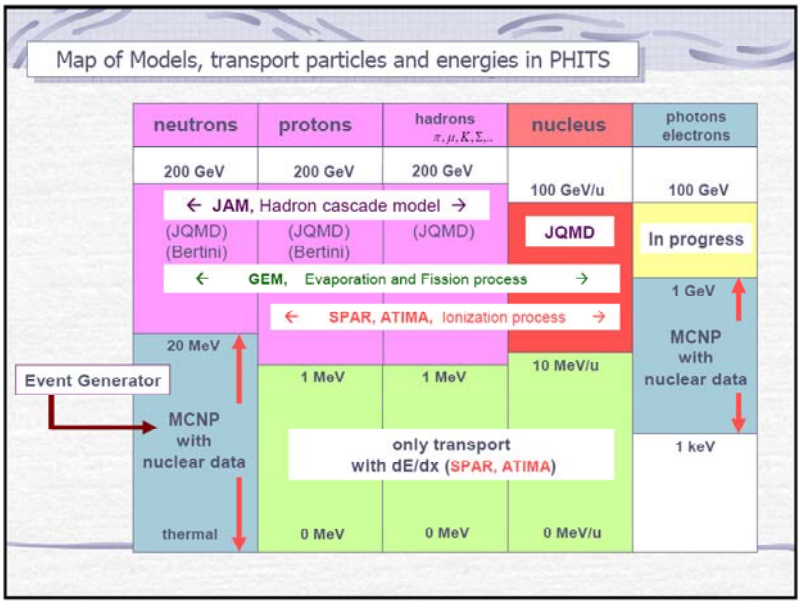

Photon Flux-to-Dose-Rate Conversion Factors

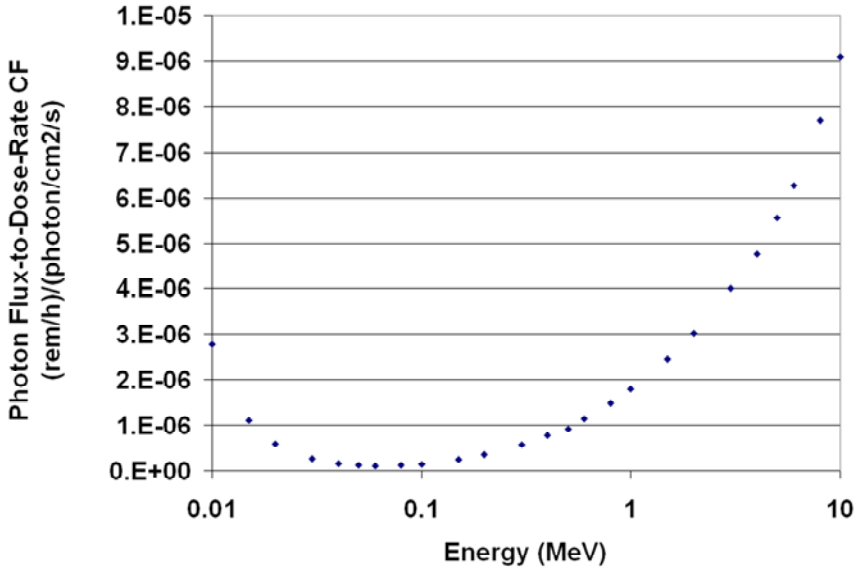

Comparison of Total Activity

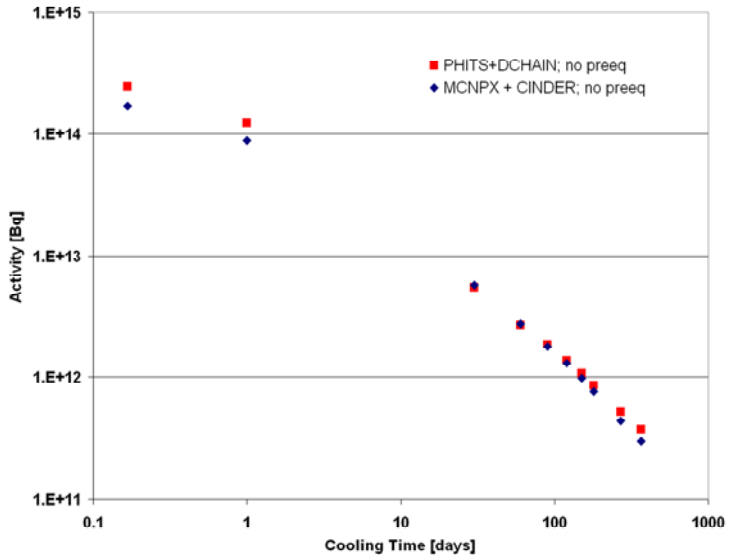

24 Managed by UT-Battelle
for the Department of Energy

Presentation_name

Gamma Source Intensity Comparison

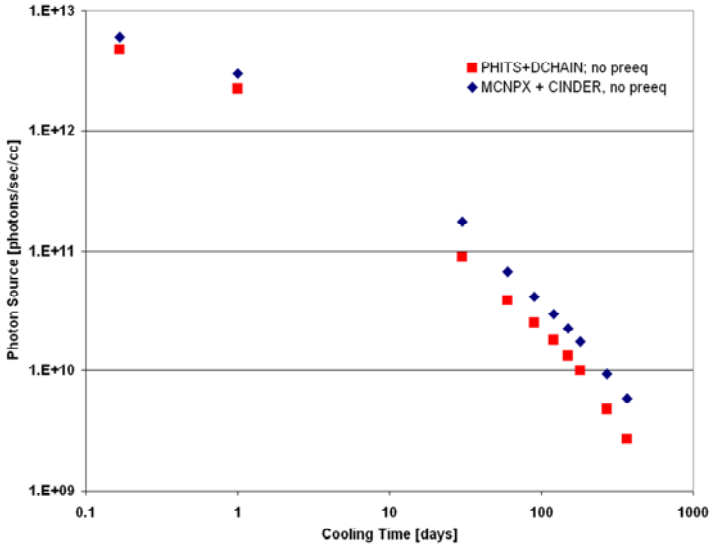

25 Managed by UT-Battelle
for the Department of Energy

Presentation_name

Decay Heat Comparison

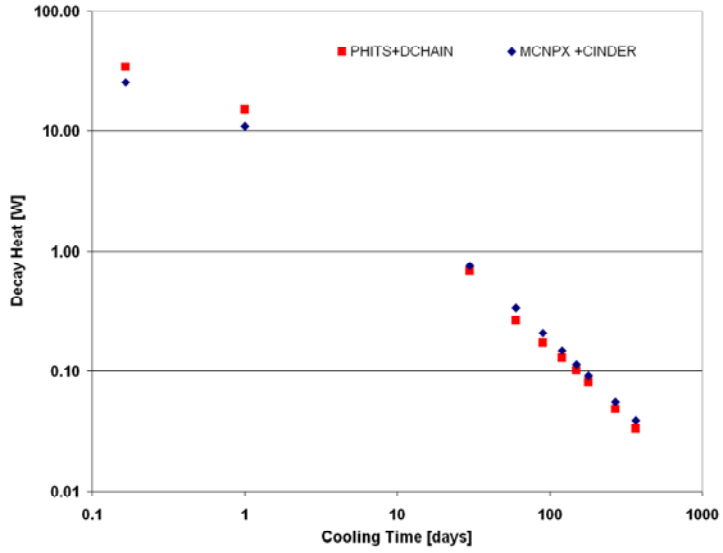

26 Managed by UT-Battelle
for the Department of Energy

Presentation_name

Gamma Source Comparison (Previous Work)

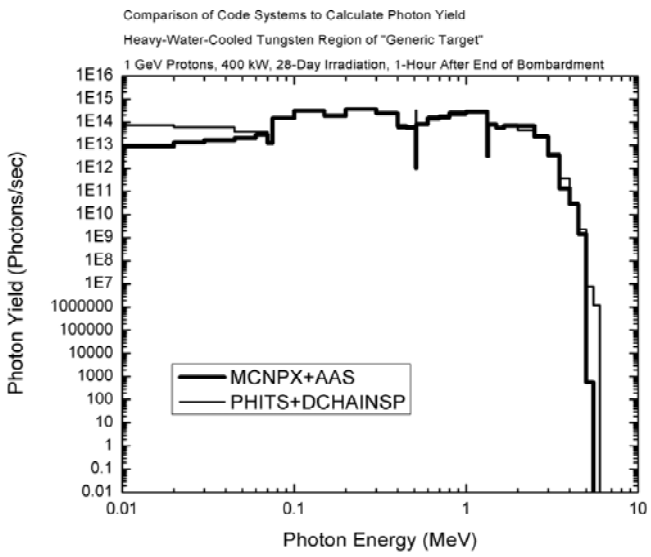

27 Managed by UT-Battelle
for the Department of Energy

Presentation_name

References

Reference for ORNL fission model and DRES evaporation model

11. J. Barish et. al., "HETFIS High-Energy Nucleon-Meson Transport Code with Fission", ORNL/TM-7882, Oak Ridge National Laboratory (July 1981). 12. L. Dresner, "EVAP - A Fortran Program for Calculating the Evaporation of Various Particles from Excited Compound Nuclei", ORNL-TM-196, Oak Ridge National Laboratory (April 1962).

Reference for RAL

10. F. Atchison, "Spallation and Fission in Heavy Metal Nuclei under Medium Energy Proton Bombardment", in Targets for Neutron Beam Spallation Sources, Jul-Conf-34, Kernforschungsanlage Julich GmbH (January 1980).

Review of ITEP experiments with targets irradiated by protons of up to 2.6 GeV energy

Yu.E. Titarenko, V.F. Batyaev, A.Yu. Titarenko,
M.A. Butko, K.V. Pavlov, S.N. Florya, R.S. Tikhonov
Institute for Theoretical and Experimental Physics (ITEP), Moscow, Russia

Abstract

The thin target experiments carried out using the ITEP proton synchrotron (Moscow, Russia) during the last decade are reviewed in detail. The experiments were aimed at determining the independent and cumulative yields of radioactive residuals in 0.04-2.6 GeV proton-irradiated thin targets. In total, 144 targets made of 22 materials ranging from ^{nat}Cr to ^{nat}U have been irradiated. Particular emphasis was laid to single-isotopic and isotope-enriched materials, such as $^{206-208}$Pb, ^{56}Fe, $^{182-186}$W, and ^{99}Tc. All in all, by the beginning of 2005 more than 10,000 yields had been determined, published, and then introduced into the EXFOR database. A fresh run of experiments with structural materials (^{56}Fe, ^{nat}Cr, ^{nat}Ni, ^{93}Nb, ^{181}Ta, and ^{nat}W) is under way. The experiments are expected to complete in 2009. The experimental procedure is described together with the techniques for, and results of, comparing with the similar data obtained at GSI (Darmstadt) and ZSR (Hannover).

Introduction

The thin target experiments[1] are aimed at verifying the interactions of primary beam protons of a given energy with target nuclei, *i.e.* the primary processes. The purpose of the verification is to check out the adequacy of describing the INC only, namely, to check on the accuracy of calculating the cross-section that characterise the nuclear interactions of high energy particles in terms of the models used in the transport code systems.

As early as 1990, the ITEP began experimenting to determine the independent and cumulative yields of residual products in thin targets via direct γ-spectrometry [1]. An Al foil-^{59}Co sample sandwich was exposed to 2 GeV proton beam at the booster of the U-70 accelerator at the Institute for High Energy Physics (Protvino, Russia). The Al foil was used to monitor the proton beam. After that, the sandwich was delivered at ITEP to be measured using a γ-spectrometer. The long period that elapsed between the irradiation end and the calculation start made the short-lived nuclides decay, so the information about production of the lattes went astray.

During the same period, the ITEP U-10 synchrotron was provided with the task-oriented extraction channel for high-energy protons of ~$1{\cdot}10^{11}$ proton/pulse intensity. Besides, a high resolution γ-spectrometer was purchased.

The techniques developed, the equipment purchased and the external beam extraction realised in the ITEP U-10 synchrotron made it possible to implement ISTC Projects Nos. 839 (1997-2000), 2002 (2002-2004), and 3266 (2006-2009) supported financially by EC, Norway and Japan and to carry out the batch measurements of the independent and cumulative yields of residuals from the thin experimental samples of different materials right at ITEP.

1 Review of experiments with thin targets

The experiments to determine the cross-sections for nuclide production in thin targets were and are made under ISTC Projects Nos. 839 (1997-2000), 2002 (2002-2004), and 3266 (2006-2009). Tables 1-4 list the targets and proton energies used in the projects. The numbers in Tables 1 and 2 for Projects 839 and 2002 that have been implemented indicate the numbers of the residual nuclide production cross-sections determined. The technical reports on the projects are accessible through the IAEA and OECD databases [2,4].

Table 1: Targets and proton energies used in ISTC Project No. 839

Proton energy [GeV]	Targets																			
	^{56}Fe	^{58}Ni	^{59}Co	^{63}Cu	^{65}Cu	^{93}Nb	^{99}Tc	^{182}W	^{183}W	^{184}W	^{186}W	^{nat}W	^{nat}Hg	^{206} Pb	^{207}Pb	^{208}Pb	^{nat}Pb	^{209}Bi	^{232}Th	^{nat}U
0.1			25	11	6		18						44	22	22	20		26	87	108
0.2			29	29	29		39	32	35	36	36		65						128	123
0.8							72	70	76	77	60								130	195
1.0*							64									114				
1.2*			41	47	54		67						103						214	226
1.5				35	36									92	93	94	93	99		
1.6			41	42	47		78	109	111	114	119		141						212	231
2.6	36	38	41	42	48	85	85					129								

* Additionally, ^{208}Pb were irradiated by 1 000 MeV proton.
** The ^{63}Cu and ^{65}Cu samples were involved in the intercalibration measurements between ITEP and JAERI.

1. We call a target thin if it satisfies the following two criteria: *i)* the energy loss of an incident particle as it traverses the target is negligible compared with its initial energy; *ii)* the free path of an incident particle is much in excess of the target length.

Table 2: Targets and proton energies used in ISTC Project No. 2002

Targets	Proton energy (GeV)										
	0.04	0.07	0.1	0.15	0.25	0.4	0.6	0.8*	1.2	1.6	2.6
^{nat}Pb	18	28	43	63	95	116	141	154	171	181	178
^{208}Pb	8	28	36	63	94	113	141	154	170	182	172
^{207}Pb	9	29	42	65	94	112	140	152	170	180	171
^{206}Pb	13	28	46	65	94	112	139	156	170	180	171
^{209}Bi	13	35	50	71	106	128	147	162	183	192	198

* Additionally, ^{197}Au were irradiated by 800 MeV proton.

Table 3: Targets and proton energies used in ISTC Project No.3266

	List of irradiation runs for beta-active nuclide production measurements										
Targets	Proton energy (GeV)										
^{56}Fe*	0.04	0.07	0.1	0.15	0.25	0.4	0.6	0.8*	1.2	1.6	2.6
^{nat}Cr	X	x	x	x	x	x	x	22	25	24	30
^{nat}Ni	X	x	x	x	x	x	x	22	25	22	26
^{93}Nb	X	x	x	x	x	x	x	24	25	21	29
^{181}Ta	X	x	x	x	x	x	x	24	25	24	29
^{nat}W	X	x	x	x	x	x	x	20	29	23	28

* Additionally, ^{56}Fe will be irradiated by 300, 500, 750, 1 000 and 1 500 MeV proton.

Table 4: List of α-active nuclide (^{148}Ga) production measurements in ISTC Project No. 3266

Targets	Proton energy (GeV)			
	0.6	0.8	1.6	2.6
^{181}Ta	x	x	x	x
^{nat}W	x	x	x	x

2 Techniques for experimental determining reaction product yields

The techniques for experimental determining the yields (cross-sections for production) of residuals are based on direct γ-spectrometry without any chemical separation of the radioactive nuclei produced by irradiation.

2.1 Spectrometer characteristics

The radioactive nuclei produced in the irradiated sampled were recorded with a GC-2518 coaxial Ge detector-based standard spectrometering circuit of a 1.8 keV resolution in the ^{60}Co 1332 keV γ-line. Figures 1 and 2 show examples of the γ-spectra of the Pb and Al foils irradiated.

2.2 Mathematical formalism used to determine the sought parameters

The formalism of presenting and, correspondingly, the techniques for experimental determining the reaction product yields (cross-sections) are based on the fact that any of the recorded reaction products of different-energy proton interactions with matter can be generated in both an examined reaction and decays of its "parent" precursors.

$$R_i^{cum/ind} = \sigma_i^{cum/ind} \cdot \hat{\Phi} \qquad i = 1,2,st \tag{1}$$

where $\sigma_1^{cum/ind}$ and $\sigma_2^{cum/ind}$ are, respectively, the cumulative and independent production cross-sections of nuclides N_1 and N_2, in experimental sample N_{Tag} exposed to protons of neutrons [barn]; $\sigma_{st}^{cum/ind}$ are the cumulative or independent monitor reaction cross-sections used to calculate the mean proton flux density [barn]; $\hat{\Phi}$ is the area- and time-averaged proton or neutron flux density [particle/(cm^2·s)].

The reaction rate definition (1) permits the double-link-chain of nuclide "parentage" $N \xrightarrow{\lambda_1} N \xrightarrow{\lambda_2}$ to be presented as a set of differential equations that describe the production and decay of the nuclides.

Figure 1: Spectra of γ-emission from Pb foils exposed to 2.6 and 0.04 GeV protons

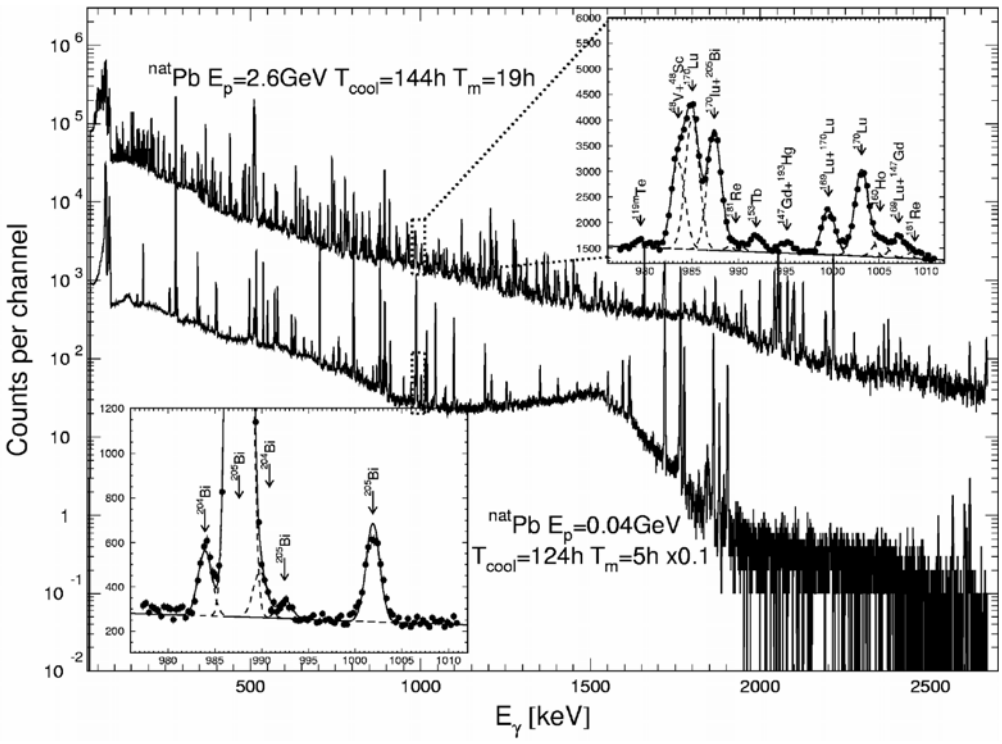

Figure 2: Spectrum of γ-emission from Al foil exposed to 2.6 GeV protons

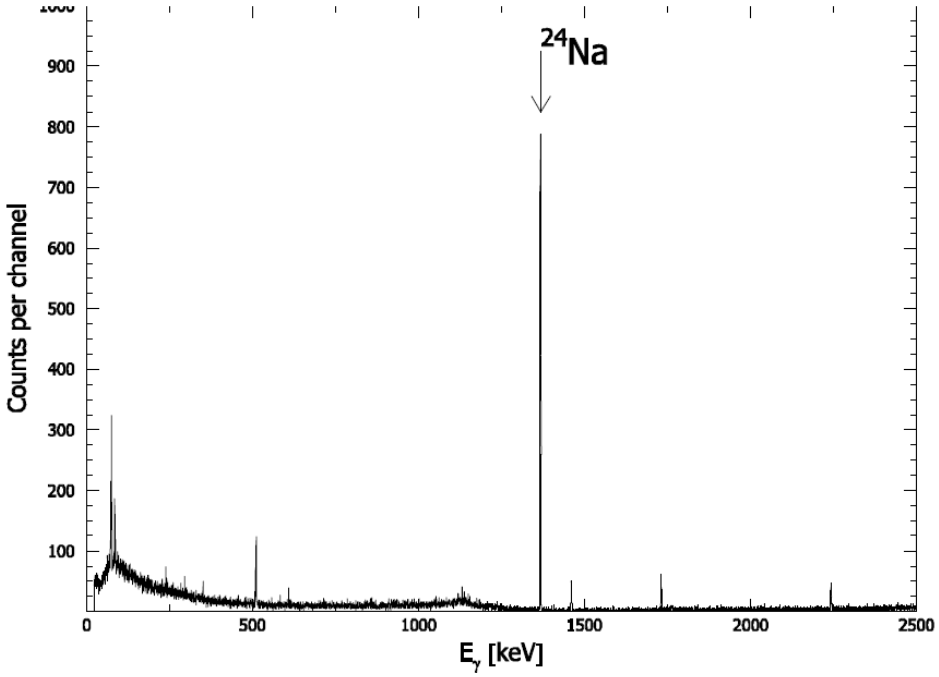

The least squares techniques were used to fit the measured points of the first and second nuclide decay curves to the decay onset (irradiation stop moment). The condition that numbers of nuclei of the first and second nuclides in the samples irradiated should be the same at the irradiation stop (*i.e.* the decay onset) permits the reaction rates to be obtained from the sets of differential equations that describe their production and decay:

$$R_1^{cum/ind} = \frac{\hat{A}_1}{N_{Tag} \cdot \eta_1 \cdot \varepsilon_1} \cdot \frac{1}{F_1} \tag{2}$$

$$R_1^{cum/ind} = \frac{\hat{A}_2^1}{N_{Tag} \cdot \eta_2 \cdot \varepsilon_2 \cdot \nu_{12}} \cdot \frac{\lambda_2 - \lambda_1}{\lambda_2} \cdot \frac{1}{F_1} \tag{3}$$

$$R_2^{cum/ind} = \left(\frac{\hat{A}_2^2}{F_2} + \frac{\hat{A}_2^1}{F_1} \cdot \frac{\lambda_1}{\lambda_2} \right) \frac{1}{N_{Tag} \cdot \eta_2 \cdot \varepsilon_2} \tag{4}$$

$$R_2^{cum} = R_2^{ind} + \nu_{12} \cdot R_2^{cum/ind} = \left(\frac{\hat{A}_2^1}{F_1} + \frac{\hat{A}_2^2}{F_2} \right) \frac{1}{N_{Tag} \cdot \eta_2 \cdot \varepsilon_2} \tag{5}$$

where $\hat{A}_1 = A_1 \cdot k_{\mu_1}$, $\hat{A}_2^1 = A_2^1 \cdot k_{\mu_2}$ and $\hat{A}_2^2 = A_2^2 \cdot k_{\mu_2}$ are the parameters determined by least squares fitting the experimental points of the decay curves of the mother and daughter nuclides (super- and subscripts 1 and 2 stand for mother and daughter, respectively); N_{Tag} is the number of nuclei in an irradiated sample; η_1 and η_2 are γ-abundancies; λ_1, and λ_2 are decay constants; ε_1 and ε_2 are absolute spectrometer effectivenesses at γ-quantum energies E_1 the first nuclide)and E_2 (the second nuclide); ν is the branching factor, *i.e.* the probability for mother to become daughter; F_1 and F_2 are functionals calculated as ($F_i = 1 - e^{-\lambda_i \cdot t_{irr}}$, where *i* = 1,2,st); t_{irr} is irradiation time.

The corrections k_μ that allow for γ-quantum absorption are determined as:

$$k_{\mu_j} = \frac{k \cdot \sigma_{tot_j} \cdot h}{1 - e^{k \cdot \sigma_{tot_j} \cdot h}} \tag{6}$$

where h is experimental sample thickness (g/cm²); σ_{tot_j} is the total interaction cross-section of γ-quanta of the *j*-th energy with matter (barn/atom); $k = \frac{N_{A_\nu}}{M} \cdot 10^{-24}$ is the coefficient of transition from dimension [barn/atom] to dimension [cm²/g], where N_{A_ν} is Avogadro number; *M* is molecular weight. The cross-sections for the *j*-th energy γ-quantum interactions with matter were borrowed from [3].

The yields (production cross-sections) of the independent and cumulative yields of residual product nuclei in an identified double-link nuclear transformation chain are calculated by normalising the respective reaction rates to the mean proton flux density:

$$\sigma_1^{cum/ind} = \frac{R_1^{cum/ind}}{\hat{\Phi}} \qquad \sigma_2^{cum/ind} = \frac{R_2^{cum/ind}}{\hat{\Phi}} \tag{7}$$

2.3 Mean proton flux density

The pioneer works determined the mean flux density of protons that irradiate a target using the $^{27}Al(p,x)^{24}Na$ reaction rate. However, the proton channel of ^{24}Na production exists alongside with the neutron channel [$^{27}Al(n,\alpha)^{24}Na$], so the use of the latter reaction underestimates the mean proton flux density. Therefore, the $^{27}Al(p,x)^{22}Na$ monitor reaction was used in the later works. The geometric dimensions of Al foils are always the same as those of the irradiated foils, so the expression of the mean proton flux density can be presented as:

$$\hat{\Phi} = \frac{R_{st}^{cum}}{\sigma_{st}^{cum}} \tag{8}$$

$$\frac{\Delta\hat{\Phi}}{\hat{\Phi}} = \sqrt{\left(\frac{\Delta R_{st}^{cum}}{R_{st}^{cum}}\right)^2 + \left(\frac{\Delta\sigma_{st}^{cum}}{\sigma_{st}^{cum}}\right)^2} \tag{9}$$

The R_{st}^{cum} value is calculated by formula (6).

Simultaneously, the ^{27}Al(p,x)^{24}Na and ^{27}Al(p,x)^{7}Be reaction cross-sections are calculated together with the ^{27}Al(n,p)^{27}Mg reaction rate in the Al foil. The latter reaction is used to estimate the neutron component rather than to monitor the proton beam.

Figure 3: The ^{27}Al(p,x)^{22}Na monitor reaction cross-section versus energy

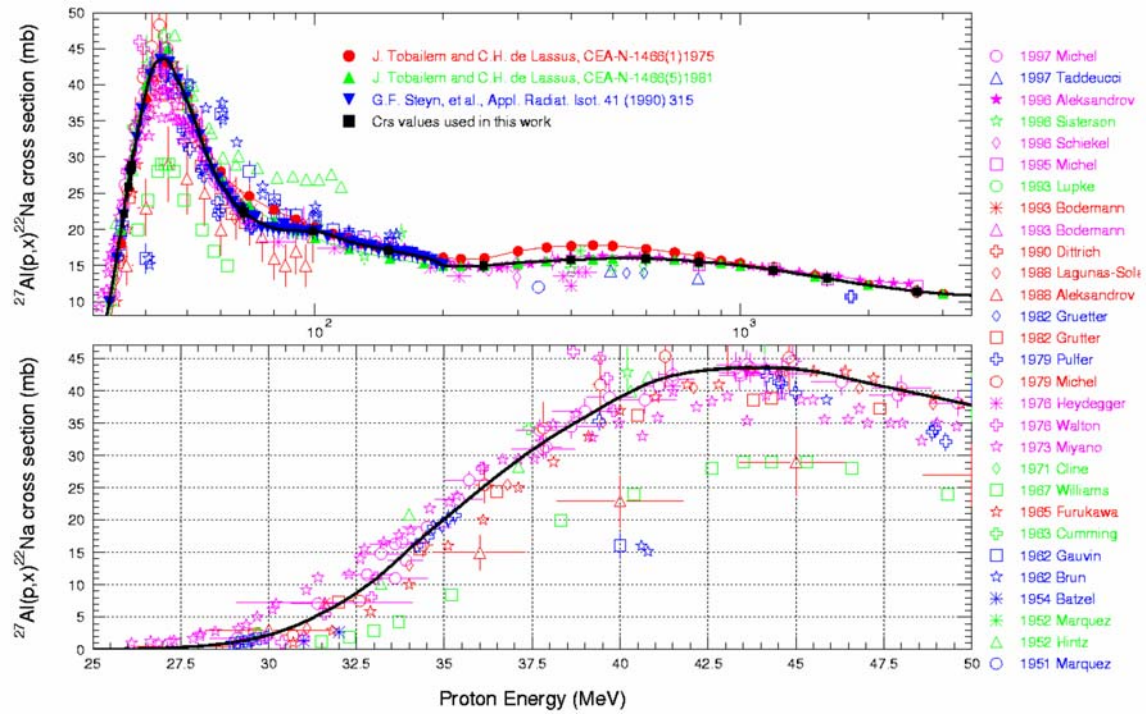

2.4 Measurement errors

Since a few $R_{ij}^{ind/cum} \pm \Delta R_{ij}^{ind/cum}$ values calculated for k different γ-lines (i = 1,2; 1 < j < k) may be averaged when calculating the mean reaction rates, it is expedient to introduce definitions for relative quantum yield and relative spectrometer effectiveness that are related to one another as:

$$\eta_{ij} = k_{\gamma_i} \cdot \eta_{ij}^{rel} \qquad \varepsilon_{ij} = k_{\varepsilon} \cdot \varepsilon_{ij}^{rel} \tag{10}$$

The $k_{\gamma_i} \pm \Delta k_{\gamma_i}$ values were borrowed from [4], while the procedure of determining the $k_{\varepsilon} \pm \Delta k_{\varepsilon}$ value can be found in [2]. In this case, the relative reaction rate for each nuclide via the factors k_{γ_i} and k_{ε} introduced, as well as the absolute reaction rates calculated via (6)-(9), can be presented as:

$$^{rel}R_{ij}^{cum/ind} = R_{ij}^{cum/ind} \cdot k_{\gamma j} \cdot k_{\varepsilon} \cdot N_{tag} \tag{11}$$

The errors in the relative reaction rates $\Delta^{rel}R_1^{cum/ind}$, $\Delta^{rel}R_2^{cum/ind}$, $\Delta^{rel}R_2^{ind}$ and $\Delta^{rel}R_2^{cum}$ are calculated via the error transfer formulas allowing for errors in all values that enter (6)-(9), (12).

The mean values of the relative independent or cumulative rates of the i-th nuclide production as inferred from j γ-lines were calculated as:

$$ {}^{rel}\overline{R}_i^{cum/ind} = \frac{\sum_{j=1}^{k} {}^{rel}R_{ij}^{cum/ind} \cdot {}^{rel}W_{ij}}{\sum_{j=1}^{k} {}^{rel}W_{ij}} \qquad {}^{rel}W_{ij} = \frac{1}{\left(\Delta^{rel}R_{ij}^{cum/ind}\right)^2} \tag{12} $$

$$ \Delta^{rel}\overline{R}_i^{cum/ind} = max\left\{\left(\Delta^{rel}\overline{R}_i^{cum/ind}\right)';\left(\Delta^{rel}\overline{R}_i^{cum/ind}\right)''\right\} \tag{13} $$

$$ \left(\Delta^{rel}\overline{R}_i^{cum/ind}\right)' = \sqrt{\frac{\sum_{j=1}^{k} {}^{rel}W_{ij}\left({}^{rel}\overline{R}_i^{cum/ind} - {}^{rel}\overline{R}_{ij}\right)^2}{(k-1)\sum_{j=1}^{k} {}^{rel}W_{ij}}} \tag{14} $$

$$ \left(\Delta^{rel}\overline{R}_i^{cum/ind}\right)'' = \sqrt{\frac{1}{\sum_{j=1}^{k} {}^{rel}W_{ij}}} \tag{15} $$

Following (13), the mean absolute independent of cumulative rates of the *i*-th nuclide production was calculated together with their errors from the respective relative reaction rates:

$$ \overline{R}_i^{cum/ind} = \frac{{}^{rel}\overline{R}_{ij}^{cum/ind}}{k_{\gamma_i} \cdot k_\varepsilon \cdot N_{tag}} \tag{16} $$

$$ \Delta\overline{R}_i^{cum/ind} = \overline{R}_i^{cum/ind} \cdot \sqrt{\left(\frac{\Delta^{rel}\overline{R}_i^{cum/ind}}{{}^{rel}\overline{R}_i^{cum/ind}}\right)^2 + \left(\frac{\Delta k_{\gamma_i}}{k_{\gamma_i}}\right)^2 + \left(\frac{\Delta k_\varepsilon}{k_\varepsilon}\right)^2 + \left(\frac{\Delta N_{tag}}{N_{tag}}\right)^2} \tag{17} $$

In case but a single γ-line is involved in calculating a reaction rate (possibly, a single line is chosen among *j* γ-lines, or else a nuclide shows but a single line [*j* = 1]), the γ-abundance of a that line ($\eta_i \pm \Delta\eta_i$) and the absolute detection effectiveness ($\varepsilon_i \pm \Delta\varepsilon_i$) were used in formulas (6)-(9), (12), so the absolute independent/cumulative reaction rate can be calculated at once.

2.5 Extra errors

The measurements were made simultaneously with the supplementary researches to reduce the errors in the eventual results, namely:

- the extracted proton beam neutron component was specified;
- the spectrometer effectiveness was studied as a function of the irradiated sample position geometry
- the γ-spectrum processing codes were optimised;
- the laboratory room background was monitored.

2.5.1 Neutron component

The neutron component was estimated as:

$$ \frac{\overline{\Phi}_n}{\overline{\Phi}_p} = \frac{\sigma_{p,x}^{^{24}Na} \Big/ \overline{\sigma}_{n,p}^{^{27}Mg}}{N^{^{24}Na} \Big/ N^{^{27}Mg} - \overline{\sigma}_{n,\alpha}^{^{24}Na} \Big/ \overline{\sigma}_{n,p}^{^{27}Mg}} \tag{18} $$

where $\overline{\sigma}_{n,p}^{^{27}Mg}$, $\overline{\sigma}_{n,\alpha}^{^{24}Na}$ are the neutron spectrum-weighted cross-sections; $\sigma_{p,x}^{^{24}Na}$ is the $^{27}Al(p,x)^{24}Na$, reaction cross-sections; N_{24Na} and N_{27Mg} are numbers of the ^{24}Na and ^{27}Mg nuclei produced in the Al samples with due allowance for their decays under irradiation.

Figures 4.1 and 4.2 show the measured neutron component of the proton beams extracted under different conditions.

Figure 4.1: Neutron component in the proton beams of different energies extracted under Project 839

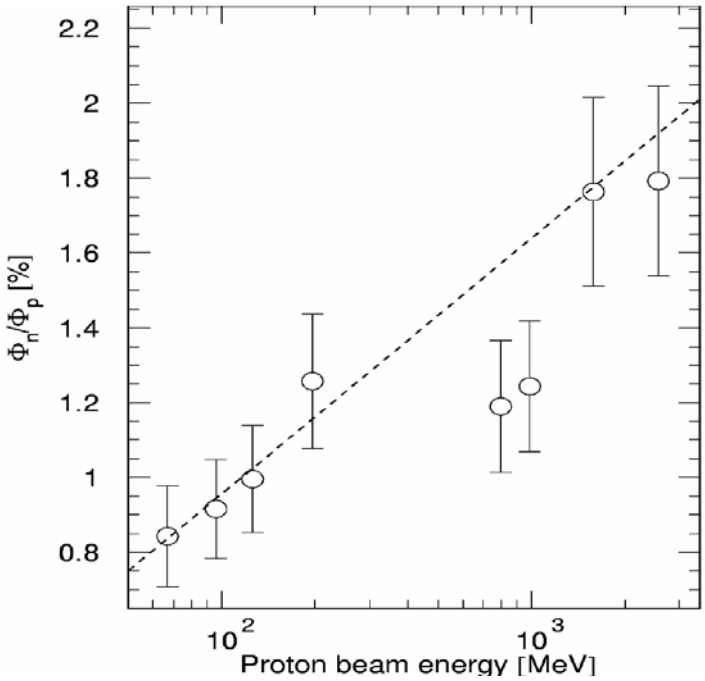

Figure 4.2: Neutron component in the proton beams of different energies extracted under Project 2002

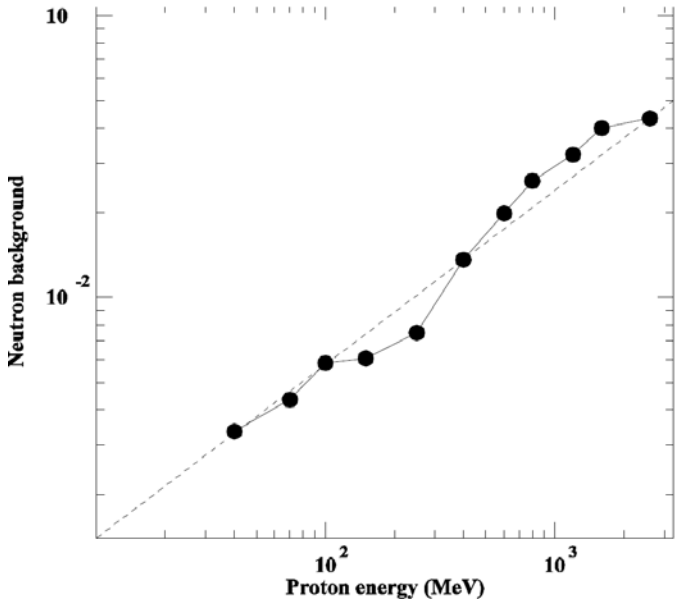

2.5.2 Spectrometer effectiveness

The analytical height-energy detection effectiveness can be presented as:

$$\varepsilon(E,H) = \varepsilon_{base}(E) \cdot \left[\frac{(q_1 + q_2 \cdot \ln E + H_{base})}{(q_1 + q_2 \cdot \ln E + H)} \right]^2 \quad (19)$$

where q_1 and q_2 are the parameters determined by fitting the experimental data. The error in the absolute spectrometer effectiveness is ranging from 4.0% to 4.5%.

Figures 5.1 and 5.2 show the results of measuring the height-energy dependence and the basic relative detection effectiveness at a 40-mm height.

2.5.3 Processing of gamma-spectra and calculations of cross-sections

The γ-spectra were processed by GENIE-2000 [5]. The sets of spectra measured having been computer processed by interactive fitting their peaks, the code examines also the pre-processing results for each of the spectra. Figures 6.1 and 6.2 show the results of pre-processing sets of spectra by GENIE-2000 in automatic mode (a) and the results of additional manual processing in interactive fitting mode (b).

The identification of γ-lines and the calculations of cross-sections for production of residuals by formulas (1)-(15) are realised via the ITEP-devised SIGMA code combined with the PCNUDAT database. Figure 7 shows the characteristic decay curves.

3 Irradiation of experimental samples

At ITEP, the above experiments are being made using the U-10 accelerator, which is a ring facility with a 25 MeV energy of proton injection into a ring and a 9.3 GeV maximum proton acceleration energy. At present, the external beams of fast and slow extraction are available with the parameters listed in Table 5.

Under ISTC Project #839 (1997-2000), the samples were exposed to the high intensity slow-extracted proton beam, thereby permitting (in combination with the available medical beam) them to be independently exposed to 2.6-0.8 GeV and 0.2-0.07 GeV protons, respectively (Figures 8 and 9).

Under ISTC Project#2002 (2002-2004) the samples were exposed to the task-oriented high intensity fast-extracted proton beam, thereby permitting them to be exposed to 0.04-2.6 GeV protons (Figure 10).

Figure 5.1: Computational height-energy simulation of the absolute detection effectiveness of the spectrometer

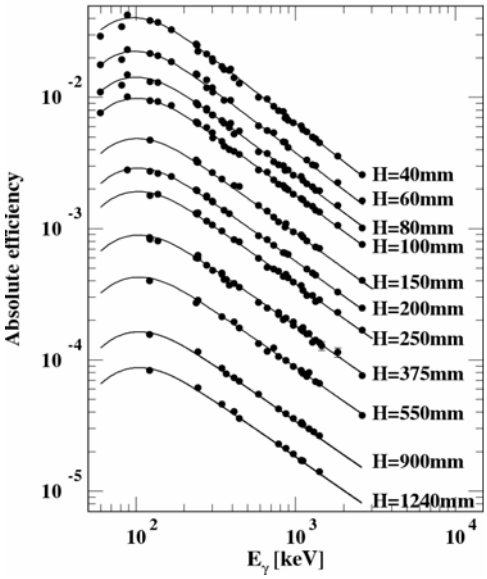

Figure 5.2: Basic relative detection effectiveness of the spectrometer at the height of 40 m and its error

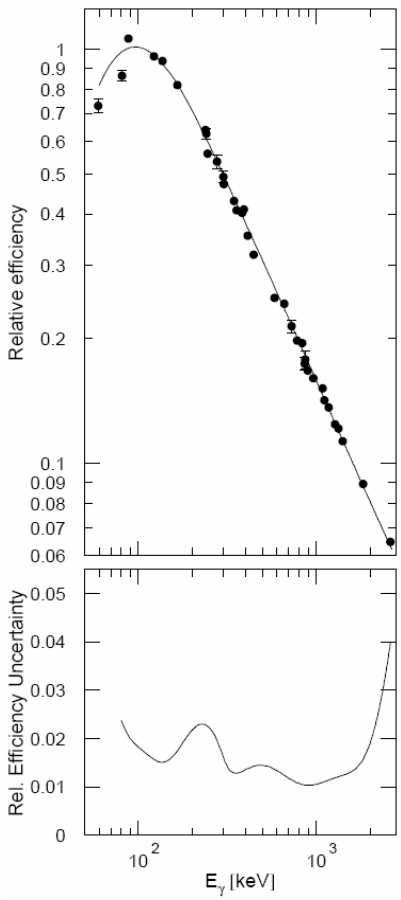

Figure 6.1: Results of primary processing a γ-spectrum by GENIE-2000 code (a) and results of additional manual processing in interactive fitting mode (b)

a b

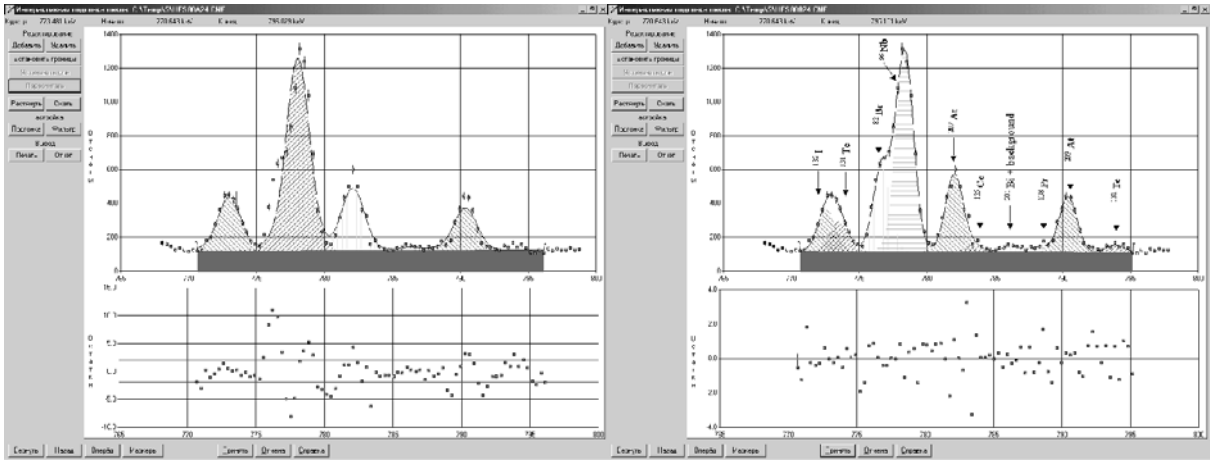

Figure 6.2: GENIE-2000 report on the processing parameters

(a) and (b) stand for the same as in Figure 6.1

(a)

(b)

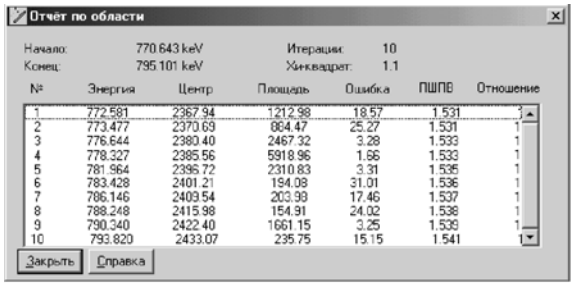

Figure 7: Characteristic examples of the decay curves of the ^{192}Hg → ^{192}Au (1), ^{188}Pt → ^{188}Ir (2), and ^{173}Ta → ^{173}Hf (3) parentages and of the independent ^{173}Ta (4) and ^{173}Ta +^{191}Pt (5)

To facilitate visualisation, the scaling factors x along Y axis and x along X axis have been introduced.

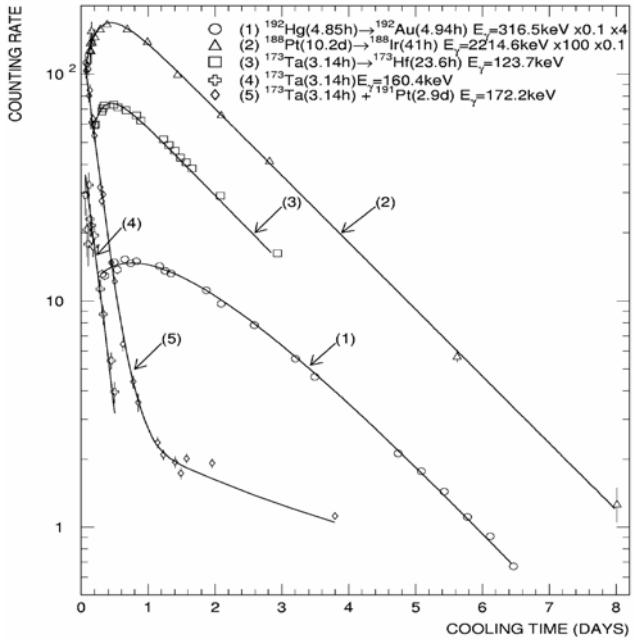

Figure 8: Schematics of the facility and of the 0.8-2.6 GeV proton beam slow extraction elements

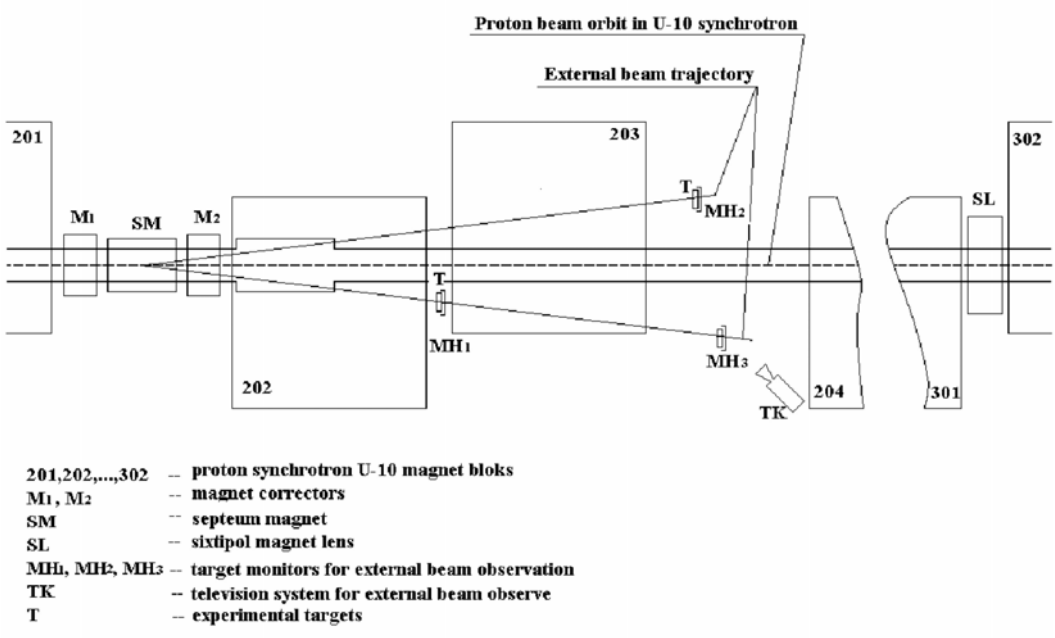

Figure 9: Schematics of the facility and of the 0.07-0.2 GeV medical proton beam fast extraction elements

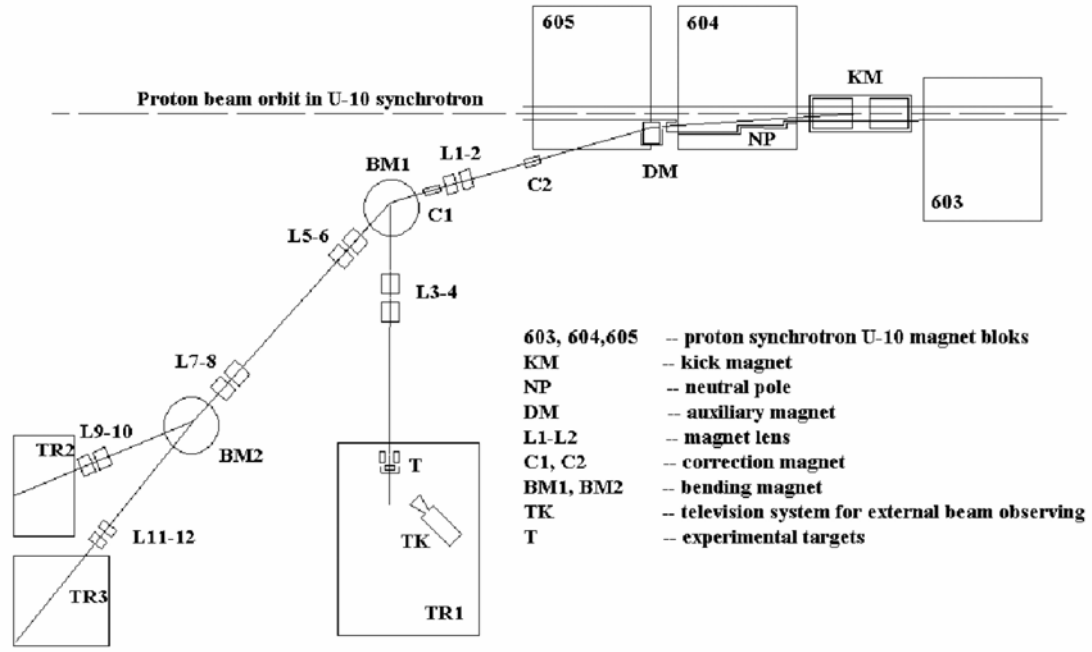

Figure 10: Schematics of the facility and of the 0.04-2.6 GeV proton beam fast extraction elements

1: Table to place the samples to be irradiated; 2: Current transformer; 3: Output flange of vacuumised proton guide; 4: Rotary magnet; 5, 6: Doublet of quadrupole lenses; 7: Septum magnet; 8, 9: Magnetic blocks of accelerator ring; 10: Kicker magnet.

Table 5: External beam parameters of the ITEP proton accelerator

Parameter	Fast extraction (medical beam)	Slow extraction (204 gaps)	Fast extraction (503 gaps)
Energy (GeV)	0.07-0.20	0.8-2.6	0.04-2.6
Intensity (proton/pulse)	~$2 \cdot 10^{9}$	~$1 \cdot 10^{11}$	~$2 \cdot 10^{11}$
Pulse duration (s)	~$0.25 \cdot 10^{-6}$	~0.3	~$1 \cdot 10^{-6}$
Pulse repetition rate (pulse/min)	~15	~15	~15
Section (mm)	Circle ∅ 20	Ellipsis ~15 × 20	Ellipsis ~10 × 15

4 Proton beam energies

The extracted proton beam energies must be known because the experiments were aimed eventually at determining the excitation functions of the independent and cumulative yields of residuals and, in particular, at finding the proton flux densities via the excitation functions of the respective monitor reactions.

Considering the invariability of the proton orbit circumference (that is of one of the main synchrotron characteristics), the proton energy can be calculated by measuring the rotation frequency of protons f_r:

$$E_0 = \frac{m_p \cdot c}{\sqrt{c^2 - L^2 \cdot f_r^2}} - m_p \tag{20}$$

where E_0 is the kinetic energy of a circulating proton; m_p = 938.26 MeV is proton mass; L = 251.21 m is the closed orbit length; c = 2.99776·10⁸ m/s is speed of light. The f_r value is multiple to the accelerating radio frequency:

$$f_a = h \cdot f_r \tag{21}$$

where h = 4 is number of harmonics; f_a is the accelerating radio frequency that varies from 1.07 MHz to 4.85 MHz. The f_a signal is formed safely, so the f_a values can well be measured up to 10^{-4} and even better. When the beam is transported to the sample to be irradiated, a small portion of the beam energy is lost for proton interaction with the transport channel structure materials, with air in the transport channel target gap, and in the target proper. The loss is allowed for as:

$$E_{sample} = E_0 - E_{loss} \tag{22}$$

where E_{sample} is the proton beam energy at the target half-thickness; E_{loss} is the energy loss for proton passage from transport channel to mid-target:

$$E_{loss} = \delta E_{mem} - \delta E_{air} - 0.5 \cdot \delta E_{sample} \tag{23}$$

where δE_{mem}, δE_{air}, and δE_{sample} are the energy losses in steel septum at the transport channel outlet, in the channel-target air gap, and in the target proper that were calculated via expression $\delta E = (dE/dx) \cdot X$ which is valid because thickness (X) of materials that the beam traverses is small and, hence, the specific loss for ionisation dE/dx can well be considered constant.

5 Techniques for calculation-experiment and experiment-experiment comparisons

As a rule, the theoretical calculations are made to simulate the independent yields of reaction products. To get the correct comparison or a general representation of the excitation functions for cumulative and supracumulative yields, it is expedient to consider the procedure of calculating them from independent calculated or experimental values of their precursors.

The general form of the radioactive nuclide transformation chain is:

Figure 11: Radioactive chain schematic

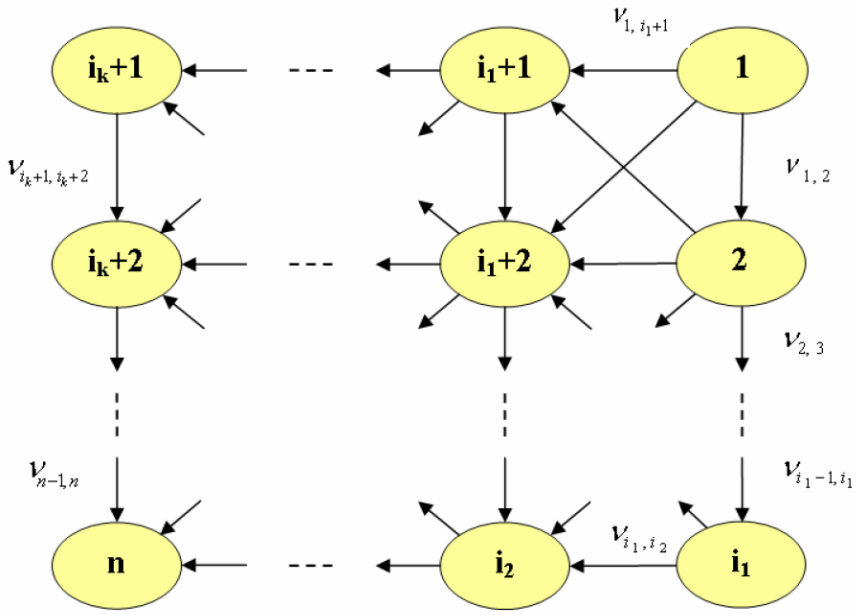

Consider a chain composed of n nuclides interconnected via β^-, ε, n, p and α transitions. Let all the chain nuclides be so numbered that a nuclide labelled a lower number will always be transformed into nuclide labelled a higher number. Then, having known the independent cross-sections for production of all the chain nuclides, we can calculate their cumulative cross-sections as:

$$\sigma_k^{cum} = \sum_{j=1}^{k} m_{kj} \cdot \sigma_j^{ind} \qquad k = 1,2,\ldots,n \tag{24}$$

$$\sigma_k^{cum} = \begin{cases} \sum_{j=1}^{k} \nu_{ik} \cdot m_{ik}, \text{ДЛЯ} & \kappa > j \\ 1, \quad \text{ДЛЯ} & \kappa = j \\ 0, \quad \text{ДЛЯ} & \kappa < j \end{cases} \tag{25}$$

where ν_{ik} are the branching factors, *i.e.* the probabilities for the *i*-th nuclide to turn into the *k*-th nuclide. The vectorial form of the expression to calculate the cumulative yields is:

$$\vec{\sigma}^{cum} = M \cdot \vec{\sigma}^{ind} \tag{26}$$

where *M* is a matrix with elements m_{kj}, $\vec{\sigma}^{cum}$ and $\vec{\sigma}^{ind}$ are vectors, whose elements are, respectively, cumulative and independent cross-sections of the chain elements:

$$\vec{\sigma}^{cum} = \begin{cases} \sigma_1^{cum} \\ \sigma_2^{cum} \\ . \\ . \\ \sigma_n^{cum} \end{cases}, \quad \vec{\sigma}^{ind} = \begin{cases} \sigma_1^{ind} \\ \sigma_2^{ind} \\ . \\ . \\ \sigma_n^{ind} \end{cases} \tag{27}$$

The branching factors ν_{ik} were borrowed from the ENSDF database of 18 decay modes of radioactive nuclide decays: β^-, $\beta^- n$, *IT*, $\varepsilon + \beta^+$, *p*, α, $\beta^+ p$, $\beta^+ \alpha$, $\beta^+ 2p$, εp, $\varepsilon\alpha$, 2ε, *n*, β^+, $2\beta^-$, $2\beta^+$, 2|e [52]. All modes that lead to identical variations of nuclear charge and mass were united into 12 groups of decays. The branching factors were taken for ground states or, if they are absent, for the first metastable state.

The comparison between the calculated and experimental excitation functions is presented both qualitatively (as plots) and quantitatively (as mean-squared deviation factors <*F*>) the latter are calculated as:

$$\langle F \rangle = 10^{\sqrt{A}}$$

where:
$$A = \left\langle \left(\log\left(\sigma_{ITEP,i} / \sigma_{X,i} \right) \right)^2 \right\rangle, \text{ X = GSI, ZSR, calc.} \tag{28}$$

$$\langle S \rangle = \frac{\sum_{i=1}^{n} \left(\sigma_{ITEP_i} / \sigma_{X_i} \right)}{n} \tag{29}$$

6 Analysis of the experiments made

The ITEP results are expedient to analyse starting from:

- the results of the ITEP and JAERI inter-calibration measurements of the residual product nuclides from ^{63}Cu and ^{65}Cu samples by the direct kinematics techniques;
- the results of five experiments with measuring the residual nuclide yields in ^{56}Fe samples exposed to 0.3, 0.5, 0.75, 1.0, 1.5 GeV protons made using direct (ITEP, ZSR) and inverse (GSI) kinematics;
- the results of four experiments with measuring the residual nuclide yields in ^{197}Au, ^{208}Pb, and ^{238}U samples exposed to 0.8, 0.5, and 1.0 GeV protons made using direct (ITEP, ZSR) and inverse (GSI) kinematics.

The data obtained at ITEP and elsewhere were quantitatively inter-compared as sets of independent experimental data by calculating the cumulative yields via independent yields as described above (Item 5) and using the mean squared deviation factor <*F*> that was calculated from (28) and used to analyse the theoretical and experimental results.

6.1 Inter-calibration measurements of residual product yields from 1.2 GeV proton-irradiated ^{63}Cu and ^{65}Cu samples

These irradiations consisted of two independent irradiation runs to expose the ^{63}Cu- and ^{65}Cu-containing sample-monitor pairs separately.

Having been irradiated, the sandwiches were labelled 1 and 2 and sent to ITEP and JAERI, respectively, to be measured there. Figure 12 presents the ITEP and JAERI results. Figure 12 and [3] present the results of measuring the residual product yield in ^{63}Cu and ^{65}Cu samples exposed to 1.2 GeV protons at ITEP (GS-2518 detector) and JAERI (VHTRC and FNS detectors).

Figure 12: Nuclide production cross-sections (mb) for ^{63,65}Cu induced with 1.2 GeV protons determined at ITEP and JAERI

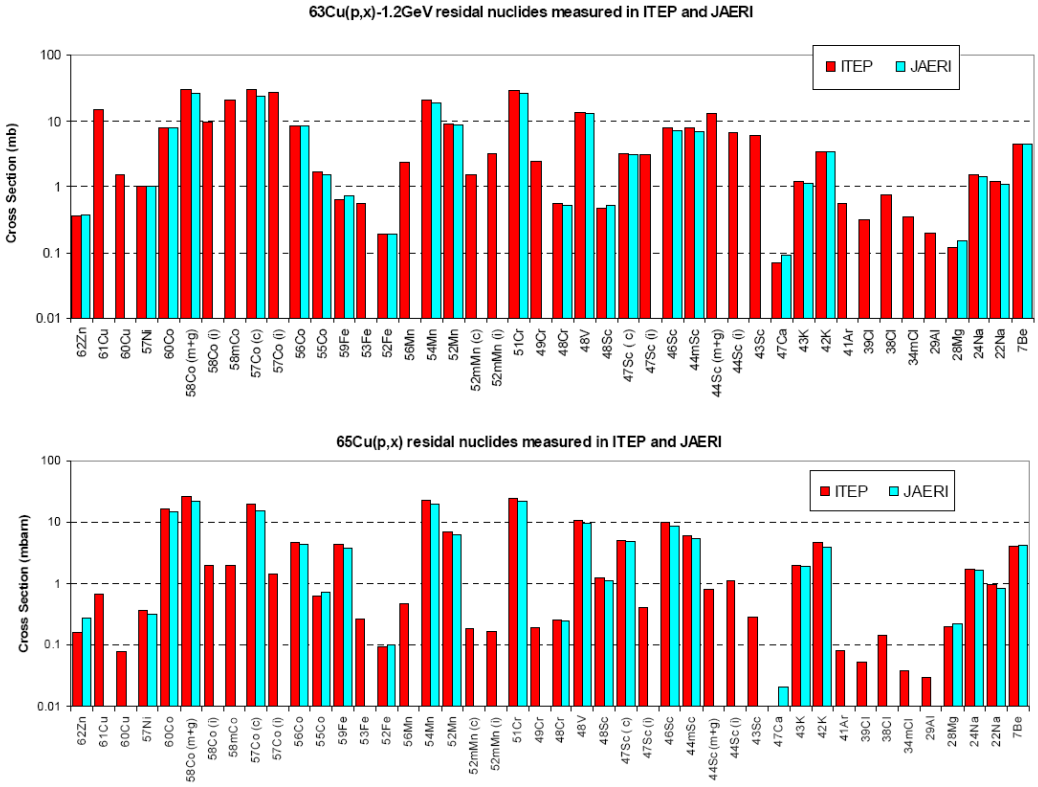

6.2 Results of measuring residual product yields in the samples with mean mass number by direct and inverse kinematics techniques

The 0.3, 0.5, 0.75, 1.0, and 1.5 proton irradiations of the mean-mass-number samples prepared by pressing the ^{56}Fe-enriched fine iron power (0.3% of ^{54}Fe, 99.5±0.1% of ^{56}Fe, 0.2% of ^{57}Fe, and <0.05% of ^{58}Fe) have given 218 independent and cumulative yields of radioactive residual product nuclei with half-lives from 6.6 min to 312 days.

The comparisons with the data obtained elsewhere were realised by analysing 41 works from EXFOR international nuclear database, in which the cross-sections for producing secondary products of nuclear reactions in ^{56}Fe exposed to different-energy protons were determined. A lot of the experimental works were broken into the following four groups:

- the data cited in the present work (black dots);
- the data obtained at GSI by inverse kinematics techniques (white dots);
- the data obtained by R. Michel (white crosses), Th. Schiekel (white triangles),and M. Fassbender (white diamonds) because the datasets obtained at those laboratories are the closest to the dataset presented here;
- the data of the remaining 32 works constitute a separate group (black asterisks).

Figure 13 shows six examples of comparing the data on the residual product yields from ^{56}Fe measured at ITEP, GSI, and ZSR. To facilitate the comparisons, the said figures present the plots of excitation functions simulated via different codes.

All the products were broken into two groups of products of spallation (A > 30) and fragmentation (A < 30). Table 6 presents the comparison results.

Figure 13: Example of comparisons among the yields of residual product nuclei from ^{56}Fe measured at ITEP (black dots), GSI (white dots), and elsewhere

The simulation results of various computational codes are also shown

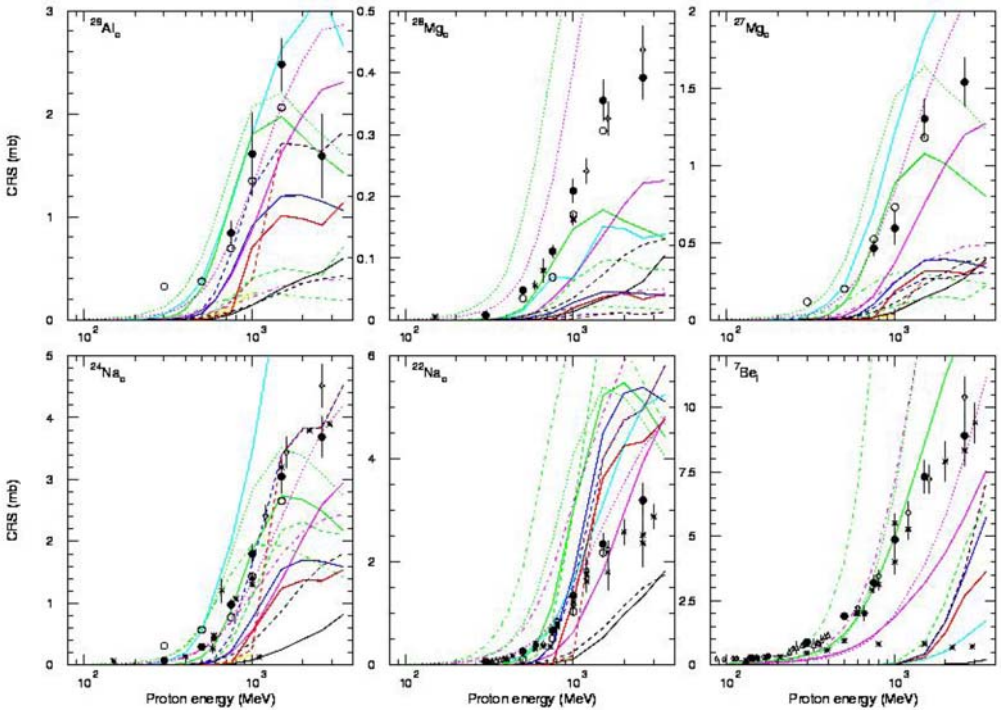

Table 6: Mean square deviation factor <F> of the ITEP and GSI data for each energy and each combination of product groups

	Product mass (A), proton energy (E_p, GeV)					All energies; all products
	300	500	750	1 000	1 500	
ITEP – GSI (A < 30)	3.14	1.93	1.33	1.25	1.14	1.35
ITEP – GSI (A > 30)	1.34	1.28	1.28	1.28	1.24	

6.3 Results of measuring the yields of residual product nuclei in samples of high mass numbers obtained by direct and inverse kinematics techniques

In the high-mass range, the direct and inverse kinematics data were compared for ^{197}Au (E_p = 0.8 GeV), ^{208}Pb (E_p = 0.5 and 1.0 GeV), and ^{238}U (E_p = 1.0 GeV). The ITEP team used U of natural composition as a ^{238}U-containing sample, and Pb enriched with ^{208}Pb (97.2% of ^{208}Pb, 1.93% of ^{207}Pb, <0.01% of ^{206}Pb and, <0.001% of ^{204}Pb) as a ^{208}Pb-containing sample. The ZSR team used Pb of natural composition.

Since the ITEP team did not measure the residual product yields in ^{238}U exposed to 1 GeV protons ^{208}Pb (E_p = 0.5), the relevant results to be compared with the GSI data were obtained by linear interpolation of the logarithms of the known experimental cross-section values for proton energies E_1 = 0.8 GeV and E_2 = 1.2 GeV:

$$\sigma_E^i = exp\left[\frac{E_2 - E}{E_2 - E_1}\cdot \ln\left(\sigma_{E_1}^i\right) + \left(1 - \frac{E_2 - E}{E_2 - E_1}\cdot \ln\left(\sigma_{E_2}^i\right)\right)\right] \quad (29)$$

where $\sigma_{E_1}^i$ and $\sigma_{E_2}^i$ are cross-sections of the i-th nuclide for proton energies E_1 and E_2.

The errors in the cross-sections obtained by interpolation were calculated as:

$$\Delta_{\sigma_{1.0}^i} = \sigma_{1.0}^i \cdot \sqrt{(\delta_{st})^2 + 0.25(\delta_{0.8}^i)^2 + 0.25(\delta_{1.2}^i)^2} \quad (29)$$

where δ_{st} is the relative error of monitor; $\delta_{0.8}^i$ and $\delta_{1.2}^i$ are relative errors in cross-sections $\sigma_{0.8}^i$ and $\sigma_{1.2}^i$ of the i-th nuclide (without the monitor error) or 0.8 GeV and 1.2 GeV, respectively.

Tables 7 and 8 and Figures 14-18 present the comparisons between ITEP and ZSR (direct γ–spectrometry) and between ITEP and GSI, ZSR and GSI (direct and inverse kinematics) for ^{197}Au.

Table 7: Independent yields of ^{nat}U(p,x) reaction at E_p = 1.0 GeV measured at ITEP and GSI

Product	$T_{1/2}$	Type	ITEP	GSI, Darmstadt
^{232}Pa	1.31 d	i	8.40 ± 0.48	6.13 ± 0.92
^{230}Pa	17.4 d	i	3.28 ± 0.26	2.88 ± 0.43
^{226}Ac	29.37 h	i	2.26 ± 0.18	1.53 ± 0.23
^{203}Pb	51.873 h	$i_{(m1 + m2 + g)}$	1.29 ± 0.23	0.06 ± 0.0060
^{201}Pb	9.33 h	$i_{(m + g)}$	4.67 ± 0.69	0.19 ± 0.02
^{200}Tl	26.1 h	i	1.43 ± 0.12	0.044 ± 0.0044
^{146}Eu	4.61 d	i	0.698 ± 0.048	0.514 ± 0.026
^{144}Pm	363 d	i	1.41 ± 0.14	1.02 ± 0.15
^{140}La	1.6781 d	i	2.89 ± 0.17	2.49 ± 0.15
…				
^{88}Y	106.65 d	I	8.57 ± 0.46	6.51 ± 0.52
^{86}Rb	18.631 d	$i_{(m + g)}$	17.1 ± 0.84	11.2 ± 0.6
^{82}Br	35.30 h	$i_{(m + g)}$	11.5 ± 0.56	8.49 ±0.51
^{78}As	90.7 m	I	7.64 ± 0.87	5.33 ±0.32
^{76}As	1.0778 d	I	6.79 ± 0.40	5.93 ±0.36
^{74}As	17.77 d	I	3.77 ± 0.26	2.84 ± 0.28
^{72}Ga	14.10 h	I	5.31 ± 0.30	3.68 ± 0.22

Table 8: Comparisons between the reaction product yields measured at ITEP and the JAERI, GSI, and ZSR measurements results

Target	Energy (GeV)	Set	<F>	<S>
^{63}Cu ^{65}Cu	1.2	ITEP/JAERI	1.11 1.22	1.03 1.02
^{56}Fe	0.3, 0.5, 0.75, 1.0, 1.5	ITEP/GSI	1.36	–
^{197}Au	0.8	ITEP/GSI GSI/ZSR ITEP/ZSR	1.54 1.56 1.28	1.45 0.88 1.17
^{208}Pb	0.5	ITEP/GSI	1.51 – all products 1.32 – spallation pr. 1.81 – fission pr.	0.98 – all products 1.12 – spallation pr. 0.71 – fission pr.
	1.0	ITEP/GSI GSI/ZSR ITEP/ZSR	1.35 1.45 1.25	– 0.79 0.90
^{238}U	1.0	ITEP/GSI	1.39	1.35

Figure 14: Nuclide production cross-sections (mb) for ^{197}Au induced with 0.8 GeV protons measured at ITEP, ZSR and GSI

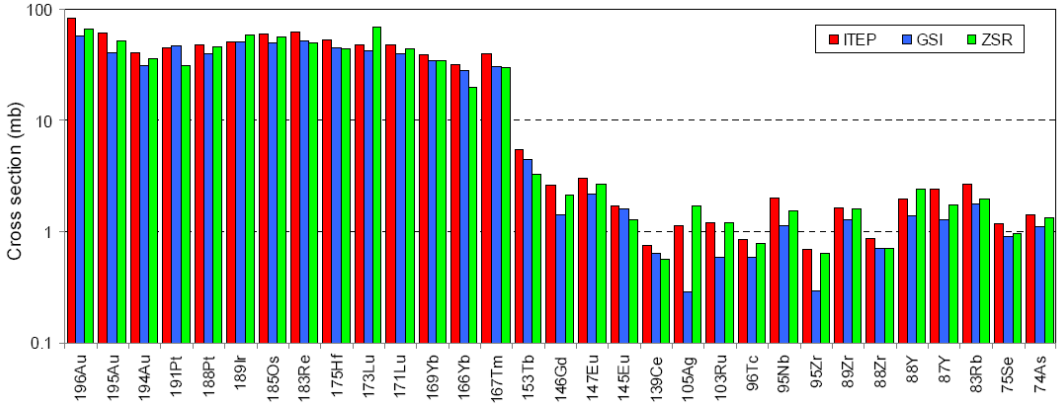

Figure 15: Nuclide production cross-sections (mb) for ^{208}Pb induced with 1.0 GeV protons measured at ITEP, ZSR and GSI

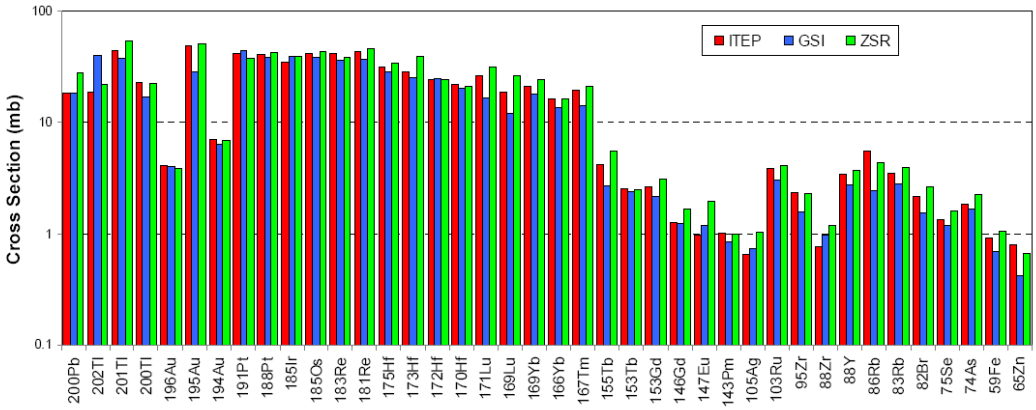

Figure 16: Fission product formation cross-sections (mb) for ^{208}Pb induced with 0.5 GeV protons measured at ITEP, ZSR and GSI

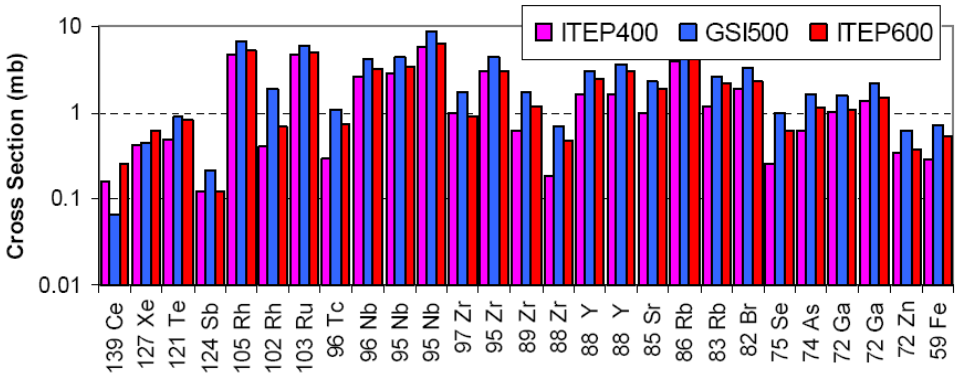

Figure 17: Comparison of Independent yields of ^{nat}U(p,x) reaction at E_p = 1.0 GeV measured at ITEP with those measured at GSI

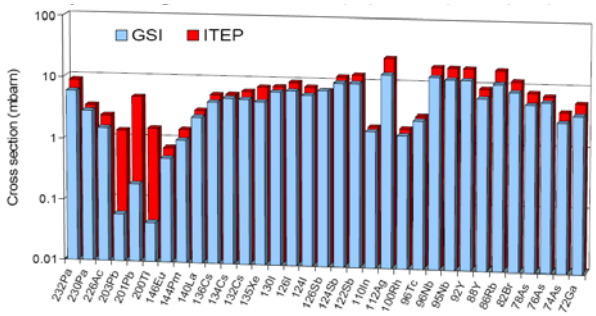

Figure 18: Comparison of independent yields of ^{197}Au(p,x) reaction at E_p = 0.8 GeV, ^{208}Pb(p,x) and ^{238}U(p,x) at E_p = 0.8 GeV measured at ITEP, ZSR and GSI together with theoretical predictions

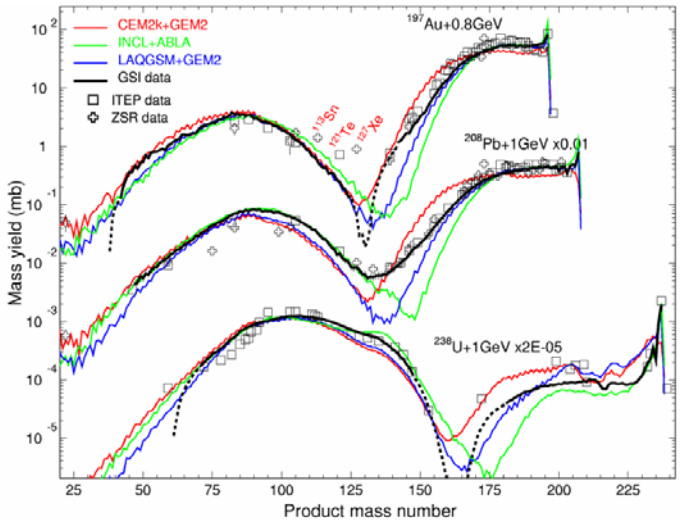

7 Conclusions

Table 8 (above) presents the complete set of comparisons between the reaction product yields measured at ITEP and the JAERI, GSI, and ZSR measurements results. Table 9 lists the direction we hope to take in the future.

Table 9: List of targets and proton energies in our future project

Targets	Proton energy (GeV)										
	0.04	0.07	0.1	0.15	0.25	0.4	0.6	0.8	1.2	1.6	2.6
^{nat}Mo	x	x	x	x	x	x	x	x	x	x	x
^{nat}Zr	x	x	x	x	x	x	x	x	x	x	x
^{nat}Ti	x	x	x	x	x	x	x	x	x	x	x
^{nat}In	x	x	x	x	x	x	x	x	x	x	x
^{115}In	x	x	x	x	x	x	x	x	x	x	x
^{112}Sn											
^{nat}Sn											
^{124}Sn											

Analysis of comparisons among the experimental data obtained at ITEP, GSI, and ZSR has shown that:

- As a whole, the convergence among three datasets is quite satisfactory (at least much better than the convergences between experiment and calculations), so all three datasets (ITEP, GSI and ZSR) must be used to verify the simulated results. However, the detailed comparison has exposed some systematic differences. For instance, the GSI data are systematically 10-15% below the ITEP data that, in turn, are systematically ~10% below the ZSR data (at the same time, the GSI data are systematically ~20% below the ZSR data).
- With the view of verifying the codes, the calculation-experiment comparisons are expedient to make using the data on a broad energy range (from ~20 MeV to 2-3 GeV) instead of the data on separate chosen energies, *i.e.* the excitation function concept must be played.
- With the above approach, each of the experimental datasets shows its own significance, namely:
  - The ZSR and ITEP data will be especially useful in the lower range of energies (~500 MeV), wherein experimenting at GSI is impossible or else the experimental results will contradict the direct kinematics data. In this case those ZSR data sets that were obtained using the stacks are particularly important, thereby permitting the near-threshold excitation functions to be obtained in some cases.
  - The GSI data are especially important when updating the methodological approaches to perfecting models and codes because those data concern the total isobaric distributions of reaction products (it should be remembered, however, that the said methodology fails to separate the ground and isomeric states of nuclei). It is also of importance that the number of GSI experiments is restricted and, therefore cannot fully satisfy the demands of theoreticians (the GSI experiments disregard the low energy range (up to 300 MeV) completely).
- The ITEP experience in comparing the results (both experiment-calculation and experiment-experiment) may underlie verification of codes.
- The ITEP team is prepared to continue studying the proton-induced reaction yields in thin targets and suggests the following target compositions to be discussed. The list may be altered and extended. We expect support from you.

References

[1] O.V. Shvedov, Yu.E. Titarenko, E.I. Karpihin, I.V. Fedorov, V.D. Kazaritsky, V.F. Batyaev, Yu.V. Kochevalin, N.V. Stepanov, *Experimental and Numerical Study of Cross-sections of Co-59 Deep Spallation Reactions Induced by 1.2-GeV Protons*, ITEP-81-93, ITEP 30-94.

[2] O.V. Shvedov, Yu.E. Titarenko, E.I. Karpihin, I.V. Fedorov, V.D. Kazaritsky, V.F. Batyaev, Yu.V. Kochevalin, N.V. Stepanov, "Experimental and Numerical Study of Cross-sections of Co-59 Deep Spallation Reactions Induced by 1.2-GeV Protons", *Proc. II Int. Sem. on Proton Accelerator Based Transmutation of Long-Lived Radioactive Wastes and Utilization of Weapon Plutonium*, Moscow, Russia, 23-27 May 1994, ITEP, Moscow, Parts I and II, 1994, 85-97.

[3] H. Takada, S. Meigo, T. Sasa, T. Fukahori, V.I. Belyakov-Bodin, G.I. Krupny, Yu.E. Titarenko, "Analysis of Reaction Rate Distributions on a Thick Tungsten Target Bombarded with Protons of 0.8 to 1.2 GeV", 4th *International Information Exchange Meeting on Actinide and Fission Product Partitioning and Transmutation*, 11-13 September, Mito, Japan, 1996, 1-11.

[4] Yu.E. Titarenko, *et al.*, *Experimental and Theoretical Study of the Yields of Residual Product Nuclei in Thin Targets Irradiated by 100-2600 MeV Protons*, IAEA, Nuclear Data Section, INDC(CCP)-434, September, 2002, *http://www-nds.iaea.org/reports/indc-ccp-434.pdf*.

[5] Yu.E. Titarenko, V.F. Batyaev, E.I. Karpikhin, R.D. Mulambetov, V.M. Zhivun, A.V. Ignatyuk, V.P. Lunev, N.N. Titarenko, Yu.N. Shubin, V.S. Barashenkov, S.V. Mulambetova, K.A. Lipatov, A.V. Belkin, N.N. Alexeev, V.A. Schegolev, Yu.M. Goryachev, V.O. Kudryashov, *Experimental and Theoretical Studies of the Yields of Residual Product Nuclei Produced in Thin Pb and Bi Targets Irradiated by 40-2600 MeV Protons*, Final Technical Report on the ISTC Project #2002, 2005, available at *www.nea.fr/html/science/egsaatif/ISTC2002-final-report.pdf*.

[6] Yu.E. Titarenko, V.F. Batyaev, V.M. Zhivun, A.B. Koldobsky, Yu.V. Trebukhovsky, E.I. Karpikhin, R.D. Mulambetov, S.V. Mulambetova, Yu.V. Nekrasov, A.Yu Titarenko, K.A. Lipatov, S.G. Mashnik, R.E. Prael, K. Gudima, M. Baznat, "Cross-sections for Nuclide Production in 1 GeV Proton-irradiated ^{208}Pb and 0.8 GeV Proton-Irradiated ^{197}Au", *Imbedded Topical AccApp'03 (Nuclear Applications of Accelerator Technology)*, *2003 Annual Meeting of the American Nuclear Society* (*ANS*), San Diego, California, USA, 1-5 June 2003, *ANS Proceedings*, pp. 1070-1073.

Experimental and theoretical study of ^{148}Gd formation in thin ^{nat}W targets induced with 0.4-2.6 GeV protons

Yu.E. Titarenko,[1] **V.F. Batyaev,**[1] **A.Yu. Titarenko,**[1] **M.A. Butko,**[1] **K.V. Pavlov,**[1]
R.S. Tikhonov,[1] **S.N. Florya,**[1] **S.G. Mashnik,**[2] **W. Gudowski**[3]
[1]Institute for Theoretical and Experimental Physics (ITEP), Moscow, Russia
[2]Los Alamos National Laboratory, Los Alamos, USA
[3]Royal Institute of Technology, Stockholm, Sweden

Abstract

Cross-sections for ^{148}Gd production in thin ^{nat}W targets induced by 0.4, 0.6, 0.8, 1.2, 1.6 and 2.6 GeV protons extracted from the ITEP accelerator complex are presented. The ^{148}Gd was measured using the alpha-spectrometry method. The detection effectiveness was calculated with the MCNPX code. Our results are compared with data obtained elsewhere and with theoretical predictions of ^{nat}W(p,x)^{148}Gd reaction by Bertini and ISABEL models from MCNPX, as well as by CEM2k+GEM2 and INCL+ABLA used here as stand-alone codes.

Introduction

During the last decade, the ITEP team carried out a broad range of experiments to determine the yields of radioactive residual product nuclei in different target and structure materials of ADS facilities exposed to 0.04-2.6 GeV protons [1-3]. The product yields were determined by the high precision gamma-spectrometry techniques using HPGe detectors. This approach is to determine the products, whose gamma-quantum yields per a decay event are significant (above ~0.1%, as a rule). However, a ponderous portion of radioactive nuclei are well-known to be exclusively the alpha- and beta-emitters that can hardly be recorded with HPGe-detectors.

In view of the above, production of some alpha-emitters is very important in practice because they induce much of the radiation hazard that arises when servicing and utilising the elements of ADS facilities. The ^{148}Gd ($T_{1/2}$ = 74.6 y) alpha-emitter produced in all heavy target materials exposed to protons above ~0.5 GeV belongs just to that type of products. It should be noted that, as of nowadays, only a single work [4] has described systematic measurements of ^{148}Gd in ^{nat}W, ^{181}Ta and ^{197}Au exposed to 0.6 and 0.8 GeV protons, which is evidently insufficient for practical applications that require, as a rule, the initial proton energy not below ~1 GeV. Therefore, the cross-sections for ^{148}Gd production in thin ^{nat}W and ^{181}Ta targets exposed to 0.4, 0.6, 0.8, 1.2, 1.6 and 2.6 GeV protons are measured at ITEP under the ISTC Project 3266 now in underway (2006-2009). The predictive power of various theoretical models is studied in line.

This work presents the preliminary results of the measurements on ^{148}Gd production in ^{nat}W.

Irradiation

The experimental samples were irradiated in fast extraction site No. 511 of the ITEP accelerator. The main parameters of the extraction can be found in [1-3]. The samples to be irradiated were stacked as 10.5-mm diameter samples. Table 1 presents the weights of ^{nat}W samples, the sequence of samples in the stacks, the irradiation time, and the proton fluences. The latter were determined via ^{27}Al(p,x)^{22}Na monitor reaction, whose cross-sections were taken using the data of [5].

Measurements

Alpha emission from ^{148}Gd was detected with an alpha-spectrometer based on a CANBERRA A300-17-AM Alpha pip detector. The alpha spectrometer was calibrated using a set of standard ^{239}Pu, ^{238}Pu and ^{226}Ra sources. Figure 1 shows some examples of the spectra measured. The domain of the spectra that correspond to energies below ~2.0 MeV is presented as both beta- and alpha-emissions from the radionuclides produced in the samples. The spectrum region between ~2.0 and 3.2 MeV is actually free of beta-component and can be used to determine the number of ^{148}Gd nuclei. The considerable extension of alpha-spectrum is explained by the short range of the ^{148}Gd-emitted 3.2 GeV alpha particles, which is ~10 mg/cm^2, that is much below the sample thickness (see Table 1). The alpha particle detection effectiveness was determined by the MCNPX code, whose input file describes the alpha detector and sample geometries and simulates the energy deposition in the detector by the alpha-particles outgoing from 10 mg/cm^2 thick surface layer of a sample. Also, ^{148}Gd was assumed to be distributed uniformly over the sample depth. Figure 1 presents also the detector response distribution obtained. Our comparison between the calculated and real spectra has demonstrated a small difference in the spectrum near the initial energy of alpha-particles. Namely, the experimental spectra demonstrate a minor curvature near 3.2 MeV, which can be explained by a small ^{48}Gd near surface density decrease due to recoil of residual nuclei during irradiation.

It can be demonstrated by comparing the spectra that the contribution of that effect should not exceed a few per cent, which agrees with the results [4] of studying the recoil effect on the basis of three ^{nat}W samples in a stack.

The ^{148}Ge production cross-sections obtained are shown in Figure 2 together with the cross-sections obtained in [4] at 0.6 and 0.8 GeV, which coincide with the data of the present work to within experimental errors.

Table 1: Main irradiation parameters

Energy (GeV)	Date of irradiation	Stack	^{nat}W mass (g)	^{27}Al(p,x)^{22}Na cross-section (mb)	Proton fluence (10^{15} p/cm^2)
0.4	18-19.10.2007	Ta-Al-W-Al	0.276	15.8 ± 1.0	1.35 ± 0.11
0.6	15-16.10.2007	Ta-Al-W-Al	0.267	16.0 ± 1.0	3.6 ± 0.3
0.8	22-25.06.2007	W-Al-Ta-Al	0.2590	15.5 ± 1.0	14.6 ± 1.1
1.2	20-22.06.2007	W-Al-Ta-Al	0.269	14.4 ± 1.0	7.5 ± 0.5
1.6	28.03-3.04.2006	W-Al-Ta-Al	0.0328	13.2 ± 1.0	5.8 ± 0.5
2.6	27.11.2006	W-Al	0.2566	11.4 ± 0.9	0.104 ± 0.009

Theoretical predictions

The predictive powers of the present-day hadron-nucleus interaction models was determined via the Bertini and ISABEL options of MCNPX [6] actively used in applied researches, in particular when designing the pilot versions of ADS facilities, and via CEM2k+GEM2 [7] and INCL4+ABLA [8] used here as stand-alone codes. The MCNPX code was used with two models: Bertini and ISABEL. All models were used for simulations of protons interactions with ^{nat}W at 18 proton energies from 0.3 to 3.5 GeV in terms of each of the models. The cumulative yields were obtained using the decay chains of radionuclides that can contribute to ^{148}Gd production. Figure 2 shows that decay chains plotted using the nuclear decay data retrieved from the ENSDF database [9]. Of 47 precursor nuclides presented, 32 may be produced in proton-^{nat}W interactions. It should be noted that, due to alpha-transitions of precursors, the energy threshold of cumulative ^{148}Gd yield production can be much below the independent yield production threshold.

Figure 1: Alpha spectrometer measured spectra of different ^{nat}W samples

Also shown is the MCNPX code-calculated spectrum from ^{148}Gd distributed uniformly over a 10 mg/cm^2 depth in ^{nat}W.

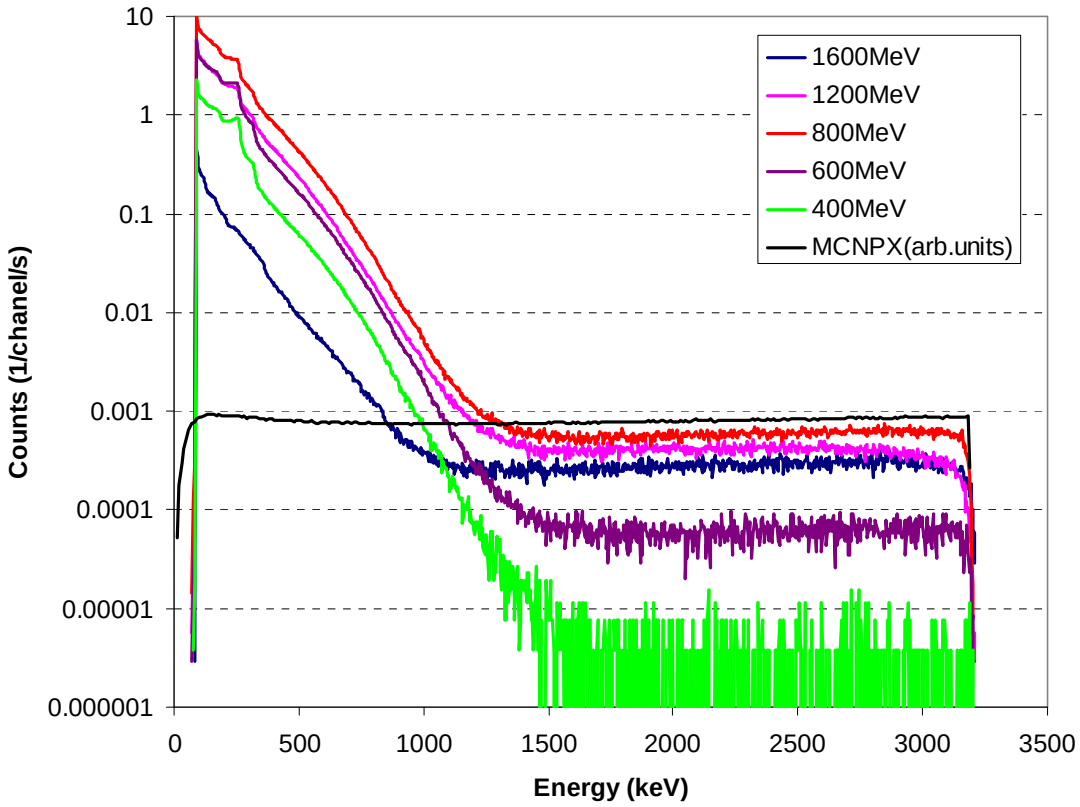

Figure 2: Decay chains of ^{148}Gd precursors

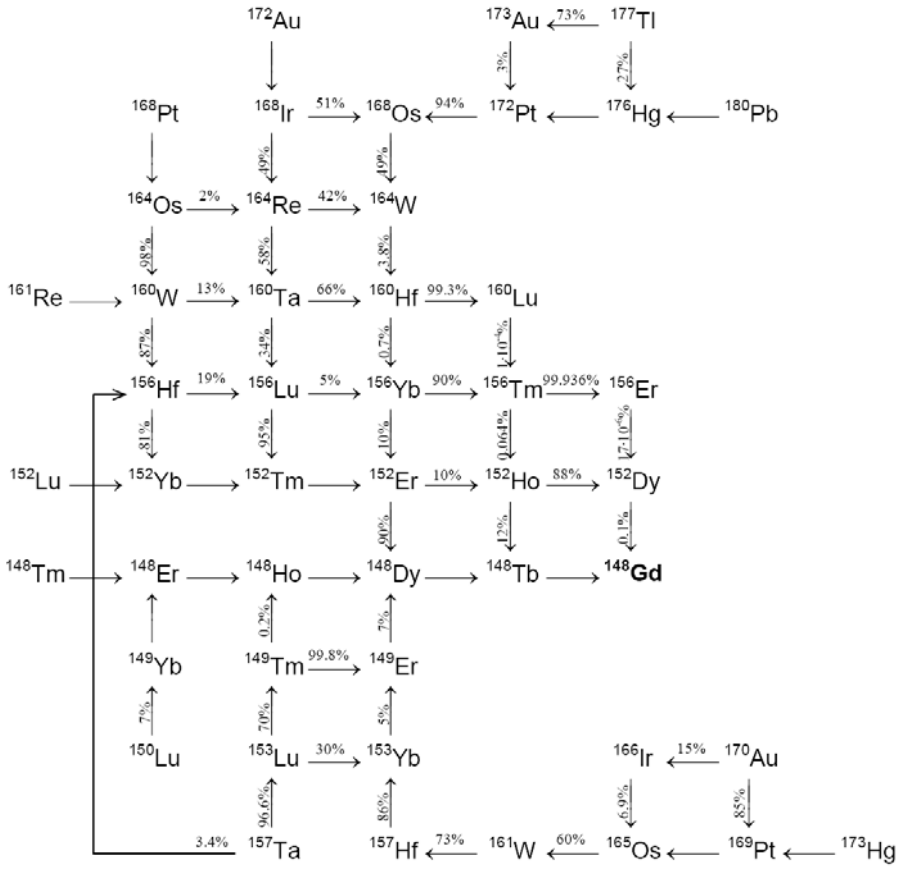

Figure 3: Experimental and calculated excitation functions of ^{148}Gd production in ^{nat}W

The data of [4] are shown for comparison

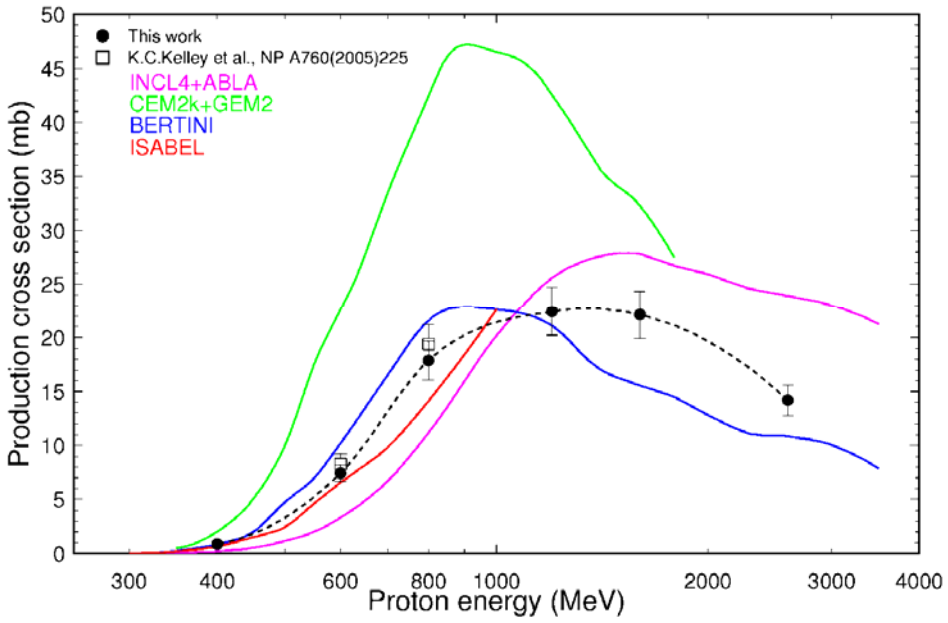

Figure 3 shows the ^{148}Gd prediction results, from which it is seen that the convergences between calculation and experiment are different at proton energies above and below 1 GeV. At energies below 1 GeV, we see a qualitative agreement of the Bertini and ISABEL results with experimental values, whereas the ^{148}Gd yield is much overestimated by the CEM2k+GEM2 code and underestimated by the INCL4+ABLA code. Besides, Bertini and ISABEL describe the energy threshold of ^{148}Gd production correctly, while the CEM2k underestimates, and INCL+ABLA overestimates that threshold. At energies above 1 GeV, the Bertini predictions are underestimated, on average, by20%, while the INCL+ABLA predictions are overestimates by the same 20%. Again on average on the energy, the CEM2k+GEM2 predictions are overestimated twofold.

Conclusion

The results displayed in Figure 3 for the experimental and calculated excitation functions of ^{148}Gd production in ^{nat}W show that:

1. the experimental data are in satisfactory agreement with the results of [4] at 0.6 and 0.8 GeV;
2. the theoretical predictions of all four codes can describe only qualitatively the excitation function form, so the codes cannot be used without validating by experimental data.

Later on, we are planning to finish the like measurements with ^{181}Ta using a broader list of theoretical codes.

Acknowledgements

The authors are grateful to A. Boudard (CEA Saclay) for providing us with INCL4+ABLA code. The research is carried out under ISTC Project #3266 [10] supported by the EC. The research is also supported by the Atomic Energy Agency of Russia and, in part, by the National Nuclear Safety Administration of the US Department of Energy in Los Angeles under contract no. DE-AC52-06NA25396.

References

[1] Yu.E. Titarenko, V.F. Batyaev, E.I. Karpikhin, R.D. Mulambetov, A.B. Koldobsky, V.M. Zhivun, S.V. Mulambetova, K.A. Lipatov, Yu.A. Nekrasov, A.V. Belkin, N.N. Alexeev, V.A. Schegolev, Yu.M. Goryachev, V.E. Luk'yashin, E.N. Firsov, *Experimental and Theoretical Study of the Yields of Residual Product Nuclei in Thin Targets Irradiated by 100-2 600 MeV Protons, Revised and updated Version of the Final Project Technical Report of ISTC 839B-99 of February 2001*, IAEA, Nuclear Data Section, Wagramer Strasse 5, A-1400 Vienna, NDC(CCP)-434, September (2002), available at *http://www-nds.iaea.org/reports/indc-ccp-434.pdf*; Yu.E. Titarenko, V.F. Batyaev, E.I. Karpikhin, R.D. Mulambetov, V.M. Zhivun, A.V. Ignatyuk, V.P. Lunev, N.N. Titarenko, Yu.N. Shubin, V.S. Barashenkov, S.V. Mulambetova, K.A. Lipatov, A.V. Belkin, N.N. Alexeev, V.A. Schegolev, Yu.M. Goryachev, V.O. Kudryashov, *Experimental and Theoretical Studies of the Yields of Residual Product Nuclei Produced in Thin Pb and Bi Targets Irradiated by 40-2 600 MeV Protons,* Final Technical Report on the ISTC Project # 2002, *nea.fr/html/science/egsaatif/ISTC2002-final-report.pdf*.

[2] Yu.E. Titarenko, O.V. Shvedov, V.F. Batyaev, E.I. Karpikhin, V.M. Zhivun, A.B. Koldobsky, R.D. Mulambetov, S.V. Kvasova, A.N. Sosnin, S.G. Mashnik, R.E. Prael, A.J. Sierk, T.A. Gabriel, M. Saito, H. Yasuda, "Cross Sections for Nuclide Production in 1 GeV Proton-irradiated ^{208}Pb", *Phys. Rev.*, *C* 65, 064610 (2002).

[3] Yu.E. Titarenko, V.F. Batyaev, A.Yu. Titarenko, M.A. Butko, K.V. Pavlov, S.N. Florya, R.S. Tikhonov, S.G. Mashnik, A.V. Ignatyuk, N.N. Titarenko, W. Gudowski, M. Tesínský, C-M.L. Persson, H. Ait Abderrahim, H. Kumawat, H. Duarte, *Cross-sections for Nuclide Production in ^{56}Fe Target Irradiated by 300, 500, 750, 1 000, 1 500, and 2 600 MeV Protons Compared with Data on Hydrogen Target Irradiation by 300, 500, 750, 1 000, and 1 500 MeV/nucleon ^{56}Fe Ions*, LANL Report LA-UR-08-2219, E-print: arXiv:0804.1260v1 [nucl-ex], submitted to PRC.

[4] K.C. Kelley, N.E. Hertel, E.J. Pitcher, M. Devlin, S.G. Mashnik, "^{148}Gd Production Cross Section Measurements for 600- and 800-MeV Protons on Tantalum, Tungsten, and Gold", *Nuclear Physics, A 760* (2005) 225-233.

[5] J. Tobailem, *Sections Efficaces des Reactions Nucleaires Indutes par Protons, Deuterons, Particles Alphas. V. Silicium*, Note CEA-N-1466(5), Saclay (1981).

[6] J.S. Hendricks, G.W. McKinney, L.S. Waters, T.L. Roberts, H.W. Egdorf, J.P. Finch, H.R. Trellue, E.J. Pitcher, D.R. Mayo, M.T. Swinhoe, S.J. Tobin, J.W. Durkee, F.X. Gallmeier, J-C. David, *MCNPX EXTENSIONS Version 2.5.0*, LANL Report LA-UR-05-2675, Los Alamos (April 2005), available at *http://mcnpx.lanl.gov/*.

[7] S.G. Mashnik, A.J. Sierk, K.K. Gudima, LA-UR-02-5185, *12th Biennial Topical Meeting of the Radiation Protection and Shielding Division of the American Nuclear Society*, Santa Fe, NM, 14-17 April 2002, nucl-th/0208048; S.G. Mashnik, K.K. Gudima, A.J. Sierk, *Proceedings of the 6th Int. Workshop on Shielding Aspects of Accelerators, Targets and Irradiation Facilities (SATIF-6)*, Stanford Linear Accelerator Center, CA, 10-12 April 2002, LA-UR-03-2261, nucl-th/0304012.

[8] A. Boudard, J. Cugnon, S. Leray, C. Volant, *Phys. Rev. C* 66 (2002) 044615; J.J. Gaimard, K-H. Schmidt, *Nucl. Phys. A531* (1991) 709; A.R. Junghans, M. de Jong, H-G. Clerc, A.V. Ignatyuk, G.A. Kudyaev, K-H. Schmidt, *Nucl. Phys. A629* (1998) 635.

[9] J.K. Tuli, *Evaluated Nuclear Structure Data File, A Manual for Preparation of Data Sets*, BNL-NCS-51655-01/02-Rev, February 2001, *http://ie.lbl.gov/databases/ENSDF-Manual.pdf*. ENSDF database is available at: *http://ie.lbl.gov/databases/ENSDFdata.exe*.

[10] ISTC Project #3266, *http://tech-db.istc.ru/istc/db/projects.nsf/all-projects/3266*.

Session III

Shielding in medical and industrial accelerator applications

Chair: B.L. Kirk

Low activation concrete project in Japan

Ken-ichi Kimura,[1] **Masaharu Kinno,**[1] **Katsumi Hayashi,**[2] **Mikio Uematsu,**[3] **Tomohiro Ogata,**[4] **Hiroichi Tomotake,**[5] **Ryouetsu Yoshino,**[6] **Mituru Sato,**[7] **Minoru Saito,**[8] **Akira Hasegawa**[9]
[1]Fujita Corporation, [2]Hitachi GE Nuclear Energy, [3]Toshiba Corporation, [4]Mitsubishi Heavy Industries, [5]Taiheiyo Cement Corporation, [6]Denki Kagaku Kogyo Co. Ltd., [7]Nippon Steel Technoresearch Corp., [8]Tohoku Electric Power Co., Inc., [9]Tohoku University

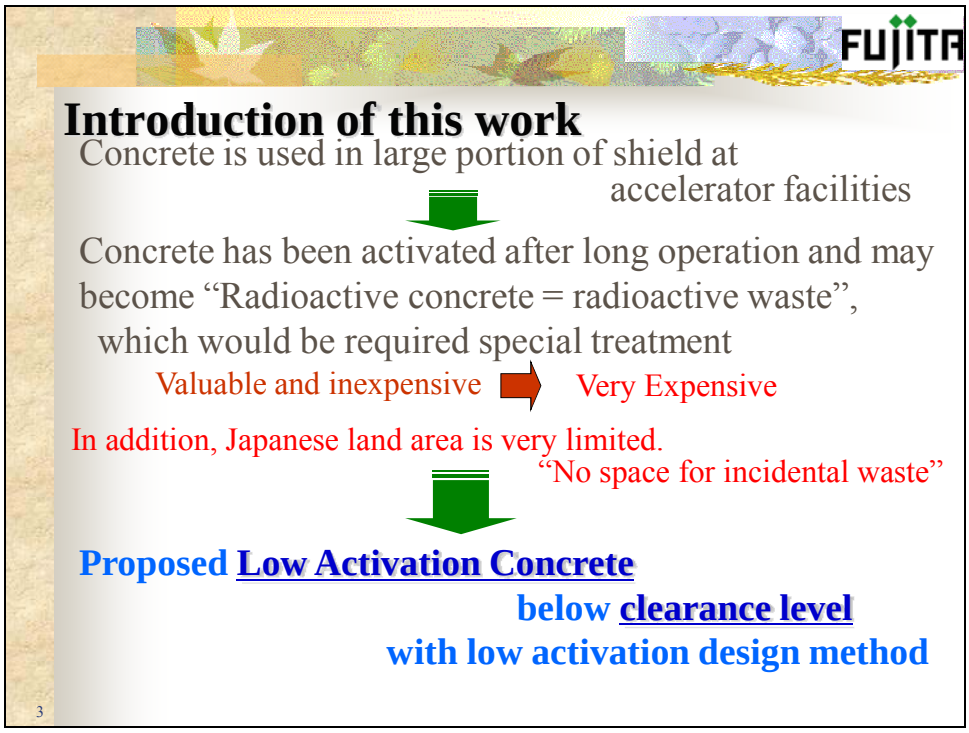

FUJITA

Classification of Radioactive Waste

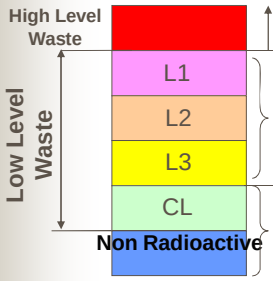

Clearance level : $\Sigma(D_i/C_i) < 1$

$\Sigma(D_i / C_i)$

D_i : Concentration of radionuclide i
C_i : Clearance level of radionuclide i

(Bq/g)

Clearance level for objected nuclides and D/C for typical ordinary concrete and low activation concrete

Nuclide		H-3	C-14	Cl-36	Fe-55	Co-60	Zn-65	Cs-134	Eu-152	Eu-154	Total
Clearance level C(B/g)		100	1	1	1000	0.1	0.1	0.1	0.1	0.1	
Di/Ci with calculated D for concrete	Ordinary	1.2-1	4.0-3	4.5-4	2.5-3	7.1	3.3-4	4.8-2	10	8.2-1	18
	1/30 Low-activation	4.8-3	2.1-3	5.3-4	2.5-5	6.4-2	6.7-5	6.7-4	4.3-1	3.5-2	0.53

Di/Ci~Di: concentration of radionuclide i, Ci: clearance level of radionuclide i, cited from IAEA-RS-G-1.7, assuming the thermal neutron $2\times10^{5}n_{th}\cdot cm^{-2}s^{-1}$, 40 yr of operation, and 6 yr of cooling.

4

FUJITA

Disposal Cost

Disposal / Material Costs Ratio

	Radioactivity Level and burial Cost[1]	Disposal Costs / Construction Costs[2] Concrete	Steel
Low Level Waste	Comparatively High Radioactivity(L1) (17,250,000yen/m^3)	2,800	250
	Low Level Waste(L2) (2,800,000yen/m^3)	460	40
	Very Low Level Waste(L3) (400,000yen/m^3)	65	5.8

1) METI comittie report 1997, 2)Assuming as 12k yen in the condition of 51% occupation

Disposal cost of radioactive waste depends on its radioactivity.

65 to 2800 for concrete
5.8 to 250 for metal

5

FUJITA

What is Clearance Level ?

- Definition of the criteria for the “trivial” radiation level which poses “negligible” risk , -10μSv/y (1/100 background)
- Determination of the line between regular waste and low level radioactive waste(LLW)
- IAEA provided international guideline for LLW, specifying “basic safety standard” (TECDOC-855)
- Reevaluated to issue RS-G-1.7 (2004)
- Introduction of CL to Japanese Low at 2005 for nuclear plants based on RS-G-1.7(IAEA) for each radioactive nuclides

6

FUJITA

Clearance level and calculated D/C

Nuclide	Clearance Level	Calculated Radioactivity		
		Andesite Concrete		1/30 LA concrete
C(Bq/g)	D(Bq/g)	D/C		D/C
H-3	100	1.21E-01		4.84E-03
C-14	1	3.96E-03		2.10E-03
Cl-36	1	4.52E-04		5.33E-04
Fe-55	1000	2.48E-03		2.48E-05
Co-60	0.1	7.07E+00		6.36E-02
Ni-59	100	5.91E-07		1.60E-07
Ni-63	100	7.00E-05		1.82E-05
Zn-65	0.1	3.34E-04		6.68E-05
Cs-134	0.1	4.80E-02		6.72E-04
Eu-152	0.1	1.02E+01		4.28E-01
Eu-154	0.1	8.23E-01		3.46E-02

Di/Ci～
Di: concentration of radionuclide i, Ci: clearance level of radionuclide i, cited from IAEA-RS-G-1.7, assuming the thermal neutron $2\times10^{5}n_{th}\cdot cm^{-2}s^{-1}$, 40 yr of operation, and 6 yr of cooling.

7

FUJITA

Activation in JPDR

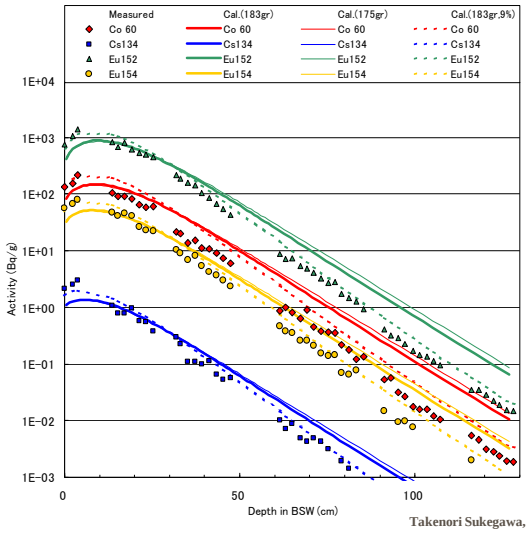

Takenori Sukegawa, et al., INDC(JPN)-164, March 1993.

8

FUJITA

Induced radioactivity at the wall of CYRIC

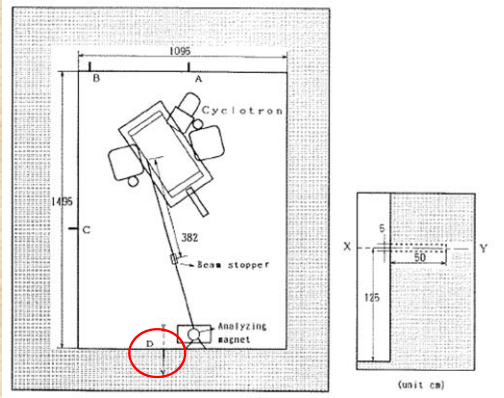

Top view of the cyclotron Side view

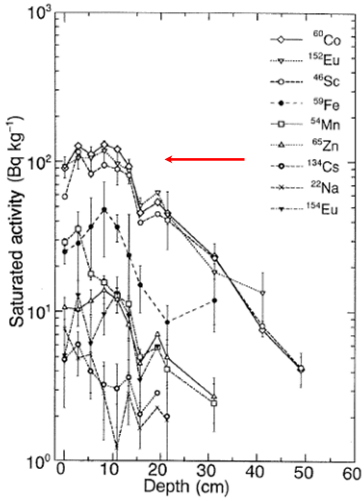

Induced radioactivity at D

9 K.Kimura et al, Health Physics, Dec. 1994, vol. 67

FUJITA

Residual Radioactivity of two types of Concrete

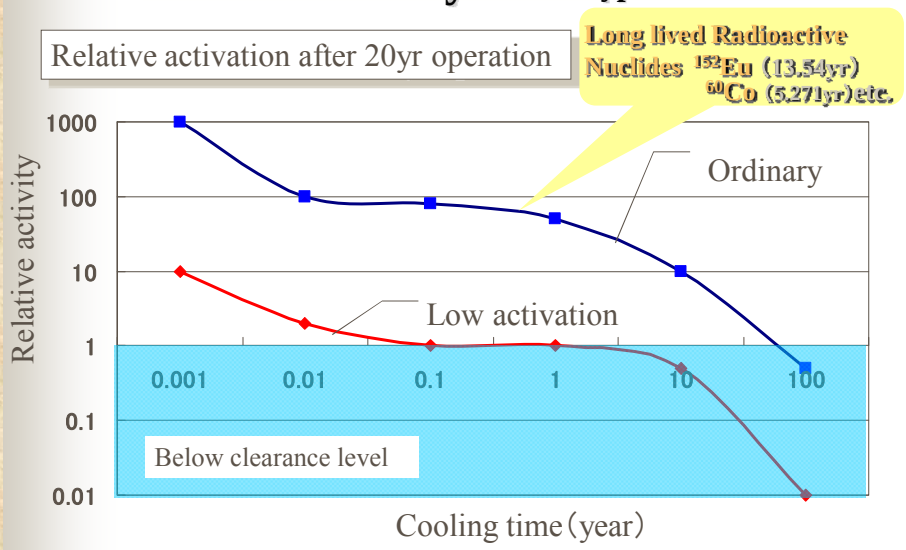

10

FUJITA

Target nuclides for low-activation in concrete

Reactor for decommissioning
- Nuclide: Eu-152, Co-60, Eu-154, H-3
- Element: Eu, Co, Li

Accelerator for decommissioning
- Nuclide: Eu-152, Co-60, Na-22, H-3, Mn-54
- Element: Eu, Co, Li, Na, Fe

Accelerator for maintenance
- Nuclide: Na-24
- Element: Na, (Mg, Al, Si)

11

FUJITA

Ways for reduction of activation in concrete

Reduction of target elements in concrete

For decommissioning:Low Eu and Low Co materials

For maintenance:Low Na

Attenuation of the (Thermal) neutron flux

Special containment in shielding concrete

High H aggregate	Serpentite and Periodite
Heavy density	Magnetite and Pyrite
Neutron absorbing material	B_4C and Colremanite

12

FUJITA

Consistent of concrete in general

Steel bar and cement are industrially manufactured

Process management required

Aggregate comes from nature (mountain, river…)

Several of data required

13

FUJITA

Containment distribution of Eu and Co for aggregate-

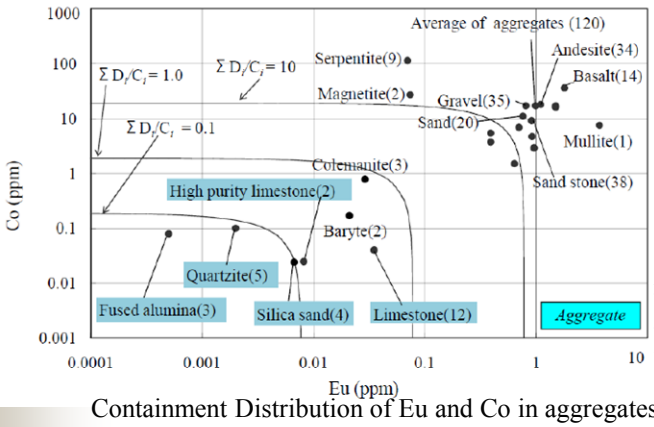

As a guideline for screening, three curved lines, ∑Di/Ci = 10, 1 and 0.1 are plotted, assuming the thermal neutron flux of 2.0E+05 $n_{th}\cdot cm^{-2}s^{-1}$, 40 years of operation, and 6 years of cooling

Containment Distribution of Eu and Co in aggregates

Limestone, quartzite, and fused alumna were selected "candidates for low-activation raw material

14

FUJITA

Containment distribution of Eu and Co for cement-

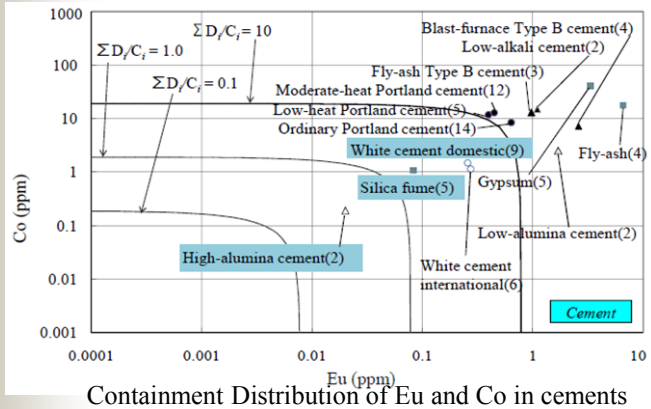

As a guideline for screening, three curved lines, ∑Di/Ci = 10, 1 and 0.1 are plotted, assuming the thermal neutron flux of 2.0E+05 $n_{th}\cdot cm^{-2}s^{-1}$, 40 years of operation, and 6 years of cooling

Containment Distribution of Eu and Co in cements

While cement and high-alumina were selected

15

FUJITA

Development of Low-Activation Reinforced Concrete design methodology (LARC) project

- 2004 Start feasibly study (4 companies)
- 2005 Adapted as IVNET (METI funds)
  Development of Low-Activation
  Reinforced Concrete design methodology (LARC)
- 2005 Start the project (9 organizations)

Tohoku University, Fujita Corporation, Hitachi-GE Nuclear Energy, Toshiba Corporation, Mitsubishi Heavy Industries, Taiheiyo Cement Corp., Denki Kagaku Kogyo Kabushiki Kaisha, Nippon Steel Technoresearch Corp., Tohoku Electric Power Co.,

16

FUJITA

Work Flow of the LARC Project

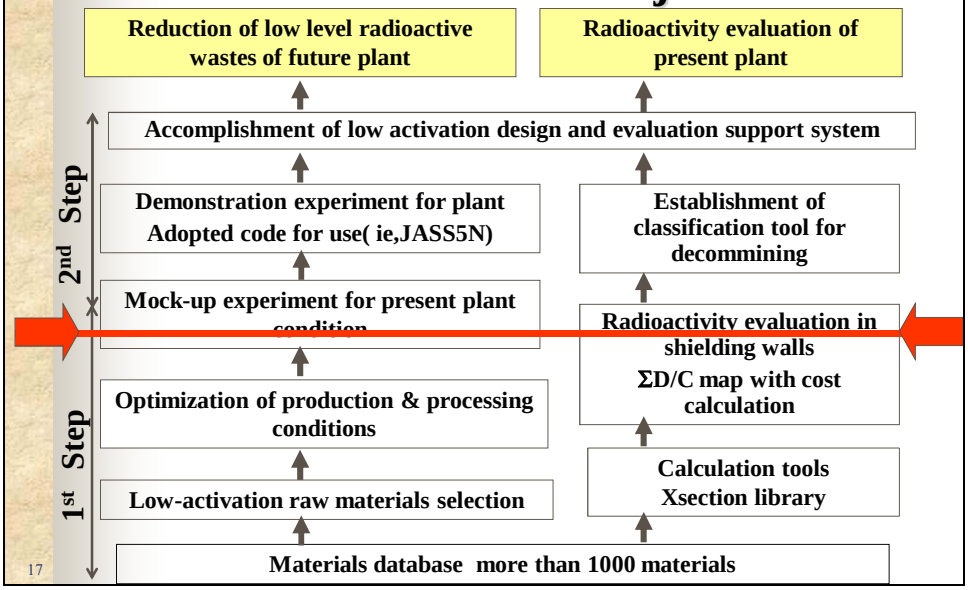

17

Three components

A.Selection of the low-activation raw material
- Establishment of the database more than 2000 raw material
- Analysis of target elements in raw materials
- Identification of materials with analyses data
- Selection and simulation of low-activation raw materials
- Low-activation Material Development Support System

B.Development of low-activation materials
- Manufacture and production evaluation and development
- Development of New cement, additive, reinforced bar
- **Manufacture of low-activation concrete :(2) by Dr.Kinno**

C.Development of low-activation Design
- Multi group X-sec library for precise activation analysis
- **Concrete activation analyses of BWR/PWR:(3)**
- **Radioactive waste disposal level mapping system:(4)**

(3) by Dr.Hayashi, and (4) by Mr. Ogata

18

Concept of the low-activation concrete

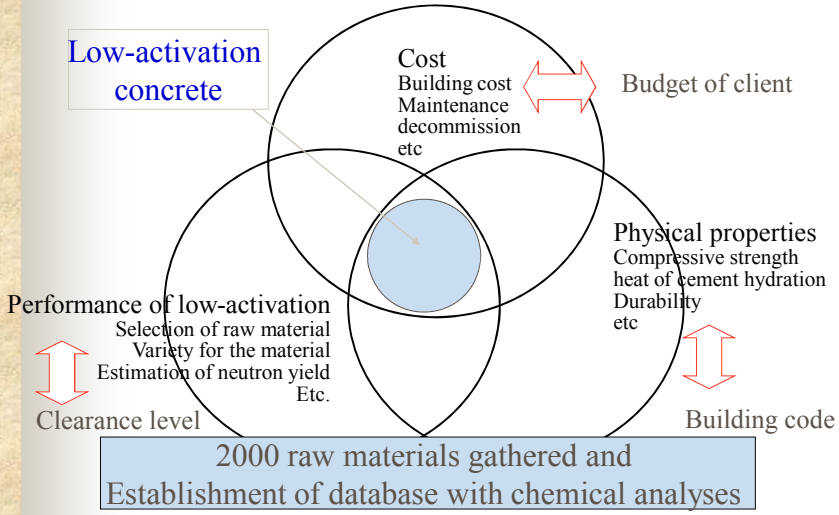

19

FUJITA

Physical properties-examples

Material	Slump(cm)	Air content(%)	Concrete temperature (°C)	Density (kg/m³)
Low-heat type I	12.5	4.6	20.7	2,340
Basic type I	13.5	3.1	21.1	2,384

Item		Condition	Low heat type concrete	Basic type concrete
Compressive strength (N/mm²)	7 days	Standard curing (20°C)	17.9	35.0
	28 days		40.2	47.8
	91 days		52.2	50.4
Young's modulus (N/mm²)	7 days	Standard curing (20°C)	23,740	27,820
	28 days		27,540	31,470
	91 days		34,820	37,960
Splitting tensile strength (N/mm²)	7 days	Sealed curing (20°C)	2.27	3.18
	28 days		3.92	3.56
	91 days		4.22	4.02
Bleeding rate (cm³/cm²)		-	0.502	0.091
Percentage of bleeding capacity (%)		-	11.4	2.3
Setting time	Initial (hr-min)	20°C	7-08	4-31
	Final (hr-min)		9-46	6-11

20

FUJITA

Lineups of low-activation concrete

Type	Aggregate	cement	Density (g/cm³)	ΣD/C ratio	Features
Basic	Limestone	White	2.39	1/31	Universal
	Limestone	Ordinary	2.35	1/10	Inexpensive
	Limestone	Ordinary w/ad	2.35	1/21	Inexpensive
	Limestone	High alumina	2.35	1/115	High performance
	Fused alumina	High alumina	2.92	1/298	High performance
Low heat	Limestone	Low heat	2.34	1/20	General
	Limestone	Low heat w/ad	2.35	1/18	Low heat
	Limestone	White w/ad	2.32	1/32	Low heat
	Limestone	LALH(New)	2.36	1/33	Low heat
	Limestone	White w/ad	2.34	1/63	Very low heat
Special	Limestone	White w/B_4C	2.35	(1/100)	Multi performance
	Serpentite +Colemanite	White		(1/1)	High H
	Sand and B_4C	Ordinary	2.19		High B (17.8w%)

21

FUJITA

Instillation of low-activation concrete to J-PARC

For reduction of induced radioactivity
Reduction of induced Na-24
Contribution ratio of the reaction*

1.0 for Na-23(n, γ)Na-24
0.02 for Mg-24(n,p)Na-24
0.01 for Al-27(n, α)Na-24
0.002 for Si(n,sp)Na-24

"Control with quantities of Sodium**"
= containment of Sodium*1.0 +
containment of Mg*0.02+
containment of Al*0.01+
containment of Si*0.002

*W.S. Gilbert, et al.,: Concrete Activation Experiment at the BEVATRON, UCRL-19368, 1969

**N. Matsuda, et al.,: A Study on Induced Activity in the Low-activationized Concrete for J-PARC, Journal of Nuclear Science and Technology, Supplement 4, Mar. 2004, p.74-77

22

FUJITA

Continuing

Requirements for raw materials

Low-Na	Limestone Aggregate
Low heat generation	Low heat Portland cement

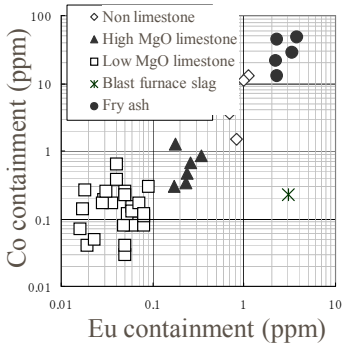

M. Miyahara, et al, "Low heat and low-activation concrete execution work –J-PARC", Cement and concrete, 2007

23

FUJITA

Activation area for PET Cyclotron room

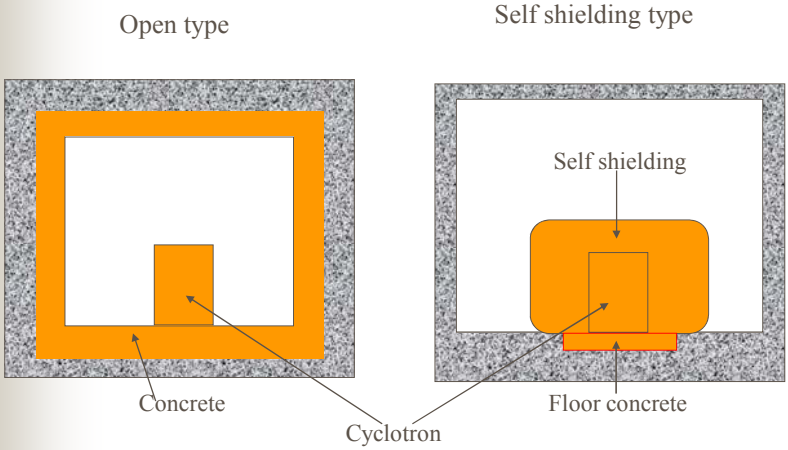

24

24

FUJITA

Basic concept to apply LAC to the self shielding facility

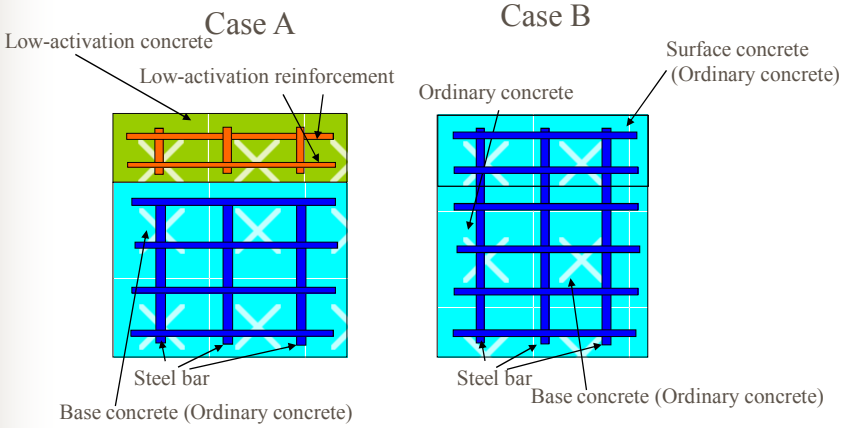

With low-activation concrete

Ordinary concrete

Floor portion of the Cyclotron facility

25

FUJITA

Estimated Residual Radioactivity for floor portion

Estimated maximum clearance level (Σ(Di/Ci)

Operation condition	Operation: 2hr/day、6d/week、20yr Cooling: 6 months
Estimated Maximum Thermal Neutron Flux (n/cm²/sec)	9.8×10^5
Referred Clearance Level	RS-G-1.7(IAEA)
Only ordinary concrete (B)	**13.5 (=required special treatment!)**
Use of Low Activation Concrete(A)	⇩
Low-Activation concrete (surface)	**0.31 (regular waste)**
Ordinary concrete (base)	**0.45 (regular waste)**

26

FUJITA

Low-Activation PCa Construction Method

Setting of the Low-Activation Concrete PCa inside cyclotron room

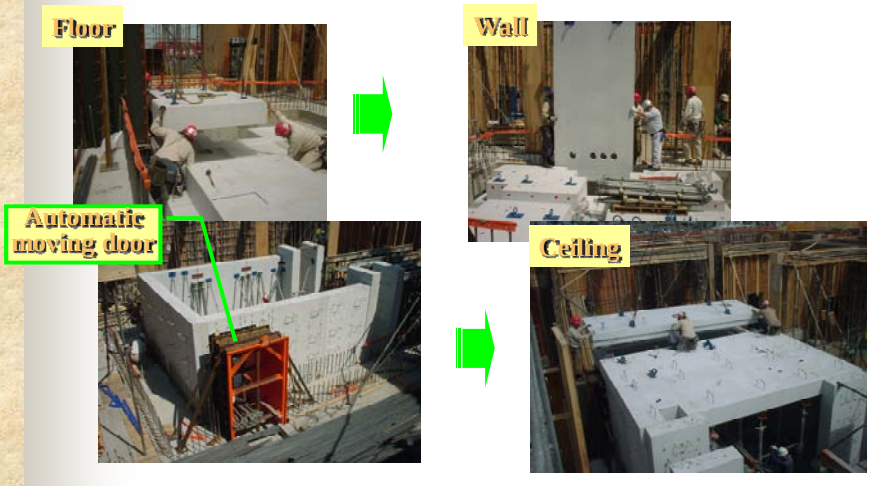

27

Low Activation PCa of the floor portion for self-shielding type cyclotron

※）Construction work of the low-activation PCa for cyclotron room in a hospital

28

Summary

- Criteria for decommissioning is “below clearance level”
- Target elements for low-activation are Eu, Co, and Na
- Low-activation concrete is required a balance of low-activation performance, physical properties, and cost.
- Introduction of LARC project
- 13 kinds of low-activation concrete are presented
- Instillation of low-activation concrete to accelerator facilities

29

Update on the activities of the Computational Medical Physics Working Group (CMPWG)

Bernadette L. Kirk
Nuclear Science and Technology Division
Oak Ridge National Laboratory
Oak Ridge, USA

Abstract

The Computational Medical Physics Working Group (CMPWG) contributes to the Shielding Aspects of Accelerators and Target Irradiation Facilities (SATIF) series of workshops through its development of shielding benchmarks of medical facilities that employ particle accelerators and general shielding due to the use of radioisotopes in the clinical setting.

Historical development

The development of software tools in the twentieth century was prompted largely by nuclear reactor analysis, nuclear weapons studies, accelerators, fusion reactors, and health physics concerns. As the fields of medical and health physics continue to grow, the implementation of these software codes in areas like radiation oncology, imaging and dosimetry becomes more pronounced.

The use of software tools in the analysis of radiation dose and its health effects has been increasing. Such tools include MCNP/MCNPX [1-3], ITS [4], TORT [5], ANISN [6], EGS4 [7-8], PENTRAN [9], GEANT4 [10], ATTILA [11], PARTISN [12] and A^{3}MCNP [13], to name a few.

CMPWG promotes the union of research encompassing nuclear engineering and medical and health physics. CMPWG was established in 2005 within the American Nuclear Society (ANS) and is hosted by three divisions of the ANS – Mathematics and Computation Division (MCD), Biology and Medicine Division (BMD), Radiation Protection and Shielding (RPSD). The website is *http://cmpwg.ans.org*.

Activities

CMPWG promotes the advancement of computational tools, experimental data, and enabling technologies which are applicable to clinical problems involving computational dosimetry. The group concentrates on a multidisciplinary approach (nuclear engineering, medical physics and health physics) for use by medical practitioners in the studies of radiation imaging, treatment and effects on human and animal life.

Benchmarking is an important endeavour of CMPWG. Where experimental results exist, efforts are made to use computational models to verify the experiments. This is to ensure that the measured dose is computed correctly by the software tools. Computational benchmarks will involve comparison between software that can model the same events. A mathematical formulation of a benchmark problem is also another important contribution of the working group.

CMPWG has held two workshops to bring the community together. The Nuclear Science and Technology Division (NSTD) of Oak Ridge National Laboratory (ORNL) sponsored CMPWG I on 26 October 2005. The workshop was held to address several key areas:

- identify the medical physics problems and experiments for computational benchmarks;
- identify the software tools, their applications, strengths and weaknesses;
- identify applications suitable for parallel computing;
- identify the roadmap for benchmarking activities.

Discussions centred on the need for experimental data, the importance of both Monte Carlo and deterministic methods, and the need to evaluate current nuclear data for medical physics applications. These activities are aimed at improving dose predictions for radiation therapy and other medical activities that utilise ionising radiation. Proceedings of the workshop are published in the ORNL report "ORNL/TM-2006/7" [14].

The University of Florida at Gainesville sponsored CMPWG II from 30 September to 3 October 2007. The focus of the workshop was on major software tools like PENTRAN, MCNP/MCNPX, GEANT4, ADEIS [15], A3MCNP and PENELOPE. In addition, emphasis on emerging needs in clinical applications of computation from medical physics practitioners, including radiotherapy, diagnostic applications, and the importance of image guided methodologies was also a major theme covered in this meeting [16].

CMPWG III is scheduled to be held at the Georgia Institute of Technology in 2009, and the next meeting is planned for Seoul, South Korea in 2011.

Conclusion

CMPWG is dedicated to advancing the research that merges nuclear engineering with computational dosimetry applications in medical and health physics. Its success will greatly depend on the invaluable contributions of the scientific community.

References

[1] Los Alamos National Laboratory, X-5 Monte Carlo Team, *MCNP – A General Monte Carlo N-particle Transport Code, Version 5 - Volume I: Overview and Theory*, LA-UR-03-1987 (April 2003, revised October 2005).

[2] D.B. Pelowitz (Ed.), *MCNPX User's Manual, Version 2.5.0*, Los Alamos National Laboratory Report, Los Alamos, New Mexico, LA-CP-05-0369 (April 2005).

[3] J.S. Hendricks, *et al.*, *MCNPX Extensions, Version 2.5.0*, Los Alamos National Laboratory Report, Los Alamos, New Mexico, LA-UR-05-2675 (April 2005).

[4] J.A. Halbleib, R.P. Kensek, T.A. Mehlhorn, G.D. Valdez, S.M. Seltzer, M.J. Berger, *ITS Version 3.0: The Integrated TIGER Series of Coupled Electron/Photon Monte Carlo Transport Codes*, Sandia National Laboratory Report, Albuquerque, New Mexico, SAND91-1634 (March 1992).

[5] W.A. Rhoades, D.B. Simpson, *The TORT Three-dimensional Discrete Ordinates Neutron/Photon Transport Code*, Oak Ridge National Laboratory Report, Oak Ridge, Tennessee, ORNL/TM-13221 (October 1997).

[6] W.W. Engle, Jr., *ANISN, A One-dimensional Discrete Ordinates Transport Code with Anisotropic Scattering,* Oak Ridge Gaseous Diffusion Plant, Oak Ridge, Tennessee, Report K-1693 (March 1967).

[7] W.R. Nelson, H. Hirayama, D.W.O. Rogers, *The EGS4 Code System*, Stanford Linear Accelerator Center Report, Stanford University, Stanford, California, SLAC-265 (December 1985).

[8] A.F. Bielajew, H. Hirayama, W.R. Nelson, D.W.O. Rogers, History, *Overview and Recent Improvements of EGS4,* Stanford Linear Accelerator Center Report, Stanford University, Stanford, California, SLAC-PUB-6499, NRC-PIRS-0436, KEK Internal 94-4 (revised 1 June 1994).

[9] G.E. Sjoden, A. Haghighat, "PENTRAN – A 3-D Cartesian Parallel Sn Code with Angular, Energy, and Spatial Decomposition", pp. 1267-1276, *Proceedings of the Joint International Conference on Mathematical Methods and Supercomputing in Nuclear Applications*, Vol. II, Saratoga Springs, NY, 6–10 October 1997, <*info@hswtech.com*>.

[10] Geant4 Collaboration, *Geant4: An Object-oriented Toolkit for Simulation in HEP*, CERN/LHCC 98-44, *http://geant4.web.cern.ch/geant4/*.

[11] Transpire, Inc., *ATTILA*, *www.transpireinc.com*.

[12] R.E. Alcouffe, R.S. Baker, J.A. Dahl, S.A. Turner, Robert Ward, *PARTISN: A Time-dependent, Parallel Neutral Particle Transport Code System*, Los Alamos National Laboratory Report, Los Alamos, New Mexico, LA-UR-05-3925 (May 2005).

[13] J.C. Wagner, A. Haghighat, "Automated Variance Reduction of Monte Carlo Shielding Calculations Using the Discrete Ordinates Adjoint Function", *Nucl. Sci. Eng.*, 128, 186-208, 1998, *http://ufttg.nre.ufl.edu/~haghigha/a3mcnp.html*.

[14] *Proceedings of the Computational Medical Physics Working Group Workshop I: CMPWG I*, ORNL/TM-2006/7, August 2006 (compiled by B.L. Kirk and A.F. Rice).

[15] *The Monte Carlo Method: Versatility Unbounded in a Dynamic Computing World*, Chattanooga, Tennessee, 17-21 April 2005, on CD-ROM, American Nuclear Society, LaGrange Park, IL (2005).

[16] Proceedings *of Computational Medical Physics Working Group Workshop II*, University of Florida, Gainesville, Florida, USA, October 2007, *http://cmpwg.ans.org*.

Session IV

Benchmarking – calculations and results

Chair: M. Brugger

Development of a database of dosimetry benchmarks for radiation transport

Dan Ilas, Bernadette L. Kirk
Oak Ridge National Laboratory
Oak Ridge, USA

Objective

- **To acquire experimental data that can be used by the scientific community to benchmark the existing or future particle transport codes.**
  - **Existing experiments published in the open literature.**
  - **No criticality safety experiments.**
  - **No new experiments envisioned.**
  - **Radiation shielding and dosimetry, health and medical physics**
  - **Photons, neutrons, electrons, protons, usually up to tens of MeVs**

3 Managed by UT-Battelle for the Department of Energy

Shielding Aspects of Accelerators and Target Irradiation Facilities, SATIF-9 April 21-23, 2008, Oak Ridge, Tennessee

Criteria for Inclusion

- **1. *Relevance*: The problem is relevant to nuclear engineers, medical or health physicist and researchers interested.**
- **2. *Simplicity*: The problem is posed in the simplest possible way that achieves the benchmarking goals and requirements.**
- **3. *Clarity and Completeness*: The problem is clearly and completely described, i.e., there are no ambiguities in the statement of the radiation source, geometry, materials, and quantities of interest.**

Criteria for Inclusion

- **4. *Traditional metrics*: The problem provides for verification of traditional metrics.**
  - **Accuracy of physics models (source, radiation transport, tallies).**
  - **Freedom from subtle geometric and material specification errors.**
  - **User competence and appropriate configuration of code options.**
- **5. *Advanced metrics*: The problem provides for tests of advanced metrics.**
  - **Execution speed and efficiency.**
  - **Scalability (parallel processing).**
  - **Robustness and reliability of the results, e.g., solution convergence.**
- **6. *Data quality*: High-quality measured data are available, preferably in the peer reviewed literature.**

Criteria for Inclusion

- **7. *Reality*: The benchmark problem design should be driven by real problems of interest in medical physics, health physics or radiation shielding.**
- **8. *Availability*: The problems and example solutions should be freely available, should contain no proprietary information, should not require license agreements, etc.**
- **9. *Collaboration*: The problems should promote collaboration between disciplines of medical and health physics, nuclear engineering, radiation shielding and computer science.**

Benchmark Format

- **Data source and credits**
- **Detailed description of the experimental benchmark**
  - **Overview of the experiment, including objectives, fields of applicability**
  - **Experimental configuration (materials, physical dimensions)**
  - **Material compositions and characteristics**
  - **Rigorous source description**
- **Experimental data**
  - **Results - Numerical data and file formats**
  - **Uncertainties**
- **Computer code input**
- **Computer code output**

Example: Electron Dose Distribution behind Heterogeneities

- **Inspired by radiation therapy activities**
- **Relevant for testing the scattering of electrons off heterogeneities**
- **Beam of 10 MeV or 18 MeV electrons impinging on a heterogeneous phantom**
- **Absorbed dose monitored at 2 depths under heterogeneity layer**

Example: Electron Dose Distribution behind Heterogeneities

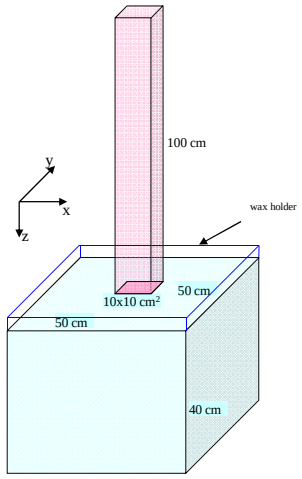

Example: Electron Dose Distribution behind Heterogeneities

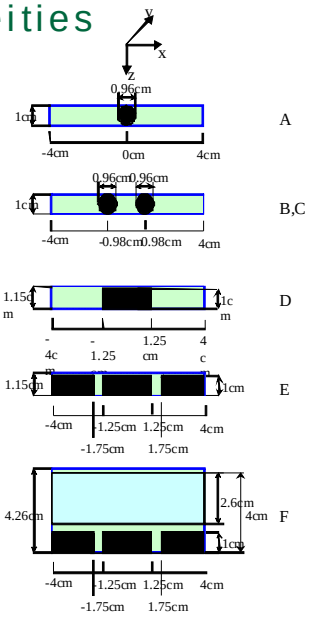

Example: Electron Dose Distribution behind Heterogeneities

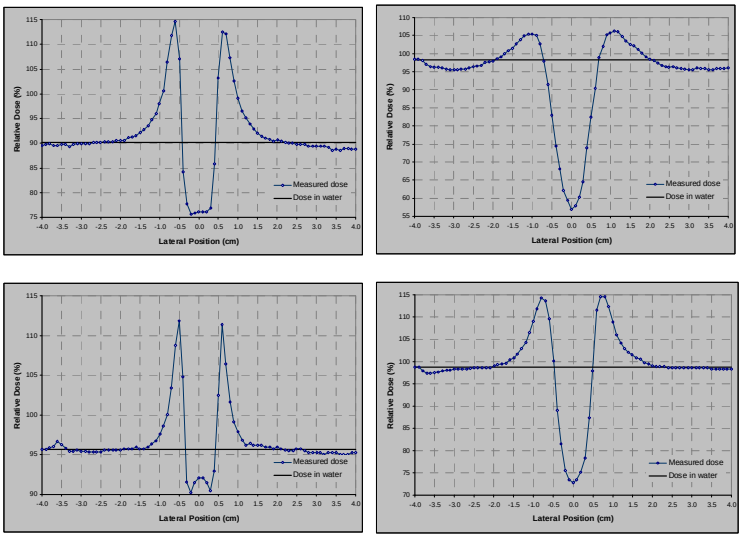

Conclusions

- **A new effort to collect experiments for benchmarking activities was started at ORNL**
- **Many experiments are old, performed with older instrumentation; authors not available anymore**
- **Description of experiments in the literature often not sufficient**
- **Search for well documented experiments continues**

Tissue equivalent proportional counter response behind the shielding of a carbon ion accelerator: Comparison between simulations and measurements

S. Rollet, P. Beck, M. Latocha, M. Wind, A. Zechner
ARC-Seibersdorf
Austria

F. Trompier
Institute for Radiological Protection and Nuclear Safety
Fontenay-aux-Roses, France

F. Wissmann
Physikalisch-TechnischeBundesanstalt
Braunschweig, Germany

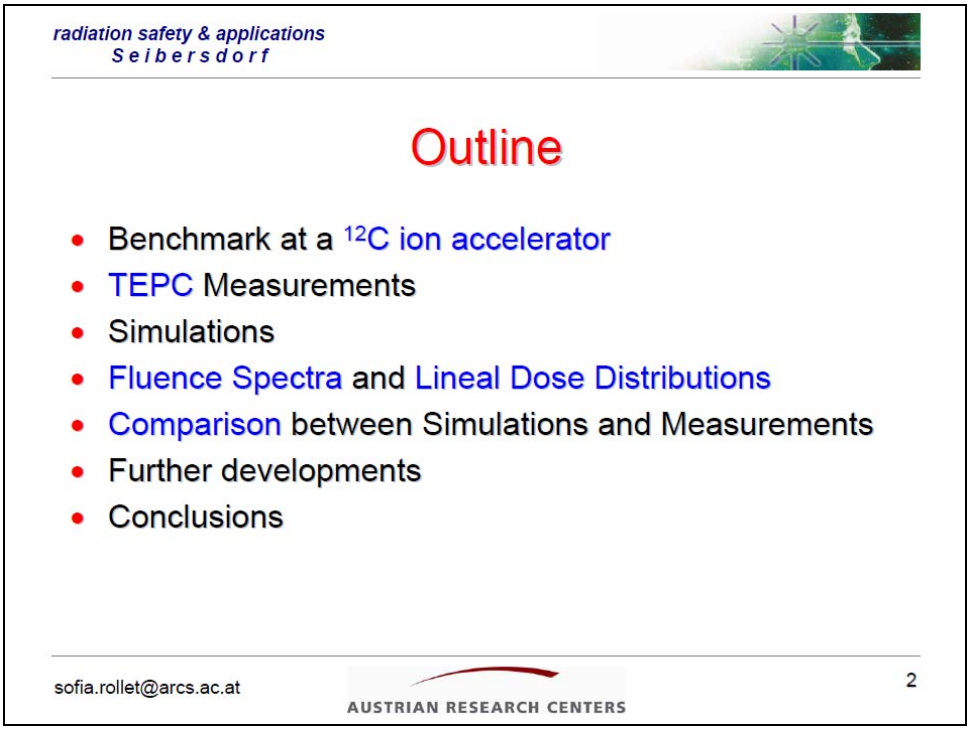

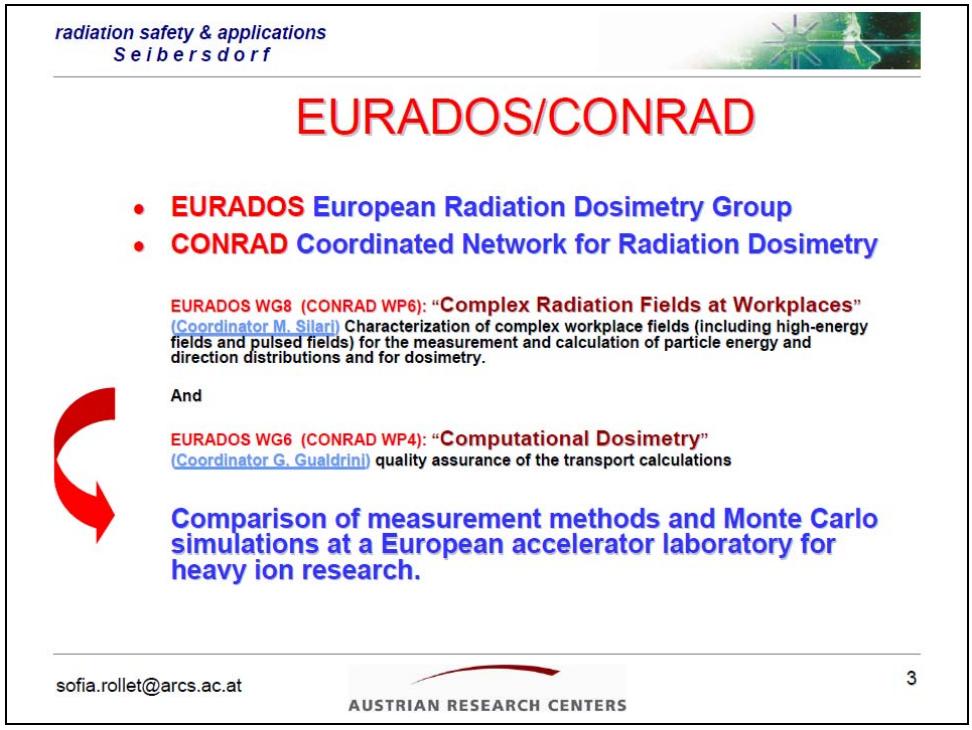
radiation safety & applications
Seibersdorf
EURADOS/CONRAD
EURADOS European Radiation Dosimetry Group
CONRAD Coordinated Network for Radiation Dosimetry
EURADOS WG8 (CONRAD WP6): "Complex Radiation Fields at Workplaces"
(Coordinator M. Silari) Characterization of complex workplace fields (including high-energy fields and pulsed fields) for the measurement and calculation of particle energy and direction distributions and for dosimetry.
And
EURADOS WG6 (CONRAD WP4): "Computational Dosimetry"
(Coordinator G. Gualdrini) quality assurance of the transport calculations
Comparison of measurement methods and Monte Carlo simulations at a European accelerator laboratory for heavy ion research.
sofia.rollet@arcs.ac.at
AUSTRIAN RESEARCH CENTERS
3

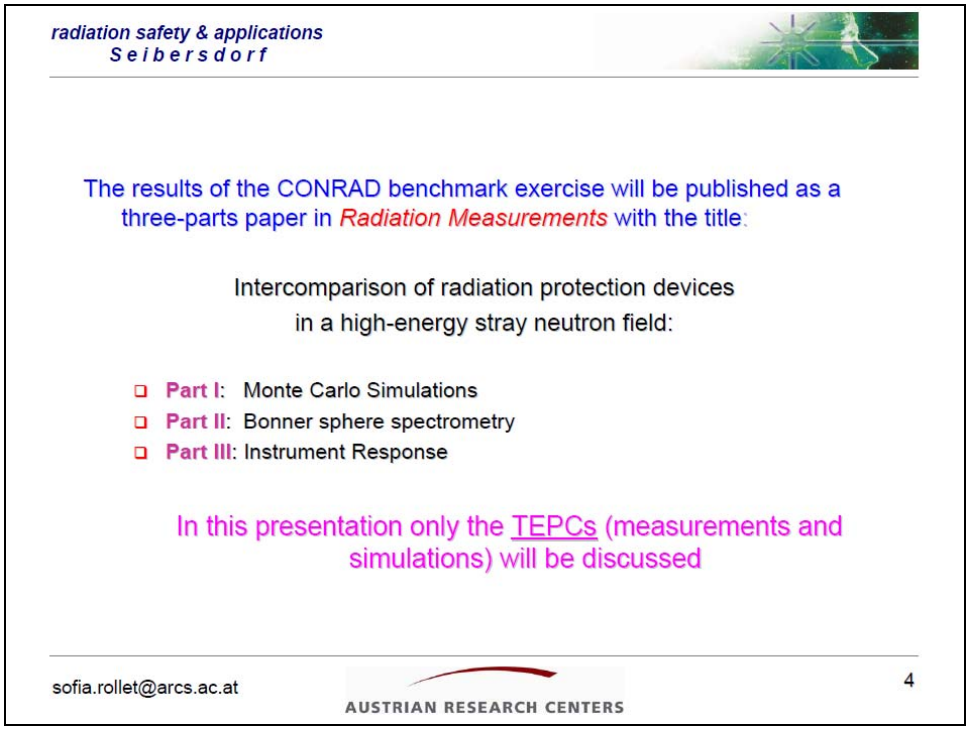
radiation safety & applications
Seibersdorf
The results of the CONRAD benchmark exercise will be published as a three-parts paper in Radiation Measurements with the title:
Intercomparison of radiation protection devices
in a high-energy stray neutron field:
Part I: Monte Carlo Simulations
Part II: Bonner sphere spectrometry
Part III: Instrument Response
In this presentation only the TEPCs (measurements and simulations) will be discussed
sofia.rollet@arcs.ac.at
AUSTRIAN RESEARCH CENTERS
4

radiation safety & applications
Seibersdorf

GSI -Darmstadt

Gesellschaft für Schwerionenforschung
Heavy Ion Research Centre – Darmstadt
Member of Helmholtz-Association

radiation safety & applications
Seibersdorf

GSI-Cave A

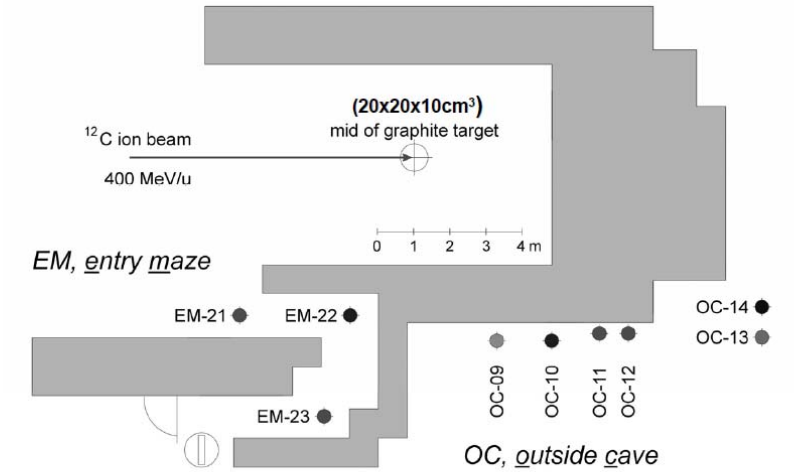

Courtesy of B. Wiegel, PTB

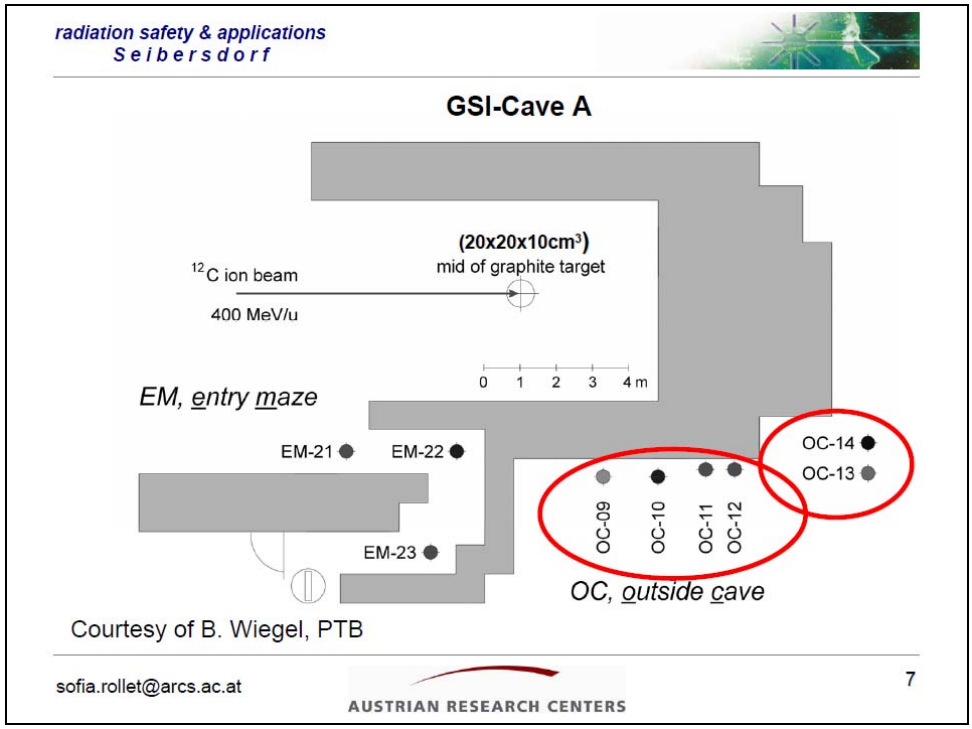
radiation safety & applications
Seibersdorf
GSI-Cave A
(20x20x10cm³)
mid of graphite target
12C ion beam
400 MeV/u
0 1 2 3 4 m
EM, entry maze
EM-21
EM-22
EM-23
OC-14
OC-13
OC-09
OC-10
OC-11
OC-12
OC, outside cave
Courtesy of B. Wiegel, PTB
sofia.rollet@arcs.ac.at
AUSTRIAN RESEARCH CENTERS
7

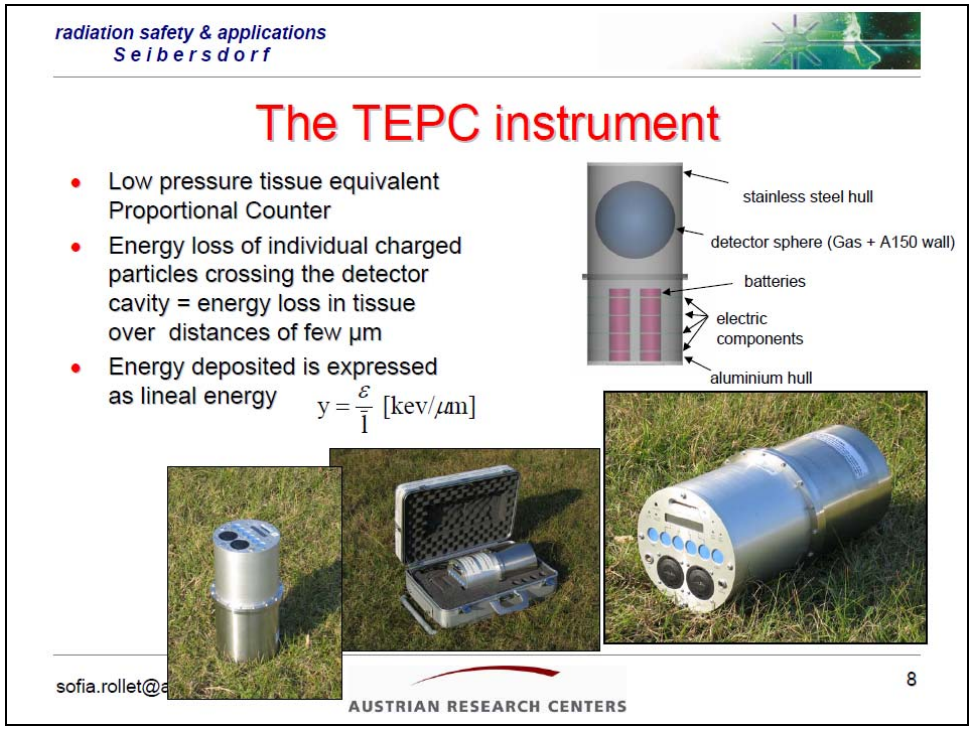
radiation safety & applications
Seibersdorf
The TEPC instrument
Low pressure tissue equivalent Proportional Counter
Energy loss of individual charged particles crossing the detector cavity = energy loss in tissue over distances of few µm
Energy deposited is expressed as lineal energy
$y = \frac{\varepsilon}{\bar{l}}$ [kev/µm]
stainless steel hull
detector sphere (Gas + A150 wall)
batteries
electric components
aluminium hull
sofia.rollet@a
AUSTRIAN RESEARCH CENTERS
8

radiation safety & applications
Seibersdorf

Measured y spectra in OC-10

y d(y) y h(y)

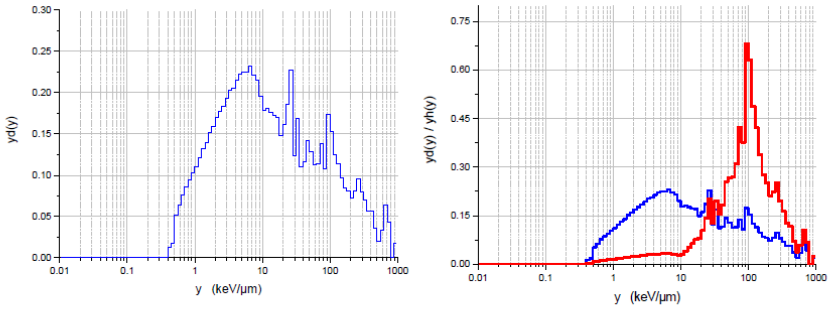

sofia.rollet@arcs.ac.at
AUSTRIAN RESEARCH CENTERS
9

radiation safety & applications
Seibersdorf

yh(y) in different positions

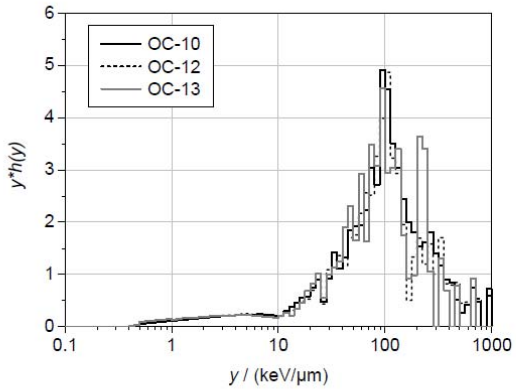

sofia.rollet@arcs.ac.at
AUSTRIAN RESEARCH CENTERS
10

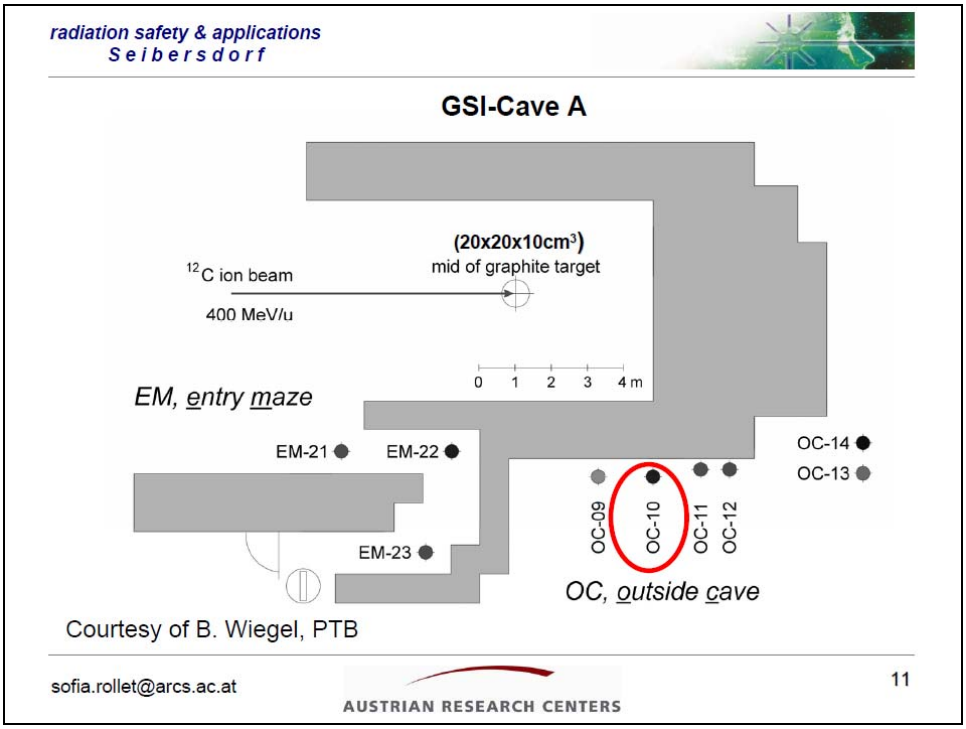
radiation safety & applications
Seibersdorf
GSI-Cave A
(20x20x10cm³)
mid of graphite target
¹²C ion beam
400 MeV/u
0 1 2 3 4 m
EM, entry maze
EM-21
EM-22
EM-23
OC-14
OC-13
OC-09
OC-10
OC-11
OC-12
OC, outside cave
Courtesy of B. Wiegel, PTB
sofia.rollet@arcs.ac.at
AUSTRIAN RESEARCH CENTERS
11

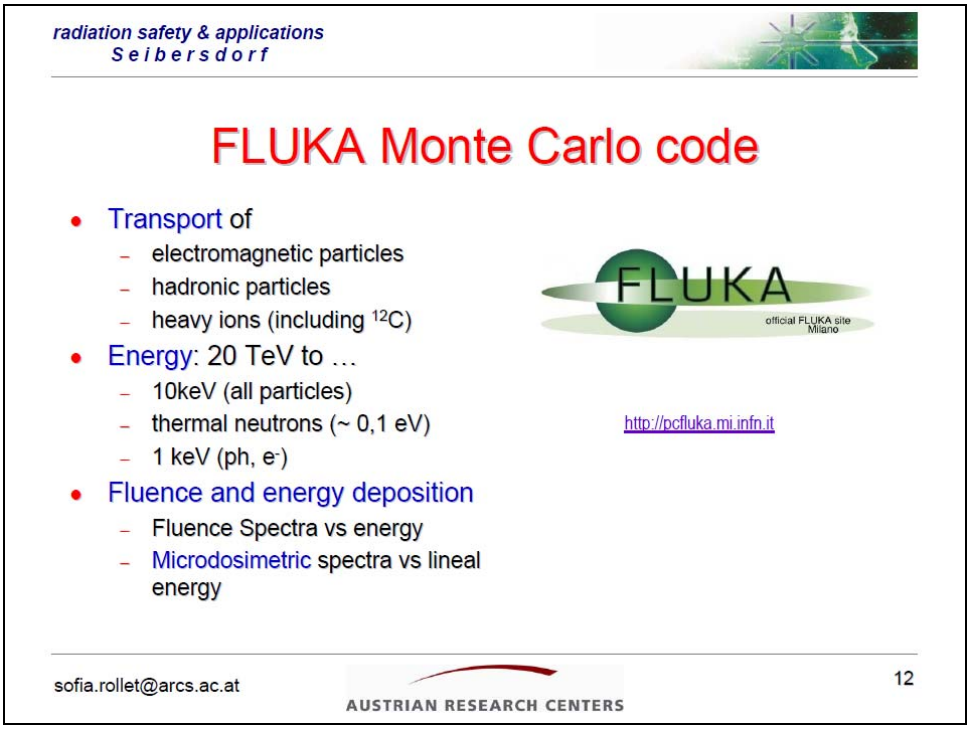
radiation safety & applications
Seibersdorf
FLUKA Monte Carlo code
Transport of
electromagnetic particles
hadronic particles
heavy ions (including ¹²C)
Energy: 20 TeV to …
10keV (all particles)
thermal neutrons (~ 0,1 eV)
1 keV (ph, e⁻)
Fluence and energy deposition
Fluence Spectra vs energy
Microdosimetric spectra vs lineal energy
FLUKA
official FLUKA site Milano
http://pcfluka.mi.infn.it
sofia.rollet@arcs.ac.at
AUSTRIAN RESEARCH CENTERS
12

radiation safety & applications
Seibersdorf

FLUKA: Fluence

Neutron Fluence at Y= -75 cm
(cm^{-2} primary $^{-1}$)

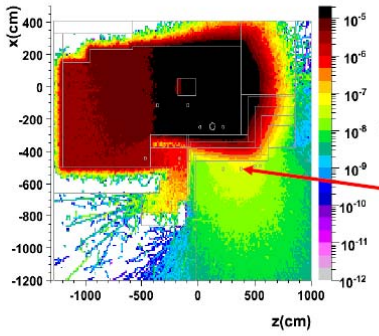

Neutron Spectral Fluence
(cm^{-2} primary $^{-1}$)

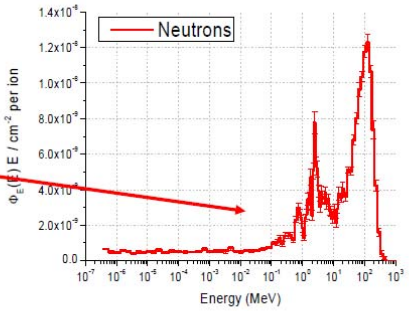

sofia.rollet@arcs.ac.at
AUSTRIAN RESEARCH CENTERS
13

radiation safety & applications
Seibersdorf

FLUKA Simulation of the TEPC

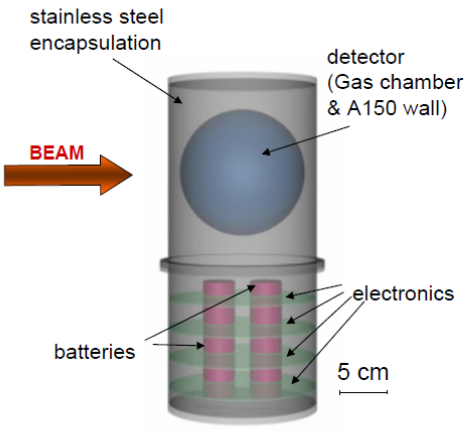

Particle Fluence (cm^{-2} primary^{-1})

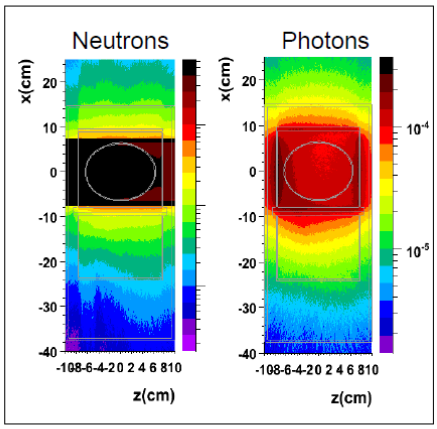

sofia.rollet@arcs.ac.at
AUSTRIAN RESEARCH CENTERS
14

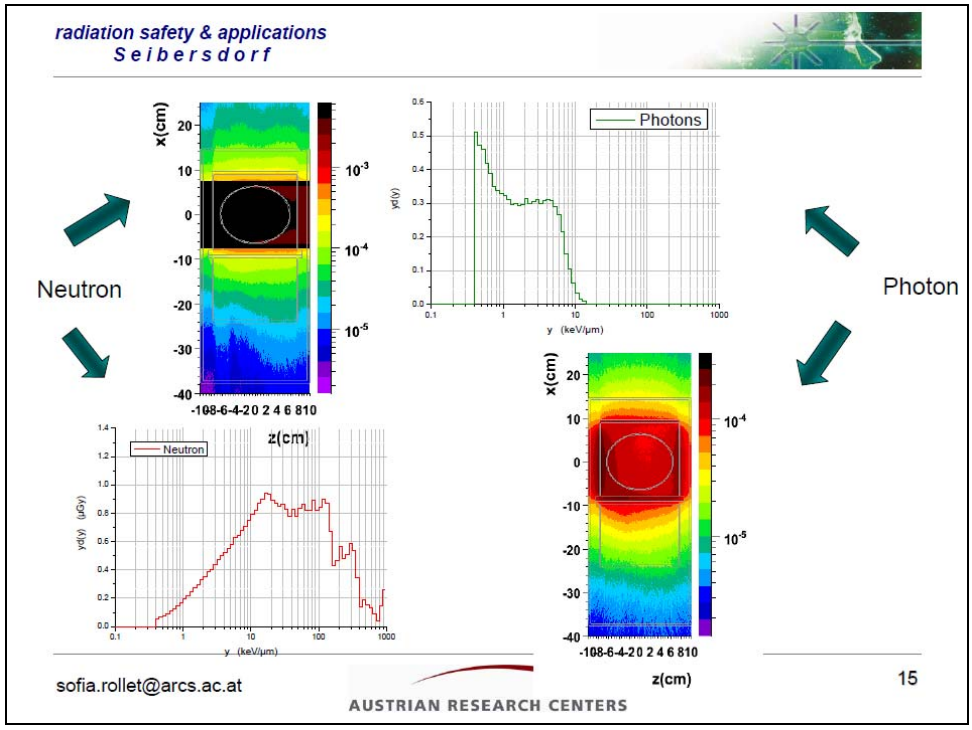
radiation safety & applications
Seibersdorf
Neutron
Photon
Photons
Neutron
x(cm)
z(cm)
yd(y)
y (keV/µm)
sofia.rollet@arcs.ac.at
AUSTRIAN RESEARCH CENTERS
15

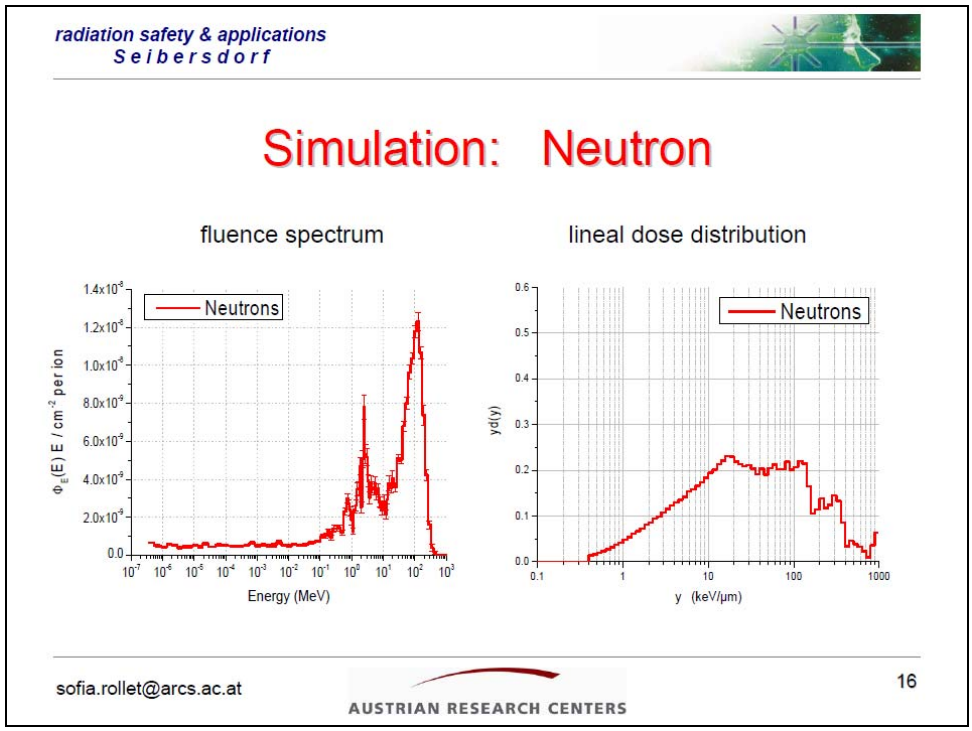
radiation safety & applications
Seibersdorf
Simulation: Neutron
fluence spectrum
lineal dose distribution
Neutrons
Energy (MeV)
yd(y)
y (keV/µm)
sofia.rollet@arcs.ac.at
AUSTRIAN RESEARCH CENTERS
16

radiation safety & applications
Seibersdorf

Simulation: Photon

fluence spectrum

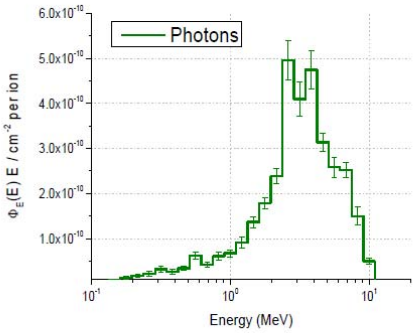

lineal dose distribution

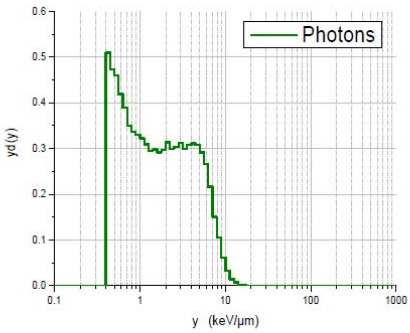

sofia.rollet@arcs.ac.at
AUSTRIAN RESEARCH CENTERS
17

radiation safety & applications
Seibersdorf

Simulation: Protons

fluence spectrum

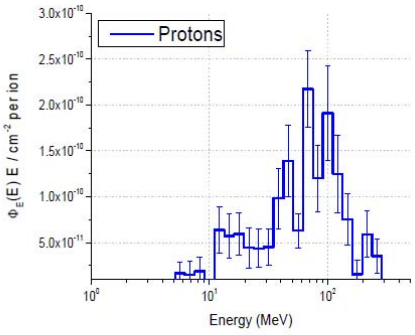

lineal dose distibution

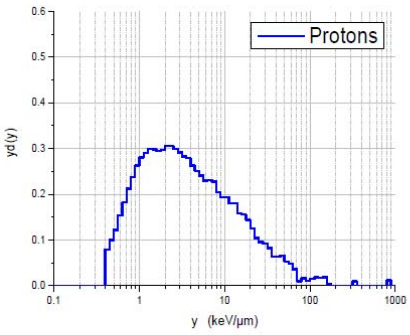

sofia.rollet@arcs.ac.at
AUSTRIAN RESEARCH CENTERS
18

radiation safety & applications
Seibersdorf

Simulated yd(y) spectrum

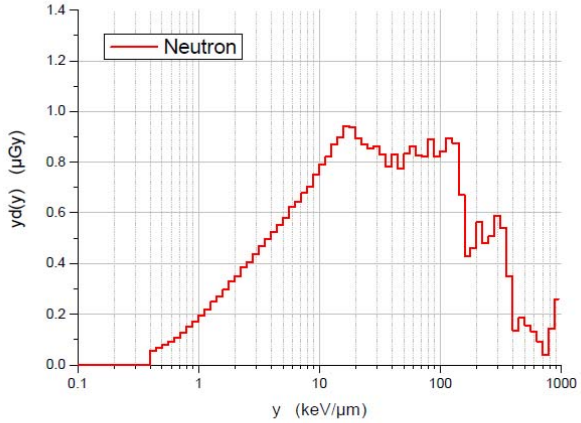

sofia.rollet@arcs.ac.at
AUSTRIAN RESEARCH CENTERS
19

radiation safety & applications
Seibersdorf

Simulated yd(y) spectrum

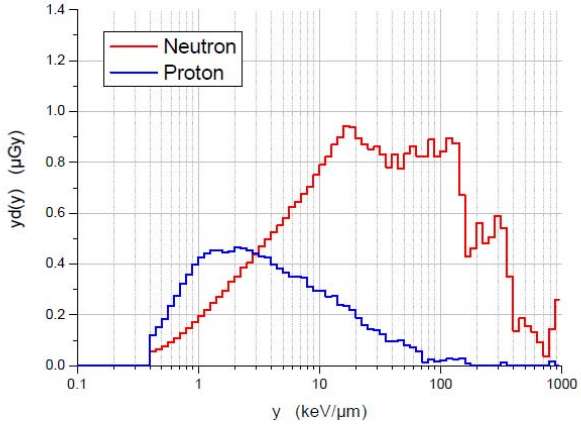

sofia.rollet@arcs.ac.at
AUSTRIAN RESEARCH CENTERS
20

radiation safety & applications
Seibersdorf

Simulated yd(y) spectrum

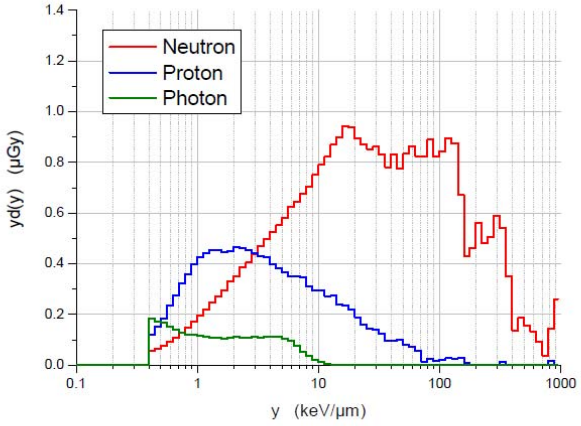

sofia.rollet@arcs.ac.at
AUSTRIAN RESEARCH CENTERS
21

radiation safety & applications
Seibersdorf

Simulated yd(y) spectrum

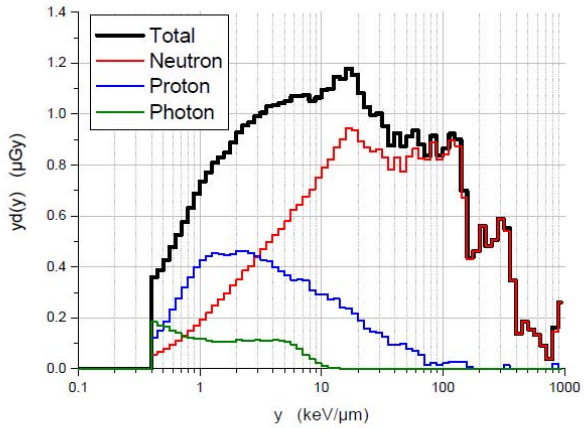

sofia.rollet@arcs.ac.at
AUSTRIAN RESEARCH CENTERS
22

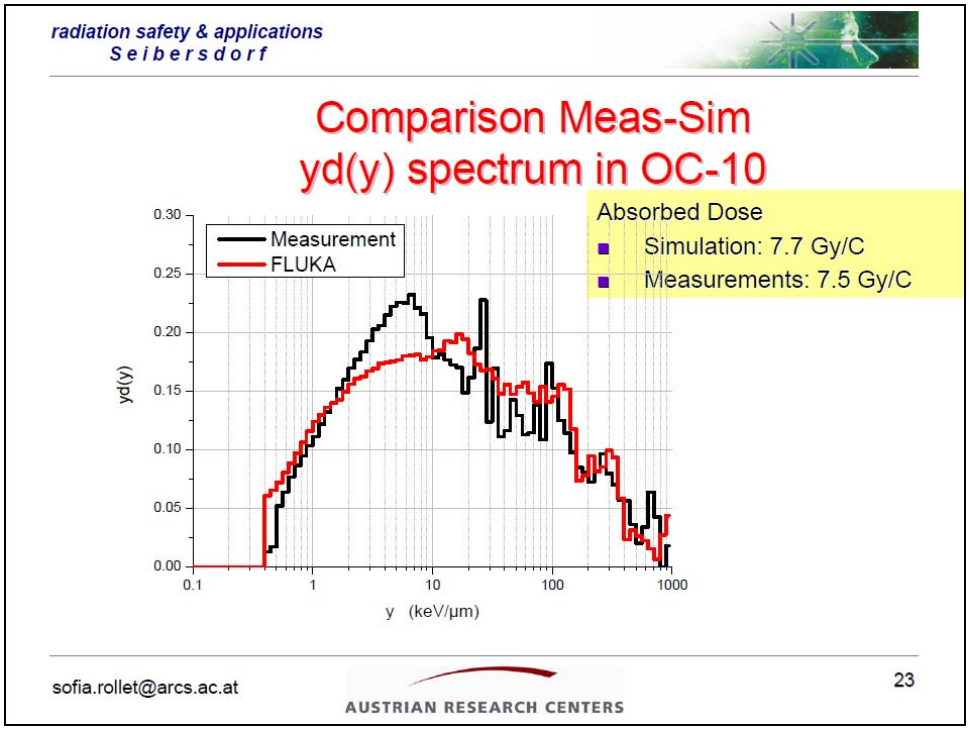
radiation safety & applications
Seibersdorf
Comparison Meas-Sim
yd(y) spectrum in OC-10
Absorbed Dose
Simulation: 7.7 Gy/C
Measurements: 7.5 Gy/C
Measurement
FLUKA
yd(y)
y (keV/µm)
sofia.rollet@arcs.ac.at
AUSTRIAN RESEARCH CENTERS
23

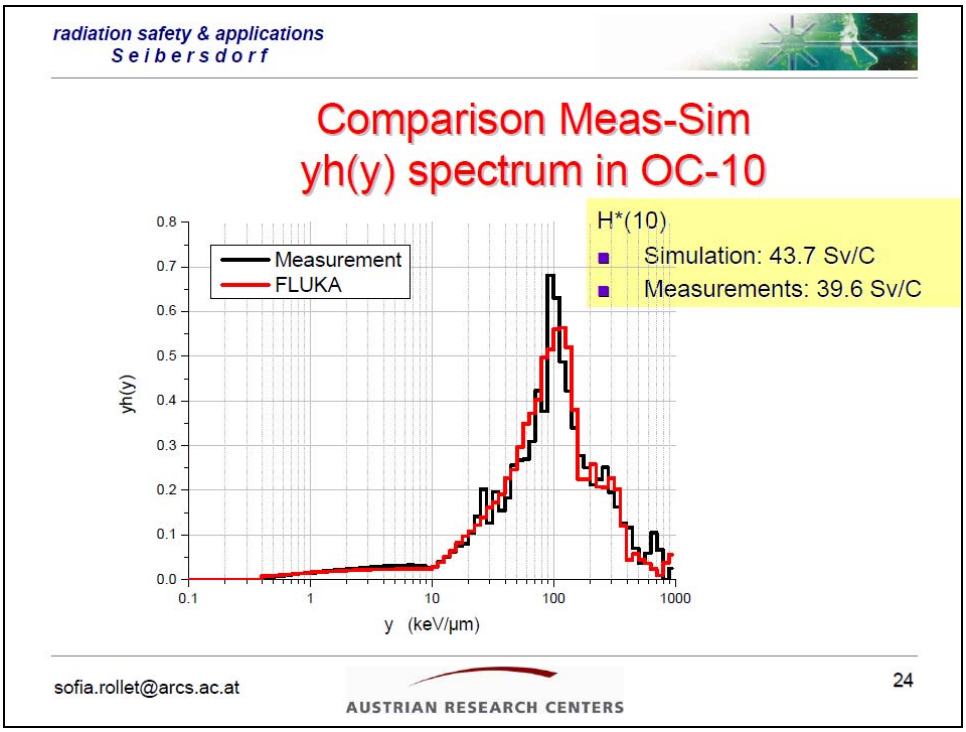
radiation safety & applications
Seibersdorf
Comparison Meas-Sim
yh(y) spectrum in OC-10
H*(10)
Simulation: 43.7 Sv/C
Measurements: 39.6 Sv/C
Measurement
FLUKA
yh(y)
y (keV/µm)
sofia.rollet@arcs.ac.at
AUSTRIAN RESEARCH CENTERS
24

radiation safety & applications
Seibersdorf

Comparison Measurements-Simulation -Ambient Dose Equivalent- (from TEPC Response)

Position OC-10	Ambient dose equivalent H*(10) Sv/C		
	H*(10)	H_low	H_high
Measurement TEPC	39.6 ± 3.7	11 %	89 %
Simulation TEPC	43.7 ± 4.3	8%	92%
Sim / Meas	**1.1** ± 0.15	**0.73**	**1.03**

sofia.rollet@arcs.ac.at
AUSTRIAN RESEARCH CENTERS
25

radiation safety & applications
Seibersdorf

Comparison Measurements-Simulation -Ambient Dose Equivalent- (from Fluence Folding with Conversion factors)

Position OC-10	Ambient dose equivalent H*(10) Sv/C			
	H*(10)			
Measurement TEPC	39.6 ± 3.7	**H_low** 11 %		**H_high** 89 %
Simulation	48.2 ± 4.8	**H_photon/H_tot** 1.3 %	**H_proton/H_tot** 2.8 %	**H_neutron/H_tot** 96 % (44% E>20MeV)
Sim / Meas	**1.22** ± 0.15			

sofia.rollet@arcs.ac.at
AUSTRIAN RESEARCH CENTERS
26

radiation safety & applications
Seibersdorf

Tissue Equivalent Proportional Counters (TEPC)

H*(10) Sv per Coulomb of SEM1 monitor

Instrument	Group	Measurement position					
		OC-9	OC-10	OC-11	OC-12	OC-13	OC-14
Hawk	ARC		39.6 ± 3.7		28.7 ± 2.7	4.05 ± 0.38	
Hawk	IRSN	29.9 ± 1.9	40 ± 3.8	37.8 ± 3.6	27.5 ± 3.0	3.9 ± 0.6	3.1 ± 0.5
TEPC/CACS	PTB				26.9 ± 2.9		3.08 ± 0.54
TEPC (2")	PTB				29.8 ± 1.5		4.49 ± 0.52

Q factors

Instrument	Group	Measurement position					
		OC-9	OC-10	OC-11	OC-12	OC-13	OC-14
Hawk	ARC		6.62 ± 0.1		6.13 ± 0.2	5.95 ± 0.2	
Hawk	IRSN	6.5 ± 0.5	6.4 ± 0.2	6.1 ± 0.3	6.1 ± 0.3	5.2 ± 0.2	5.1
		6.7 ± 0.7		6.2 ± 0.4		4.6 ± 0.2	5.1 ± 0.7
TEPC/CACS	PTB				6.1 ± 0.4		5.1 ± 0.9
TEPC (2")	PTB				3.1 ± 0.1		3.4 ± 0.5

sofia.rollet@arcs.ac.at AUSTRIAN RESEARCH CENTERS 27

radiation safety & applications
Seibersdorf

H*(10) (Sv per Coulomb of SEM1 monitor)

Class of instrument	Measurement position					
	OC-9	OC-10	OC-11	OC-12	OC-13	OC-14
Rem counters, conventional	*12.5 ± 0.4*	26.4 ± 0.07			2.95 ± 0.02	
Rem counters, extended range (a)		37.0 ± 0.07			3.95 ± 0.02	
TEPCs (b)	29.9 ± 1.9	39.8 ± 0.2	37.5 ± 0.25	29.1 ± 0.97	3.98 ± 0.08	3.2 ± 0.08
Other active instruments (c)	*21.5 ± 0.5*	*26 ± 7*		*34.8 ± 5.3*		
Passive dosemeters (d)	26.9 ± 1.5	29.9 ± 2.7	28.1 ± 5.9	27.5 ± 2.2	3.8 ± 0.3	3.05 ± 0.2
BSS	*33.0 ± 2.1*	*38.2 ± 1.3*	*35.5 ± 0.7*	*30.7 ± 2.0*	*5.1 ± 0.3*	*3.2 ± 0.27*
Monte Carlo (total)	34.8 ± 3.1	48.1 ± 2.5	44.5 ± 1.7	28.9 ± 1.4	4.4 ± 0.6	3.3 ± 0.5
Monte Carlo (neutrons)	33.4 ± 2.9	45.9 ± 2.7	42.11 ± 1.8	27.2 ± 1.3	4.1 ± 0.6	3.1 ± 0.5
Monte Carlo (neutrons < 20 MeV)	16.6 ± 1.5	21.2 ± 0.7	18.0 ± 0.8	12.8 ± 0.5	1.5 ± 0.01	1.3 ± 0.01

(a) GSI LB 6411-Pb excluded; (b) PTB Hawk excluded;
(c) Include REM-2 chamber, MDU Liulin, EPD1 and EPD2; (d) Thermal neutron detectors excluded

sofia.rollet@arcs.ac.at AUSTRIAN RESEARCH CENTERS 28

radiation safety & applications
Seibersdorf

Further Developments -1-

In collaboration with G. Taylor (NPL, Teddigton, UK)

Investigation on the dose equivalent response:

$R_h = H_{TEPC}/H^*(10)$ versus the dose fraction above the proton edge

Low energy: TEPC response dominated by proton recoil on H

Higher energy: TEPC response increasily dominated by alpha and heavier recoil (coming from Carbon in plastic rather then Oxygen in tissue) and so the TEPC is less TE

sofia.rollet@arcs.ac.at

AUSTRIAN RESEARCH CENTERS

29

radiation safety & applications
Seibersdorf

Further Developments -2-

- In collaboration with M. Reginatto (PTB,Germany) et al.

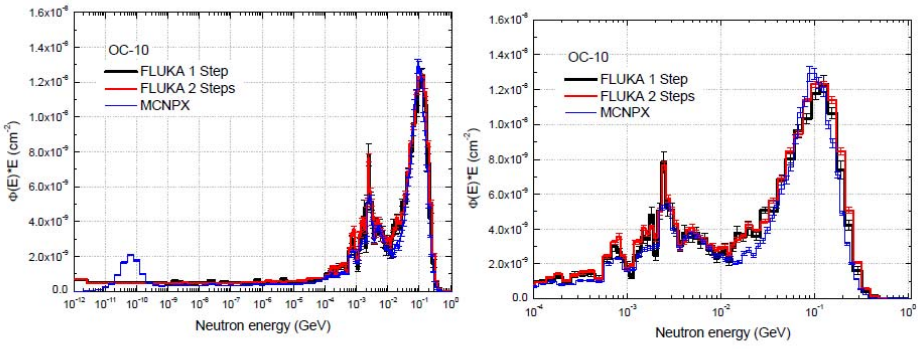

sofia.rollet@arcs.ac.at

AUSTRIAN RESEARCH CENTERS

30

radiation safety & applications
Seibersdorf

Further Developments -2-

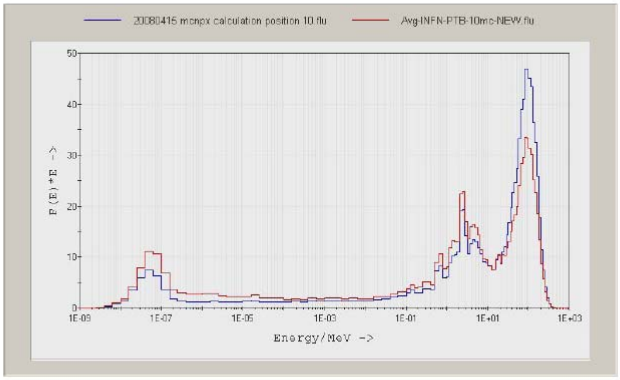

Courtesy of M. Reginatto

radiation safety & applications
Seibersdorf

Conclusion

Good agreement between simulations and measurements values for:

- Absorbed Dose:D (within 10 %)
- Dose Equivalent: H (within 10 %)

Ambient Dose Equivalent: H*(10):

- within 10% - 20% depending on the method

In general, the simulation:

- can reproduce very well the TEPC response
- can be used to assess the particles components in complex fields

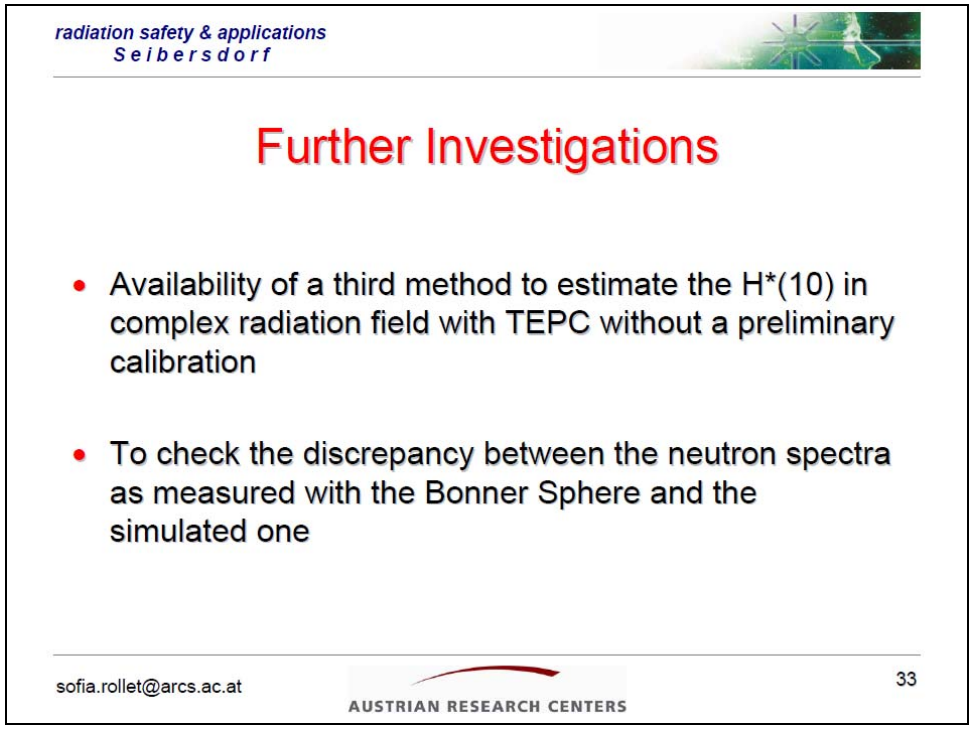
radiation safety & applications
Seibersdorf
Further Investigations
• Availability of a third method to estimate the H*(10) in complex radiation field with TEPC without a preliminary calibration
• To check the discrepancy between the neutron spectra as measured with the Bonner Sphere and the simulated one
sofia.rollet@arcs.ac.at
AUSTRIAN RESEARCH CENTERS
33

Measurements and analyses on angular distribution of dose rate around targets bombarded by 18, 25 and 34 MeV electrons

K. Kosako, K. Oishi, T. Nakamura
Shimizu Corp.

M. Takada
NIRS

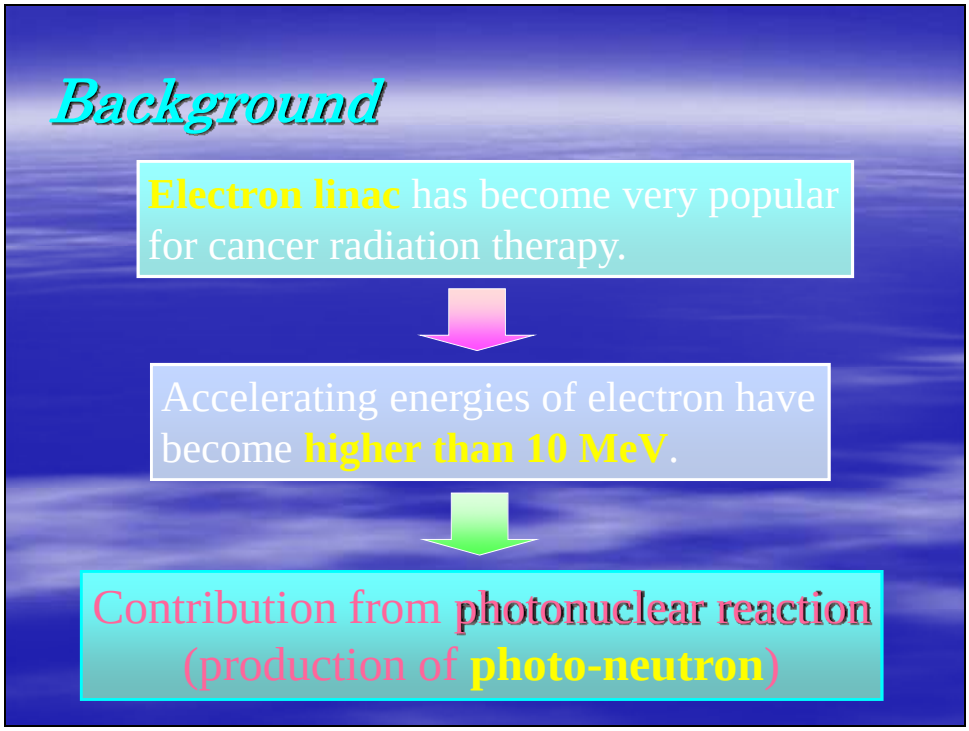

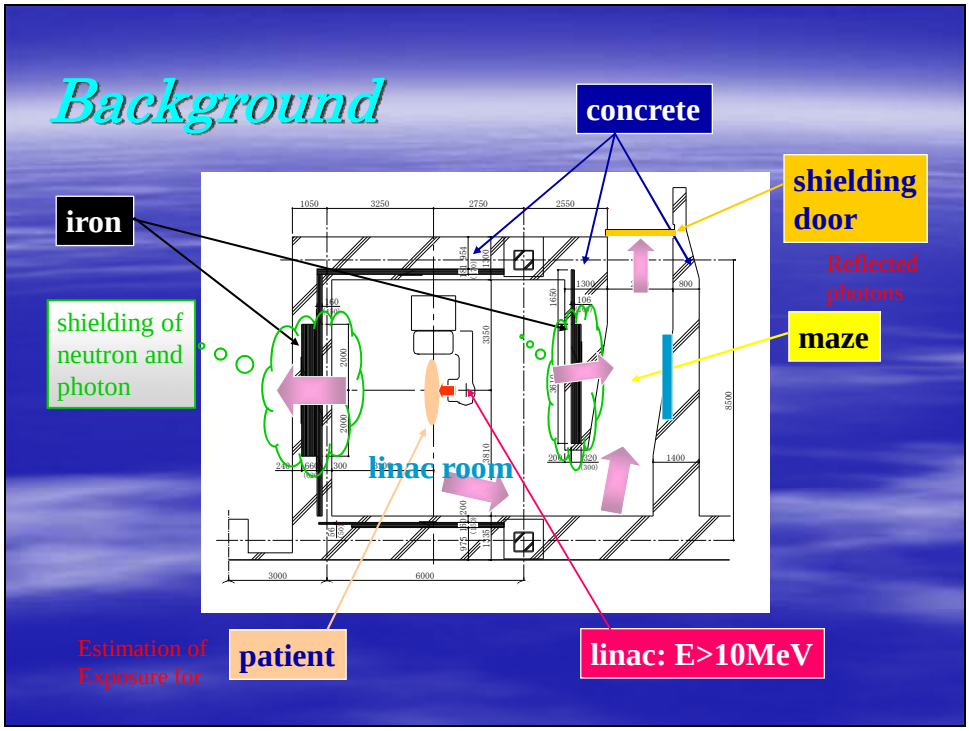
Background
concrete
iron
shielding door
Reflected photons
shielding of neutron and photon
maze
linac room
Estimation of Exposure for
patient
linac: E>10MeV

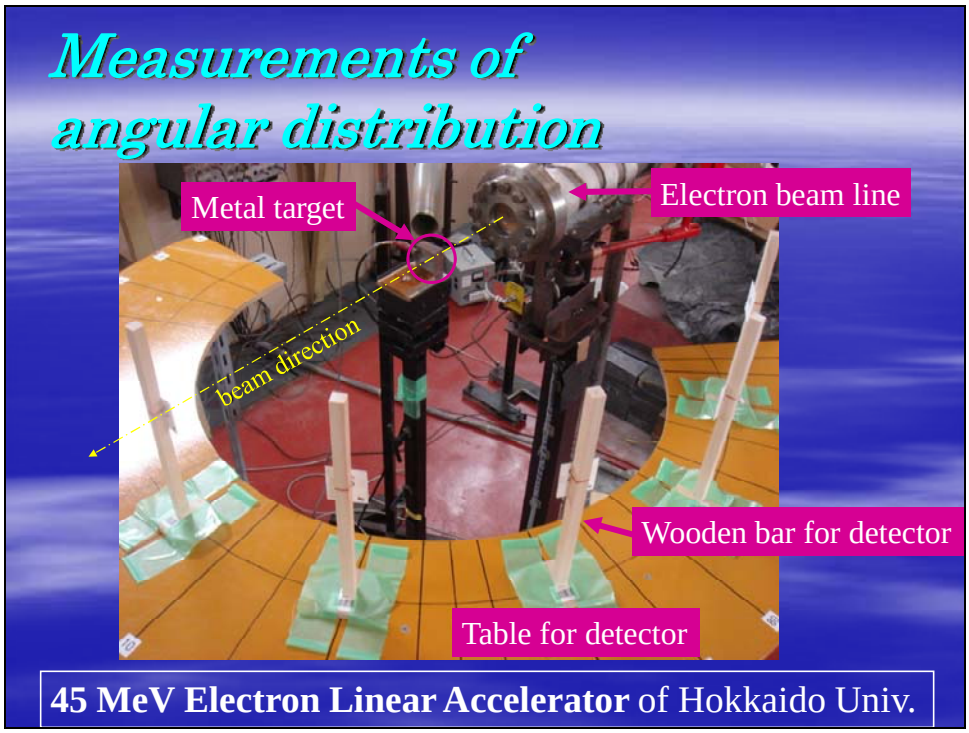
Measurements of angular distribution
Metal target
Electron beam line
beam direction
Wooden bar for detector
Table for detector
45 MeV Electron Linear Accelerator of Hokkaido Univ.

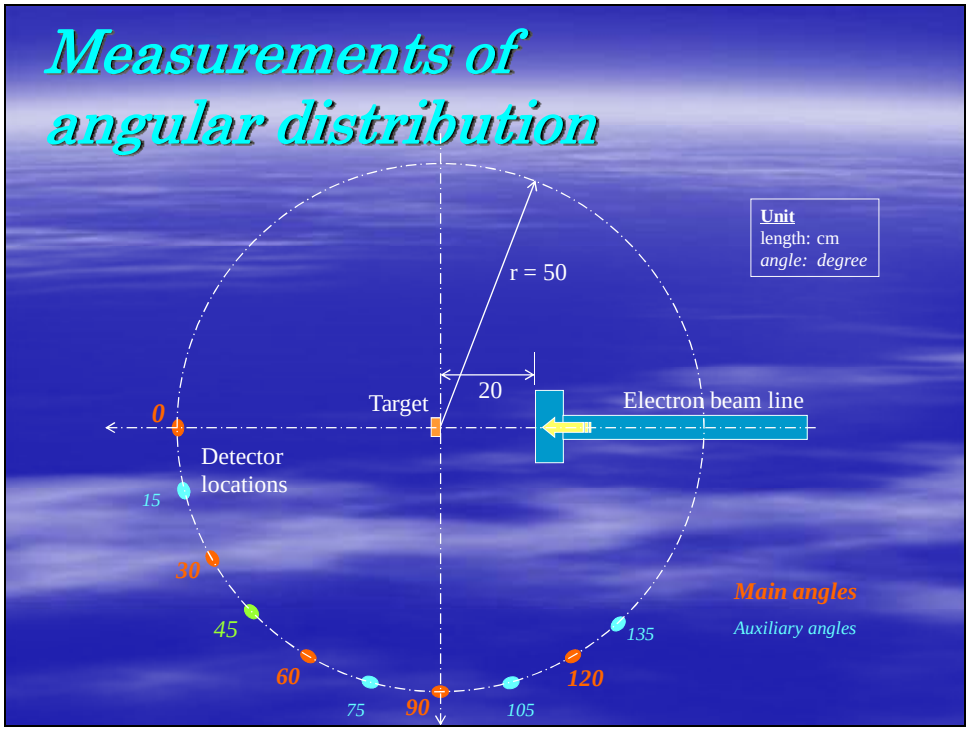
Measurements of angular distribution
Unit
length: cm
angle: degree
r = 50
20
Target
Electron beam line
Detector locations
0
15
30
45
60
75
90
105
120
135
Main angles
Auxiliary angles

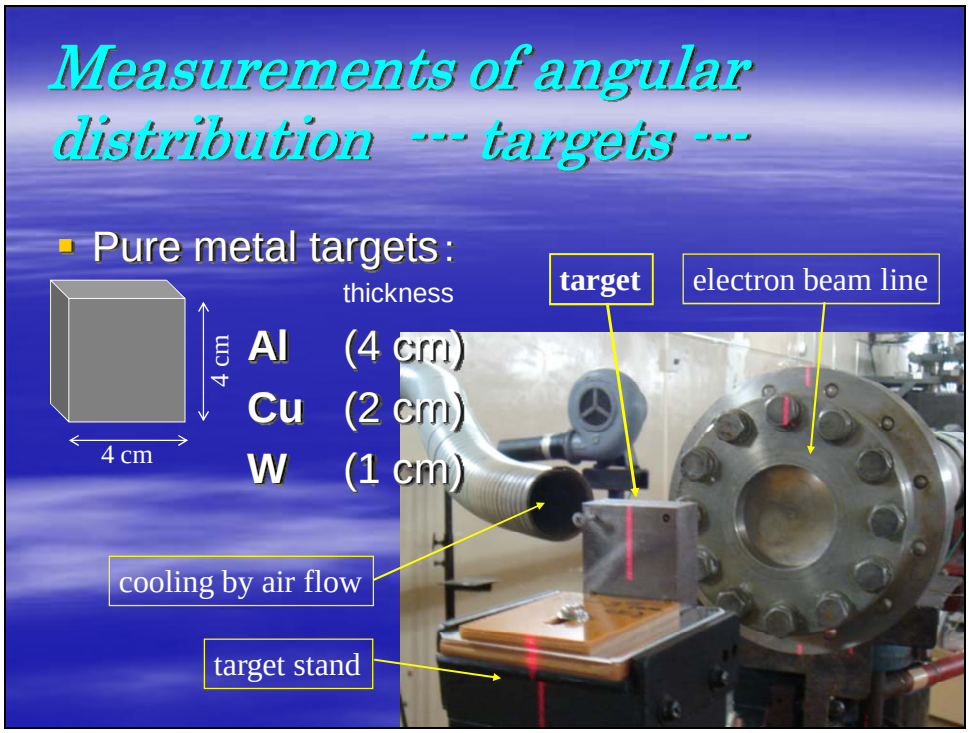
Measurements of angular distribution --- targets ---
Pure metal targets:
thickness
Al (4 cm)
Cu (2 cm)
W (1 cm)
4 cm
4 cm
target
electron beam line
cooling by air flow
target stand

Measurements of angular distribution --- detectors ---

- Neutron dose
  CR-39

- Gamma-ray dose
  Glass-dosimeter
  Ionization Chamber (farmer type:0.6cc)

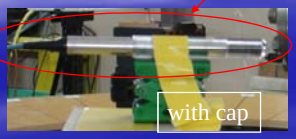

Calculation condition

needs

Photo-neutron

Monte Carlo code with photonuclear reaction
--- **MCNP5**
--- MCNPX2.5
--- MVP2

Evaluated photonuclear reaction data file : over 20 MeV
--- LA150 (LANL)
--- JENDL/PD-2004 (JAEA)
--- KAERI (KAERI)

NJOY99

Photonuclear libraries for MCNP

Calculation condition

- Transport code: MCNP5
- Cross section libraries:
  - neutron (FSXLIB-J33)
  - photon & electron (MCPLIB04 & EL3)
  - photonuclear (LA150, JENDL/PD-2004, KAERI)
- Source: electron (18, 25, 34 MeV; mono-energy)
  - beam with 1 cm-radius (Gauss spatial distr.)
- Tally: small sphere cell and point detector
  - located on angle points (0 to 135 deg.)
  - dose conversion: ICRP 1990 recommendation
  - real energy deposit in ionization chamber

Calculation condition
~ verification of Bremsstrahlung ~

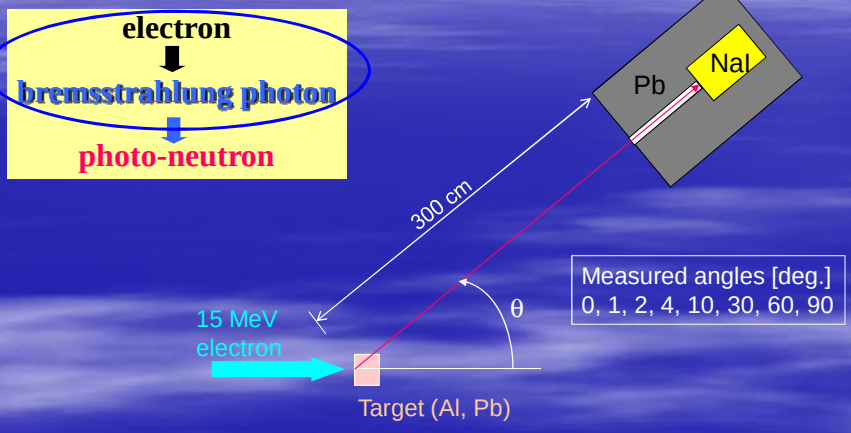

B.A.Faddegon, etc., Med. Phys. 18[4], p727-739 (1991).

Calculation condition

~ verification of Bremsstrahlung ~

Pb

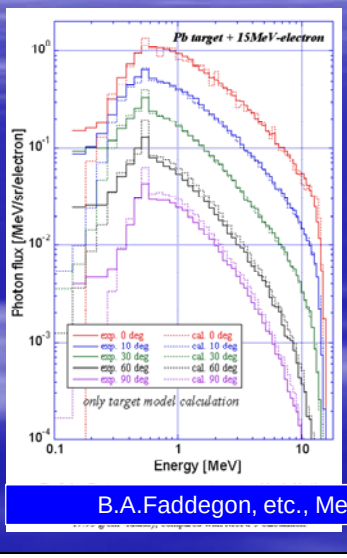

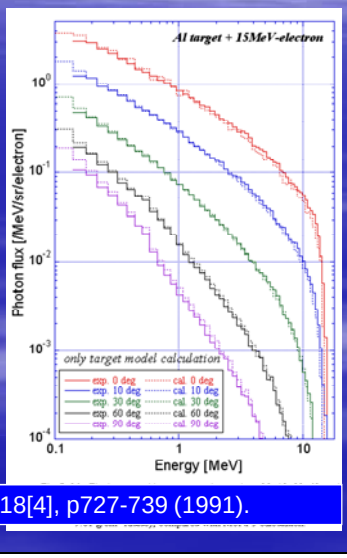

Al

B.A.Faddegon, etc., Med. Phys. 18[4], p727-739 (1991).

Results of dosimeters

~ comparison between PN libraries ~

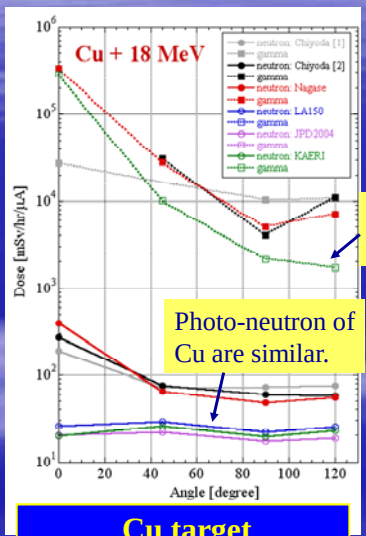

Cu target

Gamma production are completely same.

Photo-neutron of Cu are similar.

Photo-neutron of W are different.

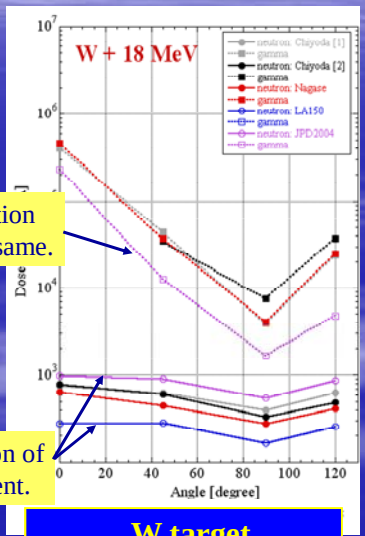

W target

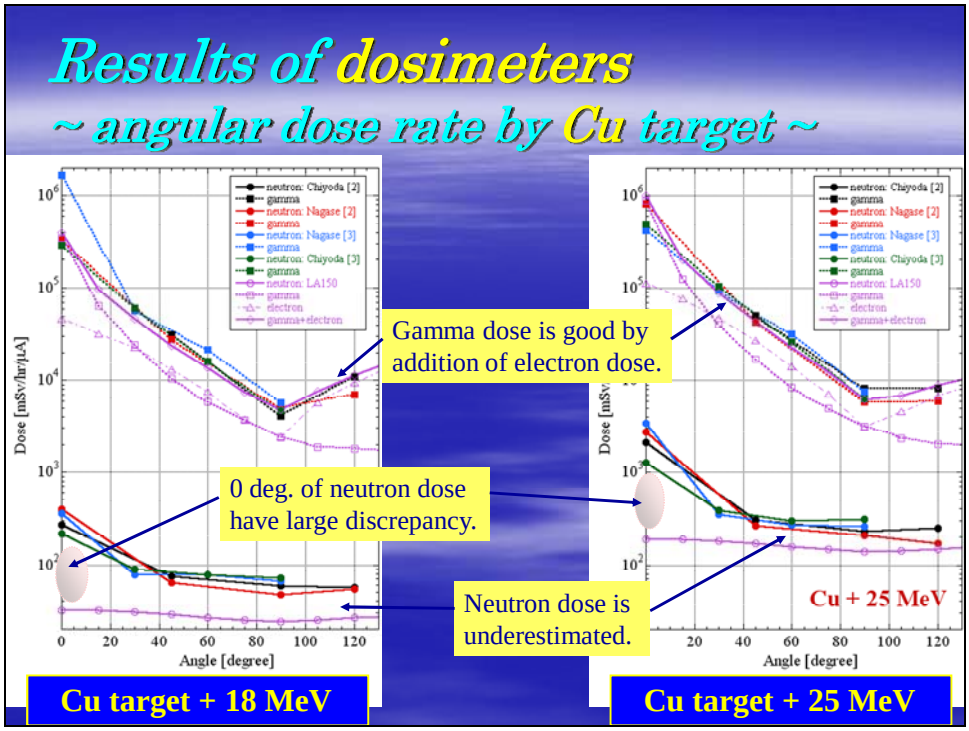
Results of dosimeters
~ angular dose rate by Cu target ~
Gamma dose is good by addition of electron dose.
0 deg. of neutron dose have large discrepancy.
Neutron dose is underestimated.
Cu + 25 MeV
Dose [mSv/hr/μA]
Angle [degree]
neutron: Chiyoda [2]
gamma
neutron: Nagase [2]
gamma
neutron: Nagase [3]
gamma
neutron: Chiyoda [3]
gamma
neutron: LA150
gamma
electron
gamma+electron
Cu target + 18 MeV
Cu target + 25 MeV

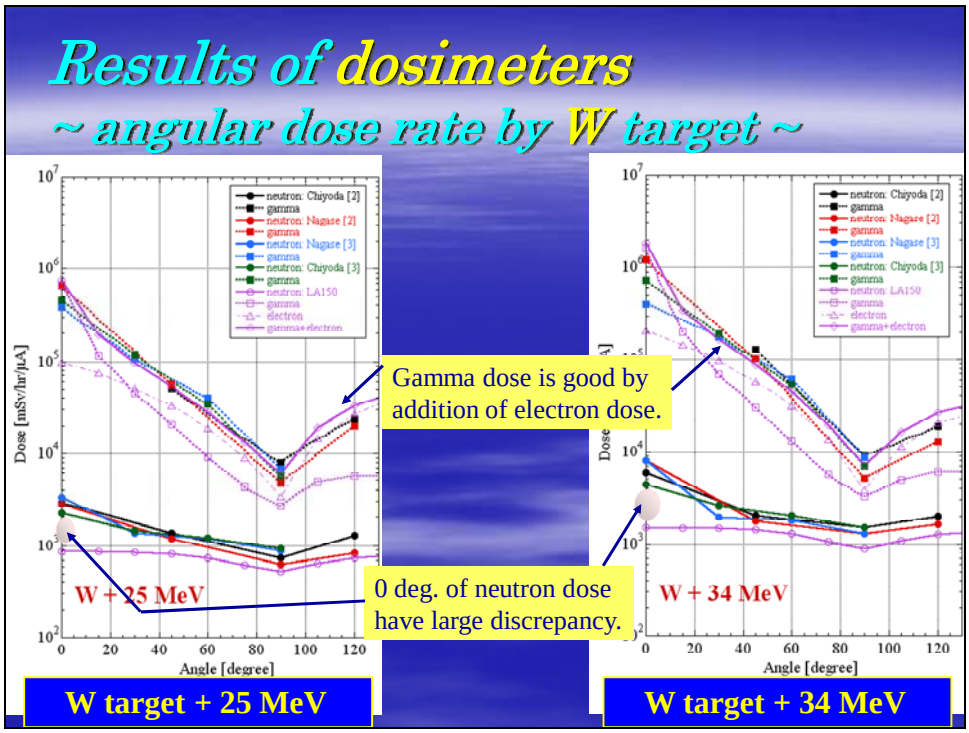
Results of dosimeters
~ angular dose rate by W target ~
Gamma dose is good by addition of electron dose.
0 deg. of neutron dose have large discrepancy.
W + 25 MeV
W + 34 MeV
Dose [mSv/hr/μA]
Angle [degree]
neutron: Chiyoda [2]
gamma
neutron: Nagase [2]
gamma
neutron: Nagase [3]
gamma
neutron: Chiyoda [3]
gamma
neutron: LA150
gamma
electron
gamma+electron
W target + 25 MeV
W target + 34 MeV

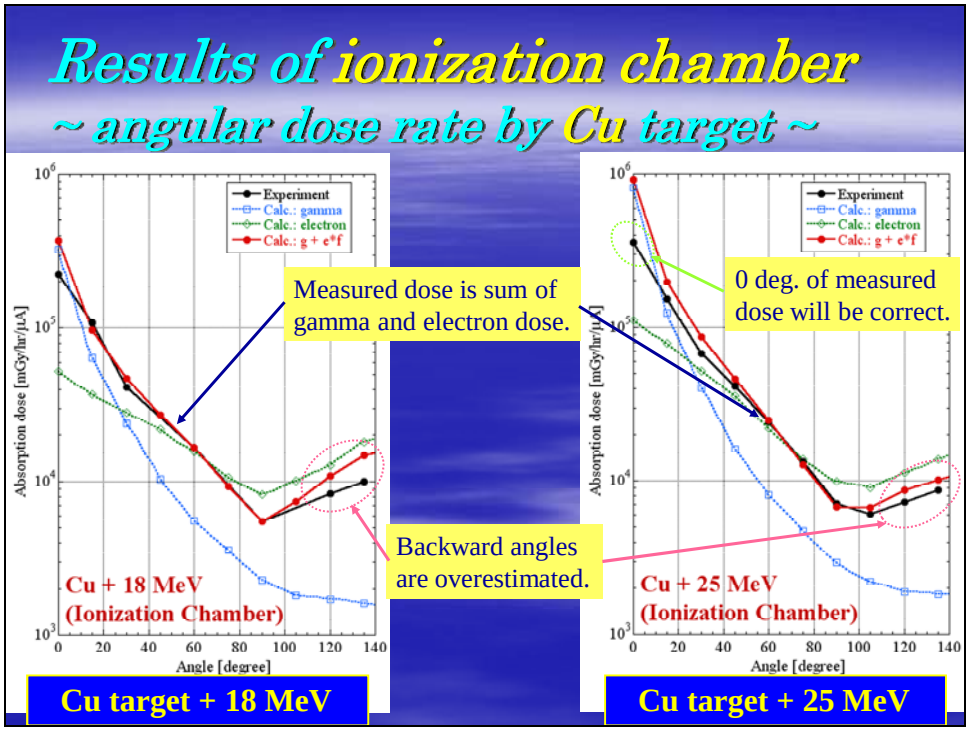
Results of ionization chamber
~ angular dose rate by Cu target ~
Experiment
Calc.: gamma
Calc.: electron
Calc.: g + e*f
Absorption dose [mGy/hr/μA]
Angle [degree]
Measured dose is sum of gamma and electron dose.
Backward angles are overestimated.
Cu + 18 MeV
(Ionization Chamber)
Cu target + 18 MeV
0 deg. of measured dose will be correct.
Cu + 25 MeV
(Ionization Chamber)
Cu target + 25 MeV

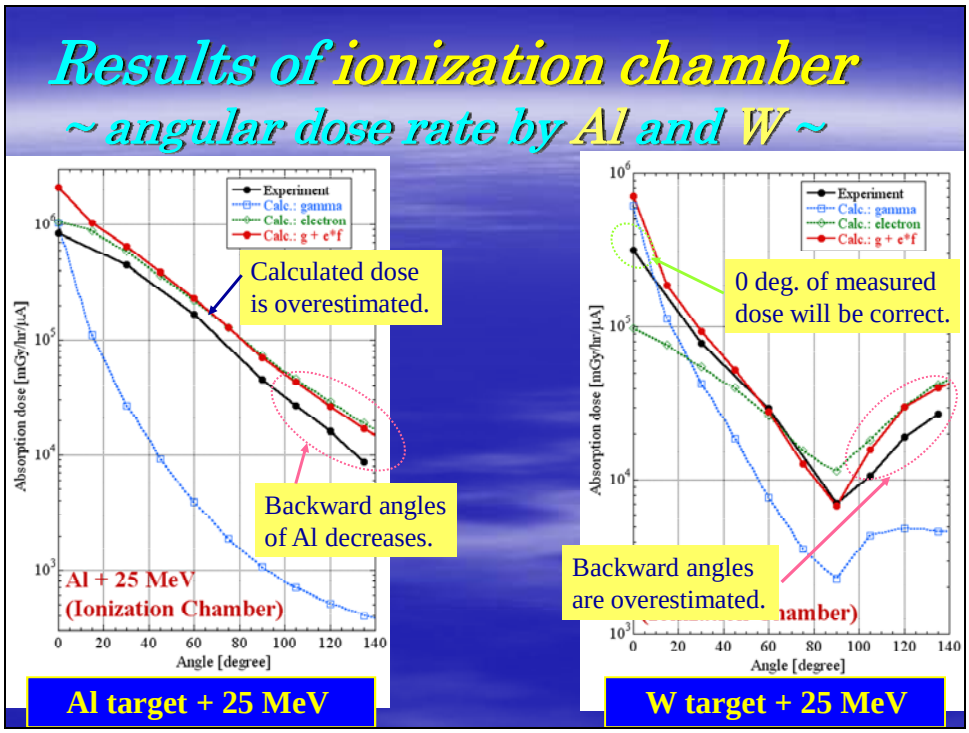
Results of ionization chamber
~ angular dose rate by Al and W ~
Experiment
Calc.: gamma
Calc.: electron
Calc.: g + e*f
Absorption dose [mGy/hr/μA]
Angle [degree]
Calculated dose is overestimated.
Backward angles of Al decreases.
Al + 25 MeV
(Ionization Chamber)
Al target + 25 MeV
0 deg. of measured dose will be correct.
Backward angles are overestimated.
W target + 25 MeV

Results ~ remarks ~

- discrepancy of neutron at 0 degree
  - charged particles from photonuclear: +5 to +50%
  - support and stand around detector: less than few %
  - photo-neutron data: no significant problem
  - confirmation of experimental reliability: in progress
- discrepancy in angular dose of neutron
  - review of photo-neutron yield: in progress
  - room scattering: +50% on Cu+18 MeV only

Summary

- Angular distribution of dose rate had been measured.
  - target: Al, Cu, W
  - energy: 18, 25, 34 [MeV] for electron
  - angle: 0, 30, (45), 60, 90 and 120 [deg.]
- MCNP5 calculations have been performed.
- Compared between experiment and calculation
  - Trend of distributions are good.
  - Gamma dose and absorption dose are good agreement.
  - Neutron dose has some discrepancies:
    - large discrepancy at 0 degree
    - underestimation of dose distribution

Results of the non-elastic reaction code BRIEFF for nuclear data and with transport code

Helder Duarte
CEA/DIF
Bruyères-le-Châtel, France

Composition of BRIEFF code

- IntraNuclear Cascade code BRIC (version 1.4: Phys. Rev. C75, 024611) down to threshold energy (version 1.5e: ND-2007 conf.)
  - incident and emitted particles: n, p, pions
  - energy range: ~1 MeV - several GeV
  - target nuclei: all (with a mass)
- Evaporation based on Weisskopf-Ewing theory
- Modified Fermi BreakUp model
- Fission model of Atchison (of 1994; temporary)

n(800 MeV) + ^{12}C → 2π + 3p + 2n + ^{8}Li*

INC stage only (BRIC)

- incident neutron
- proton
- neutron
- Δ
- π

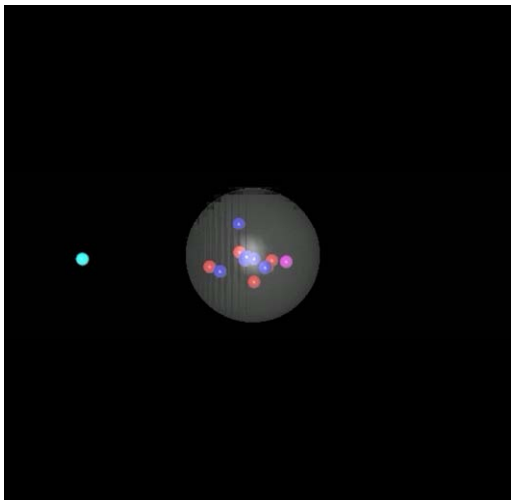

p(800 MeV) + ^{208}Pb → 3p + 5n + ^{201}Hg*

INC stage only (BRIC)

- incident proton
- proton
- neutron
- Δ
- π

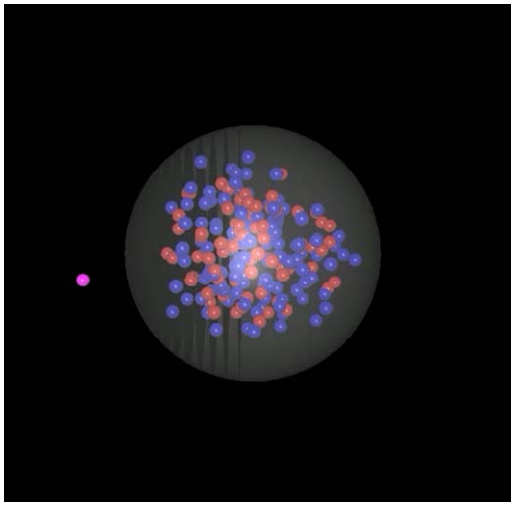

BRIC = IntraNuclear Cascade stage

- Improvements since BRIC 1.5e (ND-2007 conf.)
  - Energy levels for nucleons of target nuclei A<17.
  - Energy levels of least bound neutrons & protons for other nuclei (closed shell or not).
  - Slight modification of Pauli blocking according to least bound neutrons & protons (all nuclei), shell closure taken into account.

Description of target nuclei

Energy levels of nucleons for light nuclei

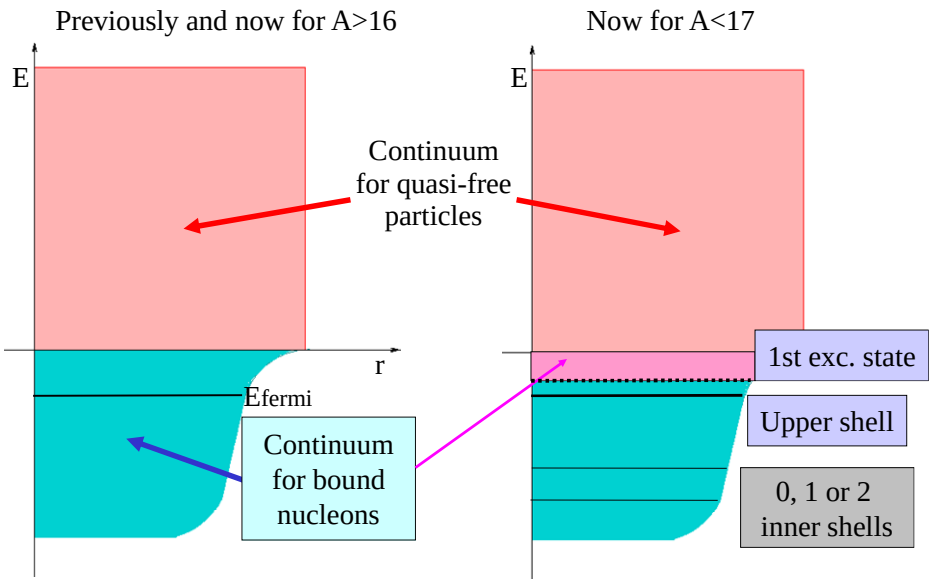

«Fermi BreakUp» model instead of evaporation for light compound nuclei (A<30)

- decay into 2 or 3 fragments of mass A<12
  - fragment in ground or discrete states (up to 30 levels)
  - probability driven by Q-value of decay channel and spin conservation
  - use Dalitz plot method for 3-body kinematics

Excitation functions

BRIEFF 1.5.4e (no levels in BRIC, ND-2007)
BRIEFF 1.5.4i (levels in BRIC for A<17)

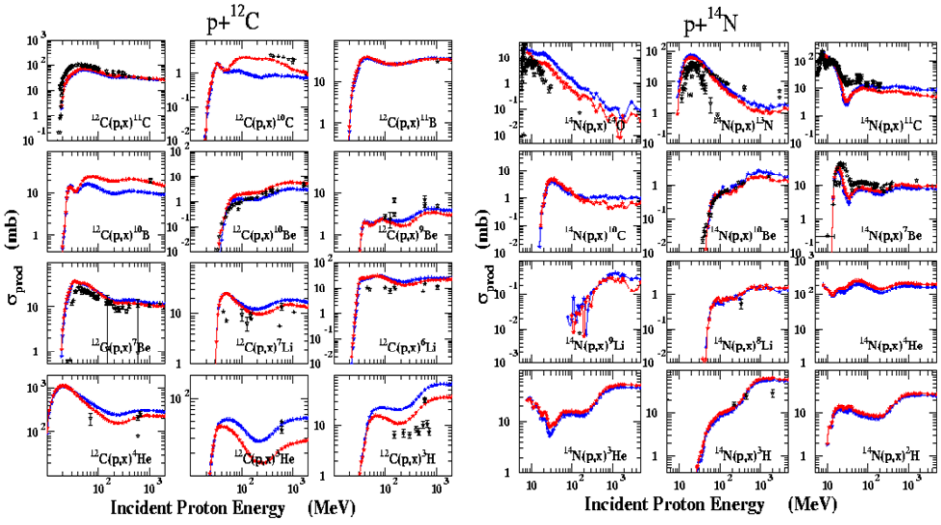

^{12}C(p,xp) at 14 and 26 MeV

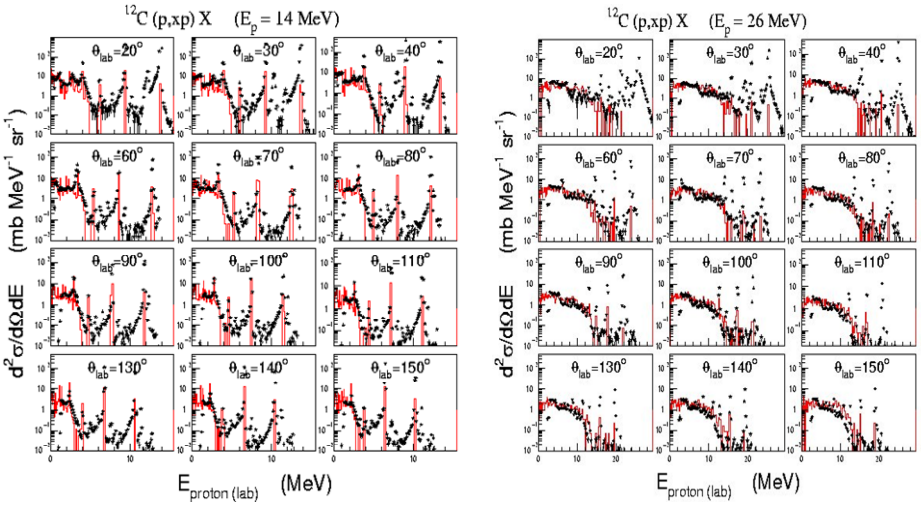

* Data of M. Harada et al., J. Nucl. Sci. Tech. 36 (1999), 313

^{12}C(p,xα) at 14 and 26 MeV

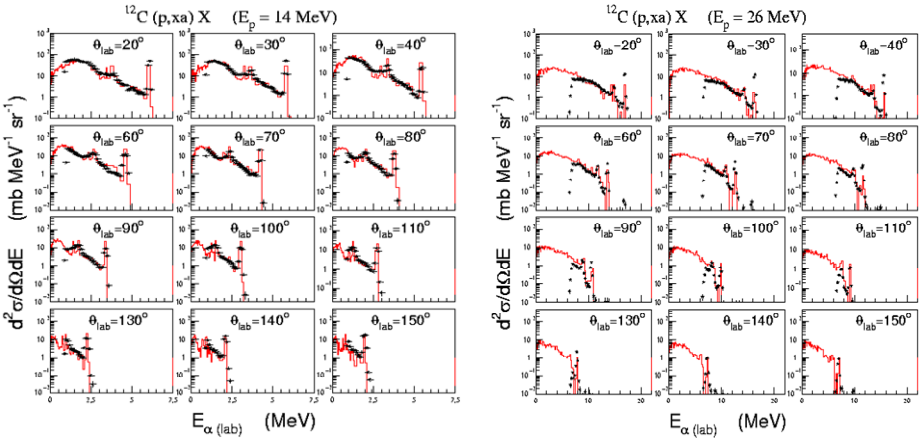

* Data of M. Harada et al., J. Nucl. Sci. Tech. 36 (1999), 313

Evaporation stage of BRIEFF

- Cross sections of compound nucleus formation calculated with BRIC (1.5a) and used in evaporation stage (in probabilities of particle emission and their energy distribution)
  - Extended from 2000 target nuclei (ND-2007 conf.) to 3300 (mainly for heavy compound nuclei).
  - Use of same potential V(r) in INC stage and in calculation of threshold energy of evaporated charged particles.

σ_{cn} : XS of compound nucleus formation

Hypothesis : no emission before time cut of INC (200 fm/c~6.7 10^{-22}s) = compound nucleus formation in INC stage

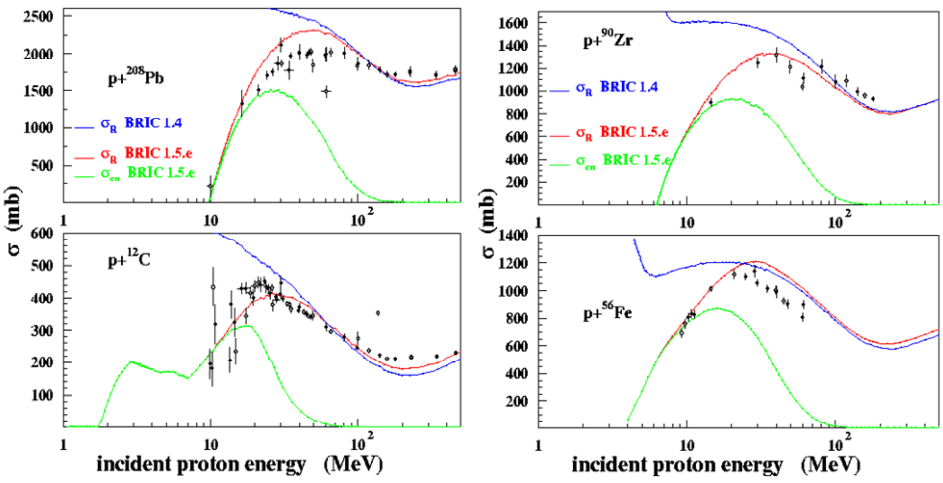

$d^2\sigma/dAdZ$ (inverse kinematics at GSI)

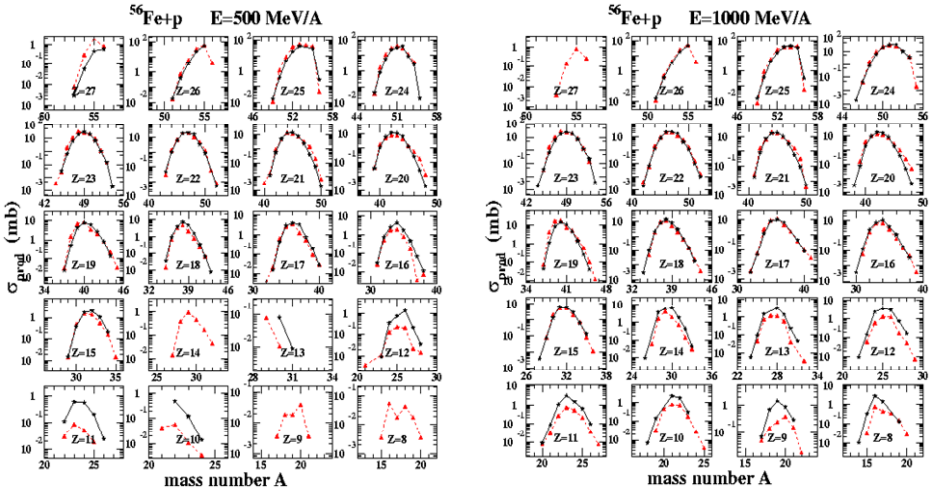

* Data of Villagrosa-Canton et al., Phys. Rev. C 75, 044603

Fission : Atchison model (RAL)

- Current fission model is a slightly modified version of first RAL model (Atchison, *Proceedings of a specialists' meeting, OECD/NEA Issy-les-Moulineaux, France (1994)*)
  - Inconsistency between our evaporation code and RAL evaporation => single factor applied to RAL fission probability to correct «discrepancy»
  - Preliminary, but problems.
  - Update of model (Atchison, Nucl. Instr. Meth. B 259, 909) or new approach needed?

$d^2\sigma/dAdZ$ (inverse kinematics at GSI)

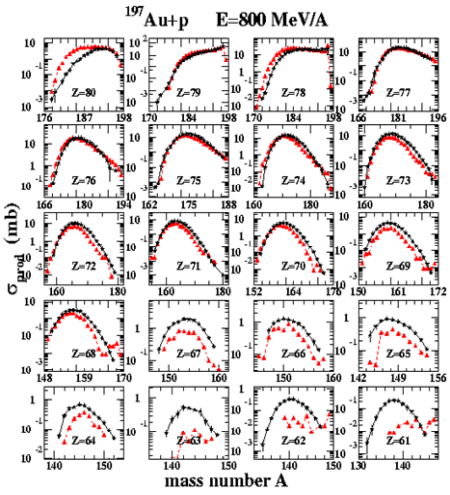

Discrepancies come mainly from fission competition (RAL model of 1994) and from lack of emission of light nuclei other than d, t, ^{3}He, α

=> (high energy) fission has to be updated or revised

* Data of Rejmund et al., Nucl. Phys. A 683 (2001), 540

$d^2\sigma/dAdZ$ (inverse kinematics at GSI)

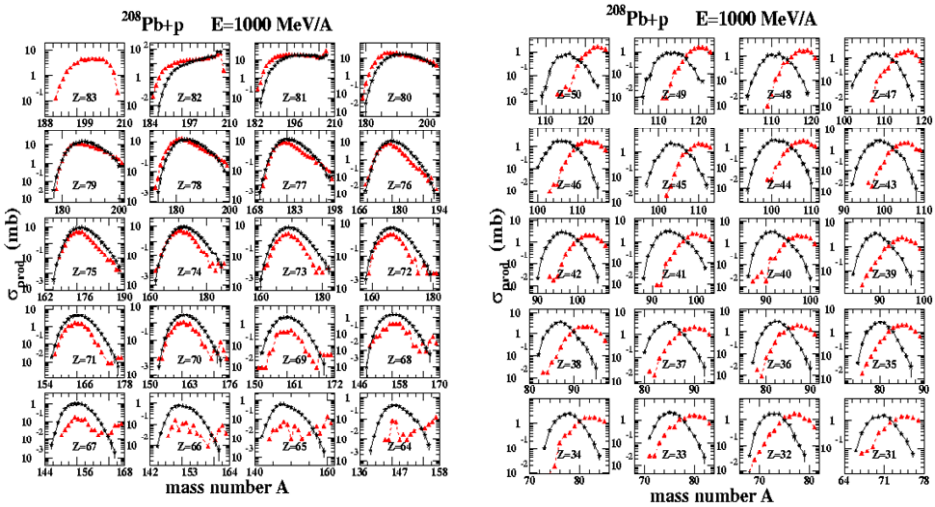

* Data of Enqvist et al., Nucl. Phys. A 686 (2001), 481

Use of BRIEFF in transport codes

- BRIEFF is incorporated into HETC-BRC
- and is incorporated into (local) MCNPX 2.5.0 (D. B. Pelowitz, ed., "MCNPX User's Manual Version 2.5.0", Los Alamos National Laboratory report, LA-CP-05-0369 (April 2005))
  - Easy way to compare to other nuclear models (Bertini-MCNPX, ISABEL-MCNPX, CEM2k, INCL4+ABLA) and LA150 libraries
  - same input file, same energy loss and straggling for charged particles ...

Neutron yields (30 MeV proton)

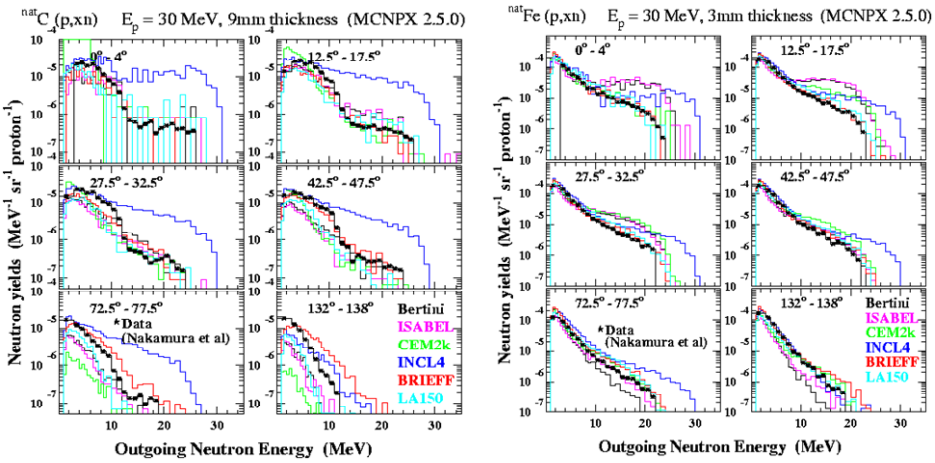

Neutron yields (50 MeV proton)

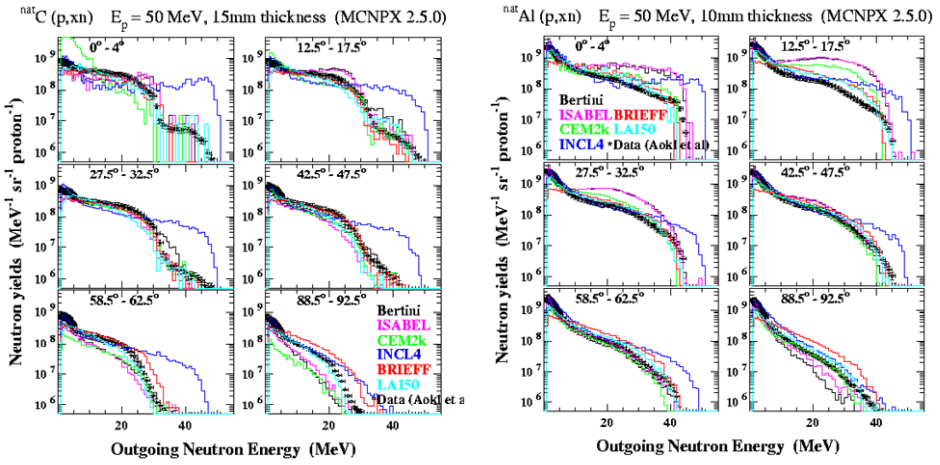

Neutrons yields (52 and 68 MeV proton)

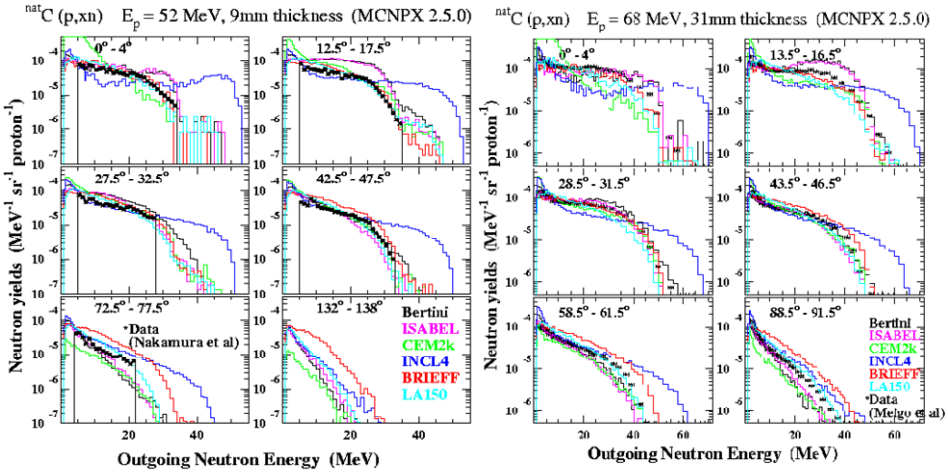

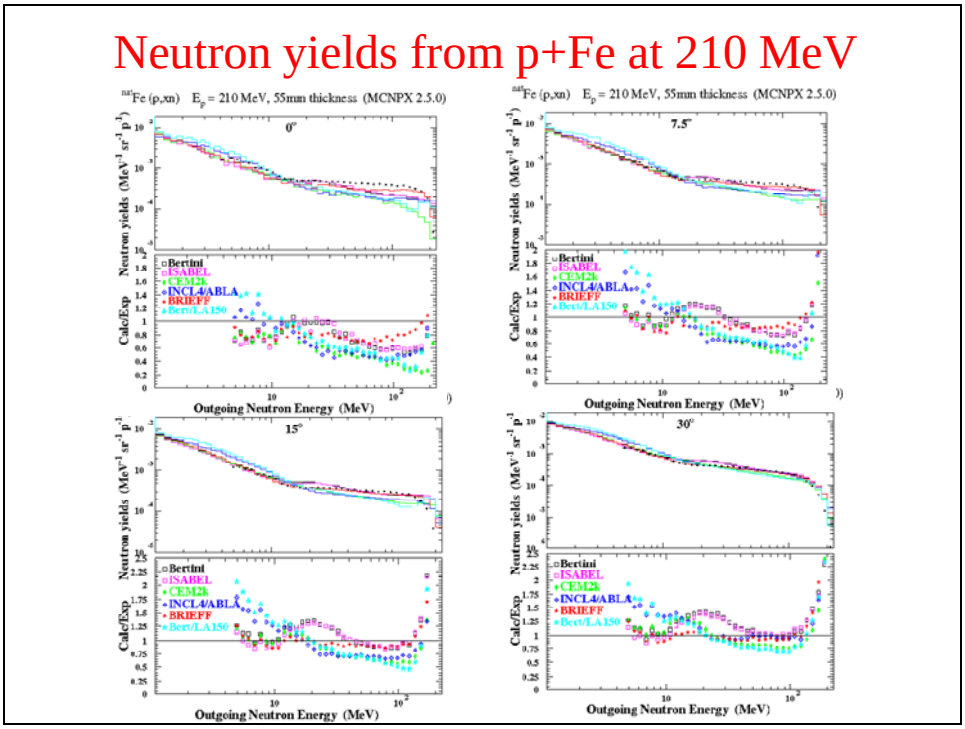
Neutron yields from p+Fe at 210 MeV
nat Fe (p,xn) Ep = 210 MeV, 55mm thickness (MCNPX 2.5.0)
0°
7.5°
15°
30°
Neutron yields (MeV-1 sr-1 p-1)
Calc/Exp
Bertini
ISABEL
CEM2k
INCL4/ABLA
BRIEFF
Bert/LA150
Outgoing Neutron Energy (MeV)

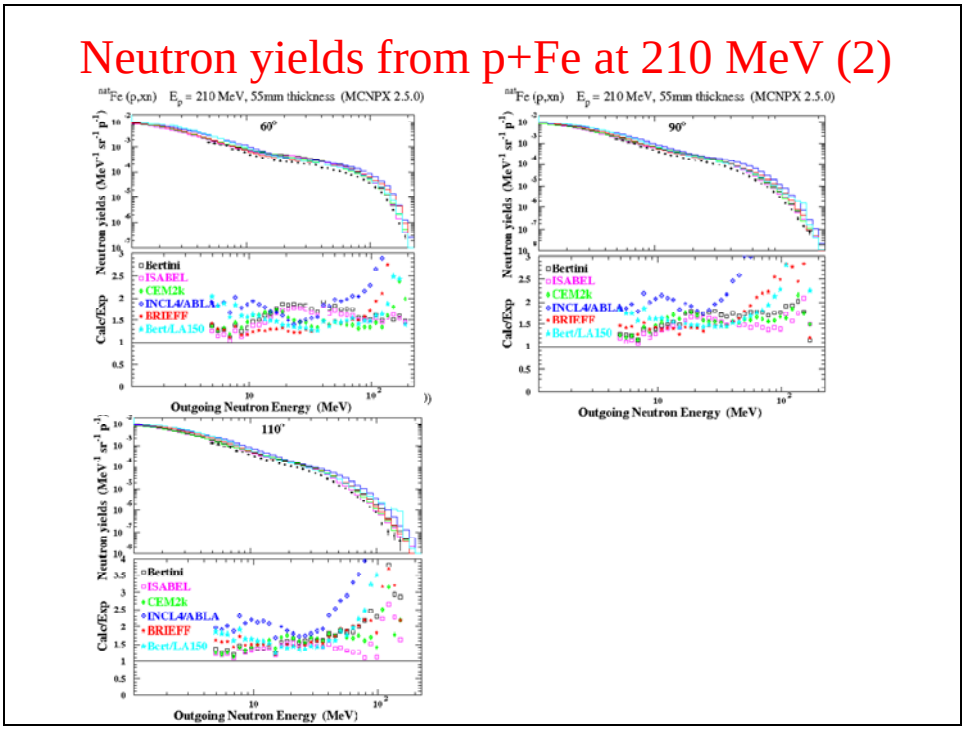
Neutron yields from p+Fe at 210 MeV (2)
nat Fe (p,xn) Ep = 210 MeV, 55mm thickness (MCNPX 2.5.0)
60°
90°
110°
Neutron yields (MeV-1 sr-1 p-1)
Calc/Exp
Bertini
ISABEL
CEM2k
INCL4/ABLA
BRIEFF
Bert/LA150
Outgoing Neutron Energy (MeV)

Neutron production at 0º (350 MeV)

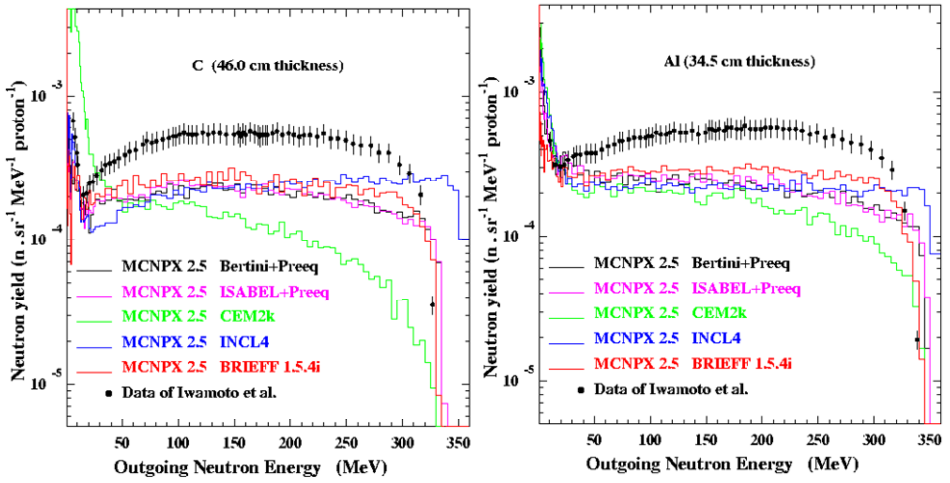

Neutron production at 0º (350 MeV)

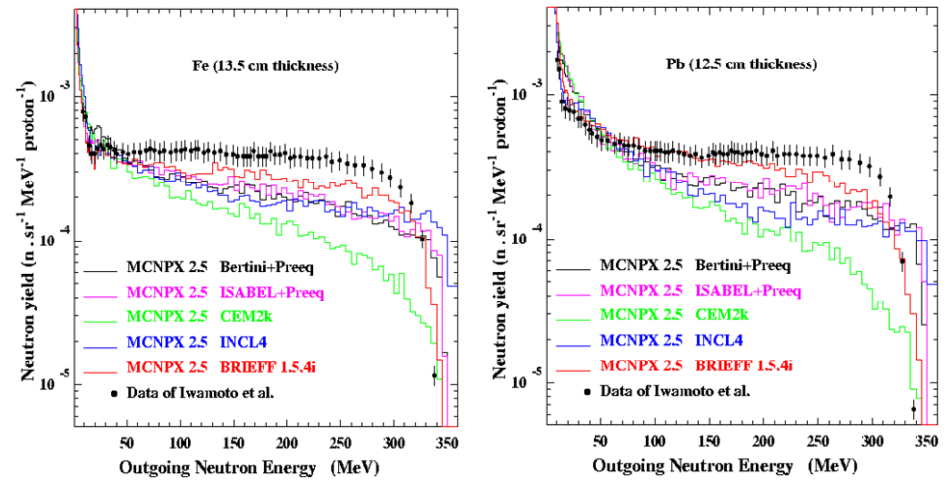

Conclusions

- In « thick » target calculation, good results of neutron yields with BRIEFF :
  - For low target mass (C) in forward direction and low intermediate energy (E_{beam}<100 MeV)
  - For medium target mass (Fe, Cu) in forward direction on wide range of energy
  - For high target mass (Pb) at very forward angle below 100 MeV (Ta,W) and high energy (350 MeV).
- Good agreement on average with LA150 libraries

Next developments?

- Use of energy levels in target nuclei in INC stage can improve BRIC modelisation (at least for low target mass A) => extension to higher A
- New Pauli blocking in INC stage (consistent with energy levels)
- Emission of/Reaction by d, t, ^{3}He, α in BRIC
- Fission model has to be revised
- Evaporation of light nuclei other than d, t, ^{3}He, α

n(800 MeV) + ^{12}C → 2π + 3p + 2n + ^{8}Li*

INC stage only (BRIC)

- incident neutron
- proton
- neutron
- Δ
- π

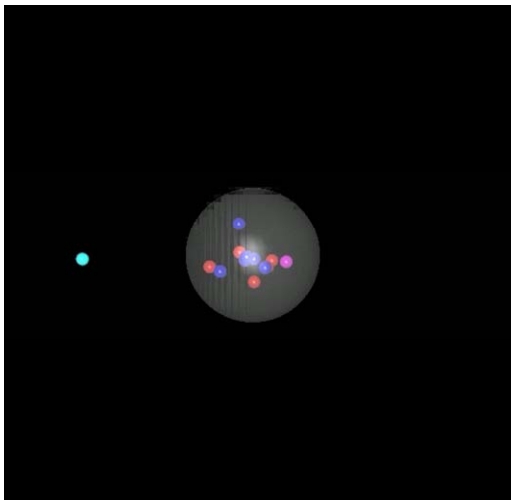

p(800 MeV) + ^{28}Si → 3p + 2n + ^{24}Mn*

INC stage only (BRIC)

- incident proton
- proton
- neutron
- Δ
- π

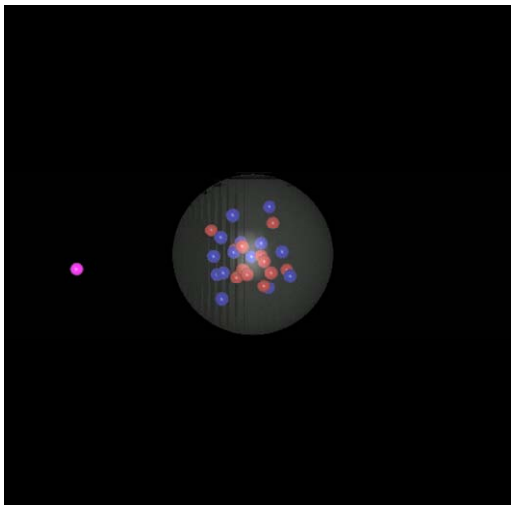

p(800 MeV) + ^{28}Si → 3p + n + ^{25}Mn*

INC stage only (BRIC)

- incident proton
- proton
- neutron
- Δ
- π

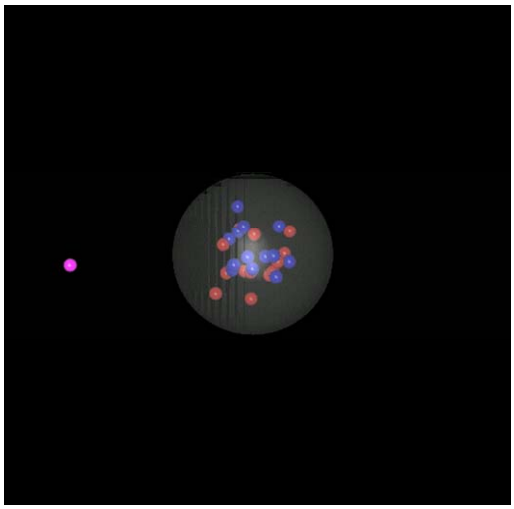

p(800 MeV) + ^{208}Pb → 3p + 5n + ^{201}Hg*

INC stage only (BRIC)

- incident proton
- proton
- neutron
- Δ
- π

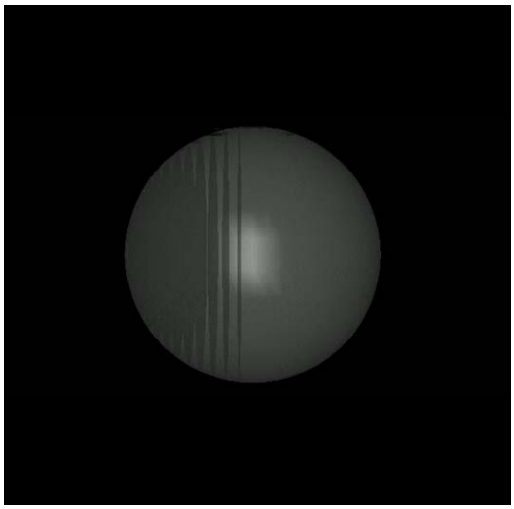

Excitation functions

BRIEFF 1.5.4e (no levels in BRIC)
BRIEFF 1.5.4i (levels in BRIC for A<20)

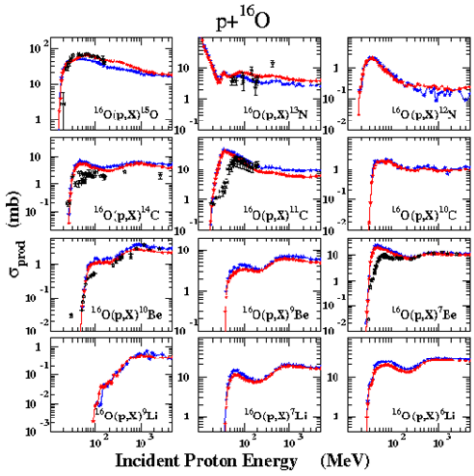

p(800 MeV) + ^{28}Si → 3p + 2n + ^{24}Mn*

INC stage only (BRIC)

- incident proton
- proton
- neutron
- Δ
- π

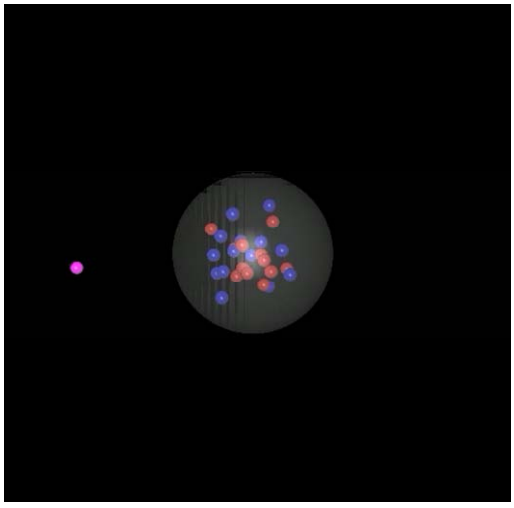

p(800 MeV) + ^{28}Si → 3p + n + ^{25}Mn*

INC stage only (BRIC)

- incident proton
- proton
- neutron
- Δ
- π

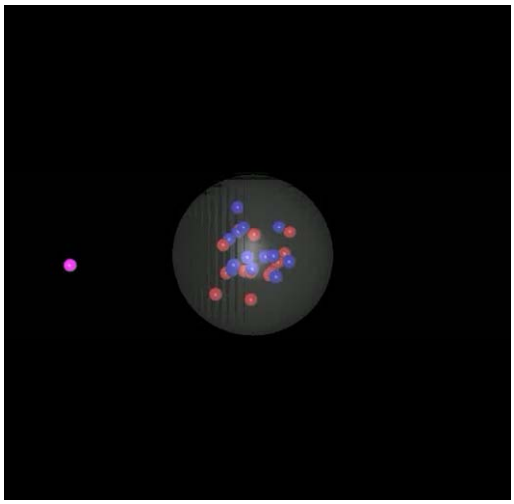

Inter-comparison of medium-energy neutron attenuation in iron and concrete (7)

H. Hirayama
KEK, High Energy Accelerator Research Organisation
Attenuation Length Sub-Working Group in Japan

From Inter-comparison at SATIF-8

- In general, the attenuation lengths calculated with various codes for mono-energy neutrons increases with the increase of neutron energy and this tendency becomes moderate above several GeVs both for iron and concrete but the values of the attenuation length are largely different from each other.
- The difference of dose increases with an increase of depth both for iron and concrete.
- The attenuation lengths for secondary neutrons from a Hg target with 3 GeV protons show a slight dependence on the emission angle for the results of all codes but the values of the attenuation length are different from each other.
- The attenuation length for secondary neutrons emitted to 90 degrees from an iron or Hg target with high energy protons reach almost a constant value above 1 GeV.
- Select suitable experiments to compare for understanding the attenuation length of secondary neutrons from high-energy protons. The results of AGS shielding experiments presented by H. Nakashima et al. will be suitable for this purpose.

Problems for an Inter-comparison (7)

- **Same Problems with an inter-comparison (6)**
- **As the new problems, the comparison with the experimental results of AGS shielding experiments presented by H. Nakashima et al. was added.**
  - **Proton (2.83 and 24 GeV)**
  - **Target Material : Mercury**
  - **Shielding Material : Steel and Concrete**
  - **Geometry : Slab Geometry**
  - **Neutron Reaction Rate**
    - $^{209}Bi(n,4n)^{206}Bi$
    - $^{209}Bi(n,6n)^{204}Bi$

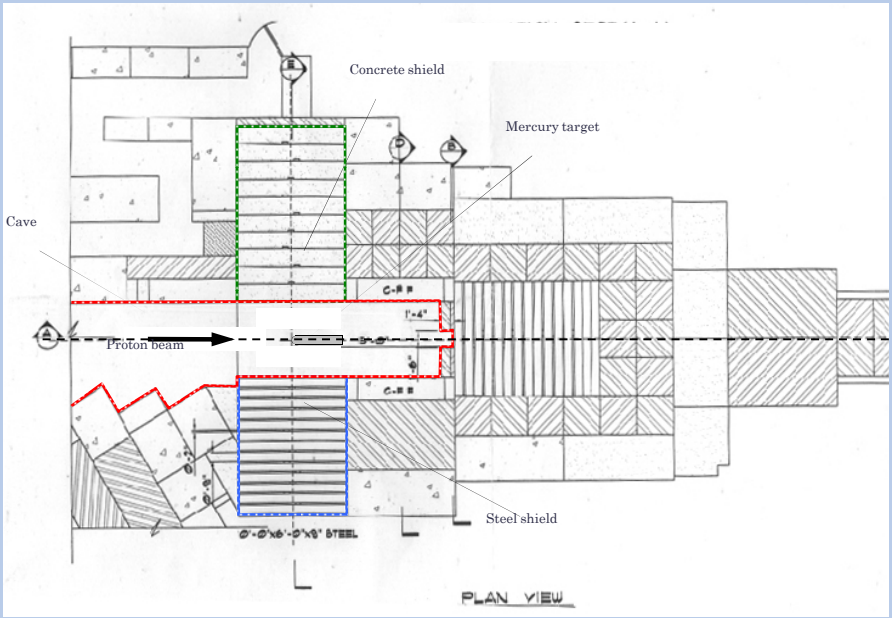

Drawings of the experimental configuration (New Problem)

Summary of contributors for Neutron attenuation calculation

Name of participants and organization	Name of computer code	Name of data base used
T. Koi. and D. Wright (SLAC)	Geant4 v9.0 p01	Library data in Geant4 v9.0 *
F. Maekawa (JAEA)	MCNPX	Library data in MCNPX, LA-150 for neutron transport below 150 MeV
F. Maekawa (JAEA)	PHITS	Library data in PHITS, JENDL-3.2 for neutron transport below 20 MeV

*Neutron cross sections are changed from the model based on J.P. Wellisch and D. Axen to the model based on JENDL High Energy File 2004 and V.S. Barashenkov.

Cross sections of JENDL High Energy File 2004 are used for the selected isotopes up 3 GeV and beyond the energy Barashenkov parameterizations are used.

Most data of elements (isotopes) in simulations for inter comparison are available from JENDL High Enegy File 2004, however if the data is not available then the Barashenkov models are used whole energy range.

(1-a) Mono-energetic neutrons (Iron)

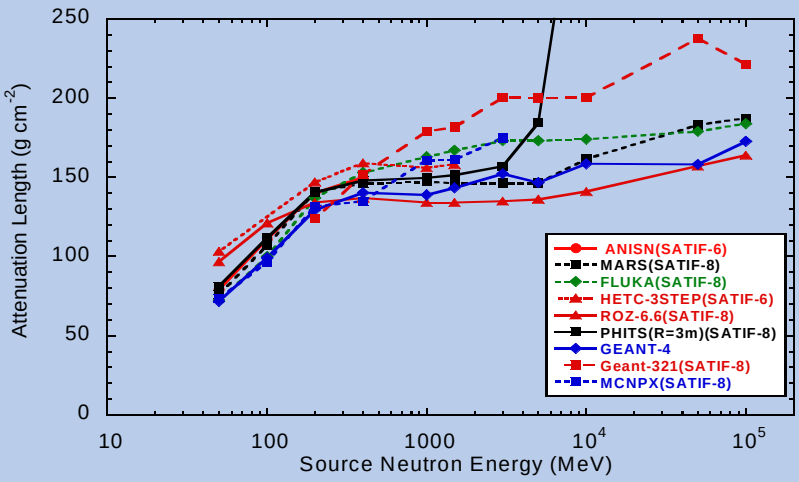

Fig. 6 Comparison of the neutron attenuation length of iron.

Note: Iron for mono energy neutrons

- The results of Geant4 close to other Monte Carlo results.
- General Tendencies are same with at SATIF-8.
  - The attenuation lengths are relatively close below 0.4 GeV.
  - The value seem to be almost constant above a few GeVs except PHITS.
  - The attenuation lengths for iron are scattered within about 50 g cm^{-2} for the energy region above 0.4 GeV. .

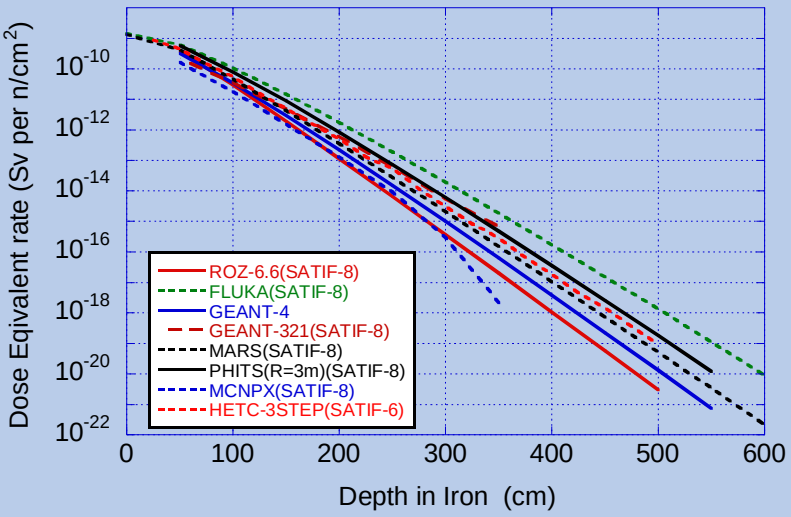

Fig. 7 Dose distribution inside iron for 1 GeV neutrons.

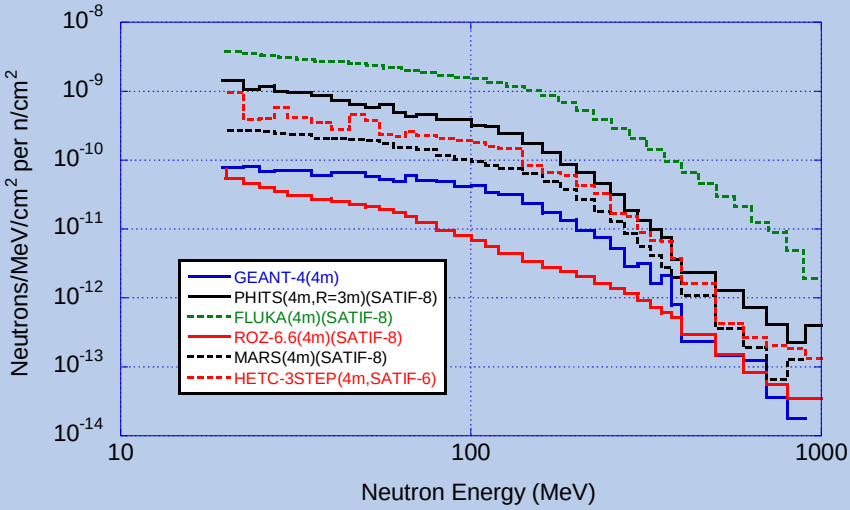

Fig. 8 Neutron spectra at 4m inside iron for 1 GeV neutrons.

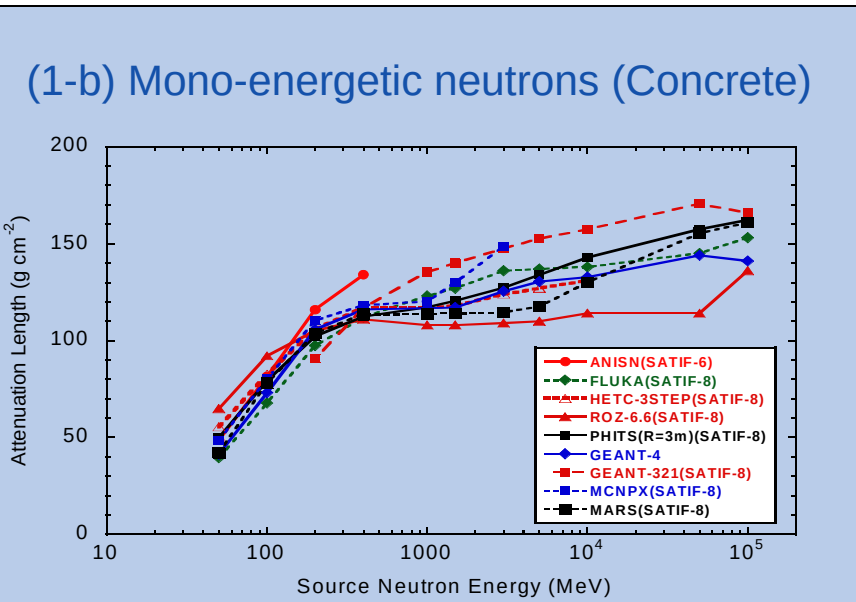

Fig. 9 Comparison of the neutron attenuation length of concrete.

Note: Concrete for mono energy neutron

- The results of Geant4 close to other Monte Carlo results.
- General Tendencies are same with at SATIF-8.
  - The differences between the attenuation lengths between each code are relatively small at low-energy region and increase with the increase of neutron energy.
  - The attenuation length have the tendency to reach an almost constant value for 12 m slab.
  - The differences are about 30 g cm^{-2} at 1 GeV and about 50 g cm^{-2} at 100 GeV, respectively.

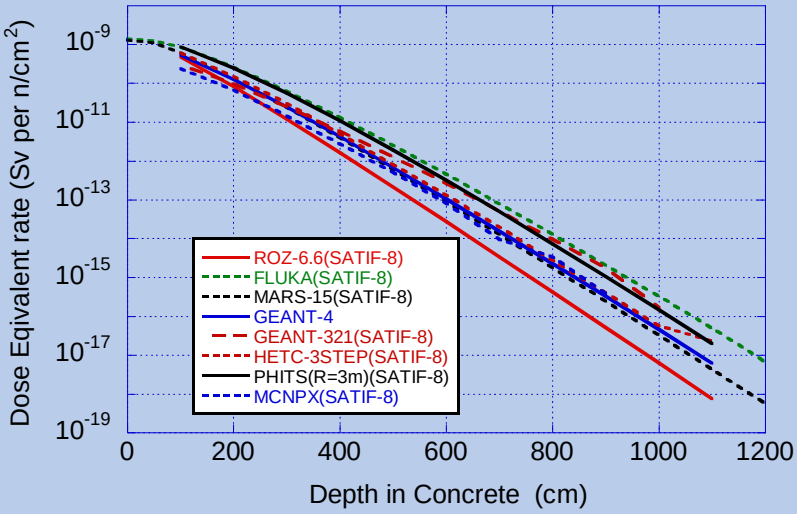

Fig. 10 Dose distribution inside concrete for 1 GeV neutrons.

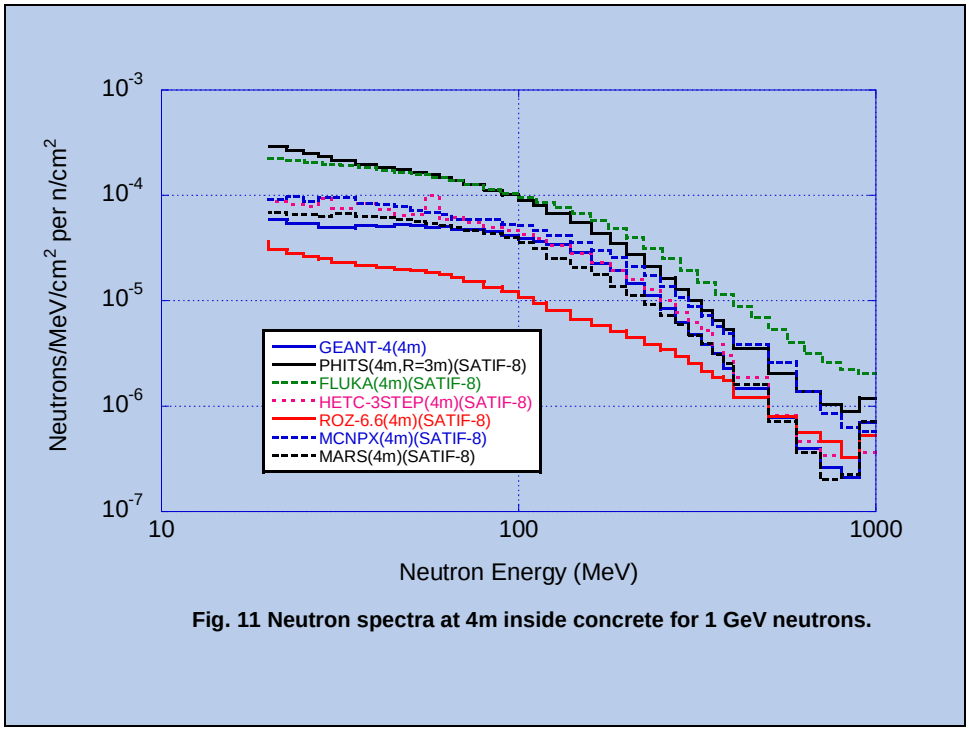

Fig. 11 Neutron spectra at 4m inside concrete for 1 GeV neutrons.

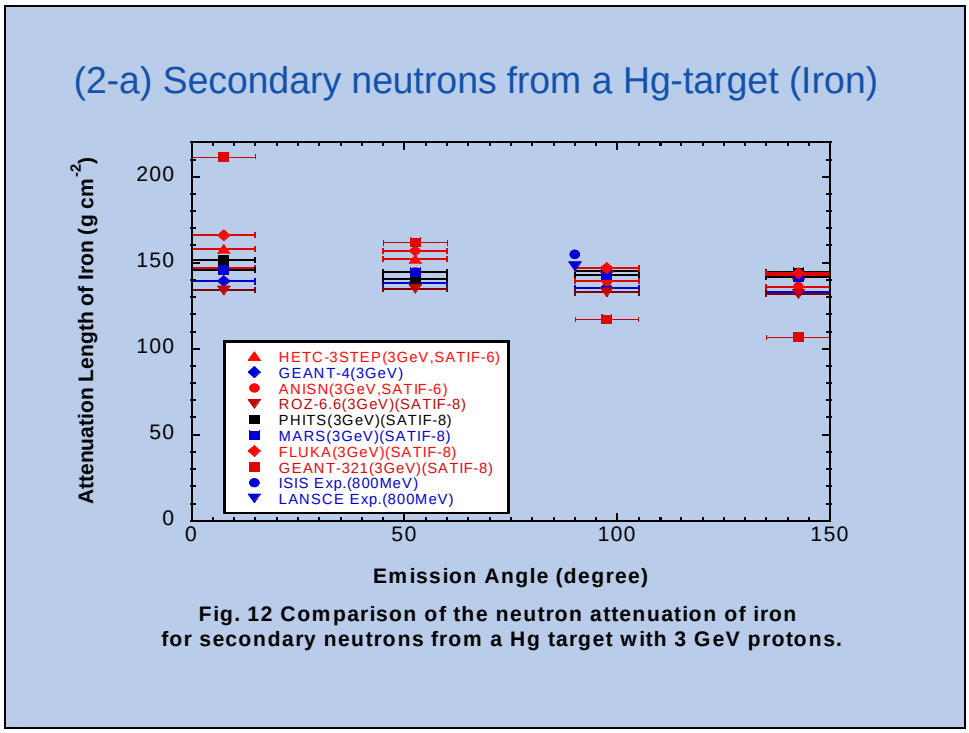

Fig. 12 Comparison of the neutron attenuation of iron for secondary neutrons from a Hg target with 3 GeV protons.

(2-b) Secondary neutrons from a Hg-target (Concrete)

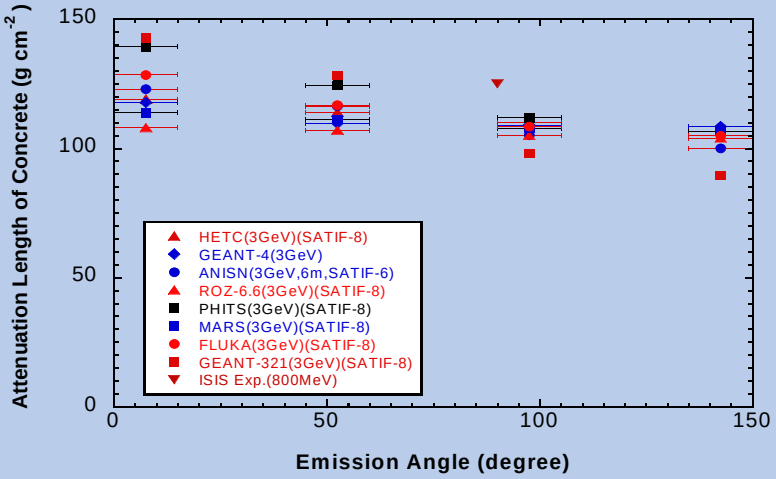

Fig. 13 Comparison of the neutron attenuation length of concrete for secondary neutrons from a Hg target with 3 GeV protons.

Attenuation Length for Secondary Neutrons from Hg Target

- General Tendencies are same with at SATIF-8.
  - In the case of iron, all results show similar weak dependence on the emission angle but their values are largely scattered between each other.
  - In the case of concrete, all results show stronger dependence on the emission angle than in the case of iron and a different dependence between the code used.

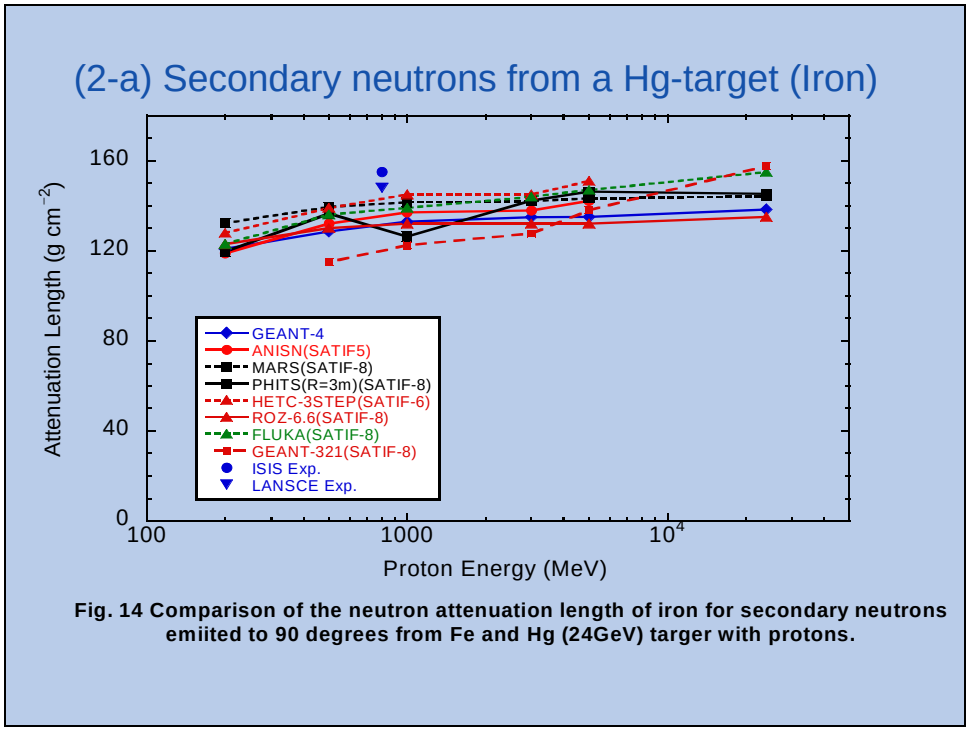

Fig. 14 Comparison of the neutron attenuation length of iron for secondary neutrons emiited to 90 degrees from Fe and Hg (24GeV) targer with protons.

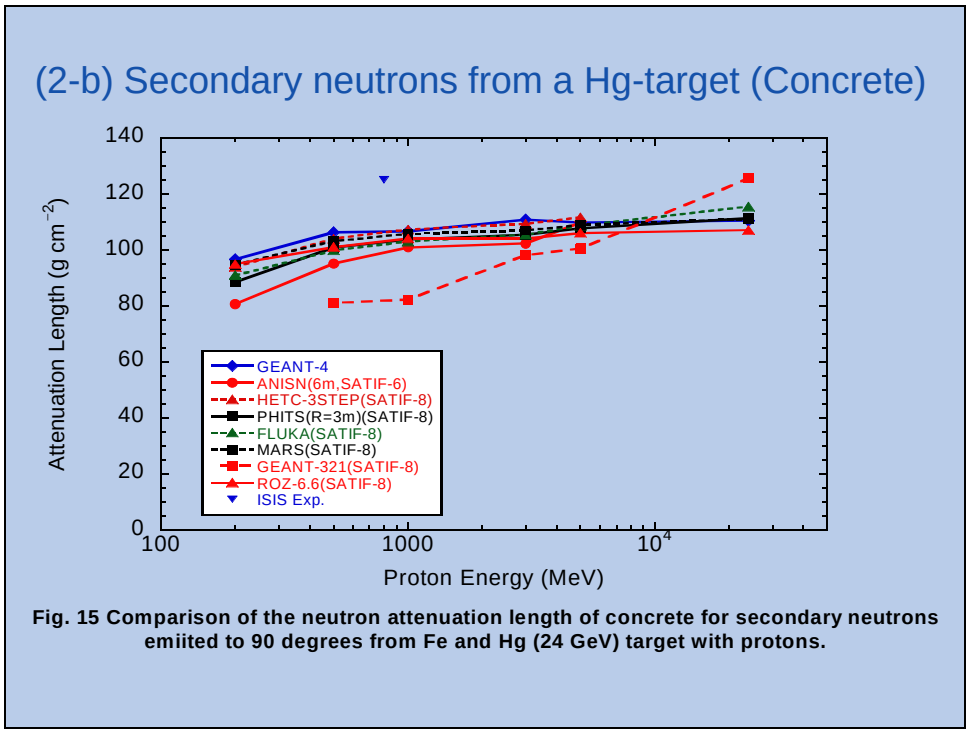

Fig. 15 Comparison of the neutron attenuation length of concrete for secondary neutrons emiited to 90 degrees from Fe and Hg (24 GeV) target with protons.

Comparison with Fe Target

- General Tendencies are same with at SATIF-8.
  - All results show similar tendency to reach an almost constant value above 1 GeV protons.
  - Values of the attenuation length almost similar except for GEANT-321.

(3-a) AGS Experiment (2.83 GeV, Iron)

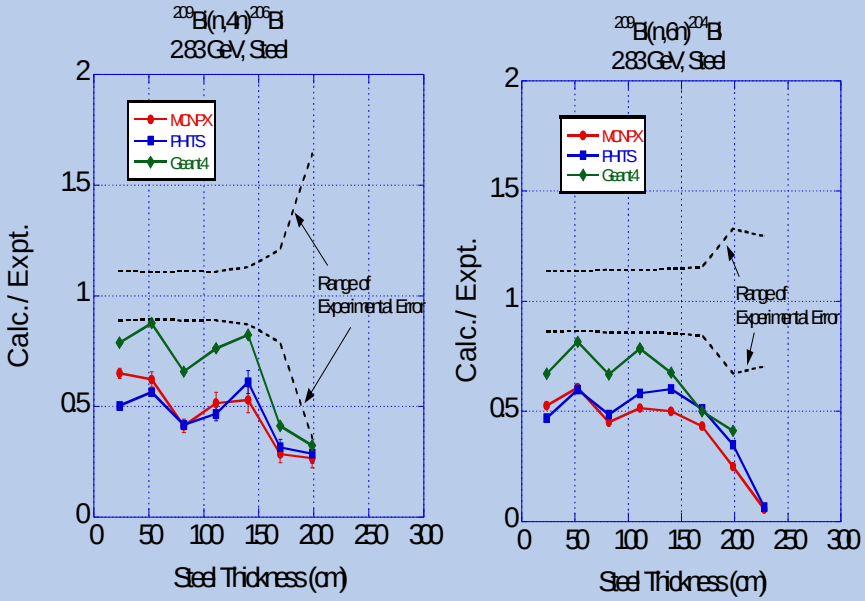

(3-a) AGS Experiment (24 GeV, Iron)

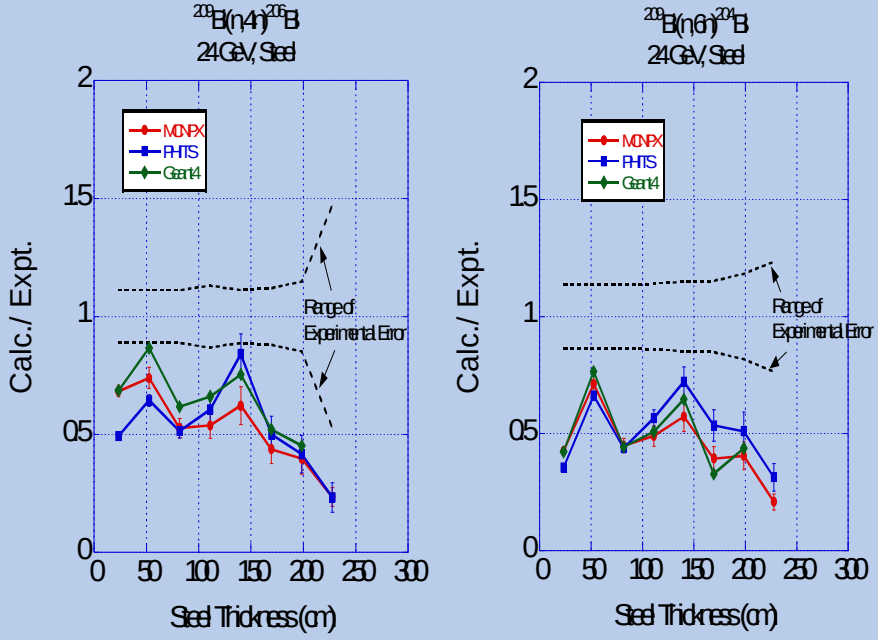

Note: Steel shield

- The calculated results are smaller than the measured ones in general.
- The results of of MCNPX and PHITS agree with each other.
- The results of Geant4 are slightly larger than these two results and closer to the measured ones for 2.83 GeV protons and are almost same for 24 GeV protons.

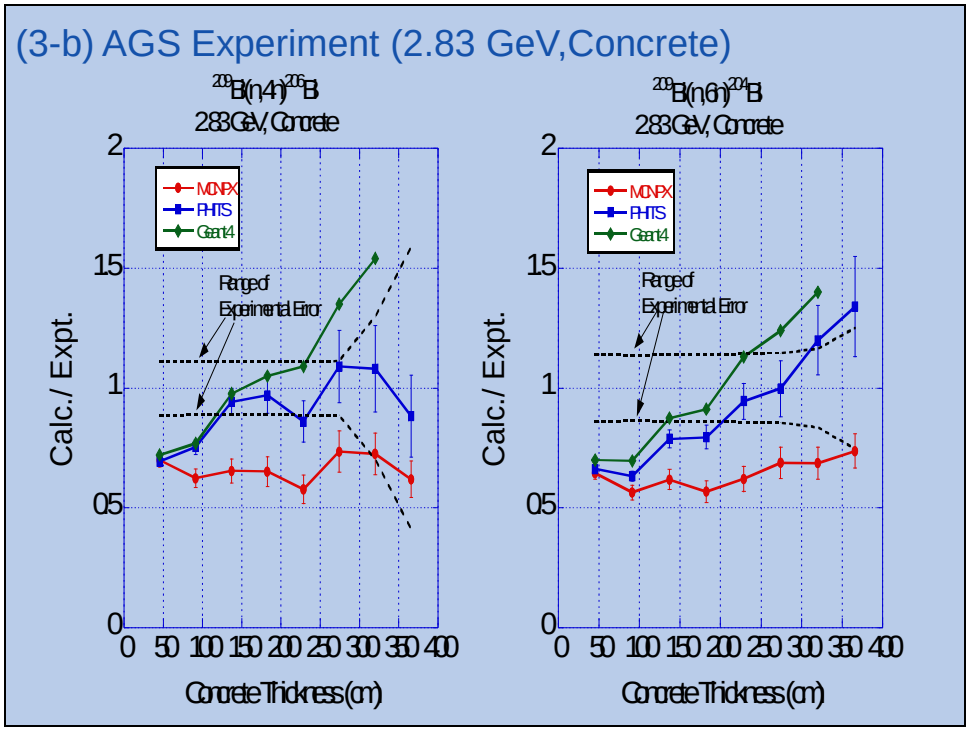
(3-b) AGS Experiment (2.83 GeV,Concrete)
209Bi(n,4n)206Bi
2.83GeV, Concrete
209Bi(n,6n)204Bi
2.83GeV, Concrete
MCNPX
PHITS
Geant4
Range of
Experimental Error
Calc./ Expt.
Concrete Thickness (cm)
0
0.5
1
1.5
2
0 50 100 150 200 250 300 350 400

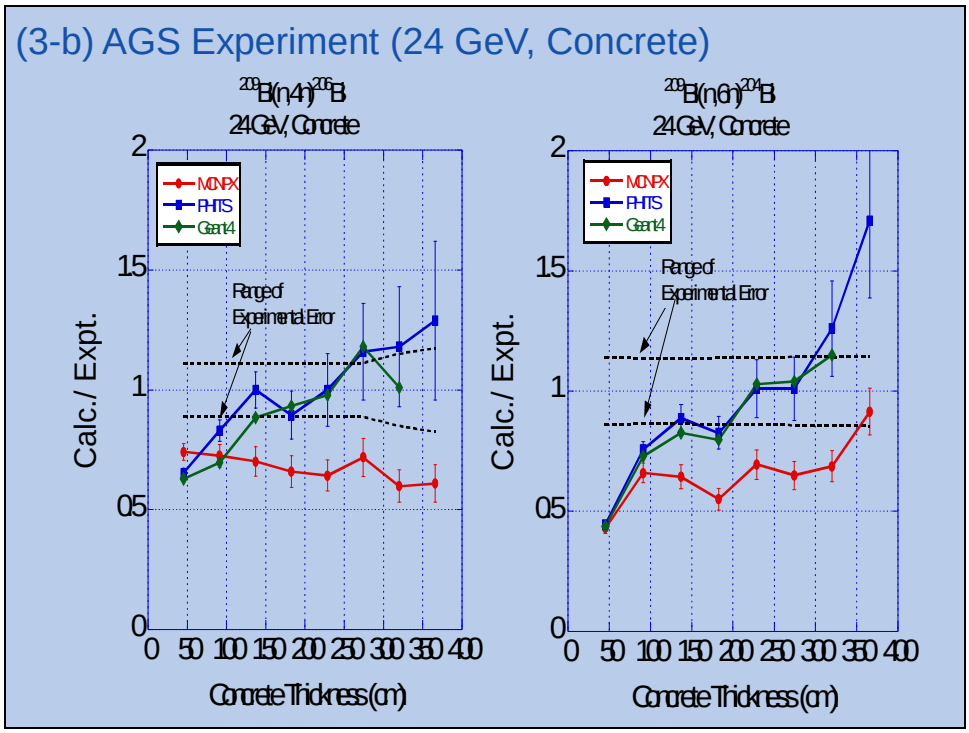
(3-b) AGS Experiment (24 GeV, Concrete)
209Bi(n,4n)206Bi
24GeV, Concrete
209Bi(n,6n)204Bi
24GeV, Concrete
MCNPX
PHITS
Geant4
Range of
Experimental Error
Calc./ Expt.
Concrete Thickness (cm)
0
0.5
1
1.5
2
0 50 100 150 200 250 300 350 400

Note: Concrete shield

- The results of PHITS and Geant4 are relatively in good agreement with the measured results.
- The results of MCNPX are smaller than these results.

Future Themes

- Study the reason for the large difference in the attenuation length and dose between codes.
  - It is desired to receive improved results from other groups.
- Study the reason of the different tendency of C/E values between codes.
  - It is desired that other groups attend this inter comparisons.

FLUKA shielding studies for the CNGS facility due to electronics damage

L. Sarchiapone, A. Ferrari, M. Brugger,
S. Roesler, P. Sala, H. Vincke, V. Vlachoudis
CERN

K. Elsener, E. Gschwendtner
(introductory slides)

Overview

- Introduction to CNGS
- 2006 Commissioning
- Residual Dose Rates Comparison
- What happened during the end of 2007
- FLUKA Calculations
- Understanding the details
- Modifications and New Shielding Design
- Final Layout and Expected Radiation Levels
- Waiting for Operation in 2008

22.04.2008 SATIF 9 - CNGS Fluka Studies 2

Why CNGS ?

⇨ Standard model of particle physics:

ν masses "ZERO"

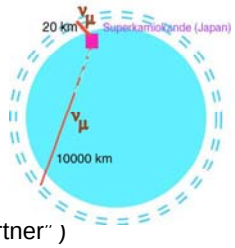

⇨ "Direct" mass measurements

⇨ upper limits

(in decay experiments measuring kinetic energy of "the partner")

$m_{\nu_e} < 2.2$ eV $m_{\nu_\mu} < 170$ keV $m_{\nu_\tau} < 15.5$ MeV

⇨ What's the problem ?

OBSERVATION 1 : SOLAR NEUTRINO "DEFICIT"

only about 50% of the ν_e expected are actually observed

(ν_e disappear "en route" over 10'000 km …)

OBSERVATION 2 : ATMOSPHERIC NEUTRINO ANOMALY"

much less ν_μ "from below" observed w.r.t. expectations

(ν_μ disappear "en route" over 10'000 km …)

22.04.2008 SATIF 9 - CNGS Fluka Studies 3

Why CNGS ?

- **ν's change flavor ! Is this possible?**
  - Yes, "if neutrinos have mass"!

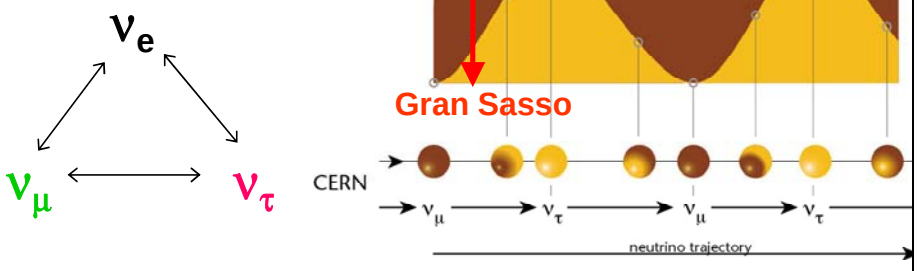

- **CNGS (CERN Neutrino Gran Sasso)**
  - **a long base-line neutrino beam facility (732km)**
  - **send ν_μ beam produced at CERN**
  - **detect ν_τ appearance in experiments at Gran Sasso**
  - **direct proof of ν_μ - ν_τ oscillation (appearance experiment)**

22.04.2008 SATIF 9 - CNGS Fluka Studies 4

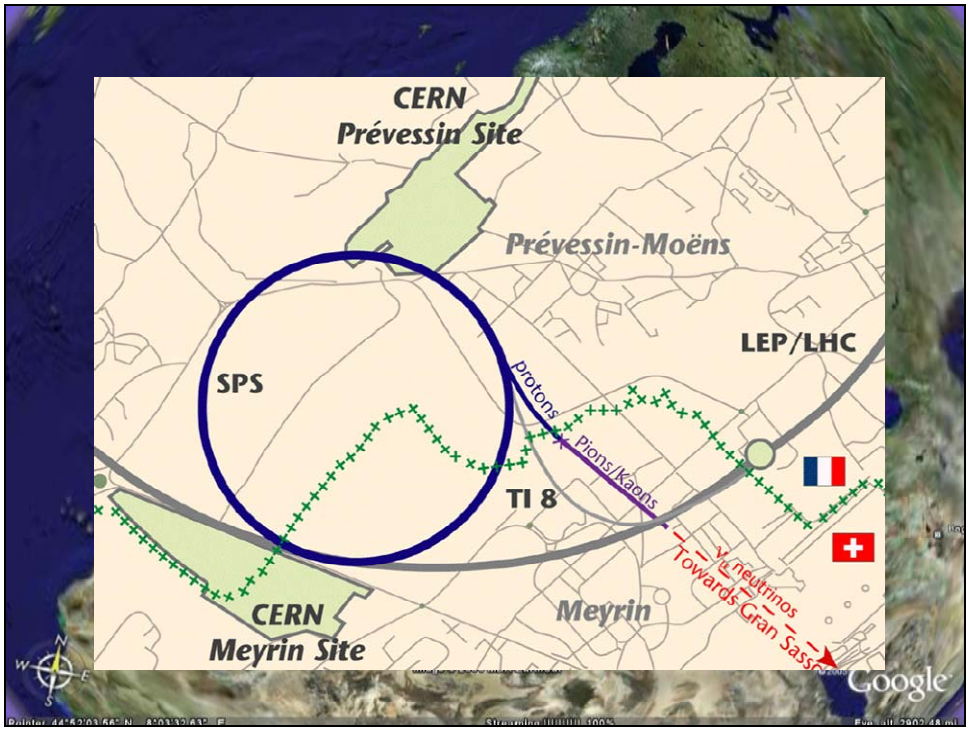
CERN
Prévessin Site
Prévessin-Moëns
LEP/LHC
SPS
protons
Pions/Kaons
TI 8
ν_μ neutrinos
Towards Gran Sasso
CERN
Meyrin Site
Meyrin
Google

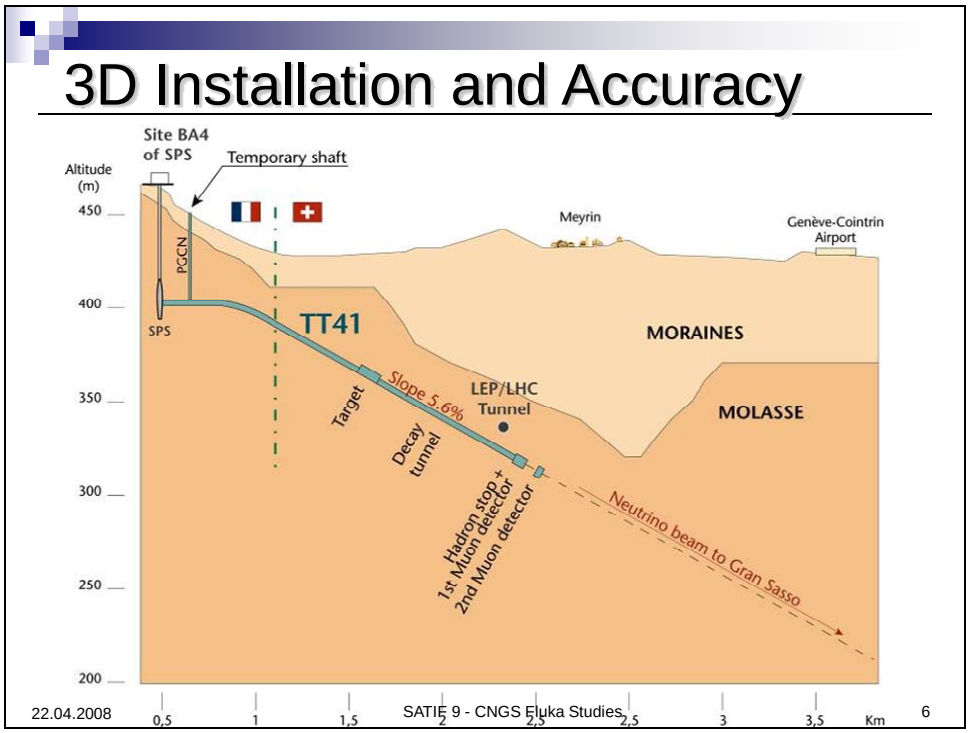
3D Installation and Accuracy
Site BA4
of SPS
Temporary shaft
Altitude
(m)
450
400
350
300
250
200
Meyrin
Genève-Cointrin
Airport
PGCN
SPS
TT41
MORAINES
LEP/LHC
Tunnel
MOLASSE
Target
Slope 5.6%
Decay
tunnel
Hadron stop +
1st Muon detector
2nd Muon detector
Neutrino beam to Gran Sasso
0,5
1
1,5
2
2,5
3
3,5
Km
22.04.2008
SATIF 9 - CNGS Fluka Studies
6

A Long Way to Go…

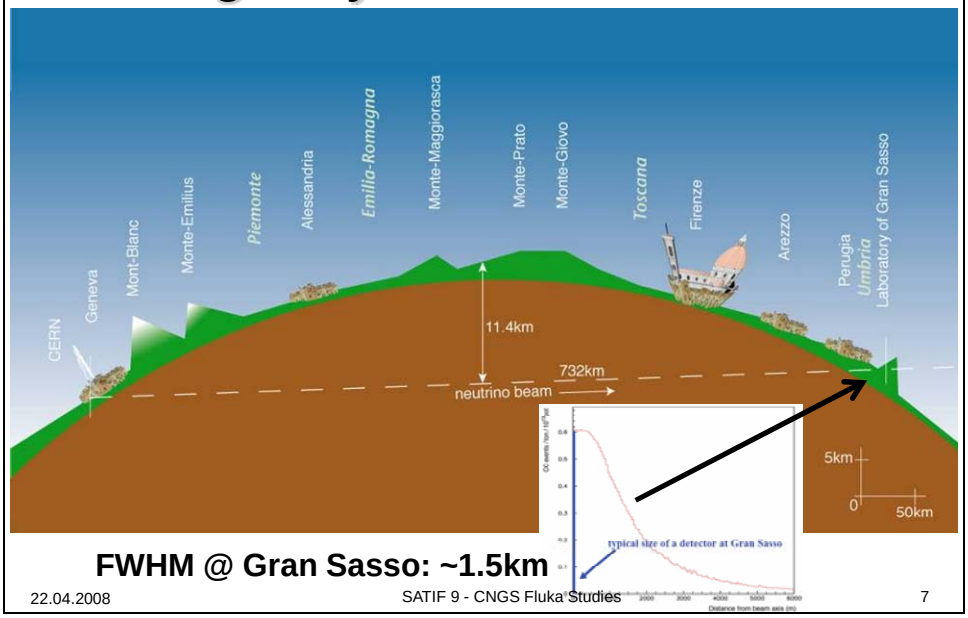

FWHM @ Gran Sasso: ~1.5km

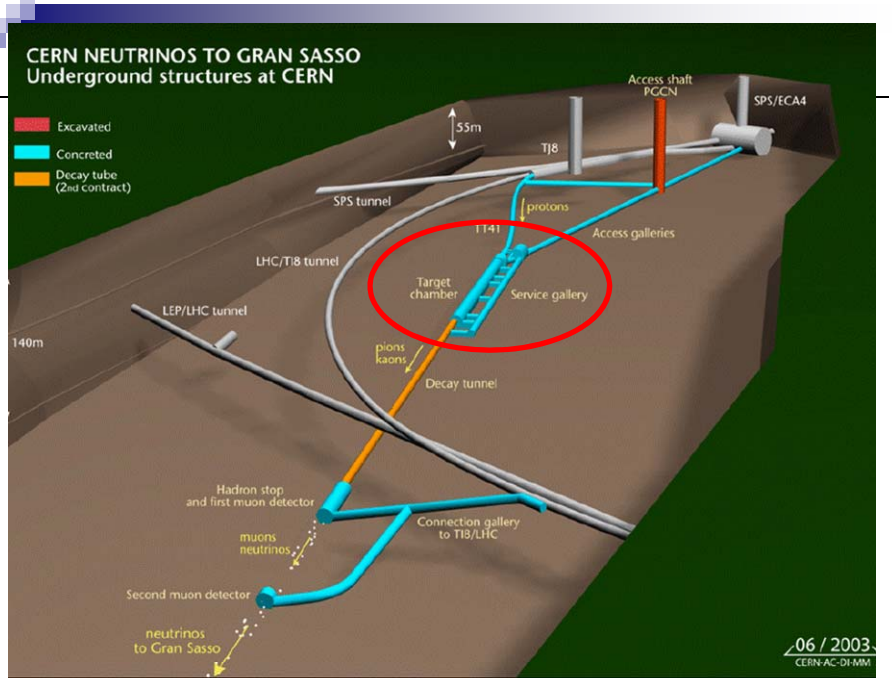

Neutrino Beam Production

- Different Stages
  - 400 GeV/c proton beam on target
  - Pion/Kaon production
  - Focusing
  - Decay
  - Muon and neutrino production
  - Hadron stop (dump)
  - Muon monitoring
  - Neutrino flight to Gran Sasso

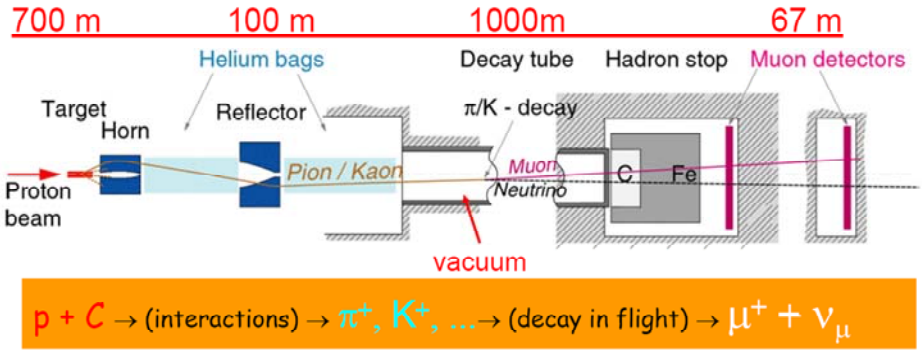

22.04.2008 SATIF 9 - CNGS Fluka Studies 9

Beam Parameters

Beam parameters	Nominal CNGS beam
Nominal energy [GeV]	400
Normalized emittance [μm]	H=12 V=7
Emittance [μm]	H=0.028 V= 0.016
Momentum spread Δp/p	0.07 % +/- 20%
# extractions per cycle	2 separated by 50 ms
Batch length [μs]	10.5
# of bunches per pulse	2100
Intensity per extraction [10^{13} p]	2.4
Bunch length [ns] (4σ)	2
Bunch spacing [ns]	5
Beta at focus [m]	hor.: 10 ; vert.: 20
Beam sizes at 400 GeV [mm]	0.5 mm
Beam divergence [mrad]	hor.: 0.05; vert.: 0.03

~500kW beam power

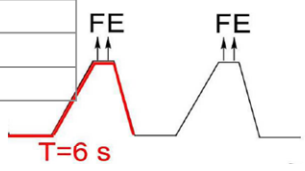

Expected beam performance: 4.5 x 10^{19} protons/year on target

22.04.2008 SATIF 9 - CNGS Fluka Studies 10

CNGS Target

- Different Stages
  - 10 cm long graphite rods, Ø = 5mm and/or 4mm
  - target rods thin / interspaced
  - target rods need to be precisely aligned (0.1 mm)
  - target needs to be cooled (particle energy deposition)

22.04.2008 SATIF 9 - CNGS Fluka Studies 11

Target Magazine (4 spare target units)

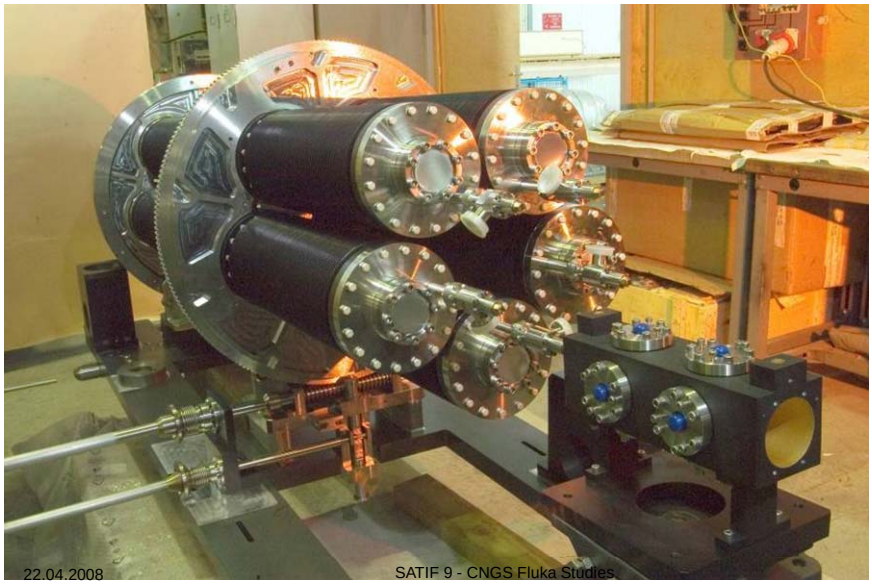

22.04.2008 SATIF 9 - CNGS Fluka Studies 12

Commissioning and First Operation

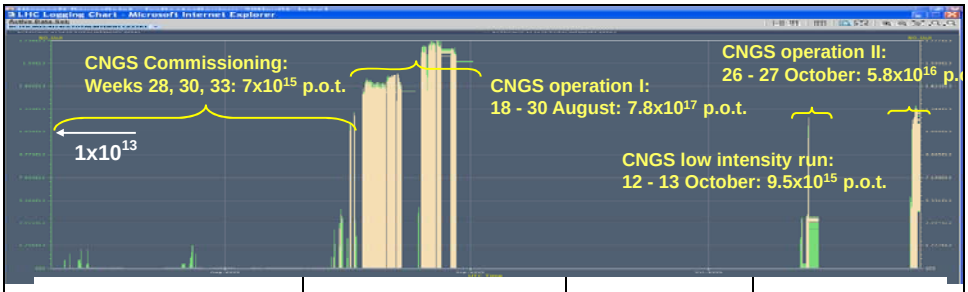

	Date	Extractions	Protons
Commissioning W28	10 – 14 Jul. 2006	300	1.3 E14
Commissioning W30	31 Jul. – 4 Aug. 2006	500	2.4 E14
Commissioning W33	14 – 18 Aug. 2006	1300	6.5 E15
Physics Operation I	18 – 30 Aug. 2006	53000	7.8 E17
Low Intensity Tests	12 – 13 Oct. 2006	2500	9.5 E15
Physics Operation II	26 – 27 Oct. 2006	8300	5.8 E16

- Maximum proton intensity reached in 2006: 3.5 $\cdot 10^{13}$/cycle at 400GeV
- While setting up high intensities for all 3 cycles, reflector leak appeared

The CNGS Reflector

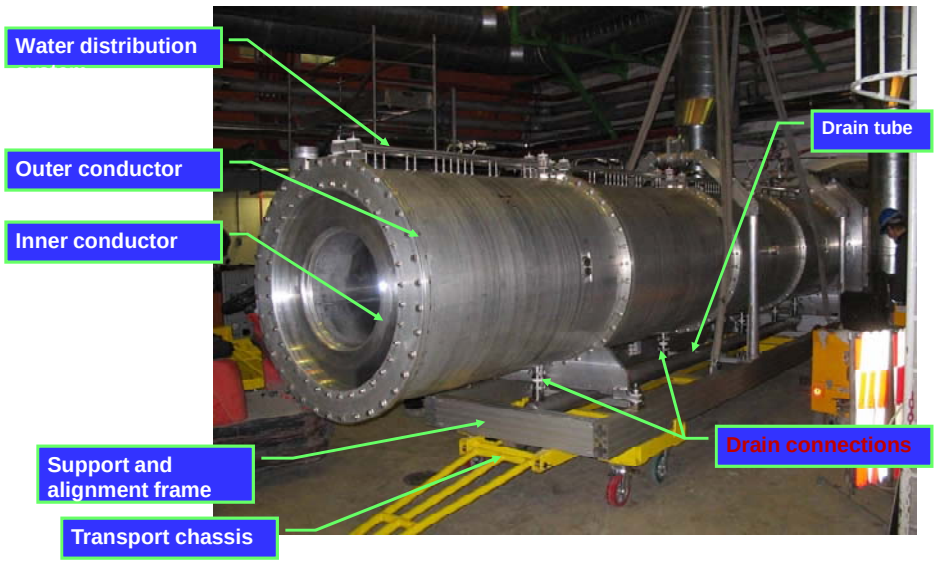

22.04.2008 SATIF 9 - CNGS Fluka Studies 16

Leaking Drain Connection

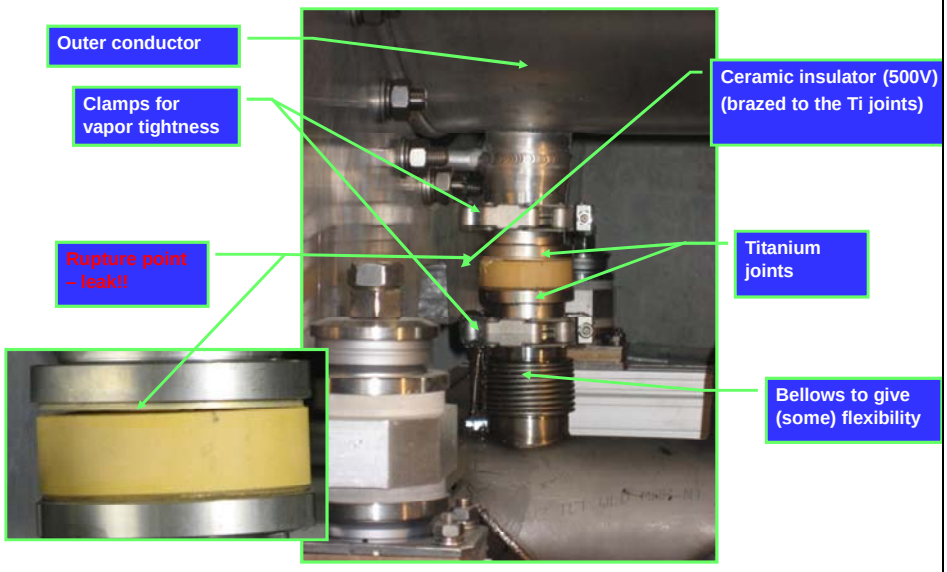

Residual Dose Rates - Benchmark

- Measurements taken in summer 2006 after phase 2 and phase 3 of the CNGS commissioning and compared to FLUKA simulations
  - Data taken along the beam line with a remotely operated detector hanging from the crane. The crane speed was manually controlled, thus certain uncertainties on the actual longitudinal scale
  - Other data taken in the aisle of TCC4 at fixed points

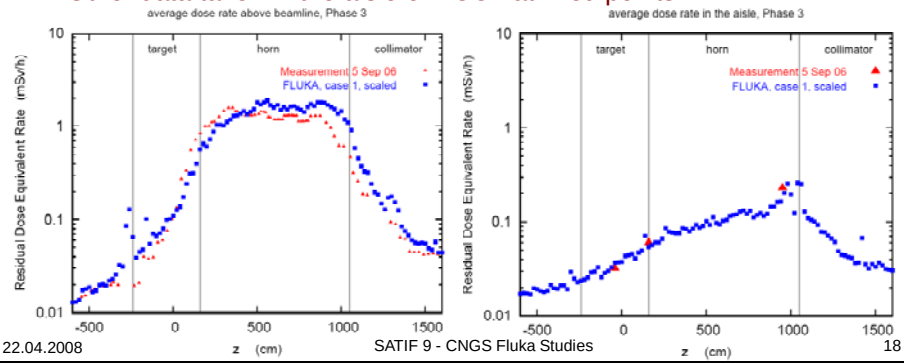

CNGS FLUKA Simulation Environment

- Detailed geometry layout around the target station
- Fully implemented tunnel and gallery structure
- Reasonably detailed geometry till the muon pits (with each BLM simulated in detail)
- Unified simulation approach:
  - for **physics** (neutrino and muon fluxes),
  - **engineering** (power deposition)
  - **prompt** (radiation damage)
  - and **residual** (maintenance and interventions) dose rates

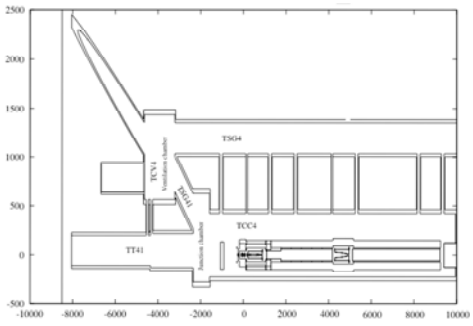

CNGS 2007 1st Commissioning Period

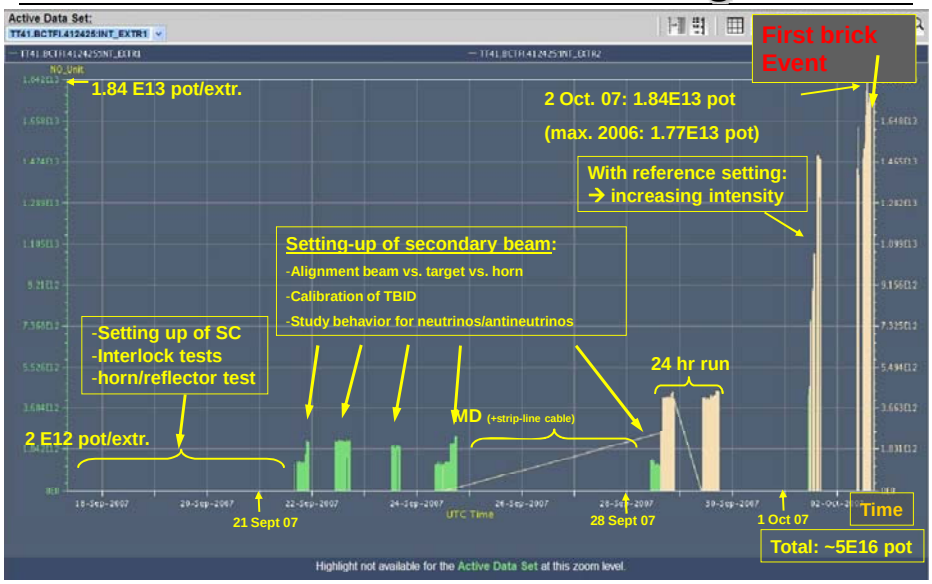

First CNGS Event inside OPERA Target

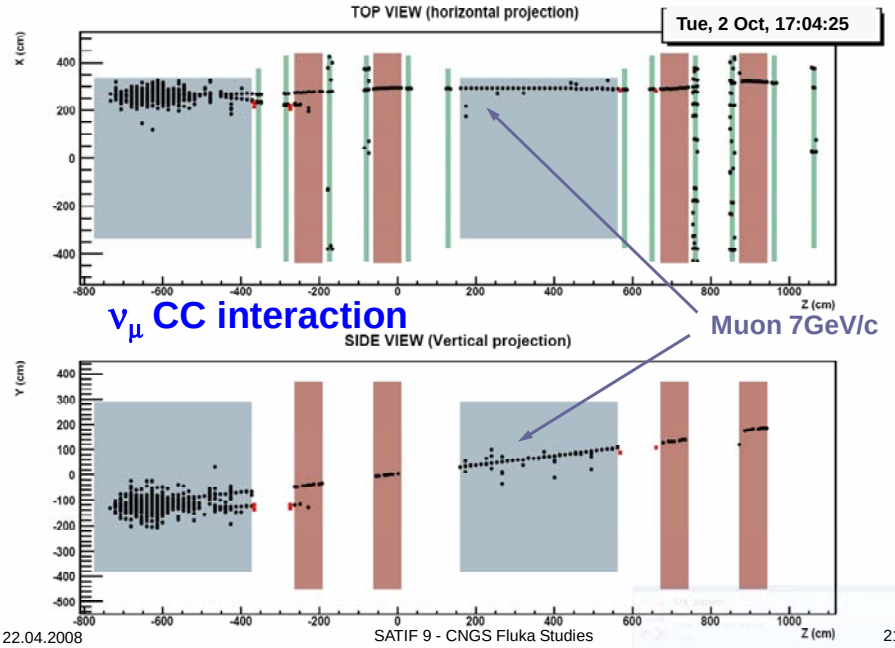

CNGS Physics Run 2007 cont.

Stop CNGS: non-standard mode of operation (access) not possible in an INB controlled facility

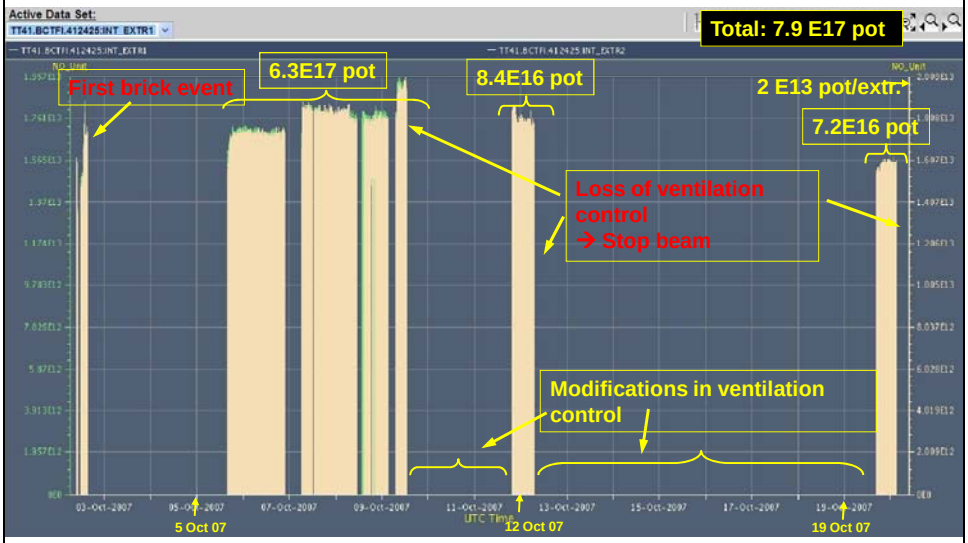

2007 and Electronics Damage

CNGS Target Chamber

Single event upsets in ventilation electronics: caused ventilation control failure and interruption of communication

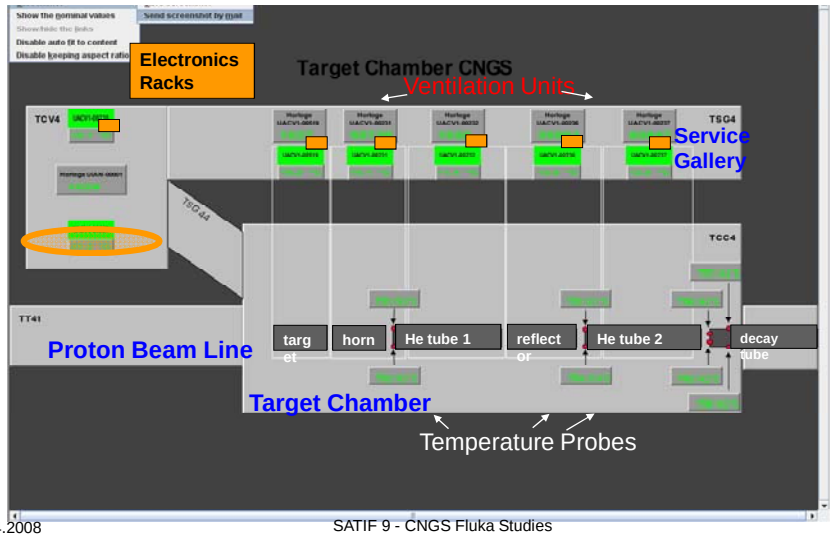

Dose Distribution – Electronics Failures

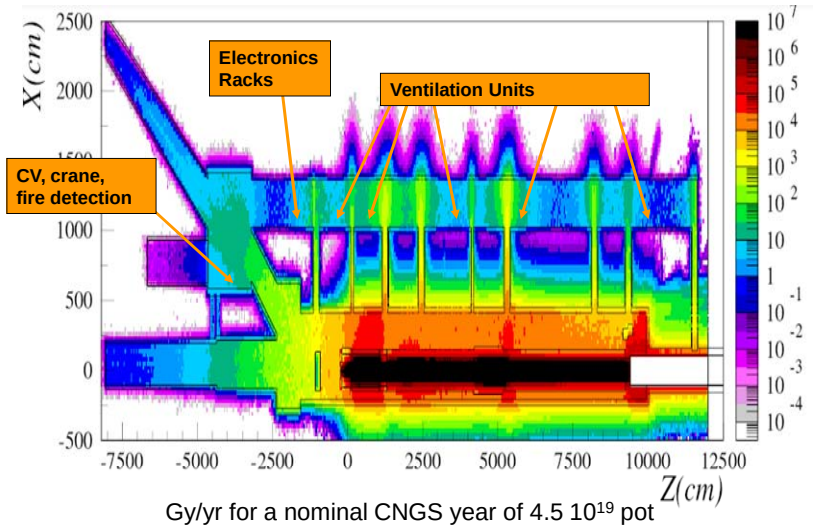

Gy/yr for a nominal CNGS year of 4.5 10^{19} pot

22.04.2008 SATIF 9 - CNGS Fluka Studies 26

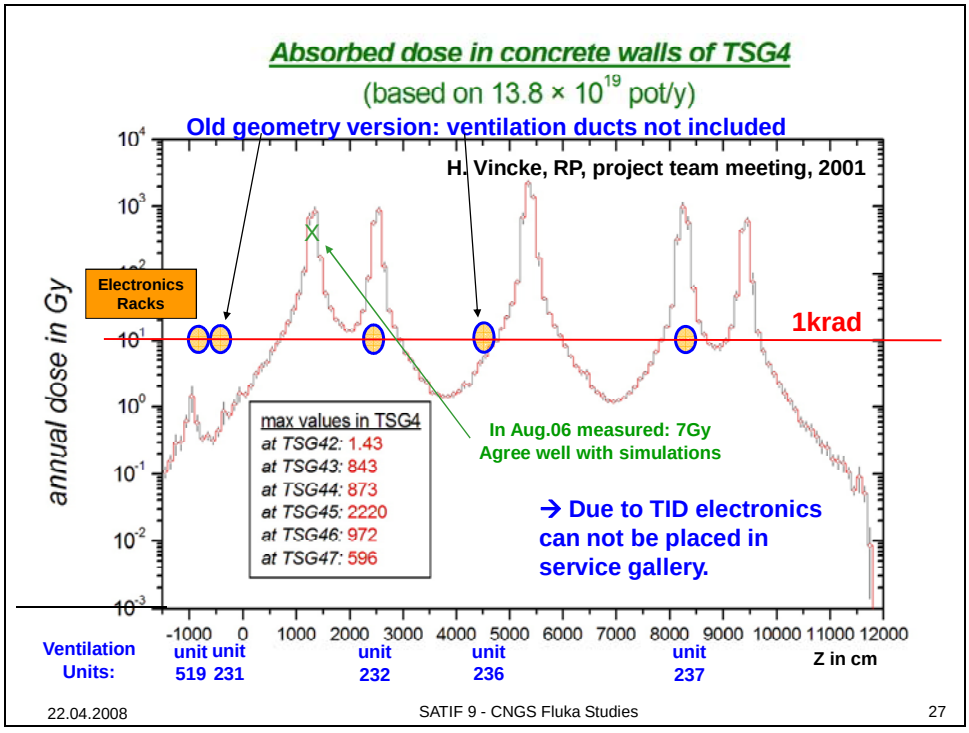

Not Only Dose …

- Dose in the service and ventilation galleries is mainly due to neutrons (and associated photons)
- Dose and neutron fluxes have a very close correlation
- **Cumulative** damage comes from
  - Energy deposition (dose)
  - Lattice displacement (1-MeV n equivalent particle fluxes)
- **Stochastic** failures can occur (SEU) and are mostly due to "high" energy hadrons (E>20 MeV)
- **No safe limit exists**, only a risk level can be determined
- Risk level for commercial electronics is poorly known and varies by orders of magnitude
- What to do, not only for ventilation units, but also for all the electronics in the galleries?

22.04.2008 SATIF 9 - CNGS Fluka Studies 28

Available Measurements - Difficulties

- **RPL** and **Alanine** dosimeters (absorbed dose)
- **RadMon** detectors (absorbed dose in Si, rough indication of 1 MeV eq. and high energy hadron fluences)
- **PMI** air ionization chambers (absorbed dose in air)
- **TLD's** (n/γ dose equivalent)

Limitations:

- Several "dose" measurements, but in different materials (Air, Si, etc.) with different sensitivities to neutrons (particularly thermal neutrons)
- Calibration performed with spectra which are not fully representative of the CNGS radiation fields
- 2 out of 3 RadMon measurements below threshold
- PMI's used for prompt doses (n+γ) while intended for residual ones → saturation and calibration problems

Simulations: Availability & Limitations

- Detailed maps exist for:
  - Dose to Equipment (Gy)
  - 1-MeV Neutron Equivalent Fluence
  - High-Energy Neutron Fluence (> 20MeV)
- Radiation gradients are very steep in many areas
  - large uncertainties in the simulated results depending on the volume used for averaging, and the exact position (often not well known)
  - ***Simulations results (in terms of comparison with the measurement) have an overall uncertainties easily as large as a factor of 2 or more***
- Adjacent galleries are all "empty" in the simulation, while in reality they are full of racks, ducts, walls etc.
  - *For example, a 10 g/cm^2 Stainless Steel layer would lower all doses in TCV4/TSG4 by a factor of ~ 2.5-3*

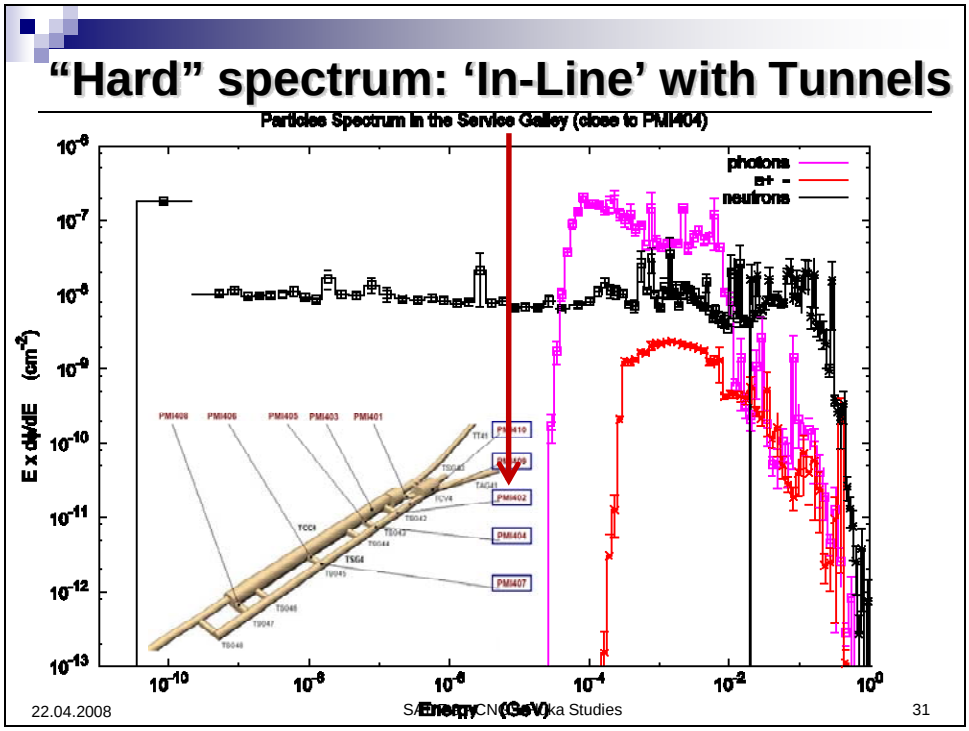
"Hard" spectrum: 'In-Line' with Tunnels
Particles Spectrum in the Service Gallery (close to PMI404)
photons
e+ -
neutrons
E x dN/dE (cm-2)
Energy (GeV)
PMI408
PMI406
PMI405
PMI403
PMI401
PMI410
PMI409
PMI402
PMI404
PMI407
22.04.2008
SATIF 9 - CNGS Fluka Studies
31

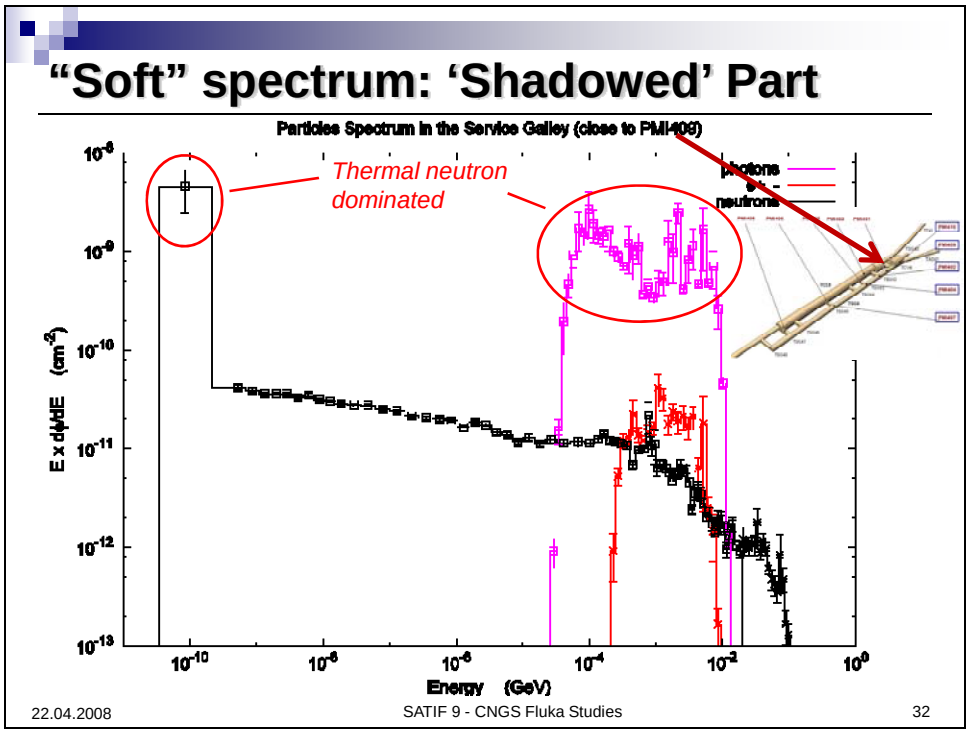
"Soft" spectrum: 'Shadowed' Part
Particles Spectrum in the Service Gallery (close to PMI409)
Thermal neutron dominated
photons
e+ -
neutrons
E x dN/dE (cm-2)
Energy (GeV)
22.04.2008
SATIF 9 - CNGS Fluka Studies
32

CNGS: RPL and Alanine Dosimeter Positions

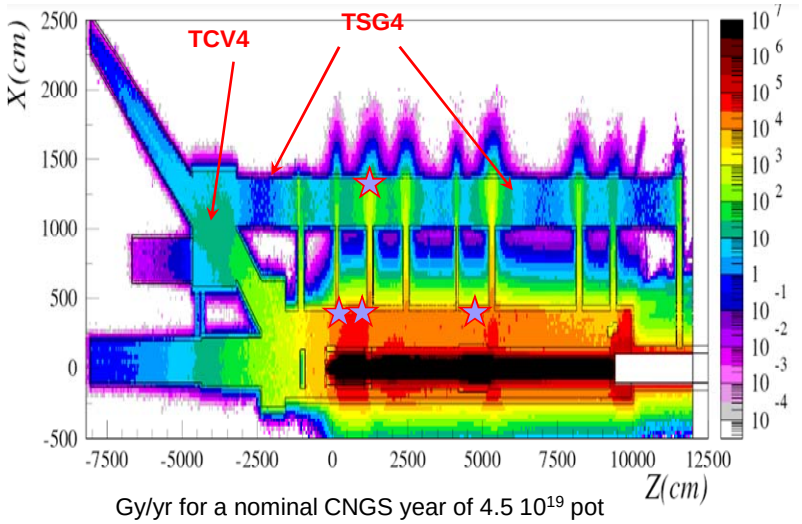

Gy/yr for a nominal CNGS year of 4.5 10^{19} pot

Alanine and RPL dosimeters: good agreement

Alanine and RPL dosimeters are in principle sensitive to both γ rays and neutrons, RPL are more sensitive to n due to some Boron content`

Detector type / position description	Exp. Value (Gy/p)	Simulation (Gy/p)
RPL: perp. horn strip lines	$1.7 \cdot 10^{-15}$	$1.2 \cdot 10^{-15}$
Alanine: perp. horn strip lines	$9.0 \cdot 10^{-16}$	
RPL: perp. refl. strip lines	$8.2 \cdot 10^{-16}$	$5.4 \cdot 10^{-16}$
Alanine: perp. refl. strip lines	$3.8 \cdot 10^{-16}$	
RPL: perp. to the target	$1.7 \cdot 10^{-15}$	$3.7 \cdot 10^{-16}$
Alanine: perp. to the target	$3.4 \cdot 10^{-16}$	
RPL: top of PMI404	$9.4 \cdot 10^{-18}$	$7.2 \cdot 10^{-18}$
Alanine: top of PMI404	$4.3 \cdot 10^{-18}$	

Hole in shielding not included in simulation

CNGS: Holes in the Target Shield (Target Motors)

RadMon Radiation Monitors - Comparison

- Absorbed dose (RadFet): sensitivity > 10^{-2} Gy
- 1 MeV equivalent neutron fluence: > 10^{10} 1 MeV n/cm^{-2}
- "High-Energetic" (roughly E > 20 MeV) hadron fluence
  - estimated counting SEU's occurring in known electronic devices, two operating modes
    - Bias 5 V: "standard" one, 1 SEU corresponds to roughly $2 \cdot 10^{8}$ h/cm^{-2} with a relatively sharp threshold around 20 MeV
    - Bias 3 V: much more sensitive, significant sensitivity also below 20 MeV
- Only two detectors installed in CNGS for the 2007 run ($7.2 \cdot 10^{16}$ pot), one (5 V) in TCV4, the other (3 V) in TSG4
  - absorbed dose: just below threshold: "confirmed" by measurement
  - 1 MeV Eq.: well below detection limit at respective locations
  - 20 MeV: **Exp. value: $2 \cdot 10^{7}$ cm^{-2} ± 30% (9 SEU's)**
    Sim. value: $2.5 \cdot 10^{7}$ cm^{-2} ± 50%

CNGS: PMI ioniz. Chambers – Only Qualitative

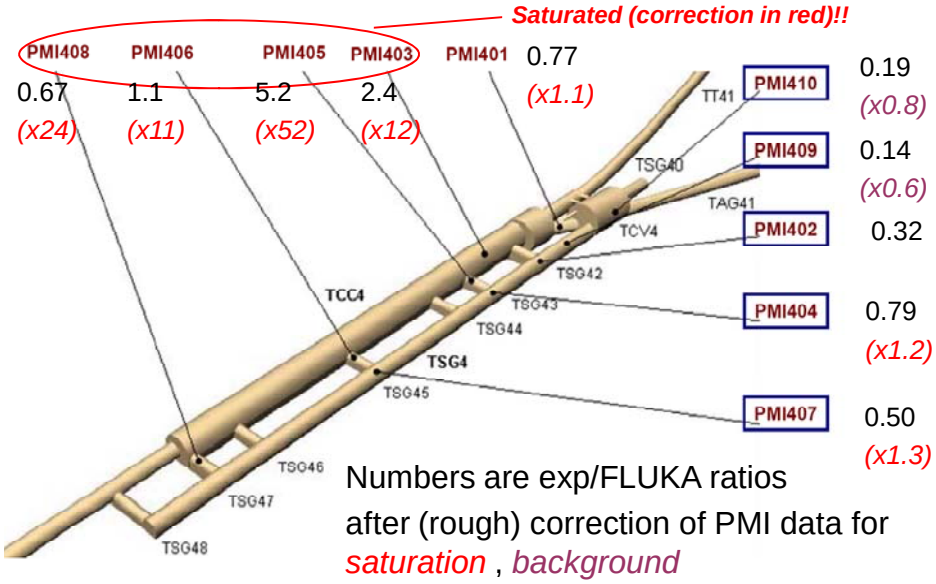

Numbers are exp/FLUKA ratios after (rough) correction of PMI data for *saturation* , *background*

TLD's: Dose Equivalent

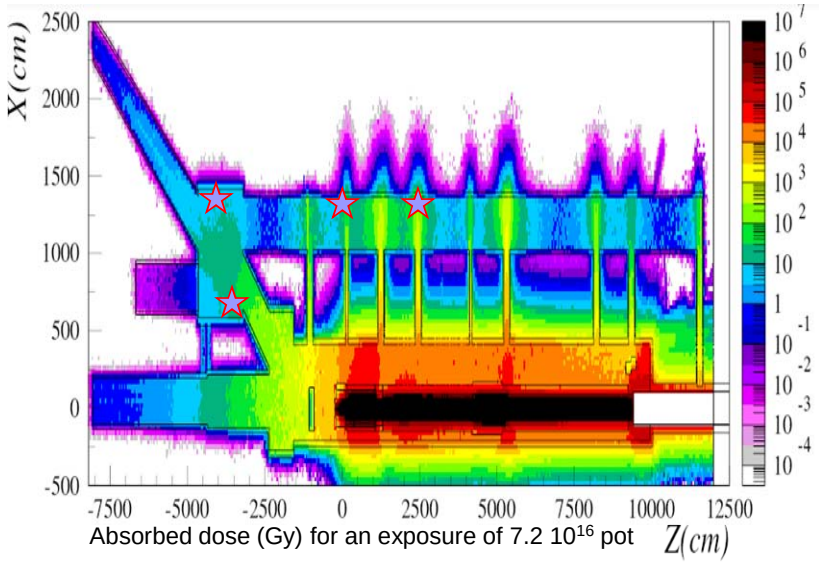

Absorbed dose (Gy) for an exposure of 7.2 10^{16} pot

TLD dosimeters

Sim. dose equivalent values (Sv) has been obtained out of calculated absorbed dose in air (Gy), **correcting for air → tissue** and weighting for the neutron quality factors with a couple of representative spectra. The related uncertainty is +/- 30% on top of the (large) statistical one

TLD / position description	Exp. Value (Sv/p)	Simulation (Sv/p)
n dose: UA232/TSG4	$2.3 \cdot 10^{-17}$	$1.3 \cdot 10^{-17}$
γ dose: UA232/TSG4	$4.3 \cdot 10^{-18}$	
n dose: UA231/TSG4	$8.1 \cdot 10^{-18}$	$2.6 \cdot 10^{-18}$
γ dose: UA231/TSG4	$2.5 \cdot 10^{-18}$	
n dose: fire detector (TCV4)	$4.0 \cdot 10^{-18}$	$2.4 \cdot 10^{-18}$
γ dose: fire detector (TCV4)	$1.2 \cdot 10^{-19}$	
n dose: pump cupboard (TCV4)	$1.3 \cdot 10^{-18}$	$6.9 \cdot 10^{-19}$
γ dose: pump cupboard (TCV4)	$5.0 \cdot 10^{-20}$	

New Shielding Design

New Shielding Layout

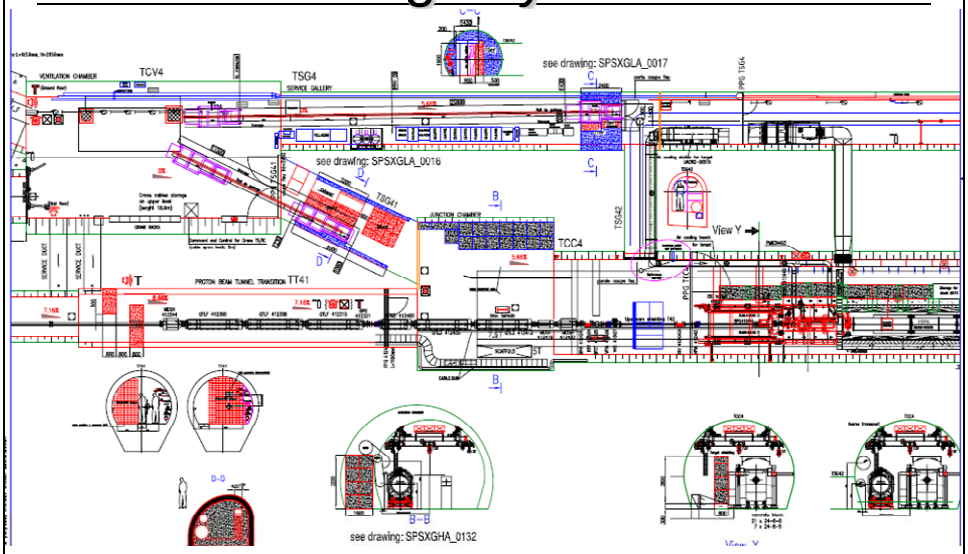

Different Shielding Options

- TSG4 plug:
  - Concrete 240 cm
  - Concrete 320 cm
  - Concrete 240 cm + Iron 20 cm
- TSG41 plug with ventilation pipes
  - Straight pipes
  - Chicane pipes
  - "Viroles"
- TT41 chicane

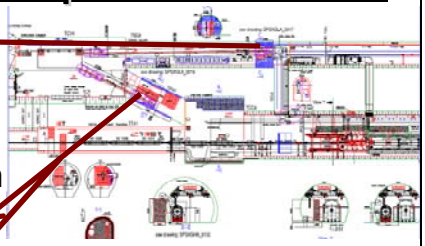

- *… and … whatever coming out of several brainstorming discussions . . .*

Getting Statistics

Biasing

- Region importance biasing for hadrons and neutrons
- Leading Particle biasing for electromagnetic showers (inside the target chamber shielding)
- "blackhole" where possible

Two-Step Approach

- First simulation to collect the spectrum of particles (mainly neutrons) moving towards the additional shielding locations
- Separate simulations to evaluate the attenuation due to each plug configuration

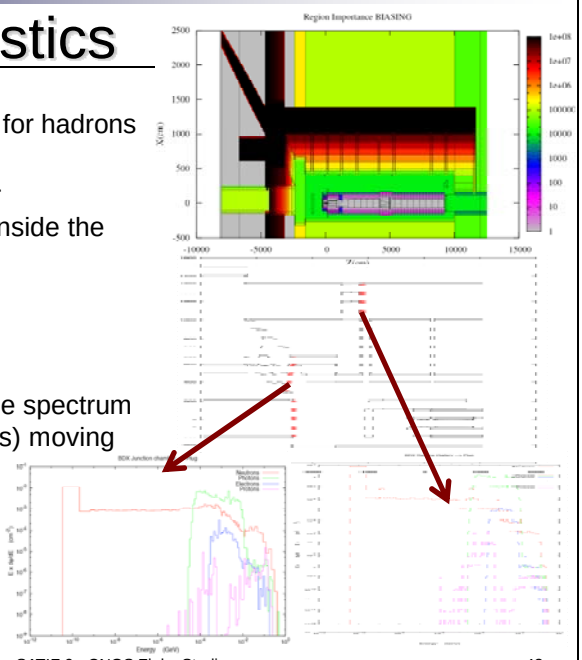

22.04.2008 SATIF 9 - CNGS Fluka Studies 43

Radiation Effects in Electronics

- **Cumulative effects**
  - **Total Ionizing Dose (TID):**
    - energy deposited by ionization per unit mass [Gy]
    - the radiation effect is referred to as surface damage
  - **Displacement Damage (NIEL):**
    - degradation of the lattice structure of silicon atoms
    - it is measured in 1 MeV neutron equivalent particles/cm2
- **Single Event Effects (SEE)**
  - Change of state of a bi-stable element caused by energetic particles
  - The SEE rate is dominated by hadrons with an energy above 20 MeV

22.04.2008 SATIF 9 - CNGS Fluka Studies 44

What are the Levels (20 MeV)

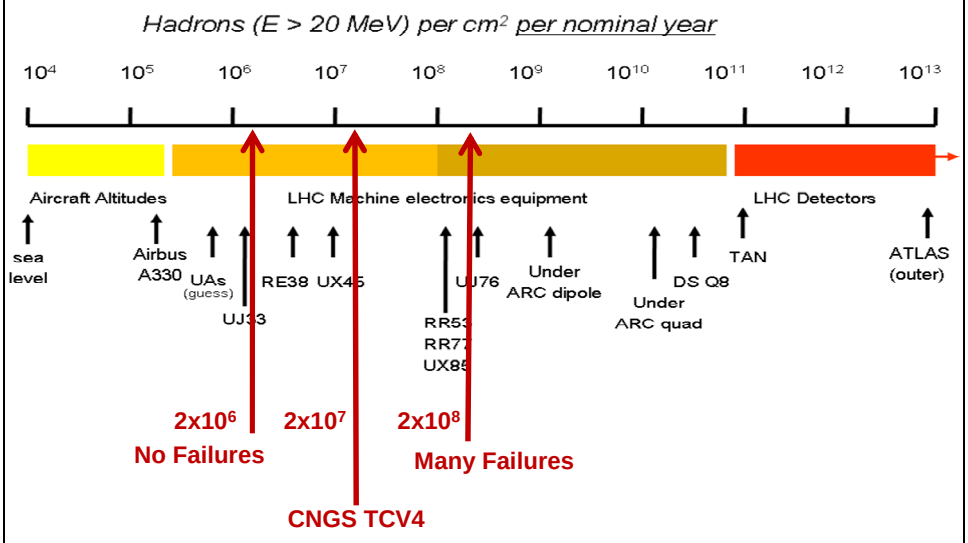

Shielding Design Studies

- Modifying the width of the plug

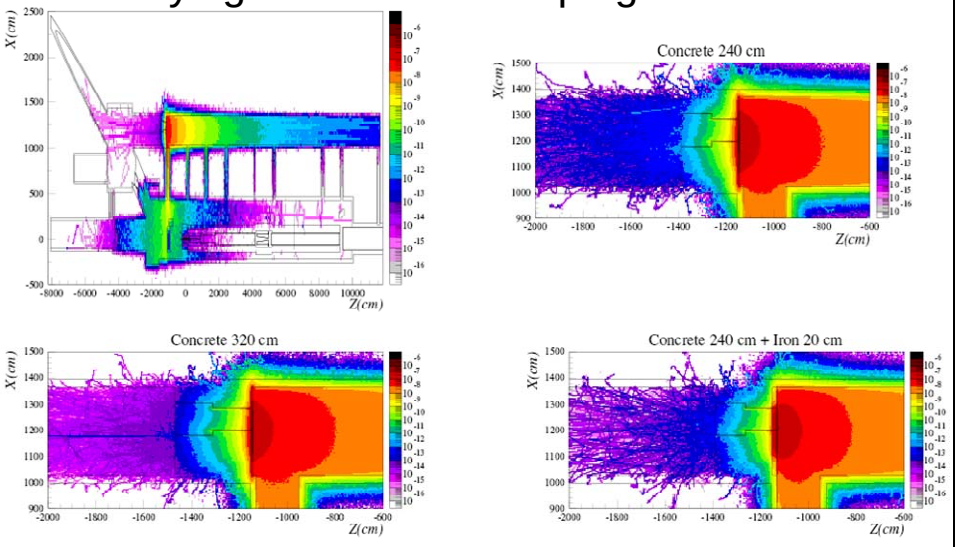

Ventilation Ducts – Design

- Plug with gaps and opening for the ventilation pipes, to be implemented in a bend tunnel -> simplification needed.

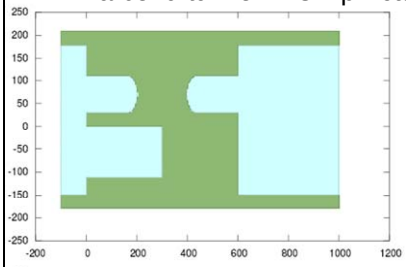

Option:
Ventilation Maze

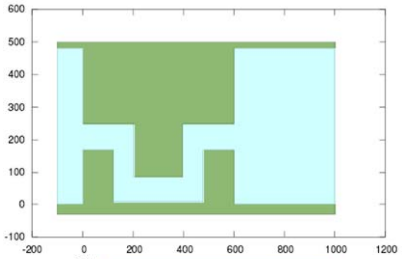

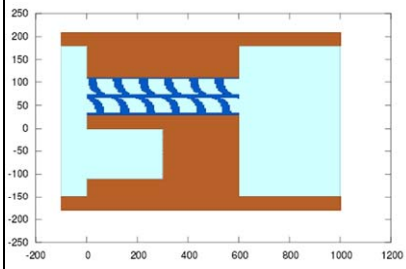

Option:
Virole Solution

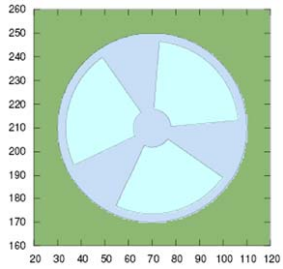

22.04.2008 SATIF 9 - CNGS Fluka Studies 47

Shielding Design Studies

- The final configuration is a “fake chicane” for one of the ventilation pipes in the movable shielding part and two (real) chicanes in the upper fix shielding part.

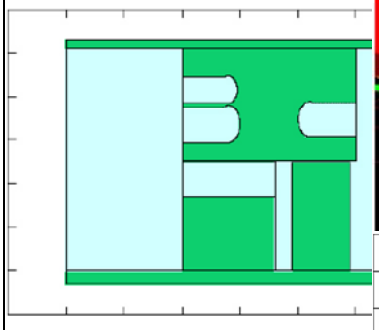

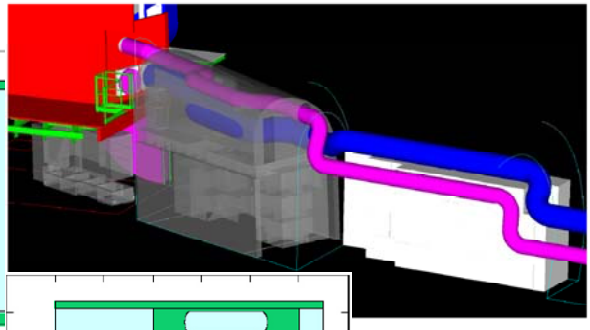

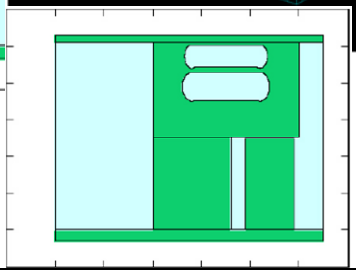

22.04.2008 48

Annual Dose (Gy)

Without Shielding

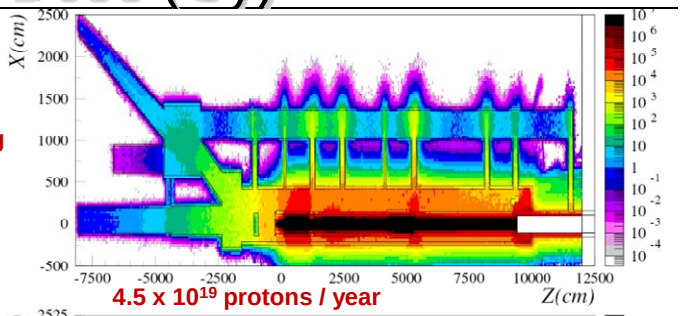

4.5 x 10^{19} protons / year

With New Shielding

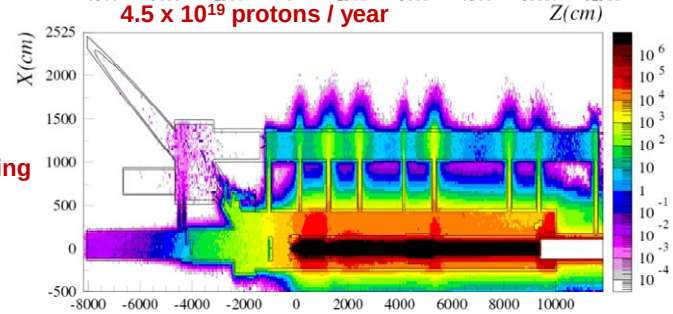

22.04.2008 SATIF 9 - CNGS Fluka Studies 49

1 MeV Equivalent Neutrons

Without Shielding

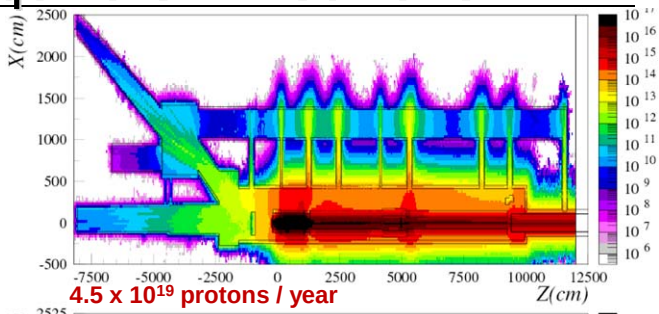

4.5 x 10^{19} protons / year

With New Shielding

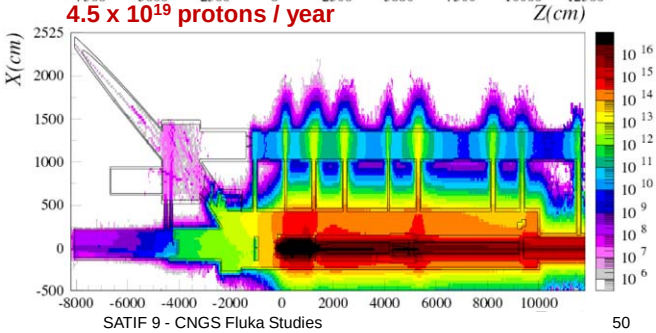

22.04.2008 SATIF 9 - CNGS Fluka Studies 50

> 20 MeV Hadron Fluence

Without Shielding

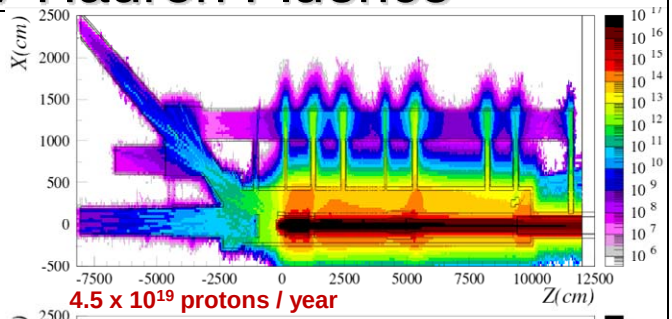

4.5 x 10^{19} protons / year

With New Shielding

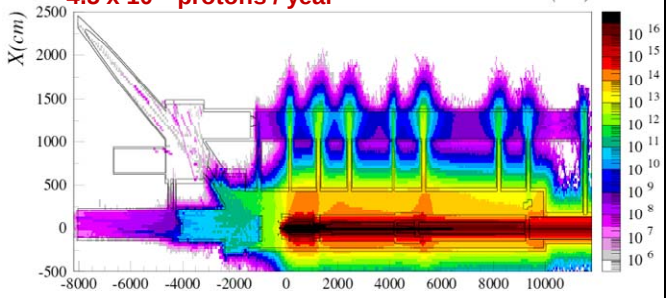

Expected Annual Values

	Dose [Gy/y]	Fluence n_{1MeV} eq. [cm^{-2}/y]	Fluence $E_h > 20MeV$ [cm^{-2}/y]
TSG4			
2007 – no shielding	1 – 10	10^9 – 10^{10}	10^7 – 10^9
Attenuation factor	10^6	10^6	10^5
Expected levels – 2008	10^{-6} – 10^{-5}	10^3 – 10^4	10^2 – 10^4
TSG41			
2007 – no shielding	1 – 100	10^{10} – 10^{12}	10^8 – 10^{11}
Attenuation factor	10^3	10^4	10^3
Expected levels – 2008	10^{-3} – 10^{-1}	10^6 – 10^8	10^5 – 10^8

all values based on 4.5E19 protons on target per year

Conclusions

- **Electronics failures** at CNGS in 2007
- **Successful comparison** of existing simulations with updated calculations, as well as available measurements
- High-energy hadron fluences caused **SEUs**
- Fast solution had to be applied, thus partly displacement of critical electronics, as well **as important additional shielding** for critical parts
- FLUKA calculations for **numerous design option** in order to determine the most efficient solution
- Expected radiation levels are **clearly below critical values**
- Similar situations will exist for the **LHC** and have to be addressed already now during the final preparation of commissioning

Session V

Dose and related issues

Chair: M. Silari

Iterative unfolding for Bonner sphere spectrometers – Sensitivity analysis and dose calculation

G. Simmer, V. Mares, E. Weitzenegger, W. Rühm
Helmholtz Zentrum München, Institute of Radiation Protection

As of January 1st 2008, the new name of our Center is:

GSF – National Research Center for Environment and Health
member of the Helmholtz Association

Institute of Radiation Protection

HelmholtzZentrum münchen
German Research Center for Environmental Health

Helmholtz Zentrum München
German Research Center for Environmental Health (HMGU)

Our addresss remains as it is: Ingolstädter Landstr. 1
D-85764 Neuherberg

Our domain changes: helmholtz-muenchen.de

Hermann Ludwig Ferdinand von Helmholtz

Born: 31 Aug 1821 in Potsdam, Germany
Died: 8 Sept 1894 in Berlin, Germany

"Helmholtz was the last great scholar whose work, in the tradition of Leibniz, embraced all the sciences, as well as philosophy and the fine arts."

HelmholtzZentrum münchen
German Research Center for Environmental Health

HELMHOLTZ ASSOCIATION

Spectrometer characteristics

- ^{3}He proportional counters: Centronics Ltd. SP9
- 15 PE-Spheres (diameter given in inch):
  2.5, 3, 3.5, 4, 4.5, 5, 5.5, 6, 7, 8, 9, 10, 11, 12, 15
- 2 PE+Pb Spheres include lead shells:
  9-1(0.5''), 9-2(1'')

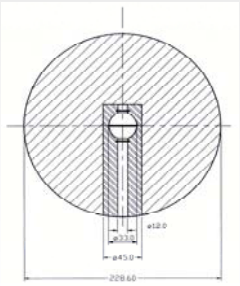

HelmholtzZentrum münchen
German Research Center for Environmental Health

HELMHOLTZ ASSOCIATION

Benchmark excercise in a workplace field

- three-year project (2005-2007) called CONRAD
  COordinated Network for RAdiation Dosimetry
- organised by WP6 of CONRAD (EURADOS WG 8)
  collaboration with WP4 (EURADOS WG 6)
- organizational framework provided by EURADOS
  European Radiation Dosimetry Group
- included both measurements and calculations

GSI Darmstadt, 2006

- aim: intercomparing the response of several types
  of radiation monitors in a well-characterised field at a high-energy particle accelerator
- to be published in Radiat. Meas., 2008 [Rollet et al., Wiegel et al., Silari et al.]

a) Department of Nuclear Engineering, Polytechnic of Milano, Via Ponzio 34/3, Milano, Italy
b) INFN Laboratori Nazionali di Frascati, Via E. Fermi 40, 00044 Frascati, Italy
c) Institute for Radiological Protection and Nuclear Safety, F-92262 Fontenay aux Roses, France
d) Paul Scherrer Institut (PSI), CH-5232 Villigen, Switzerland
e) Physikalisch-Technische Bundesanstalt, Postfach 3345, D-38023 Braunschweig, Germany
f) Strahlenbiologisches Institut, Ludwig-Maximilians-Universität München, D-80336 München, Germany
g) GSI Gesellschaft für Schwerionenforschung, Planckstraße 1, D-64291 Darmstadt, Germany
h) CERN, 1211 Geneva 23, Switzerland
i) Department of Radiation Dosimetry, Nuclear Physics Institute of the AS CR, CZ-18086 Praha, Czech Republic
j) Institute of Atomic Energy, 05-400 Otwock-Swierk, Poland
k) Polytechnic of Milan, CESNEF, Via Ponzio 34/3, 20133 Milano, Italy
l) Austrian Research Centers GmbH-ARC, 2444 Seibersdorf, Austria
m) Helmholtz Zentrum München, 85764 Neuherberg, Germany

HelmholtzZentrum münchen
German Research Center for Environmental Health

HELMHOLTZ ASSOCIATION

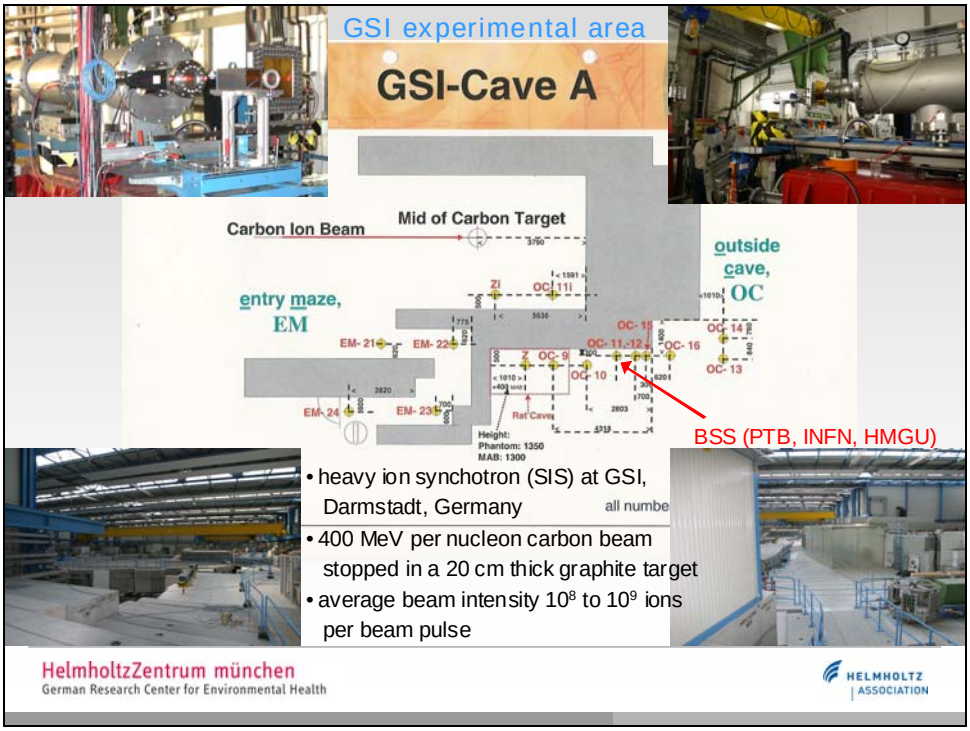
GSI experimental area
GSI-Cave A
Carbon Ion Beam
Mid of Carbon Target
entry maze,
EM
outside
cave,
OC
BSS (PTB, INFN, HMGU)
• heavy ion synchotron (SIS) at GSI, Darmstadt, Germany
• 400 MeV per nucleon carbon beam stopped in a 20 cm thick graphite target
• average beam intensity 10^8 to 10^9 ions per beam pulse
HelmholtzZentrum münchen
German Research Center for Environmental Health
HELMHOLTZ ASSOCIATION

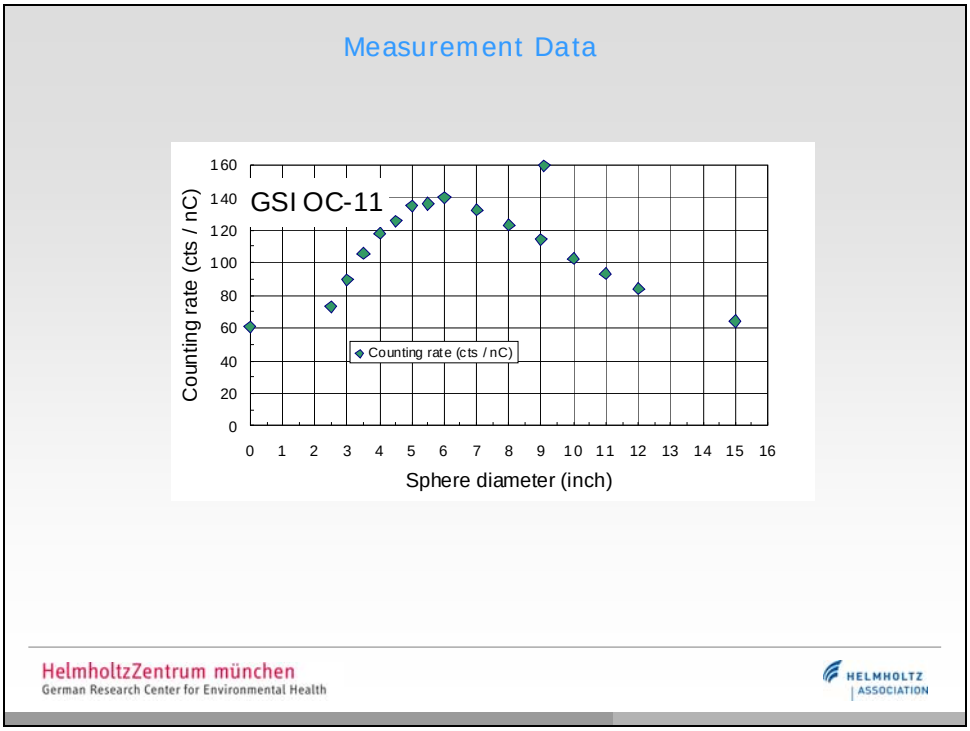
Measurement Data
GSI OC-11
Counting rate (cts / nC)
Sphere diameter (inch)
HelmholtzZentrum münchen
German Research Center for Environmental Health
HELMHOLTZ ASSOCIATION

Deconvolution of measurement data in neutron spectrometry

Convolution: $$N_k = \int R_k(E) \cdot \Phi(E) \cdot dE$$

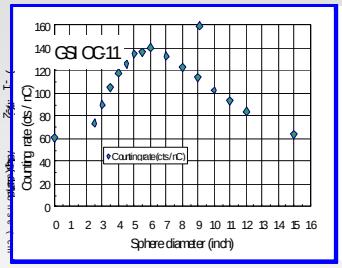

N_k count rate of k-th detector

R_k response of the k-th detector per neutron of energy E

Deconvolution: inversion process, i.e. mathematical method for determination of spectral fluence from the measurement values

Problem: non-uniqueness of deconvolution
number of measurement values (16) is much smaller than number of values (130) describing the spectrum

HelmholtzZentrum münchen
German Research Center for Environmental Health

HELMHOLTZ ASSOCIATION

Ratio of calculated and measured counts

Calculated counts = folding the response functions with the derived spectrum

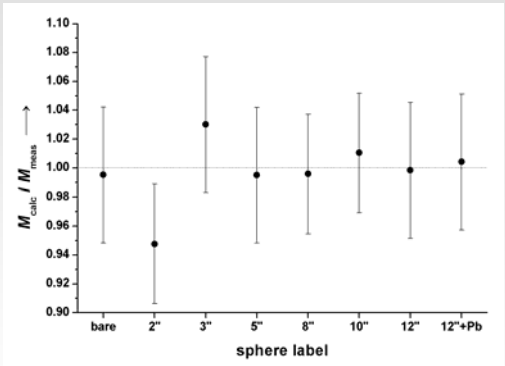

Example: counts of the active INFN-BSS at position OC-11 (R. Bedogni, A. Esposito)

HelmholtzZentrum münchen
German Research Center for Environmental Health

HELMHOLTZ ASSOCIATION

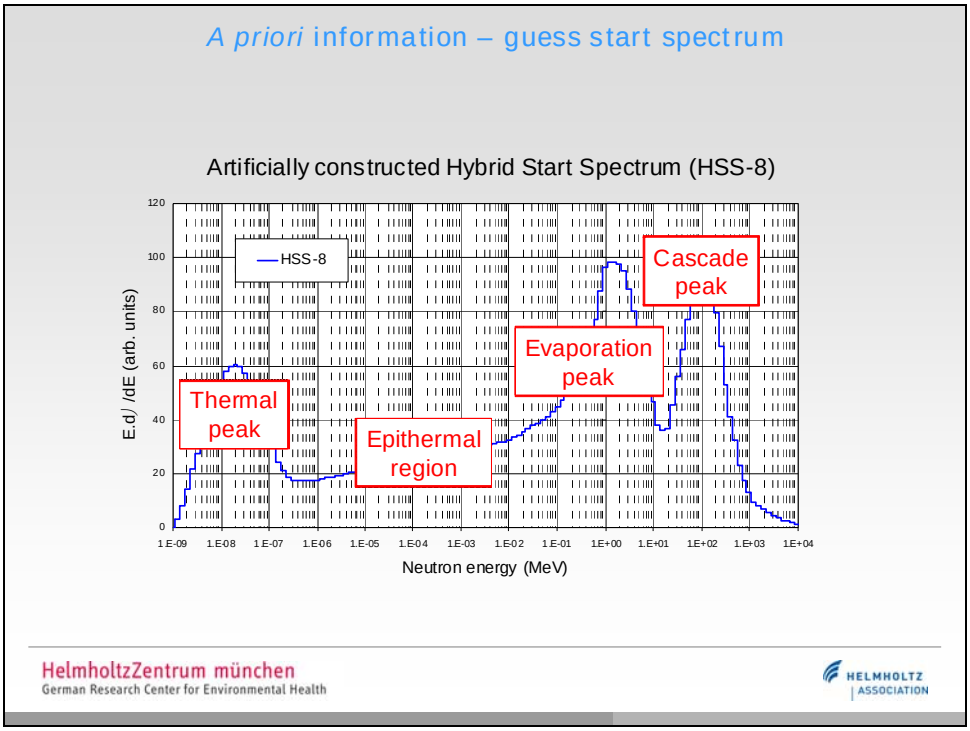
A priori information – guess start spectrum
Artificially constructed Hybrid Start Spectrum (HSS-8)
HSS-8
Cascade peak
Evaporation peak
Thermal peak
Epithermal region
E.d/ /dE (arb. units)
Neutron energy (MeV)
HelmholtzZentrum münchen
German Research Center for Environmental Health
HELMHOLTZ ASSOCIATION

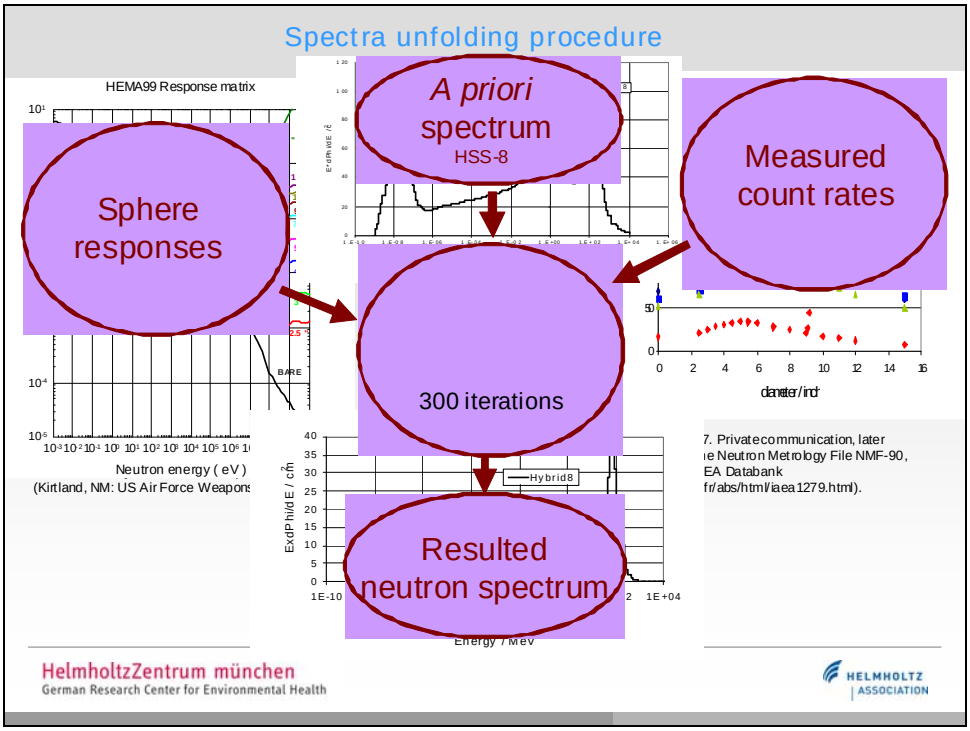
Spectra unfolding procedure
HEMA99 Response matrix
Sphere responses
A priori spectrum
HSS-8
Measured count rates
300 iterations
Resulted neutron spectrum
Hybrid8
Neutron energy (eV)
Energy / MeV
HelmholtzZentrum münchen
German Research Center for Environmental Health
HELMHOLTZ ASSOCIATION

Measurement results

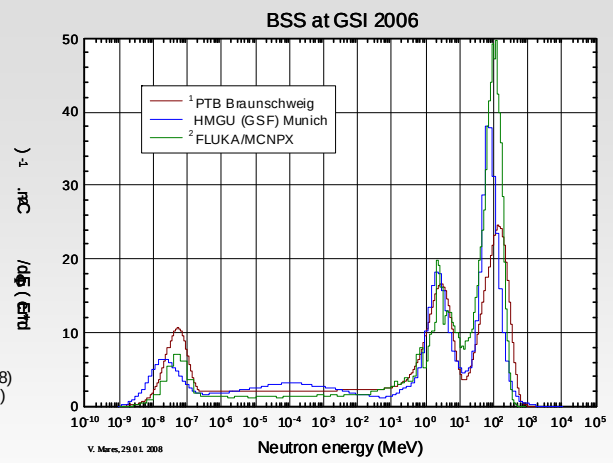

[1] Wiegel et al (2008)
[2] Rollet et al (2008)

HMGU results for OC-11

Total fluence: 142.5 cm^{-2} nC^{-1}

Total ambient dose equivalent H*(10): 36.6 Sv C^{-1}

HelmholtzZentrum münchen
German Research Center for Environmental Health

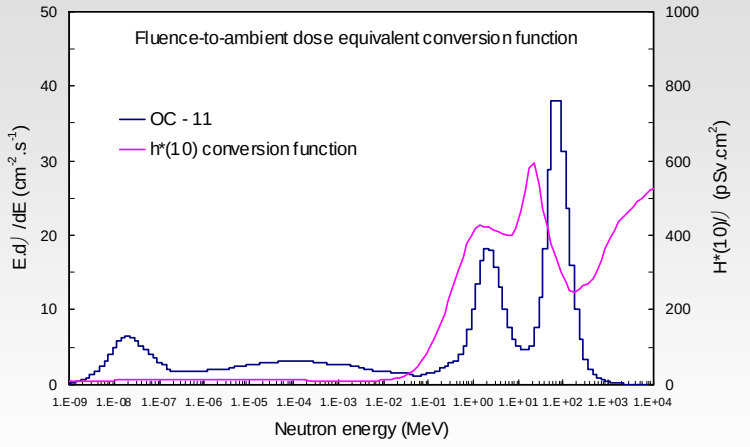

HelmholtzZentrum münchen
German Research Center for Environmental Health

Influence of the following parameters on spectrum

What is the influence of the following parameters on OC-11 output spectrum and dose?

- form of *a priori* (i.e. guess, start, input) spectra
- number of iteration steps (100, 200, ..., 1,000)
- different response matrices (HEMA99, HESA99)
- method of unfolding (unfolding program)

HelmholtzZentrum münchen
German Research Center for Environmental Health

HELMHOLTZ ASSOCIATION

Creation of hybrid start spectrum

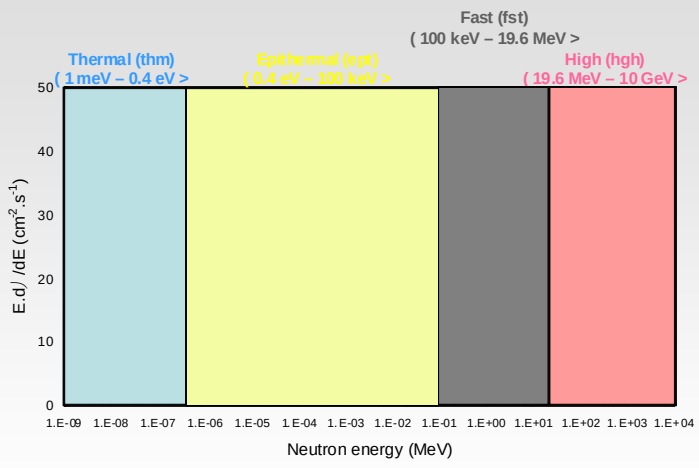

HelmholtzZentrum münchen
German Research Center for Environmental Health

HELMHOLTZ ASSOCIATION

Sensitivity analyses – variations of the thermal peak

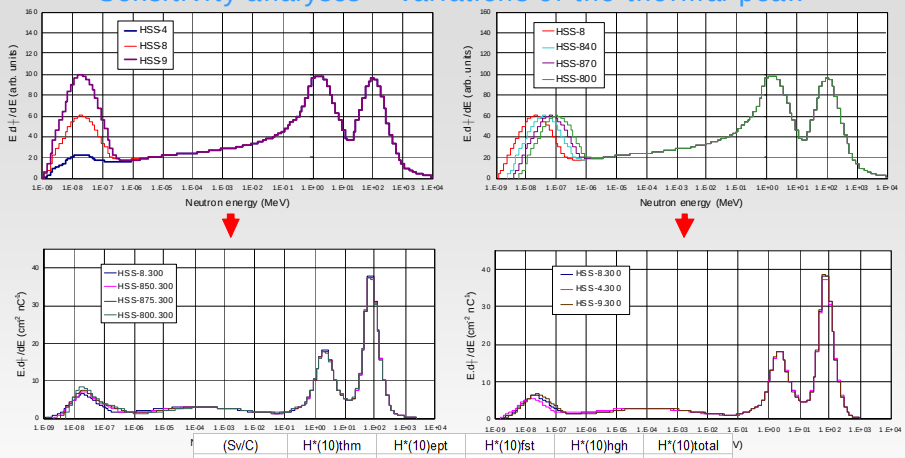

(Sv/C)	H*(10)thm	H*(10)ept	H*(10)fst	H*(10)hgh	H*(10)total
HSS-8.300	0.19	0.34	16.0	20.0	36.6
HSS-4.300	0.18	0.34	16.1	19.9	36.5
HSS-9.300	0.21	0.33	16.0	20.1	36.6
HSS-850.300	0.21	0.33	16.1	20.0	36.6
HSS-875.300	0.22	0.32	16.1	20.0	36.6
HSS-800.300	0.23	0.32	16.1	20.0	36.7
Mean	**0.21±8.7%**	**0.33±2.3%**	**16.1±0.2%**	**20.0±0.3%**	**36.6±0.2%**

HelmholtzZentrum münchen
German Research Center for Environmental Health

HELMHOLTZ ASSOCIATION

Sensitivity analyses – variations of the evaporation peak

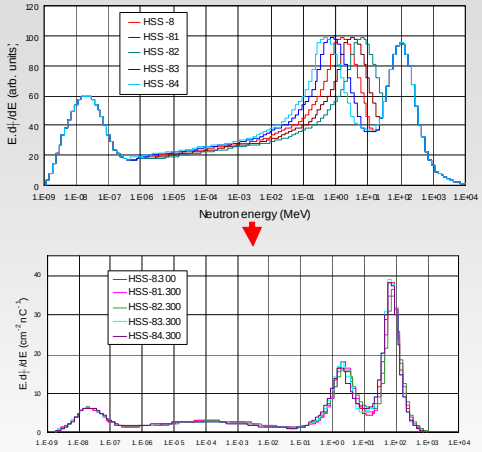

(Sv/C)	H*(10)thm	H*(10)ept	H*(10)fst	H*(10)hgh	H*(10)total
HSS-8.300	0.19	0.34	16.0	20.0	36.6
HSS-81.300	0.20	0.34	16.3	18.8	35.7
HSS-82.300	0.20	0.34	16.7	18.1	35.2
HSS-83.300	0.20	0.33	16.2	20.7	37.4
HSS-84.300	0.20	0.32	16.5	20.6	37.5
Mean	**0.20±1.1%**	**0.33±2.4%**	**16.3±1.3%**	**19.7±5.2%**	**36.5±2.5%**

HelmholtzZentrum münchen
German Research Center for Environmental Health

HELMHOLTZ ASSOCIATION

Sensitivity analyses – variations of the cascade peak

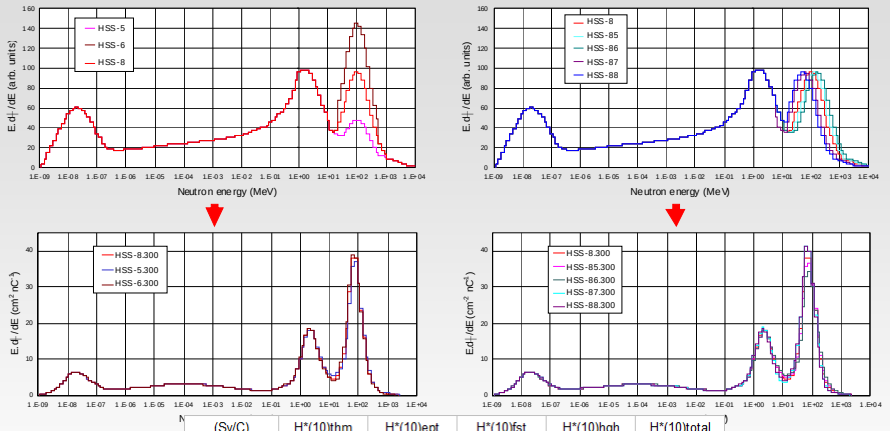

(Sv/C)	H*(10)thm	H*(10)ept	H*(10)fst	H*(10)hgh	H*(10)total
HSS-8.300	0.19	0.34	16.0	20.0	36.6
HSS-6.300	0.20	0.33	15.8	20.6	37.0
HSS-85.300	0.19	0.34	16.2	19.4	36.1
HSS-86.300	0.19	0.34	16.4	18.8	35.7
HSS-87.300	0.20	0.33	15.8	21.3	37.6
HSS-88.300	0.20	0.33	15.8	21.4	37.7
Mean	**0.20±0.8%**	**0.33±0.9%**	**16.0±1.5%**	**20.3±4.8%**	**36.8±2.0%**

HelmholtzZentrum münchen
German Research Center for Environmental Health

HELMHOLTZ ASSOCIATION

Sensitivity analyses – using different number of iterations

Number of iterations used:
100, 200, 300, ..., 900, 1 000

Based on previous experience:
n=300 optimum

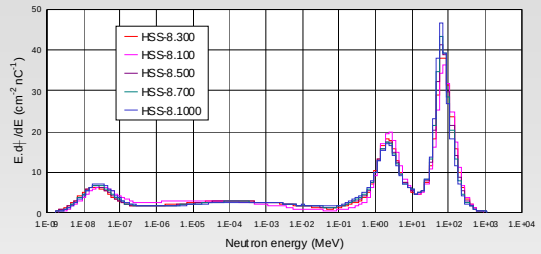

Higher number perhaps (?) better

But: too large number creates
physical unrealictic spectrum

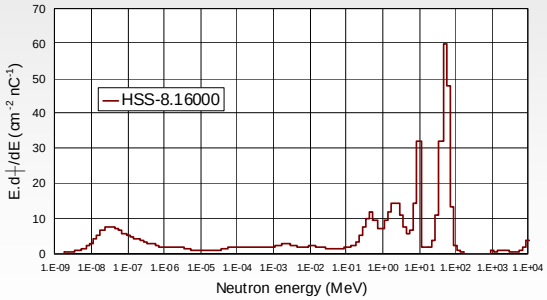

HelmholtzZentrum münchen
German Research Center for Environmental Health

HELMHOLTZ ASSOCIATION

Sensitivity analyses – using different number of iterations

H*(10) increases with increasing number of iterations

but: X^2 calculated for all energies, while dose is for E>0.1 MeV

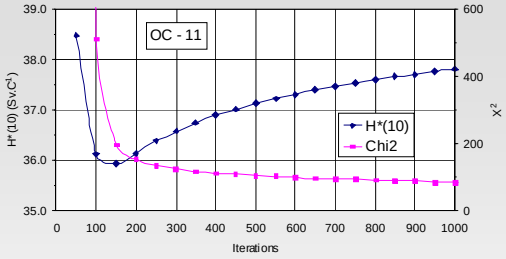

(Sv/C)	H*(10)thm	H*(10)ept	H*(10)fst	H*(10)hgh	H*(10)total
HSS-8.100	0.22	0.32	16.4	19.2	36.1
HSS-8.200	0.20	0.33	16.2	19.5	36.1
HSS-8.300	0.19	0.34	16.0	20.0	36.6
HSS-8.400	0.20	0.34	16.0	20.4	36.9
HSS-8.500	0.20	0.34	15.9	20.7	37.1
HSS-8.600	0.20	0.34	15.9	20.9	37.3
HSS-8.700	0.21	0.34	15.9	21.1	37.5
HSS-8.800	0.21	0.34	15.9	21.2	37.6
HSS-8.900	0.21	0.34	15.9	21.3	37.7
HSS-8.1000	0.22	0.33	15.9	21.4	37.8
Mean	**0.21±3.8%**	**0.33±1.6%**	**16.0±1.0%**	**20.6±3.6%**	**37.1±1.6%**

HelmholtzZentrum münchen
German Research Center for Environmental Health

HELMHOLTZ ASSOCIATION

Mean values and standard deviations

16 different *a priori* spectra
10 numbers of iterations

→ 160 unfolded spectra

Means and standard deviations calculated for each energy bin separately

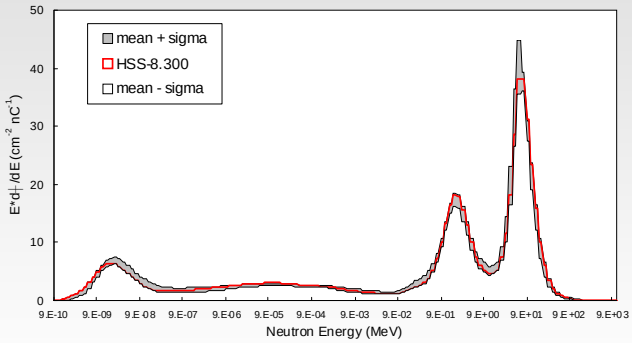

Sv/C	H*(10)thm	H*(10)ept	H*(10)fst	H*(10)hgh	H*(10)total	Φ thm	Φ ept	Φ fst	Φ hgh	Φ total
HSS-8.300	0.2	0.3	16.0	20.0	36.6	18.6	27.8	40.6	55.5	142.5
160 spectra	0.21±0.01	0.33±0.01	16.1±0.3	20.4±1.1	37.06±1.2	19.6±0.9	26.9±0.8	41.0±0.7	55.6±1.6	143.2±1.2

HelmholtzZentrum münchen
German Research Center for Environmental Health

HELMHOLTZ ASSOCIATION

Different response matrices

Two approaches to calculate the response of the Bonner spheres:

HEMA99: MCNP (E<20MeV) + MCNPH/LAHET (E>20 MeV)

HESA99: MCNP (E<20MeV) + MCNP/HADRON (E>20 MeV)

Mares et al. (1997) Radiat Prot Dosim 70: 291-294

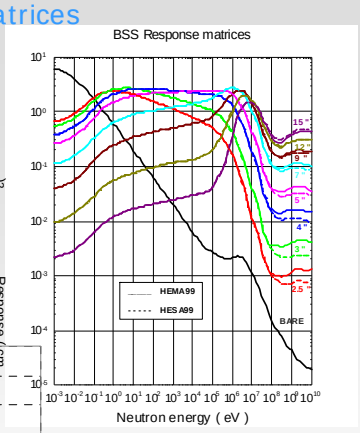

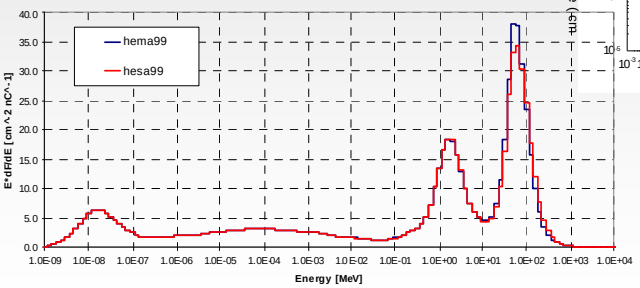

HelmholtzZentrum münchen
German Research Center for Environmental Health

HELMHOLTZ ASSOCIATION

Influence of unfolding code - 1

Idea evolved during the CONRAD meeting in Madrid 2007:

a) Use count rates measured by **different groups** with their spectrometers (number and design of spheres may differ)

b) Use corresponding response matrices

c) Unfold with **same code** (SAND) and Hybrid8 start spectrum

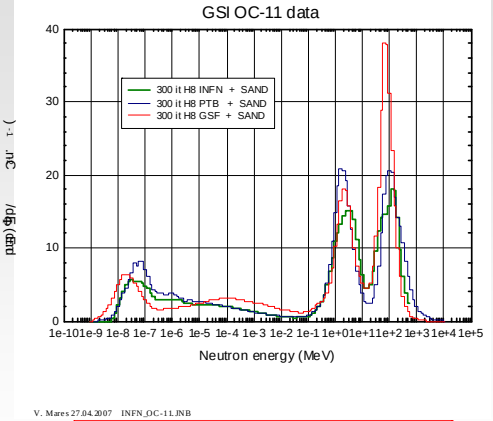

Contributing colleagues:
INFN (R. Bedogni, A. Esposito)
PTB (B. Wiegel)

Differences observed probably not due to unfolding code!!

HelmholtzZentrum münchen
German Research Center for Environmental Health

HELMHOLTZ ASSOCIATION

Influence of unfolding code - 2

a) Use **same count rates** measured by one group with own spectrometer

b) Use corresponding response matrix

c) Unfold with **different codes**

(to be done)

HelmholtzZentrum münchen
German Research Center for Environmental Health

HELMHOLTZ ASSOCIATION

Individual analysis of three groups

Total fluence F and total ambient dose equivalent $H^*(10)$ per Coulomb for OC-11 position outside Cave A and the relative contributions for four neutron energy regions.

Quantity	PTB	INFN	HMGU
F_{thm} / F / %	15.6	6.2	13.1
F_{int} / F / %	18.6	28.6	19.5
F_{fst} / F / %	30.7	33.1	28.5
F_{hgh} / F / %	35.1	32.1	38.9
$H^*(10)_{thm} / H^*$ / %	0.8	0.3	0.5
$H^*(10)_{int} / H^*$ / %	1.8	1.7	0.9
$H^*(10)_{fst} / H^*$ / %	49.8	54.3	43.8
$H^*(10)_{hgh} / H^*$ / %	47.6	43.7	54.7

HelmholtzZentrum münchen
German Research Center for Environmental Health

HELMHOLTZ ASSOCIATION

Summary and closing thoughts

- deconvolution process was analysed using MSANDB code
- start spectrum and number of iterations were varied and statistical analyses were performed
- neither spectra nor ambient dose equivalent values changed much
- HSS-8 start spectrum and 300 iterations produce reliable and stable neutron spectrum
- they could be recommended as the most suitable input parameters
- further research on other deconvolution methods is required

HelmholtzZentrum münchen
German Research Center for Environmental Health

HELMHOLTZ ASSOCIATION

THANKS

References:

Rollet, S., Agosteo, Fehrenbacher, G., Hranitzky, C., Radon, T. and Wind, M., 2008. Intercomparison of radiation protection devices in a high-energy stray neutron field. Part I: Monte Carlo simulations, to be published in Radiat. Meas., 2008

B. Wiegel, S. Agosteo, R. Bedogni, M. Caresana, A. Esposito, G. Fehrenbacher, M. Ferrarini, E. Hohmann, C. Hranitzky, A. Kasper, S. Khurana, V. Mares, M. Reginatto, S. Rollet, W. Rühm, D. Schardt, M. Silari, G. Simmer, E. Weitzenegger, 2008. Intercomparison of radiation protection devices in a high-energy stray neutron field. Part II: Bonner Sphere Spectrometry, to be published in Radiat. Meas., 2008

M. Silari, S. Agosteo, P. Beck, R. Bedogni, E. Cale, M. Caresana, C. Domingo, L. Donadille, N. Dubourg, A. Esposito, G. Fehrenbacher, F. Fernández, M. Ferrarini, A. Fiechtner, A. Fuchs, M. J. García, F. Gutermuth, S. Khurana, Th. Klages, M. Latocha, V. Mares, S. Mayer, T. Radon, H. Reithmeier, S. Rollet, H. Roos, W. Rühm, S. Sandri, D. Schardt, G. Simmer, F. Spurný, F. Trompier, C. Villa-Grasa, E. Weitzenegger, B. Wiegel, M. Wielunski, F. Wissmann, A. Zechner, M. Zielczynski. Intercomparison of radiation protection devices in a high-energy stray neutron field. Part III: Instrument response, to be published in Radiat. Meas., 2008

G. Simmer, V. Mares, E. Weitzenegger, W. Rühm, Iterative Unfolding for Bonner Sphere Spectrometers – Sensitivity Analysis and Dose Calculation, to be published in Radiat. Meas., 2008

HelmholtzZentrum münchen
German Research Center for Environmental Health

HELMHOLTZ ASSOCIATION

Dose attenuation in concrete, iron and mixed concrete-iron shields for protons with energy up to 250 MeV

S. Agosteo,[1] **M. Magistris,**[2] **A. Mereghetti,**[1,2] **M. Silari,**[2] **Z. Zajacova**[2,3]
[1]Polytechnic of Milano, Department of Nuclear Engineering, Milano, Italy
[2]CERN, Genève, Switzerland
[3]Slovak University of Technology, Bratislava, Slovak Republic

Background

This work is the Diploma thesis of Alessio Mereghetti

Published in two papers in NIM B:

S. Agosteo, M. Magistris, A. Mereghetti, M. Silari and Z. Zajacova, Shielding data for 100-250 MeV proton accelerators: double differential neutron distributions and attenuation in concrete, *Nucl. Instr. and Meth. B 265 (2007), p. 581*

S. Agosteo, M. Magistris, A. Mereghetti, M. Silari and Z. Zajacova, Shielding data for 100-250 MeV proton accelerators: attenuation of secondary radiation in thick iron and concrete/iron shields, *to be published in Nucl. Instr. and Meth. B*

21 - 23 April 2008 SATIF 9, Marco Silari 2

AIM

To provide handy data for a first assessment of shielding requirements for 100-250 MeV proton accelerator facilities, for concrete and iron as shielding material.

Brookhaven National Laboratories (USA): 200 MeV injector linac

Heidelberg (GE): proton and ion therapy (430 MeV/u)

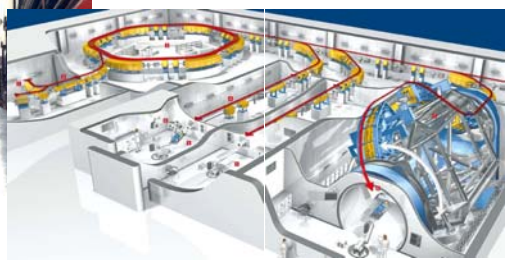

21 - 23 April 2008 SATIF 9, Marco Silari 3

Source – typical neutron distributions

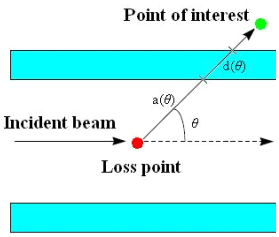

Cylindrical target: diameter and length equal to proton range in iron

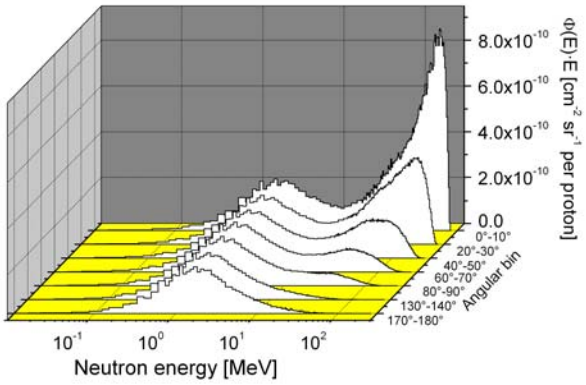

Computed neutron energy distributions from **250 MeV** protons impinging on a cylindrical iron target **7.50 cm** long and **3.75 cm** in radius.

21 - 23 April 2008 SATIF 9, Marco Silari 4

Outline

- **Preliminary** simulations:
  1. transport in a complete spherical geometry vs transport in selected directions only;
  2. scoring inside a medium instead of scoring at the external surface of the shield;
  3. cross-talk between angular bins due to neutron back-scattering;
- **Concrete**: attenuation curves, fits, dependence of fit parameters on proton energy and emission angle, comparison with experimental and computational data available in the literature
- **Iron**: attenuation curves, fits, comparison with literature data
- **Comparison** between concrete and iron as shielding materials
- 3 simple cases of **composite shielding**
- Conclusions

The simplest way

Spherical geometry with the target placed in the centre:

- Easy way of scoring: regions or surfaces can be defined **perpendicularly** to the emission direction of secondaries;
- **Every** direction can be easily scored (in a suitable angular binning);
- If a sufficiently **large radius** is chosen, problems related to curvature can be easily neglected (90 m);

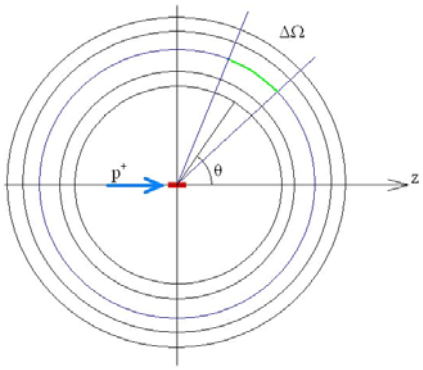

The simplest way - Problems

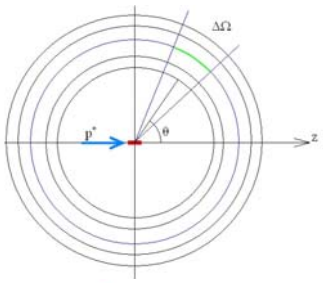

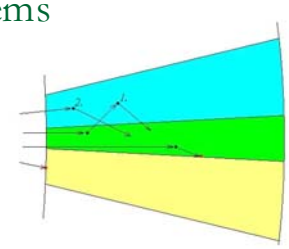

Neutron cross-talk between contiguous angular bins.

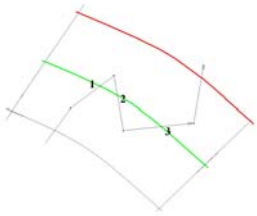

Neutron scattering across a scoring surface.

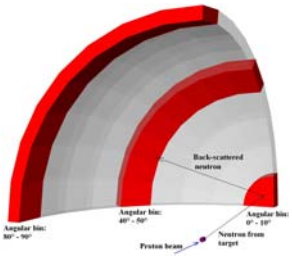

Neutron cross-talk from the inner surface of the shield

Geometry – Problem 1

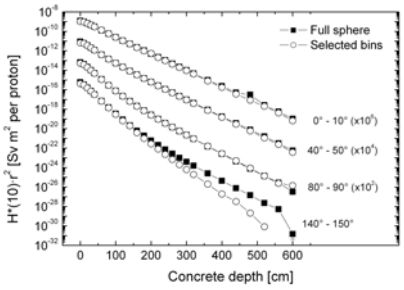

Attenuation in ordinary concrete of the total dose equivalent produced by **100 MeV** protons on a thick iron target.

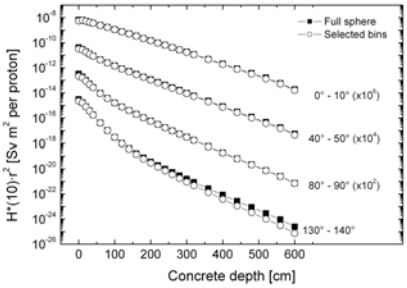

Attenuation in ordinary concrete of the total dose equivalent produced by **250 MeV** protons on a thick iron target.

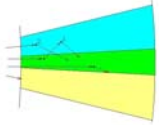

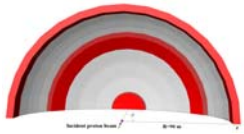

Geometry – Problem 2

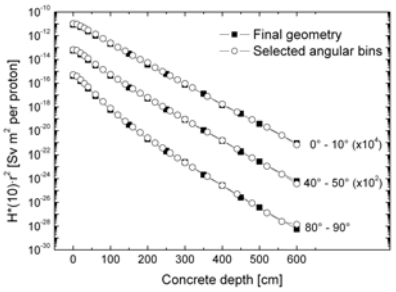

Attenuation in ordinary concrete of the total dose equivalent produced by **100 MeV** protons on a thick iron target.

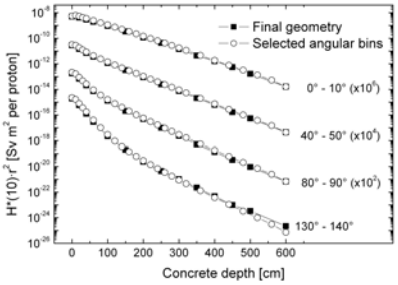

Attenuation in ordinary concrete of the total dose equivalent produced by **250 MeV** protons on a thick iron target.

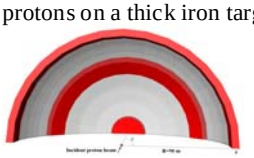

21 - 23 April 2008 SATIF 9, Marco Silari 9

Geometry – Problem 2

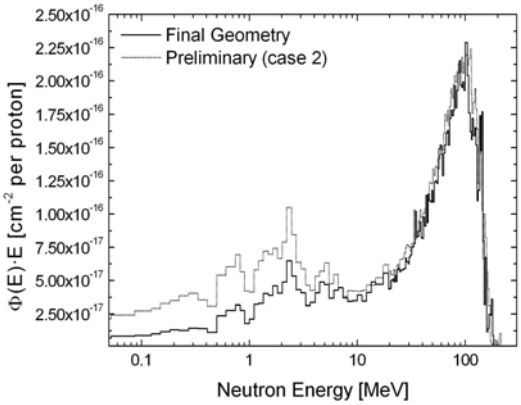

Comparison of neutron spectra between the preliminary simulations (scoring at different depths inside a unique slab of concrete) and the final geometry setting, scored after **400 cm** of concrete in the **80°-90°** angular bin, for **250 MeV** protons striking a thick iron target.

21 - 23 April 2008 SATIF 9, Marco Silari 10

Geometry – Problem 3

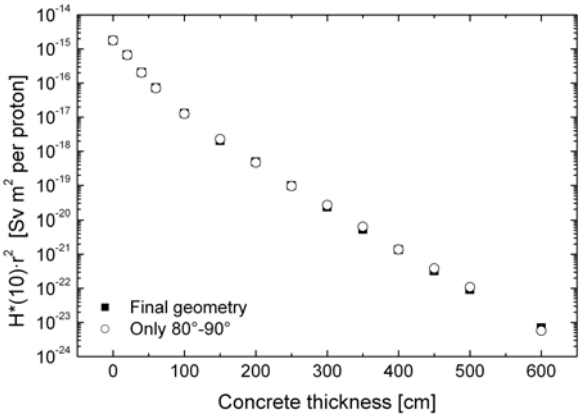

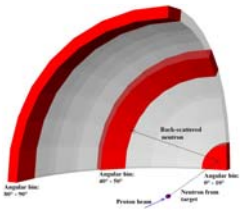

Attenuation in ordinary concrete of the total dose equivalent produced by **250 MeV** protons on a thick iron target.

21 - 23 April 2008 SATIF 9, Marco Silari 11

Concrete – Attenuation curves

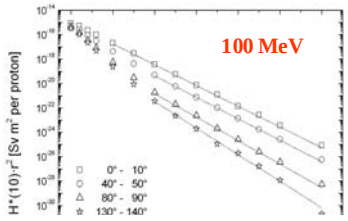

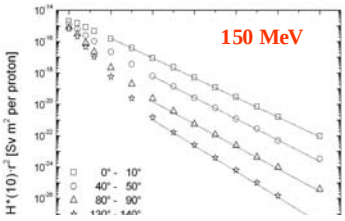

$$H(E_p,\theta,d/\lambda)=\frac{H_1(E_p,\theta)}{r^2}\exp\left[-\frac{d}{\lambda_1(\theta)g(\alpha)}\right]+\frac{H_2(E_p,\theta)}{r^2}\exp\left[-\frac{d}{\lambda_2(\theta)g(\alpha)}\right]$$

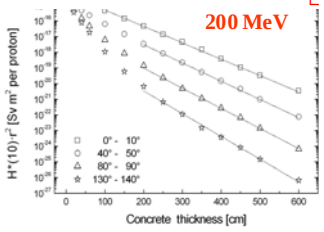

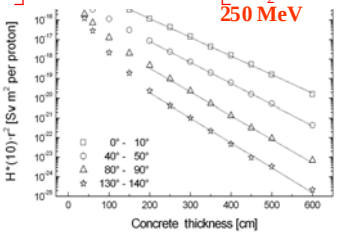

Attenuation of total dose equivalent in **ordinary concrete** for protons impinging on a thick iron target.

21 - 23 April 2008 SATIF 9, Marco Silari 12

Concrete – "Hardening" effect

Attenuation of the total dose equivalent in ordinary concrete in the **80°-90°** angular bin, from **250 MeV** protons.

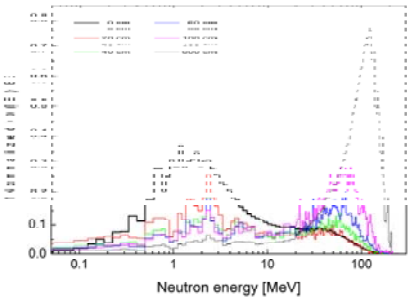

Neutron energy flunce spectra outside an ordinary concrete shield of increasing thickness, in the **80°-90°** angular bin, from **250 MeV** protons. Spectra are normalized to unity.

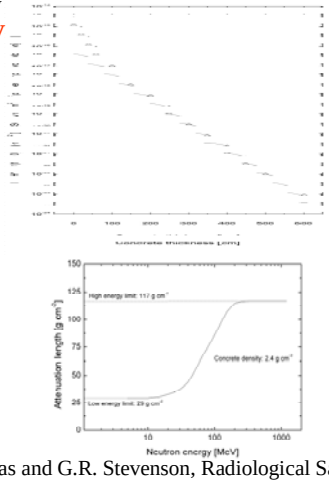

R.H. Thomas and G.R. Stevenson, Radiological Safety Aspects of the Operation of Proton Accelerators, Technical report series No. 283, IAEA, Vienna, 1988.

Concrete – Parameters fitting curves

$$\lambda_{(E_p)} = \frac{A}{1+\exp\left[\frac{\ln(P_3)-\ln(E_p)}{P_4}\right]} + B$$

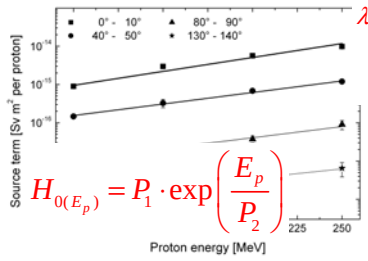

$$H_{0(E_p)} = P_1 \cdot \exp\left(\frac{E_p}{P_2}\right)$$

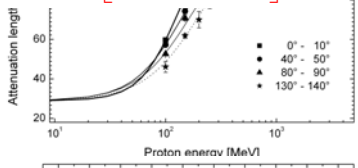

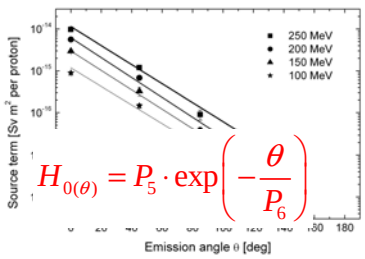

$$H_{0(\theta)} = P_5 \cdot \exp\left(-\frac{\theta}{P_6}\right)$$

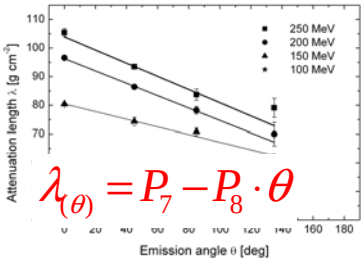

$$\lambda_{(\theta)} = P_7 - P_8 \cdot \theta$$

Concrete – Comparison with literature

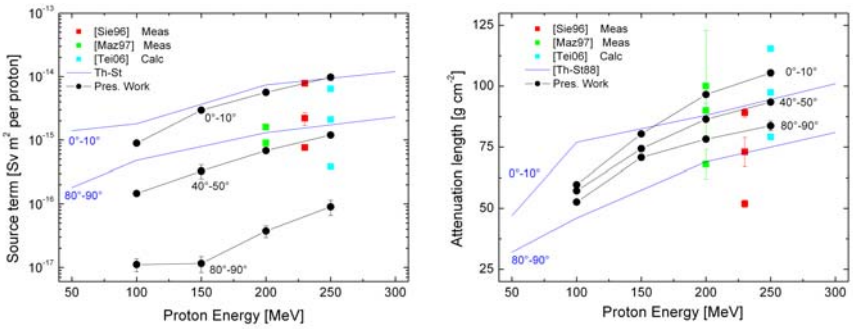

[**Sie96**] J.V. Siebers, P.M. DeLuca Jr., D.W. Pearson, Nucl. Sci. Eng. 122 (1996), p. 258. [meas.]
[**Maz97**] A. Mazal et al., Radiat. Protect. Dosim. 70 (1997), p. 429. [meas.]
[**Tei06**] S. Teichmann, Proc. of the AEN/NEA Specialists' Meeting on Shielding Aspects of Accelerators, Targets and Irradiation Facilities, Pohang Accelerator Laboratory, 22-24 May 2006, NEA/OECD (2006) (in press). [simul.]
Th-St R.H. Thomas and G.R. Stevenson, Radiological Safety Aspects of the Operation of Proton Accelerators, Technical report series No. 283, IAEA, Vienna, 1988. [ref. text]

Iron – Attenuation curves

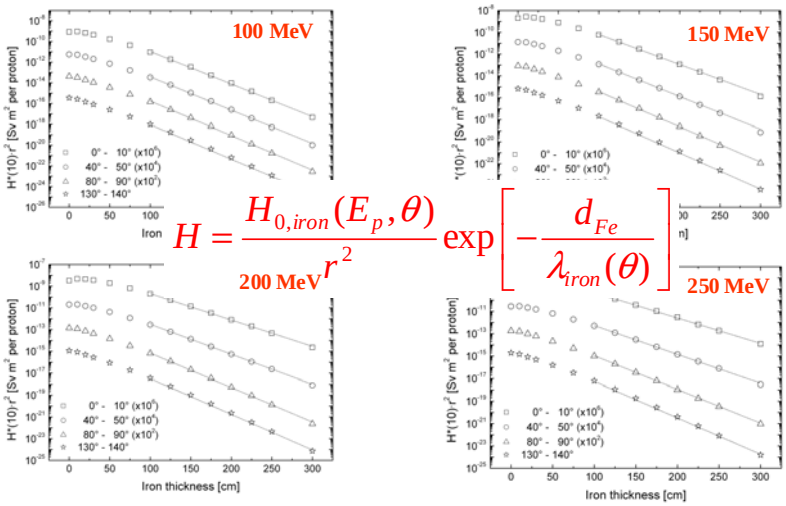

$$H = \frac{H_{0,iron}(E_p,\theta)}{200\ \text{MeV}\, r^2} \exp\left[-\frac{d_{Fe}}{\lambda_{iron}(\theta)}\right]$$

Attenuation of total dose equivalent in iron for protons impinging on an iron target thicker than the proton range.

Iron – "Softening" effect

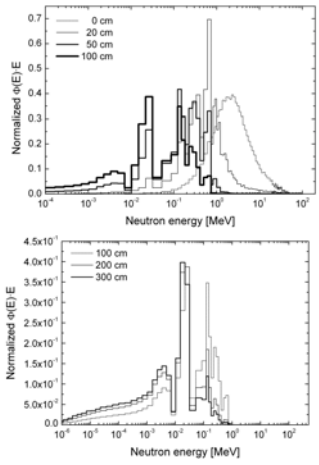

Neutron energy distributions in the **backward direction** from **100 MeV** protons, for different shield thicknesses.

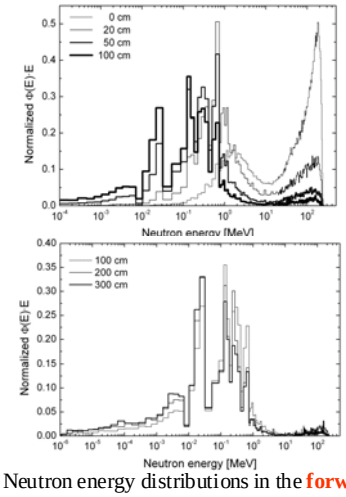

Neutron energy distributions in the **forward direction** from **250 MeV** protons, for different shield thicknesses.

Iron – Fitting parameters

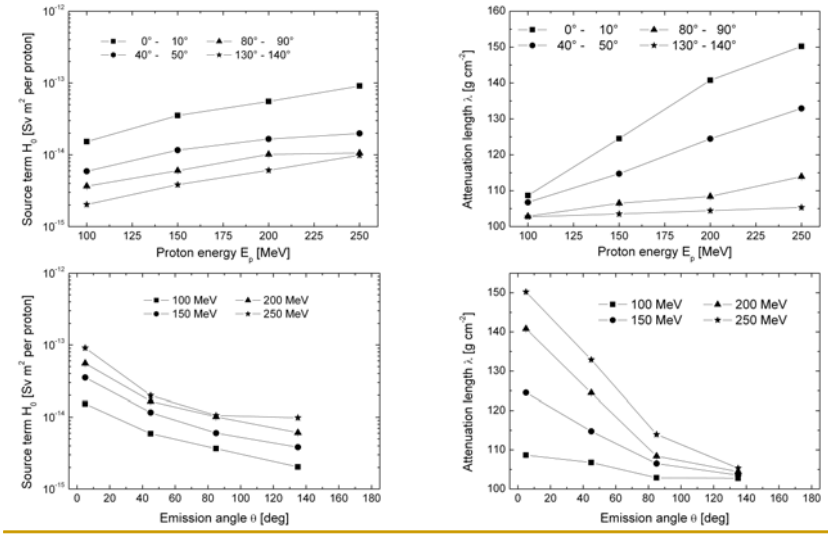

Iron – Fit curves for shallow depths

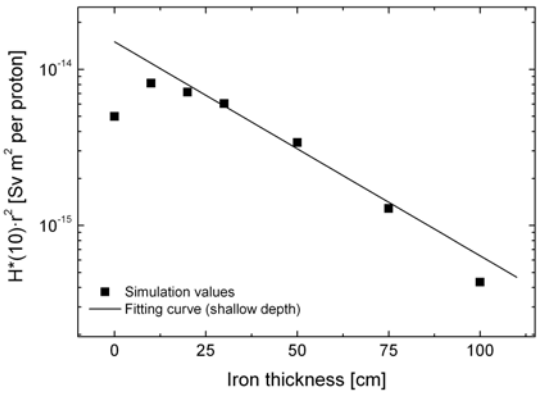

Attenuation of total dose equivalent in iron in the forward direction for **250 MeV** protons impinging on an iron target thicker than the proton range: plot for depths up to 1 m.

21 - 23 April 2008 SATIF 9, Marco Silari 19

Comparison – Concrete vs Iron

100 MeV – Backward direction

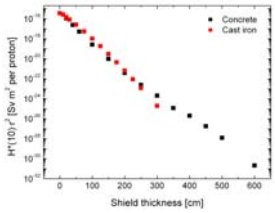

250 MeV – Forward direction

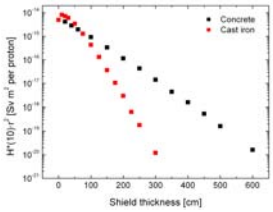

Attenuation of total dose equivalent in ordinary concrete and in iron.

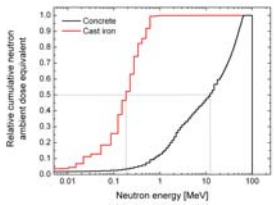

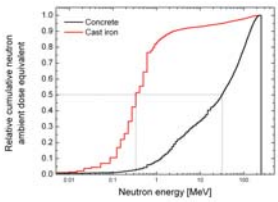

Relative cumulative neutron ambient dose equivalent versus neutron energy past a shield of concrete or iron **800 g cm^{-2}** thick.

21 - 23 April 2008 SATIF 9, Marco Silari 20

Composite shielding

Case	Angular Bin	Total ambient dose equivalent [Sv m² per proton]				
			Simple model			
			(expression 1)		(expression 2)	(expression 3)
		Simulation	Fe + DP concrete	Fe + SD concrete	Concrete only	Fe only
A	0°- 10°	5.2 x 10^{-18}	5.4 x 10^{-17}		1.2 x 10^{-16}	2.5 x 10^{-18}
	40°- 50°	2.5 x 10^{-19}	4.5 x 10^{-18}	2.7 x 10^{-18}	1.4 x 10^{-17}	1.4 x 10^{-19}
	80°- 90°	1.0 x 10^{-20}	6.9 x 10^{-19}	1.1 x 10^{-19}	4.9 x 10^{-19}	1.1 x 10^{-20}
B	0°- 10°	7.8 x 10^{-20}	8.5 x 10^{-19}		4.1 x 10^{-17}	1.9 x 10^{-19}
	40°- 50°	2.9 x 10^{-21}	4.2 x 10^{-20}	3.2 x 10^{-20}	3.7 x 10^{-18}	7.4 x 10^{-21}
	80°- 90°	1.8 x 10^{-22}	2.7 x 10^{-21}	1.1 x 10^{-21}	1.0 x 10^{-19}	3.4 x 10^{-22}
C	0°- 10°	8.5 x 10^{-18}	8.3 x 10^{-17}		4.1 x 10^{-17}	1.9 x 10^{-19}
	40°- 50°	4.2 x 10^{-19}	7.4 x 10^{-18}	2.6 x 10^{-18}	3.7 x 10^{-18}	7.4 x 10^{-21}
	80°- 90°	1.5 x 10^{-20}	1.4 x 10^{-18}	3.2 x 10^{-20}	1.0 x 10^{-19}	3.4 x 10^{-22}

Case	Layer Thicknesses [cm]	
	Cast iron	Concrete
A	100	100
B	200	50
C	50	200

$$H = \frac{H_{0,iron}(E_p,\theta)}{r^2}\exp\left[-\frac{d_{Fe}}{\lambda_{iron}(\theta)}\right]\cdot\exp\left[-\frac{L-d_{Fe}}{\lambda_{concrete}(\theta)}\right] \quad (1)$$

$$H(E_p,\theta,d/\lambda) = \frac{H_1(E_p,\theta)}{r^2}\exp\left[-\frac{d}{\lambda_1(\theta)\ g(\alpha)}\right] + \frac{H_2(E_p,\theta)}{r^2}\exp\left[-\frac{d}{\lambda_2(\theta)\ g(\alpha)}\right] \quad (2)$$

$$H = \frac{H_{0,iron}(E_p,\theta)}{r^2}\exp\left[-\frac{d_{Fe}}{\lambda_{iron}(\theta)}\right] \quad (3)$$

Composite shielding

$$H = \frac{H_{0,iron}(E_p,\theta)}{r^2}\exp\left[-\frac{z_{Fe}}{\lambda_{iron}(\theta)}\right]\cdot\exp\left[-\frac{d-z_{Fe}}{\lambda_{concrete}(\theta)}\right]$$

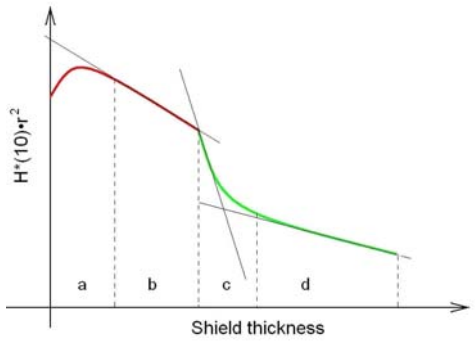

Composite shielding – case 1

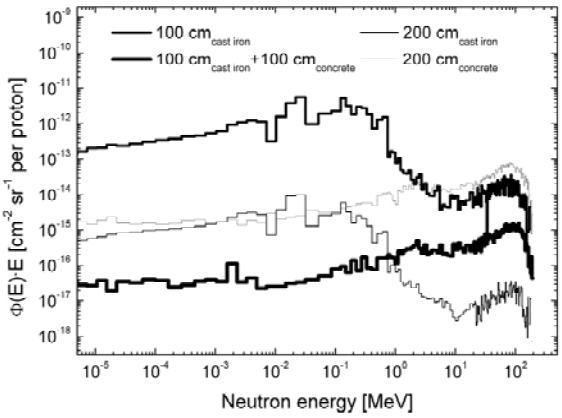

Neutron energy distributions outside: a 100 cm thick Fe shield, a composite shield made of 100 cm Fe + 100 cm concrete, a 200 cm thick shield made of either Fe or concrete, in the transverse direction **(80°-90°)** with respect to the **250 MeV** proton beam direction

21 - 23 April 2008 SATIF 9, Marco Silari 23

Composite shielding – case 2

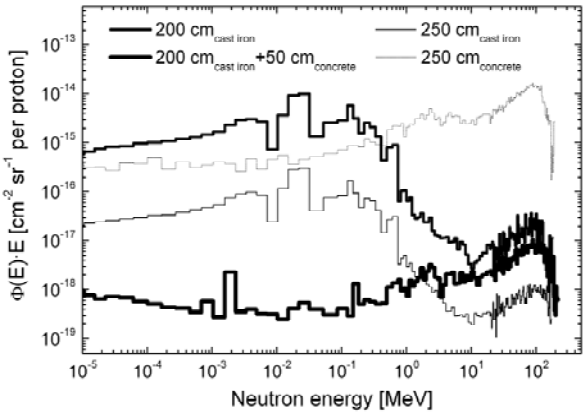

Neutron energy distributions outside: a 200 cm thick Fe shield, a composite shield made of 200 cm Fe + 50 cm concrete, a 250 cm thick shield made of either Fe or concrete, in the transverse direction **(80°-90°)** with respect to the **250 MeV** proton beam direction

21 - 23 April 2008 SATIF 9, Marco Silari 24

Composite shielding – case 3

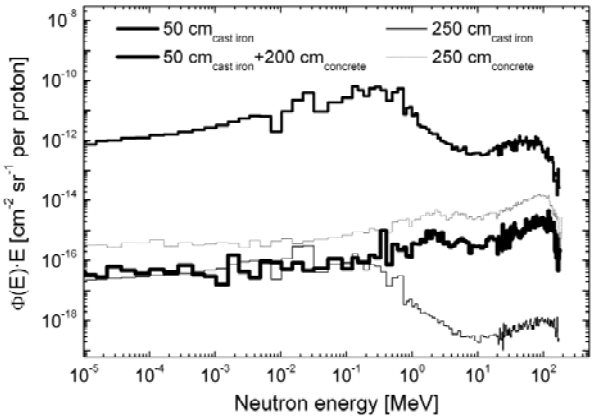

Neutron energy distributions outside: a 50 cm thick Fe shield, a composite shield made of 50 cm Fe + 200 cm concrete, a 250 cm thick shield made of either Fe or concrete, in the transverse direction **(80°-90°)** with respect to the **250 MeV** proton beam direction

21 - 23 April 2008 SATIF 9, Marco Silari 25

Conclusions

- Set of parameters for predicting ambient dose equivalent values outside shielding:
  1. Concrete: double exponential attenuation
  2. Iron: exponential attenuation with shield thickness greater than 1 m; exponential attenuation below 1 m of thickness, to be used with care
- Differences between concrete and iron in attenuating ambient dose equivalent ("hardening" and "softening" effect)
- Problems on composite shielding:
  1. neutron spectrum at equilibrium
  2. over-attenuation problem in the outer layer of concrete

21 - 23 April 2008 SATIF 9, Marco Silari 26

Appendix A – cast iron (I)

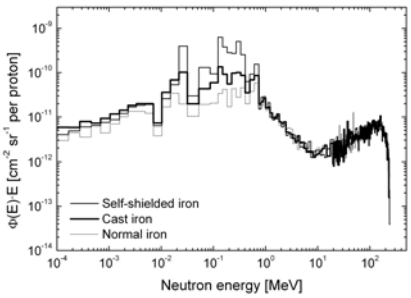

Comparison of neutron energy distributions past **100 cm** of FLUKA "normal" iron, "self-shielded" iron and "cast" iron from **250 MeV** protons, in the **forward direction**.

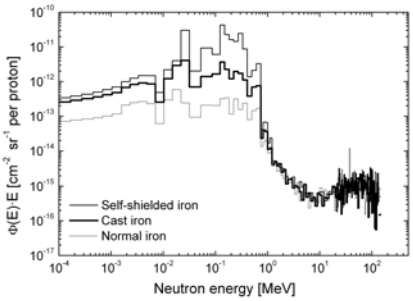

Comparison of neutron energy distributions past **100 cm** of FLUKA "normal" iron, "self-shielded" iron and "cast" iron from **250 MeV** protons, in the **backward direction**.

21 - 23 April 2008 SATIF 9, Marco Silari 27

Appendix A – cast iron (II)

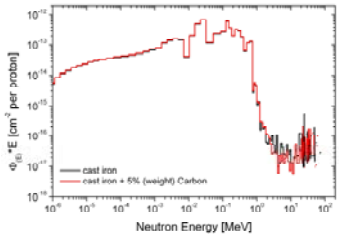

100 MeV protons
130°-140°
discrepancy: **2.6%**

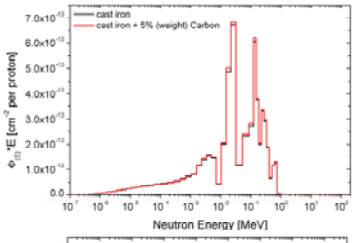

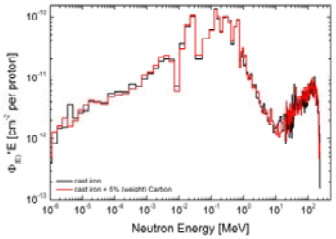

250 MeV protons
0°-10°
discrepancy: **2.3%**

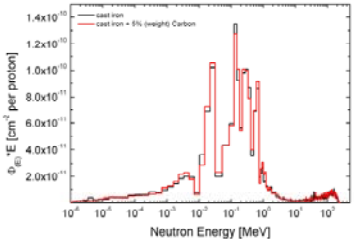

Comparison of neutron energy distributions past 100 cm of pure iron (using FLUKA "cast iron" cross section library) and adding a 5% content in weight of Carbon atoms.

21 - 23 April 2008 SATIF 9, Marco Silari 28

Appendix B – target dimensions (I)

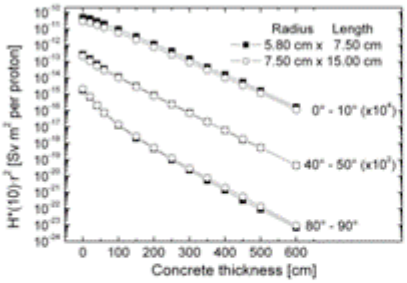

Attenuation in ordinary concrete of the total dose equivalent produced by **250 MeV** protons on two differently thick iron targets.

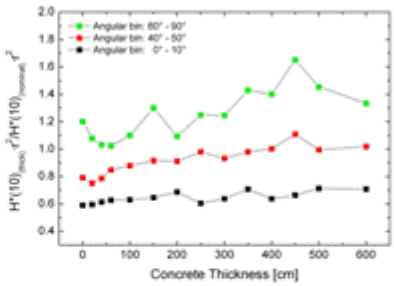

Ratio between the attenuation curves in ordinary concrete of the total dose equivalent produced by **250 MeV** protons on two differently thick iron targets.

21 - 23 April 2008 SATIF 9, Mareo Silari 29

Appendix B – target dimensions (II)

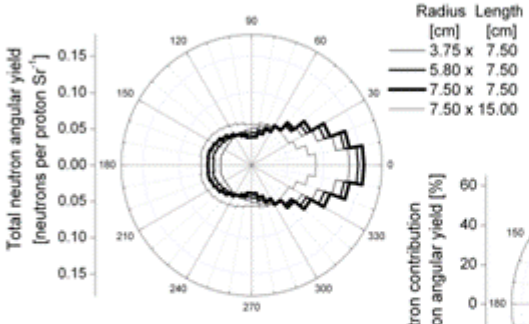

(Above) - Total neutron angular yield (neutrons per impinging proton per steradian) for four different target dimensions for **250 MeV** protons.

(Below) - Fast neutron contribution (**En>19.6 MeV**) to the total neutron angular yield for four different target dimensions for **250 MeV** protons.

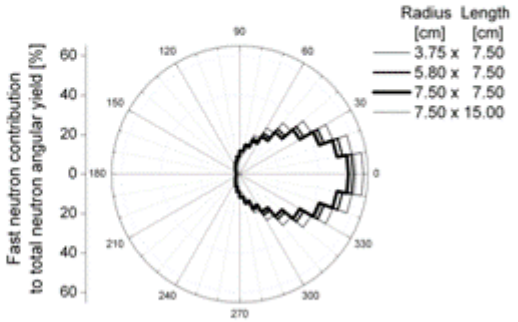

21 - 23 April 2008 SATIF 9, Mareo Silari 30

Appendix C – single particle contribution - concrete

100 MeV – 0°-10°

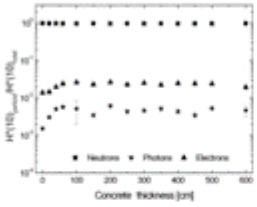

100 MeV – 130°-140°

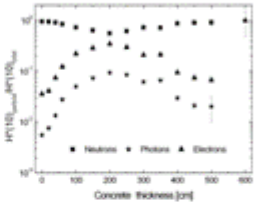

250 MeV – 0°-10°

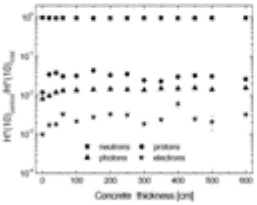

250 MeV – 130°-140°

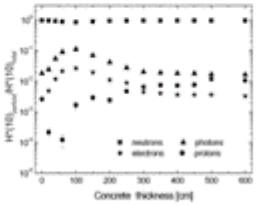

Relative contribution of the various particles to the total dose equivalent past a concrete shield of increasing thickness. Protons are not shown when their contribution is below 0.1%.

21 - 23 April 2008 SATIF 9, Maren Silari 31

Appendix C – single particle contribution - iron

100 MeV – 0°-10°

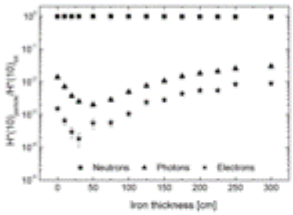

100 MeV – 130°-140°

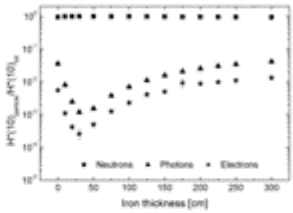

250 MeV – 0°-10°

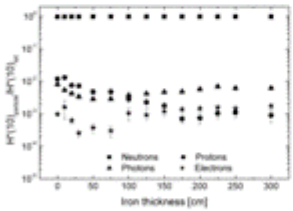

250 MeV – 130°-140°

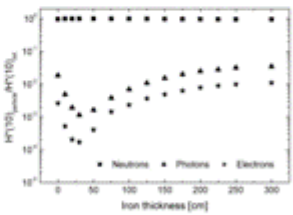

Relative contribution of the various particles to the total dose equivalent past a concrete shield of increasing thickness. Protons are not shown when their contribution is below 0.1%.

21 - 23 April 2008 SATIF 9, Maren Silari 32

Appendix D – Composite shielding – first case

	Layer Thicknesses [cm]	
Case	Cast-iron	Concrete
A	100	100
B	200	50
C	50	200

Normalized neutron energy distributions outside a composite shield made of 100 cm Fe + 100 cm concrete, and outside a 200 cm thick concrete shield, in the forward direction with respect to the **250 MeV** proton beam direction.

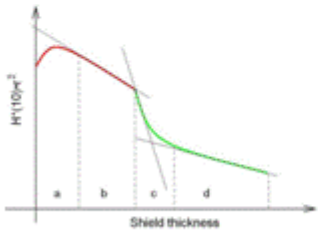

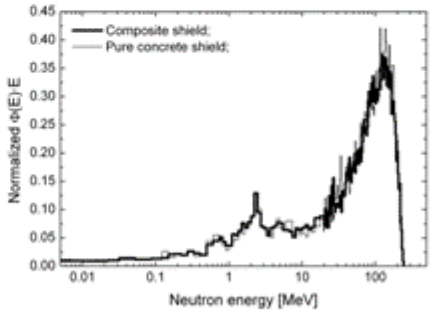

21 - 23 April 2008 SATIF 9, Marco Silari 33

Appendix D – Composite shielding – second case

	Layer Thicknesses [cm]	
Case	Cast iron	Concrete
A	100	100
B	200	50
C	50	200

Normalized neutron energy distributions outside a composite shield made of 200 cm Fe + 50 cm concrete, and outside a 250 cm thick concrete shield, in the forward direction with respect to the **250 MeV** proton beam direction.

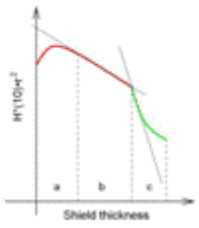

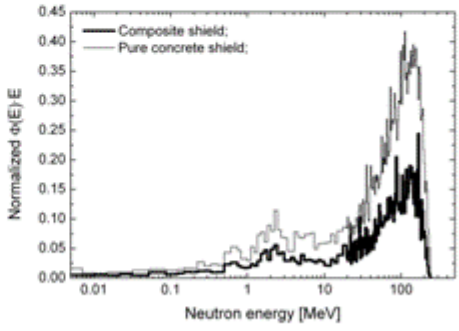

21 - 23 April 2008 SATIF 9, Marco Silari 34

Appendix D – Composite shielding – third case

	Layer Thicknesses [cm]	
Case	Cast iron	Concrete
A	100	100
B	200	50
C	50	200

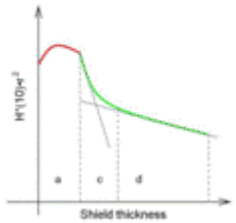

Normalized neutron energy distributions outside a composite shield made of 50 cm Fe + 200 cm concrete, and outside a 250 cm thick concrete shield, in the forward direction with respect to the 250 MeV proton beam direction.

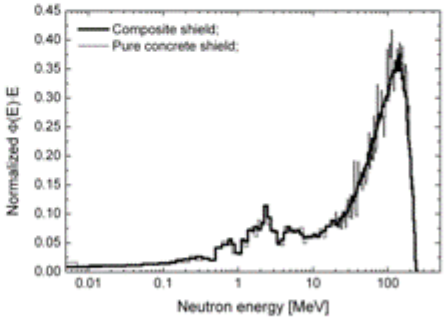

21 - 23 April 2008 SATIF 9, Marco Silari 35

Production of RIB in the EURISOL MMW target station

M. Lindroos, Y. Kadi, C. Kharoua, R. Rocca, A. Herrera, K. Samec
CERN, European Organisation for Nuclear Research

F. Groeschel, *et al.*
PSI

J. Freibergs, *et al.*
IPUL

L. Tecchio, *et al.*
INFN

F. Negoita
NIPNE

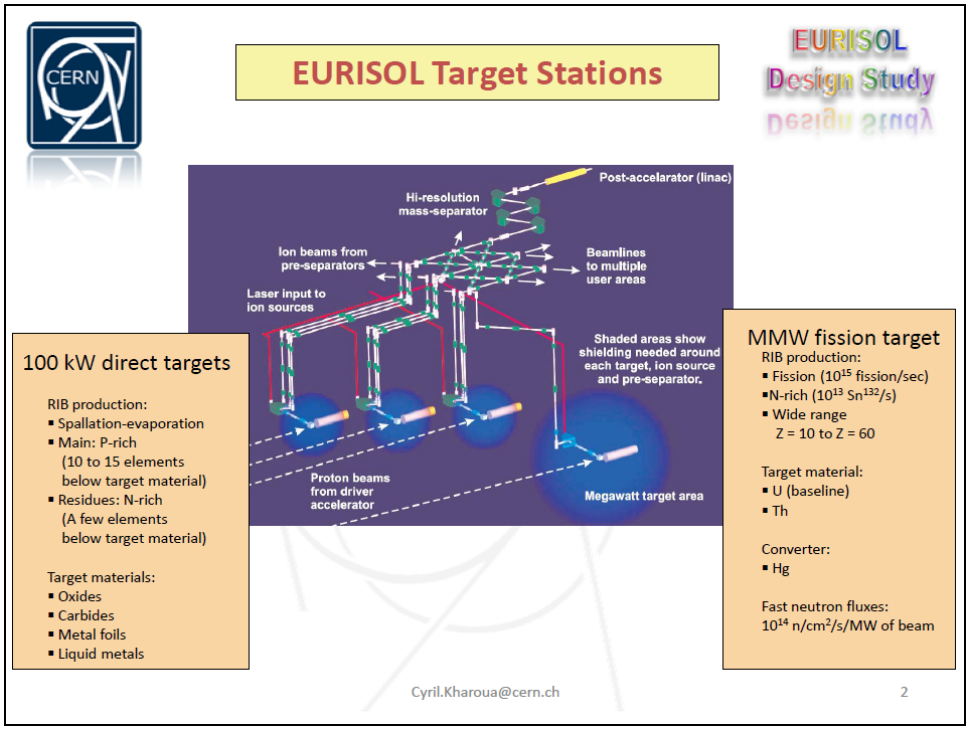

Multi-MW Liquid Hg Target

EURISOL Design Study

- Compact Hg-loop with beam widow
- Confined transverse film windowless

Deliverables:

1. Engineering study of the thermal hydraulics, fluid dynamics and construction materials of a window or window-free liquid-metal converter.
2. Study of an innovative waste management in the liquid Hg-loop e.g. by means of Hg distillation.
3. Engineering design and construction of a functional Hg-loop.
4. Off-line testing and validation of the thermal hydraulics and fluid dynamics.
5. Engineering design of the entire target station and its handling method

Window Configuration

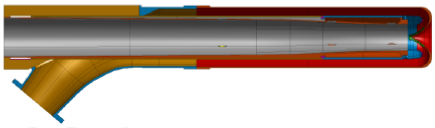

Windowless Configuration

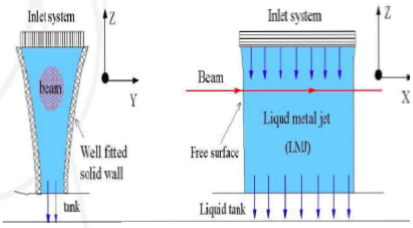

Cyril.Kharoua@cern.ch 3

PbBi against Hg – Neutron Balance

EURISOL Design Study

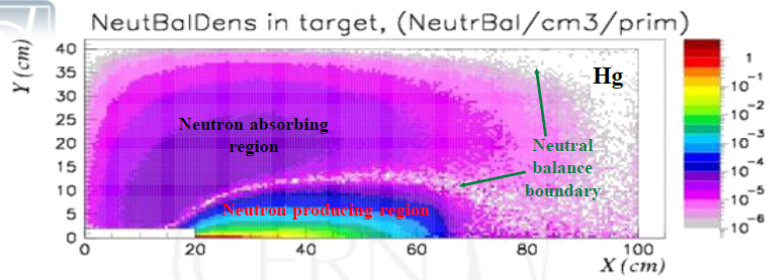

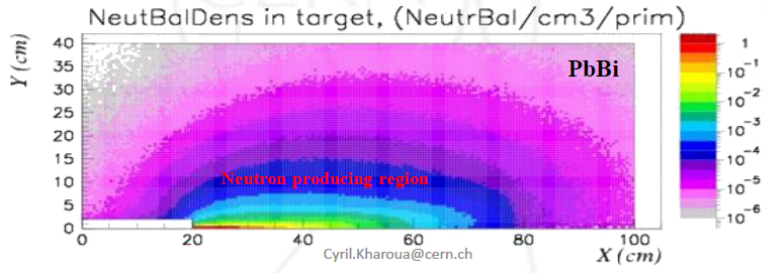

Cyril.Kharoua@cern.ch 4

PbBi against Hg – Neutron Spectra

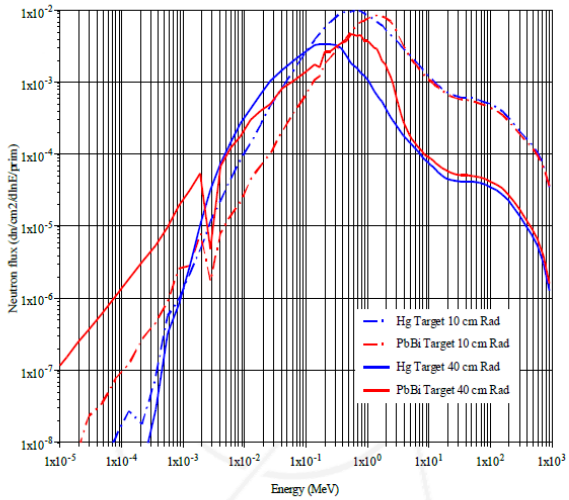

Cyril.Kharoua@cern.ch 5

The choice of Hg as a Target

- Mercury is liquid at room temperature and hence needs no auxiliary heating
- Mercury has the highest density of all heavy liquid metals and hence produces the brightest neutron source
- Mercury produces practically no alpha-emitters with any sizable life time
- Mercury has a relatively low decay heat and no long lived radioactive isotopes
- Technical feasibility of Hg purification ➡ should be verified

Cyril.Kharoua@cern.ch 6

Multi-MW Liquid Hg Target

EURISOL Design Study

- Compact Hg-loop with beam widow
- Confined transverse film windowless

Deliverables:

1. Engineering study of the thermal hydraulics, fluid dynamics and construction materials of a window or window-free liquid-metal converter.
2. Study of an innovative waste management in the liquid Hg-loop e.g. by means of Hg distillation.
3. Engineering design and construction of a functional Hg-loop.
4. Off-line testing and validation of the thermal hydraulics and fluid dynamics.
5. Engineering design of the entire target station and its handling method

Window Configuration

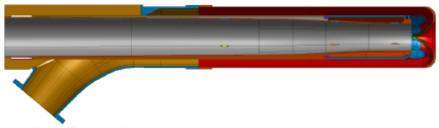

Windowless Configuration

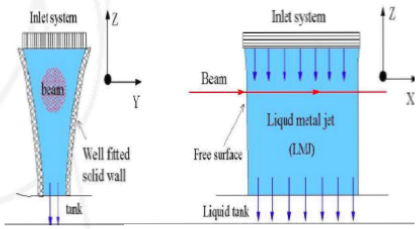

Cyril.Kharoua@cern.ch 7

Old fission target arrangment

EURISOL Design Study

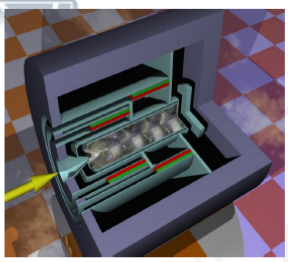

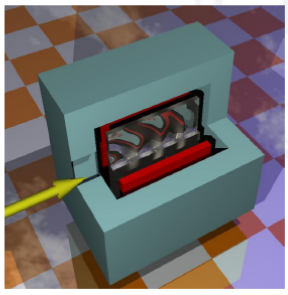

Fission density (fissions/cm^3/s/MW of beam)

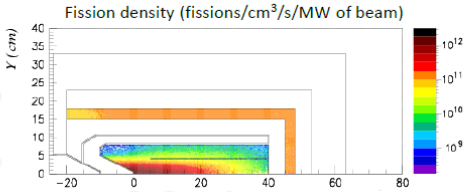

With this old design, a large number of fissions was achieved with reasonable target volumes and beam power. For example, the aimed ~10^{15} fissions/s was homogeneously produced within a 1 litre Unat target and 4 MW of proton beam power

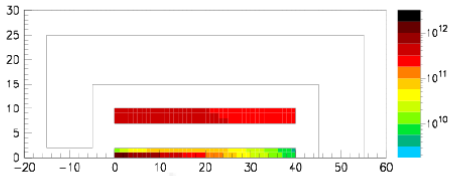

Cyril.Kharoua@cern.ch 8

New fission target arrangment

EURISOL Design Study

With this new design, a large number of fissions was achieved with a much smaller target volume. For example, the aimed ~10^{15} fissions/s was produced within a 100cm^3 of UC_x target (15g of U^{235}) and 4 MW of proton beam power.

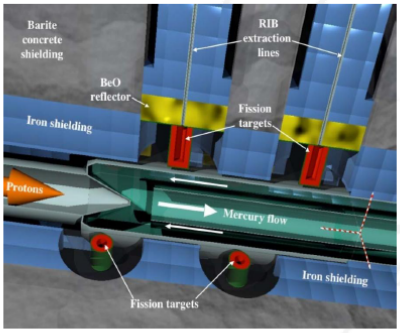

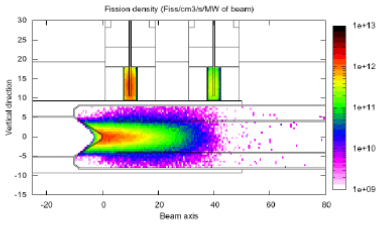

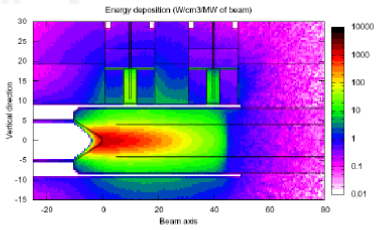

Cyril.Kharoua@cern.ch 9

Cut view of the fission target and converter : the neutron flux

EURISOL Design Study

Local enhancement due to moderator and reflector

Maximum flux coming out of the converter = few 10^{15} n/cm^2/s

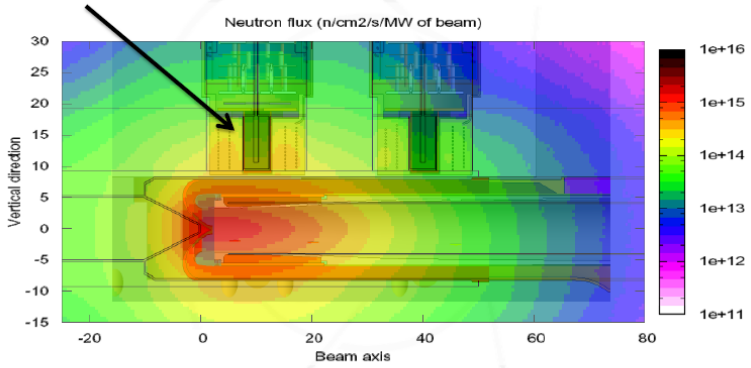

Cyril.Kharoua@cern.ch 10

Neutron Energy Spectrum vs Fission Cross-Section in Uranium

EURISOL Design Study

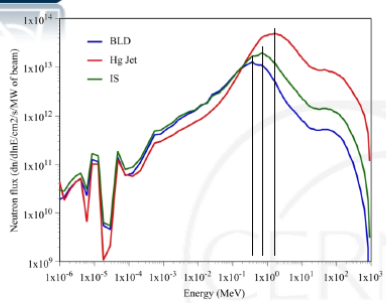

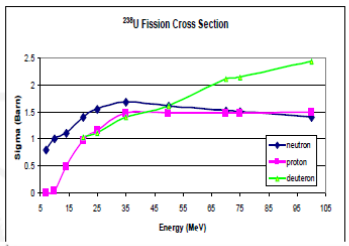

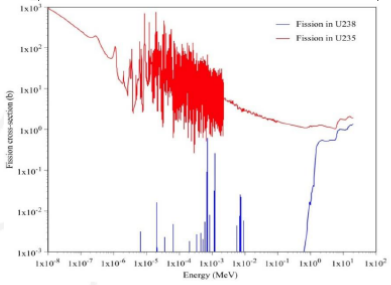

- Significantly harder spectrum for the Hg-J, with a peak neutron energy between 1 – 2 MeV, compared to 300 keV for BLD and 700 keV for IS
- Very low fission cross-section in ^{238}U below 2 MeV (~10^{-4} barns). Optimum energy: 35 MeV
- Use of natural uranium: σ_f in ^{235}U (0.7% wt.): at least 2 barns
- Further gain if neutron flux is reflected (e.g. BeO)

Cyril.Kharoua@cern.ch 11

Cut view of the fission target and converter : Fission density

EURISOL Design Study

In this new configuration the aimed 10^{15} fission/s are achieved or nearly in each target

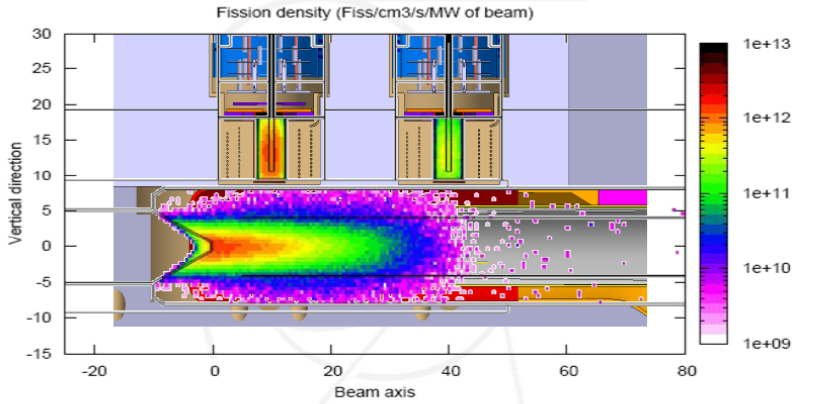

Cyril.Kharoua@cern.ch 12

Yield of the actinide target for different configuration

EURISOL Design Study

Properties of the different fuel tested

	Density [g/cm³]	Main isotope	U/C or Th/O mass ratio	atom content [at %]
POCO	0.4	^{235}U	0.5	2.49 ^{235}U
$^{nat}UC_3$	3.0	^{238}U	6.6	0.17 ^{235}U 24.83 ^{238}U
ThO_2	9.86	^{232}Th	6.4	33.33 ^{232}Th

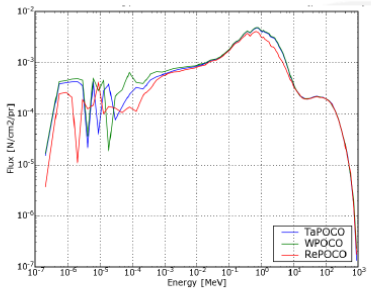

Neutron flux spectrum in the POCO fission target for different container materials

Fission rate in the actinide target for different fuel and container material

Fuel	Container	Fission Rate per target [fiss/s/4 mA]
POCO	Tantalum	1.8×10^{15}
	Tungsten	1.9×10^{15}
	Rhenium	4.9×10^{14}
$^{nat}UC_3$	Tantalum	3.8×10^{14}
	Tungsten	4.1×10^{14}
	Rhenium	1.3×10^{14}
ThO_2	Tantalum	5.8×10^{13}
	Tungsten	5.8×10^{13}
	Rhenium	5.8×10^{13}

Cyril.Kharoua@cern.ch 13

Yield of the actinide target for different configuration

EURISOL Design Study

In-target yields in a single Tantalum encased fission target for several relevant isotopes

Isotope	POCO [at/s/4mA]	$^{nat}UC_3$ [at/s/4mA]	ThO_2 [at/s/4mA]
^{74}Ni	9.72×10^{9}	8.77×10^{09}	9.73×10^{10}
^{81}Ga	7.70×10^{11}	7.70×10^{11}	6.23×10^{11}
^{90}Kr	1.03×10^{14}	2.10×10^{13}	2.95×10^{12}
^{99}Mo	1.08×10^{14}	2.27×10^{13}	1.53×10^{12}
^{132}Sn	3.19×10^{13}	1.68×10^{13}	1.58×10^{12}
^{214}Fr	na	2.50×10^{09}	7.74×10^{10}

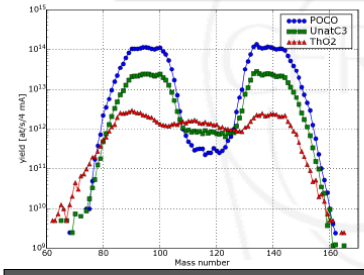

Isotopic yields obtained with the three fuels and Tantalum container as a function of mass number

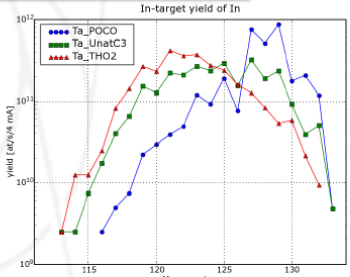

In-target Indium yield

Cyril.Kharoua@cern.ch 14

RIB Production for different converter design: Kr and Sn

EURISOL Design Study

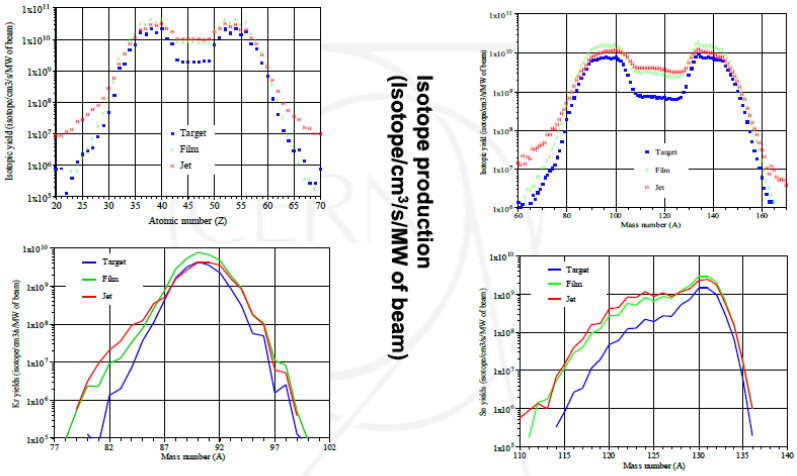

Cyril.Kharoua@cern.ch 15

Shielding of the 4 MW target

EURISOL Design Study

T. Otto & M. Felcini (CERN)

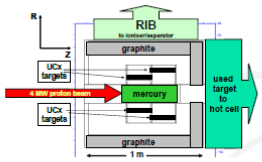

Condition for dose rates < 1 μSv/h

- 2 m of iron
- For θ = 0, 90 &180° → 9.0, 8.0 & 5.5 m of concrete
- To be complemented with earth

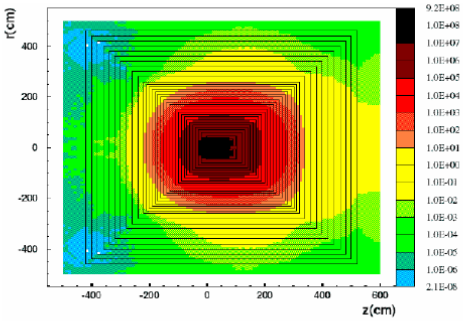

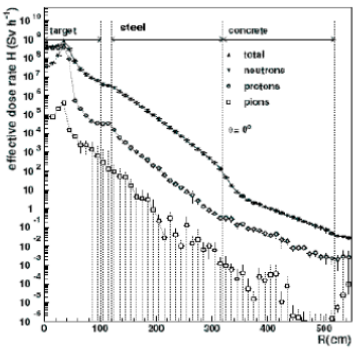

16

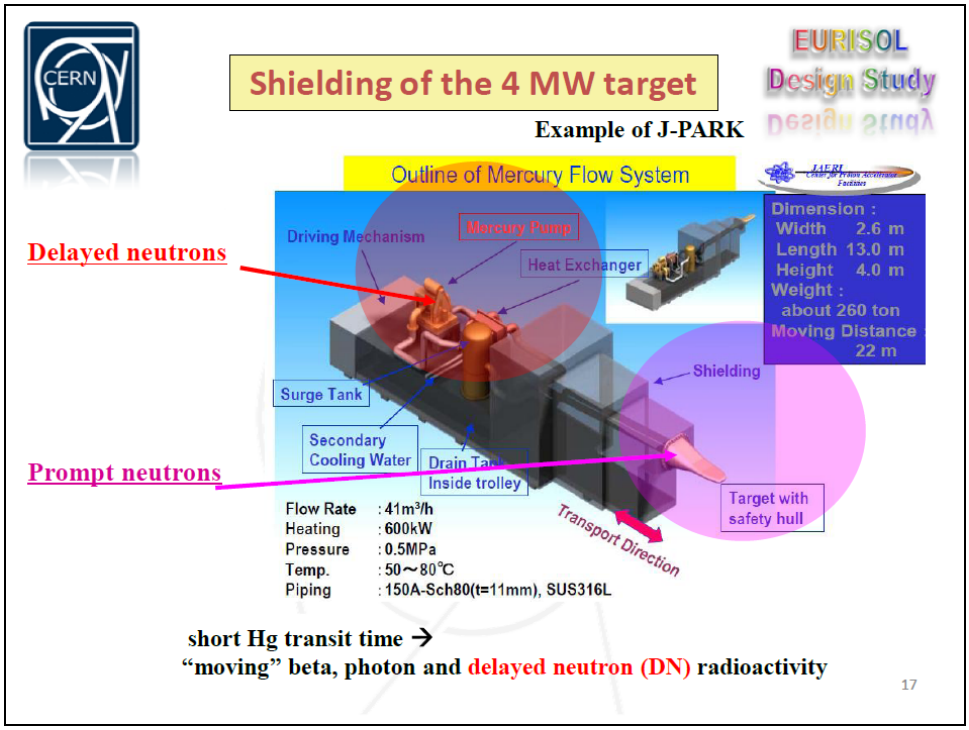
CERN
EURISOL
Design Study
Shielding of the 4 MW target
Example of J-PARK
Outline of Mercury Flow System
Delayed neutrons
Prompt neutrons
Driving Mechanism
Mercury Pump
Heat Exchanger
Dimension :
Width 2.6 m
Length 13.0 m
Height 4.0 m
Weight :
about 260 ton
Moving Distance :
22 m
Shielding
Surge Tank
Secondary
Cooling Water
Drain Tank
Inside trolley
Target with
safety hull
Transport Direction
Flow Rate : 41m³/h
Heating : 600kW
Pressure : 0.5MPa
Temp. : 50～80℃
Piping : 150A-Sch80(t=11mm), SUS316L
short Hg transit time →
"moving" beta, photon and delayed neutron (DN) radioactivity
17


CERN
EURISOL
Design Study
Hg Waste Management
18

Removal of Lu and Hf from CERN-Hg irradiated sample

EURISOL Design Study

Jörg Neuhausen et al. (PSI)

- Hf and Lu present as an oxide deposit on Hg were removed by contacting the liquid metal with oxide materials with a rough surface:
- Sintered corundum
- Molecular sieve
- Oxides stick to the surface of these materials

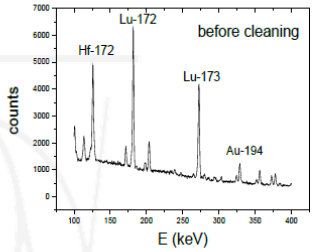

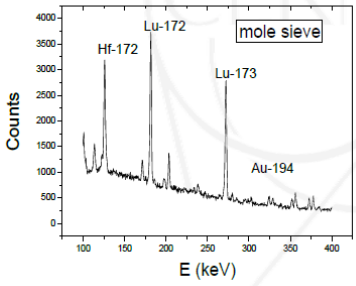

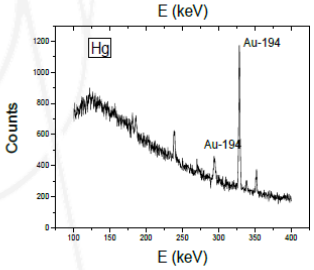

19

Activation of Hg

EURISOL Design Study

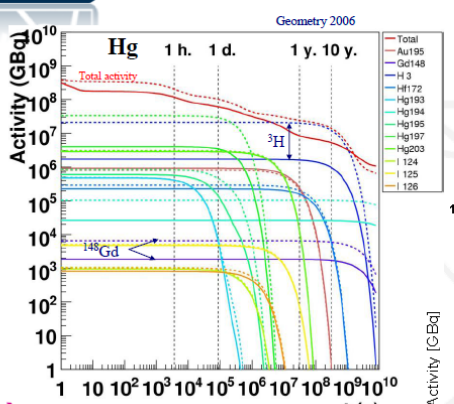

→ induced activity comparable to the research reactor + α emitters

B. Rapp et al. (CEA)

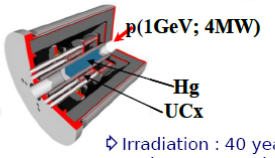

Irradiation : 40 years operation, 5000 h/year, 4MW beam power

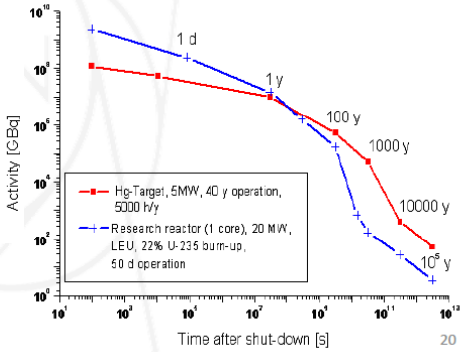

20

Disposal of liquid Hg

EURISOL Design Study

A schematic layout for liquid Hg-target disposal strategy

R. Moormann, Chiriki et al. (FZJ)

Chemical stabilization of Hg as an inorganic compound, e.g. HgS, HgSe, HgO, Hg_2Cl_2, $HgCl_2$

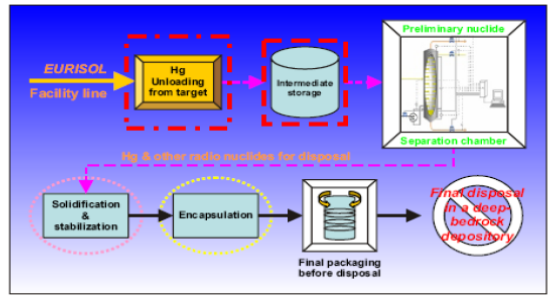

Extrapolation from laboratory scale to "industrial" scale still to be done

21

Summary and Outlook

EURISOL Design Study

- A conceptual lay-out of the new target station with all target positions and neutron facilities is proposed.
- Detailed neutronic and release studies have been carried out for different combinations of moderators and fission target composition
- Safety issues for both the fission target and proton converter are being addressed
- In parallel a detailed study of some alternative solution which would allow a much more compact geometry of the fission target arrangement is under study. (transverse film, Hg jet, etc…)

Cyril.Kharoua@cern.ch

22

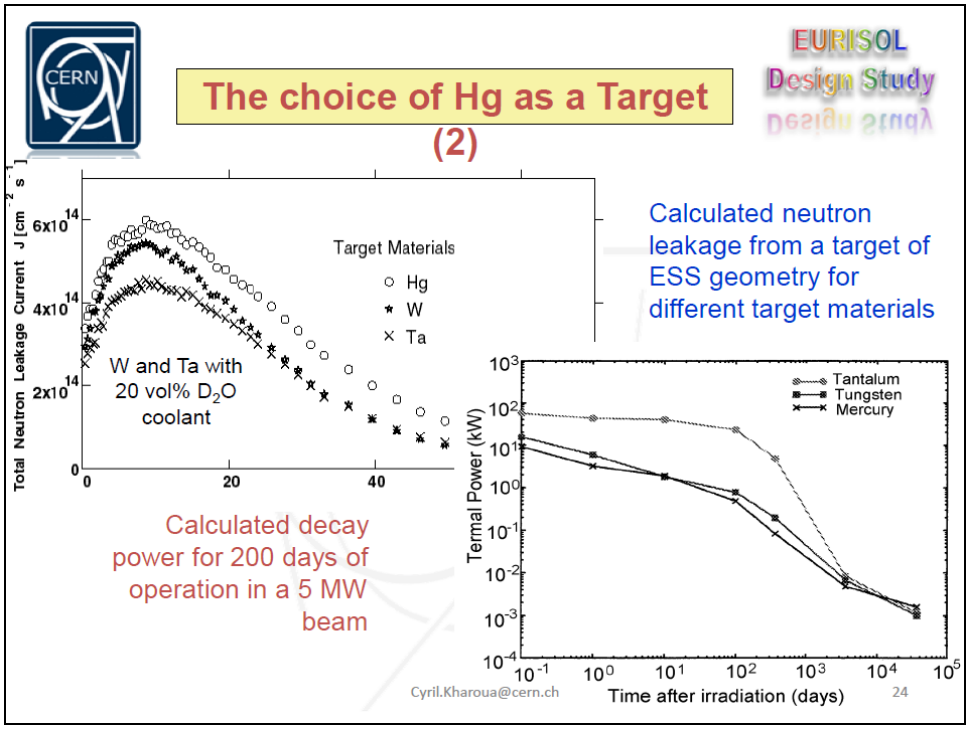
The choice of Hg as a Target
(2)
EURISOL
Design Study
Total Neutron Leakage Current J [cm⁻² s⁻¹]
6x10^14
4x10^14
2x10^14
0
0
20
40
Target Materials
Hg
W
Ta
W and Ta with
20 vol% D2O
coolant
Calculated neutron leakage from a target of ESS geometry for different target materials
Calculated decay power for 200 days of operation in a 5 MW beam
Termal Power (kW)
Tantalum
Tungsten
Mercury
Time after irradiation (days)
Cyril.Kharoua@cern.ch
24

Session VI

Status of computer codes, cross-sections and shielding data libraries

Chair: G. Muhrer

Radiation damage due to electromagnetic showers

I. Rakhno, N. Mokhov, S. Striganov
Fermilab, Batavia, Illinois, USA

Fermilab

Outline

- **Introduction**
- **Formalism:**
  - **Primary knock-on atoms ?** s_{pka}
  - **Elastic Scattering Cross Sections**
  - **Damage cross section ?** s_d
  - **Damage function ?(T)**
  - **Nuclear form-factor**
- **Calculated cross sections**
- **Conclusions**

April 22, 2008 SATIF-9, Oak Ridge, TN 2

Fermilab

Introduction

- Recent interest in high-energy lepton colliders (ILC) induced the problem of prediction of radiation damage due to electromagnetic showers in a wide energy range – from low energies up to a few hundred GeV.
- In high-flux nuclear reactors radiation damage to structural materials due to EM showers is not negligible ($E_?$= 15 MeV) and **can be comparable** to that due to neutrons (pressure vessel).
- Evaluation of e^-- and e^+-induced displacement (damage) cross sections from a few hundred keV up to 1 TeV.

April 22, 2008 SATIF-9, Oak Ridge, TN 3

Fermilab

Primary knock-on atoms – s_{pka}

- A displacement of an atom from its equilibrium position in a crystalline lattice due to irradiation ? formation of an interstitial atom and a vacancy in the lattice (***radiation damage***).
- The cross section of producing a primary knock-on atom (PKA) in elastic electron-nucleus collisions is:

$$\sigma_{pka}(E) = \int_{T_d}^{T_{max}} \frac{d\sigma(E,T)}{dT} dT$$

where E is kinetic energy of projectile, T is kinetic energy transferred to the recoil atom, T_d is the displacement energy, and T_{max} is the highest recoil energy according to kinematics.

April 22, 2008 SATIF-9, Oak Ridge, TN 4

Fermilab

Elastic Scattering cross section

- In the energy range from several keV up to 900 MeV there is a precise fitting expression for the ratio of ***Mott-to-Rutherford*** c.s., s_M/s_R, for electrons [Radiat. Phys. Chem., **45** (1995) 235]. Almost entire periodic table is covered and an average error is less than 1% when compared to exact values of s_M.
- Above 900 MeV one can use ***McKinley-Feshbach*** c.s. (2^{nd} Born approximation) which is valid when $(\alpha Z/\beta)^2 \ll 1$. Iron is the upper limit. At energies above 100 MeV one can observe small difference between s_M and s_{MF}.
- At ultra-relativistic energies an asymptotic value can be derived:

$$\sigma_{pka}(\infty) = \sigma_0 \frac{2m_e}{M} \frac{m_e c^2}{T_d}$$

Fermilab

s_{pka} for a pointlike ^{207}Pb nucleus

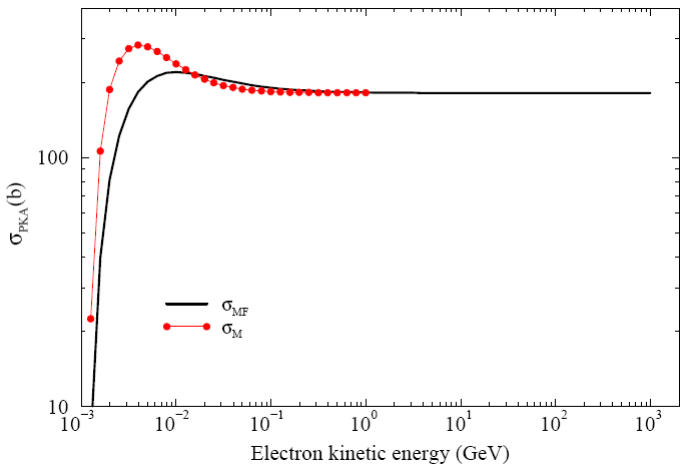

Fermilab

Displacement c.s. – s_d

A PKA can, in turn, generate a cascade of atomic displacements, energy permitting. This is taken into account via ***damage function,*** *?(T).* Number of atomic displacements per target atom (DPA) and per unit electron fluence:

$$\sigma_d(E) = \int_{T_d}^{T_{max}} \frac{d\sigma(E,T)}{dT} \nu(T) dT$$

Target atomic number, Z	T_d (eV)
13	25
22	30
29	30
41	60
42	60
73	90
74	90
82	25
All others	40

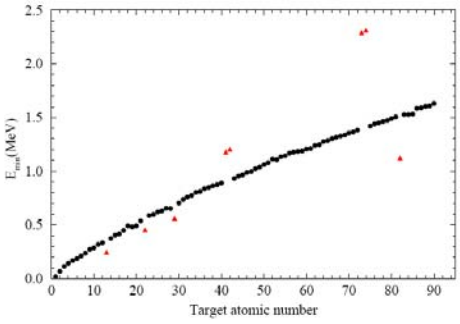

April 22, 2008 SATIF-9, Oak Ridge, TN 7

Fermilab

Damage Function ?(T)

- Modified Kinchin-Pease damage model (k(T)=0.8):

$$?(T) = \begin{cases} 0 & (T<T_d) \\ 1 & (T_d=T<2.5T_d) \\ k(T)E_d/2T_d & (2.5T_d=T) \end{cases}$$

where $E_d = T/[1+g(T, Z, A)]$. Partitioning energy loss between elastic and inelastic (dE/dx) collisions.

- At recoil energies above $2.5T_d$ the damage function, ?(T), reveals some growth with T.
- The ***displacement efficiency***, **k(T)**, is introduced as a result of simulation studies on evolution of atomic displacement cascades [J. Nucl. Math. **276** (2000) 22]. Weak dependence on target material and temperature.

April 22, 2008 SATIF-9, Oak Ridge, TN 8

Fermilab

Average Recoil Energy

according to ds_{MF}/dT (black) and ds_{M}/dT (red) for pointlike (solid) and extended (dashed) target nucleus.

Negligible difference between Gaussian and more realistic form-factors.

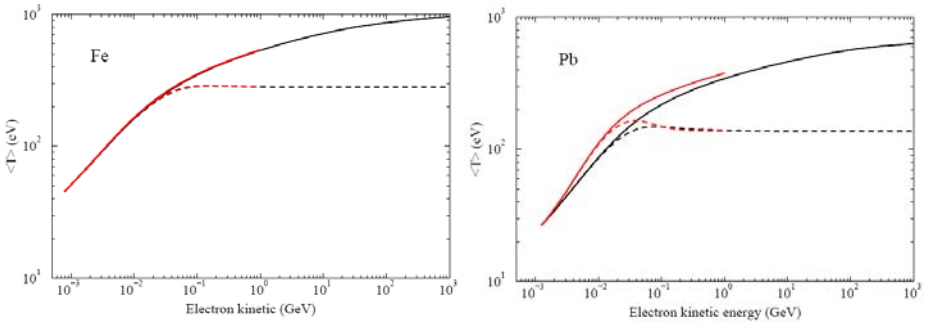

April 22, 2008 SATIF-9, Oak Ridge, TN 9

Fermilab

s_d for Iron

according to ds_{MF}/dT (lines) and ds_{M}/dT (circles) for pointlike (solid line, full circle) and extended (dashed line, open circle) target nucleus. Here k(T)=0.8

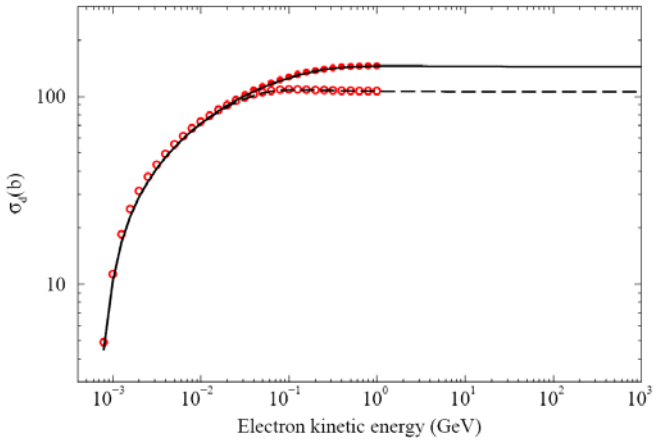

April 22, 2008 SATIF-9, Oak Ridge, TN 10

Fermilab

s_d for extended nucleus

Al (black) and Fe (red) with k(T)=0.8 (dashed) and with a realistic expression (solid) [R. Assman e.a., Proc. workshop on on materials for collimators, CERN, Sep. 5, 2007]

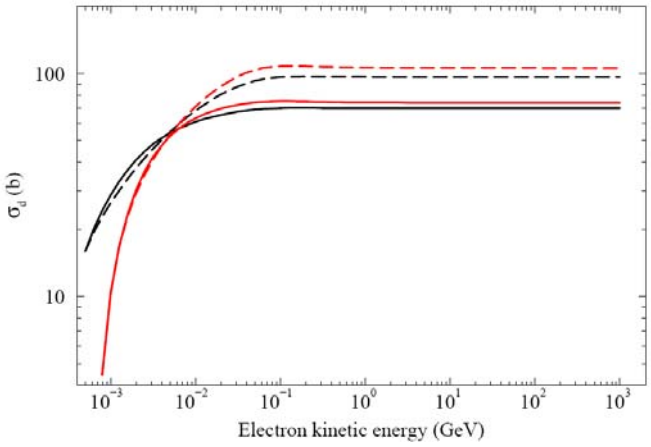

April 22, 2008 SATIF-9, Oak Ridge, TN 11

Fermilab

s_d *vs* Z

(realistic k(T), extended nucleus)

(black symbols ? T_d=40 eV)

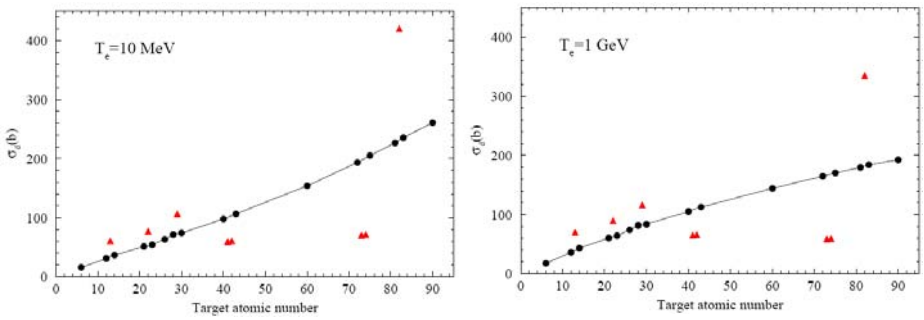

April 22, 2008 SATIF-9, Oak Ridge, TN 12

Fermilab

σ_d *vs* Z

(realistic k(T), extended nucleus, T_d=40 eV)

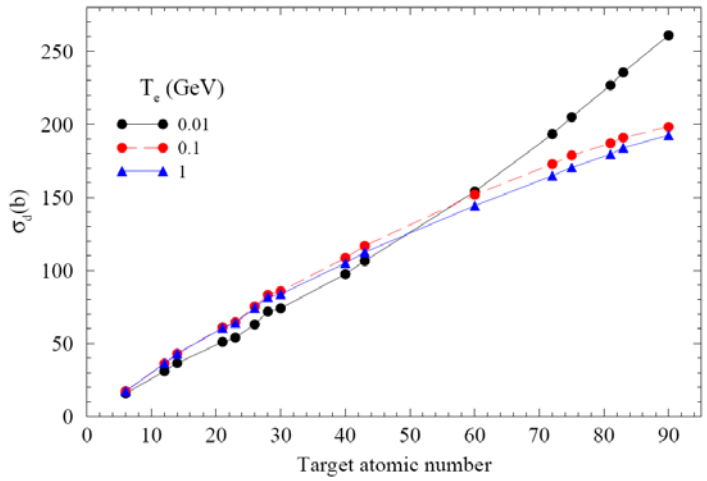

April 22, 2008 SATIF-9, Oak Ridge, TN 13

Fermilab

σ_d *for* e^- *(dashed) and* e^+ *(solid)*

(k(T)=0.8, extended nucleus, Al (black) and Fe (red))

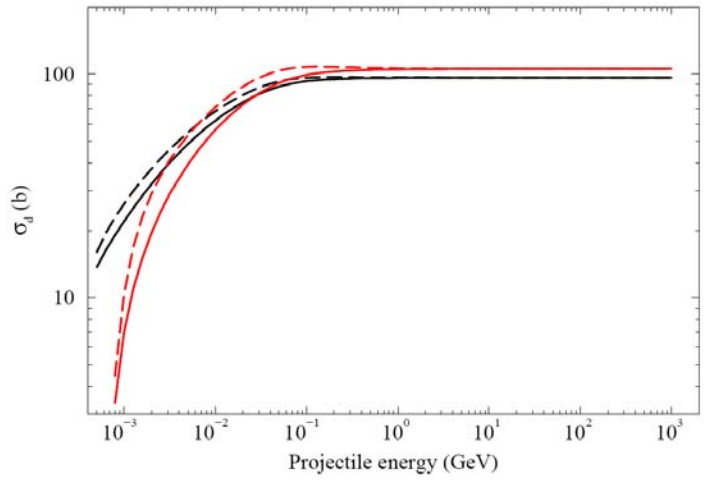

April 22, 2008 SATIF-9, Oak Ridge, TN 14

Fermilab

Conclusions

- Displacement cross sections (DPA) for electrons and positrons are calculated in the energy range from a fraction of MeV up to 1 TeV. Mott and McKinley-Feshbach differential cross sections are used.
- Importance of taking into account a nuclear form-factor is shown. Simple Gaussian form-factor is acceptable.
- For nuclei with T_d=40 eV a smooth dependence of s_d on target atomic number, Z, allows for a simple parametrization.
- Importance of taking into account a realistic displacement efficiency, k(T), is shown.

April 22, 2008 SATIF-9, Oak Ridge, TN 15

Present status of PHITS code – Event generator mode for low energy neutrons

Yukio Sakamoto,[1] **Yosuke Iwamoto,**[1] **Koji Niita,**[2] **Tatsuhiko Sato,**[1] **Norihiro Matsuda**[1]
[1]Japan Atomic Energy Agency (JAEA)
[2]Research Organisation for Information Science and Technology (RIST)

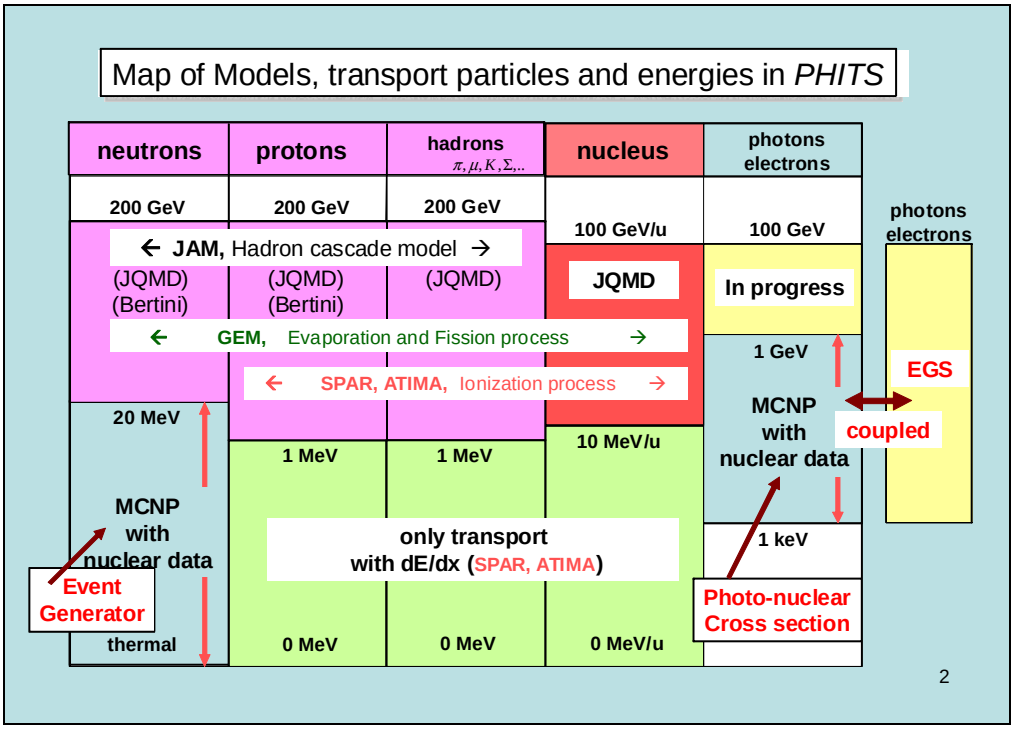

Event Generator Mode of PHITS for Low Energy Neutrons

How to estimate the deposit energy of charged particles and nuclei for neutron transport below 20 MeV

MCNP type: Transport based on Boltzmann equation with nuclear data Local Approximation (Kerma factor), Average Values

⟺

PHITS: Event Generator Mode with nucleus transport Energy Deposition in event by event Deposit energy distribution

This assumption is not valid for :

- Size of system is smaller than Range of charged particles
- Distribution is necessary instead of average value

Energy is conserved in average
No correlation

⇩

Only one-body observables

Treat all ejectiles of collisions.
Energy and Momentum are conserved in each collision.

⇩

Any observables Beyond one-body observables

3

Event Generator Mode for low energy neutrons in PHITS

Neutron data + Special Evaporation Model

We use the channel cross sections and neutron energy spectrum of the first neutron, and assume the binary decay of recoiled nucleus.

Neutron channels

capture	$\Gamma_n = 0$	charged particle and photon decay
elastic	$\Gamma_n = 0$	final state is uniquely determined
(n,n')	$\Gamma_n = 0$	charged particle and photon decay after the first neutron emission
(n,Nn')	$\Gamma_n \neq 0$	all particle and photon decay after the first neutron emission

By this model, we can determine all ejectiles (neutrons, charged particles, nucleus and photons) with keeping energy and momentum conservation. *PHITS* can transport all charged particle and nucleus down to zero energy and estimate deposit energy without local approximation (kerma factor).

4

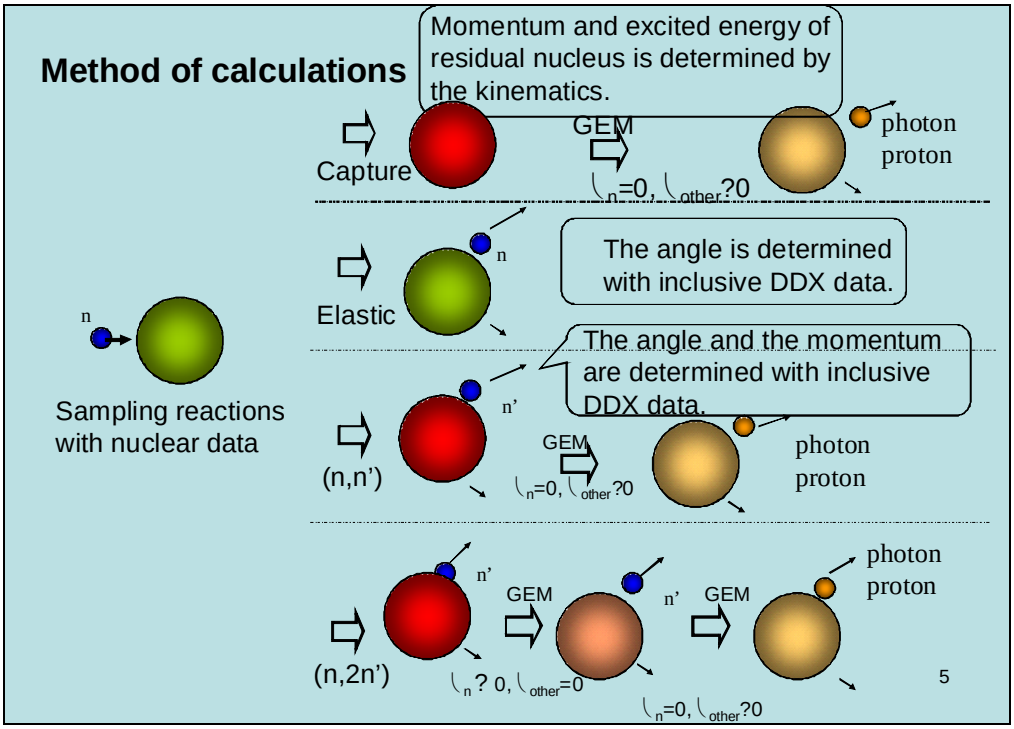
Method of calculations
Momentum and excited energy of residual nucleus is determined by the kinematics.
Capture
GEM
photon
proton
Δ_n=0, Δ_{other}?0
n
Elastic
The angle is determined with inclusive DDX data.
Sampling reactions with nuclear data
The angle and the momentum are determined with inclusive DDX data.
n'
(n,n')
GEM
Δ_n=0, Δ_{other}?0
photon
proton
n'
GEM
n'
GEM
photon
proton
(n,2n')
Δ_n? 0, Δ_{other}=0
Δ_n=0, Δ_{other}?0
5

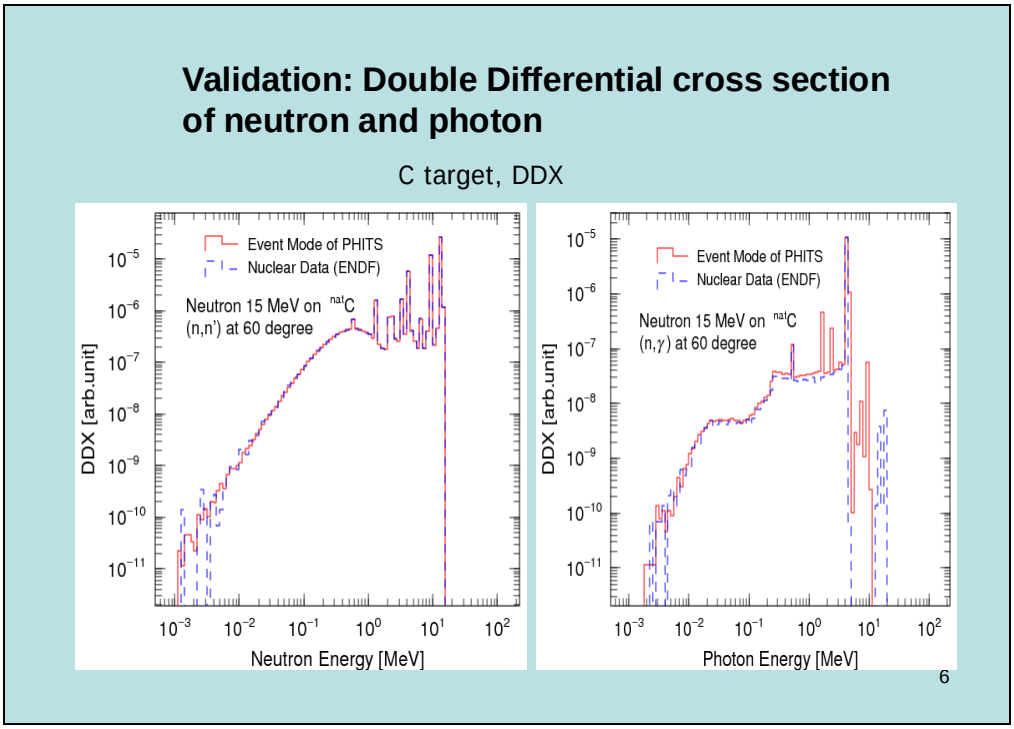
Validation: Double Differential cross section of neutron and photon
C target, DDX
Event Mode of PHITS
Nuclear Data (ENDF)
Neutron 15 MeV on natC
(n,n') at 60 degree
DDX [arb.unit]
Neutron Energy [MeV]
Event Mode of PHITS
Nuclear Data (ENDF)
Neutron 15 MeV on natC
(n,γ) at 60 degree
DDX [arb.unit]
Photon Energy [MeV]
6

Validation: Double Differential cross section of charged particles

C target, DDX

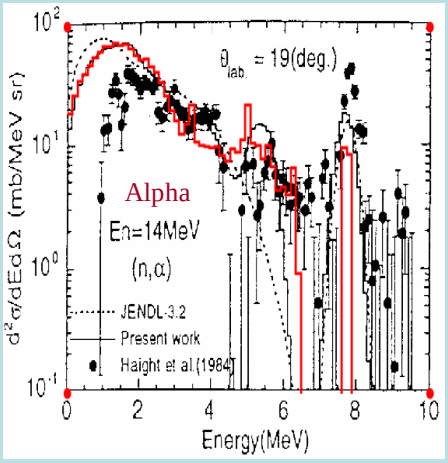

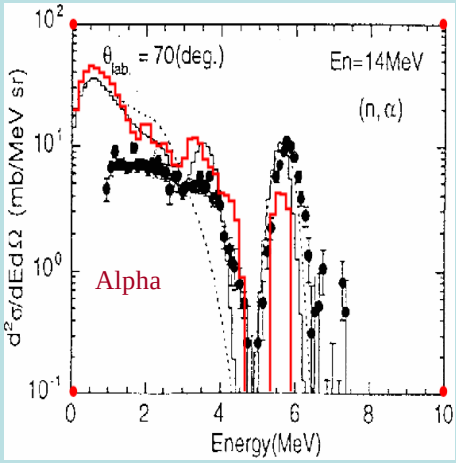

7

Validation: Double Differential cross section of charged particles and photon

9.5MeV: ^{27}Al(n,γ) at 127 deg.

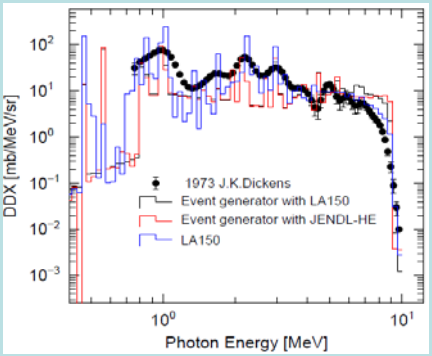

14MeV: ^{27}Al(n,xp) at 45 deg.

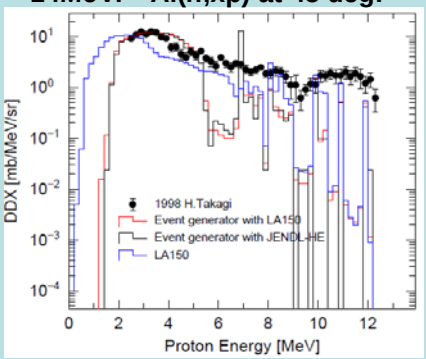

Use of inclusive neutron cross section and nuclear structure data. Calculated results with LA150 and JENDL-HE neutron data files give good agreements with experimental data.

8

Validation: Integral data (Kerma factor coefficient, total photon energy)

C target

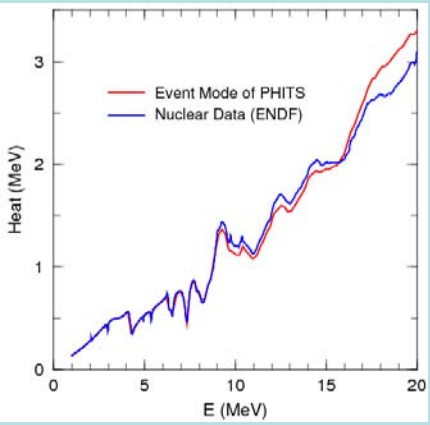

Total energy of charged particles (kerma factor)

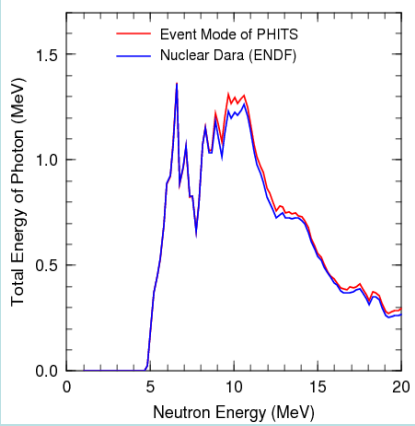

Total energy of Photon

9

Validation: Kerma coefficient of Carbon

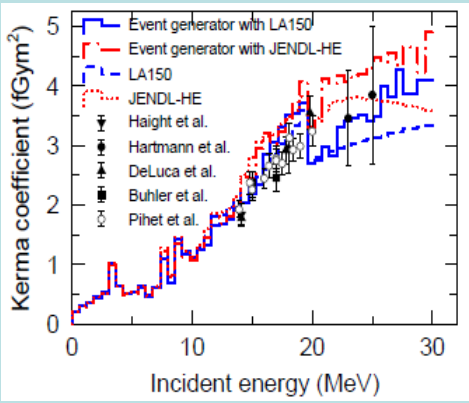

Evaluated cross section

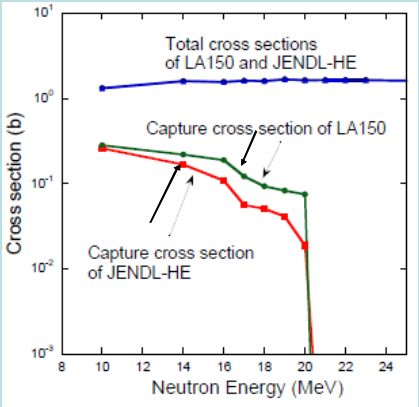

- Calculated results give good agreements below 20MeV.
- A Discontinuity at 20 MeV is appeared in kerma calculations by this work. Capture cross section are zero over 20 MeV.
- Both evaluated kerma coefficients have to be improved to connect smoothly at 20 MeV.

10

Validation: Displacement cross section

$$\sigma_{DX}(E) = \sum_i \int_{T_d}^{T_{\max}} \nu_d(T) \cdot \frac{d\sigma_d^i(T,E)}{dT} \cdot dT,$$

E: incident neutron energy
T: energy of the Primary Knock on Atom (PKA)

T_d: the atomic threshold displacement energy
Vd(T): the displacement damage function

⟹ given

$\frac{d\sigma_d^i(T,E)}{dT}$ the energy-differential cross section to be *T* at *E*

⟹ Calculation by event generator

11

Validation: Displacement cross section

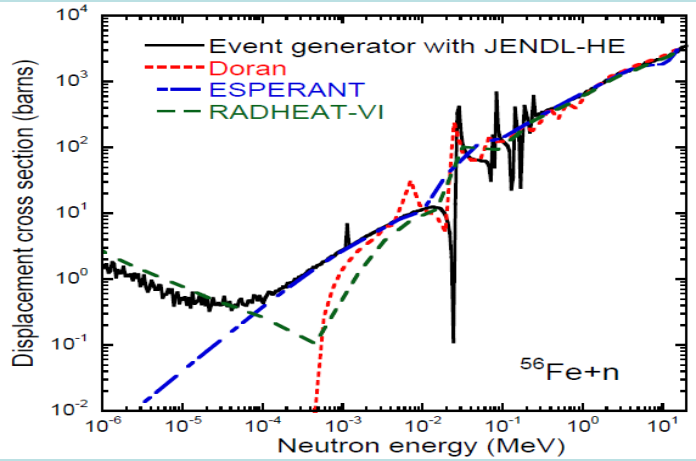

Calculated results give good agreements over 10^{-3}MeV.
Since this work and RADHEAT-VI can treat the capture reaction, the calculated values increase as neutron energy decreases below 10^{-4}MeV.

12

Application of Event Generator Mode for low energy neutrons

(1) Neutron-induced semiconductor soft error (SEU: single event upset)

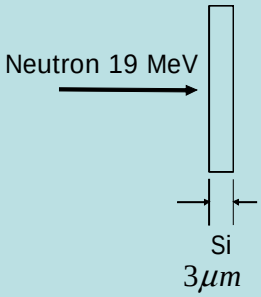

Deposit Energy Distribution by PHITS

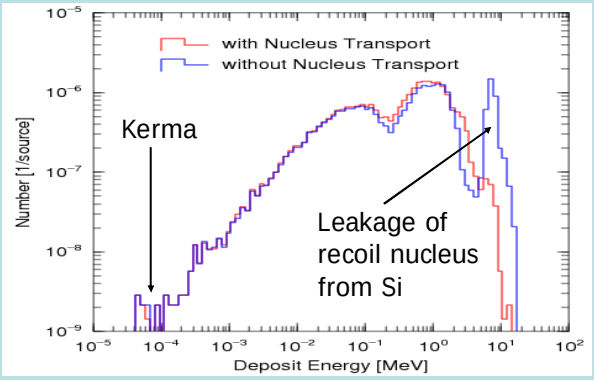

13

Application of Event Generator Mode for low energy neutrons

(2) Microdosimetric analysis of the boron-neutron capture therapy

~Energy distribution for the $^{10}B(n_{th}, \alpha)^7Li$ reaction~

$^7Li^*$ (0.84MeV) + α(1.47MeV) ^7Li (1.02MeV) + α(1.78MeV)

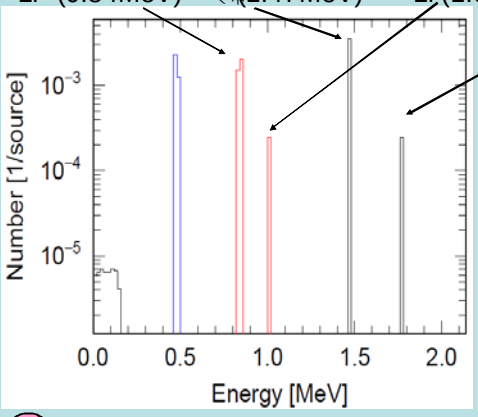

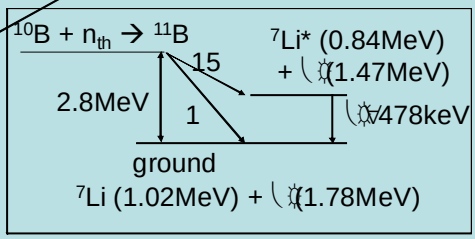

The accuracy of the energy distribution of charged particles are confirmed.

14

Application of Event Generator Mode for low energy neutrons

(3) The Kerma weighted average quality factor

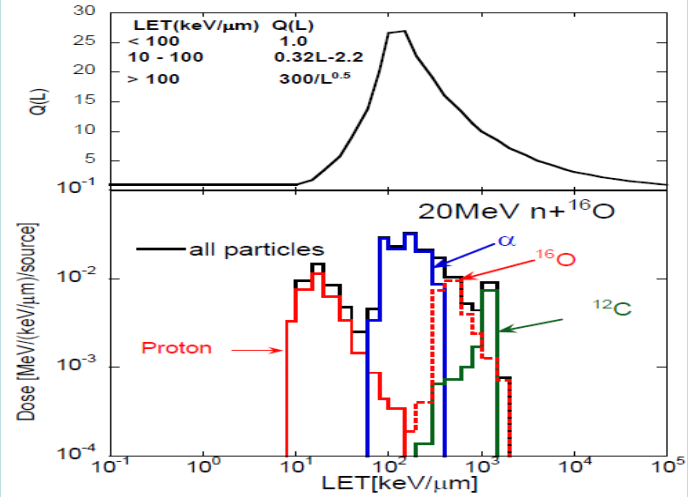

LET in water: SPAR code.

15

Application of Event Generator Mode for low energy neutrons

(3) The Kerma weighted average quality factor

$$Q = \frac{\int Q(L) D_l(L) dL}{\int D_l(L) dL}$$

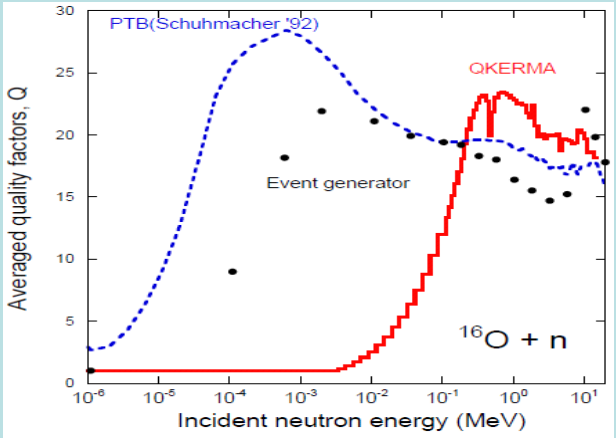

LET distributions are calculated below 20 MeV neutron incidence.
The shape of our result is somewhat similar with the result of PTB.

16

Present of PHITS

Typical Features:

◆Event Generator Mode for low energy neutrons:

- Deposit Energy (Heat) without Local Approximation.
- Deposit Energy Distribution (Beyond One-Body Observables).
- conserve the energy and momentum
- DDX, Kerma, displacement cross section: good agreement below 20 MeV.
- Its applications

Deposit energy distributions of charge particles for the $^{10}B(n_{th}, \blacklozenge)^{7}Li$ reaction , the Kerma weighted average quality factor.

◆Heavy Ion transport (JQMD and Ionizaiton Processes).
◆Low Energy Neutron Transport (By Evaluated Nuclear Data).
◆Functions of Beam Transport (Magnetic Field and the other Devices).

17

Future of PHITS

In Event Generator Mode for low energy neutrons:

Treatment of thermal neutrons, scattering law $S(\alpha,\beta)$.
Development of new frame work over 20 MeV.

Now tackled:

Photo-Nuclear Reaction
Coupled with EGS, High Energy Photon and Electron Transport

Others:

Microscopic treatment of ionization processes.
DCHAIN-SP, Radioactivity Calculation

18

Status and future plans for the Radiation Shielding and Dosimetry Experiments Database (SINBAD)

I. Kodeli, E. Sartori
OECD/NEA DB

B.L. Kirk
RSICC

SINBAD (Radiation Shielding Experiments Data Base)

- Preserve results from expensive experiments
- Validation of
  - radiation transport codes
  - cross section data
- Build confidence in methods and data used

SATIF9 2

SINBAD -Radiation Shielding Experiments Scope and Objectives

- Compilation of high quality, experiments for validation and benchmarking of computer codes and nuclear data used for radiation transport and shielding problems encompassing:
  - reactor shielding, PV dosimetry **(42)**
  - fusion blanket neutronics **(27)**
  - **accelerator shielding (15)**
- Low and inter-mediate energy particles applications.

SATIF9 3

SINBAD (Radiation Shielding Experiments Data Base)

- SINBAD data include benchmark information **in standard form**:
  (1) experimental facility and radiation source;
  (2) benchmark geometry and material composition;
  (3) detection system, measured data, and an error analysis.
- Peer review of the compilations by two scientists;
- Include graphical information on experimental geometry, measured quantities, computer code inputs for the analysis, reports used in the compilation, QA report and peer review report
- Distribution on DVD by the RSICC and the NEA Data Bank.

SATIF9 4

SINBAD - Radiation Shielding Experiments: **Contributing Institutions**

- AEAT, United Kingdom
- ARCS, Austria
- CEA, France
- CERN, Switzerland
- European Commission JRC Ispra
- ENEA, Italy
- FZKarlsruhe, Germany
- FZDresden, Germany
- Georgia-Tech, USA
- KEK, Japan
- IPPE Obninsk, Russian Federation
- IRI Delft, Netherlands
- JAEA, Japan
- Jozef Stefan Institute, Slovenia
- LBNL, USA
- LANL, USA
- Michigan State Univ., USA
- MEPhI, Moscow
- NIRS, Japan
- NIST, USA
- ORNL, USA
- PSI, Switzerland
- RAL, UK
- RIKEN, Japan
- RDIPE, Russia
- VNIITF (RFNC), Russia
- SCK-CEN Belgium
- Tohoku University
- TU Budapest ,Hungary
- TU Dresden, Germany
- University of Illinois, USA
- University of Osaka, Japan
- University of Pavia, Italy
- University of Tokyo, Japan

SATIF9 5

Accelerator Experiments by Facility

- **BEVALAC Experiment with Nb Ions on Nb & Al Targets**
- **CERN Roesti I, III: 200 GeV/c hadrons on Fe and Pb (100 cm)**
- **CERN Roesti II: 24 GeV/c protons on 100 cm Fe**
- **HIMAC - He, C, Ne, Ar, Fe, Xe, Si ions on C, Al, Cu, Pb targets**
- **HIMAC - High energy neutron (<800 MeV) measurements in iron**
- **HIMAC - High energy neutron (<800 MeV) measurements in concrete**
- **INS U-Tokyo Transmission of n,? from 52 MeV Protons through C, Fe, H2O & concrete (up to 115 cm)**
- **Osaka University Transmission of n,? from 65 MeV Protons through C, Fe, Pb & concrete (10-100 cm)**
- **ISIS Deep Penetration of Neutrons through Concrete (120cm) & Iron (60cm)**
- **MSU experiment with He & C ions on Al target**
- **PSI Neutron Spectra Generated by 590-MeV Protons on Pb Target**
- **RIKEN 70-210 MeV quasi-monoenergetic neutron spectra**
- **TEPC-FLUKA Intercomparison for aviation dose**
- **TIARA 40 & 65 MeV neutron transmission through Fe, Concrete, $(CH_2)_n$**

SATIF9 6

SINBAD -
Accelerator Radiation Shielding Experiments

Shielding Materials

- **Fe / steel (20 benchmarks)**
- **Concrete (4)**
- **Pb (3)**
- **Graphite (3)**
- **Al (5)**
- **H_2O (11), Na (5)**
- **$(CH_2)_{2n}$ (2)**
- **W (4), Nb (1), V(2)**
- **Si, SiC (3)**
- **Air (9), etc**

SATIF9 7

SINBAD – recent completed compilations or in progress and being reviewed

- AVF-75MeV - Transmission of Medium Energy Neutrons Through Concrete Shields (1991)
- Neutron Production from Thick Targets of C, Fe, Cu, and Pb by 30- and 52-MeV Protons(1982)
- CERF shielding experiment at CERN (2004)
- OKTAVIAN Mn spheres transmission experiments series
- Neutron Production from Thick Targets of Carbon, Iron, Copper, and Lead by 30- and 52-MeV Protons(1982) –
- Transmission of Medium Energy Neutrons Through Concrete Shields (1991)
- CERF shielding experiment at CERN (2004)
- CERF Radionuclide Production (2003) - CERF Residual Dose Rates (2003)
- Reaction rates inside and outside the 0.8 GeV proton-irradiated W-Na target
- IPPE neutron transmission through bismuth shell

SATIF9 8

SINBAD - work to be done

- **New review of all time of flight compilations and evaluations (see ICRS11 paper by I. Kodeli:** Lessons Learned from the TOF-benchmark Intercomparison Exercise within Eu CONRAD Project (How not to Misinterpret a TOF-benchmark)
- New review of all Accelerator Shielding Experiments
- **Reanalysis of the quality of the compiled data and benchmarks and providing a quality level for each benchmark in order to guide SINBAD user.**

SATIF9 9

SINBAD - work to be done

ACCELERATORS

Title	Organisation
68 MeV P on thick Cu target	JAERI
Neutron Yields from Stopping-Length C, Al, Fe and Depleted U Targets for 256-MeV P	LAMPF LANL-1989
Neutrons from 710-MeV Alphas Stopping in H_2O, C, Steel and Pb	SREL 1980
Photoproduction of High-Energy N in Thick Pb Targets Irradiated by 150 to 270 MeV Electrons	U-Mainz1973
Neutron Fluxes inside/around Fe Beam Stop Irradiated by 500 MeV P	KEK-1979
Reaction Rate in Thick Concrete Shield Irradiated by 6.2 GeV Protons	LBL-1965
Experiment using 4 m concrete at KENS 500 MeV Proton Accelerator	KENS/KEK
TOF N spectra & radioactivity induced in Li,Be,Cu,C,Al for 25-40 MeV d	Tohoku Univ.
Neutron spectra from 20cm Fe slab, D_2O(He3,xn) reaction at 40 MeV	NPI Rez
Residual Product Yields in Thin Targets Irradiated by 100-2600 MeV p	ITEP, Moscow
SLAC experiment using 28.7 GeV electrons	SLAC
Neutron spectra behind concrete and Fe of 120 GeV/c Hadron Beam	CERF/CERN

SATIF9 10

Conclusions

- Some valuable shielding experiments have been saved in a standard format together with the primary documents. These have been compiled and reviewed by at least 2 experts.
- Further data is being processed, in particular more accelerator and fusion relevant experiments will be added. These experiments have been identified of being of high relevance for validation of radiation transport and shielding methods and codes.
- **New contributions on benchmark experiment data, assistance in review and feedback information are welcome.**

SATIF9 11

Web page for SINBAD

SINBAD Database at RSICC:

- http://www-rsicc.ornl.gov/BENCHMARKS.html

at OECD/NEA

- http://www.nea.fr/html/science/shielding/sinbad/sinbadis.htm

SATIF9 12

Update on recent computer codes and data libraries of interest to SATIF – Status: April 2008

I. Kodeli, E. Sartori
OECD/NEA DB

B.L. Kirk
RSICC

Recently Acquired Programs and Data of Interest

- Nuclear model, resonance treatment, decay-process codes, DWBA07/DWBB07, ECIS-06, TALYS-1.0, EMPIRE-II 2.18, REFIT-2007, SAMMY-7, NJOY99.259+
- Electron-photon transport: FOTELP-2K6, PENELOPE2006 (2008 in preparation),
- General radiation transport codes: MCNP/ MCNPX, TRIPOLI-4.4, COG10
- Shielding, irradiation codes, activation: SUSD3D, EASY-2005.1
- Articles databases on radiation protection and shielding SATIF/CYCLO-RADSAFE (extended version in preparation)
- Dose rates, health physics BULK_C-12, GENII-LIN

Recent cross section data and tools

- IRDF-2002-ACE, Cross-Section Library and Spectra for Dosimetry
- ADS-LIB/V1.0, test library for Accelerator Driven Systems
- FSXLIBJ33, MCNP data library based on JENDL-3.3
- MCJEFF3.1NEA, MCNP Neutron Cross Section Library based on JEFF3.1
- VITJEFF31.BOLIB,JEFF-3.1 Multi-group Coupled (199n + 42gamma) X-Section Library
- JANIS, a Java-based nuclear data display program

Forthcoming Conferences of Interest

- Physor-2008, Interlaken, Switzerland
- M&C-2009, Saratoga Springs, NY
- SNA-2010 & MC2010, Japan
- ICRS-12 & RPSD-2012, Japan

Forthcoming Training Courses of Interest sponsored by NEA & RSICC

- MCNP/MCNPX ITN, Lisbon Portugal, 12-16 May 2008
- GEANT4, RSICC, Oak Ridge, 19-23 May 2008
- REFIT 2007 - Multi-level resonance parameter least square fit, IRMM, Geel, 2-6 June 2008
- Penelope-2008, Barcelona, Spain, 30 June - 3 July 2008
- FLUKA, Paris, 29 September - 3 October 2008
- MCNP/MCNPX, GRS, Munich, Germany, 27-31 October 2008

URLs RSICC/NEADB

- http://rsicc.ornl.gov/
- http://www.nea.fr/html/databank/

Status of cryogenic temperature scattering cross-section data

E. Sartori
OECD/NEA Data Bank

- **S(α,β) data**
  - **ENDF/B-VI, IKE, JEFF (McFarlane, Keinert/Mattes, Mounier)**
- **Multi-group data**
  - **CLES – University of Kyoto (Morishima)**

SATIF9 2

OECD/NEA Results of inquiry on cold neutron cross-section data

Request for cryogenic temperature cross-sections

Material	T=1.8K	T=4.2K	T=5-10K	T=87K	Requester
Argon				87	CERN, SLAC, FNAL
H (CH_2 bound)				87	CERN, SLAC, FNAL
Aluminium	1.8	4.2	10	87	CERN, SLAC, FNAL, PSI
Iron	1.8	4.2		87	CERN, SLAC, FNAL
Pb	1.8	4.2		87	SLAC
Ceramic(*)	1.8	4.2			FNAL
Copper	1.8	4.2			FNAL
Epoxy(**)	1.8	4.2			FNAL
G10(**)	1.8	4.2			FNAL
Helium	1.8	4.2			FNAL
Niobium	1.8	4.2			FNAL
Tin	1.8	4.2			FNAL
Titanium	1.8	4.2			FNAL
Deuterium-solid			5-10		PSI
Zirconium			10		PSI
Oxygen			5-10		PSI
CH_4-solid			5-10		PSI
H_2O (ice)					SLAC

SATIF9 3

multi-group cross-sections of moderator materials for low-energy neutron sources (140 equi-lethargy groups from 0.1 μeV to 10 MeV)

Material	Temperature (K)	Source
Liquid ^{4}He	0.1, 0.3, 0.5, 0.6, 0.7, 0.8, 0.9, 1.0, 1.5, 2.0, 2.5	Kyoto University
Liquid *ortho*-H_2	14.0, 20.4	Kyoto University
Liquid *para*-H_2	14.0, 20.4	Kyoto University
Liquid *normal*-H_2	14.0, 20.4	Kyoto University
Liquid *ortho*-D_2	18.7, 23.6	Kyoto University
Liquid *para*-D_2	18.7, 23.6	Kyoto University
Liquid *normal*-D_2	18.7, 23.6	Kyoto University
Solid CH_4	20.4, 50.0, 90.7	Kyoto University
Liquid CH_4	90.7, 111.7	Kyoto University
Liquid H_2O	278, 300, 325, 350	Kyoto University
Liquid D_2O	278, 300, 325, 350	Kyoto University

SATIF9 4

MAT numbers for the ENDF files and ID's for the ACE files

Liquid hydrogen and deuterium for the two modifications: ortho and para

Material	MAT	Temperatures (K)	ID ACE files
para Hydrogen	2	14, 16 and 20.38	pH.00t pH.01t pH.03t
ortho Hydrogen	3	14, 16 and 20.38	oH.00t oH.01t oH.03t
para Deuterium	12	19 and 23.65	pD.00t pD.01t
ortho Deuterium	13	19 and 23.65	oD.00t oD.01t

H in polyethylene (CH_2)

Material	MAT	Temperatures (K)	ID ACE files
H in CH_2	37	87, 293.6 and 350	poly.01t poly.03t poly.04t

Liquid argon

Material	MAT	Temperature (K)	ID ACE file
18-Ar	18	87	argon.01t

Aluminium face centred cubic lattice

Material	MAT	Temperatures (K)	ID ACE files
13-Al-27	61	20, 77, 87, 100, 293.6, 400	al.00t al.01 ... al.05t

SATIF9 5

ENDF/B-VI & IKE existing data

Material	Temperature (K)	Source
CH_4-s (solid methane)	22	ENDFB/VI
CH_4-l (liquid methane)	100	ENDFB/VI
D-ortho (liquid ortho deuterium)	19	ENDFB/VI
D-para (liquid para deuterium)	19	ENDFB/VI
H-ortho (liquid ortho hydrogen)	20	ENDFB/VI
H-para (liquid para hydrogen)	20	ENDFB/VI
H_2O (solid)	20, 77, 113.2, 165.2, 218.2, 248.8, 273	IKE
H_2O (liquid)	273.2, 278.2, 293.6, 308.6	IKE
Aluminium	20, 100, 293	IKE
Beryllium	100, 300	IKE
Magnesium	20, 100, 296, 773	CEA/IKE
H-para/ortho – liquid / gas	14, 16, 20.38/ 20.4, 25	IKE
D-para/ortho – liquid / gas	19, 25	IKE
CH_4 solid	31, 57, 77, 89	IKE

SATIF9 6

IKE Stuttgart

Present Status of
Evaluated Thermal Neutron Scattering Data
in the temperature range 20 K < T < 300 K
for solid and liquid moderator materials
important for design of cold neutron sources

M. Mattes and J. Keinert
IKE - University of Stuttgart

SATIF9 7

IKE Stuttgart

Graphical comparisons of evaluated data with measurements

- Aluminium
- Beryllium
- Magnesium
- liquid hydrogen (ortho and para)
- gaseous hydrogen (ortho and para)
- liquid and gaseous ortho deuterium
- light water ice

SATIF9 8

IKE Stuttgart

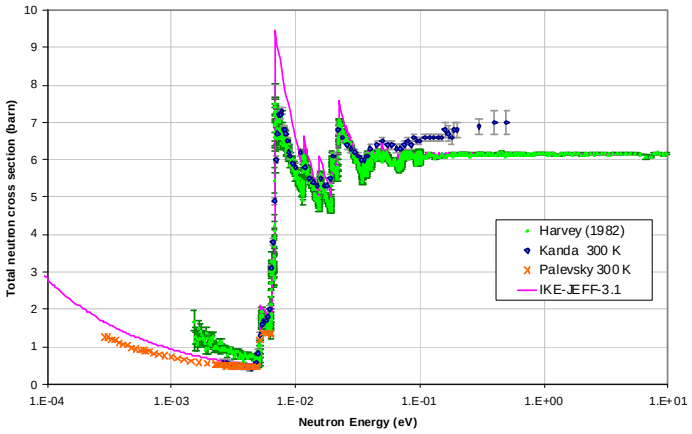

SATIF9 9

IKE Stuttgart

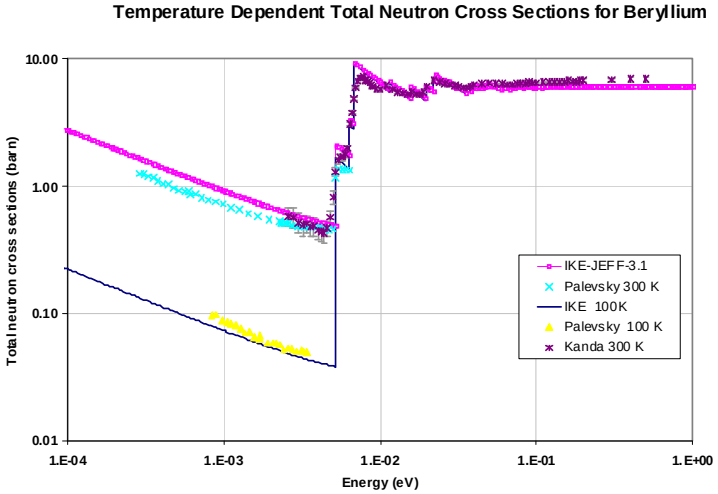

SATIF9 10

IKE Stuttgart

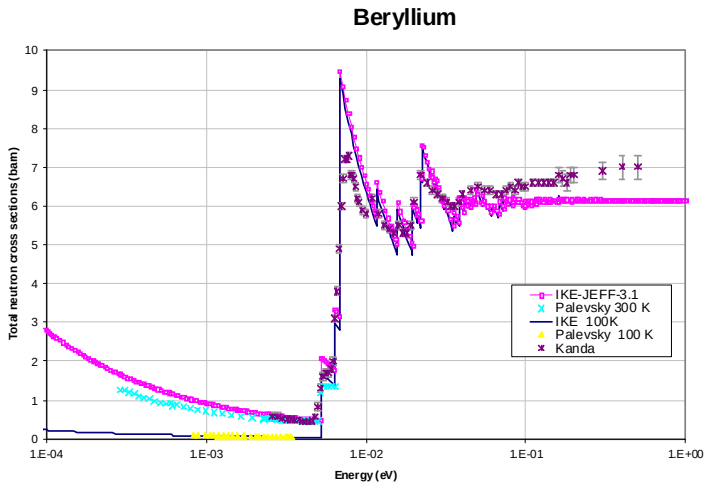

SATIF9 11

IKE Stuttgart

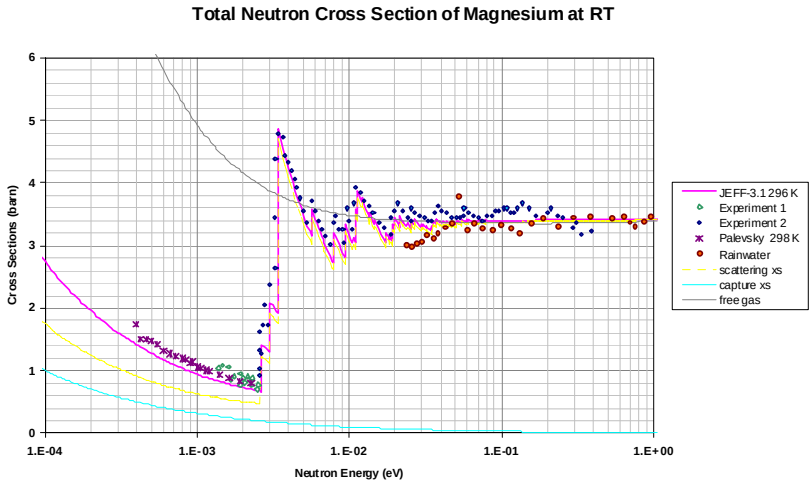

SATIF9 12

IKE Stuttgart

Total Neutron Cross Section of Magnesium

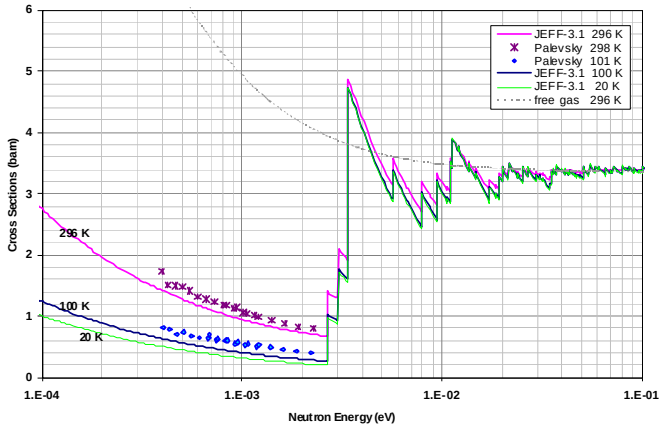

SATIF9 13

IKE Stuttgart

Total Neutron Cross Section of polycristalline Aluminium (T=293 K)

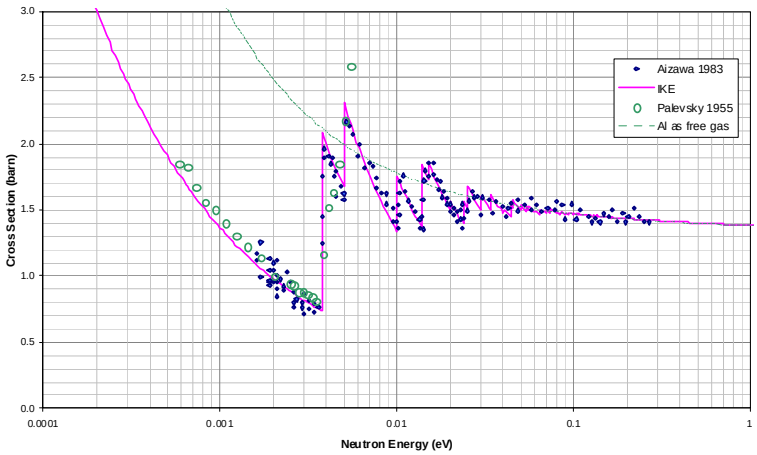

SATIF9 14

Neutron cross sections of polycrystalline aluminium at T=20K

IKE Stuttgart

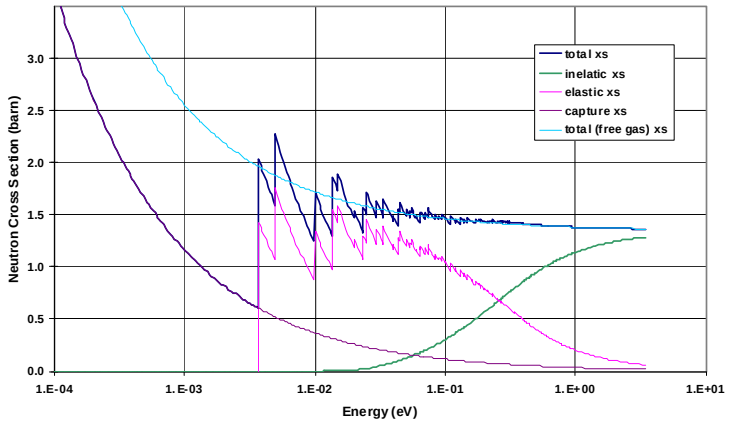

SATIF9 15

IKE Stuttgart

Total Neutron Cross Section of polycristalline Aluminium at 100 K

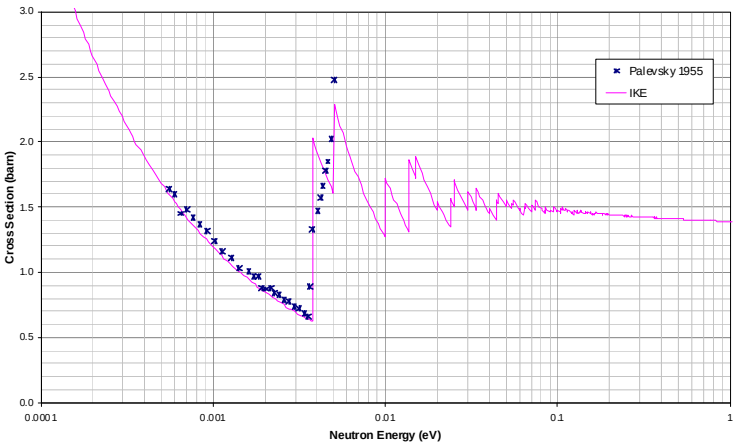

SATIF9 16

IKE Stuttgart

Aluminium - Total neutron cross section - Exp. Steyerl at 95.5K

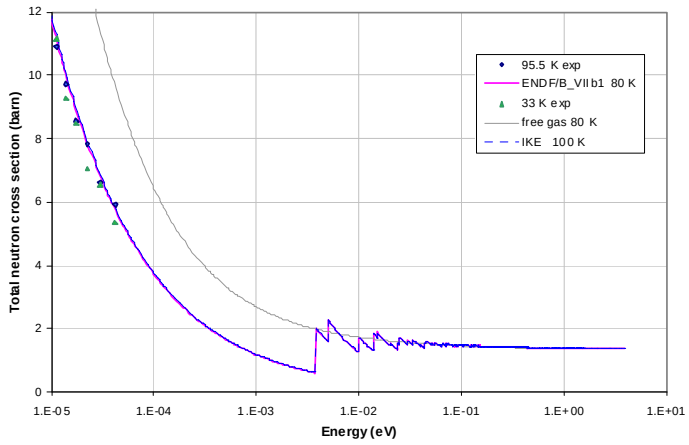

SATIF9 17

IKE Stuttgart

Aluminium - Total neutron cross section - Exp. Steyerl at 95.5K

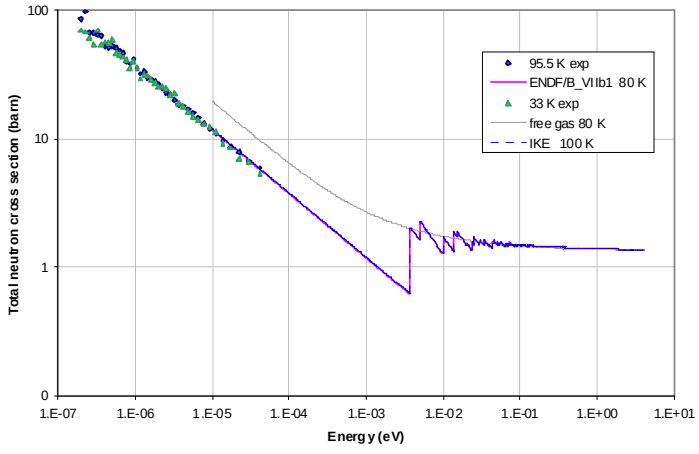

SATIF9 18

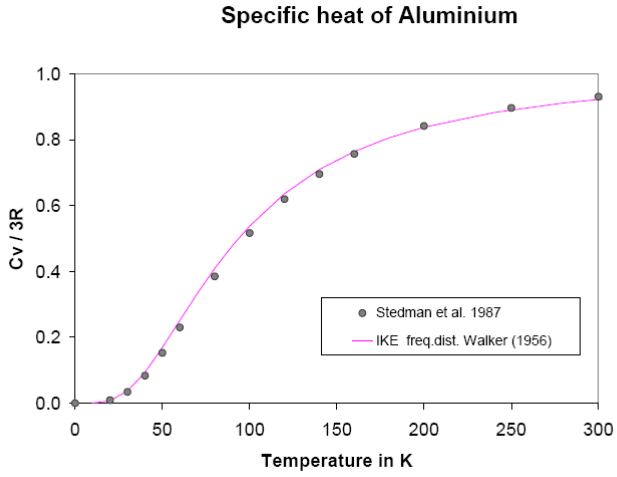

SATIF9 19

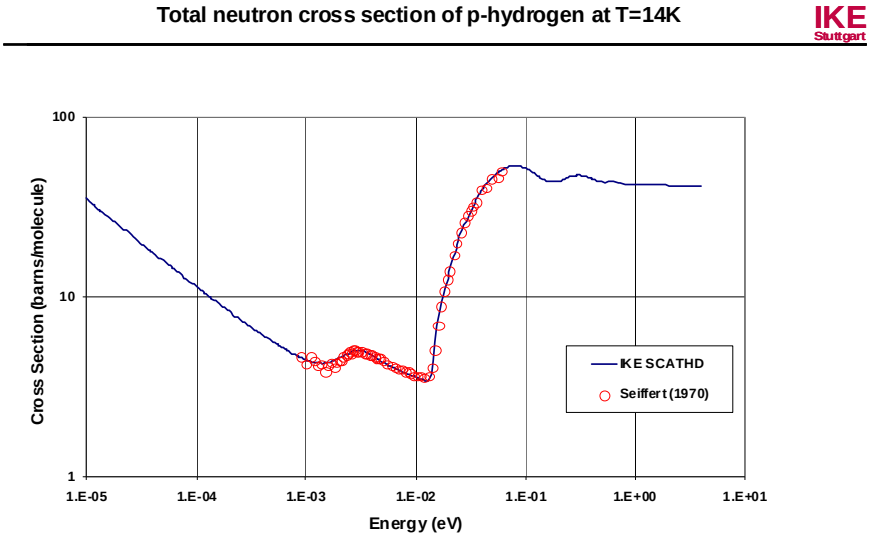

SATIF9 20

IKE Stuttgart

Total neutron cross section of liquid para-hydrogen (T = 16 K) as a function of the incident energy

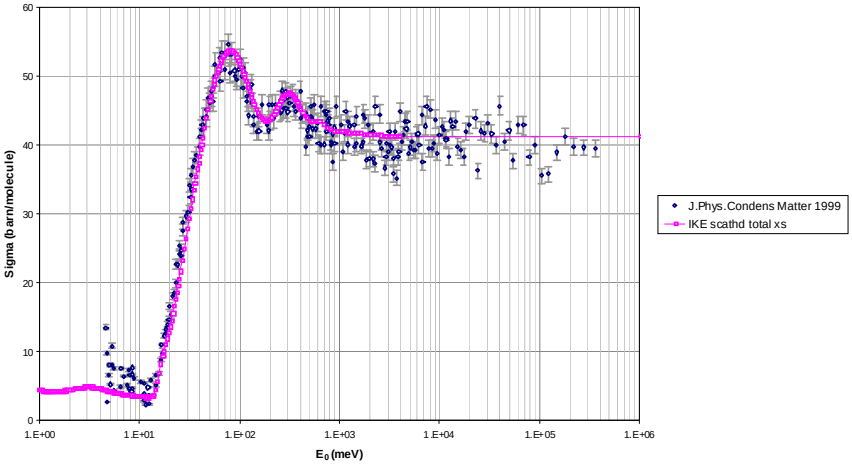

SATIF9 21

IKE Stuttgart

Total neutron cross section of liquid para-hydrogen (T = 16 K) as a function of the incident energy

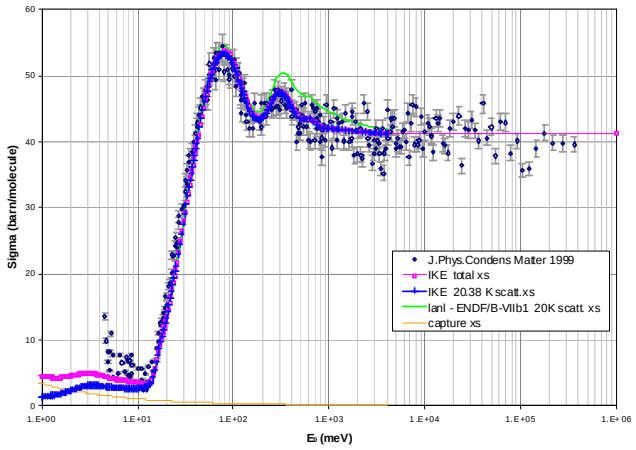

SATIF9 22

Total neutron cross section of n-hydrogen for T=16K

IKE Stuttgart

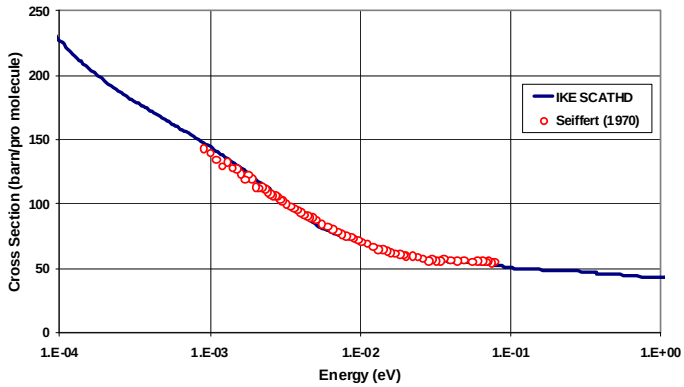

SATIF9 23

Total neutron cross section of p-hydrogen gas at T=20.4K

IKE Stuttgart

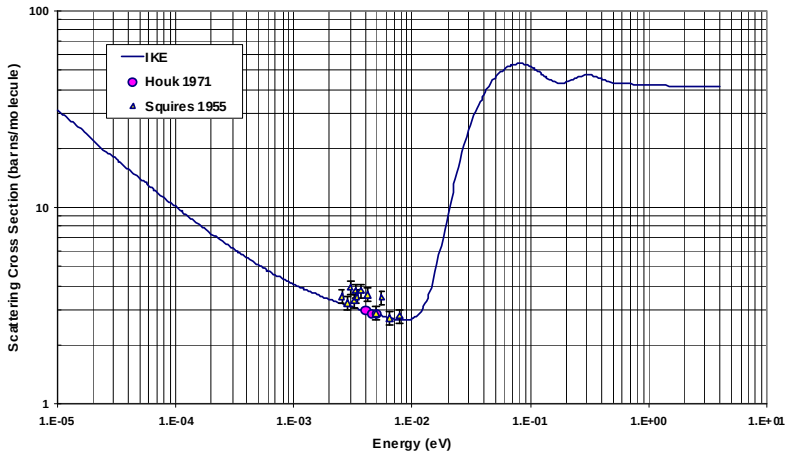

SATIF9 24

Neutron scattering cross section of o-hydrogen gas at T=20.4K

IKE Stuttgart

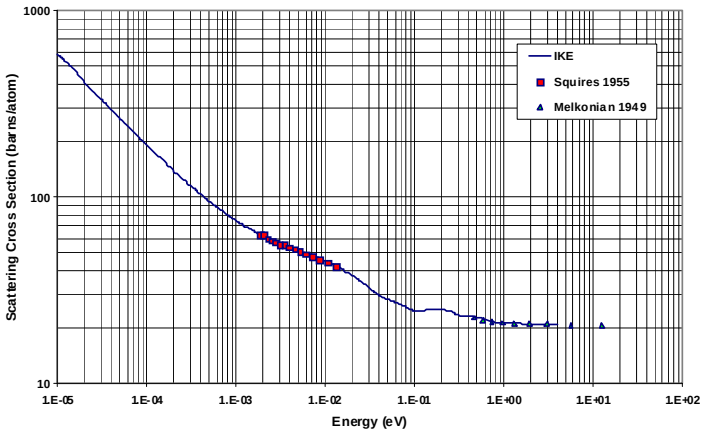

SATIF9 25

IKE Stuttgart

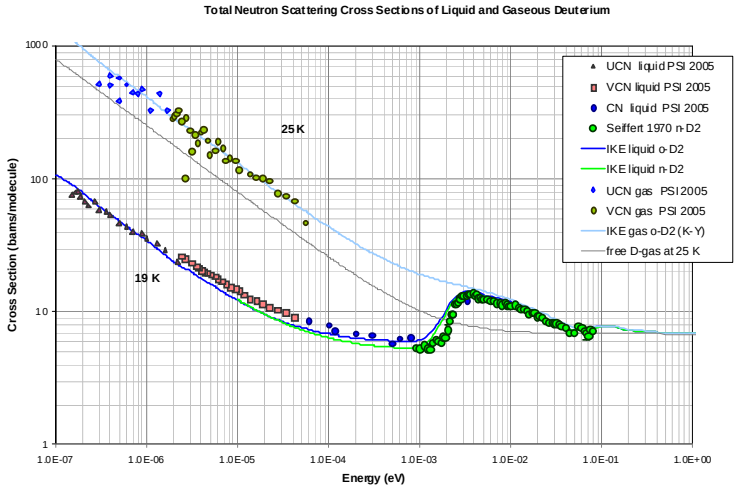

SATIF9 26

IKE Stuttgart

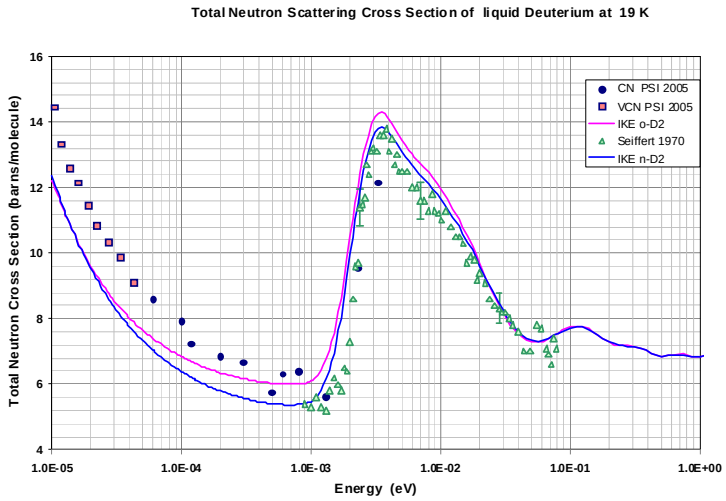

SATIF9 27

Total neutron cross section of water around T = 273K

IKE Stuttgart

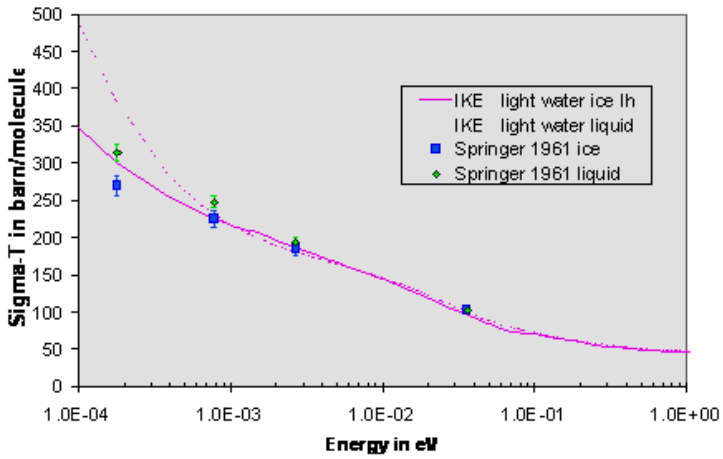

SATIF9 28

Neutron flux density spectrum in light water ice around T=20K

IKE Stuttgart

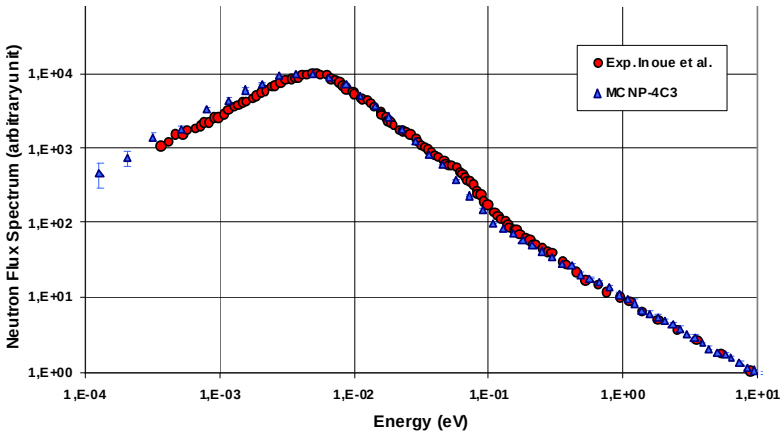

SATIF9 29

IKE Stuttgart

Neutron Cross Sections for Liquid Argon

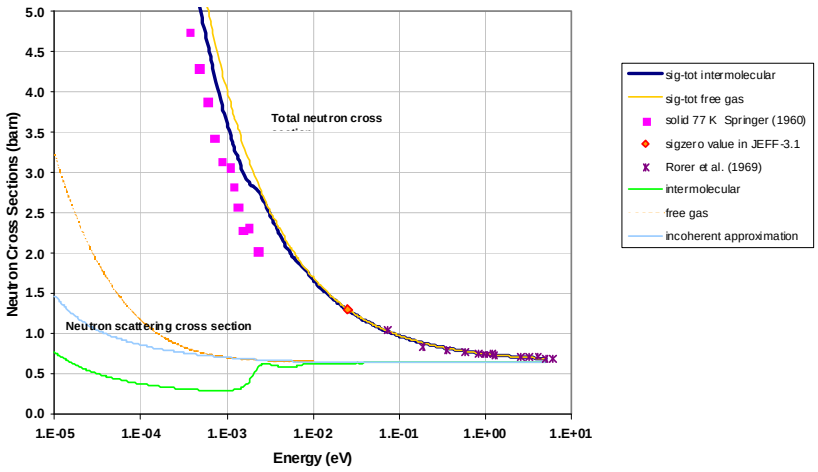

SATIF9 30

IKE
Stuttgart

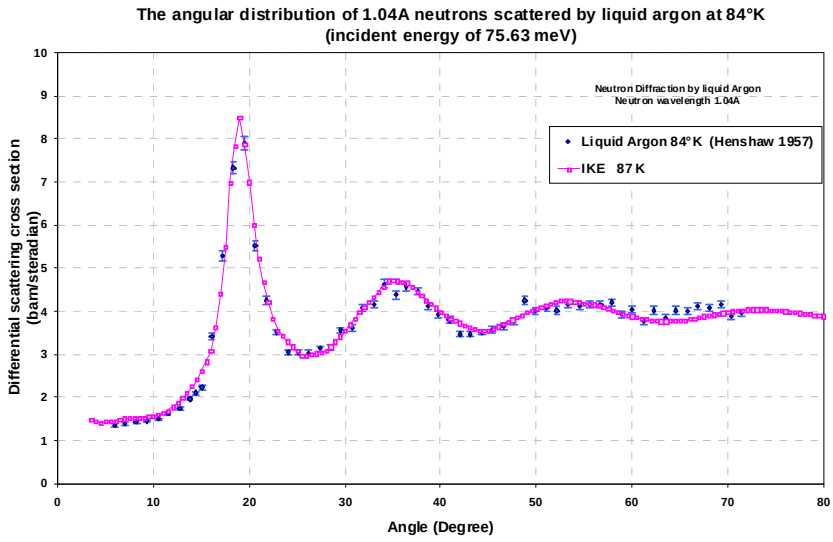

SATIF9 31

IKE
Stuttgart

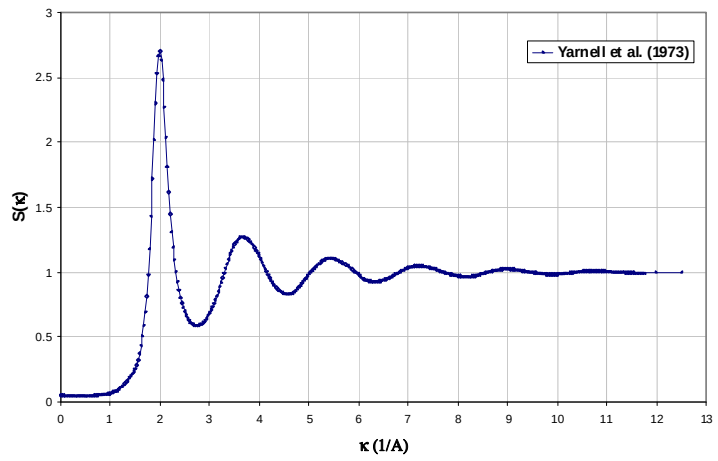

SATIF9 32

Evaluated thermal neutron scattering data of cold moderator materials from CLES and IKE

Comparisons with experimental data

M. Mattes IKE Stuttgart

SATIF9 33

References

- CLES–NEA-1775, ZZ-CLES, cross section library of moderator materials for low-energy neutron sources
- Seiffert–Messung der Streuquerschnitte vom flüssigem und festem Wasserstoff, Deuterium und Deuteriumhydrid für thermische Neutronen. EUR 4455 d (1970)
- PSI–F. Atchison et al.: Measured Total Cross Sections of Slow Neutrons Scattered by Gaseous and Liquid $^{2}H_{2}$ Phys. Rev. Letters 94,212502 (2005)
- IKE–NEA-1787, ZZ-CRYO-S(A,B)-ACE1, Scattering law and continuous energy cross section library of materials at cryogenic temperatures

SATIF9 34

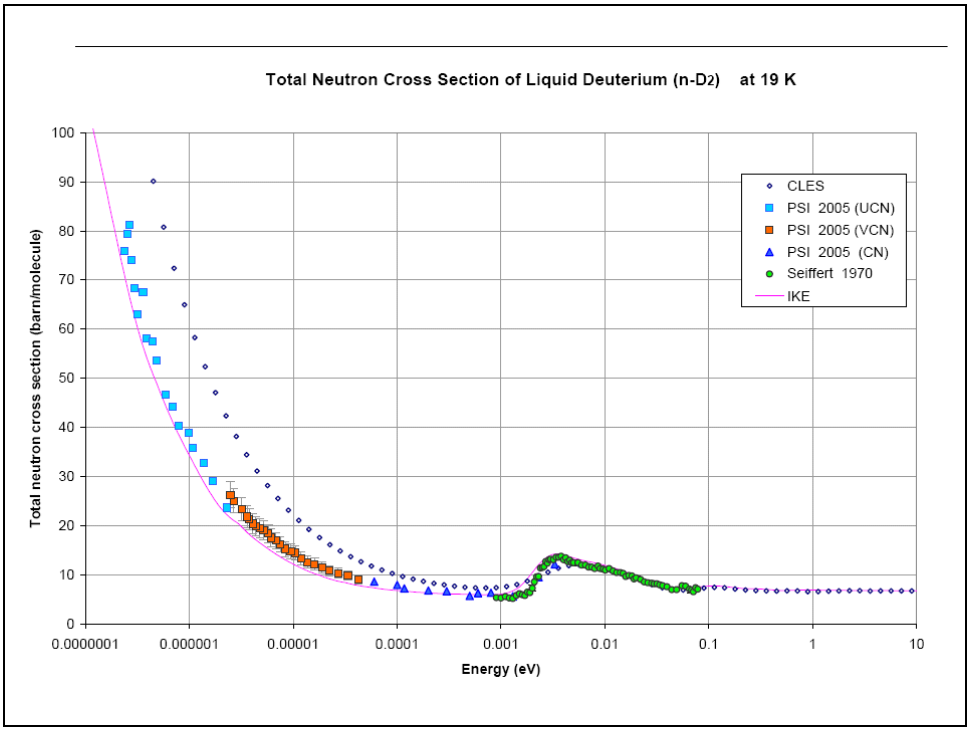
Total Neutron Cross Section of Liquid Deuterium (n-D2) at 19 K
Total neutron cross section (barn/molecule)
Energy (eV)
CLES
PSI 2005 (UCN)
PSI 2005 (VCN)
PSI 2005 (CN)
Seiffert 1970
IKE

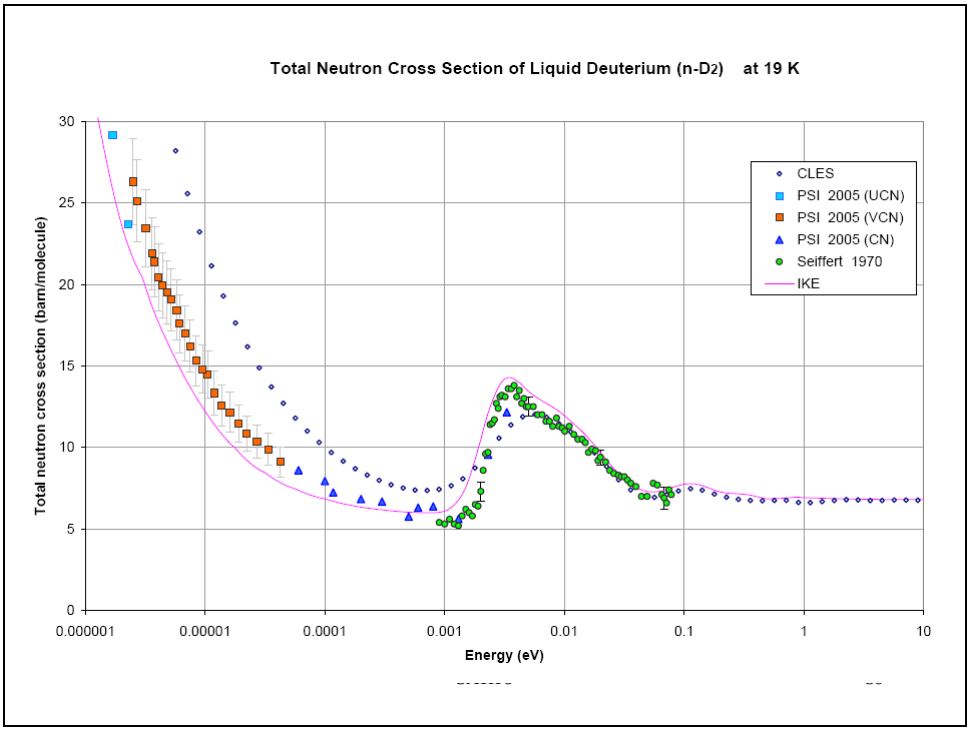
Total Neutron Cross Section of Liquid Deuterium (n-D2) at 19 K
Total neutron cross section (barn/molecule)
Energy (eV)
CLES
PSI 2005 (UCN)
PSI 2005 (VCN)
PSI 2005 (CN)
Seiffert 1970
IKE

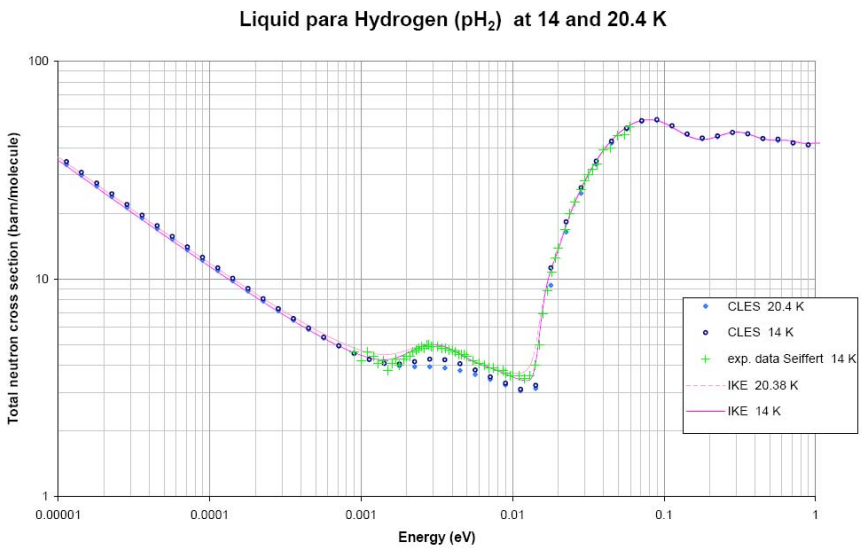

SATIF9 37

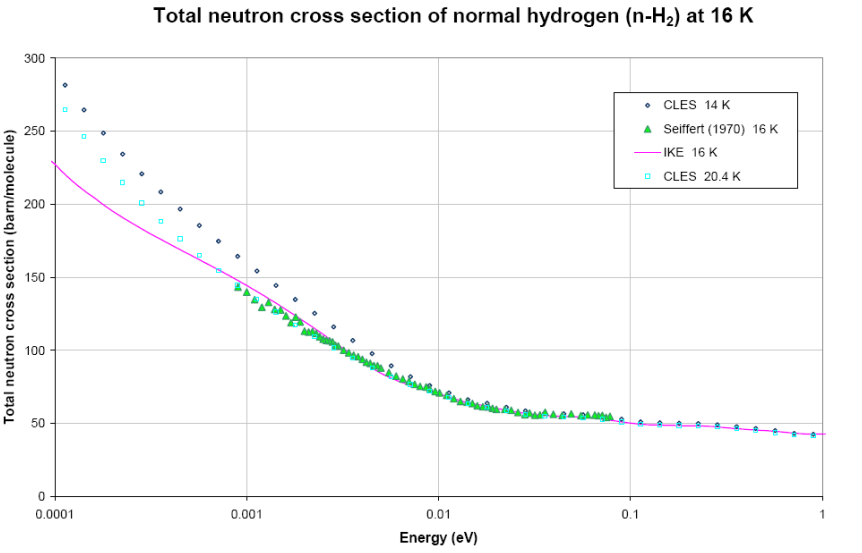

SATIF9 38

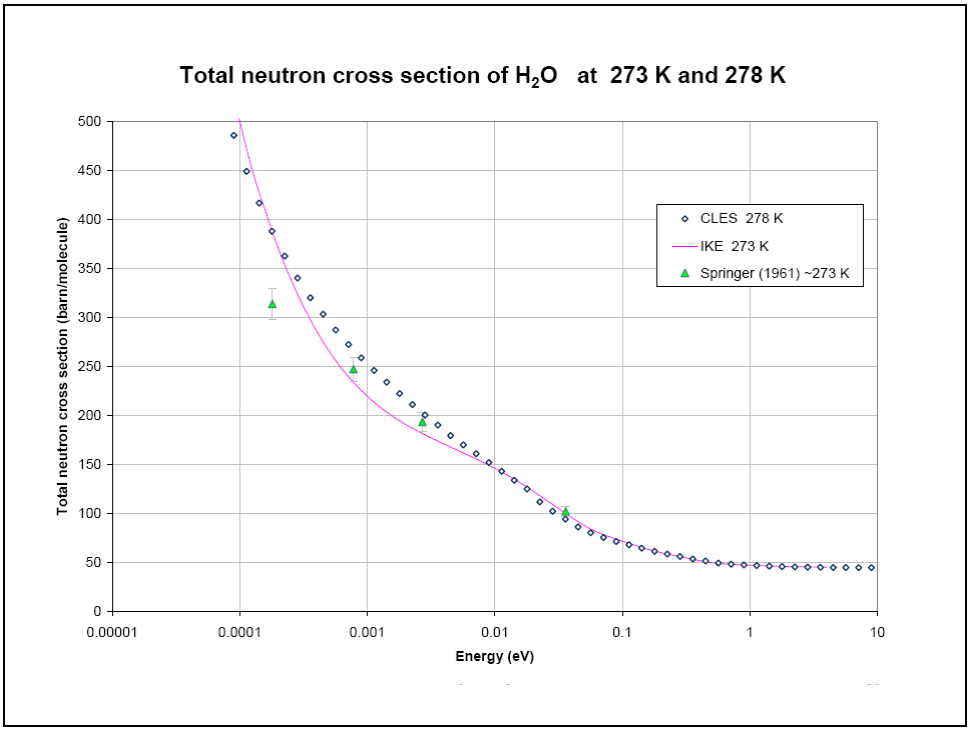
Total neutron cross section of H_2O at 273 K and 278 K
Total neutron cross section (barn/molecule)
Energy (eV)
CLES 278 K
IKE 273 K
Springer (1961) ~273 K
0
50
100
150
200
250
300
350
400
450
500
0.00001
0.0001
0.001
0.01
0.1
1
10

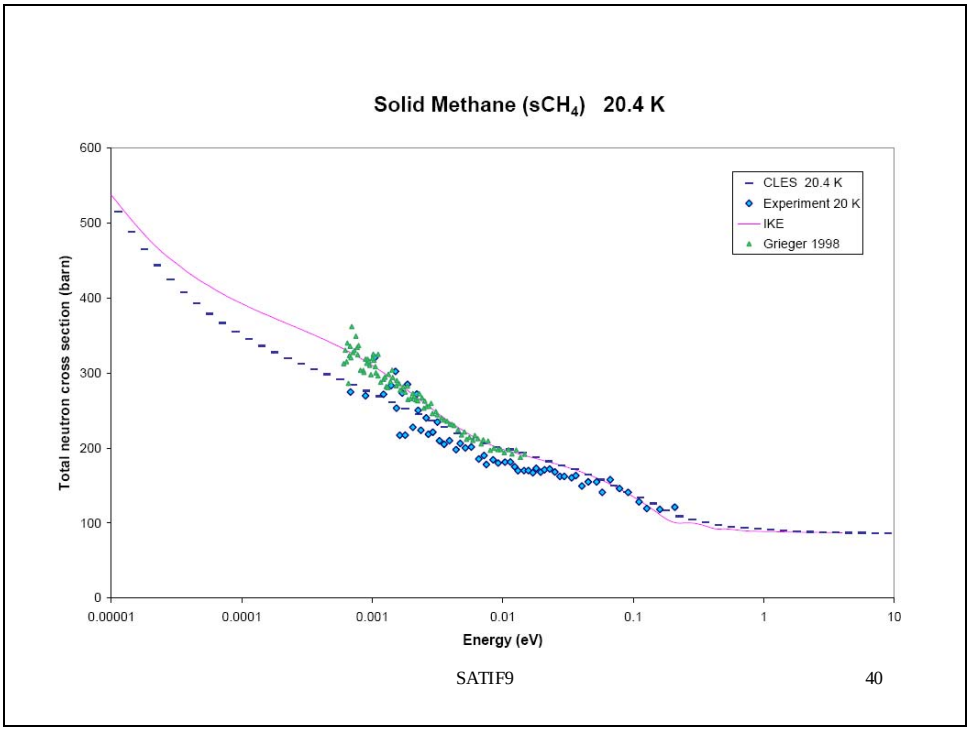
Solid Methane (sCH_4) 20.4 K
Total neutron cross section (barn)
Energy (eV)
CLES 20.4 K
Experiment 20 K
IKE
Grieger 1998
0
100
200
300
400
500
600
0.00001
0.0001
0.001
0.01
0.1
1
10
SATIF9
40

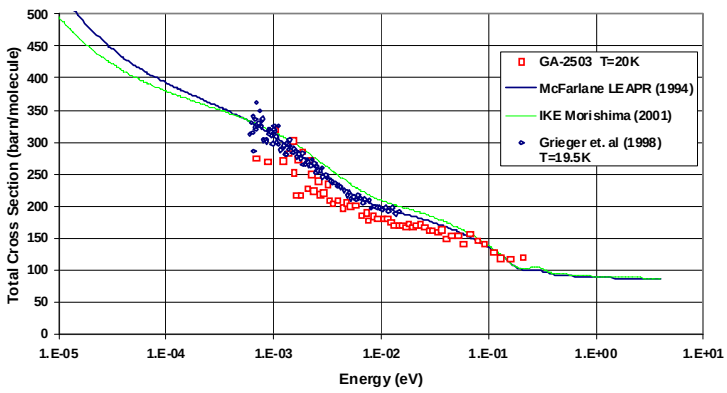

Total neutron cross section for solid methane around T=20K

SATIF9

41

Session VII

Follow-up of last SATIF agreements and actions

Discussion of the proposed content of Chapters 2.3 "Radiological standards and limits, legal dose", 2.5 "Practical aspects" and 3.6 "Environmental impact" of the "Handbook on Accelerator Shielding"

Wolfgang Dittrich
AREVA NP GmbH – NEPR-G
Erlangen, Germany

Abstract

Proposal of the content of Chapters 2.3 "Radiological standards and limits, legal dose", 2.5 "Practical aspects" and 3.6 "Environmental impact" for the Handbook on Accelerator Shielding will be presented accompanied with example outlines. A discussion is intended to help determine if the proposal meets the expectations of the SATIF participants as regards such a handbook.

Introduction

During the SATIF-8 workshop 2006 in Pohang, Korea it was decided to edit the Handbook. During autumn 2006 the team of editors (P. Vaz, N.V. Mokov) distributed a first, rough structure and proposed authors. AREVA NP GmbH accepted to contribute to Chapters 2.3, 2.5 and 3.6 and sent its contributions to the editors at beginning of 2008. This presentation should provoke a short discussion about content, depth of detail, regarded examples, etc. A copy of the proposed chapter contents follows each associated with the questions directed to the audience during the workshop. In order to avoid errors the titles of the preceding chapters are mentioned.

2 Radiation protection concepts and units

2.1 Radiation protection quantities and units

2.2 Radiation levels

2.3 Radiological standards and limits, legal dose

The radiological standards and limits as well as the legal doses in many countries follow (more or less) the recommendations of the International Commission on Radiological Protection (ICRP). This applies for example in the countries of the European Union (EU), in Japan, in the USA and in the Republic of Korea. Nevertheless, each country derived its own legal limits and other regulatory constraints on that basis. Table 2.3-1 contains some examples of this. Obviously a discussion of those limits and constraints for each country would require a separate, thick volume. Therefore in the following reference is made to the recommendations in ICRP60 [ICRP60] if not indicated otherwise. Furthermore the text refers only to the effective dose of a person since in practice this is the most common basis for shielding targets; the various dose limits for special organs, however, must also be met.

For the shielding design of an accelerator facility one can principally distinguish the following groups:

- members of the public;
- persons staying on the premises of the facility;
- persons staying in the building;
- persons working in the facility.

For members of the public the recommended annual limit of the effective dose is 1 mSv. Depending on the specific site of the accelerator facility this limit applies at the fence of the institution, in some distance outside the fence if that area is owned and controlled by the proprietor of the institution, or at a further point of reference. A limited annual occupancy for a single person can be set at these positions dependent on national regulation and on how this can be implemented unless national regulation demands the assumption of unlimited stay.

If not defined differently by the national regulation then 8 766 h/y presence is assumed at the fence or legal boundary of the premises (owner's area).

For people on the premises the annual limit of the effective dose is likewise 1 mSv, unless the fenced area is declared as being a monitored area (see Section 2.5). The annual occupancy by a person is then limited to a value either defined by national regulation or by the proprietor's controlling body.

The same applies in principle for members of the public staying in the buildings of the accelerator.

For occupationally exposed persons the annual limit is 20 mSv with a maximum of 50 mSv in a single year such that a total dose of 100 mSv is not exceeded in five consecutive years to which this single year counts. In some countries the 20 mSv per year are defined as an average value, in other countries as a maximum. This group could comprise technicians, radiation protection staff and physicians.

Many countries like Germany [G StrlSchV] but also the supra-national entity EU [EU 96/29] foresee a distinction between two subgroups of occupationally exposed persons:

- Category A – annual dose up to 20 mSv.
- Category B – annual dose up to 6 mSv.

This distinction leads practically to different scopes of medical surveillance which saves expenses for institutions and companies employing those persons.

Category A is the subgroup one would apply for workers, technicians, radiation protection staff, physicians, etc. working in radiation fields whereas category B could comprise other staff working around the beam rooms, scientific staff working only in protected experimental locations, nurses in cancer treatment centres and so on.

Consequently these limits together with additional conditions lead to first constraints which can serve as dose rate targets in shielding design. Assuming for example, a maximum 2 000 h annual stay of a category B person at a specific working place during continuous accelerator operation then a dose rate of 3 μSv/h is obtained from dividing the dose of 6 mSv by 2 000 h. The dose rate of 3 μSv/h has to be ensured with radiation protection measures like shielding if the average dose rate is higher during that period.

In addition some countries have legal dose rate limits referring to shorter time periods. For example in the USA [10CFR835] a limit of 20 μSv/h exists for the public; a controlled area is deemed to exist for dose rates above 50 μSv/h at a distance of 30 cm from radiation sources which is also defined to be a high radiation area if this dose rate exceeds 1 mSv/h (see Section 2.5). Korean regulation specifies limits of 1 mSv/week for workers and 0.1 mSv/week at locations accessible to members of the public; in addition some shielding engineers apply the constraint 10 μSv/h (20 mSv/y divided by 2 000 h/y) for shielding purposes. These lead to additional shielding targets for a facility in the country in question which could predominate.

Note: The above text describes the legal frame set by the law maker in the form of dose limits. Allowed dose rate values depend from the presence time in radiation fields. In specific cases it might be useful to consider realistic times a staff member is exposed to. For example the dose rate behind a shielding can be higher if the real beam time which is normally less than 2 000 h of annual presence (see also Section 2.5). Such an approach is applicable unless the national regulation sets strictly dose rate limits.

Table 2.3-1: Examples of legal dose limits in some countries

Country or Institution	Member of the Public:	Occupationally Exposed Person:			Remark(s)
	Maximum Annual Effective Dose in mSv	Average of Annual Effective Dose in mSv	Maximum Annual Effective Dose in mSv	Maximum Effective Dose During 5 Consecutive Years	
Canada	1		50	100	[NEA], status 2003
European Union	1		50	100	[EU 96/29], status 2007
Finland	1	20 (average of 5 consecutive years)	50		[FIN RD], status 2005
Germany	1		20 (50 in case of special authorisation)	--- (100)	[G StrlSchV], status 2007
ICRP	1	20 (average of 5 consecutive years)	50		[ICRP60]
Japan	1		50		[NEA], status 2001
Korea	1		50	100	[ISOE], status 2004
Portugal	5		50	100	[NEA], status 2003
Switzerland	1		20 (50 in case of special authorisation)	--- (100)	[CH StSV], status 2005
USA	1		50		[10CFR20], status 2005

2.4 Dose conversion coefficients and related issues

2.5 Practical aspects

Following [ICRP60] or [EU 96/29] most national regulations define radiation protection zones which are practical for structuring a building containing radiating facilities as well as for defining shielding targets within that building and for the surroundings. If not defined explicitly by those regulations constraints can be derived from the legal limits presented in Section 2.3.

ICRP, EU and many others distinguish at least between public areas, monitored areas and controlled areas:

- *Controlled area* (synonym: radiation controlled area, radiation controlled access area). These are working places of occupationally exposed workers who are required to follow well-established procedures and practices aimed specifically at controlling radiation exposures. Boundary limit could be – former procedure of ICRP, still kept by EU – 3/10 of dose limit of occupationally exposed workers; nowadays (status 1990!) ICRP recommends that the designation of controlled and supervised areas should be decided either at the design stage or locally by the operating management due to operational experience and judgement. Examples for physical boundary: entrance/exit of storage hall, building section, group of rooms. Normally the proprietor or his RP organisation will control access of persons, monitor dose rates and individual doses, keep dose records, etc.
- *Supervised area* (synonym: monitored area). Working conditions are kept under review but special procedures are not normally needed. Persons who are not occupationally exposed may stay and work there. At the boundary the limits for public are recommended to be applied if not defined otherwise by national regulation. Examples for physical boundary: fence of property, entrance/exit of building/building section. Proprietor can control presence of persons and dose rate levels in those areas.
- *Public area*. Outside the monitored (supervised) area. Nevertheless, for evidence surveys on a regular basis or long term, low-level dose monitoring could, or obtaining must be performed (depending on national regulation or requirements set by the licensing authority).

In the easiest version the public area lies outside the fence of a facility, the monitored area inside and the controlled area(s) in buildings on the monitored area. However, due to local conditions the public area could begin already at the exit of a building which itself could be a monitored area with the exception of that part containing the rooms for the accelerator and irradiation. Figure 2.5-1 describes these versions visually. Swiss regulation for example requests explicitly ≤ 0.12 μSv/h or ≤ 20 μSv/week in case of supposed permanent stay – allowing averaging over time [Teichmann].

According to Section 2.3 and the said above the constraints for these areas are or could be, respectively:

- *Public area*. 1 mSv/y to an individual member of the public; divided by the annual presence – 8 767 h/y if outside the property or for example 2 000 h/y on the property but outside the monitored area – results in 0.114 respectively 0.5 μSv/h as an average value for deriving a shielding target.
- *Monitored area*. > 1 mSv/y but less than 6 mSv/y (many EU countries according to the 3/10 limit for lower category of occupationally persons mentioned above) to an individual; divided by the annual presence – for example 1 000 h/y – results in 6 μSv/h as average value for deriving a shielding target; however – if the presence of not occupationally exposed persons is possible – the limit of 1 mSv/y for public areas may hold but together with the realistic presence time of an individual.
- *Controlled area*. > 6 mSv/y; divided by for example 2 000 h/y (a value for the annual working time used world wide for such discussions) results in 3 μSv/h as average value for deriving a shielding target – this is exactly the limit in the Finnish guide YVL 7.9 [YVL 7.9].

Figure 2.5-2 contains a set of example values for such constraints.

Figure 2.5-1: Example for the radiation protection areas of an irradiation facility with large particle energy (adapted to EU conditions)

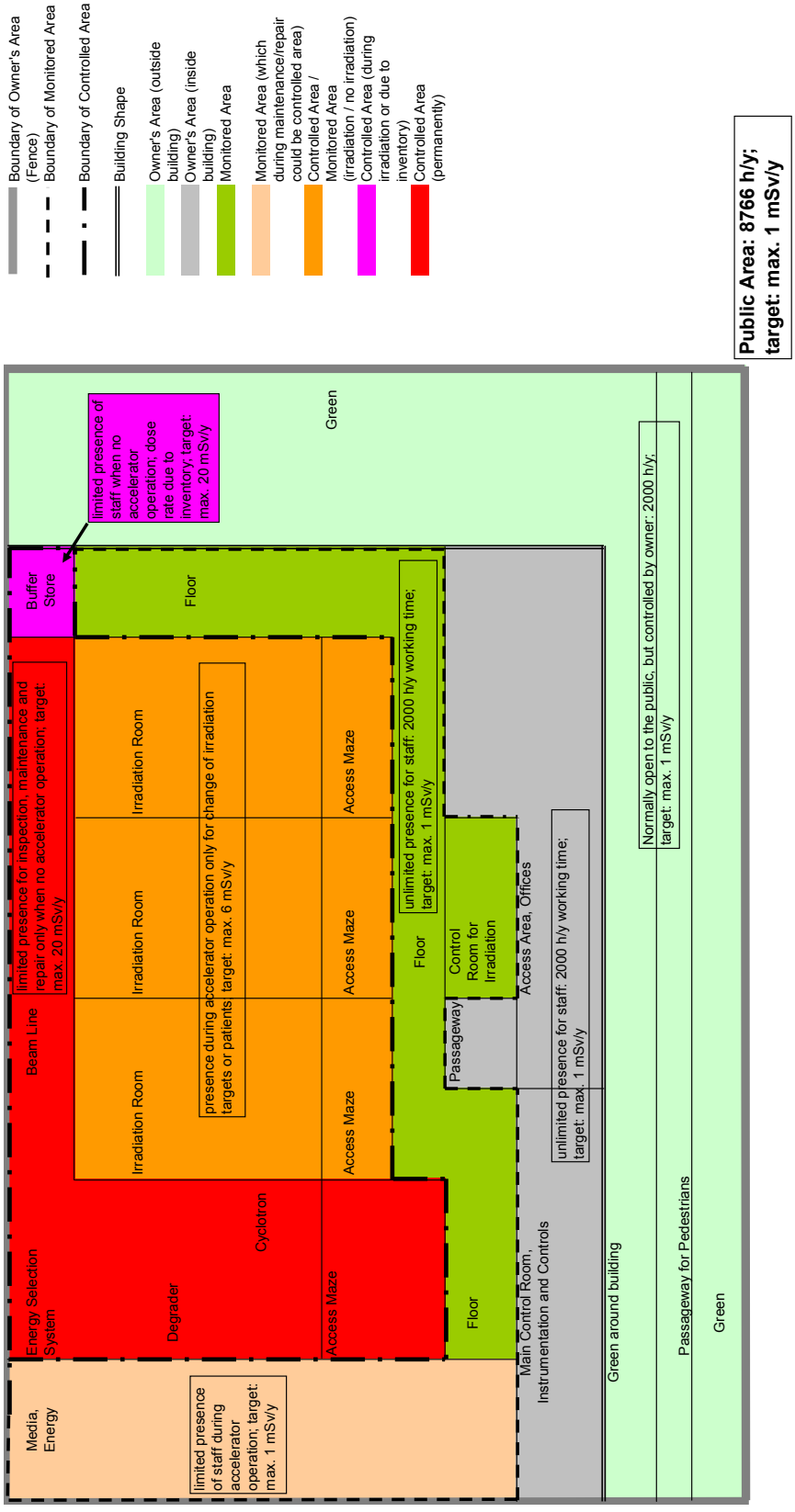

Figure 2.5-2: Example of the radiation protection constraints of an irradiation facility with large particle energy (adapted to EU conditions)

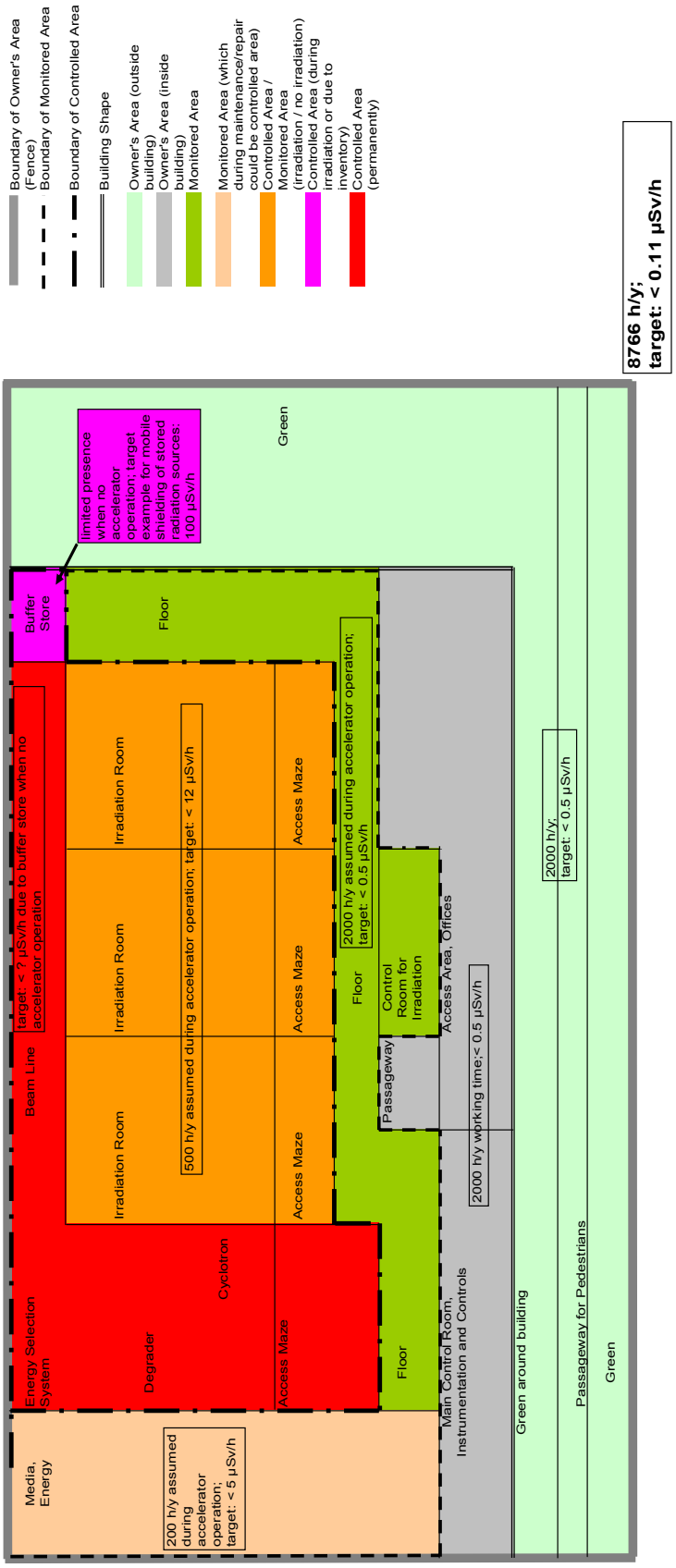

For radiation protection of personnel it proved to be useful to divide the controlled area itself in different areas classified by dose rate and zones classified by contamination. The reference values for such classification are defined in national regulations. The division into areas and zones enables the establishing of protection measures together with procedures to reduce radiation risk to personnel.

For the classification of areas by dose rate two examples for national regulation are given below: that of Switzerland and that of the USA.

Example Switzerland:

Following [HSK-R-007/d] a distinction of the controlled area is required in five area types:

- V dose rate ≤ 0.01 mSv/h (20 mSv/y / 2 000 h/y)
- W 0.01 ≤ dose rate ≤ 0.1 mSv/h
- X 0.1 ≤ dose rate ≤ 1 mSv/h
- Y 1 ≤ dose rate ≤ 10 mSv/h
- Z dose rate > 10 mSv/h

Example USA:

Following [10CFR20] in a radiation area a difference is to be made between the types:

- *Radiation area* Dose rate > 50 μSv/h in 30 cm distance from source.
- *High radiation area* Dose rate > 1 mSv/h in 30 cm distance from source (access control by means of locked doors, electronic surveillance ….).
- *Very high radiation area* Dose rate > 5 Gy/h in 1 m distance from source or wall through which radiation passes (additional measures to those for high radiation areas required to ensure that an individual is not able to gain unauthorised or inadvertent access).

In case of contamination zones both, for example Swiss and US regulations define similar rules in [HSK-R-007/d] and [10CFR835], respectively. As for shielding purposes this is of minor importance and is only mentioned here. Nevertheless, the building structure respectively the structure of the controlled area must enable measures for a suitable contamination control if needed.

In case of medical accelerator facilities specific national regulation can exist which shall be browsed for such constraints. In case of Switzerland for example [CH BeV] requires in places around irradiation rooms:

- ≤ 0.02 mSv/week in places not belonging to a controlled area;
- ≤ 0.1 mSv/week in places belonging to a controlled area.

In case of places outside the controlled area where no permanent stay is supposed and where no work locations are arranged (like waiting rooms, wardrobes, archives, stores and cellars, toilets, floors, staircases, elevator shafts, pavements, streets, green areas and gardens) these constraints may be raised by a factor 5 [CH BeV]. In locations without presence of persons during accelerator operation dose rate constraints do not exist.

Hints for a suitable building structure from the radiation protection standpoint could be found in several guides for consideration of radiation protection in the design of nuclear installations like [HSK-R-007/d] of Switzerland, [YVL7.9] and [YVL7.18] of Finland, or [KTA1301.1] of Germany.

Now – how could these constraints, rules, etc. be filled with life in the design of an accelerator facility? The subsequent description of such a proceeding uses a fictive irradiation facility equipped with a proton cyclotron as example represented in Figure 2.5-2 for illustration.

Presumably the normal situation is that the radiation protection engineer or physicist will be faced with a draft of the future facility in form of drawings and sketches provided by the architect based on the intentions of the future proprietor. This set of drawings will display the arrangement of components, rooms and supporting installation according to the knowledge of the persons involved so far. Let us assume that the radiation protection designer has been consulted at a very early stage of

the design process. Thus it may be assumed that radiation protection features such as shielding thicknesses will not require work resources for altering the already completed design, such as the arrangement and routing of technical systems like those for ventilation and power supply. Otherwise the designer will have a hard start in the project and will be beloved by fellow designers who are then faced by unexpected design changes.

The radiation protection engineer will realise the designation of the various rooms of this facility like those for beam generation, irradiation of patients or air tight sealed probes, irradiation for generation of activated substances, cooling water supply, ventilation, power supply, instrumentation and control, work shops, offices etc. Now is a good time to discuss with the proprietor as to who needs to use the facility and will work there, who needs to be protected, etc., which might lead to conclusions as follows:

1. In the beam area the technical staff – due to the radiation (gammas and betas) emitted from nuclides activated during the beam operation before – might be the most exposed group in this facility. These persons may become occupationally exposed persons of category A with an annual dose limit of 20 mSv to avoid that the operation of the facility must be interrupted because the members of this group exceed a lower dose limit during the actual calendar year. In addition the wait time before entering the beam area after any stop of operation for quick intervention could be shortened. On the other hand a person of category A causes higher costs for the employer due to the requirements of physical surveillance (dosimeters, recording of doses, special medical examination). The beam area should be defined to be a radiation controlled area and be a locked area during beam operation (it is general practice to hinder access of persons to an area with beam in operation).

2. The irradiation room will be accessed by medical staff for the care of patients or by research and laboratory staff in case of irradiation of samples. These persons are exposed to the radiation penetrating through the walls from those rooms where actual beam operation exists and to a less extent to the radiation due to the residual activation in the irradiation rooms. This group or person will be larger than that of case 1 and the employer or proprietor might intend a less expensive physical surveillance for its members. Let us assume that the decision is to put this group into category B of occupationally exposed persons with an annual dose limit of 6 mSv. This leads consequently to the requirement to shield the irradiation rooms against the beam operation in neighbouring rooms and the radiation combined with. Two of the potential constraints or shielding targets in order to meet the 6 mSv per year would be:

   – keeping the dose rate during beam operation in neighbouring rooms below 3 μSv/h which is the average dose rate considering an annual presence or working time of 2 000 h

   – or – if possible – taking benefit from a less annual presence of for example only 500 h leading to an average allowable dose rate during beam operation in neighbouring rooms below 12 μSv/h.

   According to the regulations of some countries – for example Switzerland and Germany – such rooms could be defined to be supervised areas only.

3. The accesses to areas with beam operation must be protected either by mazes or by suitable shielding plugs or shielding doors. The first alternative has the advantage that it provides significant protection even when a person is entering the first section of the maze and it never fails if designed and constructed properly. In other cases the removed plug or opened door is no longer providing any protection, and – which is very important in case of medical treatments – the action to open it needs some time which is in contradiction to the medical requirement of ease and quick access to the patient or it might fail when it must be opened to attend to the patient inside. As mazes require significant area of a building storey they must be considered as early as possible during building design.

4. Because only operating staff is working in the irradiation control room, or in the beam area during pauses, the whole interconnecting passage between the maze access points (see our example of Figure 2.5-5) could be defined to be part of the supervised area. By designing the shielding of the beam areas, irradiation rooms and mazes to be sufficiently thick, then the annual dose to an occupationally exposed worker in this area could be delimited to less than 1 mSv. This would consider a working time of 2 000 h/y leading to a constraint or shielding

target of less than 0.5 μSv/h for such walls. This layout has the advantage that no additional shielding measures have to be adopted for all other parts of the building on this level hitherto not regarded.

5. Unnecessarily thick walls [CH BeV, DIN 6847] can be avoided by exploiting national regulations or acceptance by the authorities if these allow consideration of occupancy factors or maximum annual presence times for individuals. Such rooms or areas could be rooms for services or power supply (see the example of Figure 2.5-2) to the accelerator or beam line and are therefore directly adjacent to them. Similar rooms are buffer stores for items removed from the controlled area that are awaiting further attention (clearance, waste packaging, decontamination, re-use)
6. The structural layout shall ensure that a particular restricted radiation area can only be accessed by passing through an area of the same or of less restriction.
7. A buffer room is recommended for the handling of open radioactive sources. If applicable this shall be equipped to confine any air-borne radioactivity to this room. Similar considerations can be applied to workshop areas for components removed from the controlled area for repair. Small activated items can be handled by selecting a glove box equipped with a filtered air exhaust or an extraction system into a ventilation system with discharge filters.
8. All rooms deemed to be part of the controlled area (accelerator, beam line, irradiation rooms and their mazes) and such rooms where open sources could occur (workshop areas above or rooms of potential leakage from the magnet cooling water etc) should be connected to a suitable ventilation system. This ventilation system conducts the air through HEPA filters and a monitoring system before this is discharged to the environment. Alternatively this can be coupled to an existing facility affording the same protective features. A further requirement, depending on project and national regulations for gas releases, can also be a delay line to allow sufficient radioactive decay of relatively short-lived nuclides such as C11, produced in the beam rooms by air activation, to prevent release limits from being exceeded.
9. Only when basic design features, which have influence on the building structure of an irradiation facility, have been properly defined shielding design procedures can be initiated.

3 Characterisation of radiation fields at accelerators

3.1 Beam loss in circular and linear accelerators

3.2 Target stations and beam absorbers

3.3 Prompt radiation

3.4 Residual radiation

3.5 Personal protection and monitoring

3.6 Environmental impact

In principle an accelerator facility can impact the environment by direct radiation emerging from its building walls and by radiation emerging through its roof and scattered back in the huge air volume above (which is also called skyshine in the literature). As this point is covered by the topics discussed in Section 2.5 and "please insert the no. of special shielding chapters" it is only mentioned here for completion.

During the accelerator operation the air constituents (nitrogen, oxygen, argon, carbon dioxide) are activated. These radioactive gases are transported with the ventilation system and could be finally released to the atmosphere. Some radio-nuclides have a very low half life like N16 (approx. 7 s) and decay during transport to the release point to a large extent. But some with a longer half life like C11 (approx. 21 min) and Ar41 (approx. 110 min) emerge practically undecayed. Due to the gamma radiation caused by their subsequent decay the released air plume forms a source of external

exposure to persons (gamma-submersion). The beta component of these nuclides is generally less important due to its much smaller range in air. In addition radioactive aerosols will be produced but these can be practically held back by filtering the entire air stream out of the controlled area with high efficiency particulate air filters (HEPA filters). An estimation of the production and release of radioactive gases requires not only to know the mechanism of activation (*e.g.* the activation cross-sections) but also requires consideration of the air volumes of the rooms and their ventilation rate, the distribution of flux density of activating particles together with their energy spectrum and the transport times of the radio-nuclides in the air flow. Requirements of national regulation and specific project conditions will also be considered in radiation monitoring apart from the on-line gas release determination and filter sample measurements:

- In the easiest case the new facility is an extension or modification of an already existing facility with a suitable large authorised value for the activity release. In this case the new ventilation train could be "simply" combined with the already existing controlled area exhaust train.
- Some national regulations might foresee maximum permissible concentrations for gaseous activity releases from radiation controlled areas – in this case calculational proof can be submitted to the authorities which is backed-up later by measurements.
- But in other cases it could be required to install extra long ventilation ducts, further surveillance equipment and perhaps automatic controls, or it could be required to present to the authority an environmental impact study which is time consuming or may result in delays due to legal action against the proprietor and/or licensing authority.

The cooling water for magnets itself and its potential impurities or additives might become activated. Therefore such cooling water systems should be in closed circuits. If repair or maintenance requires system draining then the radiation protection officer must first draw water samples for laboratory analysis before deciding that the water can be released into the environment – or impose restrictions. Therefore the room with the recirculation pumps and coolers of the cooling circuit should be equipped with a sump at the deepest level of all the rooms belonging to the controlled area – and the bottom of this cooling water system room should be coated with a decontaminable paint or layer. It should be possible to retain the largest cooling water train inventory within this area. As already mentioned in Section 2.5, point 8 it is recommended to connect the ventilation of that room to that of the radiation controlled area. Attention shall be paid to the ion-exchanger filter which perhaps is incorporated in the cooling water circuit for removal of impurities. This filter can collect gamma-emitting substances originated in the water, and will become a radiation source whose source strength will depend on the circumstances of the specific accelerator facility and of the cooling water circuit. One strategy treating that problem – especially in cases of presumably little water activation - is a radiation surveillance of that filter on a routine basis in order to control the activity and to be able to exchange the filter resin without large shielding efforts. If the strategy of permanent shielding of the filter is chosen the exchange method foreseen by the system designer must be examined in addition: a consequence might be a special, heavy transport shielding and additional shielding requirements for a buffer store.

The ionising particles emerging through the building base into the ground can activate the ground water and its impurities. As after travelling through diverse ground layers this water finally enters the food chain (for example as drinking water) national regulations generally specify corresponding limitations like annual dose limits for members of the public due to ingestion of radioactive contaminated water and food or derived maximum permissible concentrations in the consumption product – which here is water. The execution of such radio-ecological studies is broad topic in the literature and in many cases subject to national regulation like the US Regulatory Guide 1.109 [Reg. G. 1.1.09] or the German General Administrative Regulatory Guideline in this field [AVV]. A very simple and conservative approach – which of course should be accepted previously by the authority – is the calculation of the annual dose to man assuming his annual drinking water consumption results only from ground water irradiated over a long period – for example one year – at the most adverse point near the building and taking no credit from travel times in the ground, mixing and other effects. Then this should show that the resulting dose is less than 10 μSv/y which in several regulations is a reference value for a negligible dose contribution to members of the public (for example see § 29 of [G StrlSchV], Annex I of [EU 96/26], Articles 2, 5 and 6 of [CH StSV]); in USA the limit value is 40 μSv/y (§ 66 of [40CFR141]). The ground water impurities are determined by a recognised institution or

company appointed by the proprietor by taking water samples. Depending on the circumstances of the project under consideration a thicker concrete base or wall could be cheaper than the delay time for convincing the licensing authority to accept higher water activation. Heavy components of the accelerator, beam line and irradiation rooms require the architect to foresee a very stiff and consequently not thin concrete base in order to guarantee a highly precise position of the beam line for years to come. So such an increase might not be a major change.

In a similar way as the ground water the ground layers around and below the facility can be activated. If the licensing authority for example accepts the 10 μSv/y approach mentioned before it might accept this as a proof for the ground activation, too, and no more calculation work has to be done in this case. If this very simple approach cannot be followed, the potential activation of the soil has to be compared with reference values for soil activation or maximum permissible concentrations, whatever the licensing regulation applicable for the facility or the licensing authority requires. For performing such activation calculation one needs to know the sediment layers (like sand, clay, rock, etc.), their chemical composition by element and their density. These data are gained in advance from a suitable geological study with sample examination by a recognised institution or company.

It is the duty of the radiation protection design team to ensure that the owner of the facility take samples of soil and water at the site and performs finger-printing radiation measurements. These precautions shall be performed by a recognised institute or company prior to any site work – at least the samples shall be taken.

References

[ISOE] *Achievements and Issues in Radiation Protection in the Republic of Korea*, ISOE Asian Technical Centre, *Information Sheet, No.* 27, 2004, OECD – IAEA.

[Reg. G. 1.109] *Calculation of Annual Doses to Man from Routine Releases of Reactor Effluents for the Purpose of Evaluating Compliance with 10 CFR Part 50, Appendix I* (Rev. 1), Oct. 1977, US Nuclear Regulatory Commission.

[EU96/29] "Council Directive 96/29/EURATOM of 13 May 1996", *Official Journal of the European Communities*, *No. L 159*, 1996-06-29.

[IAEA 50-SG-D9] "Design Aspects of Radiation Protection for Nuclear Power Plants", *IAEA Safety Guide No.* 50-SG-D9, International Atomic Energy Agency, Vienna, 1985.

[AVV] *General Administrative Regulatory Guideline Concerning § 45 of the Radiation Protection Ordinance: Ascertainment of the Exposition Due to Releases of Radioactive Substances from Nuclear Plants or Installations* (Allgemeine Verwaltungsvorschrift zu § 45 Strahlenschutzverordnung: Ermittlung der Strahlenexpositon durch die Ableitung radioaktiver Stoffe aus kerntechnischen Anlagen oder Einrichtungen) from 21 February 1990, Bundesanzeiger Jahrgang 42, No. 64a, 1990-03-31, Germany.

[G StrlSchV] German Radiation Protection Ordinance (Strahlenschutzverordnung) from 2001-07-20, BGBl. I S. 1714, 2002, 1459, last change to article 2§3 section 31 of the law from 2005-09-01 (BGBl. I S. 2618).

[HSK-R-007/d] Guide HSK-R-007/d, June 1995, Switzerland.

[DIN 6847] "Medical Electron Accelerators (Medizinische Elektronenbeschleuniger-Anlagen)", *DIN* 6847 Part 2, March 1990, Deutsches Institut für Normung, Germany.

[40CFR141] *National Primary Drinking Water Regulation*, Code of Federal Regulation Title 40, Volume 19, Revision from 2001-07-01, USA.

[ICRP60] *1990 Recommendations of the International Commission on Radiological Protection*, ICRP Publication 60, Annals of the ICRP, Pergamon Press, 1991, Oxford.

[NEA] *Nuclear Legislation in OECD Countries: Regulatory and Institutional Framework for Nuclear Activities*, OECD Nuclear Energy Agency (NEA).

[10CFR835] *Occupational Radiation Protection*, 10CFR835, Code of Federal Regulation, USA.

[FIN RD] *Radiation Decree* (1512.1991), Status 2005-12-29, Finland.

[YVL7.18] *Radiation Protection Aspects in the Design of Nuclear Power Plants*, Guide 7.18, 2003-09-26, STUK – Radiation and Nuclear Safety Authority, Finland.

[KTA1301.1] *Radiation Protection Considerations for Plant Personnel in the Design and Operation of Nuclear Power Plants, Part 1: Design Safety Standards of the Nuclear Safety Standards Commission (KTA)*, KTA 1301.1, Geschaeftsstelle des Kerntechnischen Ausschusses beim Bundesamt fuer Strahlenschutz (Ed.), Post Box 10 01 49, D-38259 Salzgitter, F.R.G., November 1984.

[YVL7.9] *Radiation Protection of Nuclear Power Plant Workers*, Guide YVL 7.9, 2002-01-21, STUK – Radiation and Nuclear Safety Authority, Finland.

[Teichmann] sabine.teichmann@psi.ch, 2007-09-05.

[10CFR20] *Standards for Protection Against Radiation*, 10CFR20, Code of Federal Regulation, USA, 2005.

[CH StSV)] *Swiss Radiation Protection Ordinance* (Strahlenschutzverordnung) from 1994-06-22, Status 2000-12-19.

[CH BeV] *Swiss Accelerator Ordinance* (Beschleunigerverordnung) from 2004-12-15, status 2005-01-25.

List of participants

Austria

ROLLET, Sofia
ARCS
Systems Development Radiation Safety
Health Physics Division
ARC Seibersdorf Research GmbH
A-2444 Seibersdorf
Tel: +43 50550 2482
Fax: +43 50550 2502
Eml: sofia.rollet@arcs.ac.at

France

DUARTE, Helder
CEA Centre DAM Île-de-France
BP 12
F-91680 Bruyères-le-Châtel
Tel: +33 1 69 26 42 82
Fax: +33 1 69 26 70 63
Eml: helder.duarte@cea.fr

ENE, Daniela
CEA Saclay, Bat 703
DSM/IRFU/SPhN/MNM
F-91191 Gif-sur-Yvette Cedex
Tel: +33 1 69 08 40 91
Fax: +33 1 69 08 75 84
Eml: daniela.ene@cea.fr

JOYER, Philippe
CEA Saclay
IRFU/SIIEV – BP1
F-91191 Gif-sur-Yvette Cedex
Tel: +33 1 69 08 78 74
Fax: +33 1 69 08 92 83
Eml: philippe.joyer@cea.fr

Germany

DITTRICH, Wolfgang Max
AREVA NP GmbH
NEPR-G Strahlenschutz (Radiation Protection)
Paul-Gossen-Str. 100
D-91058 Erlangen
Tel: +49 9131 18 96535
Fax: +49 9131 18 97507
Eml: Wolfgang.Dittrich@areva.com

MARES, Vladimir
Helmholtz Zentrum München
Deutsches Forschungszentrum für
Gesundheit und Umwelt
Ingolstaedter Landstrasse 1
D-85764 Neuherberg
Tel: +49 89 3187 2652
Fax: +49 89 3187 3323
Eml: mares@helmholtz-muenchen.de

Japan

HAYASHI, Katsumi
Hitachi GE Nuclear Energy
Nuclear Plant Department
Saiwai-cho, 3-1-1, Hitachi
Ibaraki, 317-0073
Tel: +81 294 55 4501
Fax: +81 294 55 9900
Eml: katsumi.hayashi.dt@hitachi.com

HIRAYAMA, Hideo
Director, Applied Research Laboratory
High Energy Accelerator Res. Org. KEK
1-1 Oho
Tsukuba-shi, Ibaraki-ken 305-0801
Tel: +81 298 64 5451
Fax: +81 298 64 4051
Eml: hideo.hirayama@kek.jp

KIMURA, Ken-ichi
Fujita Corporation
2025-1 Ono
Atsugi-shi, Kanagawa 243-0125
Tel: +81 46 250 7095
Fax: +81 46 250 7139
Eml: kkimura@fujita.co.jp

NAKAMURA, Takashi
Professor Emeritus
Adviser of Shimizu Corp.
Naka-cho, 2-19-5-104
Musashino, Tokyo 180-0006
Tel: +81 422 54 7899
Fax: +81 422 54 7899
Eml: nakamura.takashi@shimz.co.jp

OISHI, Koji
Center for Atomic Energy Engineering
Institute of Technology
Shimizu Corporation
3-4-17 Etsyujima
Koto-ku, Tokyo 135-8530
Tel: +81 3 3820 6416
Fax: +81 3 3820 5959
Eml: koji_oishi@shimz.co.jp

SAKAMOTO, Yukio
Research Group for Applied Radiation Phys
Nuclear Science & Engineering Directorate
Japan Atomic Energy Agency
Tokai-mura, Naka-gun
Ibaraki-ken 319-1195
Tel: +81 29 282 5827
Fax: +81 29 284 3741
Eml: sakamoto.yukio@jaea.go.jp

Korea (Republic of)

LEE, Hee-Seock
Manager of Radiation Safety Group
Pohang Accelerator Laboratory
Pohang Univ. of Science and Technology
31, Nam-gu, Pohang
Gyongbuk Province, 790-784
Tel: +82 54 279 1854
Fax: +82 54 279 1799
Eml: lee@postech.ac.kr

Portugal

VAZ, Pedro
Instituto Tecnologico e Nuclear/DPRSN
Estrada Nacional 10
P-2686-953 Sacavém
Tel: +351 21 994 62 30
Fax: +351 21 994 19 95
Eml: pedrovaz@itn.pt

Russian Federation

* BATYAEV, Vyacheslav F.
Institute for Theoretical and
Experimental Physics
B. Cheremushkinskaya 25
117259 Moscow
Tel: +7 095 123 6383
Fax: +7 095 127 0543
Eml: vfb@itep.ru

* Regrets not having been able to attend.

* TITARENKO, Yury E.
Lab. of Fundamental Nuclear Physics Res.
Inst. for Theoretical & Experimental Phys
B. Cheremushkinskaya 25
117218 Moscow

Tel: +7 495 123 6383
Fax: +7 495 127 0543
Eml: Yury.Titarenko@itep.ru

Switzerland

WOHLMUTHER, Michael
Paul Scherrer Institute
WMHA/C40
CH-5232 Villigen PSI

Tel: +41 56 310 3052
Fax:
Eml: michael.wohlmuther@psi.ch

United States of America

FERGUSON, Phillip D. (Chair)
Oak Ridge National Laboratory
Spallation Neutron Source, SNS
MS 6466
Oak Ridge, TN 37830-6466

Tel: +1 865 241 5702
Fax: +1 865 574 6080
Eml: fergusonpd@ornl.gov

GALLMEIER, Franz X.
Oak Ridge National Laboratory
Building 6011, MS 6474
PO Box 2008
Oak Ridge, TN 37830

Tel: +1 865 5749675
Fax: +1 865 5746080
Eml: gallmeierfz@ornl.gov

ILAS, Dan
Oak Ridge National Laboratory
Radiation Transport and Criticality Group
Nuclear Science & Technology Division
PO Box 2008, Bldg. 5700, Rm. H334
Oak Ridge, TN 37831-6170

Tel: +1 865 576 9119
Fax: +1 865 574 3513
Eml: ilasd@ornl.gov

IVERSON, Erik B.
Oak Ridge National Laboratory
Spallation Neutron Source
Bldg. 8600, MS6475
Oak Ridge, TN 37831

Tel: +1 865 241 6970
Fax: +1 865 574 4140
Eml: iversoneb@ornl.gov

KIRK, Bernadette L.
Director
RSICC/ORNL
PO Box 2008
Bldg. 5700, MS 6171
Oak Ridge, TN 37831-6171

Tel: +1 865 574 6176
Fax: +1 865 241 4046
Eml: kirkbl@ornl.gov

LU, Wei
Oak Ridge National Laboratory
Spallation neutron Source, SNS
701 Scarboro Road
Oak Ridge, TN 37830-6474

Tel:
Fax: +1 865 574 6080
Eml: luw2@ornl.gov

MANNESCHMIDT, Jennie
RSICC/ORNL
1 Bethel Valley Road
PO Box 2008
Bldg. 5700, MS 6171
Oak Ridge, TN 37831-6171

Tel: +1 865 574 6178
Fax: +1 865 241 4046
Eml: jib@ornl.gov

* Regrets not having been able to attend.

MICKLICH, Bradley J.
Radiation Physicist
Argonne National Laboratory
Bldg. 360
9700 South Cass Avenue
Argonne, IL 60439-4814
Tel: +1 630 252 4849
Fax: +1 630 252 7722
Eml: bjmicklich@anl.gov

MUHRER, Guenter
Los Alamos National Laboratory
PO Box 1663
Los Alamos, NM, 87545
Tel: +1 505 665 8806
Fax: +1 505 665 2676
Eml: muhrer@lanl.gov

POPOVA, Irina
Oak Ridge National Laboratory
SNS
Bdg. 8600, MS 6475
Oak Ridge, TN 37830-6474
Tel: +1 865 241 5281
Fax: +1 865 574 6080
Eml: popovai@ornl.gov

RAKHNO, Igor
Fermi National Accelerator Laboratory
MS 220, PO Box 500
Batavia, IL 60510-0500
Tel: +1 630 840 6763
Fax: +1 630 840 6039
Eml: rakhno@fnal.gov

REMEC, Igor
Oak Ridge National Laboratory
PO Box 2008, MS 6363
Oak Ridge, TN 37831-6172
Tel: +1 865 574 7076
Fax: +1 865 574 9619
Eml: remeci@ornl.gov

International organisations

BRUGGER, Markus
CERN/AB
864-2D-08
CH-1211 Geneva 23
Tel: +41 22 767 6556
Fax: +41 22 766 9498
Eml: Markus.Brugger@cern.ch

KHAROUA, Cyril
CERN
AB Department – ATB group / section TCD
CH-1211 Geneva 23
Tel: +41 22 767 4857
Fax:
Eml: cyril.kharoua@cern.ch

ROESLER, Stefan
CERN
SC/RP
CH-1211 Geneva 23
Tel: +41 22 767 9891
Fax: +41 22 766 9639
Eml: Stefan.Roesler@cern.ch

SILARI, Marco
CERN
CH-1211 Geneva 23
Tel: +41 22 767 3937
Fax: +41 22 767 9360
Eml: marco.silari@cern.ch

THEIS, Christian
CERN
Geneva 23
CH-1211 Geneva
Tel: +41 22 767 8069
Fax:
Eml: Christian.Theis@cern.ch

SARTORI, Enrico (Secretariat)
OECD/NEA Data Bank
Le Seine-Saint Germain
12, boulevard des Îles
F-92130 Issy-les-Moulineaux
Tel: +33 1 45 24 10 72/78
Fax: +33 1 45 24 11 10/28
Eml: sartori@nea.fr

Annex II: Programme

Monday, 21 April

8:45 Welcome and details, *Phil Ferguson*

8:50 Opening, *Enrico Sartori*

Session 1: Source terms and related topics

Moderator: Pedro Vaz, ITN

9:00 Radiation shielding for the main injector collimation system, *Igor Rakhno* (Fermilab)

9:25 IFMIF/EVEDA accelerator nuclear safety issues and nuclear data needs, *Philippe Joyer* (CEA)

9:50 Design of the shielding of the Materials Test Station, *Guenter Muhrer* (LANL)

10:15 Break

10:30 Benchmark experiments using 140-392 MeV p-Li quasi-monoenergetic neutrons at RCNP, Osaka Univ., *Takashi Nakamura* (Tohoku University/Shimazu Corp.)

10:55 Electron linac based high energy radiation and neutron source at PAL, *Hee-Seock Lee* (PAL/POSTECH)

11:20 The multi-megawatt target station of EURISOL facility and its performance, *Cyril Kharoua* (CERN)

11:45 Complementary shielding calculations for EURISOL postaccelerator, *Daniela Ene* (CEA)

12:10 Lunch

Session 2: Measurements and calculations of induced radioactivity and activation data

Moderator: Franz Gallmeier, ORNL

13:10 An environment using nuclear inventory codes in combination with MCNPX for accelerator activation problems, *Franz Gallmeier* (ORNL)

13:35 Radiological characterisation in support of intense pulsed neutron source D&D, *Bradley J. Micklich* (ANL)

14:00 Calculation of prompt and residual dose rates of the UCN guide system, *Michael Wohlmuther* (PSI)

14:25 Simulation of the radionuclide inventories in an ISAC TRIUMF UCx target, *Igor Remec* (ORNL)

14:50 Break

15:00 Review of ITEP experiments with thin targets irradiated by protons of up to 2.6 GeV energy, *Yury Titarenko* (ITEP)

15:25 Experimental and theoretical study of ^{148}Gd formation in thin ^{nat}W targets induced with 0.4-2.6 GeV protons, *Viacheslav Batyaev* (ITEP)

16:00 SNS tour

Tuesday, 22 April

Session 3: Shielding in medical and industrial accelerator applications

Moderator: Bernadette L. Kirk, ORNL

8:30 Low activation concrete project in Japan, *Ken-ichi Kimura* (Fujita Corporation)

8:55 Activities of the Computational Medical Physics Working Group, *Bernadette L. Kirk* (ORNL)

Session 4: Benchmarking – calculations and results

Moderator: Markus Brugger, CERN

9:20 Development of a database of dosimetry benchmarks for radiation transport, *Dan Ilas*

9:45 Tissue equivalent proportional counter response behind the shielding of a carbon ion accelerator: Comparison between simulations and measurements, *Sofia Rollet* (ARC)

10:10 Measurements and analyses on angular distribution of dose rate around targets bombarded by 18, 25 and 34 MeV electrons, *Koji Oishi* (Shimizu Co.)

10:35 Break

10:45 Status of the non-elastic reaction code BRIEFF and its results with transport codes, *Helder Duarte* (CEA)

11:10 Inter-comparison of the medium-energy neutron attenuation in iron and concrete (7), *Hideo Hirayama* (KEK), presented by *Y. Sakamoto*

11:35 FLUKA shielding studies for the CNGS facility due to electronics damage, *Markus Brugger* (CERN)

12:00 Lunch

Session 5: Dose and related issues

Moderator: Marco Silari, CERN

13:00 Iterative unfolding for Bonner sphere spectrometers – sensitivity analysis and dose calculation, *G. Simmer, V. Mares, E. Weitzenegger, W. Rühm* (GSF)

13:25 Dose attenuation in concrete, iron and mixed concrete-iron shields for protons with energy up to 250 MeV, *S. Agosteo, M. Magistris, A. Mereghetti, M. Silari, Z. Zajacová*

13:50 The multi megawatt target station of EURISOL: High power deposition on the spallation and the actinides targets, *Cyril Kharoua* (CERN)

Session 6: Status of computer codes, cross-sections and shielding data libraries

Moderator: Guenter Muhrer, LANL

14:15 Radiation damage due to electromagnetic showers, *Igor Rakhno* (Fermilab)

14:40 Present status of PHITS code – event generator mode for low energy neutrons, *Yukio Sakamoto* (JAEA)

15:05 Break

15:15 Status of the International Radiations Shielding and Dosimetry Experiments (SINBAD) Database, *I. Kodeli, E. Sartori* (OECD/NEA), *B.L. Kirk* (RSICC)

15:40 Update on recent computer codes and data libraries of interest for SATIF – Status: March 2008, *I. Kodeli, E. Sartori* (OECD/NEA), *B.L. Kirk* (RSICC)

16:05 Discussion

Wednesday, 23 April

Session 7: Follow up of last SATIF agreements and actions

8:30 Discussion of the proposed content of Chapter 2.3 "Radiological standards and limits, legal dose", Chapter 2.5 "Practical aspects" and Chapter 3.6 "Environmental impact" of the "Accelerator Shielding Handbook", *Wolfgang Dittrich* (AREVA)

9:00 Discussion of the "Accelerator Shielding Handbook"

10:00 Break

10:15 Discussion including the future of SATIF

11:15 Break

11:30 Closing, *Pedro Vaz, Phil Ferguson, Enrico Sartori*

12:00 Lunch

Annex III: Structure of the "Accelerator Shielding Handbook"

N.V. Mokhov, P. Vaz
Editors

1. Introduction
2. Radiation protection concepts and units – *H. Menzel*, A. Fassò*
   - 2.1 Radiation protection quantities and units
   - 2.2 Radiation levels
   - 2.3 Radiological standards and limits, legal dose – *W. Dittrich*
   - 2.4 Dose conversion coefficients and related issues – *M. Pelliccioni, Y. Sakamoto*
   - 2.5 Practical aspects – *W. Dittrich*
3. Characterisation of radiation fields at accelerators – *S. Rokni*, A. Leuschner, W. Dittrich, M. Silari, H. Hirayama, N.V. Mokhov*
   - 3.1. Beam loss in circular and linear accelerators
   - 3.2 Target stations and beam absorbers
   - 3.3 Prompt radiation
   - 3.4 Residual radiation
   - 3.5 Personal protection and monitoring
   - 3.6 Environmental impact
4. Interactions of high-energy particles with matter – *A. Ferrari, N.V. Mokhov*, K. Niita, S. Striganov*
   - 4.1 Electromagnetic processes (ionisation, Coulomb scattering, etc.)
   - 4.2 Elastic scattering
   - 4.3 Inelastic interactions (cross-sections, multiparticle production, fragments and residual nuclei)
   - 4.4 Heavy-ion collisions
   - 4.5 Decays, capture, etc.
5. Nuclear data and event generators – *L. Waters**
   - 5.1 Cross sections – *L. Waters, S. Striganov*
   - 5.2 Evaluated libraries – *L. Waters, T. Fukahori*
   - 5.3 Event generators – *K. Gudima, S. Mashnik, K. Niita, J. Ranft, S. Striganov*

* Chapter co-ordinator.

6. Monte Carlo modelling and codes – *A. Ferrari*, A. Fassò, T. Gabriel, N.V. Mokhov, L. Waters*
   - 6.1 Monte Carlo basics
   - 6.2 Modelling coupled nuclear-electromagnetic cascades
   - 6.3 Geometry, tallies, statistics
   - 6.4 Current codes
   - 6.5 Towards efficient calculations (variance reduction, etc.)
7. Macroscopic benchmarking – *T. Nakamura**
   - 7.1 Thick target yields – *T. Nakamura, Y. Iwamoto*
   - 7.2 Shielding experiments – *T. Nakamura, S. Roesler*
   - 7.3 Deep penetration – *H. Hirayama*
   - 7.4 Electrons – *H-S. Lee*
   - 7.5 Heavy ions – *T. Nakamura, L. Heilbronn*
8. Prompt radiation: Monte Carlo and empirical approach – *K. Hayashi, M. Silari**
   - 8.1 Shielding (materials, deep penetration, etc.)
   - 8.2 Ducts and labyrinths
   - 8.3 Skyshine
9. Induced radioactivity – *S. Roesler*, I. Rakhno, M. Silari*
   - 9.1 Spallation products
   - 9.2 Components
   - 9.3 Shielding
   - 9.4 Air
   - 9.5 Ground and surface water
   - 9.6 Cooling water
10. Radiation damage and databases – *H. Schonbacher*
    - 10.1 Organic materials, composites
    - 10.2 Electronics
    - 10.3 Ceramics
    - 10.4 Metals, alloys
11. Accelerator specifics – *P. Vaz**
    - 11.1 Protons (conventional and colliders) – *H. Nakashima, S. Roesler, M. Silari*
    - 11.2 Spallation neutron sources – *T. Gabriel, F. Maekawa, A. Knapp*
    - 11.3 Electrons (conventional and colliders) – *S. Rokni, S. Roesler*
    - 11.4 Heavy ions – *T. Nakamura, Y. Uwamino, H. Iwase*
    - 11.5 Neutrino factories and muon colliders – *N.V. Mokhov*
    - 11.6 Medical applications – *N. Ipe, B. Kirk, W. Newhauser*
    - 11.7 Industrial applications – *E. Sartori, P. Vaz*

* Chapter co-ordinator.

* Chapter co-ordinator.